



Volume 13, Issue 1, March 2023
ISSN 2158-0529

IJB M

International Journal

BIOMEDICINE

INTERNATIONAL JOURNAL OF BIOMEDICINE

Aims and Scope: *International Journal of Biomedicine (IJBM)* publishes peer-reviewed articles on the topics of basic, applied, and translational research on biology and medicine. Original research studies, reviews, hypotheses, editorial commentary, and special reports spanning the spectrum of human and experimental and tissue research will be considered. All research studies involving animals must have been conducted following animal welfare guidelines such as the National Institutes of Health (NIH) Guide for the Care and Use of Laboratory Animals, or equivalent documents. Studies involving human subjects or tissues must adhere to the Declaration of Helsinki and Title 45, US Code of Federal Regulations, Part 46, Protection of Human Subjects, and must have received approval of the appropriate institutional committee charged with oversight of human studies. Informed consent must be obtained.

International Journal of Biomedicine endorses and behaves in accordance with the codes of conduct and international standards established by the Committee on Publication Ethics (COPE).

International Journal of Biomedicine (ISSN 2158-0510) is published four times a year by International Medical Research and Development Corp. (IMRDC), 6308, 12 Avenue, Brooklyn, NY 11219 USA

Customer Service: International Journal of Biomedicine, 6308, 12 Avenue, Brooklyn, NY 11219 USA; Tel: 1-917-740-3053; E-mail: editor@ijbm.org

Photocopying and Permissions: Published papers appear electronically and are freely available from our website. Authors may also use their published .pdf's for any non-commercial use on their personal or non-commercial institution's website. Users are free to read, download, copy, print, search, or link to the full texts of these articles for any non-commercial purpose. Articles from IJBM website may be reproduced, in any media or format, or linked to for any commercial purpose, subject to a selected user license.

Notice: No responsibility is assumed by the Publisher, Corporation or Editors for any injury and/or damage to persons or property as a matter of products liability, negligence, or otherwise, or from any use or operation of any methods, products, instructions, or ideas contained in the material herein. Because of rapid advances in the medical and biological sciences, in particular, independent verification of diagnoses, drug dosages, and devices recommended should be made. Although all advertising material is expected to conform to ethical (medical) standards, inclusion in this publication does not constitute a guarantee or endorsement of the quality or value of such product or of the claims made of it by its manufacturer.

Manuscript Submission: Original works will be accepted with the understanding that they are contributed solely to the Journal, are not under review by another publication, and have not previously been published except in abstract form. Accepted manuscripts become the sole property of the Journal and may not be published elsewhere without the consent of the Journal. A form stating that the authors transfer all copyright ownership to the Journal will be sent from the Publisher when the manuscript is accepted; this form must be signed by all authors of the article. All manuscripts must be submitted through the International Journal of Biomedicine's online submission and review website. Authors who are unable to provide an electronic version or have other circumstances that prevent online submission must contact the Editorial Office prior to submission to discuss alternate options (editor@ijbm.org).

IJB M

INTERNATIONAL JOURNAL OF BIOMEDICINE

Editor-in-Chief
Marietta Eliseyeva
New York, USA

Founding Editor
Simon Edelstein
Detroit, MI, USA

EDITORIAL BOARD

Mary Ann Lila
*North Carolina State University
Kannapolis, NC, USA*
Ilya Raskin
*Rutgers University
New Brunswick, NJ, USA*
Yue Wang
*National Institute for Viral Disease
Control and Prevention, CCDC
Beijing, China*
Nigora Srojidinova
*National Center of Cardiology
Tashkent, Uzbekistan*
Dmitriy Labunskiy
*Lincoln University
Oakland, CA, USA*
Randy Lieberman
*Detroit Medical Center
Detroit, MI, USA*
Seung H. Kim
*Hanyang University Medical Center
Seoul, South Korea*

Roy Beran
*Griffith University, Queensland
UNSW, Sydney, Australia*
Marina Darenskaya
*Scientific Centre for Family Health and
Human Reproduction Problems
Irkutsk, Russia*
Alexander Vasilyev
*Central Research Radiology Institute
Moscow, Russia*
Karunakaran Rohini
*AIMST University
Bedong, Malaysia*
Lev Zhivotovsky
*Vavilov Institute of General Genetics
Moscow, Russia*
Bhaskar Behera
*Agharkar Research Institute
Pune, India*
Hesham Abdel-Hady
*University of Mansoura
Mansoura, Egypt*
Tetsuya Sugiyama
*Nakano Eye Clinic
Nakagyo-ku, Kyoto, Japan*

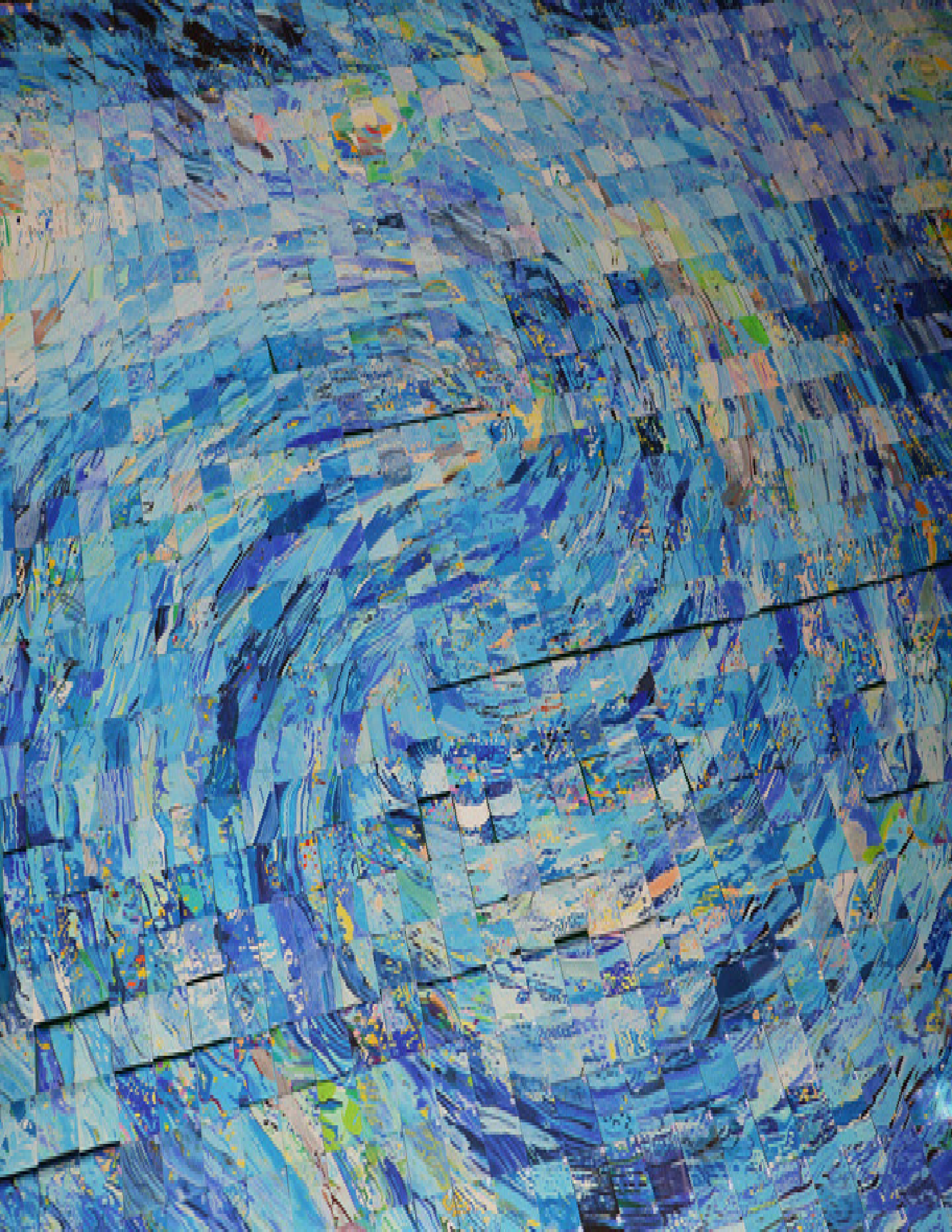
Alireza Heidari
*California South University
Irvine, California, USA*
Rupert Fawdry
*University Hospitals of Coventry &
Warwickshire Coventry, UK*
Timur Melkumyan
*Tashkent State Dental Institute
Tashkent, Uzbekistan
RUDN University, Moscow, Russia*
Shaoling Wu
*Qingdao University, Qingdao
Shandong, China*
Biao Xu
Nanjing University, Nanjing, China
Boris Mankovsky
*National Medical Academy for
Postgraduate Education
Kiev, Ukraine*
Bruna Scaggiante
*University of Trieste
Trieste, Italy*

EDITORIAL STAFF

Paul Edelstein (*Managing Editor*)
Paul Clee (*Copy Editor*)

Dmitriy Eliseyev (*Associate Editor*)
Paul Ogan (*Bilingual Interpreter*)

Arita Muhaxhery (*Editorial Assistant*)
Natalya Kozlova (*Editorial Assistant*)



IJB M

INTERNATIONAL JOURNAL OF BIOMEDICINE

www.ijbm.org

Volume 13 Issue 1 March 2023

CONTENTS

REVIEW ARTICLES

The Application of Artificial Intelligence in Detecting Breast Lesions with Medical Imaging:

A Literature Review

S. S. Alghamdi..... 9

Mesenchymal Subtype of Triple-Negative Breast Cancer: A Review of Specific Features

N. V. Krakhmal, N. N. Babyshkina, S. V. Vtorushin..... 14

Comparative Overview of Different Radiological Imaging Techniques in the Diagnosis of Pulmonary Embolism

Z. Y. Hamd..... 20

Telogen Effluvium, Diagnosis and Management: A Narrative Review

R. S. Hussein, S. B. Dayel..... 26

ORIGINAL ARTICLES

Pulmonology

Comprehensive Assessment of Cardiometabolic Risk in Patients with

Chronic Obstructive Pulmonary Disease and Obesity

E. S. Ovsyannikov, A. V. Budnevsky, L. A. Titova, A. S. Ivanova, S. A. Korchagina 31

Asthma Control in Multimorbid Patients

L. V. Tribuntseva, A. V. Budnevsky, G. G. Prozorova, et al.37

Diabetes Mellitus

Therapy Goal Achievement in Children and Adolescents with Type 1 Diabetes Mellitus in

Insulin Pump Therapy Depending on the Glucose Monitoring and Educational Programs

A. B. Tashmanova, G. N. Rakhimova, S. F. Berkinbaev, et al.....41

Trends in Prediabetes and Diabetes Prevalence in Kosovo: A Comparison of the Results of Steps Survey From 2011 and 2019

N. Ramadani, S. Hoxha-Gashi, S. Muçaj, et al.....47

Vascular Diseases

Pro- and Anti-Inflammatory Blood Cytokines Levels in Women with Moderate and

Severe Pelvic Venous Insufficiency

M. A. Darenskaya, A. A. Semendyaev, D. A. Stupin, et al.54

Internal Medicine

Impact of Cigarette Smoking on Serum Cystatin C and Creatinine Levels and MAU:

A Case-Control Study

N. M. Farah, A. M. Abbas, A. A. M. Alameen, et al.....58

Oncology

Expression of P53 and PTEN in Correlation with some Clinical and Pathological Features in Breast Cancer of Sudanese Patients

A. M. Hamad, R. M. S. Alkhatem, A. K. Algahany, et al. 62

Immunofluorescence Analysis of Erythrocyte Membranes of Cervical Cancer Patients

S. N. Mamaeva, V. A. Alekseev, N. A. Nikolaeva, et al. 69

Hematology

Analysis of NPM1 and FLT3 Mutations in Patients with Acute Myeloid Leukemia in Jeddah, Saudi Arabia: A Pilot Study

R. Alserihi, H. Ahmad, H. Alkhatabi, et al..... 73

Radiology

Characterization of Incidental Liver Lesions: Comparison of Multidetector CT versus Ultrasonography

H. E. Osman 84

Assessment of Pancreatic Duct Dilation in Patients with Pancreatic Cancer and Chronic Pancreatitis using Ultrasonography: A Retrospective Study

Z. Y. Hamd, A. Gareeballah, A. E. Abdelsalam, et al. 91

Ultrasonographic Assessment of Normal Achilles Tendon Thickness and Width in the Asymptomatic Sudanese Population

M. H. Mohammed, T. B. E. Abdalla, R. A. Abouraida, et al..... 95

Stereological Measurement of the Volume of Medulla Oblongata in Young Adults from

Magnetic Resonance Images using ImageJ Software

A. Y. Mohamed, Z. Y. Hamd, A. I. Alorainy, et al. 101

Vesicoureteral Reflux Grading using Different Imaging Techniques (MCUG, NM, and US): A Comparative Study

A. M. Omer, N. M. ALharbi, N. F. Almohammadi, et al. 106

Characterization of Primary and Malignant Liver Lesions using Texture Analysis

A. B. Mohammed, M. Garelnabi, A. Alamin, et al..... 111

Evaluation of Traumatic Knee Joint Injuries Using Magnetic Resonance Imaging

M. Elhaj, A. Elzaki, A. F. Alzain, et al. 115

Radiomorphometric Indicators, their Reliability in Detecting Early Signs of Osteoporosis in Menopausal Women

M. Shkodra-Brovina..... 120

Obstetrics and Gynecology

Association of Plasminogen Activator Inhibitor-1 4G/5G and Angiotensin-Converting Enzyme I/D Polymorphisms with Recurrent Pregnancy Loss in Sudanese Women: A Case-Control study

H. K. Ahmed, A. G. Elgoraish, S. E. Abdalla, et al. 127

Dermatology

The Impact of Single-Nucleotide Polymorphisms in Regulatory Genes on the Development of Severe Acne

A. G. Romyantsev, O. M. Demina..... 134

Dentistry

Detection of Actinobacillus actinomycetemcomitans DNA in Patients with Partial and Complete Dentures by Real-Time PCR

E. Veseli, G. Staka 141

The Color Differences in Cervical, Middle and Incisal Segments of Maxillary Frontal Teeth

T. P. Krasniqi, E. Xhajanka, Z. L. Krasniqi, et al..... 146

Vaccines and Immunization

Correlation of Herd Immunity to Measles Vaccination Rate and Disease Incidence

E. G. Haxhiu, I. Humolli, D. Pllana 151

Population Health

Correlates of Satisfaction among Hospitalized Patients in Kosovo

H. Kamberi, N. Jerliu, Genc Burazeri..... 156

Medical Education

Knowledge, Attitude, and Perception Among the Dental Students During the COVID-19 Pandemic in Kosovo

V. H. Cakolli, V. H. Hoxha, V. Ferizi, L. F. Shabani..... 161

CASE REPORT

Primary Mucinous Cystadenocarcinoma of the Testis: A Case Report and Literature Review

L. Shahini, A. Elshani, V. Cena, et al. 168

Anaplastic Pleomorphic Xanthoastrocytoma, WHO Grade 3, Located on the Hippocampal Region:

A Case Report

S. Kabashi-Muçaj, A. Mekaj, M. Petrela, et al. 172

RETRACTIONS

RETRACTED: Mitochondrial tRNALeu(UUR) Mutations in Patients with Essential Hypertension

International Journal of Biomedicine..... 177

ESC Preventive Cardiology 2023

EAPC Annual Congress



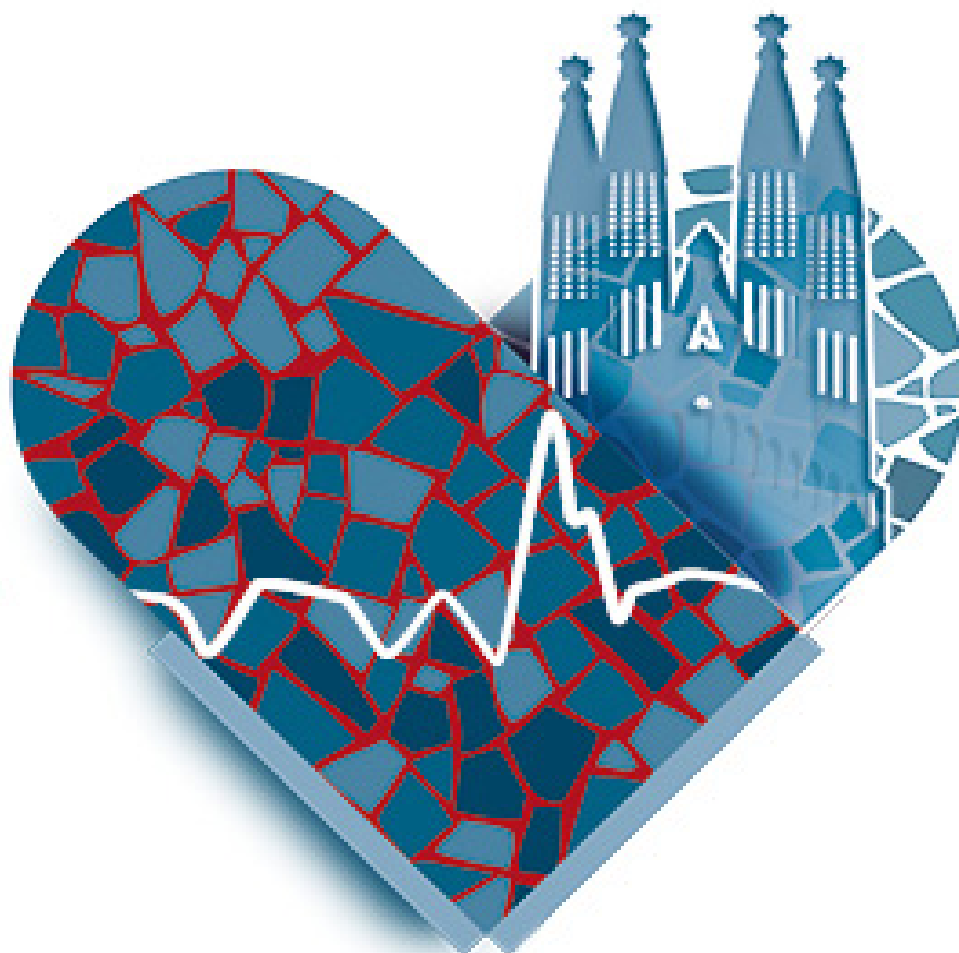
13-15 April
Malaga, Spain •

#ESCPrev2023



EHRA
European Heart
Rhythm Association

EHRA 2023



16-18 | Barcelona •
April | & Online

#EHRA2023



ESC
European Society
of Cardiology



The Application of Artificial Intelligence in Detecting Breast Lesions with Medical Imaging: A Literature Review

Salem Saeed Alghamdi*

Department of Applied Radiologic Technology, College of Applied Medical Sciences, University of Jeddah, Jeddah, Saudi Arabi

Abstract

Breast cancer is considered the most commonly diagnosed cancer among women worldwide. Several studies have shown that mammography screening could significantly decrease breast cancer mortality. Despite other screening modalities, such as MRI and ultrasound (US), mammography plays a vital role in detecting cancer and following up on it, due to its qualities and properties. The aim of this literature review is to look at recent studies that use AI with different medical imaging modalities, such as MRI, and US, in detecting breast lesions.

A literature search was carried out using Google Scholar, Semantic Scholar, medRxiv, and PubMed databases for a period of the last four years. The search terms were “breast lesion,” “breast imaging,” and “breast cancer” combined with “machine learning,” “deep learning,” and “artificial intelligence.” Among these studies, only the medical imaging related to breast lesions with AI was selected. A total of 25 articles were extracted from the following databases: 4 Google Scholar, 3 Semantic Scholar, 4 medRxiv, and 14 PubMed. Only papers related to breast lesions with medical imaging modalities were extracted, and all duplications were removed. In this study, the papers were reviewed by medical imaging professionals.

This literature review summarizes the most recent articles on utilizing artificial intelligence (AI) in detecting breast lesions for different imaging modalities: mammogram, ultrasound, and MRI. Reviewed studies showed that AI performance in detecting lesions was significant, associated with high accuracy, sensitivity, and specificity for these modalities. (**International Journal of Biomedicine. 2023;13(1):9-13.**)

Keywords: artificial intelligence • convolution neural network • machine learning • neural network artificial

For citation: Alghamdi SS. The Application of Artificial Intelligence in Detecting Breast Lesions with Medical Imaging: A Literature Review. International Journal of Biomedicine. 2023;13(1):9-13. doi:10.21103/Article13(1)_RA1.

Abbreviations

AI, artificial intelligence; AUC, area under curve; BI-RADS, Breast Imaging Reporting and Data System; DL, deep learning; CAD, computer-aided detection; CNN, convolution neural network; MRI, magnetic resonance imaging; ML, machine learning; NNA, neural network artificial; US, ultrasound.

Introduction

Breast cancer is considered the most commonly diagnosed cancer among women worldwide.^(1,2) Several studies have shown that mammography screening could significantly decrease breast cancer mortality.⁽³⁾ Despite other screening

modalities, such as MRI and ultrasound (US), mammography plays a vital role in detecting cancer and following up on it, due to its qualities and properties.⁽⁴⁾ About 20%-30% of breast cancers can be missed in mammography because of poor positioning, interpretation error, and dense parenchyma-obscuring lesions.^(5,6) By reviewing many images, radiologists have identified the mammographic differences between noncancer and cancer, and these images have been shared among radiologists, who utilized their morphological characteristics.⁽³⁾ In order to enhance the radiologists' performance, the traditional computer-aided detection (CAD) system was introduced and used in 83% of

***Contact Information:** Salem Saeed Alghamdi, Department of Applied Radiologic Technology, College of Applied Medical Sciences, University of Jeddah, Jeddah, Saudi Arabia. E-mail: ssalghamdi85@gmail.com

digital mammography examinations.⁽⁷⁾ CAD was developed to help mammogram interpretation, especially in terms of cancer detection i.e., sensitivity.⁽⁸⁻¹⁰⁾ However, CAD efficiency is controversial as some studies suggest that CAD can improve cancer detection, while large studies illustrate conflicting results for assessing the radiologist's performance in 40 facilities over four-year intervals. They found that CAD led to reduced accuracy in detecting cancer and it increased biopsy recommendations.^(11,12) Moreover, important information in CAD is susceptible to being lost when designing human-interpretation descriptors. In developed AI-based CAD, the artificial intelligence (AI) algorithms extract mammographic characteristics as descriptors. The main difference between self-learned and human-designed descriptors is the success factor of deep learning (DL) algorithms. Several studies have reported that AI could provide similar performance to medical image experts who can analyze many medical images.^(13,14) The growing interest in the application of AI in medical imaging have resulted in several newer algorithms based on DL that have been developed and utilized in digital mammography, MRI, and US. Preliminary data demonstrated that the AI system can improve the radiologist's efficiency in terms of specificity, sensitivity, and time.⁽¹⁵⁻¹⁷⁾

The aim of this literature review is to look at recent studies that use AI with different medical imaging mammograms, MRI, and US, in detecting breast lesions.

Materials and Methods

A literature search was carried out using Google Scholar, Semantic Scholar, medRxiv, and PubMed databases for a period of the last four years. The search terms were "breast lesion," "breast imaging," and "breast cancer" combined with "machine learning," "deep learning," and "artificial intelligence." Among these studies, only the medical imaging related to breast lesions with AI was selected.

Results

A total of 25 articles were extracted from the following databases: 4 Google Scholar, 3 Semantic Scholar, 4 medRxiv, and 14 PubMed. Only papers related to breast lesions with medical imaging modalities were extracted, and all duplications were removed. In this study, the papers were reviewed by medical imaging professionals. Of the extracted articles, only 3 reported on medical imaging utilized with AI: 11 mammograms, 9 US, and 5 MRI. The AI types were varied among these articles, including DL, ML, and NNA. The classification was distributed as 17 DL and 8 neural networks. The number of patients in this literature ranged from 240 to 353,879, providing data for developing the AI, including 18 retrospective data, 4 prospective data, and 3 multi-case studies (Table 1).

Discussion

Mammography

Pacilè et al.⁽¹⁸⁾ utilized 2 groups of a deep CNN named MammoScreen V1 and Therapixel, including 240 patients

(120 benign and 120 malignant tumors) with 14 radiologists. The average area under curve (AUC) across readers was 0.79 with AI, and the average variation in AUC was 0.028 by using AI; the average sensitivity was enhanced when detecting malignant tumors using AI. Kim et al.⁽³⁾ developed an AI algorithm based on a deep convolution neural networks (CNN) named ResNet-35. The data they used was collected from 5 different institutions located in the UK, USA, and South Korea. The number of all data was 170,000, including 75,000 benign and 37,000 malignant cases, with participation of 14 radiologists. By using AI, the performance of level was 0.94, which was significantly increased, compared with the radiologists' performance without AI assistance (0.81).

Moreover, AI was more sensitive in detecting cancer with masses. Frazer et al.⁽²⁰⁾ utilized multiple DL-based AI techniques, such as ResNet 50, as a backbone DL model that is pre-trained on the imageNet17 dataset. They also used 3 CNNs: inception-ResNet-V2, efficientNetB6, and NASNetLarg. The AUC was 0.89 based on 349 test cases. Another study showed that the AI reduced the false-positives for the proportion of breast screening in women from 89.9% to 62%, and the value of positive predictive recall (PPV-1) increased to 16.5%. Also, the sensitivity was enhanced for women with mass-related lesions by 98.5%.⁽²²⁾ Rodríguez-Ruiz et al.⁽²⁵⁾ used a DL-CNN system called Transpara, and the data included women from 2 institutions (in the USA and Europe). In general, the results indicate high performance in detecting cancer; with AI support, the AUC, sensitivity, and specificity were 0.89, 86%, and 79%, respectively, and the time of reviewing the case was similar between un-aided with AI (146 seconds) and aided with AI (149 seconds).

Ultrasound

Using AI applications, US demonstrated significant results. Xia et al.⁽²⁸⁾ utilized the S-detect AI system, which showed high efficiency for detecting malignant masses and was associated with high specificity, sensitivity, and accuracy of 93.8%, 95.8%, and 89.6%, respectively. Another study by Gao et al. used the RCNN network with 2 datasets from 2 different hospitals: dataset A contained 8966 nodules, and dataset B contained 2220 nodules. The number of benign cases was 788 and 929 for datasets A and B, respectively. Also, the number of malignant cases was 562 and 1291 for datasets A and B, respectively. For both datasets, the AUC of supervised learning and semi-supervised learning were: 94.2% vs. 93.7% and 92.3% vs. 92%, respectively.⁽²⁹⁾ Zhou et al.⁽³³⁾ used 3 different CNNs: Inception V3, Inception-ResNet V2, and ResNet-101 architectures with imageNet using 680 patients and 5 radiologists.

The best-performing CNN model, Inception V3, achieved an AUC of 0.89 (95% CI) in predicting the final clinical diagnosis of axillary lymph node metastasis in the independent test set. The model achieved 85% sensitivity (95% CI: 70%-94%) and 73% specificity (95% CI: 56%-85%), while the radiologists achieved 73% sensitivity (95% CI: 57%-85%) and 63% specificity (95% CI: 46%-77%).

Magnetic Resonance Imaging

A study performed by Dalmiş et al.⁽³⁵⁾ showed significant performance of AI with MRI modality. A prospective study

Table 1.

AI for detecting lesions for mammography, US and MRI.

Authors	Modality	Study type	Type of AI	Name of AI program	All data
Pacilè S. et al., 2020 ⁽¹⁸⁾	Mammography	Multi-cases retrospective study	Dual groups of deep CNNs	MammoScreen V1; Therapixel, Nice, France	241 patient cases
Kim HE et al., 2020 ⁽³⁾	Mammography	Retrospective, multireader study	Deep CNNs	ResNet-35	170,230 examinations
Rodriguez-Ruiz A, et al., 2019 ⁽¹⁹⁾	Mammography	Multi-case study	Deep learning CNNs	Transpara 1.4.0, Screenpoint Medical BV, Nijmegen, the Netherlands	2653 examinations
Fraze HM, et al., 2021 ⁽²⁰⁾	Mammography	Retrospective study Local Study & Global Study	Several DL-based AI techniques	1) ResNet50 2) Inception-ResNet-V2, EfficientNetB6 and NASNetLarge	28,694 examinations
Arasu VA, et al., 2022 ⁽²¹⁾	Mammography	Retrospective, case-cohort study	1-Mirai (MIT): leverages a ResNet 2-GMIC: used CNN	1-Mirai algorithm 2-Algorithm of Globally Aware Multiple Instance Classifier (GMIC)	329,814 patients
Kerschke L, et al., 2022 ⁽²²⁾	Mammography	Retrospective study	DL	Transpara	2957 patients
van Winkel SL., et al., 2021 ⁽²³⁾	Digital breast tomosynthesis (DBT): Mammography	Several cases	Based on deep CNNs	Transpara™ 1.6.0	360 cases
Mansour S, et al., 2021 ⁽²⁴⁾	Mammography	Prospective study	Deep CNNs	Lunit INSIGHT MMG, v. 2019	2000 mammograms
Rodriguez-Ruiz A, et al., 2019 ⁽²⁵⁾	Mammography	Retrospective, multireader, multicase study	DL CNNs	Transpara (version 1.3.0)	240 examinations
Interlenghi M, et al., 2022 ⁽²⁶⁾	Ultrasound	Retrospective study	AI	Self-developed	928 ultrasound images
Shen Y, et al., 2021 ⁽²⁷⁾	Ultrasound	Reader study	AI	Self-developed	288,767 ultrasound exams
Xia Q, et al. 2021 ⁽²⁸⁾	Ultrasound	Retrospective study	DL system	S-Detect artificial intelligence system	40 patients
Gao, Liu et al., 2021 ⁽²⁹⁾	Ultrasound	Retrospective study	DL	RCNN network	8966 nodules, 6746 nodules in Dataset A, 2220 nodules in Dataset B
Lyu SY, et al., 2022 ⁽³⁰⁾	Ultrasound	Retrospective study	Dual CNNs	AI-SONIC Breast system	92 patients
PhD XL, et al., 2022 ⁽³¹⁾	Ultrasound	Retrospective study	DL 3D CNN	3D U-net	397 participants
Mango VL, et al., 2020 ⁽³²⁾	Ultrasound	Multicenter retrospective review	ML	Koios DS for Breast, Koios Medical	900 breast lesions
Zhou LQ, et al., 2020 ⁽³³⁾	Ultrasound	Retrospective study, Multicohort study.	Deep Nueral Network, CNNs	ResNet-101 Inception-ResNet V2 Inception V3, pretrained with ImageNet	680 patients
Zhou J, et al., 2020 ⁽³⁴⁾	MRI	Retrospective study	DL CNN	ResNet50 architecture	207 patients
Dalmış MU, et al., 2019 ⁽³⁵⁾	MRI	Prospective study	DL architecture, independent CNNs	DenseNet	576 lesions
Adachi M, et al., 2020 ⁽³⁶⁾	MRI	Retrospective study	DL	RetinaNet	
Herent P, et al., 2019 ⁽³⁷⁾	MRI	Retrospective study	DL	50-layer residual neural network (ResNet-50)	335 MR images
Jiang Y, et al., 2021 ⁽³⁸⁾	MRI	Retrospective clinical reader study	Computer-assisted diagnostic MRI software	QuantX	111 examinations

associated with DL architecture used an independent CNN named DenseNet. About 576 images of lesions were used (208 benign lesions and 368 malignant lesions) from a dataset of Radboud University. The area under the ROC curve was 0.852 for the final AI system, which combines all imaging information with PI.

Another study by Adachi et al. demonstrated DL called RetinaNet that used 13 normal, 20 benign and 52 malignant cases with the participation of 4 radiologists to validate the study. The comparison between the radiologists' and AI performance was monitored. The results showed that the performance of the 4 radiologists with the AI was better than without using the AI. The AUC for the radiologists with AI was 0.925, 0.884, and 0.899, respectively. The AUC for the radiologists with AI was significantly higher than the radiologist's performance without AI ($P=0.039$).⁽³⁶⁾ Moreover, Herent et al.⁽³⁷⁾ utilized retrospective data with DL-AI that used a 50-layer residual neural network named ResNet-50. In this study, 335 MRI images were used: 212 benign lesions and 123 malignant lesions. Their model achieved a weighted mean AUC of 0.816 when using an independent challenge test. Jiang et al.⁽³⁸⁾ have evaluated whether the diagnostic performance of radiologists in differentiating cancer from noncancer with dynamic contrast, material-enhanced (DCE) breast MRI was improved when using an AI system, compared with conventionally available software. One hundred eleven women were evaluated with a total of 111 breast DCE-MRI examinations (54 malignant and 57 nonmalignant lesions). The average AUC of all readers improved from 0.71 to 0.76 ($P=0.04$) when using the AI system. The average sensitivity improved from 90% to 94% when BI-RADS category 3 was used as the cut point but not when using BI-RADS category 4a. The average specificity showed no difference when using either BI-RADS category 4a or category 3 as the cut point.

Conclusion

This literature review summarizes the most recent articles on utilizing AI in detecting breast lesions for different imaging modalities: mammogram, ultrasound, and MRI. Reviewed studies showed that AI performance in detecting lesions was significant, associated with high accuracy, sensitivity, and specificity for these modalities.

References

1. Islami F, Guerra CE, Minihan A, Yabroff KR, Fedewa SA, Sloan K, Wiedt TL, Thomson B, Siegel RL, Nargis N, Winn RA, Lacasse L, Makaroff L, Daniels EC, Patel AV, Cance WG, Jemal A. American Cancer Society's report on the status of cancer disparities in the United States, 2021. *CA Cancer J Clin.* 2022 Mar;72(2):112-143. doi: 10.3322/caac.21703.
2. Fusco R, Piccirillo A, Sansone M, Granata V, Rubulotta MR, Petrosino T, Barretta ML, Vallone P, Di Giacomo R, Esposito E, Di Bonito M, Petrillo A. Radiomics and Artificial Intelligence Analysis with Textural Metrics Extracted by Contrast-Enhanced Mammography in the Breast Lesions Classification. *Diagnostics (Basel).* 2021 Apr 30;11(5):815. doi: 10.3390/diagnostics11050815.
3. Kim HE, Kim HH, Han BK, Kim KH, Han K, Nam H, Lee EH, Kim EK. Changes in cancer detection and false-positive recall in mammography using artificial intelligence: a retrospective, multireader study. *Lancet Digit Health.* 2020 Mar;2(3):e138-e148. doi: 10.1016/S2589-7500(20)30003-0.
4. Patel BK, Lobbes MBI, Lewin J. Contrast Enhanced Spectral Mammography: A Review. *Semin Ultrasound CT MR.* 2018 Feb;39(1):70-79. doi: 10.1053/j.sult.2017.08.005.
5. Majid AS, de Paredes ES, Doherty RD, Sharma NR, Salvador X. Missed breast carcinoma: pitfalls and pearls. *Radiographics.* 2003 Jul-Aug;23(4):881-95. doi: 10.1148/rg.234025083.
6. Rawashdeh MA, Lee WB, Bourne RM, Ryan EA, Pietrzyk MW, Reed WM, Heard RC, Black DA, Brennan PC. Markers of good performance in mammography depend on number of annual readings. *Radiology.* 2013 Oct;269(1):61-7. doi: 10.1148/radiol.13122581.
7. Lehman CD, Wellman RD, Buist DS, Kerlikowske K, Tosteson AN, Miglioretti DL; Breast Cancer Surveillance Consortium. Diagnostic Accuracy of Digital Screening Mammography With and Without Computer-Aided Detection. *JAMA Intern Med.* 2015 Nov;175(11):1828-37. doi: 10.1001/jamainternmed.2015.5231.
8. Giger ML, Chan HP, Boone J. Anniversary paper: History and status of CAD and quantitative image analysis: the role of Medical Physics and AAPM. *Med Phys.* 2008 Dec;35(12):5799-820. doi: 10.1118/1.3013555.
9. Warren Burhenne LJ, Wood SA, D'Orsi CJ, Feig SA, Kopans DB, O'Shaughnessy KF, Sickles EA, Tabar L, Vyborny CJ, Castellino RA. Potential contribution of computer-aided detection to the sensitivity of screening mammography. *Radiology.* 2000 May;215(2):554-62. doi: 10.1148/radiology.215.2.r00ma15554. Erratum in: *Radiology* 2000 Jul;216(1):306.
10. Freer TW, Ulissey MJ. Screening mammography with computer-aided detection: prospective study of 12,860 patients in a community breast center. *Radiology.* 2001 Sep;220(3):781-6. doi: 10.1148/radiol.2203001282.
11. Fenton JJ, Taplin SH, Carney PA, Abraham L, Sickles EA, D'Orsi C, Berns EA, Cutter G, Hendrick RE, Barlow WE, Elmore JG. Influence of computer-aided detection on performance of screening mammography. *N Engl J Med.* 2007 Apr 5;356(14):1399-409. doi: 10.1056/NEJMoa066099.
12. James JJ, Gilbert FJ, Wallis MG, Gillan MG, Astley SM, Boggis CR, Agbaje OF, Brentnall AR, Duffy SW. Mammographic features of breast cancers at single reading with computer-aided detection and at double reading in a large multicenter prospective trial of computer-aided detection: CADET II. *Radiology.* 2010 Aug;256(2):379-86. doi: 10.1148/radiol.10091899.
13. Ehteshami Bejnordi B, Veta M, Johannes van Diest P, van Ginneken B, Karssemeijer N, Litjens G, van der Laak JAWM; the CAMELYON16 Consortium, Hermsen M, Manson QF, Balkenhol M, Geessink O, Stathonikos N, van Dijk MC, et al. Diagnostic Assessment of Deep Learning Algorithms for Detection of Lymph Node Metastases in Women With Breast Cancer. *JAMA.* 2017 Dec 12;318(22):2199-2210. doi: 10.1001/jama.2017.14585.
14. Gulshan V, Peng L, Coram M, Stumpe MC, Wu D, Narayanaswamy A, et al. Development and Validation of a Deep Learning Algorithm for Detection of Diabetic Retinopathy in Retinal Fundus Photographs. *JAMA.* 2016 Dec 13;316(22):2402-2410. doi: 10.1001/jama.2016.17216.
15. Kooi T, Litjens G, van Ginneken B, Gubern-Mérida

- A, Sánchez CI, Mann R, et al. Large scale deep learning for computer aided detection of mammographic lesions. *Med Image Anal.* 2017 Jan;35:303-312. doi: 10.1016/j.media.2016.07.007.
16. Rodríguez-Ruiz A, Krupinski E, Mordang JJ, Schilling K, Heywang-Köbrunner SH, Sechopoulos I, Mann RM. Detection of Breast Cancer with Mammography: Effect of an Artificial Intelligence Support System. *Radiology.* 2019 Feb;290(2):305-314. doi: 10.1148/radiol.2018181371.
17. Shen L, Margolies LR, Rothstein JH, Fluder E, McBride R, Sieh W. Deep Learning to Improve Breast Cancer Detection on Screening Mammography. *Sci Rep.* 2019 Aug 29;9(1):12495. doi: 10.1038/s41598-019-48995-4.
18. Pacilè S, Lopez J, Chone P, Bertinotti T, Grouin JM, Fillard P. Improving Breast Cancer Detection Accuracy of Mammography with the Concurrent Use of an Artificial Intelligence Tool. *Radiol Artif Intell.* 2020 Nov 4;2(6):e190208. doi: 10.1148/ryai.2020190208.
19. Rodríguez-Ruiz A, Lång K, Gubern-Merida A, Broeders M, Gennaro G, Clauser P, Helbich TH, Chevalier M, Tan T, Mertelmeier T, Wallis MG, Andersson I, Zackrisson S, Mann RM, Sechopoulos I. Stand-Alone Artificial Intelligence for Breast Cancer Detection in Mammography: Comparison With 101 Radiologists. *J Natl Cancer Inst.* 2019 Sep 1;111(9):916-922. doi: 10.1093/jnci/djy222.
20. Frazer HM, Qin AK, Pan H, Brotchie P. Evaluation of deep learning-based artificial intelligence techniques for breast cancer detection on mammograms: Results from a retrospective study using a BreastScreen Victoria dataset. *J Med Imaging Radiat Oncol.* 2021 Aug;65(5):529-537. doi: 10.1111/1754-9485.13278.
21. Arasu VA, Habel LA, Achacoso NS, Buist DSM, Cord JB, Esserman LJ, et al. Comparison of Mammography Artificial Intelligence Algorithms for 5-year Breast Cancer Risk Prediction. medRxiv 2022.01.05.22268746; doi: 10.1101/2022.01.05.22268746
22. Kerschke L, Weigel S, Rodríguez-Ruiz A, Karssemeijer N, Heindel W. Using deep learning to assist readers during the arbitration process: a lesion-based retrospective evaluation of breast cancer screening performance. *Eur Radiol.* 2022 Feb;32(2):842-852. doi: 10.1007/s00330-021-08217-w.
23. van Winkel SL, Rodríguez-Ruiz A, Appelman L, Gubern-Mérida A, Karssemeijer N, Teuwen J, Wanders AJT, Sechopoulos I, Mann RM. Impact of artificial intelligence support on accuracy and reading time in breast tomosynthesis image interpretation: a multi-reader multi-case study. *Eur Radiol.* 2021 Nov;31(11):8682-8691. doi: 10.1007/s00330-021-07992-w.
24. Mansour S, Kamal R, Hashem L, AlKalaawy B. Can artificial intelligence replace ultrasound as a complementary tool to mammogram for the diagnosis of the breast cancer? *Br J Radiol.* 2021 Dec;94(1128):20210820. doi: 10.1259/bjr.20210820.
25. Rodríguez-Ruiz A, Krupinski E, Mordang JJ, Schilling K, Heywang-Köbrunner SH, Sechopoulos I, Mann RM. Detection of Breast Cancer with Mammography: Effect of an Artificial Intelligence Support System. *Radiology.* 2019 Feb;290(2):305-314. doi: 10.1148/radiol.2018181371.
26. Interlenghi M, Salvatore C, Magni V, Caldara G, Schiavon E, Cozzi A, et al. A Machine Learning Ensemble Based on Radiomics to Predict BI-RADS Category and Reduce the Biopsy Rate of Ultrasound-Detected Suspicious Breast Masses. *Diagnostics (Basel).* 2022 Jan 13;12(1):187. doi: 10.3390/diagnostics12010187.
27. Shen Y, Shamout FE, Oliver JR, Witowski J, Kannan K, Park J, et al. Artificial intelligence system reduces false-positive findings in the interpretation of breast ultrasound exams. *Nat Commun.* 2021 Sep 24;12(1):5645. doi: 10.1038/s41467-021-26023-2.
28. Xia Q, Cheng Y, Hu J, Huang J, Yu Y, Xie H, Wang J. Differential diagnosis of breast cancer assisted by S-Detect artificial intelligence system. *Math Biosci Eng.* 2021 Apr 27;18(4):3680-3689. doi: 10.3934/mbe.2021184.
29. Gao Y, Liu B, Zhu Y, Chen L, Tan M, Xiao X, Yu G, Guo Y. Detection and recognition of ultrasound breast nodules based on semi-supervised deep learning: a powerful alternative strategy. *Quant Imaging Med Surg.* 2021 Jun;11(6):2265-2278. doi: 10.21037/qims-20-12b.
30. Lyu SY, Zhang Y, Zhang MW, Zhang BS, Gao LB, Bai LT, Wang J. Diagnostic value of artificial intelligence automatic detection systems for breast BI-RADS 4 nodules. *World J Clin Cases.* 2022 Jan 14;10(2):518-527. doi: 10.12998/wjcc.v10.i2.518.
31. PhD XL, Xu M, Tang G, PhD YW, Wang N, PhD DN, PhD XL, Li AH. The lesion detection efficacy of deep learning on automatic breast ultrasound and factors affecting its efficacy: a pilot study. *Br J Radiol.* 2022 Feb 1;95(1130):20210438. doi: 10.1259/bjr.20210438.
32. Mango VL, Sun M, Wynn RT, Ha R. Should We Ignore, Follow, or Biopsy? Impact of Artificial Intelligence Decision Support on Breast Ultrasound Lesion Assessment. *AJR Am J Roentgenol.* 2020 Jun;214(6):1445-1452. doi: 10.2214/AJR.19.21872.
33. Zhou LQ, Wu XL, Huang SY, Wu GG, Ye HR, Wei Q, Bao LY, Deng YB, Li XR, Cui XW, Dietrich CF. Lymph Node Metastasis Prediction from Primary Breast Cancer US Images Using Deep Learning. *Radiology.* 2020 Jan;294(1):19-28. doi: 10.1148/radiol.2019190372.
34. Zhou J, Zhang Y, Chang KT, Lee KE, Wang O, Li J, et al. Diagnosis of Benign and Malignant Breast Lesions on DCE-MRI by Using Radiomics and Deep Learning With Consideration of Peritumor Tissue. *J Magn Reson Imaging.* 2020 Mar;51(3):798-809. doi: 10.1002/jmri.26981.
35. Dalmış MU, Gubern-Mérida A, Vreemann S, Bult P, Karssemeijer N, Mann R, Teuwen J. Artificial Intelligence-Based Classification of Breast Lesions Imaged With a Multiparametric Breast MRI Protocol With Ultrafast DCE-MRI, T2, and DWI. *Invest Radiol.* 2019 Jun;54(6):325-332. doi: 10.1097/RLI.0000000000000544.
36. Adachi M, Fujioka T, Mori M, Kubota K, Kikuchi Y, Xiaotong W, Oyama J, Kimura K, Oda G, Nakagawa T, Uetake H, Tateishi U. Detection and Diagnosis of Breast Cancer Using Artificial Intelligence Based assessment of Maximum Intensity Projection Dynamic Contrast-Enhanced Magnetic Resonance Images. *Diagnostics (Basel).* 2020 May 20;10(5):330. doi: 10.3390/diagnostics10050330.
37. Herent P, Schmauch B, Jehanno P, Dehaene O, Saillard C, Balleyguier C, Arfi-Rouche J, Jégou S. Detection and characterization of MRI breast lesions using deep learning. *Diagn Interv Imaging.* 2019 Apr;100(4):219-225. doi: 10.1016/j.diii.2019.02.008.
38. Jiang Y, Edwards AV, Newstead GM. Artificial Intelligence Applied to Breast MRI for Improved Diagnosis. *Radiology.* 2021 Jan;298(1):38-46. doi: 10.1148/radiol.2020200292.

Mesenchymal Subtype of Triple-Negative Breast Cancer: A Review of Specific Features

Nadezhda V. Krakhmal^{1,2}, Natalia N. Babyshkina^{1,2}, Sergey V. Vtorushin^{1,2}

¹Department of Pathology, Siberian State Medical University Ministry of Health of Russia, Tomsk, Russia

²Department of General and Molecular Pathology, Department of Experimental Oncology, Laboratory of Molecular Oncology and Immunology, Cancer Research Institute, Tomsk National Research Medical Center of the RAS, Tomsk, Russia

Abstract

Triple-negative breast cancer (TNBC) is characterized by high invasiveness, high metastatic potential, proneness to relapse, and poor prognosis. Currently, four subtypes in the classification of TNBC are distinguished, which differ from each other in morphological manifestations, molecular genetic features, survival rates, prognosis parameters, and tumor resistance to therapy. A special place in this breast tumors group is occupied by the mesenchymal subtype, the frequency percentage of which varies from 7% to 28%, according to different data. The mesenchymal subtype of TNBC (M-TNBC) is characterized by the expression of molecular markers related to the epithelial-mesenchymal transition (EMT) program and cancer stem cells. M-TNBC has a highly aggressive behavior and worse prognosis due to its invasive and stem-like features, which correlate with metastatic dissemination and resistance to therapies. This review discusses the current knowledge regarding the mesenchymal TNBC subtype and its response to conventional therapeutic strategies. The complex approach to finding effective treatment options to restore immunocompetence in mesenchymal breast cancer patients is the final goal for further extended studies. (**International Journal of Biomedicine. 2023;13(1):14-19.**)

Keywords: triple-negative breast cancer • epithelial-mesenchymal transition • molecular markers

For citation: Krakhmal NV, Babyshkina NN, Vtorushin SV. Mesenchymal Subtype of Triple-Negative Breast Cancer: A Review of Specific Features. International Journal of Biomedicine. 2023;13(1):14-19. doi:10.21103/Article13(1)_RA2

Abbreviations

TNBC, triple negative breast cancer; **EMT**, epithelial-mesenchymal transition; **LAR**, luminal androgen receptor; **M-TNBC**, the mesenchymal subtype of TNBC; **pCR**, pathologic complete response.

Introduction

Triple-negative breast cancer (TNBC), a specific subtype of breast cancer that does not express estrogen receptor (ER) or progesterone receptor (PR) and lacks human epidermal growth factor receptor 2 (HER2) overexpression or amplification, is characterized by high invasiveness, high metastatic potential,

proneness to relapse, and poor prognosis. Recently, it has been demonstrated that TNBCs are transcriptionally heterogeneous and can be grouped into subtypes with vastly differing biologies and responses to chemotherapy and targeted therapies. The mesenchymal subtype of TNBC (M-TNBC) is characterized by the expression of molecular markers related to the epithelial-mesenchymal transition (EMT) program and cancer stem cells. M-TNBC has a highly aggressive behavior and worse prognosis due to its invasive and stem-like features, which correlate with metastatic dissemination and resistance to therapies. This review discusses the current knowledge regarding the mesenchymal TNBC subtype and its response to conventional therapeutic strategies.

*Corresponding author: Nadezhda V. Krakhmal, Department of Pathology, Siberian State Medical University Ministry of Health of Russia, Tomsk, Russia. E-mail: krakhmal@mail.ru

TNBC classifications

In 2011, The Journal of Clinical Investigation published an article entitled “Identification of human triple-negative breast cancer subtypes and preclinical models for selection of targeted therapies” by Lehmann et al.⁽¹⁾ In the presented work, the authors analyzed gene expression (GE) profiles from 21 breast cancer data sets and identified 587 TNBC cases. Cluster analysis identified 6 TNBC subtypes displaying unique GE and ontologies, including 2 basal-like (BL1 and BL2), an immunomodulatory (IM), a mesenchymal (M), a mesenchymal stem-like (MSL), and a luminal androgen receptor (LAR) subtype. Furthermore, using a GE signature derived from TNBC patient tumors, authors identified cell-line models for each TNBC subtypes and differential responses to standard-of-care chemotherapy.

A review of the literature within the framework of the designated topic showed that the smallest number of studies, and, accordingly, scientific publications among the described TNBC subtypes over the past decade, is devoted to breast tumors with a distinct “mesenchymal” molecular genetic pattern (M and MSL types).

Lehmann et al.⁽¹⁾ showed that the M subtype displays a variety of unique gene ontologies that were heavily enriched in components and pathways involved in cell motility, ECM receptor interaction, and cell differentiation pathways (Wnt pathway, anaplastic lymphoma kinase pathway, and TGF- β signaling).

The MSL subtype is enriched with genes for similar biological processes with the M subtype, including cell motility and differentiation pathways. According to Lehmann et al.,⁽¹⁾ genes representing components and processes linked to growth factor signaling pathways are unique to the MSL. So, the prevalence of cell differentiation and growth factor signaling pathways was illustrated by the expression of TGF- β signaling pathway components (*TGFB1L1*, *BGN*, *SMAD6*, *SMAD7*, *NOTCH1*, *TGFB1*, *TGFB2*, *TGFB3*, *TGFBRI*, *TGFBRII*, and *TGFBRII3*), EMT-associated genes (*MMP2*, *ACTA2*, *SNAI2*, *SPARC*, *TAGLN*, *TCF4*, *TWIST1*, *ZEB1*, *COL3A1*, *COL5A2*, *GNG11*, *ZEB2*, and decreased E-cadherin [*CDH1*] expression), growth factors (*FGF*, *IGF*, and *PDGF* pathways), and Wnt/ β -catenin signaling (*CTNNA1*, *DKK2*, *DKK3*, *SFRP4*, *TCF4*, *TCF7L2*, *FZD4*, *CAVI*, *CAV2*, and *CCND2*). In addition, it was shown that the MSL subtype was also uniquely enriched in genes involved in angiogenesis (*VEGFR2* (*KDR*), *TEK*, *TIE1*, and *EPAS1*). Thus, both M and MSL subtypes share elevated expression of genes involved in epithelial-mesenchymal-transition and growth factor pathways. Unlike the M subtype, the MSL subtype has decreased expression of genes involved in proliferation that were accompanied by enrichment in the expression of genes associated with stem cells (*ABCA8*, *PROCR*, *ENG*, *ALDH1A1*, *PER1*, *ABCBI*, *TERF2IP*, *BCL2*, *BMP2*, and *THY1*), numerous HOX genes (*HOXA5*, *HOXA10*, *MEIS1*, *MEIS2*, *MEOX1*, *MEOX2*, and *MSX1*), and mesenchymal stem cell-specific markers (*BMP2*, *ENG*, *ITGAV*, *KDR*, *NGFR*, *NT5E*, *PDGFRB*, *THY1*, and *VCAMI*).

In 2016, considering the complexity of the varying histological landscape of tumor specimens, Lehmann et al.⁽²⁾ performed histological evaluation, laser-capture

microdissection, RNA isolation, and gene expression analysis on a panel of TNBC tumors and provided significant evidence that the previously described IM and MSL TNBC subtypes represent tumors with substantial infiltrating lymphocytes and tumor-associated mesenchymal cells, respectively. Therefore, the authors refined TNBC molecular subtypes from six into four tumor-specific subtypes (TNBCtype-4: BL1, BL2, M, and LAR).⁽²⁾

It is important to point out that a year earlier, Burstein et al.⁽³⁾, based on RNA and DNA profiling analyses conducted on 198 TNBC tumors, also identified and confirmed four distinct TNBC subtypes: luminal androgen receptor, mesenchymal, basal-like immunosuppressed, and basal-like immune-activated. The description by Burstein et al.⁽³⁾ of the molecular genetic features of the isolated groups of TNBC allows us to assume that the basal-like immune-activated type correlates in its characteristics with the BL1 subtype proposed by Lehmann et al., in turn, the basal-like immunosuppressed type is similar to the BL2 according to the classification of Lehmann et al.⁽²⁾ The LAR subtype and M subtype in Burstein et al.⁽³⁾ and Lehmann et al.⁽²⁾ have similar molecular features, respectively. These data allow us to conclude that in the TNBC classification, the 4 variants described above are firmly established, among which the mesenchymal subtype, despite a significantly lower percentage of its occurrence among TNBC, occupies a special place. The presented review is devoted to the morphology, genetic and molecular features of TNBC tumors, which have a distinct “mesenchymal” profile. In addition, we attempted to reflect on the information available at this stage regarding the disease’s course, its progression parameters, resistance to therapy, and survival rates for this subtype of breast carcinoma.

Mesenchymal subtype of TNBC

Morphology and molecular genetic features

A review of literature devoted to aspects of the molecular nature and features of the clinical course of the mesenchymal subtype of TNBC (M-TNBC) suggests that the incidence of such neoplasms varies significantly.

Classification by TNBCtype-4⁽²⁾ resulted in a distribution of 35% BL1, 22% BL2, 25% M, 16% LAR, and 2% unclassified.

In a study by Harano et al.,⁽⁴⁾ among the 88 patients with TNBC, 21 (23.86%) had M-TNBC. Kim et al.⁽⁵⁾ and Hartung et al.⁽⁶⁾ defined M-TNBC in 11.5% and 16% of cases, respectively. In a study by Zhao et al.,⁽⁷⁾ the identification of the TNBC subtypes by the protein expression of AR, CD8, FOXC1, and DCLK1 detected by immunohistochemistry, found M-TNBC (AR-, CD8-, FOXC1- and DCLK1+) in 13.3% of cases (28/210). In several types of cancer, DCLK1 (Doublecortin Like Kinase 1), a microtubule-associated gene, has been recognized as a marker of cancer stem cells that may serve as a potential therapeutic target.⁽⁷⁻¹⁰⁾

Kumar et al.,⁽¹¹⁾ for the classification of TNBCs (n=245), performed immunohistochemistry on tissue microarrays for cytokeratin 5/6, 4/14 (CK5/6, CK4/14), epidermal growth factor receptor (EGFR), vimentin, E-cadherin, claudin 3 and 7, androgen receptor (AR) and aldehyde dehydrogenase. The authors identified mesenchymal type (Vimentin+, E-cadherin-, claudin 3- and 7-) in 28.6% of cases.

The morphology feature of such tumors is the presence of metaplastic signs and foci of sarcomatoid and squamous cell differentiation, specifically for dedifferentiated and aggressive metaplastic breast carcinoma.^(1,5,12-14) Although metaplastic carcinoma is a rare histological variant of breast cancer, it is known that the vast majority of such tumors have a TNBC phenotype and aggressive properties.⁽¹⁵⁾ Clinically, most TNBCs are claudin-low tumors with a high frequency of metaplastic and medullary differentiation.⁽¹⁴⁾ In other studies, it was noted that among the cases of TNBC having a molecular genetic pattern of the mesenchymal subtype, medullary carcinomas are absent, but metaplastic carcinomas occurring among them have a clearly defined fusiform, chondroid, and osteoid morphology.⁽²⁾ A distinctive morphological feature of such breast neoplasms is also the poorly cohesive pattern of tumor growth, characterized by the fact that more than 50% of carcinoma cells are scattered or discretely located in the stroma.⁽⁵⁾

Mesenchymal TNBCs are enriched in EMT-associated genes and contain a high rate of aberrations in the PI3K/AKT/mTOR pathway.⁽¹⁶⁾ However, Kumar et al.⁽¹⁷⁾ showed PIK3CA (Phosphatidylinositol-4-5-bisphosphate-3-kinase catalytic subunit- α) mutations in 16.25% (13/80) of TNBC cases. PIK3CA mutations were frequent in the LAR subtype (33.3%), followed by the unclassified type (31.5%), mesenchymal (10.5%), and BL1 (5%) subtypes. PIK3CA is an integral component of the PIK3CA/AKT signaling pathway, and the evaluation of such aberrations aims to consider them as potential therapeutic targets in the treatment of TNBC.

Hill et al.⁽¹⁸⁾ evaluated the expression of $\alpha v \beta 3$ integrin in two M-TNBC cell lines, MDA-MB-231, and BT-549, by flow cytometry. The authors observed that both cell lines express very high levels of $\alpha v \beta 3$. As known, the altered expression of $\alpha v \beta 3$ integrin has been well established as a driver of cancer progression, stemness, and metastasis. M-TNBC cells were treated with a novel peptide, ψ RGDechi, developed by authors and characterized with the ability to selectively bind and inhibit $\alpha v \beta 3$ integrin. ψ RGDechi was able to hamper adhesion, migration, and invasion of M-TNBC cells, as well as the capability of these cells to form vascular-like structures and mammospheres. In addition, the ψ RGDechi-reversed EMT program inhibited mesenchymal markers.

The literature provides evidence that the mesenchymal subtype of TNBC is also characterized by high IL6 and JAK1 mRNA expression. IL6 and JAK1 are crucial in the activation of the Janus kinase/signal transducer and activator of transcription (JAK/STAT) signaling pathway.^(7,19) The JAK/STAT signaling pathway is regarded as one of the central communication nodes in the cell function. Many papers have reported the importance of this pathway in malignancies.⁽²⁰⁻²²⁾ Zhao et al.⁽⁷⁾ found that the M subtype of TNBC showed higher mRNA expression of both IL6 and JAK1, which are crucial upstream activators of the JAK/STAT3 pathway.⁽¹⁹⁾ In addition, the phosphorylated STAT3 signature score was higher in the mesenchymal subtype than in the other subtypes of TNBC.⁽⁷⁾

The M-TNBC samples have high expression of PDGFR (platelet-derived growth factor receptor), but this subtype is

not sensitive to the corresponding targeted therapy.⁽²³⁾ Platelet-derived growth factor (PDGF) promotes cell proliferation, survival, and migration, primarily of mesenchymal origin cells.⁽²⁴⁾ Reported abnormalities of the PDGF pathway include overexpression or amplification of PDGF receptors (PDGFRs), a gain of function point mutations, or activating chromosomal translocations.

Zheng et al.⁽²⁵⁾ found the overexpression of CD155, known as poliovirus receptor (PVR) or nectin-like 5, in both TNBC cell lines and tumor tissues. CD155 was associated with a mesenchymal phenotype and a poor prognosis in breast cancer patients. CD155 knockdown induced a mesenchymal-epithelial transition in TNBC cells and suppressed TNBC cell migration, invasion, and metastasis in vitro and in vivo. Moreover, CD155 knockdown inhibited TNBC cell growth and survival, reduced IL-6, TGF- β , and Smad3 expression, and inhibited Stat3 phosphorylation. The authors concluded that CD155 contributes to the aggressive behavior of TNBC, and targeting CD155 may be beneficial to M-TNBC patients.

The study of the molecular features of TNBC cell lines with a mesenchymal phenotype made it possible to show the presence of a high expression of the AXL receptor tyrosine kinase in them. Zajac et al.⁽²⁶⁾ found that AXL controls directed cell migration, most likely by regulating cell polarity. Given the role of AXL in cancer development, metastasis, and drug resistance, AXL holds great promise as a prognostic biomarker and therapeutic target.

Analysis of the literature data showed that only a few publications are devoted to studying the relationship between different subtypes of TNBC and specific clinical parameters of patients. Kumar et al.⁽¹¹⁾ showed that M-TNBC was associated with a younger age group. In the literature, we did not find other research results regarding the characteristics of clinical parameters (primary tumor size, localization, menstrual function, the presence of a multifocal growth form, etc.) in different types of TNBC.

Lymph node metastasis and distant metastasis

M-TNBC is characterized by the expression of molecular markers related to the EMT program and cancer stem cells. It has a highly aggressive behavior and a worse prognosis due to its invasive and stem-like features that correlate with metastatic dissemination and resistance to therapies.⁽¹⁸⁾ The literature presents data indicating TNBC carcinomas' ability to form a "vascular-like" network (the phenomenon of vascular mimicry), significantly contributing to metastasis.⁽²⁷⁻²⁹⁾

In a study by Lehmann et al.,⁽²⁾ regional spread to lymph nodes occurred in 34% of TNBC. There was a significant enrichment of lymph node metastasis in LAR-TNBC, with nearly half (47%) of these patients displaying regional spread ($P=0.0278$). Lymph node involvement was lower for M-TNBC (21%). Using published datasets with metastasis-site annotations (GSE12276, GSE2034, and GSE2603), Lehmann et al.⁽²⁾ identified 124 patients with site-specific metastasis data and examined the metastatic pattern in TNBC subtypes. In TNBC, the brain, bone, and lung metastasis incidence was found in 11%, 19%, and 31%, respectively. Stratification by the TNBCs subtype did not show any statistical differences in the brain ($P=0.1238$) and lung ($P=0.0776$) metastasis.

However, the mesenchymal subtype displayed a significantly higher frequency of lung metastasis (46%) compared to all other subtypes (25%) ($P=0.0388$).

Response to therapy and prognosis

In the treatment of TNBC, given the lack of the possibility of using targeted hormonal methods, chemotherapy remains the standard of care for TNBC treatment, but unfortunately, patients frequently develop resistance.⁽³⁰⁻³³⁾ It has become evident that the development of TNBC chemoresistance is multifaceted and based on the elaborate interplay of the tumor microenvironment, drug efflux, cancer stem cells, and bulk tumor cells.⁽³⁴⁾

The mesenchymal subtype, characterized by more aggressive behavior due to increased invasive properties and more pronounced stem-like features, has a worse prognosis in terms of drug sensitivity and resistance.^(18,35) However, the data on this issue is ambiguous.

Masuda et al.⁽³⁶⁾ investigated the clinical relevancy of TNBC heterogeneity by determining pathologic complete response (pCR) rates after neoadjuvant chemotherapy based on TNBC subtypes. The pCR rate for all patients was 28% (37/130). BL1 had the highest pCR rate (52%); BL2 and LAR had the lowest pCR rates (0% and 10%, respectively), and a mesenchymal subtype had a pCR rate of 31%. However, despite its lower pCR rate, LAR had the best overall survival rate; the mesenchymal subtype had the worst.

Similar results were presented in work by Zhao S. et al.⁽⁷⁾ The authors developed an immunohistochemistry (IHC)-based approach by the protein expression of AR, CD8, FOXC1, and DCLK1 to classify TNBCs into molecular subtypes. After adjustment for other prognostic factors in multivariate analysis, the IHC-IM, IHC-LAR, and IHC-BLIS subtypes were associated with better relapse-free survival than the IHC-MES subtype (AR-, CD8-, FOXC1- and DCLK1+).

As known, carcinoma cells can undergo EMT that confers mesenchymal traits on carcinoma cells and drives their metastatic dissemination. These mesenchymal-like cells display the functional behavior of mesenchymal stromal cells. Notably, mesenchymal stromal cells can inhibit the anti-tumor immune response through either carcinoma-associated fibroblasts or bone marrow stromal cells. Experimental data have indicated their relevance in regulating cytolytic effector lymphocytes of the innate and adaptive arms of the immune system. The phenotypic and functional features of mesenchymal-like cells can support tumor growth and proliferation.⁽³⁷⁾

Dongre et al.⁽³⁸⁾ demonstrated that tumors arising from more mesenchymal carcinoma cell lines exhibiting EMT markers expressed low levels of MHC-I, high levels of PD-L1, and contained within their stroma regulatory T cells, M2 (protumor) macrophages, and exhausted CD8+ T cells. Accordingly, such tumors were less susceptible to therapeutic regimens.

In a study by Harano et al.,⁽⁴⁾ analysis of 88 cases of TNBC, taking into account the obtained data on the expression of immunomodulatory genes and the assessment of tumor-infiltrating lymphocytes (TILs), revealed 39 tumors that were identified as tumors with high expression of

immunomodulatory genes (IM+) involved in immune cellular processes. One of the important results was the complete absence of mesenchymal carcinomas among IM+ TNBC tumors.

However, some studies show no significant differences in response to neoadjuvant chemotherapy between different subtypes of TNBC, which requires further extended searches in this direction.

Conclusion

TNBC is a group of malignant tumors with pronounced intratumoral heterogeneity, characterized by an aggressive course, poor prognosis, high incidence of recurrence and metastasis, and resistance to ongoing chemotherapy. To date, there is compelling evidence that these carcinomas also differ from each other in terms of biological behavior and manifestations, as well as in terms of progression and sensitivity to therapy. TNBC accounts for 15–25% of all breast cancers.⁽²³⁾ Tumors with morphological and molecular manifestations of the mesenchymal phenotype (M-TNBC) are clearly defined in the TNBC group.^(1,39-47) The M-TNBC has a highly aggressive behavior and worse prognosis due to its invasive and stem-like features that correlate with metastatic dissemination, resistance to therapies, and poor prognosis. Finding effective treatment options for TNBC subtypes, especially M-TNBC, remains a critical clinical need.

Competing Interests

The authors declare that they have no competing interests.

References

1. Lehmann BD, Bauer JA, Chen X, Sanders ME, Chakravarthy AB, Shyr Y, et al. Identification of human triple-negative breast cancer subtypes and preclinical models for selection of targeted therapies. *J Clin Invest*. 2011;121(7):2750-67. doi: 10.1172/JCI45014.
2. Lehmann BD, Jovanović B, Chen X, Estrada MV, Johnson KN, Shyr Y, et al. Refinement of Triple-Negative Breast Cancer Molecular Subtypes: Implications for Neoadjuvant Chemotherapy Selection. *PLoS One*. 2016;11(6):e0157368. doi: 10.1371/journal.pone.0157368.
3. Burstein MD, Tsimelzon A, Poage GM, Covington KR, Contreras A, Fuqua SA, et al. Comprehensive genomic analysis identifies novel subtypes and targets of triple-negative breast cancer. *Clin Cancer Res*. 2015;21(7):1688-98. doi: 10.1158/1078-0432.CCR-14-0432.
4. Harano K, Wang Y, Lim B, Seitz RS, Morris SW, Bailey DB, et al. Rates of immune cell infiltration in patients with triple-negative breast cancer by molecular subtype. *PLoS One*. 2018;13(10):e0204513. doi: 10.1371/journal.pone.0204513.
5. Kim S, Moon BI, Lim W, Park S, Cho MS, Sung SH. Feasibility of Classification of Triple Negative Breast Cancer by Immunohistochemical Surrogate Markers. *Clin Breast Cancer*. 2018;18(5):e1123-e1132. doi: 10.1016/j.clbc.2018.03.012.

6. Hartung C, Porsch M, Stückrath K, Kaufhold S, Staeger MS, Hanf V, et al. Identifying High-Risk Triple-Negative Breast Cancer Patients by Molecular Subtyping. *Breast Care (Basel)*. 2021;16(6):637-647. doi: 10.1159/000519255.
7. Zhao S, Ma D, Xiao Y, Li XM, Ma JL, Zhang H, et al. Molecular Subtyping of Triple-Negative Breast Cancers by Immunohistochemistry: Molecular Basis and Clinical Relevance. *Oncologist*. 2020;25(10):e1481-e1491. doi: 10.1634/theoncologist.2019-0982.
8. Bailey JM, Alsina J, Rasheed ZA, McAllister FM, Fu YY, Plentz R, et al. DCLK1 marks a morphologically distinct subpopulation of cells with stem cell properties in preinvasive pancreatic cancer. *Gastroenterology*. 2014;146(1):245-56. doi: 10.1053/j.gastro.2013.09.050.
9. Liu H, Wen T, Zhou Y, Fan X, Du T, Gao T, et al. DCLK1 Plays a Metastatic-Promoting Role in Human Breast Cancer Cells. *Biomed Res Int*. 2019;2019:1061979. doi: 10.1155/2019/1061979.
10. Chandrakesan P, Yao J, Qu D, May R, Weygant N, Ge Y, et al. Dclk1, a tumor stem cell marker, regulates pro-survival signaling and self-renewal of intestinal tumor cells. *Mol Cancer*. 2017 Feb 1;16(1):30. doi: 10.1186/s12943-017-0594-y.
11. Kumar S, Bal A, Das A, Bhattacharyya S, Laroia I, Khare S, Singh G. Molecular Subtyping of Triple Negative Breast Cancer by Surrogate Immunohistochemistry Markers. *Appl Immunohistochem Mol Morphol*. 2021;29(4):251-257. doi: 10.1097/PAI.0000000000000897.
12. Hasdemir OA, Tokgöz S, Köybaşıoğlu F, Karabacak H, Yücesoy C, İmamoglu G. Clinicopathological features of metaplastic breast carcinoma. *Adv Clin Exp Med*. 2018;27(4):509-513. doi: 10.17219/acem/68293.
13. Reddy TP, Rosato RR, Li X, Moulder S, Piwnica-Worms H, Chang JC. A comprehensive overview of metaplastic breast cancer: clinical features and molecular aberrations. *Breast Cancer Res*. 2020;22(1):121. doi: 10.1186/s13058-020-01353-z.
14. Herrera Juarez M, Tolosa Ortega P, Sanchez de Torre A, Ciruelos Gil E. Biology of the Triple-Negative Breast Cancer: Immunohistochemical, RNA, and DNA Features. *Breast Care (Basel)*. 2020;15(3):208-216. doi: 10.1159/000508758.
15. González-Martínez S, Pérez-Mies B, Carretero-Barrio I, Palacios-Berraquero ML, Perez-García J, Cortés J, et al. Molecular Features of Metaplastic Breast Carcinoma: An Infrequent Subtype of Triple Negative Breast Carcinoma. *Cancers (Basel)*. 2020;12(7):1832. doi: 10.3390/cancers12071832.
16. Yam C, Mani SA, Moulder SL. Targeting the Molecular Subtypes of Triple Negative Breast Cancer: Understanding the Diversity to Progress the Field. *Oncologist*. 2017;22(9):1086-1093. doi: 10.1634/theoncologist.2017-0095.
17. Kumar S, Bal A, Das A, Loria I, Khare S, Bhattacharya S, et al. Spectrum of PIK3CA/AKT mutations across molecular subtypes of triple-negative breast cancer. *Breast Cancer Res Treat*. 2021;187(3):625-633. doi: 10.1007/s10549-021-06242-3.
18. Hill BS, Sarnella A, Capasso D, Comegna D, Del Gatto A, Gramanzini M, et al. Therapeutic Potential of a Novel $\alpha\beta_3$ Antagonist to Hamper the Aggressiveness of Mesenchymal Triple Negative Breast Cancer Sub-Type. *Cancers (Basel)*. 2019;11(2):139. doi: 10.3390/cancers11020139.
19. Balko JM, Schwarz LJ, Luo N, Estrada MV, Giltane JM, Dávila-González D, et al. Triple-negative breast cancers with amplification of JAK2 at the 9p24 locus demonstrate JAK2-specific dependence. *Sci Transl Med*. 2016 Apr 13;8(334):334ra53. doi: 10.1126/scitranslmed.aad3001. Erratum in: *Sci Transl Med*. 2019 Jan 23;11(476): PMID: 27075627; PMID: PMC5256931.
20. Brooks AJ, Putoczki T. JAK-STAT Signalling Pathway in Cancer. *Cancers (Basel)*. 2020;12(7):1971. doi: 10.3390/cancers12071971.
21. O'Shea JJ, Schwartz DM, Villarino AV, Gadina M, McInnes IB, Laurence A. The JAK-STAT pathway: impact on human disease and therapeutic intervention. *Annu Rev Med*. 2015;66:311-28. doi: 10.1146/annurev-med-051113-024537.
22. Marotta LL, Almendro V, Marusyk A, Shipitsin M, Schemme J, Walker SR, et al. The JAK2/STAT3 signaling pathway is required for growth of CD44⁺CD24⁻ stem cell-like breast cancer cells in human tumors. *J Clin Invest*. 2011 Jul;121(7):2723-35. doi: 10.1172/JCI44745.
23. Yin L, Duan JJ, Bian XW, Yu SC. Triple-negative breast cancer molecular subtyping and treatment progress. *Breast Cancer Res*. 2020;22(1):61. doi: 10.1186/s13058-020-01296-5.
24. Papadopoulos N, Lennartsson J. The PDGF/PDGFR pathway as a drug target. *Mol Aspects Med*. 2018;62:75-88. doi: 10.1016/j.mam.2017.11.007.
25. Zheng Q, Gao J, Yin P, Wang W, Wang B, Li Y, et al. CD155 contributes to the mesenchymal phenotype of triple-negative breast cancer. *Cancer Sci*. 2020;111(2):383-394. doi: 10.1111/cas.14276.
26. Zajac O, Leclere R, Nicolas A, Meseure D, Marchiò C, Vincent-Salomon A, et al. AXL Controls Directed Migration of Mesenchymal Triple-Negative Breast Cancer Cells. *Cells*. 2020;9(1):247. doi: 10.3390/cells9010247.
27. Liu TJ, Sun BC, Zhao XL, Zhao XM, Sun T, Gu Q, et al. CD133⁺ cells with cancer stem cell characteristics associates with vasculogenic mimicry in triple-negative breast cancer. *Oncogene*. 2013;32(5):544-53. doi: 10.1038/onc.2012.85.
28. Wagenblast E, Soto M, Gutiérrez-Ángel S, Hartl CA, Gable AL, Maceli AR, et al. A model of breast cancer heterogeneity reveals vascular mimicry as a driver of metastasis. *Nature*. 2015;520(7547):358-62. doi: 10.1038/nature14403.
29. Camorani S, Crescenzi E, Gramanzini M, Fedele M, Zannetti A, Cerchia L. Aptamer-mediated impairment of EGFR-integrin $\alpha\beta_3$ complex inhibits vasculogenic mimicry and growth of triple-negative breast cancers. *Sci Rep*. 2017;7:46659. doi: 10.1038/srep46659.
30. Bianchini G, Balko JM, Mayer IA, Sanders ME, Gianni L. Triple-negative breast cancer: challenges and opportunities of a heterogeneous disease. *Nat Rev Clin Oncol*. 2016;13(11):674-690. doi: 10.1038/nrclinonc.2016.66.
31. Garrido-Castro AC, Lin NU, Polyak K. Insights into Molecular Classifications of Triple-Negative Breast Cancer: Improving Patient Selection for Treatment. *Cancer Discov*. 2019;9(2):176-198. doi: 10.1158/2159-8290.CD-18-1177.
32. Marra A, Trapani D, Viale G, Criscitiello C, Curigliano G. Practical classification of triple-negative breast cancer: intratumoral heterogeneity, mechanisms of drug resistance, and novel therapies. *NPJ Breast Cancer*. 2020;6:54. doi: 10.1038/s41523-020-00197-2.
33. Dass SA, Tan KL, Selva Rajan R, Mokhtar NF, Mohd Adzmi ER, Wan Abdul Rahman WF, et al. Triple Negative

- Breast Cancer: A Review of Present and Future Diagnostic Modalities. *Medicina (Kaunas)*. 2021;57(1):62. doi: 10.3390/medicina57010062.
34. Nedeljković M, Damjanović A. Mechanisms of Chemotherapy Resistance in Triple-Negative Breast Cancer-How We Can Rise to the Challenge. *Cells*. 2019 Aug 22;8(9):957. doi: 10.3390/cells8090957. PMID: 31443516; PMCID: PMC6770896.
35. O'Connor CJ, Chen T, González I, Cao D, Peng Y. Cancer stem cells in triple-negative breast cancer: a potential target and prognostic marker. *Biomark Med*. 2018;12(7):813-820. doi: 10.2217/bmm-2017-0398.
36. Masuda H, Baggerly KA, Wang Y, Zhang Y, Gonzalez-Angulo AM, Meric-Bernstam F, et al. Differential response to neoadjuvant chemotherapy among 7 triple-negative breast cancer molecular subtypes. *Clin Cancer Res*. 2013;19(19):5533-40. doi: 10.1158/1078-0432.CCR-13-0799.
37. Poggi A, Giuliani M. Mesenchymal Stromal Cells Can Regulate the Immune Response in the Tumor Microenvironment. *Vaccines (Basel)*. 2016;4(4):41. doi: 10.3390/vaccines4040041.
38. Dongre A, Rashidian M, Reinhardt F, Bagnato A, Keckesova Z, Ploegh HL, et al. Epithelial-to-Mesenchymal Transition Contributes to Immunosuppression in Breast Carcinomas. *Cancer Res*. 2017;77(15):3982-3989. doi: 10.1158/0008-5472.CAN-16-3292.
39. Ahn SG, Kim SJ, Kim C, Jeong J. Molecular Classification of Triple-Negative Breast Cancer. *J Breast Cancer*. 2016;19(3):223-230. doi: 10.4048/jbc.2016.19.3.223.
40. Gu G, Dustin D, Fuqua SA. Targeted therapy for breast cancer and molecular mechanisms of resistance to treatment. *Curr Opin Pharmacol*. 2016;31:97-103. doi: 10.1016/j.coph.2016.11.005.
41. Kim S, Park S, Cho MS, Lim W, Moon BI, Sung SH. Strong Correlation of Indoleamine 2,3-Dioxygenase 1 Expression with Basal-Like Phenotype and Increased Lymphocytic Infiltration in Triple-Negative Breast Cancer. *J Cancer*. 2017;8(1):124-130. doi: 10.7150/jca.17437.
42. Yang F, Wang Y, Li Q, Cao L, Sun Z, Jin J, et al. Intratumor heterogeneity predicts metastasis of triple-negative breast cancer. *Carcinogenesis*. 2017;38(9):900-909. doi: 10.1093/carcin/bgx071.
43. Karaayvaz M, Cristea S, Gillespie SM, Patel AP, Mylvaganam R, Luo CC, et al. Unravelling subclonal heterogeneity and aggressive disease states in TNBC through single-cell RNA-seq. *Nat Commun*. 2018;9(1):3588. doi: 10.1038/s41467-018-06052-0.
44. Wang DY, Jiang Z, Ben-David Y, Woodgett JR, Zacksenhaus E. Molecular stratification within triple-negative breast cancer subtypes. *Sci Rep*. 2019;9(1):19107. doi: 10.1038/s41598-019-55710-w.
45. Lee YM, Oh MH, Go JH, Han K, Choi SY. Molecular subtypes of triple-negative breast cancer: understanding of subtype categories and clinical implication. *Genes Genomics*. 2020;42(12):1381-1387. doi: 10.1007/s13258-020-01014-7.
46. Nunnery SE, Mayer IA, Balko JM. Triple-Negative Breast Cancer: Breast Tumors With an Identity Crisis. *Cancer J*. 2021;27(1):2-7. doi: 10.1097/PPO.0000000000000494.
47. Mezi S, Botticelli A, Pomati G, Cerbelli B, Scagnoli S, Amirhassankhani S, et al. Standard of Care and Promising New Agents for the Treatment of Mesenchymal Triple-Negative Breast Cancer. *Cancers (Basel)*. 2021;13(5):1080. doi: 10.3390/cancers13051080.
-

Comparative Overview of Different Radiological Imaging Techniques in the Diagnosis of Pulmonary Embolism

Zuhal Y. Hamd*

*Radiological Sciences Department, College of Health & Rehabilitation Sciences,
Princess Nourah bint Abdulrahman University, Riyadh 11671, Saudi Arabia*

Abstract

Background: Imaging techniques such as chest X-ray (CXR), computed tomography pulmonary angiography (CTPA), ventilation-perfusion (V/Q) scintigraphy, and magnetic resonance imaging (MRI) are some methods used to detect and manage acute pulmonary embolism (PE). The aim of this review was a comparative analysis of the various imaging techniques used to evaluate PE.

Methods and Results: The incidence, distribution, clinical features, classification of PE and clinical assessment of the current methods for diagnosis of PE were discussed. CTPA is the gold standard for fast turnaround and accurate diagnosis. Additional probable reasons for sudden chest pain can also be learned through a CT scan. Lung perfusion anomalies can be identified and measured using dual-energy CT. Chest radiographs are only marginally beneficial, occasionally revealing PE or infarction signs, but are helpful in ruling out other possible causes of chest pain. These patients' ventilation-perfusion mismatches are evident in the V/Q scan, which has many grading schemes with conventional ranges from normal to high. While MRI, which is only available in specialist facilities and calls for higher degrees of competence, also offers accurate diagnosis.

Conclusion: Early diagnosis and treatment of PE is challenging due to asymptomatic conditions or overlapping symptoms. Diagnosis of PE in expectant mothers and those with suspected PE recurrence is typically difficult. Over-diagnosis and overtreatment, particularly regarding sub-segmental PE, and the lowered clinical suspicion threshold remain a major concern in PE diagnosis. The routine use and integration of the above diagnostic techniques need to be encouraged in clinical practice to overcome the diagnostic hurdles. The introduction of new diagnostic techniques or improved risk stratification processes might enhance the management of PE. (**International Journal of Biomedicine. 2023;13(1):20-25.**)

Keywords: pulmonary embolism • magnetic resonance imaging • computed tomography pulmonary angiography • ventilation-perfusion scan • chest radiographs

For citation: Hamd ZY. Comparative Overview of Different Radiological Imaging Techniques in the Diagnosis of Pulmonary Embolism. International Journal of Biomedicine. 2023;13(1):20-25. doi:10.21103/Article13(1)_RA3

Abbreviations

CT, computed tomography; CTPA, CT pulmonary angiography; CXR, chest X-ray; DVT, deep vein thrombosis; MRI, magnetic resonance imaging; PE, pulmonary embolism; SPECT, single-photon emission computed tomography; V/Q, ventilation-perfusion; VTE, venous thromboembolism.

Introduction

Venous thromboembolic disease (VTE) includes deep vein thrombosis (DVT) and pulmonary embolism (PE) as two distinct but often associated entities. Deep venous thrombi that have detached and embolized to the pulmonary circulation lead to the incidence of PE.⁽¹⁾ As a result of the

pulmonary vascular blockage, perfusion and gas transfer are compromised. More typically than the upper lobes, the lower lobes of the lungs are impacted, and bilateral lung participation is prevalent. Smaller emboli obstruct the peripheral arteries, while larger emboli compress in the primary pulmonary artery. A pulmonary infarction caused by peripheral PE might be seen as intra-alveolar bleeding. Dead

zone ventilation results from pulmonary artery occlusion since alveolar ventilation is greater than pulmonary capillary blood flow. Vascular obstruction of the arteries raises pulmonary vascular resistance, which exacerbates the imbalance between ventilation and perfusion. Additionally, serotonin and thromboxane, two humoral mediators produced by active platelets, can elicit vasoconstriction in unaltered lung areas. When the pulmonary artery systolic pressure increases, the right ventricular afterload also increases, leading to right ventricular dysfunction. As right ventricular failure develops, a diminished left ventricular filling may develop. Due to insufficient coronary artery filling, myocardial ischemia may advance quickly, potentially leading to hypotension, syncope, electromechanical dissociation, or abrupt death.⁽²⁾

PE is a high early-mortality-rate, acute cardiovascular disorder that can result in acute right ventricular (RV) failure, a life-threatening condition.⁽³⁾ It is the third leading cause of cardiovascular-related deaths worldwide. Therefore, rapid diagnosis and prompt therapeutic intervention are necessary for optimal management of the condition. Patients may remain asymptomatic or have symptoms that also occur in other cardiopulmonary diseases; the severity of the symptoms depends upon the duration and the level of the thrombus as well as the previous history of the patient. Diagnosis of PE still remains a challenge, wherein, under- and overdiagnosis may have serious consequences.⁽⁴⁾ Ruling out PE is significant due to the risk of bleeding upon anticoagulation therapy and the costs of treatment and management.⁽⁵⁾ Diagnosis relies on a combination of clinical assessment, diagnostic thoracic imaging, and the D-dimer test, each of which has its own benefits and limitations. Therefore, initial tests that are lower in cost and risk are conducted to exclude PE efficiently, whereas imaging tests are carried out on patients in whom PE could not be excluded upon initial assessment. Currently, the most recommended imaging technique by clinicians is CT pulmonary angiography (CTPA). However, for patients with renal insufficiency, CT is contraindicated, and lower limb venous compression ultrasound or V/Q scans are the diagnostics of choice. More recently developed novel diagnostic tests such as V/Q SPECT seem to be promising and accurate and a potential substitute for CTPA. However, further studies on PE management outcomes are warranted before it finds implementation in clinical practice. In this article, we aim to review the various diagnostic imaging techniques for PE that are well-established or novel and to provide a comparative analysis of these methods that may be used in diagnostic management tailored to patient requirements.

Incidence, distribution, classification, and clinical features of PE

Dislodging a deep vein thrombus/clot from the lower limbs can lead to PE development. The thrombus then moves to the arterial lung circulation and lodges itself, thus causing a partial or complete block.⁽⁶⁾ Acute onset chest pain presented in the emergency room is often caused by acute PE that occurs in 0.2% of individuals affected by VTE. About 5%–8% of the US population who have inherited thrombophilia are more at risk of VTE. PE remains the third leading cause of cardiovascular-related deaths, causing an annual hospitalization of 250,000

individuals in the USA alone.⁽⁷⁻⁹⁾ It is found to occur in higher numbers in males than females and can lead to chronic thromboembolic pulmonary hypertension (CTEPH) as a long-term consequence.^(10,11) Recently, the incidence of PE has increased, although deaths have decreased despite the high mortality rates associated with PE.⁽¹²⁾ Recurrent PE is seen in up to 30% of individuals within 10 years of being affected with VTE, and half of them ultimately develop long-term post-thrombotic syndrome.⁽⁸⁾ Hypertension, malignancy, obesity, and recent surgery or immobilizations are among the risk factors predisposing one to DVT and, eventually, PE.⁽¹³⁾ The clinical features of acute PE vary among individuals. A large majority of patients affected with PE may remain asymptomatic, whereas other patients may be presented with sudden death. Clinical features of acute PE commonly include dyspnea, chest pain, hypotension, cough, tachycardia, and hemoptysis. Cardiac arrest, shock, and hypotension are presented in patients with massive PE. Patients with right heart strain show notched S wave in lead V1, changes in S1Q3 and S1Q3T3 pattern, inverted T waves, and right bundle branch block in ECG.⁽¹⁴⁾ Proximal DVT causes symptoms that include edema, pain, erythema, and swelling in the lower extremities. The Wells score⁽¹⁵⁾ or the Geneva score helps stratify PE. Stratification is based on a three-tier model (>6, high risk; 2–6, moderate risk; 0–1, low risk) that helps classify risk reliably,⁽¹⁶⁾ or a two-tier model (>4 PE likely; ≤4 PE unlikely) that recommends performing a D-dimer test on patients unlikely to have PE, in contrast to a CTPA being performed in patients likely to have PE.⁽¹⁷⁾

Clinical assessment and review of current methods for the diagnosis of PE

Suspected PE initially assessed using ECG or CXR that rules out any other cause requires further testing to confirm or exclude diagnosis with a high level of certainty to overcome the consequences of anticoagulation prescription or a missed PE diagnosis. More than two decades have gone into developing diagnostic strategies to manage PE safely and non-invasively. Imaging plays a crucial role in diagnosing and managing acute PE. However, increasingly available imaging techniques and their widespread use for precise diagnosis of PE as reflected by a decrease in the prevalence of PE among suspected patients,⁽¹⁸⁾ raise public health questions that include costs and radiation hazards and treatment of very small clots that may not be clinically relevant. Therefore, D-dimer measurements and clinical probability assessment allow for ruling out PE in suspected patients without any imaging tests.

CTPA is a rapid procedure that accurately diagnoses PE and forms the first line of image modality. Other causes of acute chest pain can also be detected with CT, while dual-energy CT helps to detect and quantify lung perfusion abnormalities. Contrarily, CXR is used in evaluating other chest pain causes and can only occasionally detect PE or infarction. The V/Q scan detects ventilation-perfusion mismatches, while MRI, which is only available in specialized centers and requires expertise to be operated, provides a precise diagnosis of PE. V/Q scintigraphy was the first non-invasive procedure used to diagnose PE.⁽¹⁹⁻²¹⁾ However, a high percentage of non-

diagnostic scans result in complex diagnostic algorithms, thus decreasing acceptance of V/Q scintigraphy, compared to CTPA. Nevertheless, CTPA has drawbacks that include higher radiation dose, renal impairment, contraindications like an allergic response to iodine contrast media, and the risk of misdiagnosing non-clinically relevant PE.^(4,22) In this field, in vivo characterization of the thrombus remains a crucial challenge.⁽²³⁾

Comparative analysis of the various radiological imaging techniques employed in PE analysis

Chest Radiograph

CXR helps to detect causes of acute chest pain that include pulmonary edema, pneumonia, or pneumothorax, but is not useful in PE diagnosis. However, some radiographic abnormalities specific to PE may be seen in acute PE patients. The Fleischner sign, which refers to an enlarged pulmonary artery, occurs post its distension due to the embolus that also causes pulmonary hypertension. The Westermark sign refers to regional oligemia due to PE, which has 92% specificity and 14% sensitivity in PE diagnosis. In pulmonary infarction, a Hampton hump may be seen and has 28% PPV, 76% NPV, 22% sensitivity, and 82% specificity. Other non-specific findings comprise vascular redistribution, elevated diaphragm, and pleural effusion.⁽²⁴⁾

Computed tomography pulmonary angiography

CTPA forms the standard care for the diagnosis of PE in suspected patients and is used in clinical diagnostic algorithms.⁽⁹⁾ PIOPED II trial indicates CTPA to have 83% sensitivity and 96% specificity in accurately diagnosing PE.^(25,26) The advantages of CTPA include being rapid, minimally invasive, and readily available.⁽²⁷⁾ CTPA allows direct visualization of thrombus and can detect other etiologies causing shortness of breath as well as pain in the chest and coronary artery disease.⁽²⁸⁾ The risk of cancer owing to exposure to ionizing radiation is a concern of using CT; however, technical advances in protocols minimize the amount of ionizing radiation.⁽²⁹⁾ For patients with a poor glomerular filtration rate, the intravenous contrast material employed in CTPA may not be accepted due to its association with contrast-induced nephropathy (CIN).^(30,31) Adverse events are low, ranging between 0.2% and 0.7%.^(32,33) CTPA can detect sub-millimeter-sized, small sub-segmental pulmonary emboli and pleural effusion. A pulmonary infarct, a major consequence of acute PE, is characterized by a wedge-shaped, peripheral opacity consisting of a central ground glass and a rim of consolidation in CTPA.⁽³⁴⁾ In contrast, chronic PE is characterized by thrombus recanalization, calcification, intraluminal webs, and filling defects that adhere to the wall, forming concave surfaces and obtuse angles. The vessels in chronic PE exhibit abnormal tapering, are smaller than normal, and may be entirely cut off from the segmental vessel. Chronic PE demonstrates parenchymal changes that constitute band-like opacities, mosaic perfusion, and bronchial dilation.^(35,36) Based on several parameters, CT helps to estimate risk-stratification and the severity of PE, such as clot burden, right heart strain, and lung perfusion. Flattening of the interventricular septum, increased right ventricle/left ventricular ratio, and reflux of contrast material into the

hepatic veins and the inferior vena cava (IVC) are the features of right heart strain.⁽³⁷⁾ Scores such as the CT obstruction index and the CT severity score developed by Qanadli et al.⁽³⁸⁾ and by Mastora et al.,⁽³⁹⁾ respectively, are used to quantify the clot, but are not used in clinical practice routinely.^(40,41) Recent technological advances in CT have made low doses of radiation and concentration contrast material in CTPA acquisition feasible. Based on the body mass index of a patient, radiation doses are minimized by using minimal tube voltage and tube current.⁽⁴²⁾ Tube current modulation based on the density and thickness of the imaged area can save 26% of the radiation dose.⁽⁴³⁾ Advanced iterative reconstruction algorithms that use hybrid techniques or statistical models mitigate image noise arising due to low tube current and voltage.⁽⁴⁴⁾ Low-dose CTPA, in conjunction with the reconstruction algorithm, yields similar quality to standard-dose CTPA.⁽⁴⁵⁾ Low voltage scans reduce the requirement of contrast material by 33% but maintain diagnostic accuracy and image quality.^(46,47) Recently developed dual-source scanners permit rapid high-pitch CT acquisitions (up to 3.4) while removing gaps in data. The rapid acquisition reduces the radiation dose, volume of contrast material,^(48,49) and motion artifact, allowing free-breathing CTPA studies,⁽⁵⁰⁾ and evaluation of the coronary arteries, aorta, and pulmonary vessels.⁽⁵¹⁾ Recent CT methods use a combination of dual-source, dual-energy CT (DECT) and improved iodine detection to allow CTPA with minimal loads of contrast material, tube voltage, and tube current without substantial degradation in the quality of images.⁽⁵²⁻⁵⁴⁾ The use of X-ray tube power and IR algorithms in advanced technologies may even allow high-pitch CTPA in a large patient population while eliminating noise.⁽⁵⁵⁾

V/Q scintigraphy

This technology is a nuclear examination that makes use of a ventilation scanning procedure to determine the pattern of airflow in the lungs and a perfusion scan to map out the blood flow pattern. By analyzing images that demonstrate ventilation and perfusion in all parts of the lungs by employing radioactive tracers, the V/Q scan aids in the clinical decision process.⁽⁵⁶⁾

In cases where CTPA is either impossible or inappropriate, a V/Q scan is preferable. These cases include women who are pregnant, and persons who have renal disease, are allergic to iodinated radiocontrast agents, or cannot accommodate a CT scanner. It exposes the individuals to a 50-times lower radiation dose. A systemic evaluation of 23 prospective trials found that in a sum total of 7000 patients in whom the clinical likelihood and D-dimer evaluation were ambiguous, a normal perfusion scan may be used to safely rule out PE.⁽¹⁹⁾

The V/Q scan is a safe treatment option that most patients tolerate well. But there are some potential pitfalls which include bruising, swelling, redness, and experiencing pain at the injection site; a radioactive, isotope-induced allergic response that is treatable; and radiation exposures to the fetus, particularly in the first trimester.⁽⁵⁶⁾

One hour before the initiation of the study, a posterior-anterior and lateral chest radiograph is required. Nevertheless, in patients without deteriorating signs and symptoms, a chest radiograph taken 24 hours prior to the V/Q scans is generally

acceptable. Regional ventilation is mapped using a variety of products, such as inert gases (81mKr, 133Xe), radiolabeled aerosols 99mTc-DTPA, and 99mTc-labelled technegas.⁽⁵⁷⁾

Multiple imaging techniques are used, such as V/Q imaging with SPECT (V/Q), a regularly used protocol, and in uncommon circumstances, planar scintigraphy (V/Q) is also used. To prevent the transmission of SARS-CoV-2 during the COVID-19 epidemic, many facilities chose to perform perfusion-only scanning. Additionally, CT or CTPA may be coupled with V/Q.

Multidetector gamma cameras are used in SPECT to acquire the images and produce a three-dimensional version of the captured images. SPECT demonstrated greater sensitivity than the planar approach.⁽⁵⁸⁾ The V/Q SPECT is considered to be the second choice of the diagnostic test if the CTPA contrast and exposure to radiation are prohibited.⁽⁵⁹⁾ Low indetermination rate and higher reproducibility are two benefits of the aforementioned technique.⁽⁶⁰⁾ More sensitivity and specificity, novel methods of processing analytical data, and cutting-edge methods, such as V/Q ratio certification, are the added advantages of the said technique.⁽⁶¹⁾

For ventilation and perfusion imaging, a double gamma camera is used to acquire two-dimensional V/Q Planar image capture. Between the two consecutive scans, the patient needs to move as little as possible. When the V/Q SPECT seems not to be viable, at least four views are employed in this approach.⁽⁶²⁾ A significant disadvantage of the approach is its two-dimensional imaging. Additionally, following the embolic event, inaccurate diagnosis of segmental lung involvement, and difficulty in determining the severity of perfusion abnormalities are some of the other notable drawbacks.⁽⁴⁾

A low-dose CT scan is combined with functional SPECT imaging using the V/Q SPECT/CT Imaging Technique to offer more precise anatomical data. In actual practice, the perfusion scan is typically followed by the CT scan.⁽⁵⁹⁾ The biggest drawback of the technique is exposure to radiation. SPECT/CT has benefits that include V/Q mismatch situations, such as tumor, external vascular compression, or obstructive lung illness, and can be detected with greater accuracy than PE.⁽⁶²⁾ For non-embolic reasons, V/Q matching data seems to be better (pneumonia, pleural or pericardial effusion). Detection of PE cases is made possible where V/Q is atypically matched with a pulmonary infarction, similar to PE. Additionally, it possesses the best diagnostic precision.

Magnetic resonance imaging

By using parallel imaging for angiography procedures and pulmonary perfusion, MRI accuracy is continuously improving. This supports its usage along with other possible benefits of MRI, such as a radiation-free approach and a higher safety profile of MR contrast medium.⁽⁶³⁾

The comparative standard for investigations utilized a standard pulmonary angiography in a meta-analysis of research that used gadolinium-enhanced MR for imaging acute PE. Sensitivity values from 77% to 100% were recorded, and specificities ranged from 95% to 98%.⁽⁷⁾ Other meta-analyses found that the central and lobar arteries had 100% sensitivity for PE, the segmental arteries had 84% sensitivity, whereas the subsegmental portions had only 40% sensitivity.⁽⁶⁴⁾

The PIOPED III trial demonstrated that although 52% of patients (194 of 370) had technically subpar outcomes, technically appropriate MR angiography and venography had a sensitivity of 92% and a specificity of 96%. It was recommended that only individuals for whom comprehensive tests were contraindicated should be examined for MR pulmonary angiography, and only at centers where it is frequently performed well.⁽⁶⁵⁾ The most accurate method for determining PE, MR perfusion of the lung, was not used in this investigation, which posed a serious drawback.⁽⁶⁶⁾ Gadolinium-based contrast agents have not been shown to be safe in pregnant patients, and unaugmented MRI techniques still need to be improved to accurately assess only the central and first-order artery branches.⁽⁶⁷⁾

Conclusion

The development of diagnostic techniques during the last few years did not reduce the requirement for intrusive diagnostic testing. The existing algorithms rely on the consecutive use of the D-dimer measure, pretest probability evaluation, and, if necessary, a chest imaging examination. These methods are rather easy to understand, practical, and economical. Although these diagnostic approaches have received extensive validation, more work must be done to promote their use and integration into routine clinical practice. It is still difficult to diagnose PE in some patient populations, such as expectant mothers and those with suspected PE recurrence. The concern of overdiagnosis and overtreatment, particularly regarding sub-segmental PE, as well as the lowered clinical suspicion threshold that leads to a lower fraction of PE in suspected patients, are further challenges that may necessitate revisions of present diagnostic approaches. Some of these difficulties might be resolved with the introduction of new diagnostic techniques or improved risk stratification processes.

References

1. Lavorini F, Di Bello V, De Rimini ML, Lucignani G, Marconi L, Palareti G, et al. Diagnosis and treatment of pulmonary embolism: a multidisciplinary approach. *Multidiscip Respir Med.* 2013 Dec 19;8(1):75. doi: 10.1186/2049-6958-8-75.
2. Tarbox AK, Swaroop M. Pulmonary embolism. *Int J Crit Illn Inj Sci.* 2013 Jan;3(1):69-72. doi: 10.4103/2229-5151.109427.
3. Nachman D, Pollack A, Herzog E. Epidemiology, Pathophysiology and Predisposing Factors of Pulmonary Embolism and Deep Vein Thrombosis. In: Herzog, E. (eds) *Pulmonary Embolism.* Springer, Cham; 2022. doi: 10.1007/978-3-030-87090-4_2
4. Anderson DR, Kahn SR, Rodger MA, Kovacs MJ, Morris T, Hirsch A, et al. Computed tomographic pulmonary angiography vs ventilation-perfusion lung scanning in patients with suspected pulmonary embolism: a randomized controlled trial. *JAMA.* 2007 Dec 19;298(23):2743-53. doi: 10.1001/jama.298.23.2743.
5. Carrier M, Le Gal G, Wells PS, Rodger MA. Systematic review: case-fatality rates of recurrent venous thromboembolism and major bleeding events among patients treated for venous thromboembolism. *Ann Intern Med.* 2010 May 4;152(9):578-89. doi: 10.7326/0003-4819-152-9-201005040-00008.
6. Okada M, Kunihiro Y, Nakashima Y, Nomura T, Kudomi S, Yonezawa T, Suga K, Matsunaga N. Added value of lung

- perfused blood volume images using dual-energy CT for assessment of acute pulmonary embolism. *Eur J Radiol.* 2015 Jan;84(1):172-177. doi: 10.1016/j.ejrad.2014.09.009.
7. Raymakers AJ, Mayo J, Marra CA, FitzGerald M. Diagnostic strategies incorporating computed tomography angiography for pulmonary embolism: a systematic review of cost-effectiveness analyses. *J Thorac Imaging.* 2014 Jul;29(4):209-16. doi: 10.1097/RTI.0b013e3182999e41.
 8. Beckman MG, Hooper WC, Critchley SE, Ortel TL. Venous thromboembolism: a public health concern. *Am J Prev Med.* 2010 Apr;38(4 Suppl):S495-501. doi: 10.1016/j.amepre.2009.12.017.
 9. Goldhaber SZ, Bounameaux H. Pulmonary embolism and deep vein thrombosis. *Lancet.* 2012 May 12;379(9828):1835-46. doi: 10.1016/S0140-6736(11)61904-1.
 10. Yang S, Yang Y, Zhai Z, Kuang T, Gong J, Zhang S, et al. Incidence and risk factors of chronic thromboembolic pulmonary hypertension in patients after acute pulmonary embolism. *J Thorac Dis.* 2015 Nov;7(11):1927-38. doi: 10.3978/j.issn.2072-1439.2015.11.43.
 11. Naess IA, Christiansen SC, Romundstad P, Cannegieter SC, Rosendaal FR, Hammerstrøm J. Incidence and mortality of venous thrombosis: a population-based study. *J Thromb Haemost.* 2007 Apr;5(4):692-9. doi: 10.1111/j.1538-7836.2007.02450.x.
 12. DeMonaco NA, Dang Q, Kapoor WN, Ragni MV. Pulmonary embolism incidence is increasing with use of spiral computed tomography. *Am J Med.* 2008 Jul;121(7):611-7. doi: 10.1016/j.amjmed.2008.02.035.
 13. Previtali E, Bucciarelli P, Passamonti SM, Martinelli I. Risk factors for venous and arterial thrombosis. *Blood Transfus.* 2011 Apr;9(2):120-38. doi: 10.2450/2010.0066-10.
 14. Zhan ZQ, Wang CQ, Nikus KC, He CR, Wang J, Mao S, Dong XJ. Electrocardiogram patterns during hemodynamic instability in patients with acute pulmonary embolism. *Ann Noninvasive Electrocardiol.* 2014 Nov;19(6):543-51. doi: 10.1111/anec.12163.
 15. Gruettner J, Walter T, Lang S, Meyer M, Apfaltrer P, Henzler T, Viergutz T. Importance of Wells score and Geneva score for the evaluation of patients suspected of pulmonary embolism. *In Vivo.* 2015 Mar-Apr;29(2):269-72.
 16. Lobo SA, Fischer S. Cardiac Risk Assessment. 2022 Jul 25. In: StatPearls [Internet]. Treasure Island (FL): StatPearls Publishing; 2022 Jan-. PMID: 30725831.
 17. van Belle A, Büller HR, Huisman MV, Huisman PM, Kaasjager K, Kamphuisen PW, et al.; Christopher Study Investigators. Effectiveness of managing suspected pulmonary embolism using an algorithm combining clinical probability, D-dimer testing, and computed tomography. *JAMA.* 2006 Jan 11;295(2):172-9. doi: 10.1001/jama.295.2.172.
 18. Moore AJE, Wachsmann J, Chamarthy MR, Panjikanan L, Tanabe Y, Rajiah P. Imaging of acute pulmonary embolism: an update. *Cardiovasc Diagn Ther.* 2018 Jun;8(3):225-243. doi: 10.21037/cdt.2017.12.01.
 19. Mirza H, Hashmi MF. Lung Ventilation Perfusion Scan (VQ Scan). 2022 Oct 17. In: StatPearls [Internet]. Treasure Island (FL): StatPearls Publishing; 2022 Jan-. PMID: 33232086.
 20. Salaun PY, Couturaud F, Le Duc-Pennec A, Lacut K, Le Roux PY, Guillo P, Pennec et al. Noninvasive diagnosis of pulmonary embolism. *Chest.* 2011 Jun;139(6):1294-1298. doi: 10.1378/chest.10-1209.
 21. Lang I. Chronic thromboembolic pulmonary hypertension: a distinct disease entity. *Eur Respir Rev.* 2015 Jun;24(136):246-52. doi: 10.1183/16000617.00001115.
 22. Wiener RS, Schwartz LM, Woloshin S. Time trends in pulmonary embolism in the United States: evidence of overdiagnosis. *Arch Intern Med.* 2011 May 9;171(9):831-7. doi: 10.1001/archinternmed.2011.178.
 23. Le Roux PY, Robin P, Salaun PY. New developments and future challenges of nuclear medicine and molecular imaging for pulmonary embolism. *Thromb Res.* 2018 Mar;163:236-241. doi: 10.1016/j.thromres.2017.06.031.
 24. Jany B, Welte T. Pleural Effusion in Adults-Etiology, Diagnosis, and Treatment. *Dtsch Arztebl Int.* 2019 May 24;116(21):377-386. doi: 10.3238/arztebl.2019.0377.
 25. Moore AJE, Wachsmann J, Chamarthy MR, Panjikanan L, Tanabe Y, Rajiah P. Imaging of acute pulmonary embolism: an update. *Cardiovasc Diagn Ther.* 2018 Jun;8(3):225-243. doi: 10.21037/cdt.2017.12.01.
 26. Stein PD, Fowler SE, Goodman LR, Gottschalk A, Hales CA, Hull RD, et al.; PIOPED II Investigators. Multidetector computed tomography for acute pulmonary embolism. *N Engl J Med.* 2006 Jun 1;354(22):2317-27. doi: 10.1056/NEJMoa052367.
 27. Berdahl CT, Vermeulen MJ, Larson DB, Schull MJ. Emergency department computed tomography utilization in the United States and Canada. *Ann Emerg Med.* 2013 Nov;62(5):486-494.e3. doi: 10.1016/j.annemergmed.2013.02.018.
 28. Hassan HGEMA, Khater NH, Elia RZ. Added value of hyperdense lumen sign in prediction of acute central and peripheral pulmonary embolism on non-contrast CT chest. *Egypt J Radiol Nucl Med.* 2021;52(1):84. doi: 10.1186/s43055-021-00462-9.
 29. Woo JK, Chiu RY, Thakur Y, Mayo JR. Risk-benefit analysis of pulmonary CT angiography in patients with suspected pulmonary embolus. *AJR Am J Roentgenol.* 2012 Jun;198(6):1332-9. doi: 10.2214/AJR.10.6329. Erratum in: *AJR Am J Roentgenol.* 2013 Oct;201(4):935.
 30. Luk L, Steinman J, Newhouse JH. Intravenous Contrast-Induced Nephropathy-The Rise and Fall of a Threatening Idea. *Adv Chronic Kidney Dis.* 2017 May;24(3):169-175. doi: 10.1053/j.ackd.2017.03.001.
 31. Heller M, Krieger P, Finefrock D, Nguyen T, Akhtar S. Contrast CT Scans in the Emergency Department Do Not Increase Risk of Adverse Renal Outcomes. *West J Emerg Med.* 2016 Jul;17(4):404-8. doi: 10.5811/westjem.2016.4.28994.
 32. Beckett KR, Moriarity AK, Langer JM. Safe Use of Contrast Media: What the Radiologist Needs to Know. *Radiographics.* 2015 Oct;35(6):1738-50. doi: 10.1148/rg.2015150033.
 33. Li X, Chen J, Zhang L, Liu H, Wang S, Chen X, et al. Clinical observation of the adverse drug reactions caused by non-ionic iodinated contrast media: results from 109,255 cases who underwent enhanced CT examination in Chongqing, China. *Br J Radiol.* 2015 Mar;88(1047):20140491. doi: 10.1259/bjr.20140491.
 34. Sohoni CA. Peripheral wedge-shaped radiographic lung opacity in a young patient. *Lung India.* 2015 Mar-Apr;32(2):184-5. doi: 10.4103/0970-2113.152651.
 35. Nishiyama KH, Saboo SS, Tanabe Y, Jasinowodolinski D, Landay MJ, Kay FU. Chronic pulmonary embolism: diagnosis. *Cardiovasc Diagn Ther.* 2018 Jun;8(3):253-271.
 36. Moore AJE, Wachsmann J, Chamarthy MR, Panjikanan L, Tanabe Y, Rajiah P. Imaging of acute pulmonary embolism: an update. *Cardiovasc Diagn Ther.* 2018 Jun;8(3):225-243. doi: 10.21037/cdt.2017.12.01.
 37. Im DJ, Hur J, Han KH, Lee HJ, Kim YJ, Kwon W, Choi BW. Acute Pulmonary Embolism: Retrospective Cohort Study of the Predictive Value of Perfusion Defect Volume Measured With Dual-Energy CT. *AJR Am J Roentgenol.* 2017 Nov;209(5):1015-1022. doi: 10.2214/AJR.17.17815.
 38. Qanadli SD, El Hajjam M, Vieillard-Baron A, Joseph T, Mesurrolle B, Oliva VL, et al. New CT index to quantify arterial obstruction in pulmonary embolism: comparison with angiographic index and echocardiography. *AJR Am J Roentgenol.* 2001 Jun;176(6):1415-20. doi: 10.2214/ajr.176.6.1761415.
 39. Mastora I, Remy-Jardin M, Masson P, Galland E, Delannoy V, Bauchart JJ, Remy J. Severity of acute pulmonary embolism: evaluation of a new spiral CT angiographic score in correlation with echocardiographic data. *Eur Radiol.* 2003 Jan;13(1):29-35.

40. Furlan A, Aghayev A, Chang CC, Patil A, Jeon KN, Park B, et al. Short-term mortality in acute pulmonary embolism: clot burden and signs of right heart dysfunction at CT pulmonary angiography. *Radiology*. 2012 Oct;265(1):283-93. doi: 10.1148/radiol.12110802.
41. Yu T, Yuan M, Zhang Q, Shi H, Wang D. Evaluation of computed tomography obstruction index in guiding therapeutic decisions and monitoring percutaneous catheter fragmentation in massive pulmonary embolism. *J Biomed Res*. 2011 Nov;25(6):431-7. doi: 10.1016/S1674-8301(11)60057-2.
42. Kubo T, Lin PJ, Stiller W, Takahashi M, Kauczor HU, Ohno Y, Hatabu H. Radiation dose reduction in chest CT: a review. *AJR Am J Roentgenol*. 2008 Feb;190(2):335-43. doi: 10.2214/AJR.07.2556.
43. Mayo J, Thakur Y. Pulmonary CT angiography as first-line imaging for PE: image quality and radiation dose considerations. *AJR Am J Roentgenol*. 2013 Mar;200(3):522-8. doi: 10.2214/AJR.12.9928.
44. Ridge CA, Litmanovich D, Bukoye BA, Lin PJ, Wilcox C, Boiselle PM, Bankier AA. Computed tomography angiography for suspected pulmonary embolism: comparison of 2 adaptive statistical iterative reconstruction blends to filtered back-projection alone. *J Comput Assist Tomogr*. 2013 Sep-Oct;37(5):712-7. doi: 10.1097/RCT.0b013e31829727d2.
45. Pontana F, Henry S, Duhamel A, Faivre JB, Tacelli N, Pagniez J, et al. Impact of iterative reconstruction on the diagnosis of acute pulmonary embolism (PE) on reduced-dose chest CT angiograms. *Eur Radiol*. 2015 Apr;25(4):1182-9. doi: 10.1007/s00330-014-3393-5.
46. Bogot NR, Fingerle A, Shaham D, Nissenbaum I, Sosna J. Image quality of low-energy pulmonary CT angiography: comparison with standard CT. *AJR Am J Roentgenol*. 2011 Aug;197(2):W273-8. doi: 10.2214/AJR.10.5318.
47. Schueller-Weidekamm C, Schaefer-Prokop CM, Weber M, Herold CJ, Prokop M. CT angiography of pulmonary arteries to detect pulmonary embolism: improvement of vascular enhancement with low kilovoltage settings. *Radiology*. 2006 Dec;241(3):899-907. doi: 10.1148/radiol.2413040128.
48. Petersilka M, Bruder H, Krauss B, Stierstorfer K, Flohr TG. Technical principles of dual source CT. *Eur J Radiol*. 2008 Dec;68(3):362-8. doi: 10.1016/j.ejrad.2008.08.013.
49. Kerl JM, Lehnert T, Schell B, Bodelle B, Beeres M, Jacobi V, Vogl TJ, Bauer RW. Intravenous contrast material administration at high-pitch dual-source CT pulmonary angiography: test bolus versus bolus-tracking technique. *Eur J Radiol*. 2012 Oct;81(10):2887-91. doi: 10.1016/j.ejrad.2011.09.018.
50. Bauer RW, Schell B, Beeres M, Wichmann JL, Bodelle B, Vogl TJ, Kerl JM. High-pitch dual-source computed tomography pulmonary angiography in freely breathing patients. *J Thorac Imaging*. 2012 Nov;27(6):376-81. doi: 10.1097/RTI.0b013e318250067e.
51. Hou DJ, Tso DK, Davison C, Inacio J, Louis LJ, Nicolaou S, Reimann AJ. Clinical utility of ultra high pitch dual source thoracic CT imaging of acute pulmonary embolism in the emergency department: are we one step closer towards a non-gated triple rule out? *Eur J Radiol*. 2013 Oct;82(10):1793-8. doi: 10.1016/j.ejrad.2013.05.003.
52. Bucher AM, Kerl MJ, Albrecht MH, Beeres M, Ackermann H, Wichmann JL, et al. Systematic Comparison of Reduced Tube Current Protocols for High-pitch and Standard-pitch Pulmonary CT Angiography in a Large Single-center Population. *Acad Radiol*. 2016 May;23(5):619-27. doi: 10.1016/j.acra.2016.01.003.
53. Lu GM, Luo S, Meinel FG, McQuiston AD, Zhou CS, Kong X, et al. High-pitch computed tomography pulmonary angiography with iterative reconstruction at 80 kVp and 20 mL contrast agent volume. *Eur Radiol*. 2014 Dec;24(12):3260-8.
54. Martini K, Meier A, Higashigaito K, Saltybaeva N, Alkadhi H, Frauenfelder T. Prospective Randomized Comparison of High-pitch CT at 80kVp Under Free Breathing with Standard-pitch CT at 100kVp Under Breath-Hold for Detection of Pulmonary Embolism. *Acad Radiol*. 2016 Nov;23(11):1335-1341.
55. Meinel FG, Canstein C, Schoepf UJ, Sedlmaier M, Schmidt B, Harris BS, et al. Image quality and radiation dose of low tube voltage 3rd generation dual-source coronary CT angiography in obese patients: a phantom study. *Eur Radiol*. 2014 Jul;24(7):1643-50. doi: 10.1007/s00330-014-3194-x.
56. Parker JA, Coleman RE, Grady E, Royal HD, Siegel BA, Stabin MG, et al.; Society of Nuclear Medicine. SNM practice guideline for lung scintigraphy 4.0. *J Nucl Med Technol*. 2012 Mar;40(1):57-65. doi: 10.2967/jnmt.111.101386.
57. Roach PJ, Bailey DL, Harris BE. Enhancing lung scintigraphy with single-photon emission computed tomography. *Semin Nucl Med*. 2008 Nov;38(6):441-9.
58. Dorbala S, Ananthasubramaniam K, Armstrong IS, Chareonthaitawee P, DePuey EG, Einstein AJ, et al. Single Photon Emission Computed Tomography (SPECT) Myocardial Perfusion Imaging Guidelines: Instrumentation, Acquisition, Processing, and Interpretation. *J Nucl Cardiol*. 2018 Oct;25(5):1784-1846. doi: 10.1007/s12350-018-1283-y.
59. Roach PJ, Schembri GP, Bailey DL. V/Q scanning using SPECT and SPECT/CT. *J Nucl Med*. 2013 Sep;54(9):1588-96.
60. Leblanc M, Leveillé F, Turcotte E. Prospective evaluation of the negative predictive value of V/Q SPECT using 99mTc-Technegas. *Nucl Med Commun*. 2007 Aug;28(8):667-72. doi: 10.1097/MNM.0b013e32827a8e99.
61. Yandrapalli S, Puckett Y. SPECT Imaging. 2022 Oct 3. In: StatPearls [Internet]. Treasure Island (FL): StatPearls Publishing; 2022 Jan-. PMID: 33232084.
62. Bajc M, Neilly JB, Miniati M, Schuemichen C, Meignan M, Jonson B; EANM Committee. EANM guidelines for ventilation/perfusion scintigraphy : Part 1. Pulmonary imaging with ventilation/perfusion single photon emission tomography. *Eur J Nucl Med Mol Imaging*. 2009 Aug;36(8):1356-70.
63. Hochegger B, Ley-Zaporozhan J, Marchiori E, Irion K, Souza AS Jr, Moreira J, Kauczor HU, Ley S. Magnetic resonance imaging findings in acute pulmonary embolism. *Br J Radiol*. 2011 Mar;84(999):282-7. doi: 10.1259/bjr/26121475.
64. Oudkerk M, van Beek EJ, Wielopolski P, van Ooijen PM, Brouwers-Kuyper EM, Bongaerts AH, Berghout A. Comparison of contrast-enhanced magnetic resonance angiography and conventional pulmonary angiography for the diagnosis of pulmonary embolism: a prospective study. *Lancet*. 2002 May 11;359(9318):1643-7. doi: 10.1016/S0140-6736(02)08596-3.
65. Stein PD, Chenevert TL, Fowler SE, Goodman LR, Gottschalk A, Hales CA, et al.; PIOPED III (Prospective Investigation of Pulmonary Embolism Diagnosis III) Investigators. Gadolinium-enhanced magnetic resonance angiography for pulmonary embolism: a multicenter prospective study (PIOPED III). *Ann Intern Med*. 2010 Apr 6;152(7):434-43, W142-3. doi: 10.7326/0003-4819-152-7-201004060-00008.
66. Kluge A, Luboldt W, Bachmann G. Acute pulmonary embolism to the subsegmental level: diagnostic accuracy of three MRI techniques compared with 16-MDCT. *AJR Am J Roentgenol*. 2006 Jul;187(1):W7-14.
67. Pahade JK, Litmanovich D, Pedrosa I, Romero J, Bankier AA, Boiselle PM. Quality initiatives: imaging pregnant patients with suspected pulmonary embolism: what the radiologist needs to know. *Radiographics*. 2009 May-Jun;29(3):639-54.

*Contact Information: Assistant Professor, Dr. Zuhail Y. Hamd, PhD. Radiological Sciences Department, College of Health & Rehabilitation Sciences, Princess Nourah Bint Abdulrahman University, P.O. Box 84428, Riyadh 11671, Saudi Arabia. E-mail: zuhailhamd2019@gmail.com

Telogen Effluvium, Diagnosis and Management: A Narrative Review

Ramadan S. Hussein*, Salman Bin Dayel

*Dermatology Unit, Department of Internal Medicine, College of Medicine,
Prince Sattam Bin Abdulaziz University, Al-Kharj, Saudi Arabia*

Abstract

Telogen effluvium is a type of alopecia characterized by diffuse, frequently acute hair shedding. Another chronic type with a more gradual onset is also observed. Telogen effluvium is the most prevalent cause of non-scarring diffuse hair shedding. It is a reactive process induced by hormonal changes, metabolic stress, or drugs. An increase in telogen hair loss does not imply a reason because telogen effluvium may be confused with other hair disorders. Dermoscopy, a modern diagnostic method, can be used to distinguish a variety of hair diseases. This review discusses the putative causal variables, clinical manifestations, diagnostic techniques, and therapeutic approaches. (**International Journal of Biomedicine. 2023;13(1):26-30.**)

Keywords: telogen effluvium • trichoscopy • treatment

For citation: Hussein RS, Dayel SB. Telogen Effluvium, Diagnosis and Management: A Narrative Review. International Journal of Biomedicine. 2023;13(1):26-30. doi:10.21103/Article13(1)_RA4

Abbreviations

ATE, acute telogen effluvium; TE, telogen effluvium; CTE, chronic telogen effluvium.

Introduction

Hair is an ectodermal structure with a significant aesthetic value. Hair loss is an issue for everyone, regardless of age or gender. In a normal hair cycle, each hair on the head replaces itself after three to five years. Telogen effluvium (TE) is a prolonged transition away from the anagen phase of the hair cycle. Although some telogen hair loss is natural, severe telogen hair shedding manifests as an increase in hair loss or a dispersed decrease in hair volume. Metabolic stress, hormonal shifts, or medication may cause TE, an excessive loss of telogen, or resting hair.⁽¹⁾ Acute telogen effluvium (ATE) is the most common cause of diffuse hair shedding. Numerous other conditions that result in widespread hair loss include androgenetic alopecia, chronic telogen effluvium (CTE), loose anagen hair syndrome, anagen effluvium, a diffuse form of

alopecia areata, congenital hypotrichosis, and anomalies of the hair shaft.⁽²⁾ TE is the most prevalent hair-loss condition, and diagnosing this type of alopecia may be difficult. Trichoscopy may aid in the differential diagnosis.⁽³⁾ This article examines the etiology and treatment of TE, and the diagnostic function of trichoscopy.

Physiology of Scalp Hair Shedding

Each follicle passes through consecutive periods of development and rest, including the active hair growth (anagen), involution (catagen), and resting (telogen) phases, as part of the scalp hair cycle. During the anagen phase, every hair grows roughly 1cm each month. The overall number of follicles on a healthy scalp remains constant over time, and the percentage of follicles in the telogen stage is controlled by the duration of anagen because the telogen duration is constant. Normal scalp bronchograms have revealed that 86% of the hairs were in anagen, 1% were in catagen, and 13% were in the telogen phase, with 100-150 hairs falling out daily.⁽⁴⁾ The biological clock that controls the completion of the anagen phase and the start of the catagen/telogen phase is complicated and may be affected by a pregnancy, starvation, and other stressful events. Anagen lasts 2-8 years, catagen 4-6 weeks,

*Corresponding author: Ramadan S. Hussein. Department of Internal Medicine, College of Medicine, Prince Sattam bin Abdulaziz University, Al-Kharj, Saudi Arabia. E-mail: ramadangazeera@yahoo.com

and telogen 2-3 months. At the beginning of the catagen phase, apoptosis of hair bulb keratinocytes causes the involution of the transitory follicle below the arrector pili muscle. It takes two weeks to complete the procedure. The reduced follicle remains inactive for two more months until the next anagen cycle begins. The follicle releases dead hair (exogen) either late in telogen or early in anagen.⁽⁵⁾ However, the underlying molecular mechanisms are still emerging; it is known that the hair follicle itself contains an autonomous clock that controls its cycle. Autocrine, paracrine, and endocrine signaling systems control it. Variations in the rhythmic signal transducer of the dermal papilla and bulging zones encourage hair cycling.⁽²⁾ Wnt-family signaling molecules, FGF, TGF-, and the Hedgehog (Hh) signaling pathway influence the hair cycle. The β -catenin pathway, proteins of the Wnt family, noggin, and the transcription factor Stat3 are essential anagen inducers. In addition, SHH protein and HGF enhance anagen growth. IGF-1, VEGF, and TRH prolong the duration of the anagen phase. Polyamine spermidine is a significant catagen inhibitor and anagen prolongator. Spermidine is a powerful inducer of hair growth in humans and a previously unidentified regulator of epithelial stem cell biology. Anagen ends by simultaneously reducing anagen-supporting factors (IGF-1, HGF, and FGF-5S) and enhancing hair growth inhibitors, such as TGF- β 1, TGF- β 2, and FGF. The Dickkopf-1 (DKK-1) controls the activity of follicular keratinocytes, which play a role in the anagen-catagen transition of the hair cycle. Neurotrophins NT-3 and NT-4, retinoids, and prolactin are other chemicals that regulate the anagen-catagen transition. Prolactin, which is produced by the follicle itself, plays a role in controlling anagen and telogen initiation. Resting hair cycle control signaling remains partially understood. In contrast, telogen is likely a crucial step in controlling the hair cycle. BMP4 inhibits hair follicles in the telogen phase. The resting stage of the hair cycle is controlled by the cyclic epithelial FGF18. Exogen has own regulatory mechanisms, and it is assumed that the proteases cathepsin L and Msx-2 are its regulators.⁽⁶⁾

Pathogenesis of TE

TE is a disease state of hair follicles defined by diffuse shedding of telogen hair from the scalp, which develops approximately 3 months after a precipitating event and lasts approximately 6 months, on average. In TE, hair loss often affects not more than half of the scalp hair. Follicles are often characterized by early triggered anagen cessation. Subsequently, the follicle enters the catagen phase and turns into a telogen-like resting phase. Excessive hair loss has been observed around 2–3 months following the first insult. Multiple potential precipitants have been linked to the pathophysiology. Establishing the cause requires obtaining a pertinent history and performing appropriate laboratory tests to rule out endocrine, nutritional, and immunological disorders.⁽⁷⁾ Five functional changes affect the hair cycle, leading to more hair loss during the telogen phase:

Immediate anagen release: This is a short-onset TE, in which a trigger prematurely ends the anagen phase. It is a frequent type of TE caused by physiological stress, such as high fever episodes. During fever, cytokines trigger hair follicle keratinocyte apoptosis, beginning with catagen and

subsequently progressing to the telogen stage. Reversal is linked to regular cycle resumption

Delayed anagen release: This form of TE is often associated with postpartum hair shedding by the mother. This is caused by the high quantity of placental estrogen in circulation, which prolongs the anagen phase. The cessation of these trophic hormones during birth causes all anagen hairs to concurrently enter the catagen phase. This results in increased telogen hair loss a few months after giving birth.⁽⁸⁾

Short anagen phase: This is characterized by an idiopathic, short anagen phase that hinders the growth of long hair. It also occurs in loose anagen syndrome, familial hypotrichosis, ectodermal dysplasia, and healthy children as an independent condition, leading to resistant TE.⁽⁹⁾

Immediate telogen release: This occurs because of a shortened telogen cycle. Typically, this kind of hair loss begins 2–8 weeks after the initiation of topical minoxidil treatment. This paradoxical result occurs due to stimulation of the anagen phase, which results in the release of dormant exogen hairs.⁽⁸⁾

Delayed telogen release: Instead of shedding and returning to anagen, hair follicles of this type remain in telogen for an extended period. When teloptosis ultimately develops, a clinical indication of increased clubhair loss is detected. During the process of losing their winter coats, animals with a synchronized hair cycle experience this phenomenon. Seasonal occurrence is possible in humans.⁽⁸⁾

Clinical Features

TE was first defined as extensive hair loss beginning 2–3 months after a precipitating factor, such as surgical trauma, malnutrition, high fever, hemorrhage, or starting a new therapy. Approximately 33% of TE cases have no identifiable causes. However, ATE is often associated with emotional stress; this hypothesis has little evidence. Immediate anagen release is a functional shedding mechanism. It is unknown how these incidents at the molecular level induce hair to fall.⁽¹⁰⁾ High circulating placental hormones extend anagen, and after delivery, loss of trophic hormones leads to overdue anagen hairs entering the catagen phase. A few months later, telogen hairs are lost, producing telogen gravidarum.⁽¹¹⁾

Telogen hair loss lasting more than six months was diagnosed as CTE. This could be secondary to a variety of factors or related to a primary persistent CTE. The diagnosis can be confirmed if the link between the cause and hair shedding is reversible and repeatable.⁽¹²⁾

Primary CTE is an unexplained, self-limiting illness characterized by at least six months of elevated telogen shedding. It is prevalent in women aged between 30 and 50 years. Some episodes of CTE are preceded by ATE with a recognized cause; in the majority of cases, the cause cannot be established. CTE may be caused by any of the functional categories of TE, but it is considered to be associated with a reduced anagen of the hair cycle.⁽¹³⁾ Affected women often exhibit significant chronic shedding for various reasons for many years. They often lack a familial history of androgenetic alopecia, and physical examination indicates significant temporal recession without central portion widening; however, these standards are not rigid, and androgenetic alopecia may imitate this presenting feature.⁽¹⁴⁾

Secondary chronic telogen hair loss is often attributed to thyroid conditions, severe iron-deficiency anemia, malnutrition, and acrodermatitis enteropathica.⁽¹⁵⁾

Hyperthyroidism and hypothyroidism, as well as drug-induced hypothyroidism, may induce widespread hair shedding in about 50% and 33% of individuals, respectively. Hypothyroidism is hypothesized to impair both the epidermis and skin appendage cell division. This suppression of mitosis produces the catagen phase and slows the re-entry of telogen hairs into the anagen phase in a subset of individuals. It is unclear how hyperthyroidism causes hair loss. Hair shedding may appear months before the appearance of other symptoms. Replacement medication often stops hair loss, except for hypothyroidism with long-term atrophic hair follicles.⁽¹⁵⁾

Severe iron-deficiency anemia is associated with diffuse hair shedding. Iron insufficiency occurs in approximately 20% of cases without anemia and appears primarily at a serum ferritin level below 20 g/L. Iron is a key cofactor of DNA-synthesizing ribonuclease reductase. Iron deficiency was assumed to inhibit matrix cell proliferation. Consequently, hair follicles that lose their hair at the completion of the telogen phase could momentarily fail to re-enter the anagen phase, resulting in diffuse hair shedding with slow onset.⁽²⁾

Acrodermatitis enteropathy with zinc deficiency can result in severe TE. Nevertheless, asymptomatic zinc insufficiency without other symptoms does not result in the spread of hair loss.⁽¹⁵⁾

Rapid weight loss accompanied by acute protein-calorie deprivation may cause hair shedding. Marasmus may cause thin, dry, straight, lustreless hair that is readily plucked. Kwashiorkor causes episodes of halted hair development in which the hair either enters the telogen phase or, if less severe, the quality of the hair is affected more than its linear development, resulting in the formation of numerous Pohl Pinkus lines. The change in hair color is an additional distinguishing trait. Black hair turns brown, while brown hair becomes blonde. Kwashiorkor “flag signs” consist of this color change and periodic constriction. Deficits in essential fatty acids also cause significant hair loss and fading of hair color.⁽¹⁶⁾

Liver diseases and chronic renal failure are metabolic disorders that cause scant scalp hair. In advanced malignant illnesses, hair loss may be attributed to hypoproteinemia rather than cancer itself, although alopecia is an early sign of Hodgkin’s disease. Dermatomyositis and systemic lupus erythematosus may also induce telogen hair loss. Secondary syphilis may cause diffuse hair loss, although a typical moth-eaten sign is not usually evident.⁽¹⁷⁾

Medication-induced telogen hair shedding often begins 6–12 weeks after drug administration and continues for as long as the drug is used. Most often, it is related to quick anagen release. With acitretin, telogen hair loss is more prominent than with isotretinoin, which seems to be dose related. Retinoids seem to create a telogen anchoring defect and diminish anagen duration. Individual sensitivity exists in drug-induced TE. Retinoids, heparin, propranolol, allopurinol, captopril, and gold are all examples of drugs that have been linked to TE.⁽¹⁸⁾

Evaluation of Hair Shedding

In acute TE, the hair pull test is positive, with clumps of telogen hair easily retrieved from the vertex and scalp edge. Anagen and telogen hairs can differentiate visually. Unlike anagen hairs, telogen hairs have depigmented bulbs and no inner root sheaths. Beau’s nail line may coexist. A hair pluck trichogram often reveals more than 25% telogen hairs. A 60-second hair count test often exceeded 100 hairs (the normal value was 10 hairs). This procedure, which consists of combing the hair forward for 60 seconds over a contrasting towel before washing, may be used to evaluate the course and resolution of a condition.⁽⁵⁾

Trichoscopy is a cutting-edge diagnostic method that is straightforward and noninvasive and may be used as a convenient bedside tool for identifying common hair and scalp conditions. In addition to detecting alopecia, it may prevent needless biopsies and, if required, assist in selecting the best location for a biopsy. Moreover, trichoscopy is a useful technique for photographically assessing the therapy response at each follow-up trichoscopy in cases with ATE, revealing reduced hair density and the existence of empty follicles. Because there is no change in the hair shaft diameter and no peripilar halo, it is simple to distinguish it from androgenetic alopecia. TE is a diagnostic criterion for exclusion during trichoscopy.⁽¹⁹⁾

To rule out any further reasons for diffuse telogen hair loss, a complete blood count, iron, syphilis serology, anti-nuclear antibody, serum zinc, and, thyroid tests must be carried out.⁽⁵⁾

Although seldom necessary in acute instances, a biopsy may provide a fearful patient encouraging prognostic information. Additionally, it may rule out conditions that manifest with increased hair shedding, such as androgenetic alopecia, secondary syphilis, diffuse alopecia areata, dermatomyositis, and systemic lupus erythematosus. ATE histology demonstrates an increase in telogen hairs without inflammation, and no appreciable increase in the amount of vellus hairs, implying androgenetic alopecia.⁽⁵⁾

Drug-induced TE is diagnosed by establishing a compatible chronology between drug exposure and the development of hair shedding. Testing requires stopping the use of any suspected drugs for at least three months. If regrowth follows withdrawal and recurrence follows re-exposure, a conclusion can be drawn.⁽¹⁸⁾

CTE is frequently diagnosed based on the patient’s history and physical assessment; however, a scalp biopsy is necessary to distinguish it from androgenetic alopecia. The best scalp biopsy is a 4 mm punch biopsy obtained from the vertex for horizontal embedding. Because androgenetic alopecia is a pattern-based condition that favorably impacts the scalp’s vertex, this region has the highest diagnostic value. Scalp sample histology reveals an 8:1 anagen-to-telogen ratio, as opposed to a 14:1 ratio in a normal scalp. In CTE, the overall quantity of hair is identical to that of normal scalps, and the terminal-to-vellus hair ratio is 8:1. In androgenetic alopecia, the ratio of the terminal-to-vellus-like hair is 1.9:1.⁽²⁰⁾

General Treatment

The most crucial component of TE treatment is educating patients about their natural course. The hair cycle and link

between hair loss causes and time must be explained, and attempts should be made to determine the precise cause. Once established, this must be remedied. Stopping hair loss takes 3-6 months, and regrowth may be seen 3-6 months after elimination of the cause, although aesthetically significant regrowth can take 12-18 months.⁽²¹⁾ Typically, CTE spontaneously improves within 3-4 years. Rarely, the illness persists for more than 10 years. Stress is one of the most significant contributors to TE. There is no particular treatment that may halt the early initiation of catagen due to stress. Psychological counseling is considered the safest and most effective treatment because it is the least intrusive and requires the least effort to address psychological consequences. The patient requires a concise presentation of the diagnosis and available therapeutic alternatives. Depending on the pathophysiology of TE, potential treatment approaches include anagen induction and catagen inhibition.⁽²²⁾ Currently, no FDA-approved anagen inducer or catagen inhibitor is effective. However, catagen-inducing medicines (retinoids, beta-blockers, antithyroid, or anticoagulant therapies) and endocrine abnormalities (hyperprolactinemia, thyroid dysfunction, or hyperandrogenism) should be avoided and managed. It is also possible to commence replacement treatment for catagen-induced deficits (iron, zinc, protein, and estrogen). There is continuing debate as to whether low serum ferritin levels constitute a dietary shortage that causes hair loss.⁽¹⁸⁾ Some experts advise maintaining serum ferritin levels >40 ng/dl or 70 ng/dl to reverse severe hair loss. Effective first therapy has consisted of adequate nutritional status and 3-4 times daily oral delivery of 300 mg ferrous sulfate. Iron supplements are administered for 3-6 months until reserves are regenerated.⁽²³⁾ The efficacy of thyroxine or iron replacement on the TE outcome is limited; however, some advantages have been shown in a small number of controlled studies.⁽²⁴⁾ Some have also attempted topical minoxidil, a medicine that is a potential contender because of its ability to extend the anagen phase.⁽²⁵⁾

New Treatments

There have been reports of new cosmetic treatments for TE. It contains a leave-on technology mix (caffeine, niacin amide, panthenol, dimethazone, and an acrylate polymer (CNPDA)) that greatly improves hair diameter by 2-3 μm , increasing the cross-sectional area by around 10%. Furthermore, thicker CNPDA fibers can withstand pressure without breaking. However, the effectiveness of TE must be determined.⁽²⁶⁾ Stemoxydine is a revolutionary strategy for maintaining hair growth and cycling because it mimics hypoxic signaling. It is a strong P4H inhibitor. It can activate signaling pathways in a manner similar to hypoxia. Based on in vitro research, it has been postulated that sustaining the activity of hair follicle stem cells may require induction of hypoxic signaling. Compared with volunteers receiving a placebo, in vivo clinical investigations have demonstrated that daily topical treatment with a 5% solution for three months enhanced follicular density.⁽²⁷⁾

Conclusion

TE is the most prevalent reason for diffuse scalp hair shedding. Because ATE is a self-limiting condition, an observational strategy is required until the situation is resolved.

CTE must be established only when other types of long-standing diffuse hair shedding, such as androgenetic alopecia, are ruled out. Trichoscopy is a cutting-edge, noninvasive diagnostic method that may be used as a convenient bedside tool for identifying common hair and scalp disorders. The most crucial component of treatment is educating the patients about the natural course of TE.

Acknowledgments

This study was supported by Prince Sattam Bin Abdulaziz University (Project PSAU/2023/R/1444).

Competing Interests

The authors declare that they have no competing interests.

References

- Harrison S, Sinclair R. Telogen effluvium. *Clin Exp Dermatol.* 2002 Jul;27(5):389-5. doi: 10.1046/j.1365-2230.2002.01080.x.
- Malkud S. Telogen Effluvium: A Review. *J Clin Diagn Res.* 2015 Sep;9(9):WE01-3. doi: 10.7860/JCDR/2015/15219.6492.
- Rudnicka L, Olszewska M, Rakowska A, Kowalska-Oledzka E, Slowinska M. Trichoscopy: a new method for diagnosing hair loss. *J Drugs Dermatol.* 2008 Jul;7(7):651-4.
- KLIGMAN AM. The human hair cycle. *J Invest Dermatol.* 1959 Dec;33:307-16. doi: 10.1038/jid.1959.156.
- Messenger AG, Berker DA, Sinclair RD. Disorders of hair. In: Burns T, Breathnach S, Cox N, Griffiths C, editors. *Rook's textbook of dermatology*, 8th edition. Oxford: Blackwell Publishing; 2010:66.1- 66.100.
- Brajac I, Vičić M, Periša D, Kaštelan M. Human Hair Follicle: An Update on Biology and Perspectives in Hair Growth Disorders Treatment. *Hair Ther Transplant.* 2014;4:115. doi:10.4172/2167-0951.1000115
- Shrivastava SB. Diffuse hair loss in an adult female: approach to diagnosis and management. *Indian J Dermatol Venereol Leprol.* 2009 Jan-Feb;75(1):20-7; quiz 27-8. doi: 10.4103/0378-6323.45215.
- Wadhwa SL, Khopkar U, Nischal KC. Hair and scalp disorders. In: Valia RG, Valia AR, editors. *IADV Textbook of dermatology*, 3rd edition. Mumbai: Bhalani Publishing House; 2010:864-948.
- Sperling LC, Sinclair R. Alopecia and hair shaft abnormalities. In: Jean LB, Joseph LJ, Ronald PR, editors. *Dermatology (Bologna)*, 3rd edition. Elsevier Health Science: London, UK, 2012;(1):1098-1099.
- Grover C, Khurana A. Telogen effluvium. *Indian J Dermatol Venereol Leprol.* 2013 Sep-Oct;79(5):591-603. doi: 10.4103/0378-6323.116731.
- Sinclair R. Hair shedding in women: how much is too much? *Br J Dermatol.* 2015 Sep;173(3):846-8. doi: 10.1111/bjd.13873.
- Thai KE, Sinclair RD. Chronic telogen effluvium in a man. *J Am Acad Dermatol.* 2002 Oct;47(4):605-7. doi: 10.1067/mjd.2002.113675.

13. Gilmore S, Sinclair R. Chronic telogen effluvium is due to a reduction in the variance of anagen duration. *Australas J Dermatol*. 2010 Aug;51(3):163-7. doi: 10.1111/j.1440-0960.2010.00654.x.
 14. Sinclair R. Chronic telogen effluvium or early androgenetic alopecia? *Int J Dermatol*. 2004 Nov;43(11):842-3. doi: 10.1111/j.1365-4632.2004.02034.x.
 15. Dawber RPR, Simpson NB, Barth JH. Diffuse alopecia: Endocrine, metabolic and chemical influences on the follicular cycle. In: Dawber RPR, editor. *Diseases of the Hair and Scalp*. Blackwell Science: Oxford, UK, 1997; pp. 123–150.
 16. Kaufman JP. Letter: Telogen effluvium secondary to starvation diet. *Arch Dermatol*. 1976 May;112(5):731.
 17. Dawber RP, Simpson NB. Hair, and scalp in systemic disease. In: Dawber RP, editor. *Diseases of the Hair and Scalp*. Blackwell Science: Oxford, UK; 1997:483–527.
 18. Brodin MB. Drug-related alopecia. *Dermatol Clin*. 1987 Jul;5(3):571-9.
 19. Jain N, Doshi B, Khopkar U. Trichoscopy in alopecias: diagnosis simplified. *Int J Trichology*. 2013 Oct;5(4):170-8. doi: 10.4103/0974-7753.130385.
 20. Sinclair R, Jolley D, Mallari R, Magee J. The reliability of horizontally sectioned scalp biopsies in the diagnosis of chronic diffuse telogen hair loss in women. *J Am Acad Dermatol*. 2004 Aug;51(2):189-99. doi: 10.1016/s0190-9622(03)00045-8.
 21. Harrison S, Bergfeld W. Diffuse hair loss: its triggers and management. *Cleve Clin J Med*. 2009 Jun;76(6):361-7. doi: 10.3949/ccjm.76a.08080.
 22. Bergfeld WF, Mulinari-Brenner F. Shedding: how to manage a common cause of hair loss. *Cleve Clin J Med*. 2001 Mar;68(3):256-61. doi: 10.3949/ccjm.68.3.256.
 23. Trost LB, Bergfeld WF, Calogeras E. The diagnosis and treatment of iron deficiency and its potential relationship to hair loss. *J Am Acad Dermatol*. 2006 May;54(5):824-44. doi: 10.1016/j.jaad.2005.11.1104.
 24. McMichael A. Approach to office visits for hair loss in women. *Cutis*. 2011 Jan;87(1):8-9.
 25. Buhl AE. Minoxidil's action in hair follicles. *J Invest Dermatol*. 1991 May;96(5):73S-74S. doi: 10.1111/1523-1747.
 26. Davis MG, Thomas JH, van de Velde S, Boissy Y, Dawson TL Jr, Iveson R, Sutton K. A novel cosmetic approach to treat thinning hair. *Br J Dermatol*. 2011 Dec;165 Suppl 3:24-30. doi: 10.1111/j.1365-2133.2011.10633.x.
 27. Rathman-Josserand M, Bernard BA, Misra N. Hair Density Recovery: New Insights in Hair Growth Biology—L'Oreal Research: O 10: The Niche of Human Hair Follicle Stem Cells: A Specific Environment. *Int J Trichology*. 2014;6:113–139.
-

Comprehensive Assessment of Cardiometabolic Risk in Patients with Chronic Obstructive Pulmonary Disease and Obesity

Evgeniy S. Ovsyannikov*, Andrey V. Budnevsky, Lilia A. Titova,
Anastasia S. Ivanova, Sofia A. Korchagina

Voronezh State Medical University named after N.N. Burdenko
Voronezh, Russia

Abstract

Background: Currently, comorbid patients with chronic obstructive pulmonary disease (COPD) and obesity are becoming increasingly common in clinical practice. The objective of this study was to conduct a comparative analysis of indicators of various types of body metabolism (carbohydrate, lipid, adipokine profile) in COPD patients with obesity and normal body weight.

Methods and Results: The study included 86 patients with COPD (GOLD 3-4, group D). The diagnosis of COPD was established in accordance with GOLD, revision 2021. The patients were divided into two groups. Group 1 consisted of 43 COPD patients with NBW [31(72.7%) men and 12(27.3%) women aged 43 to 75 years (mean age of 62.40 ± 8.83 years)] and Group 2 consisted of 43 COPD patients with obesity [32(77.27%) men and 11(22.73%) women aged 48 to 72 years (mean age of 62.94 ± 5.96 years)]. All patients underwent an analysis of the composition of the body by the bioelectrical impedance method. Blood levels of total cholesterol (TC), triglycerides (TG), high-density lipoprotein cholesterol (HDL-C), and low-density lipoprotein cholesterol (LDL-C) were determined by the enzymatic colorimetric method. The glucose level was determined by the glucose oxidant method. The serum adipokine levels (leptin, adiponectin, resistin), as well as testosterone and immunoreactive insulin, were determined using ELISA. To assess insulin resistance, the HOMA-IR index was calculated. To determine cardiovascular risk, the visceral adiposity index (VAI) was calculated according to the formula, which considers body mass index, triglycerides, HDL-C, and waist circumference.

The level of HDL-C was significantly lower ($P=0.0000$), and the levels of TC ($P=0.0479$), LDL-C ($P=0.0020$), glucose ($P=0.0020$), immunoreactive insulin ($P=0.0000$), and HOMA-IR index ($P=0.0000$), were significantly higher in Group 2 than in Group 1. As for the content of adipose tissue hormones, the leptin level was significantly higher in Group 2 ($P=0.0000$) than in Group 1, while there were no statistically significant differences between groups in the level of resistin ($P=0.4996$). The adiponectin level was significantly lower in Group 2 than in Group 1 ($P<0.0001$). The VAI level in Group 2 was significantly higher than in Group 1 (2.13 ± 1.56 and 1.18 ± 0.41 , respectively, $P=0.0002$). In contrast, the testosterone level was significantly lower in Group 2 than in Group 1 (10.59 ± 6.94 nmol/l and 20.02 ± 12.25 nmol/l, respectively, $P=0.0000$).

Conclusion: The high metabolic activity of adipose tissue in patients with COPD and obesity is directly related to the progression of comorbid conditions. (*International Journal of Biomedicine*. 2023;13(1):31-36.)

Keywords: COPD • cardiometabolic risk • body mass index • leptin

For citation: Ovsyannikov ES, Budnevsky AV, Titova LA, Ivanova AS, Korchagina SA. Comprehensive Assessment of Cardiometabolic Risk in Patients with Chronic Obstructive Pulmonary Disease and Obesity. *International Journal of Biomedicine*. 2023;13(1):31-36. doi:10.21103/Article13(1)_OA1

Abbreviations

BMI, body mass index; **COPD**, chronic obstructive pulmonary disease; **CHF**, chronic heart failure; **HC**, hip circumference; **HOMA-IR**, Homeostasis Model Assessment of Insulin Resistance; **HDL-C**, high-density lipoprotein cholesterol; **LDL-C**, low-density lipoprotein cholesterol; **NBW**, normal body weight; **TC**, total cholesterol; **TG**, triglycerides; **VAI**, visceral adiposity index; **WC**, waist circumference.

Introduction

Currently, comorbid patients with chronic obstructive pulmonary disease (COPD) and obesity are becoming increasingly common in clinical practice.^(1,2) This combined pathology causes difficulties in managing such patients and in assessing the prognosis and outcomes of the disease.^(1,3,4)

COPD is one of the leading global health problems, which significantly increases the number of deaths.^(1,2) As is known, both endogenous factors and the impact of environmental factors play a role in the development of COPD.⁽⁵⁾ About 2.75 million people die from COPD every year, which is 4.8% of all causes of death.⁽⁵⁾ The main causes of death in patients with COPD are cardiovascular diseases (25%) and tumors of various localization (mainly lung cancer, 20%-33%); other causes account for up to 30% of cases.⁽⁵⁾

Obesity is a chronic disease caused by an excess of adipose tissue, which can significantly reduce health and alter the functionality of various organs, including the lungs.^(6,7) Excessive deposition of fat in the abdomen can lead to malposition of the diaphragm and subsequent reduction in lung volume, leading to an increased need for ventilation and an increased susceptibility to respiratory diseases, including COPD.^(6,8) The altered secretion profile of adipokines from dysfunctional adipose tissue in obesity contributes to low-grade systemic inflammation, impairing lung immune response and promoting airway hyperresponsiveness.⁽⁶⁻⁸⁾

But now there is also evidence of the “obesity paradox.”⁽⁹⁾ Twenty years ago, Gruberg and coworkers observed better outcomes in overweight and obese patients with coronary heart disease undergoing percutaneous coronary intervention compared with very lean patients (BMI < 18.5 kg/m²) and those with BMI within the normal range. This unexpected phenomenon was described as “an obesity paradox.”⁽¹⁰⁾ Following this, more research on the obesity paradox in various conditions has been conducted. It is known that overweight or obese patients initially have a greater resource of lean muscle mass, and therefore, better tolerate its loss than patients with COPD and normal body weight (NBW), resulting in their higher chances of survival.⁽¹¹⁻¹³⁾

Excess body weight in combination with COPD leads to an increased risk of developing diseases, primarily of the cardiovascular system.⁽⁷⁾ There is evidence that the combination of low muscle mass and abdominal obesity may adversely affect the cardiometabolic risk profile in COPD, even in NBW individuals.⁽⁷⁾

Objective: to conduct a comparative analysis of indicators of various types of body metabolism (carbohydrate, lipid, adipokine profile) in COPD patients with obesity and normal body weight.

Materials and Methods

The study included 86 patients with COPD (GOLD 3-4, group D). The diagnosis of COPD was established in accordance with GOLD, revision 2021. The patients were divided into two groups. Group 1 consisted of 43 COPD patients with NBW [31(72.7%) men and 12(27.3%) women aged 43 to 75 years (mean age of 62.40 ± 8.83 years)]

and Group 2 consisted of 43 COPD patients with obesity [32(77.27%) men and 11(22.73%) women aged 48 to 72 years (mean age of 62.94 ± 5.96 years)]. Groups 1 and 2 were comparable in terms of gender ($\chi^2=1.658$; $P=0.224$) and age ($P=0.628$). The main criterion for diagnosing NBW or obesity was BMI (kg/m²). According to WHO recommendations, a BMI of 18.5-24.99 kg/m² corresponds to NBW, ≥ 30 kg/m² corresponds to obesity.

The criteria for exclusion from the study were: 1) participation of the patient in any intervention study, 2) COPD in the acute stage, 3) concomitant diseases of the lungs, such as confirmed or suspected malignant lung disease or other disease of the respiratory system such as lung tumor, pulmonary fibrosis, interstitial pulmonary fibrosis, tuberculosis, sarcoidosis, bronchial asthma, bronchiolitis obliterans, bronchiectasis, 4) concomitant diseases of other organs and systems, such as acute cardiac pathology, CHF Stage IIA and higher, and chronic renal or hepatic insufficiency.

Basic therapy for COPD included a long-acting anticholinergic drug or a long-acting β_2 -agonist in combination with a long-acting anticholinergic drug, or a long-acting β_2 -agonist in combination with an inhaled glucocorticosteroid (GCS). Patients used short-acting β_2 -agonists as needed.⁽¹⁴⁾

Functional and biochemical tests

All patients in the study groups underwent an analysis of the composition of the body by the bioelectrical impedance method using a fat mass analyzer BC-555 (Tanita Corporation, Tokyo, Japan). The percentages of fat, water, MM, and bone mass were evaluated.

Blood levels of TC, TG, HDL-C, and LDL-C were determined in the venous blood by the enzymatic colorimetric method. The glucose level was determined by the glucose oxidant method. The serum adipokine levels (leptin, adiponectin, resistin), as well as testosterone and immunoreactive insulin, were determined using ELISA. To assess insulin resistance, the HOMA-IR index was calculated using the formula: $HOMA-IR = \text{fasting insulin } (\mu\text{U/ml}) \times \text{fasting glucose (mmol/l)} / 22.5$.⁽¹⁵⁾ To determine cardiovascular risk, the VAI was calculated according to the formula, which considers BMI, TG, HDL-C, and WC. The value of VAI for men: $VAI = (WC / 39.68 + (1.88 \times BMI)) \times (TG / 1.03) \times (1.31/HDL-C)$. The value of VAI for women: $VAI = (WC/36.58 + (1.89 \times BMI)) \times (TG/0.81) \times (1.52/HDL-C)$.⁽¹⁶⁾

Statistical analysis was performed using STATGRAPHICS Plus 5.1. For descriptive analysis, results were presented as mean ± standard deviation (SD). Inter-group comparisons were performed using One-Way ANOVA. Group comparisons with respect to categorical variables were performed using chi-square test. Pearson's correlation coefficient (r) was used to determine the strength of the relationship between the two continuous variables. A probability value of $P < 0.05$ was considered statistically significant.

The study was conducted in accordance with ethical principles of the WMA Declaration of Helsinki (1964, ed. 2013) and approved by the Ethics Committee of Voronezh State Medical University named after N. N. Burdenko. Written informed consent was obtained from all participants.

Results

Groups 1 and 2 were comparable in relation to the use of long-acting anticholinergics ($P=0.6494$), long-acting β_2 -agonists ($P=0.8801$), inhaled corticosteroids ($P=0.8784$), and short-acting β_2 -agonists ($P=0.1735$).

The results of a comparative analysis of an anthropometric examination with the determination of BMI, HC, WC, as well as the body composition of COPD patients are presented in Table 1. In Group 2, a relationship between increased BMI and a high WC/HC ratio ($r=5.34$, $P=0.004$) and a high fat percentage ($r=6.29$, $P=0.001$) was determined, which may indirectly indicate metabolic disorders associated with excess fat tissues in the body. The results of assessing the percentage of water content in patients of both groups are interesting. Thus, in Group 1 patients, the water percentage in the body was significantly higher than in Group 2 patients ($P=0.0000$). At the same time, there were no significant differences between groups in the indicator of the percentage of muscle mass.

Table 1.

Comparative characteristics of body composition parameters in COPD patients in study groups.

Index	Group 1 (n=43)	Group 2 (n=43)	P-value
BMI, kg/m ²	23.02±1.93	35.28±5.94	0.0000
% fat	16.72±7.91	40.62±10.32	0.0000
% of muscle mass	44.72±9.58	48.26±22.36	0.3427
% of water	53.56±4.02	42.65±12.06	0.0000
% of bone mass	4.09±1.15	6.24±4.76	0.0051
WC, cm	85.92±12.79	124.90±12.74	0.0000
HC, cm	95.30±4.76	102.58±21.91	0.0362
WC/HC	0.90±0.12	1.30±0.58	0.0000

The prevalence of diabetes mellitus in Group 2, 14(31.8%), was significantly higher than in Group 1, 0(0%) ($P=0.0000$). Hypertension in Group 2 was also significantly more common than in Group 1 [36(81.81%) and 21(47.72%), respectively ($P=0.0001$). Groups 1 and 2 did not significantly differ in the frequency of occurrence of coronary heart disease and CHF ($P>0.05$ in both cases).

Changes in lipid profile, insulin sensitivity, and adipokine status were detected only in Group 2 (Tables 2 and 3). In particular, the level of HDL-C was significantly lower ($P=0.0000$), and the levels of TC ($P=0.0479$), LDL-C ($P=0.0020$), glucose ($P=0.0020$), immunoreactive insulin ($P=0.0000$), and HOMA-IR index ($P=0.0000$), were significantly higher in Group 2 than in Group 1. As for the content of adipose tissue hormones, the leptin level was significantly higher in Group 2 ($P=0.0000$) than in Group 1, while there were no statistically significant differences between groups in the level of resistin ($P=0.4996$). The adiponectin level was significantly lower in Group 2 than in Group 1

($P<0.0001$). The VAI level in Group 2 was significantly higher than in Group 1 (2.13 ± 1.56 and 1.18 ± 0.41 , respectively, $P=0.0002$). In contrast, the testosterone level was significantly lower in Group 2 than in Group 1 (10.59 ± 6.94 nmol/l and 20.02 ± 12.25 nmol/l, respectively, $P=0.0000$).

Table 2.

Comparative characteristics of carbohydrate metabolism parameters and adipokine levels in COPD patients in study groups.

Index	Group 1 (n=43)	Group 2 (n=43)	P-value
Glucose, mmol/l	5.34±1.10	7.32±1.21	0.0000
Insulin, mcME/ml	11.34±4.24	28.46±3.54	0.0000
HOMA-IR	2.69±1.82	7.76±1.09	0.0000
Resistin, ng/ml	9.38±4.92	8.61±5.59	0.4996
Leptin, ng/ml	13.32±10.81	45.58±29.47	0.0000
Adiponectin, µg/ml	32.21±4.15	26.57±4.42	<0.0001

Table 3.

Comparative characteristics of lipid profile parameters in COPD patients in the study groups.

Index	Group 1 (n=43)	Group 2 (n=43)	P-value
TC, mmol/l	5.36±1.54	6.20±2.27	0.0479
LDL-C, mmol/l	3.48±1.84	4.87±2.18	0.0020
HDL-C, mmol/l	1.28±0.30	1.04±0.40	0.0023
TG, mmol/l	0.96±0.14	1.12±0.72	0.1563

Discussion

Consistent with the data obtained in our study, it is possible to describe obesity in COPD patients as a metabolically “active” state. This is confirmed as a direct indicator of metabolic disorders (the correlation of increased BMI with the percentage of body fat), and an indirect indicator (an increased WC/HC ratio). It can be concluded that the high metabolic activity of visceral fat becomes a key factor in the development of diseases associated with obesity and the development of complications.

In the course of body composition analysis, it was found that patients with COPD and obesity had a higher percentage of fat and a lower percentage of water content than the non-obese COPD group. Changes in muscle mass parameters were not statistically significant. It is worth mentioning that various studies have shown that sarcopenia, muscle wasting, and low muscle strength are associated with an increase in inflammatory biomarkers, a decrease in lung function, and, because of all the above, a drop in the quality of life and a worse prognosis.⁽¹⁷⁾ However, at the same time, there are studies with a completely opposite result: some authors argue that a higher BMI has a positive relationship with FEV1, and the higher the BMI, the better the lung function.⁽¹⁸⁾

It must be remembered that COPD is a chronic disease, the development and progression of which are influenced by concomitant pathology. Thus, according to scientists, the combination of COPD with various diseases of the cardiovascular system is reflected in the deterioration of the prognosis, which ultimately increases mortality.⁽¹⁹⁾ Special attention in this context should be given to hyperlipidemia, which is one of the risk factors for cardiovascular diseases.⁽²⁰⁾ Given the prevalence of hyperlipidemia in patients with COPD, it can be concluded that it may play some role in the pathophysiology of COPD,⁽²⁰⁾ which, however, requires further clarification. Our study found a significant decrease in HDL-C, and an increase in TC, LDL-C and TG in obese patients with COPD, compared with normal-weight COPD patients.

As is known, VAI is a more specific and sensitive examination tool than BMI. VAI is considered a reliable indicator of the increased risk of cardiometabolic diseases in patients.⁽²¹⁾ According to the results of our study, this indicator was significantly higher in COPD patients with obesity, which indicates a higher functional activity of visceral adipose tissue in this group of subjects.

In recent years, there has been an active search for biomarkers that would allow diagnosing exacerbations of COPD at an earlier stage, which would allow for maintaining a higher lung function in a patient. However, the results of such studies are somewhat inconsistent and sometimes contradictory.⁽²²⁾ The role of adipokines involved in various metabolic processes, systemic inflammatory reactions, and atherogenesis is discussed. There is evidence that patients with COPD and bronchial asthma are characterized by a higher level of these markers.⁽²²⁾ Thus, the dysregulation of adipokines may have an impact on the course of patients with these diseases. According to the results of our study, the average values of leptin concentration are significantly higher in the group of patients with COPD and obesity, which probably causes a higher activity of systemic inflammation in this group.

It has been suggested that inflammation mediated by alveolar macrophages may be inhibited by adiponectin, which thus exerts a protective effect on the respiratory system. It is known that obesity, especially central obesity, is associated with an increase in inflammatory factors such as IL-6 and TNF- α ,⁽²³⁾ which have a negative impact on lung function and, as a result, increase morbidity and mortality.⁽²⁴⁾ According to some researchers, genetically induced adiponectin deficiency in mice resulted in increased expression of TNF- α , defining an emphysema-like phenotype.⁽²⁵⁾ However, no full-fledged studies that determine the place of adiponectin as a prognostic factor in COPD have been conducted. Our study showed that obese COPD patients had lower mean adiponectin levels than normal-weight COPD patients.

In addition to the above, it is worth mentioning that metabolic syndrome is one of the factors that worsen the course and prognosis of COPD.^(24,26) It is known that patients with COPD have an increased prevalence of metabolic syndrome, compared with the general population (21%-62%), with the highest prevalence of metabolic syndrome observed

in the early stages of COPD.⁽²⁷⁾ Immediate manifestations of deterioration in the course of this combination of diseases: a more predictable decrease in FEV1 in percent, increased dyspnea, and increased use of inhaled steroids.⁽²⁸⁾ Data from some studies suggest that diabetes is more common in patients with respiratory diseases than emphysema on a CT scan.⁽²⁹⁾ It has been suggested that both the direct effect of hyperglycemia and the support of systemic inflammation in insulin resistance have a negative effect on lung function.⁽³⁰⁾ Our study found higher insulin levels in obese COPD patients than in normal-weight COPD patients. In addition, high HOMA-IR values were indicative of insulin resistance.

The role of systemic inflammation as an important cause of hypogonadism should also be noted. The following chain of events is observed: men with COPD often suffer from hypoxemia, have many comorbidities, and are exposed to long-term exposure to glucocorticoids,⁽³¹⁾ which increases the risk of developing hypogonadism. It is known that testosterone deficiency exacerbates COPD symptoms in two ways: 1) by a direct effect on the respiratory muscles; 2) by reducing overall strength and physical performance.⁽³²⁾ All this leads to a decrease in FEV1 and FVC. Recent studies have shown that low circulating testosterone levels are associated with adverse respiratory outcomes.⁽³²⁾ Our data support lower serum testosterone levels in patients with COPD and obesity.

Conclusion

The high metabolic activity of adipose tissue in patients with COPD and obesity is directly related to the progression of comorbid conditions. Patients with COPD and obesity are more likely to have comorbidities like diabetes mellitus and hypertension, which further determines cardiac outcomes. It is necessary to evaluate VAI in patients with COPD and obesity, since early diagnosis and timely preventive measures can improve the prognosis in terms of comorbidity. The role of adipokines in the COPD pathogenesis needs additional study that may open novel therapeutic strategies for COPD. The management of patients with COPD and obesity should be carried out comprehensively,^(33,34) with pulmonologists, cardiologists, and endocrinologists involved in the diagnostic and treatment process.

Competing Interests

The authors declare that they have no competing interests.

References

1. Christenson SA, Smith BM, Bafadhel M, Putcha N. Chronic obstructive pulmonary disease. *Lancet*. 2022 Jun 11;399(10342):2227-2242. doi: 10.1016/S0140-6736(22)00470-6.

*Corresponding author: Prof. Evgeniy S. Ovsyannikov, Ph.D., Sc.D. Department of faculty therapy, Voronezh State Medical University named after N.N. Burdenko. Voronezh, Russia. E-mail: ovses@yandex.ru

2. WHO: Chronic obstructive pulmonary disease (COPD) [May; 2022]. Available from: [https://www.who.int/news-room/fact-sheets/detail/chronic-obstructive-pulmonary-disease-\(copd\)](https://www.who.int/news-room/fact-sheets/detail/chronic-obstructive-pulmonary-disease-(copd))
3. Chuchalin AG, Avdeev SN, Aisanov ZR, Belevskii AS, Leshchenko IV, Meshcheryakova NN, Ovcharenko SI, Shmelev EI. Russian Respiratory Society. Federal Guidelines on Diagnosis and Treatment of Chronic Obstructive Pulmonary Disease. *Pul'monologiya*. 2014;(3):15-36. doi:10.18093/0869-0189-2014-0-3-15-54. [In Russian].
4. Budnevsky AV, Ovsyannikov ES, Labzhanina NB. [Chronic obstructive pulmonary disease concurrent with metabolic syndrome: Pathophysiological and clinical features]. *Ter Arkh*. 2017;89(1):123-127. doi: 10.17116/terarkh2017891123-127. [Article in Russian].
5. Global Initiative for Chronic Obstructive Lung Disease (GOLD). Global Strategy for the Diagnosis, Management, and Prevention of Chronic Obstructive Pulmonary Disease: 2022 Report. Available from: <https://goldcopd.org/2022-gold-reports/>
6. Pazarlı AC. The role of anthropometric measurements in identifying cardiometabolic diseases in obstructive sleep apnea syndrome. *Tuberk Toraks*. 2022 Sep;70(3):287-292. English. doi: 10.5578/tt.20229708.
7. Beijers R, van de Boven C, van den Borst B, Franssen FME, Wouters EFM, Schols AMWJ. Normal Weight but Low Muscle Mass and Abdominally Obese: Implications for the Cardiometabolic Risk Profile in Chronic Obstructive Pulmonary Disease. *J Am Med Dir Assoc*. 2017 Jun 1;18(6):533-538. doi: 10.1016/j.jamda.2016.12.081.
8. Palma G, Sorice GP, Genchi VA, Giordano F, Caccioppoli C, D'Oria R, Marrano N, Biondi G, Giorgino F, Perrini S. Adipose Tissue Inflammation and Pulmonary Dysfunction in Obesity. *Int J Mol Sci*. 2022 Jul 1;23(13):7349. doi: 10.3390/ijms23137349.
9. Lavie CJ, De Schutter A, Parto P, Jahangir E, Kokkinos P, Ortega FB, Arena R, Milani RV. Obesity and Prevalence of Cardiovascular Diseases and Prognosis-The Obesity Paradox Updated. *Prog Cardiovasc Dis*. 2016 Mar-Apr;58(5):537-47. doi: 10.1016/j.pcad.2016.01.008.
10. Gruberg L, Weissman NJ, Waksman R, et al. The impact of obesity on the short-term and long-term outcomes after percutaneous coronary intervention: the obesity paradox? *J Am Coll Cardiol* 2002;39:578-584
11. Giri Ravindran S, Saha D, Iqbal I, Jhaveri S, Avanthika C, Naagendran MS, Bethineedi LD, Santhosh T. The Obesity Paradox in Chronic Heart Disease and Chronic Obstructive Pulmonary Disease. *Cureus*. 2022 Jun 5;14(6):e25674. doi: 10.7759/cureus.25674.
12. Samuleeva YuV, Zadionchenko VS, Li VV, Adasheva TV, Samorukova EI, Pikhlak AE, Logachev VA, Sokolova LB. [Obesity and metabolic disorders in COPD patients: opportunities for phenotyping]. *PULMONOLOGIYA*. 2014;(5):32-38. doi: 10.18093/0869-0189-2014-0-5-32-38. [Article in Russian].
13. Ovsyannikov ES, Budnevsky AV, Titova LA, Ivanova AS, Kachur AS. The Peculiarities of Six-Minute Walk Test in Patients with Chronic Obstructive Pulmonary Disease, Some with Normal Weight and Some Overweight. *International Journal of Biomedicine*. 2022;12(4):530-534. doi:10.21103/Article12(4)_OA1.
14. Aisanov ZR, Avdeev SN, Arkhipov VV, Belevskii AS, Leshchenko IV, Ovcharenko SI, Shmelev EI, Chuchalin AG. National Clinical Guidelines on Diagnosis and Treatment of Chronic Obstructive Pulmonary Disease: A Clinical Decision-Making Algorithm. *Pul'monologiya*. 2017;27(1):13-20. doi: 10.18093/0869-0189-2017-27-1-13-20 [In Russian].
15. Matthews DR, Hosker JP, Rudenski AS, Naylor BA, Treacher DF, Turner RC. Homeostasis model assessment: insulin resistance and beta-cell function from fasting plasma glucose and insulin concentrations in man. *Diabetologia*. 1985 Jul;28(7):412-9. doi: 10.1007/BF00280883.
16. Pérez ÁN, Álvarez G, Sanchez Tomero JA, Barril G. Body mass index (BMI), visceral adiposity index (VAI), and concicity index (CI) as predictors of cardiovascular risk. *Clinical Nutrition*. 2018;37(Suppl 1):S104. doi:10.1016/j.clnu.2018.06.1398
17. Martínez-Luna N, Orea-Tejeda A, González-Islas D, Flores-Cisneros L, Keirns-Davis C, Sánchez-Santillán R, Pérez-García I, Gastelum-Ayala Y, Martínez-Vázquez V, Martínez-Reyna Ó. Association between body composition, sarcopenia and pulmonary function in chronic obstructive pulmonary disease. *BMC Pulm Med*. 2022 Mar 26;22(1):106. doi: 10.1186/s12890-022-01907-1.
18. Sun Y, Milne S, Jaw JE, Yang CX, Xu F, Li X, Obeidat M, Sin DD. BMI is associated with FEV₁ decline in chronic obstructive pulmonary disease: a meta-analysis of clinical trials. *Respir Res*. 2019 Oct 29;20(1):236. doi: 10.1186/s12931-019-1209-5.
19. Budnevsky AV, Malysh EY. [Clinico-Pathogenetic Relationship of Cardiovascular Diseases and Chronic Obstructive Pulmonary Disease]. *Kardiologiya*. 2017 Apr;57(4):89-93. PMID: 28762911. [Article in Russian].
20. Yang HY, Hu LY, Chen HJ, Chen RY, Hu CK, Shen CC. Increased Risk of Chronic Obstructive Pulmonary Disease in Patients with Hyperlipidemia: A Nationwide Population-Based Cohort Study. *Int J Environ Res Public Health*. 2022 Sep 28;19(19):12331. doi: 10.3390/ijerph191912331.
21. Khanna D, Rehman A. Pathophysiology of Obesity. 2022 Jun 11. In: *StatPearls* [Internet]. Treasure Island (FL): StatPearls Publishing; 2022 Jan.
22. Vassiliou AG, Vitsas V, Kardara M, Keskinidou C, Michalopoulou P, Rovina N, Dimopoulou I, Orfanos SE, Tsoukalas G, Koutsoukou A, Kotanidou A. Study of inflammatory biomarkers in COPD and asthma exacerbations. *Adv Respir Med*. 2020;88(6):558-566. doi: 10.5603/ARM.a2020.0188.
23. Provotorov VM, Budnevskii AV, Semenkova GG, Shishkina ES. [Proinflammatory Cytokines in Combination of Coronary Heart Disease and Chronic Obstructive Pulmonary Disease]. *Klin Med (Mosk)*. 2015;93(2):5-9. [Article in Russian].
24. Lavie CJ, Milani RV. Obesity and cardiovascular disease: the hippocrates paradox? *J Am Coll Cardiol*. 2003 Aug 20;42(4):677-9. doi: 10.1016/s0735-1097(03)00784-8.
25. Summer R, Little FF, Ouchi N, Takemura Y, Aprahamian T, Dwyer D, Fitzsimmons K, Suki B, Parameswaran H, Fine A, Walsh K. Alveolar macrophage activation and an emphysema-like phenotype in adiponectin-deficient mice. *Am J Physiol Lung Cell Mol Physiol*. 2008 Jun;294(6):L1035-42. doi: 10.1152/ajplung.00397.2007.
26. Kozhevnikova SA, Budnevskiy AV, Ovsyannikov ES, Belov VN. [Particularity of the clinical course and quality of

- life of patients with chronic obstructive pulmonary disease on the background of the metabolic syndrome]. *Medical News of North Caucasus*. 2017;12(1):20–23. doi:10.14300/mnnc.2017.12006. [Article in Russian].
27. Piazzolla G, Castrovilli A, Liotino V, Vulpi MR, Fanelli M, Mazzocca A, Candigliota M, Berardi E, Resta O, Sabbà C, Tortorella C. Metabolic syndrome and Chronic Obstructive Pulmonary Disease (COPD): The interplay among smoking, insulin resistance and vitamin D. *PLoS One*. 2017 Oct 24;12(10):e0186708. doi: 10.1371/journal.pone.0186708.
28. Díez-Manglano J, Barquero-Romero J, Almagro P, Cabrera FJ, López García F, Montero L, Soriano JB; Working Group on COPD; Spanish Society of Internal Medicine. COPD patients with and without metabolic syndrome: clinical and functional differences. *Intern Emerg Med*. 2014 Jun;9(4):419–25. doi: 10.1007/s11739-013-0945-7.
29. Park SS, Perez Perez JL, Perez Gandara B, Agudelo CW, Rodriguez Ortega R, Ahmed H, Garcia-Arcos I, McCarthy C, Geraghty P. Mechanisms Linking COPD to Type 1 and 2 Diabetes Mellitus: Is There a Relationship between Diabetes and COPD? *Medicina (Kaunas)*. 2022 Aug 1;58(8):1030. doi: 10.3390/medicina58081030.
30. Cazzola M, Rogliani P, Calzetta L, Lauro D, Page C, Matera MG. Targeting Mechanisms Linking COPD to Type 2 Diabetes Mellitus. *Trends Pharmacol Sci*. 2017 Oct;38(10):940-951. doi: 10.1016/j.tips.2017.07.003.
31. Balasubramanian V, Naing S. Hypogonadism in chronic obstructive pulmonary disease: incidence and effects. *Curr Opin Pulm Med*. 2012 Mar;18(2):112-7. doi: 10.1097/MCP.0b013e32834feb37.
32. Baillargeon J, Urban RJ, Zhang W, Zaiden MF, Javed Z, Sheffield-Moore M, Kuo YF, Sharma G. Testosterone replacement therapy and hospitalization rates in men with COPD. *Chron Respir Dis*. 2019 Jan-Dec;16:1479972318793004. doi: 10.1177/1479972318793004.
33. Budnevsky AV, Isaeva YV, Malysh EY, Kozhevnikova SA. [Pulmonary rehabilitation as an effective method for optimizing therapeutic and preventive measures in patients with chronic obstructive pulmonary disease concurrent with metabolic syndrome]. *Ter Arkh*. 2016;88(8):25-29. doi: 10.17116/terarkh201688825-29. [Article in Russian].
34. Budnevskiy AV, Tsvetikova LN, Ovsyannikov ES, Goncharenko OV. [A role of melatonin for occurrence of chronic obstructive pulmonary disease]. *Pulmonologiya*, 2016, 26(3), 372–378. doi:10.18093/086990189920166266333722378 [Article in Russian].
-

Asthma Control in Multimorbid Patients

Ludmila V. Tribuntseva, Andrey V. Budnevsky, Galina G. Prozorova, Svetlana A. Kozhevnikova, Irina A. Olysheva, Evgeniy S. Ovsyannikov*, Tatiana A. Chernik

Voronezh State Medical University named after N.N. Burdenko
Voronezh, Russia

Abstract

Background: The aim of this study was to evaluate the asthma control in multimorbid patients to personalize asthma treatment.

Methods and Results: The study involved 237 asthma patients (51 men and 186 women) aged 18 to 78 years (mean age of 52.6 ± 1.3 years). All patients were divided into 3 groups: Group 1 included 59(24.9%) patients with normal body weight, Group 2 included 69(29.1%) overweight patients, and Group 3 had 109(46.0%) obese patients. The mean BMI was of 23.14 ± 2.84 kg/m², 27.60 ± 2.58 kg/m², and 35.82 ± 10.23 kg/m² in Groups 1, 2, and 3, respectively ($F=65.572$, $P=0.0000$). Research methods included numerical rating scale (NRS) for a qualitative assessment of the severity of asthma clinical symptoms, asthma control questionnaire (ACQ-5) to assess asthma control, asthma quality of life questionnaire (AQLQ). Comorbidities were analyzed according to medical records.

The mean number of comorbidities among all studied patients was 4.31 ± 0.27 : 55(23.2%) people had ≤ 2 comorbidities, 118(49.8%) people had 3-5 comorbidities, and 64(27.0%) people had ≥ 6 comorbidities. The Group 3 patients had significantly more comorbidities than patients of Groups 1 and 2 ($P=0.000$). The mean value of the ACQ-5 results was 0.97 ± 0.32 , 1.06 ± 0.53 , and 1.82 ± 0.55 in Groups 1, 2, and 3, respectively ($F=77.1896$, $P=0.0000$). The level of AC, according to the ACQ-5, had a positive correlation with the number of comorbidities ($r=0.5418$, $P<0.05$) and a negative correlation with all scales of the AQLQ: activity limitation ($r=-0.6376$, $P<0.05$), symptoms ($r=-0.6577$, $P<0.05$); emotional function ($r=-0.4535$, $P<0.05$); environmental stimuli ($r=-0.4529$, $P<0.05$), and general QOL ($r=-0.6504$, $P<0.05$).

The asthma course is negatively affected by multimorbidity, which is most pronounced in obese patients. An increase in the number of comorbidities significantly worsens AC in patients of all studied groups, while the worst control level was observed in obese patients. A personalized program for managing multimorbid asthma patients should be developed and implemented, considering the multivariate assessment of treatable signs of disease. (**International Journal of Biomedicine. 2023;13(1):37-40.**)

Keywords: asthma control • multimorbidity • body mass index

For citation: Tribuntseva LV, Budnevsky AV, Prozorova GG, Kozhevnikova SA, Olysheva IA, Ovsyannikov ES, Chernik TA. Asthma Control in Multimorbid Patients. International Journal of Biomedicine. 2023;13(1):37-40. doi:10.21103/Article13(1)_OA2

Abbreviations

AC, asthma control; ACQ, asthma control questionnaire; AQLQ, asthma quality of life questionnaire; BMI, body mass index; CAD, coronary artery disease; COPD, chronic obstructive pulmonary disease; DM, diabetes mellitus; ENT, ear, nose, and throat; NBW, normal body weight; NRS, numerical rating scale; OA, osteoarthritis; QOL, quality of life.

Introduction

Asthma is a disease with a global burden. About 348 million patients worldwide suffer from asthma.⁽¹⁾ Despite the stepwise asthma treatment algorithm developed over almost 30 years, including modern immunobiological treatments of

stages 4-5, there is still a low level of asthma control (AC) around the world; in fact, 57% of European patients have no control over the disease. According to the results of the NIKA multi-center observational study in Russia, well-controlled asthma was found in 23% of patients, partly controlled and uncontrolled asthma was diagnosed in 25% and 42% of

patients, respectively.⁽²⁾ Worldwide, there is a trend toward an increase in the number of patients with asthma among middle-aged and older people with a high incidence of comorbidities. The presence of comorbidities not only impairs AC but contributes to more frequent visits to medical care and reduces the quality of life (QOL) and response to standard treatment.⁽³⁾

Epidemiological data show that obesity, which has a pandemic distribution throughout the world, is not only associated with asthma but also precedes its development.⁽⁴⁾ Obese individuals have an increased risk of developing hypertension, diabetes mellitus (DM), osteoarthritis (OA), oncological diseases, and asthma, which creates difficulties in the rational choice of pathogenetic treatment of obesity with comorbidities.⁽⁵⁾ In this regard, a comprehensive assessment of multimorbidity, especially obesity, is a relevant track of a multivariate individual assessment of asthma patients to ensure the highest possible levels of AC.

The aim of this study was to evaluate the AC in multimorbid patients to personalize asthma treatment.

Materials and Methods

The study involved 237 asthma patients (51 men and 186 women) aged 18 to 78 years (mean age of 52.6±1.3 years). The diagnosis of asthma was established in accordance with GINA 2022 criteria. Obesity was diagnosed with BMI ≥30 kg/m².

Patients with acute respiratory infections and asthma exacerbation within the previous 3 months were excluded from the study. Excluded criteria also included active malignant neoplasms of any localization, the presence of other diseases of the respiratory system, decompensated somatic diseases, including mental disorders and severe brain lesions, pregnancy and lactation, and severe infectious diseases.

Research methods included:

1. Numerical rating scale (NRS) for a qualitative assessment of the severity of asthma clinical symptoms (shortness of breath, feeling of suffocation, cough)

2. Asthma Control Questionnaire (ACQ-5) to assess AC

3. Asthma Quality of Life Questionnaire (AQLQ) (authorized Russian version)⁽⁶⁾ in 5 domains: activity limitation, symptoms, emotional function, environmental stimuli, general QOL

Statistical analysis was performed using STATGRAPHICS Plus 5.1. For descriptive analysis, results were presented as mean±standard deviation (SD). Inter-group comparisons were performed using One-Way ANOVA. Group comparisons with respect to categorical variables were performed using chi-square test. Pearson's correlation coefficient (r) was used to determine the strength of the relationship between the two continuous variables. A probability value of $P < 0.05$ was considered statistically significant.

The study was conducted in accordance with ethical principles of the WMA Declaration of Helsinki (1964, ed. 2013) and approved by the Ethics Committee of Voronezh State Medical University named after N. N. Burdenko. Written informed consent was obtained from all participants.

Results

The 237 asthma patients were divided into 3 groups: Group 1 included 59(24.9%) NBW patients, Group 2 included 69(29.1%) overweight patients, and Group 3 had 109(46.0%) obese patients. The mean BMI was of 23.14±2.84 kg/m², 27.60±2.58 kg/m², and 35.82±10.23 kg/m² in Groups 1, 2, and 3, respectively ($F=65.572$, $P=0.0000$).

All groups were comparable by sex and age: Group 1 (15 (25.4%) men and 44(74.6%) women, mean age of 52.17±1.37 years; Group 2 (12(17.4%) men and 57(82.6%) women, mean age of 52.12±1.17 years; Group 3 (24(22%) men and 85(78%) women, mean age of 54.04±0.94 years.

The mean number of comorbidities among all studied patients was 4.31±0.27: 55(23.2%) people had ≤ 2 comorbidities, 118(49.8%) people had 3-5 comorbidities, and 64(27.0%) people had ≥6 comorbidities. The Group 3 patients had significantly more comorbidities than patients of Groups 1 and 2 (Table 1).

Table 1.

The number of comorbidities among the study groups

Group	≤2	3-5	≥6	P-value
Group 1 (n=59)	29(49.2)	20(33.9%)	10(16.9%)	0.000
Group 2 (n=69)	23(33.3)	32(46.4%)	14(20.3%)	
Group 3 (n=109)	3(2.7)	66(60.6%)	40(36.7%)	

The range of comorbidities identified in all examined patients was wide: OA, hypertension, DM, allergic diseases, rhinitis, other ENT pathology, CAD, and gastroesophageal reflux disease. It should be noted that OA prevailed in Group 3, as well as hypertension, DM, CAD, allergic diseases, rhinitis, and other ENT pathology (Table 2)

Table 2.

The number of main comorbidities among the study groups

Comorbidity	Group 1 (n=59)	Group 2 (n=69)	Group 3 (n=109)	P-value
Hypertension	43	35	94	0.000
CAD	-	-	28	0.000
DM	-	-	23	0.000
OA	49	34	108	0.000
Allergic diseases	33	20	48	0.008
Rhinitis	41	32	53	0.014

According to the results of the ACQ-5 test, in Group 3, there were significantly more patients with uncontrolled asthma (74/68% patients). In contrast, in Groups 1 and 2 uncontrolled asthma was found in 3(5%) patients and 15(22%) patients, respectively. Of the 237 patients included in the study, 33(13.9%) had controlled asthma: 13 patients in

Group 1 and 20 in Group 2. Partially controlled asthma was found in 112(47.2%) patients: 43, 34, and 35 in Groups 1, 2, and 3, respectively. The mean value of the ACQ-5 results was 0.97 ± 0.32 , 1.06 ± 0.53 , and 1.82 ± 0.55 in Groups 1, 2, and 3, respectively ($F=77.1896$, $P=0.0000$).

In our study, the AC level was assessed depending on the number of comorbidities. With an increase in the number of comorbidities, patients of all groups had lower AC. In Groups 2 and 3, with ≥ 6 comorbidities, asthma had an uncontrolled course, and the worst control level was observed in Group 3.

All patients underwent an assessment of the severity of clinical symptoms according to the NRS data. Patients in Groups 2 and 3 suffered significantly more from shortness of breath and coughing than Group 1 patients. The mean score of dyspnea was 2.3 ± 2.02 points, 3.8 ± 2.94 points, and 4.2 ± 2.23 points in Groups 1, 2, and 3, respectively ($F=12.1755$, $P=0.0000$). The mean score of coughs was 1.9 ± 1.93 , 3.3 ± 2.43 , and 2.9 ± 2.26 in Groups 1, 2, and 3, respectively ($F=6.5925$, $P=0.0016$). There were no significant differences in the symptom of suffocation between the groups (3.2 ± 1.56 points, 3.9 ± 2.86 points, and 3.8 ± 2.20 points in Groups 1, 2, and 3, respectively [$F=1.7743$, $P=0.1719$]). At the same time, the analysis of the ACQ-5 showed that for patients of Group 3, physical activity restriction was a more distressing symptom than existing respiratory problems. These data again confirm that in patients with asthma and multimorbidity, individual symptoms of comorbidities may prevail over respiratory complaints, negatively affecting AC. A comparison of the disease-specific QOL indicators, using the AQLQ, revealed a significantly negative effect of asthma on activity, symptoms, and general QOL in patients with obesity (Fig.1).

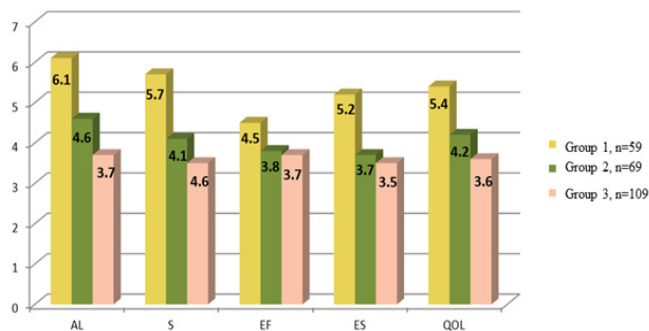


Fig. 1. QOL indicators according to the AQLQ in patients in the study groups

AL - activity limitation; S - symptoms; EF - emotional function; ES - environmental stimuli; QOL - general QOL

The conducted correlation analysis confirmed the data. We found statistically significant relationships between the estimated indicators. The level of AC, according to the ACQ-5, had a positive correlation with the number of comorbidities ($r=0.5418$, $P<0.05$) and a negative correlation with all scales of the AQLQ: activity limitation ($r=-0.6376$, $P<0.05$), symptoms ($r=-0.6577$, $P<0.05$); emotional function ($r=-0.4535$, $P<0.05$); environmental stimuli ($r=-0.4529$, $P<0.05$), and general QOL ($r=-0.6504$, $P<0.05$).

Our data are comparable with the results of clinical trials. In a study by Weatherburn et al.,⁽⁷⁾ 62.6% of the examined asthma patients had at least 1 comorbidity, and 16.3% had 4 or more comorbidities. Wardzyńska et al.⁽⁸⁾ found that among 93 patients with asthma aged >65 years and 78 patients aged 30-50 years, there was a high incidence of chronic comorbidities (an average of 8.4 and 4.7, respectively).

Currently, asthma is not considered a classic multimorbid condition; researchers often pay attention only to a combination of diseases with common or similar etiological and pathogenetic factors. According to recent publications, the most common comorbid conditions in asthma are diseases of the upper respiratory tract, chronic sinusitis, obesity, and depression.⁽⁹⁻¹¹⁾ Thus, only a multicomplex assessment of an asthma patient with an uncontrolled course makes it possible to determine the tools for influencing AC for the selection of personalized treatment in each individual case.⁽¹²⁻¹⁴⁾

The negative effect of obesity on AC is confirmed by the authors, who showed that physiological changes in lung function occur in visceral obesity: a decrease in vital capacity and residual lung volume, an increase in chest rigidity, and the development of dyspnea. And in patients with abdominal obesity, the expiratory reserve volume and functional capacity of the lungs are significantly reduced.⁽¹⁵⁾

A study by Tomisa et al.⁽¹⁶⁾ found that most of the 12,000 patients with asthma had at least 1 comorbidity (the most common - obesity, COPD, and CAD). An increase in the number of comorbidities significantly increased the risk of uncontrolled asthma. Other factors that also had a significant negative effect on AC were female gender, age 46-65 years, high BMI, long smoking history, and a long history of asthma.

Thus, currently, in most asthma patients, it is not possible to achieve complete control of the disease. This dictates the need to form a new approach to asthma treatment aimed at treatable traits of diseases that are characterized by clinical significance for a particular patient. Given this approach to managing asthma patients, we identified clinically significant, identifiable signs that contribute to the lack of AC. These include multimorbidity, especially in combination with obesity. In the group of patients with obesity, there were significantly more comorbidities than in patients who were not obese nor overweight. In multimorbid asthma patients, individual symptoms of comorbidities were prevalent over respiratory complaints, which negatively affects AC, making it difficult to achieve, and which must be considered when developing personalized algorithms for treating asthma in this group of patients.

Conclusions:

1. The asthma course is negatively affected by multimorbidity, which is most pronounced in obese patients. An increase in the number of comorbidities significantly worsens AC in patients of all studied groups, while the worst control level was observed in obese patients.

2. A personalized program for managing multimorbid asthma patients should be developed and implemented, considering the multivariate assessment of treatable signs of disease.

Competing Interests

The authors declare that they have no competing interests.

References

1. Global Initiative for Asthma. Global Strategy for Asthma Management and Prevention, 2021. Available from: www.ginasthma.org.
2. Arkhipov VV, Grigoryeva EV, Gavrishina EV. [Control of bronchial asthma in Russia: results of NIKA multi-center observational study]. *Pulmonologiya*. 2011;(6):87-93. (In Russ.) doi: 10.18093/0869-0189-2011-0-6-87-93. [Article in Russian].
3. Mindlis I, Wisnivesky JP, Wolf MS, O'Connor R, Federman AD. Comorbidities and depressive symptoms among older adults with asthma. *J Asthma*. 2022 May;59(5):910-916. doi: 10.1080/02770903.2021.1887890.
4. Van Huisstede A, Castro Cabezas M, van de Geijn GJ, Mannaerts GH, Njo TL, Taube C, Hiemstra PS, Braunstahl GJ. Underdiagnosis and overdiagnosis of asthma in the morbidly obese. *Respir Med*. 2013 Sep;107(9):1356-64. doi: 10.1016/j.rmed.2013.05.007.
5. Stepanova YeV, Loranskaya ID, Rakitskaya LG, Mamedova LD. [Obesity as the Omni-Factor for Serious Diseases]. *Effektivnaya Farmakoterapiya*. 2019;15(18):68-77. doi: 10.33978/2307-3586-2019-15-18-68-77. [Article in Russian].
6. Juniper EF, Buist AS, Cox FM, Ferrie PJ, King DR. Validation of a standardized version of the Asthma Quality of Life Questionnaire. *Chest*. 1999 May;115(5):1265-70. doi: 10.1378/chest.115.5.1265.
7. Weatherburn CJ, Guthrie B, Mercer SW, Morales DR. Comorbidities in adults with asthma: Population-based cross-sectional analysis of 1.4 million adults in Scotland. *Clin Exp Allergy*. 2017 Oct;47(10):1246-1252. doi: 10.1111/cea.12971.
8. Wardzyńska A, Kubsik B, Kowalski ML. Comorbidities in elderly patients with asthma: Association with control of the disease and concomitant treatment. *Geriatr Gerontol Int*. 2015 Jul;15(7):902-9. doi: 10.1111/ggi.12367.
9. Cazzola M, Rogliani P, Ora J, Calzetta L, Matera MG. Asthma and comorbidities: recent advances. *Pol Arch Intern Med*. 2022 Apr 28;132(4):16250. doi: 10.20452/pamw.16250.
10. Ermolova AV, Budnevsky AV, Yu ME, Ovsyannikov ES, Drobysheva ES. [BRONCHIAL ASTHMA AND METABOLIC SYNDROME]. *Klin Med (Mosk)*. 2015;93(6):44-9. [Article in Russian].
11. Provotorov VM, Budnevsky AV, Filatova YI. [Clinical manifestations of asthma during combination therapy using ceruloplasmin]. *Ter Arkh*. 2016;88(3):36-39. doi: 10.17116/terarkh201688336-39. [Article in Russian].
12. Provotorov VM, Budnevsky AV, Filatova YI, Perfil'eva MV. [ANTIOXIDANT THERAPY OF BRONCHIAL ASTHMA]. *Klin Med (Mosk)*. 2015;93(8):19-22. [Article in Russian].
13. Budnevsky AV, Isaeva YV, Malysh EY, Kozhevnikova SA. Legochnaya reabilitatsiya kak effektivnyi metod optimizatsii lechebno-profilakticheskikh meropriyatii u bol'nykh khronicheskoi obstruktivnoi bolezniyu legkikh s metabolicheskim sindromom [Pulmonary rehabilitation as an effective method for optimizing therapeutic and preventive measures in patients with chronic obstructive pulmonary disease concurrent with metabolic syndrome]. *Ter Arkh*. 2016;88(8):25-29. doi: 10.17116/terarkh201688825-29. [Article in Russian].
14. Tsvetkova LN, Budnevsky AV, Ovsyannikov ES, Kudashova EA. Melatonin: Possibilities for use in the treatment of asthma. *Ter Arkh*. 2017;89(3): 112–115. (In Russ.) doi: 10.17116/terarkh2017893112-115.
15. Masa JF, Pépin JL, Borel JC, Mokhlesi B, Murphy PB, Sánchez-Quiroga MÁ. Obesity hypoventilation syndrome. *Eur Respir Rev*. 2019 Mar 14;28(151):180097. doi: 10.1183/16000617.0097-2018.
16. Tomisa G, Horváth A, Santa B, Keglevich A, Tamási L. Epidemiology of comorbidities and their association with asthma control. *Allergy Asthma Clin Immunol*. 2021 Sep 22;17(1):95. doi: 10.1186/s13223-021-00598-3.

*Corresponding author: Prof. Evgeniy S. Ovsyannikov, PhD, ScD. Department of faculty therapy, Voronezh State Medical University named after N.N. Burdenko. Voronezh, Russia. E-mail: ovses@yandex.ru

Therapy Goal Achievement in Children and Adolescents with Type 1 Diabetes Mellitus in Insulin Pump Therapy Depending on the Glucose Monitoring and Educational Programs

Akmaral B. Tashmanova^{1,2*}, Gulnara N. Rakhimova³, Salim F. Berkinbaev²,
Madina E. Mansurova¹, Kamilla B. Srailova²

¹Kazakh National University named after Al-Farabi, Almaty, Kazakhstan

²Kazakh National Medical University named after S. D. Asfendiyarov, Almaty, Kazakhstan

³Center for the Development of Advanced Training of Medical Workers of the Ministry of Health of the Republic of Uzbekistan, Tashkent, Uzbekistan

Abstract

Background: Education and treatment programs can help children and adolescents with type 1 diabetes (T1D), and their parents, to independently carry out the necessary measures to achieve the treatment goals. In this regard, it seems extremely relevant to develop and evaluate the effectiveness of a training-modified program, considering national characteristics for children and adolescents with T1D who are devoted to using insulin pumps for insulin administration. The purpose of this work was to evaluate the effectiveness of a modified training program in achieving target levels of glycemia in children and adolescents with T1D on insulin pump therapy in Almaty.

Methods and Results: Our study included 125 children and adolescents with T1D who were divided into 2 groups. The main group (MG), with a modified educational program, consisted of 68 children and adolescents with T1D who studied quarterly at the “School of T1D.” The comparison group (CG) consisted of 57 children and adolescents with T1D who were on outpatient and inpatient treatment in different clinics and were trained in the “School of T1D” by the traditional method. All surveyed children and adolescents took a training course 2-3 times a year (each session 5 days long) from 2018 to 2021.

The patients of MG and CG were divided into 2 subgroups depending on the method of assessing glycemia: self-monitoring blood glucose (SMBG) using an individual glucometer and FreeStyle Libre Glucose Sensor (FSLGS) for continuous glucose monitoring (CGM). The modified program included the installation of Flash monitoring and a strategy to increase time in the target range, as well as calculating the insulin bolus dose in bread units, calculated in national dishes, then monitoring treatment correction.

After a year of training, the frequency of achieving target levels of HbA1c ($\leq 7.0\%$) increased to 60.5% compared to 30.6% at the initial stage in the main subgroup with SMBG and 66.4% versus 28.7% in the main subgroup with the FSLGS for CGM; it was significant in both cases ($P=0.01$). In the comparison subgroups, achieving target levels of HbA1c was less pronounced and not significant (46.2% compared to 29.5% at the initial stage in the subgroup with SMBG and 51.1% compared to 29.1% at the initial stage in the subgroup with the FSLGS for CGM, $P>0.05$ in both cases).

Conclusion: CGM and modified learning significantly contribute to the management of T1D, are associated with lower HbA1c levels and longer stay in the time-in-range, and increase the commitment of patients and their parents to the self-control of glucose. (*International Journal of Biomedicine*. 2023;13(1):41-46.)

Keywords: type 1 diabetes • pediatrics • continuous glucose monitoring • glycosylated hemoglobin

For citation: Tashmanova AB, Rakhimova GN, Berkinbaev SF, Mansurova ME, Srailova KB. Therapy Goal Achievement in Children and Adolescents with Type 1 Diabetes Mellitus in Insulin Pump Therapy Depending on the Glucose Monitoring and Educational Programs. *International Journal of Biomedicine*. 2023;13(1):41-46. doi:10.21103/Article13(1)_OA3

Abbreviations

ADA, American Diabetes Association; **BC**, bolus calculator; **CSII**, continuous subcutaneous insulin infusion; **CGM**, continuous glucose monitoring; **FSLGS**, FreeStyle Libre Glucose Sensor; **HbA1c**, glycosylated hemoglobin; **SMBG**, self-monitoring blood glucose; **TIR**, time-in-range; **TBR**, time below range; **T1D**, type 1 diabetes.

Introduction

Continuous subcutaneous insulin infusion (CSII) is gradually being introduced into traditional clinical practice, facilitated by the availability of modern, reliable insulin pumps, increased clinical experience with pump therapy, a strong evidence base for the effectiveness of pump therapy, and the development of national guidelines on diabetes management.^(1,2)

In the world, insulin pump therapy is used quite widely: up to 34% of patients with type 1 diabetes (T1D) in the USA and up to 25% in Europe use insulin pumps to administer insulin.⁽³⁾

The incidence and prevalence of T1D vary significantly in different countries. In Almaty, Kazakhstan, the prevalence of T1D was 1.2 and the incidence 13.2 per 100,000 child population. Among the children of Almaty, the number of pump users has been progressively increasing and, by 2020, amounted to 281 children and adolescents.⁽⁴⁾

Education and treatment programs can help children and adolescents with T1D, and their parents, to independently carry out the necessary measures to achieve the treatment goals, thereby sharing responsibility for the effectiveness of therapy between the doctor and the patient. Most studies on the application of this method state a significant positive trend in 1-2 years after training.^(5,6)

The ADA Standards of Care in Diabetes recommend that all children and adolescents with T1D perform self-monitoring of glucose levels 6–10/day using self-monitoring blood glucose (SMBG) or continuous glucose monitoring (CGM), including the periods before meals, before going to bed, and as needed in certain situations (exercise, symptoms of hypoglycemia).^(3,7,8)

In 2017, the CGM Consensus for Patient Education was published,⁽⁹⁾ requiring all patients to receive training on how to interpret and respond to their glucose data.

Today in the world, there are several programs for patients with CGM. The first was the SPECTRUM (Structured Patient Education and Treatment Program for Self-Reliant Continuous Glucose Monitoring) patient education and treatment program for CGM users. The SPECTRUM program included 110 patients. As a result of training, knowledge about the CGM system improved by 43%, study participants mastered almost all practical skills in working with the system, and patients showed a decrease in HbA_{1c} levels.^(10,11)

The Dynamic GM training program for children and adolescents with T1D who are CGM users was based on a review of international guidelines for structured learning for CGM users.⁽¹²⁾ The program included children and adolescents with T1D (n=50) (mean age of 10.2 years, mean disease duration of 5.2 years). The training was conducted by a nurse or trainer. The total time of classes was 10 hours, lasting 6 months.

The results of the Flash program, a self-management-based treatment and education program developed in Germany aimed at educating patients using the FreeStyle Libre system, is built on a different principle. The Flash program lasts 6 weeks and includes 4 sessions. This program was evaluated in

a randomized, open-label study with a control group to study the impact of education on patients with diabetes on glycemic control parameters. The results of the Flash program showed a more pronounced decrease in HbA_{1c} in patients from the Flash training program than in the control group (69.6% and 54.6%, respectively, $P=0.003$).^(13,14)

Currently, in some countries, when transferring patients to CSII, appropriate selection and training are often not carried out, which leads to many errors in handling devices and decompensation of diabetes, even in those patients who were compensated using syringe pens. Monitoring patients receiving this expensive type of treatment is also chaotic, without considering the characteristics of these patients and the opportunities that an insulin pump gives an endocrinologist.^(15,16)

In this regard, it seems extremely relevant to develop and evaluate the effectiveness of a training-modified program, considering national characteristics for children and adolescents with T1D who are devoted to using insulin pumps for insulin administration. The learning process should consider the individual psychological characteristics of patients, traditional-national nutritional characteristics, and modern methods of intensive care and monitoring of blood glucose concentration with a glucometer or FreeStyle Libre glucose sensor (FSLGS).

The purpose of this work was to evaluate the effectiveness of a modified training program in achieving target levels of glycemia in children and adolescents with T1D on insulin pump therapy in Almaty.

Materials and Methods

Our study included 125 children and adolescents with T1D who were divided into 2 groups. The main group (MG), with a modified educational program, consisted of 68 children and adolescents with T1D who studied quarterly at the “School of T1D.” The comparison group (CG) consisted of 57 children and adolescents with T1D who were on outpatient and inpatient treatment in different clinics and were trained in the “School of T1D” by the traditional method. The groups did not differ in age or duration of the disease (Table 1).

Table 1.

General characteristics of patients on CSII

Variable	Modified educational program	Traditional educational program	P-value
Age, yrs.	12.0 [8;16]	13.0 [7;16]	0.209
Experience of diabetes, yrs.	6.7 [4;14]	7.2 [5;16]	0.181
HbA _{1c} , % before training	8.7 [7.0;9.8]	9.0 [8.1;10.0]	>0.05

The patients of MG and CG were divided into 2 subgroups depending on the method of assessing glycemia:

MG1(n=35) and CG1 (n=30): Patients performed SMBG using an individual glucometer.

MG2 (n=33) and CG2 (n=27): Patients used FSLGS for CGM.

The training was conducted in the “School for T1D” (the Children’s Clinical Hospital #2) on an outpatient basis. All surveyed children and adolescents took a training course 2-3 times a year (each session 5 days long) from 2018 to 2021. The modified program included the following steps: 1- familiarization lesson and setting individual goals, 2- prevention of hypo-hyperglycemia, 3- installation of Flash monitoring and a strategy to increase time in the target range, 4 and 5 lessons included calculating the insulin bolus dose in bread units (BU), calculated in national dishes, then monitoring treatment correction.⁽¹⁷⁻¹⁹⁾

All subjects were tested based on a modified questionnaire, including 30 key questions on self-monitoring glucose during insulin pump therapy, on sensors, and on counting BU before and after training.⁽¹⁸⁻²⁰⁾

Compensation was assessed based on the determination of the level of HbA1c by the immunochemical method using DCA Vantage Analyzer (Siemens Healthcare Diagnostics). The method for determining HbA1c corresponds to the NGSP certificate (The National Glycohemoglobin Standardization Program).

Statistical analysis was performed using STATISTICA version 8 (StatSoft Inc., USA). For descriptive analysis, results are presented as median (Me), first quartile (Q1), and third quartile (Q3). Differences of continuous variables were tested by the Mann-Whitney *U*-test. Group comparisons with respect to categorical variables are performed using the chi-square test. A probability value of $P < 0.05$ was considered statistically significant.

This study was approved by the Ethics Committee of the Kazakh National University named after Al-Farabi (Almaty, Kazakhstan). Written informed consent was obtained from the parent/guardian/relative of each patient.

Results and Discussion

When evaluating the training effectiveness using a questionnaire, it was found that patients in the MG (an average T1D duration of 6.7[4;14] years), before training, could correctly answer questions only in 16%-20% of cases. After 6 months and after one year after training, correct answers were obtained in 80%-90% of cases. During the observation period, CG patients (an average T1D duration of 7.2[5;16] years) had a low level of correct answers, from 20% to 37%. Patients of the CG were more likely to be admitted to the intensive care unit both before and after traditional training.

At the time of transfer from the regimen of multiple insulin injections to CSII, MG and CG did not significantly differ from each other in the degree of compensation of carbohydrate metabolism (Table 2).

Six months after training and switching from multiple insulin injections to CSII, the HbA1 level showed a greater decrease in the MG1 and MG2 than in the dynamics in the CG1 and CG2. At the same time, a more pronounced reduction in the HbA1 level was noted in CG2 than in CG1 (8.0% [6.2;8.3] vs. 8.8% [8.2;9.5], $P < 0.01$). After one year, the HbA1c level

was significantly lower in MG subgroups, especially in MG2, compared to CG1 and CG2. At the same time, a more pronounced decrease in the HbA1c level was found in CG2 compared to CG1 (7.6% [7.4;8.0] vs. 7.8% [7.5;8.5], $P < 0.05$) (Table 3).

Table 2.

Clinical characteristics of patients on CSII depending on the method of assessing glycemia and the type of training at the initial stage

Variable	Modified educational program		<i>P</i>	Traditional educational program		<i>P</i>
	MG1	MG2		CG1	CG2	
Age, yrs.	10.0 [6;15]	12.0 [8;16]	0.56	9.7 [6;16]	13.0 [9.5;17]	
Experience of T1D, yrs.	6.6 [7;14]	8.4 [6;14]	0.21	7.1 [5;15]	9.2 [7.5;15]	0.12
HbA _{1c} , %	8.1 [7.4;9.6]	7.7 [8.0;9.2]	0.69	9.3 [8.4;10.3]	8.9 [7.7;9.0]	>0.05

Table 3.

Dynamics of HbA1c (%) in the study subgroups.

Training phase	Modified educational program			Traditional educational program		
	MG1	<i>P</i>	MG2	CG1	<i>P</i>	CG2
At the time of transfer to CSII (I)	8.1 [7.4;9.6]	>0.05	7.7 [8.0;9.2]	9.3 [8.4;10.3]	<0.05	8.9 [7.7;9.0]
6 months after	7.6 [6.7;8.0]	>0.05	7.3 [6.1;7.6]	8.8 [8.2;9.5]	<0.01	8.0 [6.2;8.3]
12 months after (II)	7.4 [6.3;8.2]	>0.05	7.1 [6.0;7.4]	7.8 [7.5;8.5]	<0.05	7.6 [7.4;8.0]
<i>P</i> _{I-II}	<0.05		<0.05	<0.05		<0.05

Before switching to CSII, the frequency of achieving target levels of HbA1c ($\leq 7.0\%$) in MG1 and MG2 was 30.6% and 28.7%, respectively, versus 29.5% and 29.1% in CG1 and CG2, respectively (Table 4). After a year of training, the frequency of achieving target levels of HbA1c in MG1 increased to 60.5%, compared to 30.6% at the initial stage ($P = 0.01$). In MG2, similar dynamics were also seen, and the target values were achieved in 66.4% of patients versus 28.7% at the initial stage ($P < 0.01$). In subgroups CG1 and CG2, a similar trend was observed, but without significant dynamics (Table 4).

Glycemia was evaluated according to reports obtained by downloading data from insulin pumps to a personal computer using CareLink Personal software ver. 7.0 (Medtronic BV,

USA). Additionally, glycemia indicators were evaluated according to the data of reports obtained by downloading data from the FSLGS using the software (Figure 1).

Table 4.

The frequency of achieving target levels of HbA1c in study subgroups

Variable	Modified educational program			Traditional educational program			P	P
	MG1 (n=35)	P	MG2 (n=33)	CG1 (n=30)	P	CG2 (n=27)		
Before switching to CSII	30.6%	>0.05	28.7%	29.5%	>0.05	29.1%	>0.05	>0.05
6 months after	42.7%	>0.05	47.5%	34.6%	>0.05	38.4%	>0.05	>0.05
12 months after	60.5%	>0.05	66.4%	46.2%	>0.05	51.1%	>0.05	>0.05
P	0.01		<0.01	>0.05		>0.05		

found that patients in the CG used a bolus calculator less frequently than in the MG (5.9±3.0 vs. 7.1±3.4, P=0.040) and administered self-calculated bolus (“in mind”) more often or calculated using different Internet sites.

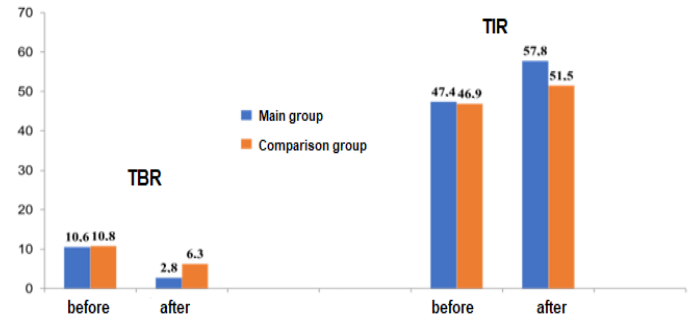


Fig. 2. Dynamics of TBR (%) and TIR (%) before and after the training programs.

Table 5.

The frequency of bolus calculator use in the study groups and subgroups.

Group	Number of the bolus calculator use per day			P-value
	Total	SMBG	FSLGS	
MG (n=68)	7.1±3.4	6.2±3.1 (n=35)	7.9±3.7 (n=33)	0.044
CG (n=57)	5.9±3.0	5.3±2.9 (n=30)	6.7±3.2 (n=27)	0.089
P-value	0.040	0.234	0.190	

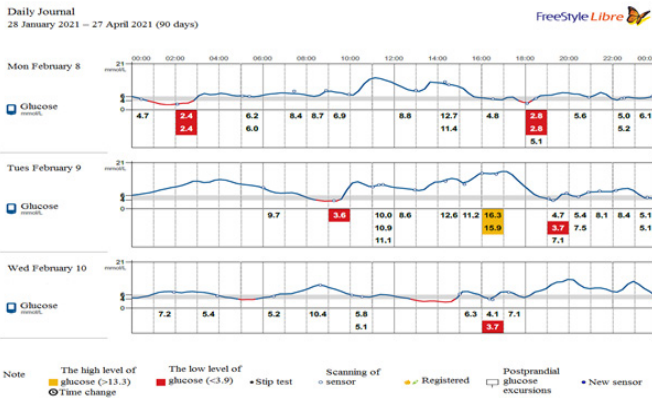


Fig. 1. Glycemic values according to the FreeStyle Libre sensor report.

The introduction of training-modified programs for patients with T1D in the MG contributed to a more significant improvement in glycemic control than in the CG. Thus, there was an increase in the time-in-range (TIR) from 47.4% to 57.8% in the MG and from 46.9% to 51.5% in CG (P<0.001). Time below range (TBR) decreased from 10.6% to 2.8% in the MG and from 10.8% to 6.3% in the CG (P<0.001) (Fig. 2). The modified training program has contributed to more regular use of CGM data by patients, a reduced need for routine glucometry, and improved use of continuous subcutaneous insulin infusion.

Based on the reports obtained when loading data from insulin pumps into a computer, we analyzed the frequency of bolus calculator use as one of the factors affecting the compensation of carbohydrate metabolism (Table 5). It was

Conclusions

1. In children and adolescents with T1D of the main group with modified learning, after one year of observation, the average level of HbA1c achieved 7.4% [6.3;8.2] in the subgroup with self-monitoring blood glucose and 7.1% [6.0;7.4] in the subgroup with the FreeStyle Libre Glucose Sensor for continuous glucose monitoring. Children and adolescents with T1D of the comparison group with standard learning achieved compensation after one year of observation by a lesser degree (HbA1c of 7.8% [7.5.;8.5] in the subgroup with self-monitoring blood glucose and 7.6% [7.4;8.0] in the subgroup with the FreeStyle Libre Glucose Sensor for continuous glucose monitoring). The FreeStyle Libre Glucose Sensor for continuous glucose monitoring was more effective in both groups.

2. After a year of training, the frequency of achieving target levels of HbA1c (≤7.0%) increased to 60.5% compared

to 30.6% at the initial stage in the main subgroup with self-monitoring blood glucose and 66.4% versus 28.7% in the main subgroup with the FreeStyle Libre Glucose Sensor for continuous glucose monitoring; it was significant in both cases ($P=0.01$). In the comparison subgroups, achieving target levels of HbA1c was less pronounced and not significant (46.2% compared to 29.5% at the initial stage in the subgroup with self-monitoring blood glucose and 51.1% compared to 29.1% at the initial stage in the subgroup with the FreeStyle Libre Glucose Sensor for continuous glucose monitoring, $P>0.05$ in both cases).

3. Continuous glucose monitoring and modified learning significantly contribute to the management of T1D, are associated with lower HbA1c levels and longer stay in the time-in-range, and increase the commitment of patients and their parents to the self-control of glucose.

Sources of Funding

This work was funded by Committee of Science of Republic of Kazakhstan AP09260767 “Development of intellectual information-analytical system for assessing the health of students in Kazakhstan” (2021-2022).

Competing Interests

The authors declare that they have no competing interests.

References

- Ibragimova LI, Philippov YI, Mayorov AY. Insulin pump therapy in type 1 diabetes mellitus: education effectiveness and quality of life. *Diabetes mellitus*, 2012, 15(1), 35-40. doi: 10.14341 / 2072-0351-5977.
- Mayorov AY, Surkova EV, Motovilin OG, Mel'nikova OG, Shishkova YuA. [Education of diabetic patients: synthesis of evidence-based medicine and psychological approach]. *Diabetes mellitus*. 2011;14(1):46-52. [Article in Russian].
- DiMeglio LA, Acerini CL, Codner E, Craig ME, Hofer SE, Pillay K, Maahs DM. ISPAD Clinical Practice Consensus Guidelines 2018: Glycemic control targets and glucose monitoring for children, adolescents, and young adults with diabetes. *Pediatr Diabetes*. 2018 Oct;19 Suppl 27:105-114. doi: 10.1111/pedi.12737.
- Almaty City Branch “Republican Center for Electronic Health” of the Ministry of Health of the Republic of Kazakhstan. Available from: <http://riac-almaty.kz/index.php/ru/>
- Galstyan GR, Maiorov AY, Dvoinishnikova OM, Bessmertnaya YG, Milenkaya TM, Sunsov YI, Antsiferov MB, Dedov II. [Long-term results of therapeutic education of patients with type 1 diabetes mellitus]. *Probl Endokrinol (Mosk)*. 2005 Jun 15;51(3):50-55. doi: 10.14341/probl200551350-55. [Article in Russian].
- Mensing C, Boucher J, Cypress M, Weinger K, Mulcahy K, Barta P, Hosey G, Kopher W, Lasichak A, Lamb B, Mangan M, Norman J, Tanja J, Yauk L, Wisdom K, Adams C.

National standards for diabetes self-management education. *Diabetes Care*. 2007 Jan;30 Suppl 1:S96-S103. doi: 10.2337/dc07-S096.

- American Diabetes Association. 7. Diabetes Technology: Standards of Medical Care in Diabetes-2020. *Diabetes Care*. 2020 Jan;43(Suppl 1):S77-S88. doi: 10.2337/dc20-S007. Erratum in: *Diabetes Care*. 2020 Aug;43(8):1981.
- American Diabetes Association. Addendum. 7. Diabetes Technology: Standards of Medical Care in Diabetes-2020. *Diabetes Care* 2020;43(Suppl. 1):S77-S88. *Diabetes Care*. 2020 Aug;43(8):1981. doi: 10.2337/dc20-ad08c. Epub 2020 Jun 5. Erratum for: *Diabetes Care*. 2020 Jan;43(Suppl 1):S77-S88.
- Danne T, Nimri R, Battelino T, Bergenstal RM, Close KL, DeVries JH, Garg S, Heinemann L, Hirsch I, Amiel SA, Beck R, Bosi E, Buckingham B, Cobelli C, Dassau E, Doyle FJ 3rd, Heller S, Hovorka R, Jia W, Jones T, Kordonouri O, Kovatchev B, Kowalski A, Laffel L, Maahs D, Murphy HR, Nørgaard K, Parkin CG, Renard E, Saboo B, Scharf M, Tamborlane WV, Weinzimer SA, Phillip M. International Consensus on Use of Continuous Glucose Monitoring. *Diabetes Care*. 2017 Dec;40(12):1631-1640. doi: 10.2337/dc17-1600.
- Gehr B, Holder M, Kulzer B, Lange K, Liebl A, Sahm C, von Sengbusch S, Schlüter S, Siegmund T, Thurm U, Ziegler R, Freckmann G, Heinemann L; SPECTRUM Group. SPECTRUM. *J Diabetes Sci Technol*. 2017 Mar;11(2):284-289. doi: 10.1177/1932296816661735.
- Schlüter S, Freckmann G, Heinemann L, Wintergerst P, Lange K. Evaluation of the SPECTRUM training programme for real-time continuous glucose monitoring: A real-world multicentre prospective study in 120 adults with type 1 diabetes. *Diabet Med*. 2021 Feb;38(2):e14467. doi: 10.1111/dme.14467.
- Pemberton JS, Kershaw M, Dias R, Idkowiak J, Mohamed Z, Saraff V, Barrett TG, Krone R, Uday S. DYNAMIC: Dynamic glucose management strategies delivered through a structured education program improves time in range in a socioeconomically deprived cohort of children and young people with type 1 diabetes with a history of hypoglycemia. *Pediatr Diabetes*. 2021 Mar;22(2):249-260. doi: 10.1111/pedi.13155. Epub 2021 Jan 15. Erratum in: *Pediatr Diabetes*. 2022 Feb;23(1):166-168.
- Phelan H, Lange K, Cengiz E, Gallego P, Majaliwa E, Pelicand J, Smart C, Hofer SE. ISPAD Clinical Practice Consensus Guidelines 2018: Diabetes education in children and adolescents. *Pediatr Diabetes*. 2018 Oct;19 Suppl 27:75-83. doi: 10.1111/pedi.12762.
- Hermanns N, Ehrmann D, Schipfer M, Kröger J, Haak T, Kulzer B. The impact of a structured education and treatment programme (FLASH) for people with diabetes using a flash sensor-based glucose monitoring system: Results of a randomized controlled trial. *Diabetes Res Clin Pract*. 2019 Apr;150:111-121. doi: 10.1016/j.diabres.2019.03.003.

*Corresponding author: Dr. Akmaral B. Tashmanova. Kazakh National University named after Al-Farabi. Kazakh National Medical University named after S. D. Asfendiyarov. Almaty, Kazakhstan. E-mail: akmaralbaymatovna@mail.ru

15. NICE: National Institute for Clinical Excellence. NICE Technology Appraisal Guidance No 60. Guidance on the use of patient-education models for diabetes. Published: 26 April 2003 Last updated: 01 August 2015. Available from: <https://www.nice.org.uk/guidance/ng17>
 16. Plank J, Köhler G, Rakovac I, Semlitsch BM, Horvath K, Bock G, Kraly B, Pieber TR. Long-term evaluation of a structured outpatient education programme for intensified insulin therapy in patients with Type 1 diabetes: a 12-year follow-up. *Diabetologia*. 2004 Aug;47(8):1370-5. doi: 10.1007/s00125-004-1456-x.
 17. Ismailov S, Rakhimova G, Tashmanova A, Abdurazakova Z. [Evaluation of Clinical and Metabolic Parameters of Efficiency of Long-term Training and Achievement of Target Levels of Type 1 Diabetes Mellitus Therapy in Children and Adolescents]. *INTERNATIONAL JOURNAL OF ENDOCRINOLOGY (Ukraine)*. 2014;(6.62):19–23. doi: 10.22141/2224-0721.6.62.2014.76930. [Article in Russian].
 18. Rakhimova GN, Ismailov SI, Alimova NU, Tashmanova AB, Alieva AV. [Type 1 diabetes mellitus in children and adolescents]. *Methodological manuals for children, adolescents, and their parents*. Tashkent, 2012. [In Russian].
 19. Rakhimova G.N, Ismailov SI, Alimova NU, Akbarov AZ, Tashmanova AB, Alieva AV. [National standards of care for children and adolescents with type 1 diabetes]. *Methodological recommendation*. Tashkent, 2013. [In Russian].
 20. Tashmanova A, Ismailov S, Rakhimova G, Abdurazakova Z. [Evaluating the Efficacy of New Structured Program for Teaching Patients with Diabetes Mellitus Type 1 in the Republic of Uzbekistan]. *INTERNATIONAL JOURNAL OF ENDOCRINOLOGY (Ukraine)*. 2014.(1.57):46–50. doi:10.22141/2224-0721.1.57.2014.76401. [Article in Russian].
-

Trends in Prediabetes and Diabetes Prevalence in Kosovo: A Comparison of the Results of Steps Survey From 2011 and 2019

Naser Ramadani^{1,2}, Sanije Hoxha-Gashi^{1,2*}, Sefedin Muçaj^{1,2}, Ajkuna Hoxha⁴,
Naim Jerliu^{1,2}, Josipa Kern³

¹Faculty of Medicine, University of Prishtina "Hasan Prishtina", Prishtina, Kosovo

²National Institute of Public Health of Kosovo, Prishtina, Kosovo

³School of Medicine, University of Zagreb, Zagreb, Croatia

⁴Biochemistry Clinic, University Clinical Center of Kosovo, Prishtina, Kosovo

Abstract

Background: Some years ago, chronic diseases were considered to be a problem for the wealthy and elderly population. Today, chronic conditions affect the poor, young, and middle-aged people in high-income countries. The global prevalence of diabetes mellitus (DM) has been continuously growing for over half a century and has reached pandemic proportions. In the present study, we aimed to estimate the trends in prediabetes and DM prevalence and to determine related risk factors among Kosovo people from 2011 to 2019.

Methods and Results: A population-based survey was conducted among people aged 18-69 from April 2018 to June 2019 and those aged 15-64 using the WHO STEPs instrument. Detailed findings on the magnitude of DM and impaired fasting blood glucose (FBG) are presented in this paper.

Prevalence of prediabetes in 2011 at 15-64 years was 6.0% (95% CI: 4.6% - 7.9%), and in 2019 at 18-69 years was 6.1% (95% CI: 5.3% - 7.1%), not a significant difference ($P>0.05$). To avoid bias from different ages, we compared prevalence by age groups. Only in the age group of 35-44 we found a significant difference in the prevalence of prediabetes. In this age group, the prevalence of prediabetes was 2.4% (95% CI: 0.9% - 6.1%) in 2011 and 2.7% (95% CI: 0.9% - 6.1%) in 2019. In 2019, the prevalence of prediabetes was higher among males than in 2011, when females prevailed.

Prevalence of DM in 2011 at 15-64 years was 7.7% (95% CI: 6.0% - 9.7%), and in 2019 at 18-69 years was 7.9% (95% CI: 6.9% - 9.0%), not a significant difference ($P>0.05$). In the age groups of 45-54 and 55-64, we found a significant difference in the prevalence of DM by years. The prevalence of DM at 45-54 years was 13.5% (95% CI: 9.2% - 19.5%) in 2011 and 7.8% (95% CI: 6.0% - 10.2%) in 2019 ($P=0.032$). The prevalence of DM at 55-64 years was 21.6% (95% CI: 15.8% - 28.9%) in 2011 and 13.2% (95% CI: 10.6% - 16.3%) in 2019 ($P=0.015$). The prevalence of DM was higher among females in 2011 and 2019.

Conclusion: Results from 2 STEPS in Kosovo show that we have no significant increase in the prevalence of prediabetes and DM in total. At the same time, we found a significant decrease in DM in the age group 45-64. (**International Journal of Biomedicine. 2023;13(1):47-53.**)

Keywords: prediabetes • diabetes • Kosovo adults • STEPS survey

For citation: Ramadani N, Hoxha-Gashi S, Muçaj S, Hoxha A, Jerliu N, Kern J. Trends in Prediabetes and Diabetes Prevalence in Kosovo: A Comparison of the Results of Steps Survey From 2011 and 2019. International Journal of Biomedicine. 2023;13(1):47-53. doi:10.21103/Article13(1)_OA4

Abbreviations

DM, diabetes mellitus; **FBG**, fasting blood glucose; **IFG**, impaired fasting glycemia; **NCDs**, non-communicable diseases; **WHO**, World Health Organization.

Introduction

Diabetes mellitus (DM) has emerged as one of the most severe and prevalent chronic diseases of our time, causing potentially fatal, disabling, and expensive complications and reducing life expectancy.⁽¹⁾ The global DM prevalence in 20-79-year-olds in 2021 was estimated to be 10.5% (536,6 million people), and is predicted to rise to 12.2% (783,2 million) in 2045. A large proportion of diabetics (80.6%, 432,7 million) live in low- and middle-income countries. Global DM-related health expenditures were estimated at 966 billion USD in 2021 and are projected to reach 1,054 billion USD by 2045.⁽²⁾ The rising prevalence of DM has been attributed primarily to population aging, rapid urbanization, and the increasing prevalence of risk factors such as obesity, poor diet, smoking, and alcohol consumption.⁽³⁻⁵⁾ To combat the growing threat of DM, the United Nations Resolution 61/225 in 2006 encouraged all nations to develop national policies for DM prevention, care, and treatment.⁽⁶⁾ The ability to measure the distribution of DM (prevalence and incidence) and its determinants and consequences, including complications and premature death, is a common denominator for achieving this goal and demonstrating the impact of new policies. DM is the leading non-communicable disease in Kosovo, according to annual reports from the Department of Statistics at the National Institute of Public Health of Kosovo.⁽⁷⁾ Type 2 diabetes affects more than 90% of people with DM. After cardiovascular diseases and cancers, the most common cause of premature death among Kosovo residents is DM.⁽⁸⁾

The WHO created the STEPwise approach⁽⁹⁾ to address the need for standardized data on a few key risk factors, allowing countries to have small amounts of high-quality data for comparison between and within countries, as well as the ability to measure trends in these risk factors over time. In this context, the WHO STEPS approach to NCD risk-factor surveillance is an excellent example of an integrated and phased approach that many countries have used and tested. It enables countries to create a detailed risk profile for their national populations. STEPS in Kosovo was conducted for the first time in 2011,⁽¹⁰⁾ and the second time in 2019.

In the present study, we aimed to estimate the trends in prediabetes and DM prevalence and to determine related risk factors among Kosovo people from 2011 to 2019.

Materials and Methods

The survey was conducted using the WHO STEPwise approach to NCD risk-factor surveillance (STEPS). In each of the 2 STEPS (2011 and 2019), we used 3 STEPS to gather information. STEP 1 measures behavioral risk factors, STEP 2 covers physical measurements, and STEP 3 includes the measurement of biochemical characteristics (blood glucose and total cholesterol). In this paper are presented only results from STEP 3 glucose measurement.

In STEPS-2011, STEP 3 was planned for 1000 participants, and 796(79.6%) agreed to participate. In STEPS-2019, 2800 residents aged 18-69 years were randomly selected for the survey, and 2539(90.7%) agreed to participate.

Sampling

Two-stage probability sampling using stratification procedures was used to prepare the sample. The sample size will be calculated using the following formula and assumptions:

$$n = \frac{Z^2 \times P \times (1 - P)}{d^2}$$

d - margin of error 0.05, P - probability 0.5, Z - confidence level 95%; design effect of 1.5.

For STEPS 2019, we used 4 groups; for STEPS 2011, we used 8 groups. A 75% response rate is expected.⁽¹¹⁾

Biochemical Measurements

A mobile laboratory was used in data collection. The mobile laboratory contained the logistics and human resources required, including an Accutrend Plus and all materials required for blood glucose testing. Fasting samples were taken to measure blood glucose using the dry method. Participants were instructed to fast overnight for 12 hours, and diabetic patients on medication were reminded to bring their medicine/insulin with them and take their medicine after providing the blood sample.

IFG was defined as either capillary whole blood value ≥ 5.6 mmol/L – < 6.1 mmol/L. Raised FBG was defined as either capillary whole blood value ≥ 6.1 mmol/L.

Data collection and quality control

The questionnaires were adapted and translated into Albanian and back translated into English to ensure their validity. To ensure the high quality of data, the group of 45 field workers (public health professionals of NIPHK) conducted three days of training for field data collectors and supervisors.

Statistical analysis

For STEPS-2011, statistical analysis was undertaken using SPSS version 22.0. Data are presented as percentage and 95% confidence interval (CI). Mann-Whitney U test was used to compare means of 2 groups of variables not normally distributed. The frequencies of categorical variables were compared using Pearson's chi-squared test or Fisher's exact test (2-tail), when appropriate. A probability value of $P < 0.05$ was considered statistically significant.

Data for STEPS-2019 were weighted. Weights were assigned to account for the following factors: selection probability, nonresponse, and gender and age differences between the sample and the target population. Data analysis was conducted in Epi Info,⁽¹²⁾ version 3.5.1 (Centers for Disease Control and Prevention, Atlanta, Ga), and prevalence rates with corresponding 95% CIs were estimated. The results were considered statistically significant if there was no overlap between 2 CIs of the compared groups (e.g., males vs. females) or $P < 0.05$ if they were tested with the Chi test or Fisher exact test.

Results

A population-based survey was conducted among people aged 18-69 from April 2018 to June 2019 and those aged 15-64 using the WHO STEPs instrument. Detailed findings on the magnitude of DM and impaired FBG are presented in this

paper. By gender, more respondents were female than male (50.3% in 2011 vs. 59.0% in 2019); adults aged 25-44 were 39.5% in 2011 and 32.6% in 2019; rural residents were 56.5% in 2011 and 59.0% in 2019; illiteracy was 2.9% in 2011 and 3.8% in 2019 (Table 1).

Table 1.
Socio-demographic and behaviors characteristics of the study population, Kosovo STEPS survey 2011 and 2019.

Characteristics	STEPS 2011	STEPS 2019
	n=796 (%)	n=2539 (%)
Age groups (years)		
15-24	163 (20.5)	*229 (9.0)
25-34	165 (20.7)	328 (12.9)
35-44	150 (18.8)	500 (19.7)
45-54	170 (21.4)	613 (24.1)
55-64	148 (18.6)	539 (21.2)
65-69	-	330 (13.0)
Gender		
Male	396 (49.7)	1042 (41.0)
Female	400 (50.3)	1497 (59.0)
Residence		
Rural	450 (56.5)	1499 (59.0)
Urban	346 (43.5)	1040 (41.0)
Educational status		
Illiterate	23 (2.9)	96 (3.8)
Up to primary education	222 (27.9)	1064 (41.9)
Up to secondary education	398 (50.0)	868 (34.2)
Higher education	153 (19.2)	510 (20.1)
Marital status		
Never married	224 (28.1)	386 (15.2)
Currently married	546 (68.6)	1945 (76.6)
Separated/divorced	3 (0.4)	20 (0.8)
Widowed and cohabitating	23 (2.9)	188 (7.4)
BMI		
Underweight	-	33 (1.3)
Normal weight	363 (45.6)	669 (26.3)
Overweight	138 (17.3)	1045 (41.2)
Obese	295 (37.1)	767 (30.2)
Current smoking		
Yes	197 (24.7)	648 (25.5)
No	599 (75.3)	1891 (74.5)
Current alcohol use**		
Yes	61 (7.7)	294 (11.6)
No	735 (92.3)	2245 (88.4)

*18-24 years; **One who has drunk alcohol in the past 30 days

In 2011, 27.9% of respondents had finished primary school, and 68.6% were married. In 2019, 41.9% had completed primary school, and 76.6% were married. In 2019, we had more overweight people (41.2% vs. 17.4%) and current alcoholic drinkers (7.4% vs. 11.6%) than in 2011.

When interpreting the results of the previous 2011 study, it should be noted that the target population in 2011 was different from that of the current STEPS survey (15-64 years in the 2011 survey, 18-69 years in the 2019 survey) and that the 2011 survey was not weighted. To compare the prevalence trend of prediabetes and DM from 2011 to 2019 in Kosovo, we used unweighted data from STEPS-2011 and STEPS-2019. Tables 2 and 3 contain unweighted data. To compare the prevalence of prediabetes and DM in Kosovo with other countries, we used weighted data from STEPS-2019 (Tables 4-6).

Table 2.
Prevalence of prediabetes in Kosovo, stratified by socio-demographic and behavioral characteristics, 2011 and 2019 (unweighted data).

Characteristics	Prevalence of prediabetes				
	STEPS 2011 n=796		STEPS 2019 n=2539		P
	Total n	n (%; 95% CI)	-	n (%; 95% CI)	
Age groups (years)					
15-24	163	1 (0.6; 0.1-3.4)	*229	2 (0.9; 0.2-3.1)	0.999
25-34	165	4 (2.4; 0.9-6.1)	328	9 (2.7; 1.5-5.1)	0.834
35-44	150	11 (7.3; 4.1-12.7)	500	16 (3.2; 2.0-5.1)	0.046
45-54	170	13 (7.6; 4.5-12.6)	613	41 (6.7; 5.0-8.9)	0.790
55-64	148	19 (12.8; 8.4-19.2)	539	51 (9.5; 7.3-12.2)	0.294
65+	-	-	330	37 (11.2; 8.2-15.1)	-
Gender					
Male	396	22 (5.6; 3.7-8.3)	1042	70 (6.7; 5.4-8.4)	0.494
Female	400	26 (6.5; 4.5-9.4)	1497	86 (5.7; 4.7-7.0)	0.652
Residence					
Rural	450	26 (6.5; 4.0-8.3)	1499	85 (5.7; 4.6-7.0)	0.931
Urban	346	22 (5.6; 4.2-9.4)	1040	71 (6.8; 5.4-8.5)	0.858
BMI					
Underweight	-	-	33	1 (3.0; 0.5-15.3)	-
Normal	363	11 (3.0; 1.7-5.3)	669	23 (3.4; 2.3-5.1)	0.866
Overweight	138	24 (17.4; 12.0-24.6)	1045	62 (5.9; 4.7-7.5)	0.000
Obese	295	13 (4.4; 2.6-7.4)	767	68 (8.9; 7.1-11.1)	0.020
Current smoking					
Yes	197	12 (6.1; 3.5-10.3)	648	40 (6.1; 4.6-8.3)	0.966
No	599	36 (6.0; 4.4-8.2)	1891	116 (6.1; 5.1-7.3)	0.989
Current alcohol use**					
Yes	61	4 (6.6; 2.6-15.7)	294	14 (4.8; 2.9 -7.8)	0.526
No	735	44 (6.0; 4.5-7.9)	2245	142 (6.3; 5.4 -7.4)	0.809
Total	796	48 (6.0; 4.6-7.9)	2539	156 (6.1; 5.3 -7.1)	0.974

**One who has drunk alcohol in the past 30 days

Prevalence of prediabetes in 2011 at 15-64 years was 6.0% (95% CI: 4.6% - 7.9%), and in 2019 at 18-69 years was 6.1% (95% CI: 5.3% - 7.1%), not a significant difference ($P>0.05$). To avoid bias from different ages, we compared prevalence by age groups. Only in the age group of 35-44 we found a significant difference in the prevalence of prediabetes. In this age group, the prevalence of prediabetes was 2.4% (95% CI: 0.9% - 6.1%) in 2011 and 2.7% (95%CI: 0.9% - 6.1%) (95%CI: 0.9% - 6.1%) in 2019. In 2019, the prevalence of prediabetes was higher among males than in 2011, when females prevailed (Table 2).

Table 3.
Prevalence of diabetes in Kosovo, stratified by socio-demographic and behavioral characteristics, 2011 and 2019 (unweighted data)

Characteristics	Prevalence of diabetes					P
	STEPS 2011 n=796		STEPS 2019 n=2539		-	
	Total n	n (%; 95% CI)		n (%; 95% CI)		
Age groups (years)						
15-24	163	-	229	3 (1.3; 0.4- 3.8)	-	
25-34	165	2 (1.2; 0.3 - 4.3)	328	6 (1.8; 0.8-3.9)	0.724	
35-44	150	4 (2.7; 1.0-6.7)	500	16 (3.2; 2.0 - 5.1)	0.950	
45-54	170	23 (13.5; 9.2 - 19.5)	613	48 (7.8; 6.0 - 10.2)	0.032	
55-64	148	32 (21.6; 15.8 - 28.9)	539	71 (13.2; 10.6-16.3)	0.015	
65+	-	-	330	56 (17.0; 13.3-21.4)	-	
Gender						
Male	396	25 (6.3; 4.3 - 9.2)	1042	79 (7.6; 6.1-9.3)	0.474	
Female	400	36 (9.0; 6.6 -12.2)	1497	121 (8.1; 6.8-9.6)	0.624	
Residence						
Rural	450	41 (5.2; 6.8 - 12.1)	1499	123 (8.2; 6.9 - 9.7)	0.610	
Urban	346	20 (2.5; 3.8 - 8.8)	1040	77 (7.6; 6.0 - 9.2)	0.366	
BMI						
Underweight	-	-	33	2 (6.1; 1.7 - 19.6)	-	
Normal	363	13 (3.6; 2.1-6.0)	669	20 (3.0; 1.9 - 4.6)	0.740	
Overweight	138	20 (14.5; 9.6-21.3)	1045	80 (7.7; 6.2 - 9.4)	0.010	
Obese	295	28 (9.5; 6.6-13.4)	767	98 (12.8; 10.6-15.3)	0.168	
Current smoking						
Yes	197	18 (9.1; 5.9-14.0)	648	41 (6.3; 4.7 - 8.5)	0.231	
No	599	43 (7.2; 5.4-9.5)	1891	159 (8.4; 7.2-9.7)	0.381	
Current alcohol use**						
Yes	61	4 (6.6; 2.6-15.7)	294	9 (3.1; 1.6 - 5.7)	0.250	
No	735	57 (7.8; 6.0-9.9)	2245	191 (8.5; 7.4 - 9.7)	0.572	
Total	796	61 (7.7; 6.0 - 9.7)	2539	200 (7.9; 6.9 - 9.0)	0.904	

**One who has drunk alcohol in the past 30 days

Prevalence of DM in 2011 at 15-64 years was 7.7% (95% CI: 6.0% - 9.7%), and in 2019 at 18 - 69 years was

7.9% (95% CI: 6.9% - 9.0%), not a significant difference ($P>0.05$). To avoid bias from different ages, we compared prevalence by age groups. In the age groups of 45-54 and 55-64, we found a significant difference in the prevalence of DM by years. The prevalence of DM at 45-54 years was 13.5% (95% CI: 9.2% - 19.5%) in 2011 and 7.8% (95%CI: 6.0%-10.2%) in 2019 ($P=0.032$). The prevalence of DM at 55-54 years was 21.6% (95% CI: 15.8% - 28.9%) in 2011 and 13.2% (95% CI: 10.6% - 16.3%) in 2019 ($P=0.015$). The prevalence of DM was higher among females in 2011 and 2019 (Table 3).

The age-sex standardized population-based mean FBG for 2539 participants was 4.6mmol/L (95% CI: 4.5-4.7 mmol/L). There were no significant differences in mean FBG by age and gender (Table 4).

Table 4.
Fasting blood glucose (mmol/L): Kosovo STEPS survey 2019 (weighted data)

Mean fasting blood glucose (mmol/L)									
Age Group (years)	Men			Women			Both Sexes		
	n	Mean	95% CI	n	Mean	95% CI	n	Mean	95% CI
18-44	420	4.3	4.2 - 4.4	637	4.4	4.2 - 4.5	1057	4.3	4.2-4.4
45-69	622	5.3	5.1 - 5.6	860	5.5	5.2 - 5.8	1482	5.4	5.2-5.6
18-69	1042	4.6	4.5 - 4.7	1497	4.7	4.5 - 4.8	2539	4.6	4.5-4.7

The overall age-sex standardized population-based prevalence of IFG (prediabetes) in 2542 participants was 3.7% (95% CI: 2.7% - 4.6%). The IFG prevalence was higher in men than women, 4.0% (95% CI: 2.4% - 5.7%) vs 3.3% (95% CI: 2.3% - 4.2%), (Table 5).

Table 5.
Prevalence of IFG: Kosovo STEPS survey 2019

Age Group (years)	Men			Women			Both Sexes		
	n	%	95% CI	n	%	95% CI	n	%	95% CI
18-44	420	2.6	0.4 - 4.7	637	1.8	0.8-2.7	1057	2.2	0.9-3.4
45-69	622	7.9	6.5 -10.1	863	7.1	5.2-8.9	1485	7.5	6.0-8.9
18-69	1042	4.0	2.4 - 5.7	1500	3.3	2.3-4.2	2542	3.7	2.7-4.6

In both men and women participants, the prevalence of raised FBG or currently on medication for DM was 4.3% (95% CI: 3.3% - 5.4%). Although the prevalence was higher in women than men, 5.1% (95% CI: 3.5 - 6.8%) vs. 3.5% (95% CI: 2.4% - 4.6%), the differences were not statistically significant ($P>0.05$). The prevalence of the raised FBG increased with age (Table 6).

Table 6.**Prevalence of raised FBG or currently on medication for DM.**

Raised blood glucose or currently on medication for diabetes									
Age Group (years)	Men			Women			Both Sexes		
	n	%	95% CI	n	%	95% CI	n	%	95% CI
18-44	420	1.2	0.3-2.1	637	2.2	0.2-4.1	1057	1.7	0.6-2.8
45-69	622	9.5	6.9-12.1	863	12.6	10.1-15.2	1485	11.1	9.1-13.0
18-69	1042	3.5	2.4-4.6	1500	5.1	3.5-6.8	2542	4.3	3.3-5.4

Currently on medication for diabetes									
Age Group (years)	Men			Women			Both Sexes		
	n	%	95% CI	n	%	95% CI	n	%	95% CI
18-44	458	0.2	-0.1-0.5	682	1.3	-0.5-3.0	1040	0.7	-0.2-1.6
45-69	657	7.0	4.7-9.2	898	8.9	6.8-10.9	1555	7.9	6.3-9.5
18-69	1115	2.0	1.4-2.7	1580	3.3	1.8-4.8	2695	2.7	1.8-3.5

Discussion

According to the WHO, one of the significant development challenges of the twenty-first century is the mortality and morbidity caused by NCDs. More than 36 million people die each year due to NCDs worldwide, with 15 million of them dying very young, between the ages of 30 and 70. Most premature deaths result from 4 main NCDs: cardiovascular diseases, cancer, DM, and chronic obstructive pulmonary disease.⁽¹³⁾ The diabetes disease burden is high and rising in every country, fueled by a global increase in obesity and unhealthy lifestyles. According to the most recent estimates, the prevalence of DM was 11.1% in 2019 and is expected to rise to 13% by 2045.⁽¹⁴⁾ Results from 2 STEPS in Kosovo show that we have no significant increase in the prevalence of prediabetes and DM in total. The prevalence of prediabetes in 2011 among those 15-64 years old was 6.0% (95% CI: 4.6% - 7.9%) and 6.1% (95% CI: 5.3% - 7.1%), respectively, and there were no significant changes among 18-69 years in 2019 ($P>0.05$). Also, we have no significant increase in the prevalence of DM in total. The prevalence of DM in 2011 among 15-64 years was 7.7% (95% CI: 6.0% - 9.7%), and 7.9% (95% CI: 6.9% - 9.0%) among 18-69 years in 2019.

We have a 0.2% increase in the prevalence of DM. This increase was attributed to the older age group of adults included in STEPS-2019. Because we compare the prevalence by age groups, we found a significant decrease in DM in the age group 45-64.

The overall age-sex standardized population-based prevalence of prediabetes in 2019 was 3.7% (95% CI: 2.7%-4.6%), higher in men than women [4.0% (95% CI: 2.4% - 5.7%) vs 3.3% (95% CI: 2.3% - 4.2%)]; but the weighted prevalence of DM in 2019 was 4.3% (95% CI: 3.3% - 5.4%), higher in women than men, 5.1% (95% CI: 3.5 - 6.8%) vs 3.5% (95%

CI: 2.4% - 4.6%), $P>0.05$. The prevalence of DM increases with age. The prevalence of DM in Kosovo, according to weighted 2019 data, was lower than the global DM prevalence in adults aged 20-79 years, standardized to 2021: 10.5% (95% CI: 8.3% - 12.0%), 10.8% in men, and 10.2% in women. In our study the higher prevalence of DM was among women. In IDF Diabetes Atlas 2021, it was presented that prevalence increases with age, with the highest prevalence (24.0%) observed at 75-79 years.

Our study also showed an increase in the prevalence of DM with age. By 2030 and 2045, world-age standardized DM prevalence is projected to increase to 13.3% and 13.9% in the Middle East and North Africa region and 5.1% and 5.2% in the African region. The region-stratified DM prevalence is calculated for several countries, displaying the countries with the most diabetic patients in 2019. Kosovo has a DM prevalence like the prevalence in low-income countries.⁽¹⁵⁾

According to the CDC,⁽¹⁶⁾ the age-adjusted prevalence of total DM increased significantly among adults aged 18 and older between 2001 and 2020. Estimates of total DM prevalence ranged from 10.3% in 2001-2004 to 13.2% in 2017-2020.

According to the diabetes registry for 2019, the number of new cases of DM in the Republic of North Macedonia was 5,378, a rate of 259,24/100,000, while the total prevalence was 89,964 cases, a rate of 4336.66/100,000.⁽¹⁷⁾ It is assumed that this figure is much higher. Every year, up to 4000 new cases are investigated in Albania, with a total prevalence of approximately 80,000.⁽¹⁸⁾

As in other European countries, an increase in the prevalence of DM with age resulted in growing morbidity and mortality due to NCDs and, accordingly, increasing financial and social requirements for the national health system. These problems will become more severe if the health systems are not adequately adapted and relevant measures are not taken.

According to gender, the prevalence for both types of DM was the highest among women at over 50%, and the most affected age group for both types of DM was over 60 years old.

The focus of public health in the future will continue to be directed toward scientific research, supervision, development, and implementation of techniques to eliminate or reduce the action of factors harmful to health, as well as laws to preserve and enhance the progress of individual and community health.

NCDs now make up 7 of the world's top 10 causes of death, according to WHO's 2019 Global Health Estimates.⁽¹⁹⁾ This is an increase from 4 of the 10 leading causes in 2000. The new data cover the period from 2000 to 2019, inclusive. These 7 causes accounted for 44% of all deaths or 80% of the top 10. However, all NCDs together accounted for 74% of deaths globally in 2019. Lower-middle-income countries have the most disparate top 10 causes of death: five non-communicable, 4 infectious, and one injury. DM is a rising cause of death in this income group: it has moved from the 15th to the ninth leading cause of death, and the number of deaths from this disease has nearly doubled since 2000.

Conclusion

This research provides reliable evidence regarding the high burden of DM among the adult population in Kosovo. It is urgent to treat this critical burden on the health system. Newly diagnosed cases of DM in people should not be neglected, and early treatment should be offered to avoid complications. The reasons for uncontrolled DM in Kosovo require further research and innovative strategies for addressing this population. The prevention of DM should have a high priority in the development plans of public health in Kosovo to prevent increased economic costs. Effective preventive interventions are required, and healthcare systems must be prepared to detect and manage DM and its complications.

Limitations of the study

There are some limitations to this study. It is a cross-sectional study design that restricts the causality of relationships. However, the study's large sample size makes the results conclusive. Another limitation was that we used capillary blood samples instead of venous blood glucose estimations and measured blood glucose with a glucometer device.^(20,21) However, blood glucose quality-control checks were performed on a regular basis. Furthermore, only FBG levels were used to diagnose DM and prediabetes.

Funding

The STEPs in 2011 was financed by the French Embassy in Kosovo and the National Institute of Public Health of Kosovo (NIPHK) to support the doctoral thesis for Sanije Hoxha-Gashi in Medical School, University of Zagreb, Zagreb, Croatia.

The STEPS survey 2019 was organized by the Ministry of Health, NIPHK, and WHO with the technical assistance of WHO and AQH (Accessible Quality Healthcare).

Acknowledgments

The authors would like to thank the French Embassy in Kosovo for its financial and technical support for STEPS 2011. The authors would also like to thank the WHO in Geneva and the WHO office in Prishtina for their technical and financial support and AQH for their financial support for STEPS 2019.

Ethical considerations

Ethical Approval for STEPS 2011 received from Ethical Committee of Medical Faculty, University of Prishtina, number 4483. For STEPS 2019, the protocol was approved by the Committee on Ethical Issues, Kosovo Doctors Chamber nr. 06/2018. Written informed consent was obtained before participants were enrolled in the study, in accordance with ethical norms [WHO. Standards and operational guidance for ethics review of health-related research with human participants. Guidance document. 29 September 2011].

Competing Interests

The authors declare that they have no competing interests.

References

1. Heald AH, Stedman M, Davies M, Livingston M, Alshames R, Lunt M, Rayman G, Gadsby R. Estimating life years lost to diabetes: outcomes from analysis of National Diabetes Audit and Office of National Statistics data. *Cardiovasc Endocrinol Metab.* 2020 Jun 2;9(4):183-185. doi: 10.1097/XCE.0000000000000210.
2. International Diabetes Federation (IDF). *IDF Diabetes Atlas 2021.* International Diabetes Federation; 2021. Available from: <https://diabetesatlas.org/atlas/tenth-edition/>
3. WHO. *World health statistics 2021: monitoring health for the SDGs, sustainable development goals.* Geneva: World Health Organization; 2021.
4. Fottrell E, Ahmed N, Shaha SK, Jennings H, Kuddus A, Morrison J, Akter K, Nahar B, Nahar T, Haghparast-Bidgoli H, Khan AKA, Costello A, Azad K. Distribution of diabetes, hypertension and non-communicable disease risk factors among adults in rural Bangladesh: a cross-sectional survey. *BMJ Glob Health.* 2018 Nov 12;3(6):e000787. doi: 10.1136/bmjgh-2018-000787.
5. NCD Risk Factor Collaboration (NCD-RisC). *Worldwide trends in diabetes since 1980: a pooled analysis of 751 population-based studies with 4.4 million participants.* *Lancet.* 2016 Apr 9;387(10027):1513-1530. doi: 10.1016/S0140-6736(16)00618-8. Epub 2016 Apr 6. Erratum in: *Lancet.* 2017 Feb 4;389(10068):e2.
6. United Nations. *Resolution adopted by the General Assembly on 20 December 2006. 61/225. World Diabetes Day; 2006.* Available from: https://www.wddj.jp/pdf/UN_Resolution.pdf
7. National Institute of Public Health of Kosovo. Department of Health Statistics. *Health statistics report. Report of survey on risk factors for chronic disease. Prishtina. 2011-2021.*
8. Statistical Office of Kosovo. *Causes of death in Kosovo 2018 and 2019.* Prishtina, December 2020.
9. World Health Organization. *STEPwise approach to NCD risk factor surveillance (STEPS).* (Last accessed 06.01.2022). Available from: <https://www.who.int/teams/noncommunicable-diseases/surveillance/systems-tools/steps>
10. Gashi S. *Prevalence of chronic diseases risk factors and specific health determinants in a transitional country- The case of Kosovo.* School of Medicine, University of Zagreb. Dissertation, Zagreb 2018.
11. WHO STEPs surveillance manual: the WHO STEPwise approach to chronic disease risk factor surveillance. Geneva: World Health Organization. Available from: <https://www.who.int/teams/noncommunicable-diseases/surveillance/systems-tools/steps/manuals>

**Corresponding author: Sanije Hoxha-Gashi, Faculty of Medicine, University of Prishtina "Hasan Prishtina," Prishtina, Kosovo. E-mail: Sanije.Gashi@uni-pr.edu*

12. Epi Info [download and information page]. Atlanta (GA): Centers for Disease Control and Prevention (Available from: <https://www.cdc.gov/epiinfo/index.html>).
 13. World Health Organization. Tackling NCDs: 'best buys' and other recommended interventions for the prevention and control of noncommunicable diseases. World Health Organization; 2017.
 14. Saeedi P, Petersohn I, Salpea P, Malanda B, Karuranga S, Unwin N, Colagiuri S, Guariguata L, Motala AA, Ogurtsova K, Shaw JE, Bright D, Williams R; IDF Diabetes Atlas Committee. Global and regional diabetes prevalence estimates for 2019 and projections for 2030 and 2045: Results from the International Diabetes Federation Diabetes Atlas, 9th edition. *Diabetes Res Clin Pract.* 2019 Nov;157:107843. doi: 10.1016/j.diabres.2019.107843.
 15. Alam S, Hasan MK, Neaz S, Hussain N, Hossain MF, Rahman T. Diabetes Mellitus: insights from epidemiology, biochemistry, risk factors, diagnosis, complications and comprehensive management. *Diabetology.* 2021 Apr 16;2(2):36-50.
 16. Centers for Disease Control and Prevention. National Diabetes Statistics Report website. Available from: <https://www.cdc.gov/diabetes/data/statistics-report/index.html>
 17. Institute for Public Health of the Republic N. Macedonia, Center for statistical processing health data, publication and education, Skopje 2019-2020.
 18. Institute of Public Health, National Report on Non-Communicable Diseases, Mortality, Injury and Risk Factors. Tirana 2019.
 19. World Health Organization. WHO global health estimates: 2000-2019. Available from: <https://www.who.int/news-room/fact-sheets/detail/the-top-10-causes-of-death>
 20. Tirimacco R, Tideman PA, Dunbar J, Simpson PA, Philpot B, Laatikainen T, Janus E. Should capillary blood glucose measurements be used in population surveys? *International Journal of Diabetes Mellitus.* 2010 Apr 1;2(1):24-7.
 21. Carstensen B, Lindström J, Sundvall J, Borch-Johnsen K, Tuomilehto J; DPS Study Group. Measurement of blood glucose: comparison between different types of specimens. *Ann Clin Biochem.* 2008 Mar;45(Pt 2):140-8.
-

Pro- and Anti-Inflammatory Blood Cytokines Levels in Women with Moderate and Severe Pelvic Venous Insufficiency

Marina A. Darenskaya^{1*}, Andrey A. Semendyaev², Dmitriy A. Stupin^{1,2}, Sergey I. Kolesnikov¹, Natalya V. Semenova¹, Konstantin V. Pesterev², Lyubov I. Kolesnikova¹

¹Scientific Centre for Family Health and Human Reproduction Problems, Irkutsk, the Russian Federation

²Irkutsk State Medical University, Irkutsk, the Russian Federation

Abstract

The aim of this study was to determine the blood levels of pro- and anti-inflammatory cytokines in patients with moderate and severe pelvic venous insufficiency (PVI).

Methods and Results: One hundred and four women with PVI and 30 healthy women (control group [CG]) of reproductive age were examined. The patients with PVI (main group [MG]) were divided into 2 subgroups according to the severity of the disease: MG-moderate (n=63) and MG-severe (n=41). The concentration of pro-inflammatory cytokines (IL-1 β , IL-2, IL-6, IL-8), and anti-inflammatory interleukins IL-4 and IL-10 were assessed by enzyme immunoassay using monoclonal antibody panels. Measurements were performed on a microplate photometer. Data analysis showed higher values of pro-inflammatory factors (IL-1 β , IL-6, and IL-8) in the MG-moderate than in the CG. The MG-severe, compared with the CG, had high levels of IL-1 β , IL-2, IL-6, IL-8, and low IL-10 concentration. In addition, patients of the MG-severe had higher levels of IL-2 than patients of the MG-moderate ($P=0.045$). The IL-6/IL-10 ratio was characterized by higher values in the MG-moderate and MG-severe than in the CG ($P<0.0001$). The patients of the MG-severe also had higher levels of the IL-6/IL-10 ratio than patients of the MG-moderate ($P=0.020$).

Conclusion: In patients with PVI with increasing severity of varicose veins, the pro- and anti-inflammatory cytokine balance is progressively disturbed toward the dominance of pro-inflammatory components. The control of these changes in patients is an important component of the design of therapeutic measures and prevention of morphofunctional disorders occurring with the progression of the disease. (**International Journal of Biomedicine. 2023;13(1):54-57.**)

Keywords: pelvic venous insufficiency • women • cytokines

For citation: Darenskaya MA, Semendyaev AA, Stupin DA, Kolesnikov SI, Semenova NV, Pesterev KV, Kolesnikova LI. Pro- and Anti-Inflammatory Blood Cytokines Levels in Women with Moderate and Severe Pelvic Venous Insufficiency. International Journal of Biomedicine. 2023;13(1):54-57. doi:10.21103/Article13(1)_OA5

Abbreviations

AP-1, activating protein-1; HIF, hypoxia-inducible factor 1; IL, interleukins; MCP, monocyte chemoattractant protein-1; NADPH, nicotinamide adenine dinucleotide phosphate; NF- κ B, nuclear factor kappa-light-chain-enhancer of activated B cells; PVI, pelvic venous insufficiency; TGF- β , Transforming growth factor beta; VCAM-1, vascular cell adhesion molecule 1.

Introduction

Pelvic venous insufficiency (PVI) in women is characterized by a high prevalence (25%-60% of cases), the risk of reproductive disorders (15%-25%), and the ineffectiveness of

treatment measures (recurrence in 5%-100%).^(1,2) Diagnosis of primary PVI in women is complicated due to the lack of specific clinical symptoms and laboratory criteria typical of the initial manifestations of the pathological process.^(3,4) Even severe forms of the disease can be characterized by an asymptomatic course or the presence of “acute abdomen” syndrome.⁽⁴⁾ The clinical manifestations of this pathological condition include the following: the presence of chronic pelvic pain, dyspareunia, cyclic and acyclic bleeding, infertility, and other symptoms.⁽⁵⁻⁷⁾ The disease onset is characterized by venous hypertension,

*Corresponding author: Prof. Marina A. Darenskaya, PhD, ScD. Scientific Centre for Family Health and Human Reproduction Problems, Irkutsk, the Russian Federation. E-mail: marina_darenskaya@inbox.ru

venous insufficiency valve, retrograde blood flow through the ovarian veins, and venous-venous discharge of the gonadal vein pool.^(2,8) The formation of venous insufficiency is associated with regional hemodynamic disorders, excessive formation of cellular metabolic products, and inflammatory phenomena in the venous wall.^(4,9,10,11) An important component of inflammatory reactions in this pathology is the insufficiency of the immune system.^(2,12,13) Immunological dysfunction can promote varicose vein transformation and ultimately determine the course of the disease. Evaluation of immune reactivity changes in patients with PVI at different stages of the disease is relevant.

In this regard, the aim of our work was to determine the blood levels of pro- and anti-inflammatory cytokines in patients with moderate and severe PVI.

Materials and Methods

Design of study

One hundred and four women with PVI and 30 healthy women (control group [CG]) of reproductive age were examined. The patients with PVI (main group [MG]) were divided into 2 subgroups according to the severity of the disease: MG-moderate (n=63) and MG-severe (n=41).

Common criteria for inclusion in the MG and CG: reproductive age (20-45 years), signed informed consent. Main criteria for inclusion in the MG: a confirmed diagnosis of primary PVI based on the results of ultrasound examination with duplex angioscanning; exclusion criteria: the presence of concomitant somatic pathology, gynecological diseases, and organic lesions in the pelvis. Main criteria for inclusion in the CG are the absence of acute, or exacerbation of, chronic diseases and the absence of pathological changes in the venous system. Common exclusion criteria for both groups: pregnancy and intake of venotonic, angioprotective antioxidant drugs or synthetic analogs of female sex hormones (hormonal contraceptives) during the last 6 months

Biochemical measurements

The concentration of pro-inflammatory cytokines (IL-1 β , IL-2, IL-6, IL-8), and anti-inflammatory interleukins IL-4 and IL-10 were assessed by enzyme immunoassay using monoclonal antibody panels (JSC "Vector-Best", Novosibirsk, Russia). Measurements were performed on a microplate photometer (MultiskanAscent, Finland). The IL-6/IL-10 ratio, reflecting the balance of pro- and anti-inflammatory cytokines, was also calculated.

Statistical analysis was performed using STATISTICA 10.0 software package (Stat-Soft Inc, USA). The normality of distribution of continuous variables was tested by the Kolmogorov-Smirnov test with the Lilliefors correction and Shapiro-Wilk test. The F-test for equality of two variances was applied. For descriptive analysis, results are presented as median (Me), interquartile range (IQR; 25th to 75th percentiles). Differences of continuous variables departing from the normal distribution, even after transformation, were tested by the Mann-Whitney U-test. A probability value of $P < 0.05$ was considered statistically significant.

The study was conducted in accordance with ethical principles of the WMA Declaration of Helsinki (1964, ed.

2013) and approved by the Ethics Committee at the Scientific Centre for Family Health and Human Reproduction Problems (Irkutsk, Russia). Written informed consent was obtained from all participants.

Results and Discussion

Data analysis showed higher values of pro-inflammatory factors (IL-1 β , IL-6, and IL-8) in the MG-moderate than in the CG (Table 1). The MG-severe, compared with the CG, had high levels of IL-1 β , IL-2, IL-6, IL-8, and low IL-10 concentration (Table 1). In addition, patients of the MG-severe had higher levels of IL-2 than patients of the MG-moderate ($P=0.045$). The IL-6/IL-10 ratio was characterized by higher values in the MG-moderate and MG-severe than in the CG ($P < 0.0001$) (Fig. 1). The patients of the MG-severe also had higher levels of the IL-6/IL-10 ratio than patients of the MG-moderate ($P=0.020$) (Fig. 1).

Table 1.

Pro- and anti-inflammatory cytokines levels (pg/ml) in female patients with moderate and severe PVI.

Parameters	CG (n=30) (1)	MG-moderate (n=63) (2)	MG-severe (n=41) (3)	P-value
IL-1 β	124.70 (113.88;131.15)	157.00 (149.26;166.20)	168.00 (151.34;175.91)	1-2 (0.040) 1-3 (0.032) 2-3 (>0.05)
IL-2	39.63 (33.25;45.74)	47.78 (42.13;58.45)	59.80 (53.42;68.62)	1-3 (0.039) 2-3 (0.045) 1-2 (>0.05)
IL-6	2241 (3147;3380)	5358 (5249;5541)	5574 (5495;5780)	1-2 (<0.001) 1-3 (0.009) 2-3 (>0.05)
IL-8	1151 (1075;1217)	2417 (2210;2726)	3792 (3561;4053)	1-2 (0.034) 1-3 (0.011) 2-3 (>0.05)
IL-4	793.76 (762.58;825.38)	789.57 (750.63;831.42)	751.44 (738.16;788.29)	1-2 (>0.05) 1-3 (>0.05) 2-3 (>0.05)
IL-10	1145.72 (1067.43;1271.58)	762.19 (735.17;801.94)	522.43 (475.26;560.81)	1-3 (0.037) 1-2 (>0.05) 2-3 (>0.05)

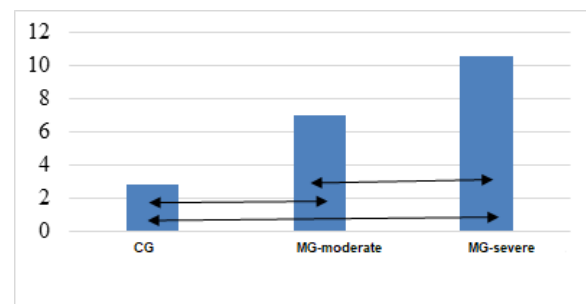


Fig. 1. Values of the IL-6/IL-10 ratio in the groups

↔ (statistically significant differences).

The findings indicated a pronounced imbalance of pro- and anti-inflammatory factors in patients with increasing degrees of PVI. Thus, the moderate form was characterized by increased values of IL-1 β , IL-6, and IL-8, compared to controls.

It was established that the pathological changes in pelvic veins in women are induced by the presence of congestive venous hemodynamics arising due to disturbances of venous outflow.⁽¹³⁾ Reduced laminar flow velocity and blood stasis reduce tangential tension and contribute to overstretching of the vascular wall.⁽⁴⁾ These changes, as well as associated hypoxia, can trigger a cascade of biochemical processes contributing to variceal transformation.⁽¹⁴⁻¹⁶⁾ It is difficult to find the initiating event in the chain of events since the vein wall may already be altered by the time of clinical manifestations. Undoubtedly, the decisive influence is exerted by the combined effect of external provoking factors and genetic features, which, over time, lead to a condition in which hemodynamic disorders are already chronic.^(1,3,4)

Thus, it was found that in response to chronic vascular wall deformation, there is an induction of expression of a wide range of genes responsible for cell proliferation, apoptosis, and migration, regulation of vascular tone, degradation and reorganization of extracellular matrix, inflammation, angiogenesis, and other processes.^(2,17) The induction pathways include activating the NADPH-oxidase enzyme complex on the membranes of endothelial and smooth muscle cells. This leads to the generation of reactive oxygen species, which are also inducers of intracellular signal transduction pathways.⁽¹⁸⁾ The developing hypoxia activates specific transcription factors.

These events trigger the work of the key transcription factors AP-1, HIF-1 α , HIF-2 α , NF- κ B, which control dozens of genes.⁽¹⁹⁾ In particular, such genes include genes of matrix metalloproteinases responsible for proteolysis of extracellular matrix components, as well as genes of pro-inflammatory cytokines and chemokines, that stimulate the proliferation and differentiation of B- and T-lymphocytes (IL-6 and IL-12) and attract monocytes/macrophages, neutrophils, eosinophils, basophils and lymphocytes (IL-8 and MCP-1) to the inflammation focus.⁽²⁰⁾ The accession of the inflammatory process can aggravate venous wall damage due to leukocytic aggression, which leads to the progression of venous framework integrity disorders.⁽¹²⁾

Cytokines, low-mass proteins synthesized mainly by leukocytes, as well as by mononuclear phagocytes and other tissue cells in picomolar and nanomolar concentrations, are also actively involved in this process.⁽²¹⁾ Pro-inflammatory cytokines are produced predominantly by activated macrophages and are involved in enhancing inflammatory reactions.⁽²⁰⁾ In our study, further aggravation of the pathological process (severe form of the PVI) was characterized by more pronounced manifestations of cytokine imbalance. In this case, we noted a greater involvement of pro-inflammatory factors (IL-1 β , IL-2, IL-6, IL-8), as well as a decreased concentration of the anti-inflammatory component—IL-10. In this case, we can suggest a cytokine-pronounced damaging effect on the veins. Pro-inflammatory cytokines, as well as adhesion molecules, especially TGF- β , IL-6, IL-8, and VCAM-1 are the cause of

venous valve insufficiency, which has been shown in several studies.^(12,22-24)

High levels of IL-6/IL-10 ratio with increasing severity of PVI should also be noted. This ratio characterizes the prevalence of pro-inflammatory reactions in the body over anti-inflammatory ones at the systemic level. It is assumed that high cytokine activity mediates impaired regulation of extracellular matrix degradation processes, modification of its components (collagen and elastin), and reduction of smooth muscle cells, which aggravates the pathological process.^(25,26)

Conclusion

Thus, in patients with PVI with increasing severity of varicose veins, the pro- and anti-inflammatory cytokine balance is progressively disturbed toward the dominance of pro-inflammatory components. The control of these changes in patients is an important component of the design of therapeutic measures and prevention of morphofunctional disorders occurring with the progression of the disease.

This work was performed with the use of equipment of the Collective Research Center "Centre for the development of progressive personalized health technologies" SC FHHRP, Irkutsk.

Competing Interests

The authors declare that they have no competing interests.

References

1. Riding DM, Hansrani V, McCollum C. Pelvic vein incompetence: clinical perspectives. *Vasc Health Risk Manag.* 2017 Nov 27;13:439-447. doi: 10.2147/VHRM.S132827.
2. Khilnani NM, Meissner MH, Learman LA, Gibson KD, Daniels JP, Winokur RS, Marvel RP, Machan L, Venbrux AC, Tu FF, Pabon-Ramos WM, Nedza SM, White SB, Rosenblatt M. Research Priorities in Pelvic Venous Disorders in Women: Recommendations from a Multidisciplinary Research Consensus Panel. *J Vasc Interv Radiol.* 2019 Jun;30(6):781-789. doi: 10.1016/j.jvir.2018.10.008.
3. Khatri G, Khan A, Raval G, Chhabra A. Diagnostic Evaluation of Chronic Pelvic Pain. *Phys Med Rehabil Clin N Am.* 2017 Aug;28(3):477-500. doi: 10.1016/j.pmr.2017.03.004.
4. Barge TF, Uberoi R. Symptomatic pelvic venous insufficiency: a review of the current controversies in pathophysiology, diagnosis, and management. *Clin Radiol.* 2022 Jun;77(6):409-417. doi: 10.1016/j.crad.2022.01.053.
5. Daniels JP, Champaneria R, Shah L, Gupta JK, Birch J, Moss JG. Effectiveness of Embolization or Sclerotherapy of Pelvic Veins for Reducing Chronic Pelvic Pain: A Systematic Review. *Journal of Vascular Surgery: Venous and Lymphatic Disorders.* 2017;5(1):144. doi:10.1016/j.jvsv.2016.10.007
6. Gus AI, Khamoshina MB, Cherepanova MA, Bachurina SM, Semendyaev AA, Stupin DA. Diagnosis and treatment

- of varicose veins of the small pelvis in women. Novosibirsk: Nauka; 2014;136. [In Russian].
7. Gus AI, Kolesnikova LI, Semendyaev AA, Stupin DA, Shcherbatykh AV, Kalyagin AN, et al. [Optimizing management strategy in women with pelvic varicose veins]. *Obstetrics and Gynecology*. 2019;4:58-64. doi: 10.18565/aig.2019.4.58-64. [Article in Russian].
8. Bendek B, Afuape N, Banks E, Desai NA. Comprehensive review of pelvic congestion syndrome: causes, symptoms, treatment options. *Curr Opin Obstet Gynecol*. 2020 Aug;32(4):237-242. doi: 10.1097/GCO.0000000000000637.
9. Kolesnikova LI, Semendyaev AA, Stupin DA, Darenskaya MA, Grebenkina LA, Natyaganova LV, et al. [The Intensity of Lipid Peroxidation Processes in Women with Primary Varicose Veins of the Pelvic Depending on the Stage of the Disease]. *Annals of the Russian Academy of Medical Sciences*. 2018;73(4):229-235. doi: 10.15690/vramn1005. [Article in Russian].
10. Darenskaya MA, Stupin DA, Semendyaev AA, Kolesnikov SI, Shcherbatykh AV, Tolkachev KS, Kolesnikova LI. Pelvic venous insufficiency: lipid peroxidation levels in ovarian venous blood. *Biomedical Research and Therapy*. 2022;9(2):4884-48913 doi: 10.15419/bmrat.v9i2.730
11. Darenskaya MA, Stupin DA, Semendyaev AA, Kolesnikov SI, Grebenkina LA, Shcherbatykh AV, et al. [Peripheral and regional blood bloodstreams lipid peroxidation comparative analysis in women with pelvic venous disorder]. *Klinicheskaya Laboratornaya Diagnostika (Russian Clinical Laboratory Diagnostics)*. 2022;67(7):374-380 (in Russ.). doi: 10.51620/0869-2084-2022-67-7-374-380. [Article in Russian].
12. Golovina VI, Seliverstov EI, Efremova OI, Zolotukhin IA. [Cytokines in Pathogenesis of Varicose Veins]. *Flebologiya*. 2021;15(2):117-126. doi: 10.17116/flebo202115021117. [Article in Russian].
13. Balabuszek K, Toborek M, Pietura R. Comprehensive overview of the venous disorder known as pelvic congestion syndrome. *Ann Med*. 2022 Dec;54(1):22-36. doi: 10.1080/07853890.2021.2014556.
14. Kolesnikova LI, Semendyaev AA, Stupin DA, Darenskaya MA, Grebenkina LA, Natyaganova LV, et al. On the opportunities of using the indices of lipid peroxidation - antioxidant defense system in the diagnostics of varicose veins of small pelvis in women. *Acta Biomedica Scientifica (East Siberian Biomedical Journal)*. 2020;5(1):14-20. DOI: 10.29413/ABS.2020-5.1.2. [Article in Russian].
15. Kolesnikova LI, Kolesnikov SI, Darenskaya MA, Grebenkina LA, Nikitina OA, Lazareva LM, Suturina LV, Danusevich IN, Druzhinina EB, Semendyaev AA. Activity of LPO Processes in Women with Polycystic Ovarian Syndrome and Infertility. *Bull Exp Biol Med*. 2017 Jan;162(3):320-322. doi: 10.1007/s10517-017-3605-5.
16. Kolesnikova LI, Gus AI, Taranenko AV, Semendyaev AA, Stupin DA, Shcherbatykh AV, et al. [Informativeness of estimating cd34 expression in the development of pelvic varicose veins in women]. *Obstetrics and Gynecology*. 2019;2:120-125. doi: 10.18565/aig.2019.2.120-125. [Article in Russian].
17. Szary C, Wilczko J, Zawadzki M, Grzela T. Hemodynamic and Radiological Classification of Ovarian Veins System Insufficiency. *J Clin Med*. 2021 Feb 8;10(4):646. doi: 10.3390/jcm10040646.
18. Riding DM, Hansrani V, McCollum C. Pelvic vein incompetence: clinical perspectives. *Vasc Health Risk Manag*. 2017 Nov 27;13:439-447. doi: 10.2147/VHRM.S132827.
19. Seryapina YUV, Sevost'Yanova KS, Tulupov AA, Morozov VV, Shevela AI. [The genetic predictors of varicose veins of small pelvis: a pilot study]. *Flebologiya*. 2018;12(1):25-29. doi: 10.17116/flebo201812125-29. [Article in Russian].
20. Spath P, Tisato V, Gianesini S, Tessari M, Menegatti E, Manfredini R, Occhionorelli S, Secchiero P, Zamboni P. The calendar of cytokines: Seasonal variation of circulating cytokines in chronic venous insufficiency. *JRSM Cardiovasc Dis*. 2017 Sep 8;6:2048004017729279. doi: 10.1177/2048004017729279.
21. Sayer GL, Smith PD. Immunocytochemical characterisation of the inflammatory cell infiltrate of varicose veins. *Eur J Vasc Endovasc Surg*. 2004 Nov;28(5):479-83. doi: 10.1016/j.ejvs.2004.07.023.
22. Danusevich IN, Lazareva LM, Nemchenko UM. [Characteristics of the main links of immunity and endometrial cytokines in women with reproductive disorders]. *Yakut Medical Journal*. 2022;1(77):79-83. doi: 10.25789/YMJ.2022.77.20. [Article in Russian].
23. Danusevich IN, Lazareva LM, Nemchenko UM, Kolesnikova LI. Endometrial cytokines in women with reproductive disorders. *International Journal of Biomedicine*. 2021;11(4):526-531. doi: 10.21103/Article11(4)_OA20
24. Darenskaya MA, Semendyaev AA, Stupin DA, Grebenkina LA, Danusevich IN, Kolesnikova LI, Kolesnikov SI. Activity of Antioxidant Enzymes in the Regional Blood Flow during Pelvic Venous Disorders in Women. *Bull Exp Biol Med*. 2020 Oct;169(6):747-750. doi: 10.1007/s10517-020-04970-y.
25. Golovina VI, Seliverstov EI, Efremova OI, Zolotukhin IA. [The role of cytokines in the pathogenesis of varicose veins]. *Phlebology*. 2021;15(2):117-126. doi: 10.17116/flebo202115021117. [Article in Russian].
26. Karzakova LM, Kudryashov SI, Lutkova TS, Sokolova EV, Sidorov IA. *Fundamentals of General Immunology: Tutorial*. Cheboksary: Chuvash Univ Publishing, 2020;200. [In Russian].

Impact of Cigarette Smoking on Serum Cystatin C and Creatinine Levels and MAU: A Case-Control Study

Nizar M. Farah¹, Anass M. Abbas^{2*}, Ayman Ali Mohammed Alameen², Manar G. Shalabi², Abozer Y. Elderderly², Lienda Basheir Eltayeb³, Asaad Ma. Babker⁴, Hatem Mohamed⁵, Abdullah I Aedh⁶

¹Department of Hematology, Faculty of Medical Laboratory Sciences, Al Neelain University, Sudan

²Department of Clinical Laboratory Sciences, College of Applied Medical Sciences, Jouf University, KSA

³Department of Medical Laboratory Sciences, College of Applied Medical Sciences, Prince Sattam Bin Abdulaziz University, Alkharj, 11942, Saudi Arabia

⁴Department of Medical Laboratory Sciences, College of Health Sciences, Gulf Medical University, Ajman, UAE

⁵Department of Medical Education, College of Medicine, Najran University, Najran, Saudi Arabia

⁶Najran University Hospital, Najran University, Najran, Saudi Arabia

Abstract

Background: Smoking-related hemodynamic events may adversely influence renal function. The aim of this study was to evaluate renal impairment biomarkers among healthy people influenced by cigarette smoke.

Methods and Results: In this case-control study, 90 subjects were enrolled: 60 were smokers, and 30 were non-smokers (apparently healthy control). Serum CysC was measured using a semi-automated, specific protein analyzer Mispai-2 (Germany). Serum creatinine and MAU were assayed in the fully automated biochemistry analyzer (Mindray BS380). The mean concentration of CysC was significantly higher in cigarette smokers than in non-smokers (0.793 ± 0.125 vs. 0.619 ± 0.103 , $P=0.000$). Also, the mean of MAU and serum creatinine levels were significantly higher in cigarette smokers than in non-smokers (18.33 ± 3.41 vs. 12.70 ± 0.517 , 1.06 ± 0.161 vs. 0.810 ± 0.058 , respectively, $P=0.000$ in both cases). The mean concentration of CysC and MAU was significantly greater in heavy smokers than in light smokers ($P=0.000$ and $P=0.001$, respectively). Serum CysC and MAU levels were positively correlated with the age of cigarette smokers ($r=0.734$ and $r=0.730$, respectively; $P=0.000$ in both cases) and the duration of smoking ($r=0.773$ and $r=0.790$, respectively; $P=0.000$ in both cases).

Conclusion: cigarette smoking increases the specific renal biomarkers considered risk factors for renal impairment. Using such inflammatory biomarkers as diagnostic tools can be a necessary precaution in the development of chronic kidney disease caused by smoking and in the avoidance of acute renal consequences linked to cigarette smoking. (*International Journal of Biomedicine*. 2023;13(1):58-61.)

Keywords: cigarette smoking • inflammatory biomarkers • chronic kidney disease

For citation: Farah NM, Abbas AM, Alameen AAM, Shalabi MG, Elderderly AY, Eltayeb LB, Babker AM, Mohamed H, Aedh AI. Impact of Cigarette Smoking on Serum Cystatin C and Creatinine Levels and MAU: A Case-Control Study. *International Journal of Biomedicine*. 2023;13(1):58-61. doi:10.21103/Article13(1)_OA6

Abbreviations

CKD, chronic kidney disease; CysC, cystatin C; ESRD, end-stage renal disease; MAU, microalbuminuria.

Introduction

The fight against cigarette smoking is a global challenge. Worldwide, 1.2 billion people smoked in 2000, a number that is projected to increase to 1.6 billion by 2030.⁽¹⁾ The 21st century is likely to see 1 billion tobacco deaths, most of them in low-income countries.⁽²⁾ Chronic cigarette consumption is harmful in both active and passive smokers. It has a role in the initiation and progression of chronic kidney disease (CKD), type 2 diabetes mellitus, diabetic nephropathy, and cardiovascular complications of diabetes mellitus. It is also evident that chronic kidney failure raises the risk of cardiovascular morbidity and mortality; thus, tobacco use can be considered as a factor that induces or aggravates processes that diminish life quality or even shorten life expectancy. Noteworthy is the human “memory for smoking”, namely, the harmful effects of tobacco consumption do not last only until the cessation of cigarette smoking but even for many years.⁽¹⁾

A recent preliminary report suggests that smoking-related hemodynamic events may have an acute influence on renal function⁽³⁾ and be a risk factor for the development and progression of CKD in the community,⁽⁴⁾ which is a risk factor for end-stage renal disease (ESRD).⁽⁵⁾ Regarding the adverse effect of smoking on renal biomarkers, many studies suggest a higher prevalence of microalbuminuria in smokers compared to non-smokers and raise the possibility of renal glomerular injury.⁽⁶⁾ Microalbuminuria (MAU) (urinary albumin excretion of 30-300 mg/day) is an early sign of renal damage. It is demonstrated that renal risk is elevated even in the high normal range of MAU<30 mg/day.⁽⁷⁾

Cystatin C (CysC) is a basic protein with a molecular weight of 13 kDa and is a member of the cysteine protease inhibitor family that is measurable in body fluids. The glomerulus completely filters it, and its concentration is closely correlated with the glomerular filtration rate. Serum CysC levels are less affected by biological factors and rise 1–2 days earlier than creatinine in the setting of acute kidney injury. Therefore, CysC can be used as an alternative renal biomarker to creatinine because it is filtered in the glomeruli and is reabsorbed in the proximal tubule, where it is completely catabolized.^(8,9) Serum creatinine level is commonly used to estimate renal function.⁽¹⁰⁾

The aim of this study was to evaluate renal impairment biomarkers among healthy people influenced by cigarette smoke.

Materials and Methods

In this case-control study, 90 subjects were enrolled: 60 were smokers, and 30 were non-smokers (apparently healthy control). All subjects were referred to Elriada Specialized Center in Khartoum state from June to December 2020. Exclusion criteria were diabetes mellitus, hypertension, obesity, alcoholism, and diagnosed diseases.

Serum CysC was measured using a semi-automated, specific protein analyzer Mispai-2 (Germany). Serum creatinine and MAU were assayed in the fully automated biochemistry analyzer (Mindray BS380).

Statistical analysis was performed using statistical software package SPSS version 21.0 (Armonk, NY: IBM Corp.). For descriptive analysis, results are presented as mean (M) ± standard deviation (SD). Inter-group comparisons were performed using Student’s t-test. Pearson’s Correlation Coefficient (r) was used to determine the strength of the relationship between the two continuous variables. A probability value of $P<0.05$ was considered statistically significant.

This study was approved by the Ethical Committee of the Al-Neelain University (Sudan). All participants provided written informed consent.

Results

The mean concentration of CysC was significantly higher in cigarette smokers than in non-smokers (0.793 ± 0.125 mg/L vs. 0.619 ± 0.103 mg/L, $P=0.000$). Also, the mean of MAU and serum creatinine levels were significantly higher in cigarette smokers than in non-smokers (18.33 ± 3.41 mg/L vs. 12.70 ± 0.517 mg/L, 1.06 ± 0.161 mg/dL vs. 0.810 ± 0.058 mg/dL, respectively, $P=0.000$ in both cases) (Table 1).

Table 1.

Mean concentrations of CysC, MAU and serum creatinine among cigarette smokers and non-smokers

Parameters	Smokers	Non-smokers	P-value
CysC, mg/L	0.793±0.125	0.619±0.103	0.000
MAU, mg/L	18.33±3.41	12.70±0.517	0.000
Creatinine, mg/dL	1.06±0.161	0.810±0.058	0.000

The mean concentration of CysC and MAU was significantly greater in heavy smokers than in light smokers ($P=0.000$ and $P=0.001$, respectively) (Table 2).

Table 2.

Mean concentrations of CysC, MAU and serum creatinine among light and heavy smokers

Parameters	Light smokers	Heavy smokers	P-value
CysC, mg/L	0.715±0.12	0.848±0.10	0.000
MAU, mg/L	16.71±2.51	19.49±3.51	0.001
Creatinine, mg/dL	1.06±0.19	1.06±0.14	0.883

In addition, serum CysC and MAU levels were positively correlated with the age of cigarette smokers ($r=0.734$ and $r=0.730$, respectively; $P=0.000$ in both cases) (Figures 1 and 2) and the duration of smoking ($r=0.773$ and $r=0.790$, respectively; $P=0.000$ in both cases) (Figures 3 and 4).

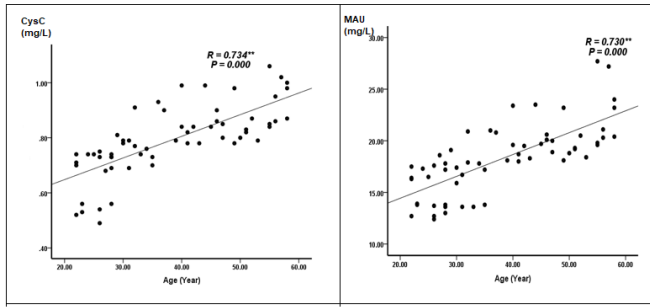


Fig 1. Correlation between CysC and age.

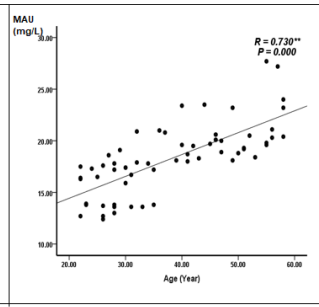


Fig. 2. Correlation between MAU and age.

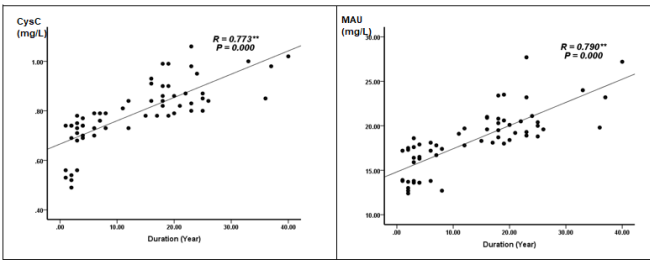


Fig. 3. Correlation between CysC and duration of smoking.

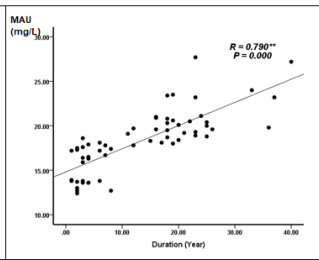


Fig. 4. Correlation between MAU and duration of smoking.

Discussion

In our study, the mean concentrations of CysC, MAU, and serum creatinine levels were significantly higher in cigarette smokers than in non-smokers ($P=0.000$ in all cases). Also, serum CysC and MAU levels were positively correlated with the age of cigarette smokers and the duration of smoking ($P=0.000$ in both cases). Many previous research studies showed similar findings in creatinine level and MAU.⁽¹¹⁻¹⁴⁾ In a study by Pinto-Sietsma et al.,⁽¹⁴⁾ after adjustment for several potential confounding factors, persons who smoked 20 or fewer cigarettes/d and persons who smoked more than 20 cigarettes/d, respectively, showed a dose-dependent association between smoking and MAU (relative risk, 1.92 [CI 95%: 1.54-2.39] and 2.15 [CI 95%: 1.52-3.03]). In a study by Yoon,⁽¹⁵⁾ current smoking was associated with a higher risk of proteinuria (urine dipstick for albuminuria $\geq 1+$) than non-smoking (odds ratio=1.380, $P<0.001$). Gupta et al.⁽¹⁶⁾ showed that among 80 smokers, 73(91.25%) had MAU >20 mg/L, and MAU level was directly related to the amount of smoking (pack-years). Similar data were obtained in a study by Abdallah et al.⁽¹⁷⁾ Yamada et al.⁽¹⁸⁾ showed that serum CysC was higher in smokers and obese subjects. In contrast, serum creatinine was lower in smokers and slender subjects.

Conclusion

Cigarette smoking increases the specific renal biomarkers considered risk factors for renal impairment. Using such inflammatory biomarkers as diagnostic tools can be a necessary precaution in the development of chronic

kidney disease caused by smoking and in the avoidance of acute renal consequences linked to cigarette smoking.

Competing Interests

The authors declare that they have no competing interests.

References

1. Halmi R. Role of Cigarette Smoke in Chronic Kidney Disease. University of Pécs, Faculty of Medicine, 2nd Department of Internal Medicine, Pécs, Hungary, 2013. Available from: https://aok.pte.hu/docs/phd/file/dolgozatok/2013/Halmi_Richard_PhD_dolgozat.pdf
2. Jha P, Chaloupka FJ, Moore J, Gajalakshmi V, Gupta PC, Peck R, et al., editors. In: Disease Control Priorities in Developing Countries. 2nd edition. Washington (DC): The International Bank for Reconstruction and Development. The World Bank; 2006. Chapter 46.
3. Gambaro G, Verlato F, Budakovic A, Casara D, Saladini G, Del Prete D, Bertaglia G, Masiero M, Checchetto S, Baggio B. Renal impairment in chronic cigarette smokers. *J Am Soc Nephrol.* 1998 Apr;9(4):562-7. doi: 10.1681/ASN.V94562.
4. Yacoub R, Habib H, Lahdo A, Al Ali R, Varjabedian L, Atalla G, Kassis Akl N, Aldakheel S, Alahdab S, Albitar S. Association between smoking and chronic kidney disease: a case control study. *BMC Public Health.* 2010 Nov 25;10:731. doi: 10.1186/1471-2458-10-731.
5. Orth SR, Hallan SI. Smoking: a risk factor for progression of chronic kidney disease and for cardiovascular morbidity and mortality in renal patients--absence of evidence or evidence of absence? *Clin J Am Soc Nephrol.* 2008 Jan;3(1):226-36. doi: 10.2215/CJN.03740907.
6. Hammer Y, Cohen E, Levi A, Krause I. The Relationship between Cigarette Smoking and Renal Function: A Large Cohort Study. *Isr Med Assoc J.* 2016 Sep;18(9):553-556.
7. Koroshi A. Microalbuminuria, is it so important? *Hippokratia.* 2007 Jul;11(3):105-7.
8. Lassus J, Harjola VP. Cystatin C: a step forward in assessing kidney function and cardiovascular risk. *Heart Fail Rev.* 2012 Mar;17(2):251-61. doi: 10.1007/s10741-011-9242-6.
9. Andersen TB, Jødal L, Erlandsen EJ, Morsing A, Frøkiær J, Brøchner-Mortensen J. Detecting reduced renal function in children: comparison of GFR-models and serum markers. *Pediatr Nephrol.* 2013 Jan;28(1):83-92. doi: 10.1007/s00467-012-2268-8.
10. Knight EL, Verhave JC, Spiegelman D, Hillege HL, de Zeeuw D, Curhan GC, de Jong PE. Factors influencing serum cystatin C levels other than renal function and the impact on renal function measurement. *Kidney Int.* 2004 Apr;65(4):1416-21. doi: 10.1111/j.1523-1755.2004.00517.x.

*Corresponding author: Anass M. Abbas. Department of Clinical Laboratory Sciences, College of Applied Medical Sciences, Jouf University, KSA. E-mail: anasseen@hotmail.com

11. Ahmed MME, Sabah AO, Aziz Jawad A. The effect of smoking cigarette on kidney functions among Sudanese peoples. *International Journal of Development Research*. 2015;5(5):4473-4475.
 12. Ishizaka N, Ishizaka Y, Toda E, Shimomura H, Koike K, Seki G, Nagai R, Yamakado M. Association between cigarette smoking and chronic kidney disease in Japanese men. *Hypertens Res*. 2008 Mar;31(3):485-92. doi: 10.1291/hypres.31.485.
 13. Halimi JM, Giraudeau B, Vol S, Cacès E, Nivet H, Lebranchu Y, Tichet J. Effects of current smoking and smoking discontinuation on renal function and proteinuria in the general population. *Kidney Int*. 2000 Sep;58(3):1285-92. doi: 10.1046/j.1523-1755.2000.00284.x.
 14. Pinto-Sietsma SJ, Mulder J, Janssen WM, Hillege HL, de Zeeuw D, de Jong PE. Smoking is related to albuminuria and abnormal renal function in nondiabetic persons. *Ann Intern Med*. 2000 Oct 17;133(8):585-91. doi: 10.7326/0003-4819-133-8-200010170-00008.
 15. Yoon HJ, Park M, Yoon H, Son KY, Cho B, Kim S. The differential effect of cigarette smoking on glomerular filtration rate and proteinuria in an apparently healthy population. *Hypertens Res*. 2009 Mar;32(3):214-9. doi: 10.1038/hr.2008.37.
 16. Gupta RK, Gupta R, Maheshwari VD, Mawliya M. Impact of smoking on microalbuminuria and urinary albumin creatinine ratio in non-diabetic normotensive smokers. *Indian J Nephrol*. 2014 Mar;24(2):92-6. doi: 10.4103/0971-4065.127893.
 17. Abdallah EM, Modawe GA, Shrief NM. Assessment of Creatinine and Microalbuminuria in Sudanese Smoker. *Sch Bull*. 2016;2(3):153-156
 18. Yamada Y, Noborisaka Y, Ishizaki M, Yamazaki M, Honda R, Yokoyama H, Kakuma T. Different association of cigarette smoking with GFR estimated from serum creatinine and that from serum cystatin C in the general population. *Clin Exp Nephrol*. 2015 Aug;19(4):669-77. doi: 10.1007/s10157-014-1058-y.
-

Expression of P53 and PTEN in Correlation with some Clinical and Pathological Features in Breast Cancer of Sudanese Patients

Abubaker M. Hamad^{1,2}, Rania Mahjoub Ser Alkhatem², Asaad K. Algahany³,
Hussain G. Ahmed^{4,5}, Abdulaziz Alfahed⁶, Hisham Ali Waggiallah⁶

¹College of Health Sciences, AL-Rayan Colleges, Madinah Al Munawwarah, Kingdom of Saudi Arabia

²Department of Histopathology and Cytopathology, Faculty of Medical Laboratory Sciences,
University of Gezira, Wad Madani, Sudan

³Department of Basic Sciences, Preparatory Year Deanship, Prince Sattam Bin Abdulaziz University,
Alkharj 11942, Saudi Arabia

⁴Department of Pathology, College of Medicine, University of Hail, Hail, Saudi Arabia

⁵Department of Histopathology and Cytology, Faculty of Medical Laboratory Sciences,
University of Khartoum, Khartoum, Sudan

⁶Department of Medical Laboratory Science, College of Applied Medical Science,
Prince Sattam Bin Abdulaziz University, Alkharj 11942, Saudi Arabia

Abstract

The goal of our study was to determine the expression and phosphorylation of PTEN at residues Ser380/Thr382/383, as well as the nuclear expression of p53 in Sudanese patients with breast cancer in association with clinicopathological aspects of breast cancer.

Methods and Results: This retrospective, descriptive study was carried out in Wad-Madani, Gezira state in Sudan, from January 2015 to August 2016. A total of 179 biopsies were taken at random from patients with breast lesions. Two blocks were obtained for each patient. One came from a malignant lesion (Group A), whereas the other came from the margin adjacent to healthy tissue (Group B). Immunohistochemistry and immunofluorescent histochemistry were performed on two separate slides. We found a statistically significant difference in the frequency of immunohistochemical expression of p53 and phosphorylation of PTEN between the cancerous breast tissue and adjacent normal tissue. P53 and PTEN exhibited a significant relationship with each other and the grade of tumor, indicating their importance in the aggressiveness of breast lesions. It should also be emphasized that there is an association between p53 expression and lymph node metastasis, which indicates the involvement of p53 mutation in the metastasis of breast cancer. (**International Journal of Biomedicine. 2023;13(1):62-68.**)

Keywords: PTEN • p53 • breast cancer • immunohistochemistry

For citation: Hamad AM, Alkhatem RMS, Algahany AK, Ahmed HG, Alfahed A, Waggiallah HA. Expression of P53 and PTEN in Correlation with some Clinical and Pathological Features in Breast Cancer of Sudanese Patients. International Journal of Biomedicine. 2023;13(1):62-68. doi:10.21103/Article13(1)_OA7.

Abbreviations

DFS, dermatofibrosarcoma; **DCI**, ductal carcinoma in situ; **FHC**, fibrous histiocytoma; **IDC**, invasive ductal carcinoma; **ILC**, invasive lobular carcinoma; **PD**, Paget's disease.

Introduction

Breast cancer⁽¹⁾ is the most common female malignancy and the second leading cause of mortality in women worldwide. In addition to its heterogeneity, BC incidence is increasing

globally, putting a financial strain on both developed and developing countries.^(2,3) Many risk factors, including genetic predisposition, have been linked to the etiology of breast cancer,⁽⁴⁾ including previous history of breast tumors in the same person or in his/her family⁽⁵⁾ or even malignancies other

than breast tumors,⁽⁶⁾ as well as levels of hormones over a lifetime (e.g., estrogen increase and decrease cycle, hormone replacement treatment),⁽⁷⁾ which are raising the possibility of breast cancer. Moreover, physical inactivity, obesity, and alcohol drinking all contribute to an elevated risk of breast cancer.^(8,9)

Economically developing countries, like Sudan, account for over 60% of all breast cancer fatalities worldwide.⁽¹⁰⁾ Breast cancer is a serious issue in Sudan, where it is characterized by early onset, late presentation, and poor resources. However, screening for high-risk individuals is inexpensive.⁽¹¹⁾

The tumor protein p53 (p53) is the primary regulator of human genome stability through cell cycle regulation. The most common genetic alteration in breast cancer is mutations of the *TP53* gene.^(12,13) Immunohistochemical staining for p53 is used as a surrogate for mutational analysis in the diagnostic workup of carcinomas of multiple sites. Strong and diffuse immunopositivity of p53 is generally interpreted as likely indicating a *TP53* gene mutation.⁽¹⁴⁾ Phosphatase and tensin homolog (*PTEN*) is a tumor-suppressor gene, and phagocytosis mutations in the *PTEN* gene have been linked to various malignancies, including breast cancer.^(15,16) It has been demonstrated in a mouse model that a 20% reduction in the *PTEN* expression can result in high penetrance breast cancer.⁽¹⁷⁾ Yang et al. found that phosphorylation of PTEN at residues Ser380/Thr382/383 resulted in the loss of phosphatase activity and tumor-suppressor function.⁽¹⁸⁾

The goal of our study was to determine the expression and phosphorylation of PTEN at residues Ser380/Thr382/383, as well as the nuclear expression of p53 in Sudanese patients with breast cancer in association with clinicopathological aspects of breast cancer.

Materials and Methods

This retrospective, descriptive study was carried out in Wad-Madani, Gezira state in Sudan, from January 2015 to August 2016. A total of 179 biopsies (fixed in a 10% neutral buffered formalin) were taken at random from patients with breast lesions. Two blocks were obtained for each patient. One came from a malignant lesion (Group A), whereas the other came from the margin adjacent to healthy tissue (Group B). Histologically, malignant samples were classified as ductal carcinoma in situ (DCI), invasive ductal carcinoma (IDC), invasive lobular carcinoma (ILC), sarcoma, and others. The histology sections had been previously diagnosed for all breast lesions in the Research Laboratory of the Faculty of Medicine at the University of Gezira.

Three serial sections (4 mm thick) were taken from each of the 179 biopsies using a Leica RM2125 RT rotary microtome. Immunohistochemistry and immunofluorescent histochemistry were performed on two separate slides.

P53 immunohistochemistry technique

We used CONFIRM anti-p53 (DO-7) Primary Antibody ((IgG1, kappa). Catalog Number: 800-2912. Species: Mouse. Localization: Nuclear. Regulatory Status: IVD. Ventana Medical System, Inc. 1910E, Tucson, Arizona, USA.

PTEN immunofluorescent histochemistry technique

We used PTEN pSer380/pThr382/383 rabbit polyclonal antibody, Aff – Purified (Cat. # AP02355PU-N). OriGene Technologies, Inc. Rockville, MD, USA.

Statistical analysis was performed using statistical software package SPSS version 23.0 (Armonk, NY: IBM Corp.). Group comparisons were performed using chi-square test with Yates correction. Inter-group comparisons were performed using Student's t-test. A probability value of $P < 0.05$ was considered statistically significant.

Ethical approvals were obtained from the research center at Faculty of Medical Laboratory Sciences, University of Gezira (Wad Madani, Sudan). The data was only used for study purposes without individual details identifying the participant.

Results

For this retrospective, descriptive study, the 179 histological biopsies were obtained from patients with breast lesions. The ages of the patients (174/97.2% females and 5/2.8% males) ranged from 13 to 95 years, with a mean age of 50.2 years (Table 1). Our sample population was divided as follows: 120(67.0%) samples were obtained in 2015 and 59(33.0%) in 2016. From 179 biopsies, 68(38.0 %) lesions were from the right breast, 63(35.0%) from the left breast, 1(0.6%) from both sides, and the remaining 47(26.3%) without indication of the affected side.

Table 1.

The age distribution of the study population.

Age group	Frequency	Percent	Valid Percent	Mean age
<30 years	11	6.1%	6.3%	50.20
31-40	46	25.7%	26.4%	
41-50	52	29.1%	29.9%	
51-60	26	14.5%	14.9%	
>61	39	21.8%	22.4%	
Missing	5	2.8%	-----	
Total	179	100%	100%	

All tissue specimens had previously been histopathologically identified as having either malignant or benign pathological conditions. We took histopathological sections from two blocks in each sample, one from the lesion and the other from the normal part of the tissue. All specimens were then immunohistochemically examined for P53 and PTEN.

The 179 breast lesions were all malignant tumors: DCI (10/5.6%), IDC (151/84.4%), ILC (6/3.4%), sarcoma (9/5.0%), and others (3/1.7%). In terms of malignancy grade, there was Grade I (4/2.2%), Grade II (74/41.3%), and Grade III (69/38.5%), and 1(0.6%) was the anaplastic case. Furthermore, 31(17.3%) cases had no determined grade mentioned.

In terms of infiltration, 165(92.2%) were infiltrating malignancies, and 14(7.8%) were in situ malignancies. Metastasis of malignancy to lymph nodes was detected in only 18(10.1%) cases. In terms of histological sites, we found the following: ducts (150/83.8%), lobules (17/9.5%), nipples (PD) (2/1.1%), and medullary carcinoma (7/3.9%). Basal cell carcinoma was detected in only 1(0.6%) case, fibrous histiocytoma in only 1(0.6%) case, and dermatofibrosarcoma (DFS) protuberans also in 1(0.6%) case.

Regarding histological form, we found the following: papillary (4/2.2%), mucinous (5/2.8%), cribriform (3/1.7%), phyllodes tumor (6/3.4%), and nonspecific histological form (161/89.9%). Our cases were divided into four types of cancerous cells: carcinoma (138/77.1%), adenocarcinoma (37/20.7%), sarcoma (3/1.7%), and lymphoma (1/0.6%) (Table 2). As shown in Table 3, there was an increase in the expression of p53, phosphorylation of PTEN, and Nuclear PTEN expression (Nuclear PTEN) in Group A, compared to Group B. There were statistically significant differences between Group A and Group B for all three parameters studied (PTEN, P53, and Nuclear PTEN) (Table 4).

Table 2

The demographic data and BC characteristics.

Sex		Total				
Female	Male	179				
174	5					
Year						
2015	2016					
120	59					
Grade						
Grade I	Grade II	Grade III	Anaplastic	No Grade		
4	74	69	1	31		
Lymph node metastasis						
Absent		Present				
161		18				
Histological site						
Ductal	Lobular	Nipple	Medullary	Basal cell	FHC	DFS protuberans
150	17	2	7	1	1	1

Table 3.

Expression of nuclear p53, PTEN, and Nuclear PTEN.

	Group A			Group B		
	PTEN	p53	Nuclear PTEN	PTEN	p53	Nuclear PTEN
Negative	16	20	3	69	87	56
Positive	163	159	176	110	92	123
Total	179					

Table 4.

T-test for Groups A and B.

Variables	Groups	T	P-value
PTEN	Group A - Group B	12.654	0.000
p53	Group A - Group B	12.948	0.000
Nuclear PTEN	Group A - Group B	11.568	0.000

We found that phosphorylation of PTEN at residues Ser380/Thr382/383 was increased in Group A in association with the histopathological grade of breast cancer ($P=0.005$) and the histological site of the lesion ($P=0.026$). However, there was no significant relationship between PTEN mutation in cancerous tissue and the following variables: year of sample collection, sex, patient's age group, and metastasis to lymph nodes (Table 5).

The same analysis was performed for p53 expression in cancerous tissue (Group A). A significant relationship was found only between the presence of p53 expression and the metastasis to lymph nodes ($P=0.037$). However, there was no significant relationship between P53 expression and the following variables: year of sample collection, sex, patient's age group, the histopathological grade of breast cancer and the histological site of the lesion (Table 6).

Our analysis revealed the relationship between the type of breast cancer diagnosis and sex ($P=0.001$), age group ($P=0.037$), grade of lesions ($P=0.000$), and histological site ($P=0.000$) (Table 7).

Discussion

Breast cancer is the leading cause of cancer morbidity and mortality among women in developing countries.⁽¹⁹⁾ Breast cancer remains the most common type of cancer in Sudan, despite the fact that it accounted for only 22.9% of all cancers in Sudan in 1959, when the first report about cancer in Sudan, "Malignant epithelial tumors in the Sudanese," was published by Hickey⁽²⁰⁾ following a lecture presented to the Royal College of Surgeons, England on 13 March 1958.

Due to a lack of adequate awareness and screening programs,⁽²¹⁻²²⁾ Sudanese women are still suffering from advanced stages of breast cancer. The average age ranged from 41 to 50 years. The majority of cases within our study were ductal lesions at the later stages (Grade III) with metastasis to lymph nodes. Most patients in this study were of menopausal age, and the clinical course of the disease at that time appeared to be similar to that of European women.⁽²²⁾ However, a recent study found possible differences in breast cancer between Sudanese women in Central Sudan and women in Northern Italy.

Our findings are nearly consistent with previous research, which found that Sudanese patients were premenopausal in age, had larger tumors at more advanced stages and grades, and were frequently positive for nodal metastases, when compared

to Italian patients. The expression of estrogen receptors varied between the two groups, with most Sudanese patients' tumors

expressing no receptors. These clinicopathological and patient characteristics are now widespread in Sudan.⁽²²⁾

Table 5.
The relationship between PTEN mutation in Group A and demographic data

Variables		PTEN (Group A)			P-value
		Negative	Positive	Total	
Year	2015	8	112	120	0.070
	2016	8	51	59	
	Total	16	163	179	
Sex	Female	15	159	174	0.458
	Male	1	4	5	
	Total	16	163	179	
Age group	<30 years	3	8	11	0.418
	31-40	3	43	46	
	41-50	6	46	52	
	51-60	2	24	26	
	>61	2	37	39	
	Total	16	163	174	
Lymph node metastasis	No Lymph Node Metastasis	15	146	161	0.712
	Lymph Node Metastasis	1	17	18	
	Total	16	163	179	
Grade	Grade I	0	4	4	0.005
	Grade II	5	69	74	
	Grade III	4	65	69	
	Anaplastic	0	1	1	
	No Grade	7	24	31	
	Total	16	163	179	
Histological site	Ductal	13	137	150	0.026
	Lobular	1	16	17	
	Nipple (Paget's disease)	0	2	2	
	Medullary	1	6	7	
	Basal cell	0	1	1	
	Fibrous Histiocytoma	1	0	1	
	DFS protuberans	0	1	1	
	Total	16	163	179	

Table 6.
The relationship between p53 expression in Group A and demographic data

Variables		P53 (Group A)			P-value
		Negative	Positive	Total	
Year	2015	13	107	120	0.945
	2016	7	52	59	
	Total	20	159	179	
Sex	Female	20	154	174	0.705
	Male	0	5	5	
	Total	20	159	179	
Age group	<30 years	2	9	11	0.676
	31-40	3	43	46	
	41-50	8	44	52	
	51-60	1	25	26	
	>61	6	33	39	
	Total	20	154	174	
Lymph node metastasis	No Lymph Node Metastasis	19	142	161	0.037
	Lymph Node Metastasis	1	17	18	
	Total	20	159	179	
Grade	Grade I	1	3	4	0.102
	Grade II	11	63	74	
	Grade III	4	65	69	
	Anaplastic	0	1	1	
	No Grade	4	27	31	
	Total	20	159	179	
Histological site	Ductal	19	131	150	0.148
	Lobular	0	17	17	
	Nipple (Paget's disease)	0	2	2	
	Medullary	0	7	7	
	Basal cell	1	0	1	
	Fibrous Histiocytoma	0	1	1	
	DFS protuberans	0	1	1	
	Total	20	159	179	

Table 7.
The relationship between the type of BC diagnosis and demographic data.

Variables		Diagnosis						P-value
		DCI	IDC	ILC	Sarcoma	Other	Total	
Year	2015	4	104	5	6	1	120	0.214
	2016	6	47	1	3	2	59	
	Total	10	151	6	9	3	179	
Sex	Female	10	149	5	8	2	174	0.001
	Male	0	2	1	1	1	5	
	Total	10	151	6	9	3	179	
Age group	<30 years	0	10	0	1	0	11	0.037
	31-40	5	37	0	2	2	46	
	41-50	4	43	0	5	0	52	
	51-60	1	23	1	1	0	26	
	>61	0	33	5	0	1	39	
	Total	10	146	6	9	3	174	
Lymph node metastasis	No Lymph Node Metastasis	10	135	6	8	2	161	0.456
	Lymph Node Metastasis	0	16	0	1	1	18	
	Total	10	151	6	9	3	179	
Grade	Grade I	1	3	0	0	0	4	0.000
	Grade II	3	66	4	1	0	74	
	Grade III	1	65	1	1	1	69	
	Anaplastic	0	0	0	1	0	1	
	No Grade	5	17	1	6	2	31	
	Total	10	151	6	9	3	179	
Histological site	Ductal	9	135	0	6	0	150	0.000
	Lobular	0	8	6	1	2	17	
	Nipple (PD)	1	0	0	0	1	2	
	Medullary	0	7	0	0	0	7	
	Basal cell	0	1	0	0	0	1	
	FHC	0	0	0	1	0	1	
	DFS Protuberans	0	0	0	1	0	1	
	Total	10	151	6	9	3	179	

The current study found a difference that is statistically significant in mutation frequency for p53 and phosphorylation of PTEN between the cancerous breast tissue and adjacent normal tissue, and this was applied to all parameters studied. Our results are consistent with findings in previous studies performed by Gang et al.⁽²³⁾ for P53, and Miao et al.⁽²⁴⁾ and Alam et al.⁽²⁵⁾ for PTEN and Nuclear PTEN.

We discovered a statistically significant relationship between PTEN phosphorylation and tumor grade due to PTEN inactivation. This is supported by Al-Subhi et al.⁽²⁶⁾ and Khan et al.⁽²⁷⁾ We did not detect a significant relationship between p53 expression in cancerous breast tissue and such factors as sex, age group, tumor grade, or histological site of the breast lesion. These findings were consistent with the data of Pan et al.⁽²⁸⁾ However, we found a link between p53 expression and lymph node metastasis, indicating an aggressive form of breast cancer. This was consistent with Payandeh et al.⁽²⁹⁾

The current study found a significant correlation between breast cancer diagnosis and patient gender. It goes without saying that breast cancer is more inherent in women. Breast cancer diagnosis was statistically strongly correlated with tumor grade and histological site. We also found that most cases were Grade II and ductal lesions, which was consistent with Fu et al.⁽³⁰⁾ We also discovered a statistically significant relationship between diagnosis and age group. This is supported by Efirid et al.⁽³¹⁾ So, among women >65 years of age, 75% had well or moderately differentiated tumors and only 16% had lymph node invasion. Most tumors in this age group were ≤ 2 cm (67%). Approximately 17% of older women had the more aggressive triple-negative breast cancer (HR-/HER2-).⁽³¹⁾ At the same time, there was no statistically significant link between breast cancer diagnosis and lymph node metastasis. However, Yun et al.⁽³²⁾ found that the presence of symptoms, triple-negative breast cancer subtype, larger size mass on breast ultrasonography (>10 mm), and higher Breast Imaging Reporting and Data System category on breast ultrasonography ($\geq 4c$) were positively associated with axillary lymph node metastasis.

P53 and PTEN can be used as breast cancer diagnostic and prognostic markers. We advocate for a comprehensive national program of breast cancer awareness and screening for the entire Sudanese population, as well as the creation of a freely accessible dataset portal for all cancers. Given the sociological, cultural, and educational considerations discussed above, screening and surveillance protocols may be appropriate, but they must be designed with great care and sensitivity.

Conclusion

We found a statistically significant difference in the frequency of immunohistochemical expression of p53 and phosphorylation of PTEN between the cancerous breast tissue and adjacent normal tissue. P53 and PTEN exhibited a significant relationship with each other and the grade of tumor, indicating their importance in the aggressiveness of breast lesions. It should also be emphasized that there is an association between p53 expression and lymph node

metastasis, which indicates the involvement of p53 mutation in the metastasis of breast cancer.

Acknowledgments

This publication was supported by the Deanship of Scientific Research at Prince Sattam bin Abdulaziz University.

Competing Interests

The authors declare that they have no competing interests.

References

- Fahad Ullah M. Breast Cancer: Current Perspectives on the Disease Status. *Adv Exp Med Biol.* 2019;1152:51-64. doi: 10.1007/978-3-030-20301-6_4. PMID: 31456179.
- Fagundo-Rivera J, Gómez-Salgado J, García-Iglesias JJ, Gómez-Salgado C, Camacho-Martín S, Ruiz-Frutos C. Relationship between Night Shifts and Risk of Breast Cancer among Nurses: A Systematic Review. *Medicina (Kaunas).* 2020 Dec 10;56(12):680. doi: 10.3390/medicina56120680.
- Alghamdi A, Balkhi B, Alqahtani S, Almotairi H. The Economic Burden Associated with the Management of Different Stages of Breast Cancer: A Retrospective Cost of Illness Analysis in Saudi Arabia. *Healthcare (Basel).* 2021 Jul 18;9(7):907. doi: 10.3390/healthcare9070907.
- Palmer JR, Polley EC, Hu C, John EM, Haiman C, Hart SN, et al. Contribution of Germline Predisposition Gene Mutations to Breast Cancer Risk in African American Women. *J Natl Cancer Inst.* 2020 Dec 14;112(12):1213-1221. doi: 10.1093/jnci/djaa040. Erratum in: *J Natl Cancer Inst.* 2020 Oct 1;112(10):1071.
- van den Broek JJ, Schechter CB, van Ravesteyn NT, Janssens ACJW, Wolfson MC, Trentham-Dietz A, Simard J, Easton DF, Mandelblatt JS, Kraft P, de Koning HJ. Personalizing Breast Cancer Screening Based on Polygenic Risk and Family History. *J Natl Cancer Inst.* 2021 Apr 6;113(4):434-442. doi: 10.1093/jnci/djaa127.
- Ji F, Yang CQ, Li XL, Zhang LL, Yang M, Li JQ, et al. Risk of breast cancer-related death in women with a prior cancer. *Aging (Albany NY).* 2020 Apr 6;12(7):5894-5906. doi: 10.18632/aging.102984.
- Olsson HL, Olsson ML. The Menstrual Cycle and Risk of Breast Cancer: A Review. *Front Oncol.* 2020 Jan 24;10:21. doi: 10.3389/fonc.2020.00021.
- Padovano F, Mariani G, Ferdeghini M. Hybrid Imaging for Breast Malignancies. In: Volterrani D, Erba P, Carrió I, Strauss H., Mariani G. (Eds.) *Nuclear Medicine Textbook.* Springer, Cham; 2019:543-570.
- Schairer C, Hablas A, Eldein IAS, Gaafar R, Rais H, Mezlini A, et al. Risk factors for inflammatory and non-inflammatory breast cancer in North Africa. *Breast Cancer Res Treat.* 2020 Nov;184(2):543-558. doi: 10.1007/s10549-020-05864-3.
- Marima R, Francies FZ, Hull R, Molefi T, Oyomno M, Khanyile R, et al. MicroRNA and Alternative mRNA Splicing Events in Cancer Drug Response/Resistance: Potent Therapeutic Targets. *Biomedicines.* 2021 Dec 2;9(12):1818. doi: 10.3390/biomedicines9121818.
- Salih AM, Alam-Elhuda DM, Alfaki MM, Yousif AE, Nouradyem MM. Developing a risk prediction model for breast cancer: a Statistical Utility to Determine Affinity of Neoplasm (SUDAN-CA Breast). *Eur J Med Res.* 2017 Sep 29;22(1):35. doi: 10.1186/s40001-017-0277-6.
- Kaur K, Manjari M, Rai V, Madhukar M. Evaluation of correlation of tumor markers with tumor grading in breast carcinoma patients. *J Adv Med Dent Scie Res.* 2016 Sep; 4(5):131-136.
- Lee SK, Bae SY, Lee JH, Lee HC, Yi H, Kil WH, et al. Distinguishing Low-Risk Luminal A Breast Cancer Subtypes with Ki-67 and p53 Is More Predictive of Long-Term Survival. *PLoS One.* 2015 Aug 4;10(8):e0124658. doi: 10.1371/journal.pone.0124658.
- Yemelyanova A, Vang R, Kshirsagar M, Lu D, Marks MA, Shih IeM, Kurman RJ. Immunohistochemical staining patterns of p53 can serve as a surrogate marker for TP53 mutations in ovarian carcinoma: an immunohistochemical and nucleotide sequencing analysis. *Mod Pathol.* 2011 Sep;24(9):1248-53. doi: 10.1038/modpathol.2011.85.
- Li C, Xu B, Miu X, Deng Z, Liao H, Hao L. Inhibition of miRNA-21 attenuates the proliferation and metastasis of human osteosarcoma by upregulating PTEN. *Exp Ther Med.* 2018 Jan;15(1):1036-1040. doi: 10.3892/etm.2017.5477.
- Lin Fde M, Bacchi CE, Baracat EC, Carvalho FM. Loss of PTEN expression and AKT activation in HER2-positive breast carcinomas. *Rev Bras Ginecol Obstet.* 2014 Aug;36(8):340-6.
- Alimonti A, Carracedo A, Clohessy JG, Trotman LC, Nardella C, Egia A, Salmena L, Sampieri K, Haveman WJ, Brogi E, Richardson AL, Zhang J, Pandolfi PP. Subtle variations in Pten dose determine cancer susceptibility. *Nat Genet.* 2010 May;42(5):454-8. doi: 10.1038/ng.556.
- Yang Z, Xie C, Xu W, Liu G, Cao X, Li W, et al. Phosphorylation and inactivation of PTEN at residues Ser380/Thr382/383 induced by *Helicobacter pylori* promotes gastric epithelial cell survival through PI3K/Akt pathway. *Oncotarget.* 2015 Oct 13;6(31):31916-26. doi: 10.18632/oncotarget.5577.
- Ng'ida FD, Kotoroi GL, Mwangi R, Mabelele MM, Kitau J, Mahande MJ. Knowledge and practices on breast cancer detection and associated challenges among women aged 35 years and above in Tanzania: a case in Morogoro Rural District. *Breast Cancer (Dove Med Press).* 2019 May 28;11:191-197. doi: 10.2147/BCTT.S199889.
- HICKEY BB. Malignant epithelial tumours in the Sudanese. *Ann R Coll Surg Engl.* 1959 May;24(5):303-22.
- Fadhil I, Alkhalawi E, Nasr R, Fouad H, Basu P, Camacho R, Alsaadoon H. National cancer control plans across the Eastern Mediterranean region: challenges and opportunities to scale-up. *Lancet Oncol.* 2021 Nov;22(11):e517-e529. doi: 10.1016/S1470-2045(21)00410-1.
- Elamin A, Ibrahim ME, Abuidris D, Mohamed KE, Mohammed SI. Part I: cancer in Sudan—burden, distribution,

*Corresponding authors: Dr. Hisham Ali Waggiallah, Department of Medical Laboratory Sciences, College of Applied Medical Sciences, Prince Sattam Bin Abdulaziz University. E-mail: hishamwagg30@hotmail.com

- and trends breast, gynecological, and prostate cancers. *Cancer Med.* 2015 Mar;4(3):447-56. doi: 10.1002/cam4.378.
23. Gang Z, Zhong L, Xiao-meng L, Jun-hua Z, Yong C, Xing Z. Expression of P53, PTEN and S100A4 in invasive ductal breast cancer and the clinical significance. *J Chitwan Med College.* 2016;6(2):49-55.
24. Miao Y, Zheng W, Li N, Su Z, Zhao L, Zhou H, Jia L. MicroRNA-130b targets PTEN to mediate drug resistance and proliferation of breast cancer cells via the PI3K/Akt signaling pathway. *Sci Rep.* 2017 Feb 6;7:41942. doi: 10.1038/srep41942.
25. Alam MS, Jerah ABA, Ashraf AM, Kumaresan K, Eisa ZM, Mikhail NT. Promoter Methylation and Loss of Expression of PTEN Gene in Breast Cancer Patients from Saudi Population. *J Clin Exp Oncol.* 2017; 6(7):6 -11.
26. Al-Subhi N, Ali R, Abdel-Fatah T, Moseley PM, Chan SYT, Green AR, et al. Targeting ataxia telangiectasia-mutated- and Rad3-related kinase (ATR) in PTEN-deficient breast cancers for personalized therapy. *Breast Cancer Res Treat.* 2018 Jun;169(2):277-286. doi: 10.1007/s10549-018-4683-4.
27. Khan F, Esnakula A, Ricks-Santi LJ, Zafar R, Kanaan Y, Naab T. Loss of PTEN in high grade advanced stage triple negative breast ductal cancers in African American women. *Pathol Res Pract.* 2018 May;214(5):673-678. doi: 10.1016/j.prp.2018.03.020.
28. Pan Y, Yuan Y, Liu G, Wei Y. P53 and Ki-67 as prognostic markers in triple-negative breast cancer patients. *PLoS One.* 2017 Feb 24;12(2):e0172324. doi: 10.1371/journal.pone.0172324.
29. Payandeh M, Sadeghi M, Sadeghi E, Madani SH. Expression of p53 Breast Cancer in Kurdish Women in the West of Iran: a Reverse Correlation with Lymph Node Metastasis. *Asian Pac J Cancer Prev.* 2016;17(3):1261-4.
30. Fu D, Zuo Q, Huang Q, Su L, Ring HZ, Ring BZ. Molecular Classification of Lobular Carcinoma of the Breast. *Sci Rep.* 2017 Mar 17;7:43265. doi: 10.1038/srep43265.
31. Efir JT, Hunter S, Chan S, Jeong S, Thomas SL, Jindal C, Biswas T. The Association between Age, Comorbidities and Use of Radiotherapy in Women with Breast Cancer: Implications for Survival. *Medicines (Basel).* 2018 Jun 25;5(3):62. doi: 10.3390/medicines5030062.
32. Yun SJ, Sohn YM, Seo M. Risk Stratification For Axillary Lymph Node Metastases in Breast Cancer Patients: What Clinicopathological and Radiological Factors of Primary Breast Cancer Can Predict Preoperatively Axillary Lymph Node Metastases? *Ultrasound Q.* 2017 Mar;33(1):15-22. doi: 10.1097/RUQ.0000000000000249.
-

Immunofluorescence Analysis of Erythrocyte Membranes of Cervical Cancer Patients

Sargylana N. Mamaeva¹, Vladislav A. Alekseev², Nadezhda A. Nikolaeva¹,
Tatyana A. Krylova¹, Aya A. Gabysheva¹, Alexandr N. Pavlov¹, Irina V. Kononova²,
Georgy V. Maksimov³

¹M.K. Ammosov North-Eastern Federal University, Yakutsk, Sakha (Yakutia) Republic, Russia

²Yakut Scientific Center of Complex Medical Problems, Yakutsk, Sakha (Yakutia) Republic, Russia

³Lomonosov Moscow State University, Moscow, Russia

Abstract

Currently, cervical cancer (CC) is one of the most common oncological diseases. In this regard, it is necessary to develop new research methods for a more detailed study of the occurrence and development of the disease at the molecular and cellular levels, as well as to improve the effectiveness of treatment and form a deeper understanding of the causes of relapses. The aim of this work was to study nanoparticles localized on the erythrocyte membrane—presumably HPV 16, 18, before and after radiation therapy, in patients with CC.

To study the surface of red blood cells by the SEM method, venous blood samples from 17 patients with a confirmed diagnosis of CC were prepared in thin layers evenly applied to a dry, fat-free glass slide, which was dried at room temperature. To detect nanoparticles on the surface of erythrocytes by the immunofluorescence assay, we developed a special protocol for preparing erythrocyte masses from patients diagnosed with CC. As a result of using a new method of sample preparation for immunofluorescence assay and using SEM, the hypothesis of the viral nature of nanoparticles localized on the surface of the blood erythrocytes of patients with CC was confirmed: Particles of HPV 16 and 18 are located on the cytoplasmic membrane of erythrocytes. Studies suggest that viruses attach to the erythrocyte membrane, which seems to influence the development of CC, its recurrence, and metastasis. (*International Journal of Biomedicine*. 2023;13(1):69-72.)

Keywords: cervical cancer • immunofluorescence assay • erythrocyte • HPV • scanning electron microscope

For citation: Mamaeva SN, Alekseev VA, Nikolaeva NA, Krylova TA, Gabysheva AA, Pavlov AN, Kononova IV, Maksimov GV. Immunofluorescence Analysis of Erythrocyte Membranes of Cervical Cancer Patients. *International Journal of Biomedicine*. 2023;13(1):69-72. doi:10.21103/Article13(1)_OA8

Abbreviations

CC, cervical cancer; HPV, human papillomavirus; IFA, immunofluorescence assay; SEM, scanning electron microscope

Introduction

Currently, cervical cancer (CC) is one of the most common oncological diseases. Epidemiological and virological studies have revealed that 95% of all squamous cell cancers of the cervix are caused by human papillomavirus (HPV) and contain HPV-DNA 16,18. By the end of 2020, according to the International Agency for Research on Cancer

GLOBOCAN, CC was among the top 10 cancers (using estimates of morbidity and mortality). In 2020, 604,127 new cases and 341,831 deaths were registered.^(1,2)

An even more significant increase in the incidence of CC is expected despite the development of new comprehensive prevention measures to control CC, methods of early diagnosis, and the development of high-tech therapy. In addition, there are frequent recurrences of

CC after various types of radical treatment, including after radiation therapy in the early stages of the disease and the phenomenon of metastasis, which complicates therapy and affects the survival of patients.⁽³⁻⁸⁾

Note that now there is no clear explanation for the recurrence of this disease. In this regard, it is necessary to develop new research methods for a more detailed study of the occurrence and development of the disease at the molecular and cellular levels, as well as to improve the effectiveness of treatment and form a deeper understanding of the causes of relapses.

According to the results of studies of red blood cells from CC patients using scanning electron microscopy (SEM), obtained by the authors previously, nanoparticles were found on the surface of erythrocytes, the sizes of which were comparable to those of HPV16, 18, and other viruses.⁽⁹⁾ In this regard, it became necessary to identify these nanoparticles, determine their nature, and explain the dependence of erythrocyte morphology on radiation therapy. It has been suggested that nanoparticles localized on the surface of erythrocytes before, during, and after radiation therapy could be viruses and vesicles.⁽¹⁰⁾

In addition, the authors previously established the dependence of these particles' number, morphology, and size on the radiation therapy stages. The appearance of a large number of nanoparticles during radiation therapy and their change (up to complete disappearance at the end of therapy) in the blood (both on erythrocytes and in plasma)—the sizes of which were determined as continuous values, in contrast to nanoparticles that were detected before radiation therapy, the sizes of which were determined as discrete values—can be considered as factors in the reaction of the human body to exposure to ionizing radiation during radiation therapy. In some patients (with stages 3 and 4 of cancer), the presence of membrane-bound nanoparticles is probably due to structures on the erythrocyte surface that existed even before radiation therapy. These nanoparticles are likely viruses. Both viruses that remain in the blood after therapy and vesicles localized on the surface of the erythrocyte membrane may be provocative factors for disease relapses. The appearance of a large number of vesicles in the blood during radiation therapy may be associated, in particular, with altered properties of the membranes of dysmorphic erythrocytes.⁽¹⁰⁾

The aim of this work was to study nanoparticles localized on the erythrocyte membrane—presumably HPV 16, 18, before and after radiation therapy, in patients with CC. The results of such a study will allow us in the future to evaluate the immunological role of erythrocytes in the development of the disease.

Materials and Methods

This study used venous blood samples from 17 patients with a confirmed diagnosis of CC before and after radiation therapy. The scheme of radiation therapy was described in detail in our previous work.⁽¹⁰⁾

To study the surface of red blood cells by the SEM method, venous blood samples were prepared in thin layers

evenly applied to a dry, fat-free glass slide, which was dried at room temperature. To detect nanoparticles on the surface of erythrocytes by the immunofluorescence analysis, we developed a special protocol for preparing erythrocyte masses from patients diagnosed with CC.

Sample preparation

Blood samples collected in tubes containing EDTA were centrifuged for 5 minutes at 600g. The supernatant was drained, and the precipitate was placed in a 15 ml centrifuge tube for further washing with a phosphate buffer (PBS). We mainly took the central part of the sediment without touching the upper boundary of the phases and the bottom of the tube, where various nucleated cells and other blood elements were concentrated. After the transfer of the erythrocyte fraction, the total volume of the suspension was brought to 10ml using PBS, after which the samples were centrifuged for 5 minutes at 600g. The phosphate buffer washing procedure was repeated 3-4 times. The cells were fixed with 1% paraformaldehyde solution in PBS. A fixing solution was added to the washed sediment, bringing the total volume to 10ml, and then gently mixed by turning the test tube several times and incubating for 15 minutes at room temperature. The fixing solution was removed by centrifugation under the same conditions, and the precipitate was washed 2 times with FACS solution (2% veal serum in PBS). At this stage, the samples were ready for immunofluorescence analysis.

Immunofluorescence assay

This method is widely used in modern cellular and molecular biology and is described in sufficient detail in many works. In our case, the suspension of a fixed sample was diluted with a FACS solution in a ratio of 1:3 (250:750 μ l, respectively); then 100 μ l of the diluted sample was transferred to a clean Eppendorf-type tube, and 1 μ l of primary antibodies was carefully added, followed by incubation overnight at +4 °C. Mouse monoclonal antibodies against HPV protein types 1, 6, 11, 16, 18, and 31 MAB837 (Sigma-Aldrich) were used as primary antibodies. After incubation, the sample was centrifuged for 5 minutes at 800 g; the supernatant was drained and washed 3 times with FACS solution. To the sample dissolved in 500 μ l of FACS solution was added 2 μ l of secondary antibodies, which were goat polyclonal antibodies against mouse immunoglobulin H and L chains conjugated with fluorescein (Stemcell Technologies, cat. # 60138FI).

Dry smears were prepared after an hour of incubation of samples with antibodies and visualized using an AxioVert.A1 microscope with a FITC fluorescent filter.

Scanning electron microscopy

SEM was used to investigate the morphology and surface of red blood cells in CC patients before and after radiation therapy. A high-resolution SEM JSM-7800F (Japanese Electron Optics Laboratory, JEOL, Japan) equipped with a Schottky thermal field emission cathode, a super hybrid objective lens, and a Gentle Beam system was used. The smears were examined at an accelerating voltage of 1.3 kV and a focal length of 4.0 mm using the Gentle Beam system.

The study was conducted in accordance with ethical principles of the WMA Declaration of Helsinki (1964, ed. 2013) and approved by the Ethics Committee of the M.K. Ammosov North-Eastern Federal University (protocol No. 13 of April 4, 2018, decision No. 2). Written informed consent was obtained from each patient.

Results

In this work, in parallel, examinations of the same samples of whole venous blood of CC patients were carried out using different methods: 1) study of the morphology of erythrocytes of dry smears using the SEM method; 2) study of erythrocytes by the MFA method.

Figure 1 shows an SEM image of the red blood cell surface of a dry blood smear of a CC patient. Nanoparticles were detected on erythrocytes, the sizes of which are comparable to those of HPV 16,18.

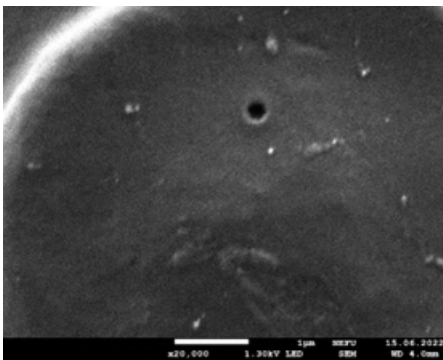


Fig. 1. SEM image of the erythrocyte surface at 20,000x

Figure 2 (before radiation therapy) shows images of erythrocytes of the erythrocyte mass obtained based on a new protocol we developed for sample preparation in a CC patient.

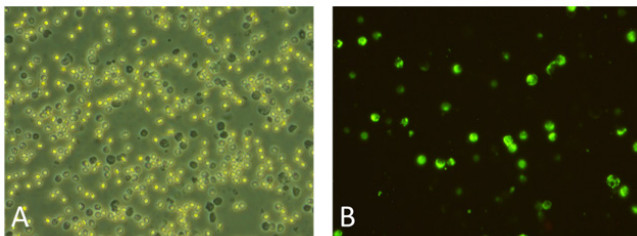


Fig. 2. Micrographs of erythrocytes of a patient with cervical cancer (400x). (A) phase contrast; (B) fluorescent mode.

These images were obtained using a fluorescent microscope at various magnifications and microphotography conditions: with phase contrast and in fluorescent mode. The images show a glow on the surface of some red blood cells, thereby confirming the authors' assumptions that the nanoparticles observed in the SEM images may be viral particles.

To detect the nucleus-containing cells, the samples were also stained with Hoechst 33342 dye; however, we did not detect glowing nuclei in the ultraviolet spectrum, which indicates the luminous elements we detected are erythrocytes. In addition, it was found that the luminescence on the surface of erythrocytes is observed in patient samples before and after radiation therapy, i.e., these particles were present even before radiation therapy and were in no way associated with exposure to ionizing radiation.

As a result of using a new method of sample preparation for immunofluorescence analysis and using SEM, the hypothesis of the viral nature of nanoparticles localized on the surface of the blood erythrocytes of patients with CC was confirmed: Particles of HPV 16 and 18 are located on the cytoplasmic membrane of erythrocytes.

Studies suggest that viruses attach to the erythrocyte membrane, which seems to influence the development of CC, its recurrence, and metastasis.

Discussion

Our previous studies lacked sufficient results in favor of identifying nanoparticles on the surface of erythrocytes as viruses. The results of this study are an additional link in the definition of these nanoparticles as viruses. Another group of researchers has shown that surface receptors and ligands of exosomes are responsible for the distribution and attachment of exosomes to target cells and extracellular matrix.^(11,12) Consequently, exosomes circulating in the blood and attached to blood cells do not undergo immediate fusion with cells but remain exosomes attached to the cell surface for some time. The role of circulating exosomes attached to the surface of erythrocytes in the spread of the tumor remains unclear; however, convincing evidence has been obtained that RNA and proteins included in such particles can play an important role in the diagnosis of cancer.^(13,14)

Based on the results of this work and that of other researchers, it can be argued that the HPV can attach and be transported to the surface of red blood cells, affecting their morphology and biophysical properties, possibly playing a decisive role in the development of the disease, and have an impact on the results of therapy and relapses of the disease.

Significant evidence has also recently been obtained indicating that HPV may play a role in developing CC. However, the data linking CC with chronic HPV infection were contradictory, which led to a lack of consensus.⁽¹⁵⁾ We plan to conduct more focused research to confirm the results of our study.

Sources of Funding

This study financial supported by the State Assignment (Grant No. FSRG-2021-0014).

Acknowledgments

This study was supported by "The Fund of Target Capital Management M. K. Ammosov North-Eastern Federal University."

Competing Interests

The authors declare that they have no competing interests.

References

1. MISKAWAAN. Global Cancer Facts and Figures 2021. Available at: <https://miskawaanhealth.com/cancer/global-cancer-statistics/>
2. WHO. Cancer Today. Available at: <https://gco.iarc.fr/today/home>
3. Lushnikova PA, Sukhikh ES, Izhevsky PV, Sutygina YN, Tatarchenko MA, Pyzhova IB. [Modern Techniques for Cervical Cancer Radiotherapy]. Creative surgery and oncology. 2021;11:58-67. doi: 10.24060/2076-3093-2021-11-1-58-67. [Article in Russian].
4. Tazhibayeva KN, Sadykova AD, Tasboltayeva DT, Ormanov AN, Kaldygozova GE. Ways to improve the diagnosis and detection of cervical cancer and recurrence risk. Oncology and radiology of Kazakhstan, 2021; №4 (62): 24-27. doi: 10.52532/2663-4864-2021-4-62-24-27
5. Shakirova EZ, Zidikhanov DI. [Salvage hysterectomy after radiotherapy for cervical cancer: A literature review]. Tumors of female reproductive system. 2021;17(3):121-7. doi: 10.17650/1994-4098-2021-17-3-121-127. [Article in Russian].
6. Kreinina YM, Shevchenko LN, Kaskulova MK, Dykina AV, Smyslov AY, Trotsenko SD, et al. [Actual technologies of conformal radiation therapy in modern programs of treatment of relapses of cervical cancer, uterine body and ovaries]. Oncogynecology. 2020;2(34): 60-70. doi: 10.52313/22278710-2020-2-60. [Article in Russian].
7. Mansurova GB, Saidova KA, Razakov AR, Talybova SA, Agzamov OA, Chen et al. Analysis of factors influencing the recurrence of cervical cancer. Clinical and Experimental Oncology. 2018;1(3):15-18.
8. Shumeikina AO, Vavilov KV, SamoiloVA EA, Mansurova AS, Ponomarenko AG. The possibilities of using stereotactic radiation therapy for the treatment of recurrent cervical cancer. Materials of the VIII St. Petersburg International Cancer Forum "White Nights 2022." Tumors of the female reproductive system: radiation therapy. Issues of Oncology. 2022;3(68):231-232.
9. Mamaeva SN, Kononova IV, Ruzhansky M, Nikiforov PV, Nikolaeva NA, Pavlov AN et al. The use of scanning electron microscopy and atomic force microscopy to study the formation of nanoparticles on the surface of erythrocytes in patients with cervical cancer. International Journal of Biomedicine. 2020; 10(1):70-75. doi: 10.21103/Article10(1)_OA12
10. Mamaeva SN, Kononova IV, Nikolaeva NA, Pavlov AN, Semenova MN, Maksimov GV. Determination of Blood Parameters using Scanning Electron Microscopy as a Prototype Model for Evaluating the Effectiveness of Radiation Therapy for Cervical Cancer. International Journal of Biomedicine.. 2021;11(1):32-38. doi: 10.21103/Article11(1)_OA6
11. Tamkovich SN, Yunusova NV, Tugutova E, Somov AK, Proskura KV, Kolomiets LA, Stakheeva MN, Grigor'eva AE, Laktionov PP, Kondakova IV. Protease Cargo in Circulating Exosomes of Breast Cancer and Ovarian Cancer Patients. Asian Pac J Cancer Prev. 2019 Jan 25;20(1):255-262. doi: 10.31557/APJCP.2019.20.1.255.
12. Tamkovich SN, Bakakina YS, Tutanov OS, Somov AK, Kirushina NA, Dubovskaya LV, et al. Proteomic analysis of circulating exosomes in healthcare and breast cancer. Russian Journal of Bioorganic Chemistry. 2017;43(2):126-134. doi: 10.1134/S1068162017020157
13. Tamkovich S, Tutanov O, Efimenko A, Grigor'eva A, Ryabchikova E, Kirushina N, Vlassov V, Tkachuk V, Laktionov P. Blood Circulating Exosomes Contain Distinguishable Fractions of Free and Cell-Surface-Associated Vesicles. Curr Mol Med. 2019;19(4):273-285. doi: 10.2174/1566524019666190314120532.
14. Zhang W, Ou X, Wu X. Proteomics profiling of plasma exosomes in epithelial ovarian cancer: A potential role in the coagulation cascade, diagnosis and prognosis. Int J Oncol. 2019 May;54(5):1719-1733. doi: 10.3892/ijo.2019.4742.
15. Islam MS, Chakraborty B, Panda CK. Human papilloma virus (HPV) profiles in breast cancer: future management. Ann Transl Med. 2020 May;8(10):650. doi: 10.21037/atm-19-2756.

*Corresponding author: Sargylana Mamaeva, Ph.D. M.K. Ammosov North-Eastern Federal University, Yakutsk, Sakha (Yakutia) Republic, Russia. E-mail: sargylana_mamaeva@mail.ru

Analysis of *NPM1* and *FLT3* Mutations in Patients with Acute Myeloid Leukemia in Jeddah, Saudi Arabia: A Pilot Study

Raed Alserihi¹, Hameeda Ahmad², Heba Alkhatabi^{1,2}, Talal Qadah¹, Shahad W. Kattan³, Elrashed B. Yasin⁴, Haitham M. H. Qutob⁴, Waleed M. Bawazir^{1,5}, Abeer Fakhr-Eldeen^{6,7}, Manal S. Fawzy^{8,9*}, Ahmad S. Barefah^{5,10}

¹Department of Medical Laboratory Technology, Faculty of Applied Medical Sciences, King Abdulaziz University, Jeddah 21589, Saudi Arabia

²Center of Excellence in Genomic Medicine Research (CEGMR), King Abdulaziz University, Jeddah 80200, Saudi Arabia

³Department of Medical Laboratory, College of Applied Medical Sciences, Taibah University, Yanbu, Saudi Arabia

⁴Department of Medical Laboratory Technology, Faculty of Applied Medical Sciences, King Abdulaziz University, Rabigh 25732, Saudi Arabia

⁵Hematology Research Unit, King Fahad Medical Research Center, King Abdulaziz University, Jeddah, Saudi Arabia

⁶Department of Clinical Pathology, Faculty of Medicine, Sohag University, Sohag, Egypt

⁷Department of Pathology, Faculty of Medicine, Northern Border University, Arar, Saudi Arabia

⁸Department of Biochemistry, Faculty of Medicine, Northern Border University, Arar, Saudi Arabia

⁹Department of Medical Biochemistry and Molecular Biology, Faculty of Medicine, Suez Canal University, Ismailia, Egypt

¹⁰Hematology Department, Faculty of Medicine, King Abdulaziz University, Jeddah 21589, Saudi Arabia

Abstract

Background: The outcome of acute myeloid leukemia (AML) is influenced by ethnicity, geographic variations, and the patient's molecular profile. We aimed to explore the mutation frequencies of the nucleophosmin 1 (*NPM1*) and the FMS-like tyrosine kinase 3 (*FLT3*) internal tandem duplication (ITD) or tyrosine kinase domain (TKD) with correlation to the cytogenetic profiles in patients with AML.

Methods and Results: Bone marrow/whole blood samples from 33 patients with AML were screened for *NPM1/FLT3*-ITD mutations by fragments analysis using a GeneScan analyzer. Depending on the fragment size, the *NPM1* and *FLT3* wild type (Wt) (170 bp and 330 bp) vs. mutated (170/174 bp and 330/351 bp) alleles, respectively, can be distinguished. The allelic ratio of *FLT3*-ITD⁺ was calculated. *FLT3*-TKD⁺ mutation was detected by Sanger sequencing. Samples were tested for chromosomal aberrations. According to the French-American-British (FAB) classification, the predominant type in the present cohort was AML-M5, accounting for 30.3%. *NPM1*⁺, *FLT3*-ITD⁺, and double mutations were found in 12.1%, 3.1%, and 6.1% of cases, respectively. The combined *NPM1*⁺/*FLT3*-ITD⁺/*FLT3*-TKD⁺ profile was presented in one patient (3.1%). The dual positivity group (*NPM1*⁺/*FLT3*⁺) significantly had a higher WBC count with a median of $81.3 \times 10^3/\mu\text{L}$. A total of 63.6% of patients had abnormal cytogenetics. The *NPM1*⁺/*FLT3*-ITD⁺ patients had normal karyotypes. Patients with *NPM1*⁺/*FLT3*⁺ showed complex karyotype (24%) and t(8;21) (8%). The *FLT3*-ITD⁺ patient had trisomy 8.

Conclusion: The frequency of *NPM1/FLT3* mutations in the study cohort showed less rate than in other studies with a distinct pattern. Due to the preliminary nature of the present work, more extensive screening is warranted to evaluate their usefulness as prognostic indicators in this region. (International Journal of Biomedicine. 2023;13(1):73-83.)

Keywords: acute myeloid leukemia • *FLT3* • *NPM1* • sequencing

For citation: Alserihi R, Ahmad H, Alkhatabi H, Qadah T, Kattan SW, Yasin EB, Qutob HMH, Bawazir WM, Fakhr-Eldeen A, Fawzy MS, Barefah AS. Analysis of *NPM1* and *FLT3* Mutations in Patients with Acute Myeloid Leukemia in Jeddah, Saudi Arabia: A Pilot Study. International Journal of Biomedicine. 2023;13(1):73-83. doi:10.21103/Article13(1)_OA9

Abbreviations

AML, acute myeloid leukemia; **FLT3**, FMS-like tyrosine kinase 3; **ITD**, internal tandem duplication; **NPM1**, Nucleophosmin 1; **TKD**, tyrosine kinase domain.

Introduction

AML is one of the hematopoietic tumors caused by the atypical production and differentiation of myeloblasts in the bone marrow.⁽¹⁾ In 2017, AML accounted for 23.1% of the total leukemia cases with a current global incidence rate equal to 0.9-2.8 cases per 10⁵ men and 0.4-2.2 per 10⁵ women, raising the possibility of becoming one of the primary, worldwide public health concerns.^(2,3)

According to the Saudi Cancer Registry, 2016, the leukemia age-standardized rate was 3.6 per 10⁵ men and 3.0 per 10⁵ women⁽⁴⁾ with a slightly variable incidence of AML per Saudi Arabia regions, as the Eastern Region showed the highest rate of cases.⁽⁵⁾

The etiopathology of AML is heterogeneous and caused by different environmental and genetic aberrations associated with diverse outcomes.⁽⁶⁾ Accumulating evidence indicates that the genetic profile alterations of patients with AML are considered essential workup for stratifying cases into “favorable, intermediate, or adverse prognostic risk groups,” according to the 2017 European LeukemiaNet (ELN) guidelines, and are the strongest predictors of patients’ outcome and planning therapeutic strategies.⁽⁷⁻⁹⁾

Among the molecular studies that are essential for AML case-risk stratification are the nucleophosmin 1 (*NPM1*) and FMS-like tyrosine kinase 3 (*FLT3*) mutations.⁽¹⁰⁾ The phosphoprotein *NPM1* is implicated in regulating the function and stability of various nuclear proteins and several intracellular activities, such as stress response, DNA replication/recombination, transcription, repair, preribosomal particle transport, centromere duplications, and the stability of tumor suppressor genes (Figure 1A).⁽¹¹⁻¹³⁾

NPM1 is predominantly localized in the nucleolus and is thought to function as a molecular chaperone of proteins, facilitating the transport of ribosomal proteins through the nuclear membrane.⁽¹⁴⁻¹⁵⁾ The role of *NPM1* in human cancer has received a new spotlight with the discovery of mutations of exon 12 of *NPM1* in approximately 30% of adult de novo AML, and in 50–60% in those with a normal karyotype.^(16,17) The latest updates of the World Health Organization (WHO) classification of myeloid neoplasm recognized AML with mutated *NPM1* as a distinct diagnostic entity.⁽¹⁸⁾

Several different types of mutations exist in exon 12 of the *NPM1* gene. The most common type (called type A), representing about 70%–80% of all mutations, features a four-base pair nucleotide (TCTG) insertion at the position encoding the 288th amino acid residue, resulting in a frameshift of the downstream sequence.⁽¹⁹⁾ As a consequence, the C-terminal amino acid sequence 286DLWQWWRKSL-COOH changes to 286DLCLAVEEVSLRK-COOH. The mutant *NPM1* in AML leads to the cytoplasmic dislocation of *NPM1*.^(20,21) Interestingly, this type of mutation has been reported to have a favorable prognosis within the context of other specific genetic changes in AML cases.^(20,22-24)

The *FLT3* is a member of the class III receptor tyrosine kinase family that is generally expressed on early myeloid cell precursors and plays a central role in controlling the survival, proliferation and differentiation of hematopoietic cells (Figure 1B).⁽²⁵⁾ The in-frame internal tandem duplication (ITDs) and missense point mutation (D835) in the tyrosine kinase domain (TKD) are the most frequent activating mutations (i.e., lead to constitutive function of the TK receptor) explored in patients with AML.^(25,26) The latter mutations have been associated with AML’s poor prognosis for increased relapse risk and/or reduced overall survival.⁽²⁷⁾ Also, it is worth noting that the abnormal *FLT3* kinase activation is one of the putative therapeutic targets in AML.⁽²⁸⁾

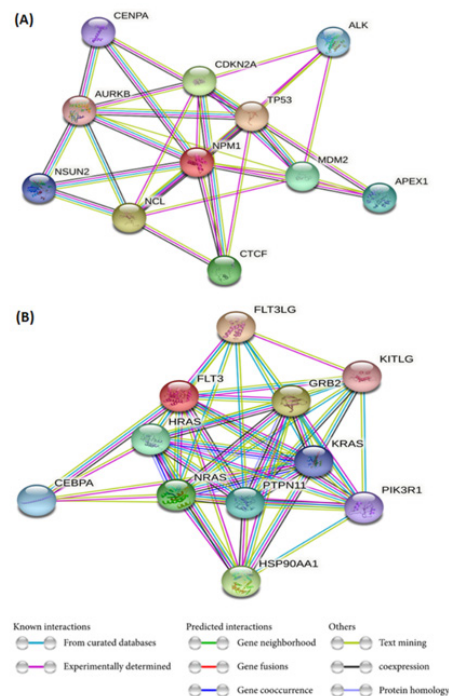


Figure 1. The STRING analysis of *NPM1* and *FLT3* with the predicted functional partners. Each node represents a protein produced by a single gene locus. Edges represent protein-protein associations. (A) The *NPM1* interacts with the tumor suppressor protein p53 (*TP53*), the major nucleolar protein nucleolin (*NCL*), cyclin-dependent kinase inhibitor 2A (*CDKN2A*), the transcriptional repressor (*CTCF*), the E3 ubiquitin-protein ligase Mdm2 (*MDM2*), the DNA-(apurinic or apyrimidinic site) lyase (*APEX1*), the *ALK* tyrosine kinase receptor (*ALK*), the *NOP2/Sun* RNA methyltransferase family member 2 (*NSUN2*), the Histone H3-like centromeric protein A (*CENPA*), and Aurora kinase B (*AURKB*) to mediate several cellular processes, including cell apoptosis, chromatin decondensation, transcriptional regulation, cellular response to oxidative stress, proper spindle assembly, and chromosome segregation, among others. (B) The *FLT3* interacts with the *Fms*-related tyrosine kinase 3 ligand (*FLT3LG*), the growth factor receptor-bound protein 2 (*GRB2*), the heat shock protein HSP 90-alpha (*HSP90AA1*), the proto-oncogene (*NRAS*), the GTPases (*HRAS* and *KRAS*), the Tyrosine-protein phosphatase non-receptor type 11 (*PTPN11*), the CCAAT/enhancer-binding protein alpha (*CEBPA*), the Phosphoinositide-3-kinase regulatory subunit alpha/beta/delta (*PIK3R1*), and the Kit legend (*KITLG*), to stimulate the proliferation of early hematopoietic cells, cell maturation, structural maintenance, associate cell surface growth factor receptors with the Ras signaling pathway, coordinate proliferation arrest and the differentiation of myeloid progenitors, among others. [data source: <https://string-db.org>, version 11.5] (last accessed 20 Sep 2022).

Cytogenetic abnormalities are detected in 50%–61% of AML patients at diagnosis.⁽²⁹⁾ For patients with normal karyotype, either the reverse transcriptase-polymerase chain reaction (RT-PCR) technique or the fluorescent in situ hybridization (FISH) is essential to detect any cryptic rearrangement of the relevant locus.⁽³⁰⁾ Based on the cytogenetic findings for AML patients, they are classified into three groups for their prognostic risk: (i) favorable group with balanced translocations, including t(15;17), t(8;21), inv(16) or t(16;16); (ii) intermediate risk group with normal karyotype, t(9;11) with no additional abnormalities, or isolated +8; (iii) adverse risk group with t(6;9), inv(3), or complex karyotype (more than three chromosomal abnormalities).⁽²⁹⁻³¹⁾

As molecular genotyping and cytogenetic studies have an increasingly measurable impact on clinical decision-making for patients with AML, and there are limited related studies in our region, we were inspired to evaluate the molecular profiles of *NPM1* and *FLT3* mutations and correlate the results with the clinical and cytogenetic findings in a cohort of AML cases referred for molecular investigation in our hospital.

Materials and Methods

A total of 33 patients with AML referred to King Abdulaziz University Hospital from 2017 to 2020 were enrolled in the study. They have confirmed cases of AML based on the revised version of the myeloid neoplasms and acute leukemia definition of the WHO 2016 classification. Patients who started the treatment regimen and/or have low-quality extracted DNA were excluded.

The study was conducted in accordance with the Declaration of Helsinki and approved by the Research Bioethics Committee of the Center of Excellence in Genomic Medicine Research (CEGMR). Written informed consent was obtained from patients (or the participant's parent/guardian) before collecting the data.

NPM1 and FLT3-ITD fragment analysis and mutation detection

A total of 5mL of blood/bone marrow were collected on EDTA and sodium heparin tubes for molecular and cytogenetic testing, respectively. Genomic DNA was isolated using the QIAamp DNA Kit (Cat# 51304, Qiagen, Hilden, Germany) following the manufacturer-supplied protocol. Nucleic acid concentration at 260nm and purity ratio at 260/280nm were determined by a NanoDrop 2000c spectrophotometer (Thermo Scientific, Waltham, MA, USA). The extracted DNA samples were stored at -70°C until use. PCR analysis for the extracted DNA was done using GoTaq® Green Master Mix (Cat# M7122, Promega, Madison, USA), which contains two types of identification dyes that allow monitoring of PCR product progress during the gel electrophoresis (<https://worldwide.promega.com/resources/protocols/product-information-sheets/g/gotaq-green-master-mix-m712-protocol/>). The PCR reaction was carried out in a 25-µL reaction volume containing 10µL GoTaq Green Master Mix and 1.0µL (10 pmol) of each primer, with 100ng genomic DNA completed to the final volume by the DNAsae- free distilled water. Appropriate negative (no template) and positive controls for both genes

in each run were applied. The primers applied in the PCR reaction (Table 1) were designed by OligoPerfect™ Designer (ThermoFisher Scientific), available at www.lifetechnologies.com, in CEGMR laboratory. The forward *FLT3* and the reverse *NPM1* primers were labeled with FAM and HEX dyes, respectively. These dyes are excited by the dual-mode argon laser of the 3500 Series Genetic Analyzer (Applied Biosystems), and the detector identifies the intensity of the emitted fluorescence during the capillary electrophoresis.

Table 1.

The applied primer sequences of the studied NPM1 and FLT3 genes

Gene name	Primer sequences (5' to 3')
NPM1-F	GTT TCT TTT TTT TTT TTT CCA GGC TAT TCA AG
NPM1-R	HEX-CAC GGT AGG GAA AGT TCT CAC TCT GC
FLT3-F	FAM-AGC AAT TTA GGT ATG AAA GCC AGC TA
FLT3-R	CTT TCA GCA TTT TGA CGG CAA CC
FLT3-D835H- F	CCG CCA GGA ACG TGC TTG
FLT3-D835H-R	GCA GCC TCA CAT TGC CCC

F: forward; *R*: reverse; *D835H*: the first nucleotide G of DNA sequence coding for D835H is substituted with C, resulting in an Aspartate to Histidine amino-acid change.

Capillary electrophoresis and data analysis

After the samples were amplified, each PCR product was loaded on the 3500 Series Genetic Analyzer with an internal lane size standard GeneScan™ 500 LIZ™ Size Standard (Life Technologies, USA) to normalize differences in electrophoretic mobility between injections or gel lanes and to allow for automatic sizing of the products.^(32,33) The analyzer performs fragment sizing during data collection, and the data were managed by GeneScan® Analysis Software. The sample electropherograms showed fluorescence intensity as a function of fragment size. Depending on the fragment size, the *NPM1* and *FLT3* wild type (Wt) (170 bp and 330 bp) vs. mutated (170/174 bp and 330/351 bp) alleles, respectively, can be distinguished.

FLT3-ITD⁺ allelic ratio calculation

The allelic ratio of *FLT3-ITD⁺* was calculated by the following formula: [mutated allele peak area/(mutated allele peak area + Wt allele peak area)].⁽³⁴⁾ The allelic ratio of *FLT3-ITD⁺* can be used to specify the prognosis of *FLT3-ITD⁺* carrier patients following the ELN recommendations. Patients with a high allelic ratio (≥ 0.5) have a poor prognosis, while patients with a low allelic ratio (< 0.5) have a favorable prognosis, particularly if combined with *NPM1* mutation.⁽⁷⁾

FLT3-TKD⁺ mutation detection by DNA sequencing

The purified PCR products were cycle sequenced in an ABI 3500/3500XL Genetic analyzer using BigDye® Terminator version 3.1 Cycle Sequencing Kit (Applied Biosystems, USA) on ABI 3730XL Gene Analyzer (Applied Biosystems, USA) following the manufacturer's protocol. Briefly, the master mix for cycle sequencing included 2µl sequencing buffer (5x), 1µl Big Dye Terminator ready

reaction premix, 1 µl for either primer (3.2 pmol) (Table 1), and 5 µl nuclease-free water to be added to 1 µl of purified PCR (10 µl) product. The ready-made pGEM®-3Zf⁺ DNA and M13 forward primer (Applied Biosystems) were applied as control during the sequencing analysis. The cycle sequencing conditions were the first stage of initial denaturation at 95°C for 1 min, then 35 cycles each of denaturation at 96°C for 10 sec, annealing at 59°C for 5 sec, and extension at 60°C for 4 min, followed by cooling stage for 10 min at 4 °C. The sequencing results were analyzed by FinchTV Software and compared to the *FLT3* sequence on the ensemble (<https://useast.ensembl.org/>).

Chromosomal analysis

Karyotyping was carried out for all cases according to the International System for Human Cytogenetic Nomenclature⁽³⁵⁾ to detect structural and numerical abnormalities using CytoVision Software v3.6 (Leica Biosystems, USA). For each case, 20 metaphases were analyzed, and in the case of mosaicism, the number was raised to 50 metaphases. Based on the cytogenetic findings, the patients were classified into three groups for their prognostic risk.⁽³¹⁾

Statistical analysis was performed using GraphPad Prism 7.0 and statistical software package SPSS version 20.0 (Armonk, NY: IBM Corp.). The normality of distribution of continuous variables was tested by the Shapiro-Wilk test. Baseline characteristics were summarized as frequencies and percentages for categorical variables. Continuous variables with normal distribution were presented as mean (standard deviation [SD]); non-normal variables were reported as median. Means of 2 continuous normally distributed variables were compared by independent samples Student's t test. Group comparisons with respect to categorical variables are performed using chi-square test. A probability value of $P < 0.05$ was considered statistically significant.

The study was conducted according to the guidelines of the Declaration of Helsinki and approved by the Research Bioethics Committee of the Center of Excellence in Genomic Medicine Research (CEGMR) (approval no. 06-CEGMR-Bioeth2019).

Results

The mean age of AML patients was 36.7±20.6 years, and 63.6% of patients were men (Table 2). According to the French-American-British (FAB) classification, the predominant type in the present cohort was AML-M5, accounting for 30.3%, followed by the AML-M4 at 9.1% and the AML-M3 at 6.1%. AML-M1, M2, M6, and therapy-related AML patients each accounted for 3%, while the remaining 42.4% were not classified.

NPM1 and FLT3 mutational profile

Following a screening of the study participants using fragment analysis and sequencing, the majority of patients (25/75.8%) had wild-type *NPM1/FLT3*, one patient (3.1%) had *FLT3-ITD*⁺, four (12.1%) patients had *NPM1*⁺, two (6.1%) had combined *NPM1*⁺ with *FLT3-ITD*⁺ and one patient (3.1%) had combined *NPM1*⁺/*FLT3-ITD*⁺/*FLT3-TKD*⁺ profile. Examples of an electropherogram of FLT3 and NPM1 results are shown

in Figure 2. The Sequencing result of one *FLT3-TKD* case is shown in Figure 3. In the combined *NPM1*⁺/*FLT3-ITD*⁺ group, the allelic ratio of *FLT3-ITD* was calculated as explained previously, to conclude the prognostic impact of *FLT3-ITD*⁺. The calculated ratios for the three patients were 0.48, 0.23, and 0.37, respectively.

Cytogenetic study findings

Out of 33 AML patients investigated, 12(36.3%) patients had normal karyotypes (Table 2). The t(8;21) was presented in 9.1% of cases, inv(16) in 6.1%, del(7) in 6.1%, and the other types of cytogenetic abnormalities represented 3.1% of cases for each. The complex karyotype (more than three chromosomal abnormalities) was found in 18.2% of cases (Table 2).

Table 2.

Demographic and clinical data of the study patients with AML

Parameters		n=33	
Age	Age (Mean ± SD), years	36.7±20.6	
Sex	Male : Female	21:12	
CBC	WBC (Mean ± SD), (cell//µL)	32.5±31.7	
	Blast (Mean ± SD), count (%)	41.1±32.8	
AML Subtypes	M1	1(3.1%)	
	M2	1(3.1%)	
	M3	2(6.1%)	
	M4	3(9.1%)	
	M5	10(30.3%)	
	M6	1(3.1%)	
	Therapy-related AML	1(3.1%)	
	Not Classified	14(42.4%)	
	Cytogenetics	Normal	12(36.3%)
		Complex	6(18.2%)
t(8;21)		3(9.1%)	
inv(16)		2(6.1%)	
del(7)		2(6.1%)	
t(8;21), -Y		1(3.1%)	
t(8;21), del (9)		1(3.1%)	
t(15;17)		1(3.1%)	
+8		1(3.1%)	
del(13)		1(3.1%)	
t(1;11)		1(3.1%)	
t(18,22), trisomy 22		1(3.1%)	
+9, ins(11)	1(3.1%)		

CBC: complete blood count; WBC: white blood cells; complex: more than 3 chromosomes have abnormality; t: translocation; inv: inversion; del: deletion; ins: insertion.

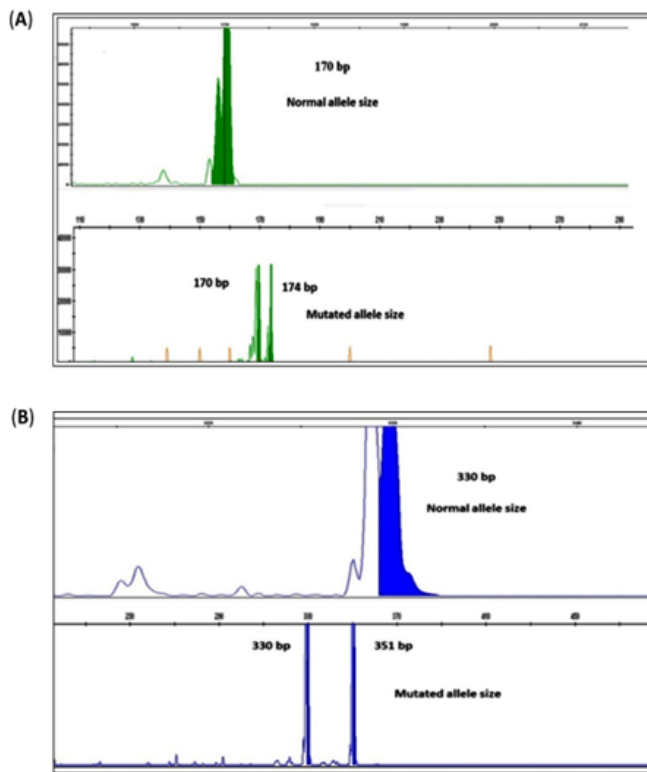


Figure 2. An example of an electropherogram for *NPM1* and *FLT3* alleles. (A) For *NPM1*, the electropherogram shows one peak of 170 bp in Wt *NPM1* (upper panel) and two peaks of 170 bp and 174 bp in the case of heterozygous *NPM1* mutation (lower panel). (B) For *FLT3-ITD*, the electropherogram shows one peak of 330 bp in wild-type (Wt) *FLT3* (upper panel) and two peaks of 330 bp and 351 bp in the case of heterozygous *FLT3-ITD*⁺ (lower panel).

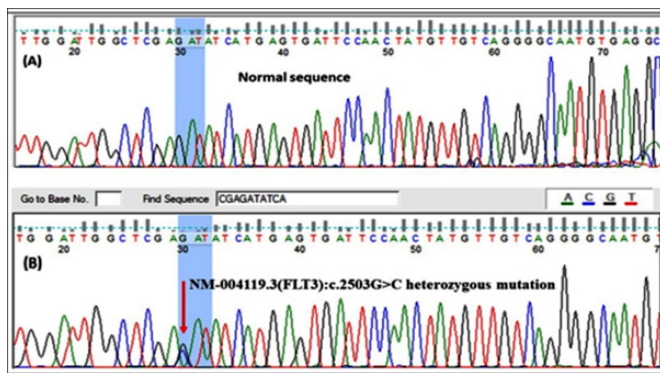


Figure 3. An example of *FLT3-TKD* Sequencing results. (A) Normal sequence. (B) Heterozygous *FLT3-TKD* mutation, in which the first nucleotide G of D835 is substituted with C, resulting in an Aspartate to Histidine amino-acid change (D835H).

Association of *NPM1* and *FLT3* mutational profiles with the clinical characteristics

Based on the *NPM1* and *FLT3* mutational profiles of the study participants, patients were classified into four different groups: *NPM1*⁻/*FLT3*⁻ (Wt), *NPM1*⁺, *FLT3*⁺, and dual positivity group *NPM1*⁺/*FLT3*⁺. Carriers of both gene mutant alleles had the highest median age of 42 (a range of 37-63). Males predominated in all subgroups. Carriers of either dual wild or mutant alleles of both study genes exhibited 60% (15/25) and 66.6% (2/3) mortality rates, respectively (Table 3).

Table 3.

The clinical features among different mutational profiles in the study cohort

	<i>NPM1</i> ⁻ / <i>FLT3</i> ⁻ n = 25	<i>NPM1</i> ⁺ n = 4	<i>FLT3-ITD</i> ⁺ n = 1	<i>NPM1</i> ⁺ / <i>FLT3-ITD</i> ⁺ n = 3
Median age	35	22.5	14	42
Age range	5-76	9-38	14	37-63
Male: Female	15:10	3:1	1:0	2:1
M1	1(4%)	-	-	-
M2	1(4%)	-	-	-
M3	1(4%)	-	-	1(33.3%)
M4	3(12%)	-	-	-
M5	8(32%)	1(25%)	-	1(33.3%)
M6	1(4%)	-	-	-
Therapy related	-	-	-	-
NOS*	-	1(25%)	-	-
Unknown classification	10(40%)	2(50%)	1(100%)	1(33.3%)
Favorable risk karyotype	7(28%)	1(25%)	-	-
Intermediate risk karyotype	8(32%)	2(50%)	1(100%)	3(100%)
Un-favorable risk karyotype	8(32%)	1(25%)	-	-
Death	15(60%)	2(50%)	-	2(66.6%)
In remission	7(28%)	1(25%)	1	1(33.3%)
Without remission	3(12%)	1(25%)	-	-

*Not otherwise specified, according to the WHO classification of AML.

The subgroups were compared according to the CBC results (Figure 4). The dual positivity group (*NPM1*⁺/*FLT3*⁺) significantly had a higher WBC count with a median of $81.3 \times 10^3/\mu\text{L}$ compared to other groups: Wt ($20.9 \times 10^3/\mu\text{L}$), $P=0.008$; *NPM1*⁺ ($16.26 \times 10^3/\mu\text{L}$), $P=0.036$. Also, the *FLT3*⁺ subgroup showed a significantly higher WBC median than the *NPM1*⁺ subgroup ($P=0.029$) (Figure 4A).

Furthermore, the combined mutations subgroup (*NPM1*⁺/*FLT3*⁺) significantly had a higher blast count (88.5%) in the peripheral blood compared to other subgroups (Wt subgroup (34%), $P=0.024$; *FLT3*⁺ (39%), $P=0.009$; *NPM1*⁺ (35%), $P=0.049$) (Figure 4B). The *NPM1*⁺ subgroup had the highest Hb level among the other subgroups, and there was a significant difference between the Wt subgroup and *NPM1*⁺ subgroup ($P=0.002$) (Figure 4E). Regarding the count of RBCs and platelets, there were no significant differences between the different subgroups (Figure 4C&D).

The clinical association between the mutations and the cytogenetic findings

A total of 63.6% of patients had abnormal cytogenetics. The most common abnormality was complex karyotype, found in the Wt-*NPM1*⁻/*FLT3*⁻ group only (Table 4). The *FLT3-ITD*⁺ patient had trisomy 8. The *NPM1*⁺ group had two patients with normal karyotype, one patient with t(8;21), and one patient with del(13). The *NPM1*⁺/*FLT3-ITD*⁺ group had normal karyotypes in all patients (Table 4). The cytogenetic abnormalities of prognostic significant and molecular mutations results are summarized in Table 3.

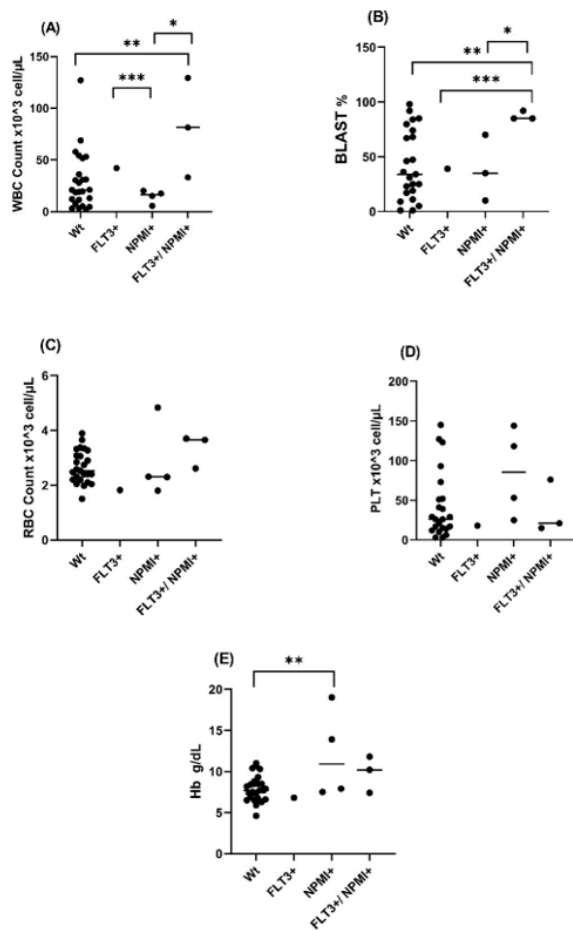


Figure 4. Comparison of the hematological parameters among the different AML subgroups. (A) White blood cell (WBC) count, * $P=0.036$, ** $P=0.008$, *** $P=0.029$, (B) Blast percentage, * $P=0.049$, ** $P=0.024$, *** $P=0.009$, (C) Red blood cell (RBC) count, (D) Platelet (PLT) count, and (E) Hemoglobin (Hb) concentration, ** $P=0.002$. An unpaired *t*-test was applied.

Table 4.

Cytogenetic findings frequencies among different mutation profiles in the study cohort

	NPM1 ⁻ / FLT3 ⁻ n = 25	NPM1 ⁺ n = 4	FLT3-ITD ⁺ n = 1	NPM1 ⁺ / FLT3-ITD ⁺ n = 3
Normal karyotype	7(28%)	2(50%)	0	3(100%)
Complex karyotype	6(24%)	0	0	0
t(8;21)	2(8%)	1(25%)	0	0
inv(16)	2(8%)	0	0	0
del(7)	2(8%)	0	0	0
t(8;21,-Y)	1(4%)	0	0	0
t(8;21), del(9)	1(4%)	0	0	0
t(15;17)	1(4%)	0	0	0
Trisomy 8	0	0	1(100%)	0
del(13)	0	1(25%)	0	0
Trisomy 9, ins(11)	1(4%)	0	0	0
t(1;11)	1(4%)	0	0	0
t(18,22), trisomy 22	1(4%)	0	0	0

Complex: more than 3 chromosomes have abnormality;
t: translocation; inv: inversion; -: loss; del: deletion; ins: insertion.

Discussion

Recent evidence supports the diagnostic/prognostic utility of molecular aberrations for AML cases.⁽²⁹⁾ The *NPM1* and *FLT3* mutations are the most common genetic mutations in AML, associated with a favorable prognosis in the case of the *NPM1* mutation and a poor prognosis in the *FLT3*.^(21,36) Unravelling the prevalence of these mutations in patients with AML is greatly valuable in predicting patients' prognosis, planning for the appropriate therapeutic regimen, and monitoring patients' response to the therapy.^(37,38) In this sense, we aimed to explore *NPM1* and *FLT3* mutation frequencies and features in our tertiary health center.

In this study, the most frequent FAB leukemia subtype was M5, which agrees with another study in Jeddah, which indicated that this subtype is common in the Saudi⁽³⁹⁾ population. Meanwhile, other studies showed M3 as the most frequent AML subtype.⁽⁴⁰⁾ In Egypt, Jordan, and Pakistan, M2 was reported to be the most frequent subtype.⁽⁴⁰⁻⁴³⁾

The *NPM1* mutation was implicated in apoptosis and cell cycle regulation in AML. The related mutation shifts the NPM1 protein, which is essential for the stability of FBW7 γ (important in the degradation of the oncoprotein MYC) and ARF (important in the stability of P53), to the cytoplasm with subsequent malignant transformation. This occurs because the mutated NPM will bind and enhance degradation of the above-mentioned proteins, contributing to attenuation of the oncosuppressor pathway and augmentation of oncogenic mechanisms augmentation in the cell.⁽⁴⁴⁾

For the *NPM1* mutation, the frequency in the present study was 21% (including the combined cases with FLT3; 9%). This rate is higher than reported by Alrajeh et al.,⁽⁴⁰⁾ with a 12% recorded frequency rate. Other studies reported a range between 6%-48.6% for *NPM1* mutation frequency (Table 5).⁽⁴⁵⁻⁵¹⁾ This variation could be attributed to the differences in the ethnicity and epidemiology of AML in different countries.

Table 5.

Prevalence of *NPM1* mutations in AML in other studies

Authors	Country	Number of patients	% <i>NPM1</i> mutation
Alsobhi et al. ⁽³⁹⁾	Saudi Arabia (Jeddah)	87	11.5%
Alrajeh et al. ⁽⁴⁰⁾	Saudi Arabia (Riyadh)	100	12%
Wang et al. ⁽⁴⁵⁾	China	76	26.3%
Haferlach et al. ⁽⁴⁶⁾	Germany	805	48.6%
Dalal et al. ⁽⁴⁷⁾	Canada	83	46%
Daver et al. ⁽⁴⁸⁾	USA	145	16%
Chauhan et al. ⁽⁴⁹⁾	India	161	21%
Marshall et al. ⁽⁵⁰⁾	South African	160	7.5%
Koczkodaj et al. ⁽⁵¹⁾	Poland	50	6%
Rubio et al. ⁽⁶⁵⁾	Argentina	216	4.2%

For the *NPM1*⁺ group, which was reported to have a favorable outcome, the patients showed a poor prognosis, which seems to differ from other studies. However, this finding confirms that AML prognosis is variable and depends on the clinical features of the patients, such as “patient age, performance status, and comorbidities,” as well as a constellation of “leukemia-specific genetic features.”^(52,53)

The second gene studied in the current work is coding for the FLT3 receptor protein. On ligand binding, this receptor synergizes with other interleukins and growth factors in the bone marrow to stimulate the progenitor cells to survive, proliferate and differentiate.⁽⁵⁴⁾ The pro-survival function of FLT3 may be mediated by phosphorylation of the proapoptotic BAD protein, by induction of the anti-apoptotic BCL-2, or by preventing the induction of the proapoptotic BAX. FLT3 receptor with ITD initiates the activation of the Ras and PI3K pathways in a similar way to the wild-type receptor, although STAT5 may play a more critical role in *FLT3-ITD*⁺ signaling.⁽⁵⁵⁾ *FLT3-ITD*⁺ has also been shown to inhibit the Forkhead transcription factor (FOXO3) function, thereby inhibiting induction of the proapoptotic BIM protein.⁽⁵⁶⁾

The *FLT3-ITD* mutation found in exons 14 and 15 of the gene results in the addition of many amino acids in the juxta membrane domain that impact the auto-inhibitory function of the FLT3 receptor. The length of the duplicated region varies from 3bp to 400bp, but always, the resultant transcripts are in-frame. Approximately 20%–30% of AML patients carry the *FLT3-ITD* mutation in the *FLT3* gene, which leads to uncontrolled cellular proliferation, survival, and differentiation through constitutive activation of *FLT3*.^(36,57,58)

The total frequency of *FLT3-ITD* in the current study was 12% (including the combined cases with *NPM1*). This number is consistent with other studies that stated *FLT3* more commonly occurs in patients with mutated *NPM1* than Wt *NPM1*.^(59,60) Alrajeh et al.⁽⁴⁰⁾ and Gari et al.⁽⁶¹⁾ reported frequencies of 9% (9/100) and 11.6% (15/129), respectively. In contrast, Alsobhi et al.⁽³⁹⁾ reported a frequency of 4.6% (4/87) (Table 6). However, the frequency was lower (2.3%) in Jastaniah et al.⁽⁶²⁾ The reason for this discrepancy could be due to the difference in sample size and the age of the study participants as the later study, for example, enrolled children only. The study frequency for *FLT3-ITD*⁺ was lower than in other countries. The reported range in the literature was between 8% and 47%. This difference could be due to the variable epidemiology of AML in different countries. (Table 6).^(41,45-51,63-68)

The patient with the *FLT3-ITD*⁺ mutation alone had trisomy and was in remission. Different factors can impact the prognosis of patients with the *FLT3-ITD*⁺ mutation, including patient age, the number of *FLT3* mutations the same patient has, co-excising mutations, and the type of chemotherapy used.⁽⁵⁸⁾ The patient with the *FLT3-ITD*⁺ mutation in the current study was 14 years old. In elderly patients with AML carrying the *FLT3-ITD*⁺ mutation, the survival rate is low due to many factors, including the increased risk of having high-risk cytogenetic abnormalities (i.e., monosomy 5, monosomy 7, or complex karyotypes) or resistant disease and poor performance status.⁽⁴⁸⁾ However, here, it is difficult to determine the mutation impact based on only one patient, and it can be considered a limitation in the current study.

Table 6.

Summary of the prevalence of *FLT3* mutations in patients with AML in other studies

Authors	Country	Number of patients	% FLT3
Alsobhi et al. ⁽³⁹⁾	Saudi Arabia (Jeddah)	87	4.6% ITD
Alrajeh et al. ⁽⁴⁰⁾	Saudi Arabia (Riyadh)	100	9 % ITD
Ishfaq et al. ⁽⁴¹⁾	Pakistan	55	13.3% ITD
Wang et al. ⁽⁴⁵⁾	China	76	19.7% ITD
Haferlach et al. ⁽⁴⁶⁾	Germany	805	27.2% ITD
Dalal et al. ⁽⁴⁷⁾	Canada	83	47%
Daver et al. ⁽⁴⁸⁾	USA	390	12% ITD
Chauhan et al. ⁽⁴⁹⁾	India	161	25% ITD
Marshall et al. ⁽⁵⁰⁾	South Africa	160	12% ITD
Koczkodaj et al. ⁽⁵¹⁾	Poland	50	8% ITD
Gari et al. ⁽⁶¹⁾	Saudi Arabia (Jeddah)	129	11.62% ITD 8.5% TKD
Zaker et al. ⁽⁶³⁾	Iran	212	18% ITD
Stirewalt et al. ⁽⁶⁴⁾	USA	140	34 % ITD
Rubio et al. ⁽⁶⁵⁾	Argentina	216	10.2% ITD 7.9% TKD
Kumsaen et al. ⁽⁶⁶⁾	Thailand	52	19.2 % ITD
Perry et al. ⁽⁶⁷⁾	France	126	20.6% ITD 12.7% TKD
Kandeel et al. ⁽⁶⁸⁾	Egypt	257	21.7 % ITD
Fröhling et al. ⁽⁷²⁾	Germany	523	32% ITD 14% TKD
Bacher et al. ⁽⁷³⁾	Germany	3082	4.8% TKD

The prognosis of *NPM1*⁺/*FLT3-ITD*⁺ patients was determined according to the calculated *FLT3-ITD*⁺ mutated allelic ratio, which showed low allelic ratios for all patients. In contrast to Lyu et al.,⁽³⁴⁾ who considered a low ratio a good prognosis, two patients with a low allelic ratio died in our study. This event agrees with others, where a low mutated allelic ratio was not associated with a favorable prognosis.^(7,34,69) Further studies for patients with *NPM1*⁺/*FLT3-ITD*⁺ mutations are recommended to investigate the impact of allelic ratio on patients' prognosis.

The second most common type of *FLT3* mutation is found on exon 20, and it is a missense point mutation that occurs within the activation loop of the TKD of the receptor. This mutation is found in 5%-10% of the patients with AML and currently has no clinically significant impact.⁽³⁶⁾

In the present study, only one patient had the *FLT3-TKD* mutation, and interestingly, it was combined with mutated *NPM1*⁺/*FLT3-ITD*⁺. There was no adverse effect of the three mutations on the prognosis, as the patient was in remission status. A study by Boddu et al. found that the effect of combining the triple mutations has equivalent survival. Further studies are also recommended to investigate the effect of this type of three combined mutations.⁽⁷⁰⁾

For the *FLT3-TKD* mutation, the frequency was 3%, combined with *NPM1*⁺ and *FLT3-ITD*⁺. In Saudi Arabia, three studies for *FLT3-TKD* were found, and one of these studies was for AML in childhood, in which the frequency was 4.2%.⁽⁶²⁾ The second study included only five AML patients, and the rate was

40%.⁽⁷¹⁾ Gari's group found *FLT3-TKD* in 8%.⁽⁶¹⁾ Internationally, the rate was as follows: Argentina -7.9%, France - 12.7%, and Germany - 4.8% and 14% in two different studies (Table 6).^(72,73)

By comparing the available laboratory parameters among patient subgroups with different genetic profiles, we found that the WBC count and blast percentage were high in the *NPM1*⁺/*FLT3-ITD*⁺ and *FLT3-ITD*⁺ subgroups. Similarly, Marshal and colleagues had the same findings and traced this increment to the presence of the *FLT3* mutation, which results in continuous proliferation and a decrease in the apoptosis of cells.^(50,59)

The chromosomal analysis showed abnormal karyotypes in 63.6% of the cases. The most frequent karyotype result was the complex karyotype (18%). In Alrajeh's study,⁽⁴⁰⁾ the abnormal karyotype percentage was 64%, which is very close to our percentage; however, the difference was that the most frequent cytogenetic abnormalities were trisomy 8 and trisomy 21, representing 8% for each. Another study,⁽³⁹⁾ reported t(15;17) and complex karyotype as the most frequent abnormalities, with 17.2% and 13.8%, respectively.

Although the small sample size could limit the present study, the findings reflected our patients' genetic profiles regarding two common mutations that are helpful to be incorporated into the routine workup of the patients to pave the way for personalized medicine in AML in this region.

It is recommended that patients of intermediate risk group, based on karyotyping analysis with *Wt-NPM1/FLT3* genes, be further subjected to screening of other molecular mutations with prognostic significance, such as *IDH1*, *IDH2*, *WT1*, and *c-KIT*.^(31,36,74)

Conclusion

The prevalence of *FLT3* was found to be similar to that of other studies conducted in Saudi Arabia and lower than found in international studies. However, *NPM1* frequency was higher than in other Saudi studies. The *FLT3* mutation was primarily found combined with the *NPM1* mutation. Furthermore, the *FLT3* mutation was associated with increased WBC and blast percentages. Although AML with non-mutated *FLT3* or *NPM1* was the most prominent genetic subgroup of the present cohort, the *NPM1*⁺/*FLT3-ITD*⁺ subgroup was associated with normal karyotype, which agrees with other studies. The complex karyotype is the most frequent cytogenetic abnormality in the study cohort. Further molecular work for other gene mutations with prognostic significance in AML is strongly recommended to complete the big picture.

Acknowledgments

The authors would like to thank all study participants, King Abdulaziz University Hospital, and the Center of Excellence in Genomic Medicine Research (CEGMR) for providing the facilities to perform the current work.

Competing Interests

The authors declare that they have no competing interests.

References

- Döhner H, Weisdorf DJ, Bloomfield CD. Acute Myeloid Leukemia. *N Engl J Med*. Sep 17 2015;373(12):1136-52. doi:10.1056/NEJMra1406184
- Miranda-Filho A, Piñeros M, Ferlay J, Soerjomataram I, Monnereau A, Bray F. Epidemiological patterns of leukaemia in 184 countries: a population-based study. *Lancet Haematol*. Jan 2018;5(1):e14-e24. doi:10.1016/S2352-3026(17)30232-6
- Dong Y, Shi O, Zeng Q, Lu X, Wang W, Li Y, Wang Q. Leukemia incidence trends at the global, regional, and national level between 1990 and 2017. *Exp Hematol Oncol*. 2020 Jun 19;9:14. doi: 10.1186/s40164-020-00170-6.
- Alahmari B, Alzahrani M, Al Shehry N, Tawfiq O, Alwasaidi T, Alhejazi A, Bakkar M, Al Behainy A, Radwi M, Alaskar A. Management Approach to Acute Myeloid Leukemia Leveraging the Available Resources in View of the Latest Evidence: Consensus of the Saudi Society of Blood and Marrow Transplantation. *JCO Glob Oncol*. 2021 Jul;7:1220-1232. doi: 10.1200/GO.20.00660.
- Bawazir A, Al-Zamel N, Amen A, Akiel MA, Alhawiti NM, Alshehri A. The burden of leukemia in the Kingdom of Saudi Arabia: 15 years period (1999-2013). *BMC Cancer*. Jul 17 2019;19(1):703. doi:10.1186/s12885-019-5897-5
- Shallis RM, Wang R, Davidoff A, Ma X, Zeidan AM. Epidemiology of acute myeloid leukemia: Recent progress and enduring challenges. *Blood Rev*. 07 2019;36:70-87. doi:10.1016/j.blre.2019.04.005
- Döhner H, Estey E, Grimwade D, Amadori S, Appelbaum FR, Büchner T, Dombret H, Ebert BL, Fenaux P, Larson RA, Levine RL, Lo-Coco F, Naoe T, Niederwieser D, Ossenkoppele GJ, Sanz M, Sierra J, Tallman MS, Tien HF, Wei AH, Löwenberg B, Bloomfield CD. Diagnosis and management of AML in adults: 2017 ELN recommendations from an international expert panel. *Blood*. 2017 Jan 26;129(4):424-447. doi: 10.1182/blood-2016-08-733196.
- Tallman MS, Wang ES, Altman JK, Appelbaum FR, Bhatt VR, Bixby D, Coutre SE, De Lima M, Fathi AT, Fiorella M, Foran JM, Hall AC, Jacoby M, Lancet J, LeBlanc TW, Mannis G, Marcucci G, Martin MG, Mims A, O'Donnell MR, Olin R, Peker D, Perl A, Pollyea DA, Pratz K, Prebet T, Ravandi F, Shami PJ, Stone RM, Strickland SA, Wieduwilt M, Gregory KM; OCN; Hammond L, Ogburn N. Acute Myeloid Leukemia, Version 3.2019, NCCN Clinical Practice Guidelines in Oncology. *J Natl Compr Canc Netw*. 2019 Jun 1;17(6):721-749. doi: 10.6004/jnccn.2019.0028.
- Heuser M, Ofran Y, Boissel N, Brunet Mauri S, Craddock C, Janssen J, Wierzbowska A, Buske C; ESMO Guidelines Committee. Electronic address: clinicalguidelines@esmo.org. Acute myeloid leukaemia in adult patients: ESMO Clinical Practice Guidelines for diagnosis, treatment and follow-up. *Ann Oncol*. 2020 Jun;31(6):697-712. doi: 10.1016/j.annonc.2020.02.018.
- Takahashi S. Current findings for recurring mutations in acute myeloid leukemia. *J Hematol Oncol*. 2011 Sep 14;4:36. doi: 10.1186/1756-8722-4-36.
- Falini B, Nicoletti I, Martelli MF, Mecucci C. Acute myeloid leukemia carrying cytoplasmic/mutated nucleophosmin (NPMc+ AML): biologic and clinical features. *Blood*. Feb 01 2007;109(3):874-85. doi:10.1182/blood-2006-07-012252
- Gregory TK, Wald D, Chen Y, Vermaat JM, Xiong Y, Tse W. Molecular prognostic markers for adult acute myeloid leukemia with normal cytogenetics. *J Hematol Oncol*. Jun 02

2009;2:23. doi:10.1186/1756-8722-2-23

13. Catalano G, Niscola P, Banella C, Diverio D, Trawinska MM, Fratoni S, Iazzoni R, De Fabritiis P, Abruzzese E, Noguera NI. NPM1 Mutated, BCR-ABL1 Positive Myeloid Neoplasms: Review of the Literature. *Mediterr J Hematol Infect Dis.* 2020 Nov 1;12(1):e2020083. doi: 10.4084/MJHID.2020.083.

14. Dumber TS, Gentry GA, Olson MO. Interaction of nucleolar phosphoprotein B23 with nucleic acids. *Biochemistry.* 1989 Nov 28;28(24):9495-501. doi: 10.1021/bi00450a037.

15. Cordell JL, Pulford KA, Bigerna B, Roncador G, Banham A, Colombo E, Pelicci PG, Mason DY, Falini B. Detection of normal and chimeric nucleophosmin in human cells. *Blood.* 1999 Jan 15;93(2):632-42.

16. Falini B, Brunetti L, Sportoletti P, Martelli MP. NPM1-mutated acute myeloid leukemia: from bench to bedside. *Blood.* 2020 Oct 8;136(15):1707-1721. doi: 10.1182/blood.2019004226.

17. Grimwade D, Ivey A, Huntly BJ. Molecular landscape of acute myeloid leukemia in younger adults and its clinical relevance. *Blood.* 2016 Jan 7;127(1):29-41. doi: 10.1182/blood-2015-07-604496.

18. Arber D.A., Brunning R.D., Le Beau M.M., Falini B., Vardiman J.W., Porwit A., Thiele J., Foucar K., Dohner H., Bloomfield C.D. Acute myeloid leukaemia with recurrent genetic abnormalities. In: Swerdlow SH, Campo E, Harris NL, Jaffe ES, Pileri SA, Stein H, et al., editors. *WHO Classification of Tumors of Hematopoietic and Lymphoid Tissue.* International Agency for Research on Cancer; Lyon, France. 2017:141-142.

19. Verhaak RG, Goudswaard CS, van Putten W, Bijl MA, Sanders MA, Hagens W, Uitterlinden AG, Erpelinck CA, Delwel R, Löwenberg B, Valk PJ. Mutations in nucleophosmin (NPM1) in acute myeloid leukemia (AML): association with other gene abnormalities and previously established gene expression signatures and their favorable prognostic significance. *Blood.* 2005 Dec 1;106(12):3747-54. doi: 10.1182/blood-2005-05-2168.

20. Koh Y, Park J, Bae EK, Ahn KS, Kim I, Bang SM, Lee JH, Yoon SS, Lee DS, Lee YY, Park S, Kim BK. Non-A type nucleophosmin 1 gene mutation predicts poor clinical outcome in de novo adult acute myeloid leukemia: differential clinical importance of NPM1 mutation according to subtype. *Int J Hematol.* 2009 Jul;90(1):1-5. doi: 10.1007/s12185-009-0350-1.

21. Haslam K, Chadwick N, Kelly J, Browne P, Vandenberghe E, Flynn C, Conneally E, Langabeer SE. Incidence and significance of FLT3-ITD and NPM1 mutations in patients with normal karyotype acute myeloid leukaemia. *Ir J Med Sci.* 2010 Dec;179(4):507-10. doi: 10.1007/s11845-010-0567-2.

22. Schnittger S, Schoch C, Kern W, Mecucci C, Tschulik C, Martelli MF, Haferlach T, Hiddemann W, Falini B. Nucleophosmin gene mutations are predictors of favorable prognosis in acute myelogenous leukemia with a normal karyotype. *Blood.* 2005 Dec 1;106(12):3733-9. doi: 10.1182/blood-2005-06-2248

23. Pazhakh V, Zaker F, Alimoghaddam K, Atashrazm F. Detection of nucleophosmin and FMS-like tyrosine kinase-3 gene mutations in acute myeloid leukemia. *Ann Saudi Med.* 2011 Jan-Feb;31(1):45-50. doi: 10.4103/0256-4947.75778.

24. Park BG, Chi HS, Park SJ, Min SK, Jang S, Park CJ, Kim DY, Lee JH, Lee JH, Lee KH. Clinical implications of non-A-type NPM1 and FLT3 mutations in patients with normal karyotype acute myeloid leukemia. *Acta Haematol.* 2012;127(2):63-71. doi: 10.1159/000331509.

25. Grafone T, Palmisano M, Nicci C, Storti S. An overview

on the role of FLT3-tyrosine kinase receptor in acute myeloid leukemia: biology and treatment. *Oncol Rev.* 2012 Apr 17;6(1):e8. doi: 10.4081/oncol.2012.e8.

26. Abu-Duhier FM, Goodeve AC, Wilson GA, Gari MA, Peake IR, Rees DC, Vandenberghe EA, Winship PR, Reilly JT. FLT3 internal tandem duplication mutations in adult acute myeloid leukaemia define a high-risk group. *Br J Haematol.* 2000 Oct;111(1):190-5. doi: 10.1046/j.1365-2141.2000.02317.x.

27. Motyckova G, Stone RM. The role of molecular tests in acute myelogenous leukemia treatment decisions. *Curr Hematol Malig Rep.* 2010 Apr;5(2):109-17. doi: 10.1007/s11899-010-0049-7.

28. Kindler T, Lipka DB, Fischer T. FLT3 as a therapeutic target in AML: still challenging after all these years. *Blood.* 2010 Dec 9;116(24):5089-102. doi: 10.1182/blood-2010-04-261867.

29. Pourrajab F, Zare-Khormizi MR, Hashemi AS, Hekmatimoghaddam S. Genetic Characterization and Risk Stratification of Acute Myeloid Leukemia. *Cancer Manag Res.* 2020;12:2231-2253. doi:10.2147/CMAR.S242479

30. Kassem N, Hamid AA, Attia T, Baathallah S, Mahmoud S, Moemen E, Safwat E, Khalaf M, Shaker O. Novel mutations of the nucleophosmin (NPM-1) gene in Egyptian patients with acute myeloid leukemia: a pilot study. *J Egypt Natl Canc Inst.* 2011 Jun;23(2):73-8. doi: 10.1016/j.jnci.2011.09.003. Epub 2011 Oct 13. Erratum in: *J Egypt Natl Canc Inst.* 2012 Jun;24(2):105.

31. Slovak ML, Kopecky KJ, Cassileth PA, Harrington DH, Theil KS, Mohamed A, Paietta E, Willman CL, Head DR, Rowe JM, Forman SJ, Appelbaum FR. Karyotypic analysis predicts outcome of preremission and postremission therapy in adult acute myeloid leukemia: a Southwest Oncology Group/Eastern Cooperative Oncology Group Study. *Blood.* 2000 Dec 15;96(13):4075-83.

32. Durney BC, Criehtfield CL, Holland LA. Capillary electrophoresis applied to DNA: determining and harnessing sequence and structure to advance bioanalyses (2009-2014). *Anal Bioanal Chem.* 2015 Sep;407(23):6923-38. doi: 10.1007/s00216-015-8703-5.

33. Kristoff CJ, Bwanali L, Veltri LM, Gautam GP, Rutto PK, Newton EO, Holland LA. Challenging Bioanalyses with Capillary Electrophoresis. *Anal Chem.* 2020 Jan 7;92(1):49-66. doi: 10.1021/acs.analchem.9b04718.

34. Lyu M, Liao H, Shuai X, Jin Y, Su J, Zheng Q. The prognosis predictive value of FMS-like tyrosine kinase 3-internal tandem duplications mutant allelic ratio (FLT3-ITD MR) in patients with acute myeloid leukemia detected by GeneScan. *Gene.* 2020 Feb 5;726:144195. doi: 10.1016/j.gene.2019.144195.

35. Simons A, Shaffer LG, Hastings RJ. Cytogenetic Nomenclature: Changes in the ISCN 2013 Compared to the 2009 Edition. *Cytogenet Genome Res.* 2013;141(1):1-6. doi:10.1159/000353118

36. Renneville A, Roumier C, Biggio V, Nibourel O, Boissel N, Fenaux P, Preudhomme C. Cooperating gene mutations in acute myeloid leukemia: a review of the literature. *Leukemia.* 2008 May;22(5):915-31. doi: 10.1038/leu.2008.19.

37. Coles EC, Colita A, Momanu R, Berbec N, Ivanescu AM, Oprea M, Jardan D, Jardan C, Arghir A, Coriu D, Lupu AR. Importance of assessing cytogenetic and molecular risk factors in acute myeloid leukemia therapy. *J Med Life.* 2012 Oct-Dec;5(Spec Issue):36-43.

38. Zhou JR, Zhang X, Zhao YL, Yang JF, Zhang JP, Cao XY, Lu Y, Liu DY, Lyu FY, Ouyang J, Lu PH. [Clinical characteristics and prognosis of 34 cases of acute myeloid leukemia with FLT3

- internal tandem duplication and MLL gene rearrangement]. *Zhonghua Xue Ye Xue Za Zhi*. 2018 Sep 14;39(9):751-756. doi: 10.3760/cma.j.issn.0253-2727.2018.09.010. [Article in Chinese].
39. Alsobhi E, Farahat F, Daghistani M, Awad K, Al-Zahran O, Al-Saiari A, Koshak F. Overall survival of adult acute myeloid leukemia based on cytogenetic and molecular abnormalities during 5 years in a single center study. *Saudi Med J*. 2019 Nov;40(11):1171-1176. doi: 10.15537/smj.2019.11.24584.
40. Alrajeh A, Abalkhail H, Khalil S. Cytogenetics and molecular markers of acute myeloid leukemia from a tertiary care center in Saudi Arabia. *Journal of Applied Hematology*. 2017;8(2):68-74. doi:10.4103/joah.joah_57_16
41. Ishfaq M, Malik A, Faiz M, Sheikh I, Asif M, Khan MN, Qureshi MS, Zahid S, Manan A, Arooj M, Qazi MH, Chaudhary A, Alqahtani MH, Rasool M. Molecular characterization of FLT3 mutations in acute leukemia patients in Pakistan. *Asian Pac J Cancer Prev*. 2012;13(9):4581-5. doi: 10.7314/apjcp.2012.13.9.4581.
42. Adnan-Awad S, Gaber O, Eltokhy SA, Mourad D, Amer M, Kandeel EZ, Eldesouky I. FLT3-ITD Mutations in Egyptian Patients of Acute Myeloid Leukemia: Correlation with Cytogenetic, FAB Subgroups and Prognosis. *Clin Lab*. 2017 May 1;63(5):1027-1034. doi: 10.7754/Clin.Lab.2017.170121.
43. Halahleh K, Taqash A, Abdelkhalq H, Manasrah M, Marie L, Al-Rabi K. Analysis of FLT3-Activating Mutations in Patients With Acute Myelogenous Leukemia in Jordan: Association With FAB Subtypes and Identification of Subgroups With Poor Prognosis. *Clin Lymphoma Myeloma Leuk*. 2021 Jul;21(7):e588-e597. doi: 10.1016/j.clml.2021.02.006.
44. Di Fiore PP. Playing both sides: nucleophosmin between tumor suppression and oncogenesis. *J Cell Biol*. 2008 Jul 14;182(1):7-9. doi: 10.1083/jcb.200806069.
45. Wang L, Xu WL, Meng HT, Qian WB, Mai WY, Tong HY, Mao LP, Tong Y, Qian JJ, Lou YJ, Chen ZM, Wang YG, Jin J. FLT3 and NPM1 mutations in Chinese patients with acute myeloid leukemia and normal cytogenetics. *J Zhejiang Univ Sci B*. 2010 Oct;11(10):762-70. doi: 10.1631/jzus.B1000052.
46. Haferlach T, Bacher U, Alpermann T, Haferlach C, Kern W, Schnittger S. Amount of bone marrow blasts is strongly correlated to NPM1 and FLT3-ITD mutation rate in AML with normal karyotype. *Leuk Res*. 2012 Jan;36(1):51-8. doi: 10.1016/j.leukres.2011.04.026.
47. Dalal BI, Mansoor S, Manna M, Pi S, Sauro GD, Hogge DE. Detection of CD34, TdT, CD56, CD2, CD4, and CD14 by flow cytometry is associated with NPM1 and FLT3 mutation status in cytogenetically normal acute myeloid leukemia. *Clin Lymphoma Myeloma Leuk*. 2012 Aug;12(4):274-9. doi: 10.1016/j.clml.2012.01.003.
48. Daver N, Liu Dumlaio T, Ravandi F, Pierce S, Borthakur G, Pemmaraju N, Nazha A, Faderl S, Jabbour E, Garcia-Manero G, Cortes J, Kantarjian H, Quintás-Cardama A. Effect of NPM1 and FLT3 mutations on the outcomes of elderly patients with acute myeloid leukemia receiving standard chemotherapy. *Clin Lymphoma Myeloma Leuk*. 2013 Aug;13(4):435-40. doi: 10.1016/j.clml.2013.02.021.
49. Chauhan PS, Ihsan R, Singh LC, Gupta DK, Mittal V, Kapur S. Mutation of NPM1 and FLT3 genes in acute myeloid leukemia and their association with clinical and immunophenotypic features. *Dis Markers*. 2013;35(5):581-8. doi: 10.1155/2013/582569.
50. Marshall RC, Tlagadi A, Bronze M, Kana V, Naidoo S, Wiggill TM, Carmona SC. Lower frequency of NPM1 and FLT3-ITD mutations in a South African adult de novo AML cohort. *Int J Lab Hematol*. 2014 Dec;36(6):656-64. doi: 10.1111/ijlh.12204.
51. Koczkodaj D, Zmorzyński S, Michalak-Wojnowska M, Wąsik-Szczepanek E, Filip AA. Examination of the FLT3 and NPM1 mutational status in patients with acute myeloid leukemia from southeastern Poland. *Arch Med Sci*. 2016 Feb 1;12(1):120-8. doi: 10.5114/aoms.2015.49811.
52. Peterlin P, Renneville A, Ben Abdelali R, Nibourel O, Thomas X, Pautas C, de Botton S, Raffoux E, Cayuela JM, Boissel N, Terré C, Celli-Lebras K, Castaigne S, Preudhomme C, Gardin C, Dombret H. Impact of additional genetic alterations on the outcome of patients with NPM1-mutated cytogenetically normal acute myeloid leukemia. *Haematologica*. 2015 May;100(5):e196-9. doi: 10.3324/haematol.2014.115576.
53. DiNardo CD, Cortes JE. Mutations in AML: prognostic and therapeutic implications. *Hematology Am Soc Hematol Educ Program*. 2016 Dec 2;2016(1):348-355. doi: 10.1182/asheducation-2016.1.348.
54. Kiyoi H, Yanada M, Ozekia K. Clinical significance of FLT3 in leukemia. *Int J Hematol*. 2005 Aug;82(2):85-92. doi: 10.1532/IJH97.05066.
55. Markovic A, MacKenzie KL, Lock RB. FLT-3: a new focus in the understanding of acute leukemia. *Int J Biochem Cell Biol*. 2005 Jun;37(6):1168-72. doi: 10.1016/j.biocel.2004.12.005.
56. Choudhary C, Müller-Tidow C, Berdel WE, Serve H. Signal transduction of oncogenic Flt3. *Int J Hematol*. 2005 Aug;82(2):93-9. doi: 10.1532/IJH97.05090.
57. El Fakih R, Rasheed W, Hawsawi Y, Alsermani M, Hassanein M. Targeting FLT3 Mutations in Acute Myeloid Leukemia. *Cells*. 2018 Jan 8;7(1):4. doi: 10.3390/cells7010004.
58. Abou Dalle I, Ghorab A, Patel K, Wang X, Hwang H, Cortes J, Issa GC, Yalniz F, Sasaki K, Chihara D, Price A, Kadia T, Pemmaraju N, Daver N, DiNardo C, Ravandi F, Kantarjian HM, Borthakur G. Impact of numerical variation, allele burden, mutation length and co-occurring mutations on the efficacy of tyrosine kinase inhibitors in newly diagnosed FLT3- mutant acute myeloid leukemia. *Blood Cancer J*. 2020 May 4;10(5):48. doi: 10.1038/s41408-020-0318-1.
59. Döhner K, Schlenk RF, Habdank M, Scholl C, Rücker FG, Corbacioglu A, Bullinger L, Fröhling S, Döhner H. Mutant nucleophosmin (NPM1) predicts favorable prognosis in younger adults with acute myeloid leukemia and normal cytogenetics: interaction with other gene mutations. *Blood*. 2005 Dec 1;106(12):3740-6. doi: 10.1182/blood-2005-05-2164.
60. Thiede C, Koch S, Creutzig E, Steudel C, Illmer T, Schaich M, Ehninger G. Prevalence and prognostic impact of NPM1 mutations in 1485 adult patients with acute myeloid leukemia (AML). *Blood*. 2006 May 15;107(10):4011-20. doi: 10.1182/blood-2005-08-3167.
61. Gari M, Abuzenadah A, Chaudhary A, Al-Qahtani M, Banni H, Ahmad W, Al-Sayes F, Lary S, Damanhour G. Detection of FLT3 oncogene mutations in acute myeloid leukemia using conformation sensitive gel electrophoresis. *Int J Mol Sci*. 2008 Nov;9(11):2194-2204. doi: 10.3390/ijms9112194.
62. Jastaniah W, Al Ghemlas I, Al Daama S, Ballourah W, Bayoumy M, Al-Anzi F, Al Shareef O, Alsultan A, Abrar MB, Al Sudairy R. Clinical characteristics and outcome of childhood

- de novo acute myeloid leukemia in Saudi Arabia: A multicenter SAPHOS leukemia group study. *Leuk Res.* 2016 Oct;49:66-72. doi: 10.1016/j.leukres.2016.08.009.
63. Zaker F, Mohammadzadeh M, Mohammadi M. Detection of KIT and FLT3 mutations in acute myeloid leukemia with different subtypes. *Arch Iran Med.* 2010 Jan;13(1):21-5.
64. Stirewalt DL, Kopecky KJ, Meshinchi S, Appelbaum FR, Slovak ML, Willman CL, Radich JP. FLT3, RAS, and TP53 mutations in elderly patients with acute myeloid leukemia. *Blood.* 2001 Jun 1;97(11):3589-95. doi: 10.1182/blood.v97.11.3589. Erratum in: *Blood* 2001 Aug 15;98(4):924.
65. Rubio P, Campos B, Digiorge JA, Gallego MS, Medina A, Rossi JG, Felice MS, Alonso CN. NPM1, FLT3 and CEBPA mutations in pediatric patients with AML from Argentina: incidence and prognostic value. *Int J Hematol.* 2016 Nov;104(5):582-590. doi: 10.1007/s12185-016-2064-5.
66. Kumsaen P, Fucharoen G, Sirijerachai C, Chainansamit SO, Wisanuyothin N, Kuwatjanakul P, Wiangnon S. FLT3-ITD Mutations in Acute Myeloid Leukemia Patients in Northeast Thailand. *Asian Pac J Cancer Prev.* 2016;17(9):4395-4399.
67. Perry M, Bertoli S, Rocher C, Hayette S, Ducastelle S, Barraco F, Labussière-Wallet H, Salles G, Recher C, Thomas X, Paubelle E. FLT3-TKD Mutations Associated With NPM1 Mutations Define a Favorable-risk Group in Patients With Acute Myeloid Leukemia. *Clin Lymphoma Myeloma Leuk.* 2018 Dec;18(12):e545-e550. doi: 10.1016/j.clml.2018.06.006.
68. Kandeel EZ, El Sayed G, Elsharkawy N, Eldin DN, Nassar HR, Ibrahiem D, Amin R, Hanafi M, Khalil M, Kamel A. Impact of FLT3 Receptor (CD135) Detection by Flow Cytometry on Clinical Outcome of Adult Acute Myeloid Leukemia Patients. *Clin Lymphoma Myeloma Leuk.* 2018 Aug;18(8):541-547. doi: 10.1016/j.clml.2018.05.014.
69. Sakaguchi M, Yamaguchi H, Najima Y, Usuki K, Ueki T, Oh I, et al. Prognostic impact of low allelic ratio *FLT3*-ITD and *NPM1* mutation in acute myeloid leukemia. *Blood Adv.* 2018 Oct 23;2(20):2744-2754. doi: 10.1182/bloodadvances.2018020305.
70. Boddu P, Kantarjian H, Borthakur G, Kadia T, Daver N, Pierce S, Andreeff M, Ravandi F, Cortes J, Kornblau SM. Co-occurrence of *FLT3*-TKD and *NPM1* mutations defines a highly favorable prognostic AML group. *Blood Adv.* 2017 Aug 17;1(19):1546-1550. doi: 10.1182/bloodadvances.2017009019.
71. FM A-D, Rashid Mir R, Javid J, Sharaf F, Burrow N. Optimization of allele specific PCR (AS-PCR) for the early detection of FLT3 (D835Y) mutation in Acute Myeloid Leukemia patients at Tabuk, Saudi Arabia. *International Journal of Advanced Research (IJAR).* 2017;5(1):817-822. doi:10.21474/ijar01/2819
72. Fröhling S, Schlenk RF, Breitnick J, Benner A, Kreitmeier S, Tobis K, Döhner H, Döhner K; AML Study Group Ulm. Acute myeloid leukemia. Prognostic significance of activating FLT3 mutations in younger adults (16 to 60 years) with acute myeloid leukemia and normal cytogenetics: a study of the AML Study Group Ulm. *Blood.* 2002 Dec 15;100(13):4372-80. doi: 10.1182/blood-2002-05-1440.
73. Bacher U, Haferlach C, Kern W, Haferlach T, Schnittger S. Prognostic relevance of FLT3-TKD mutations in AML: the combination matters--an analysis of 3082 patients. *Blood.* 2008 Mar 1;111(5):2527-37. doi: 10.1182/blood-2007-05-091215.
74. Yohe S. Molecular Genetic Markers in Acute Myeloid Leukemia. *J Clin Med.* 2015 Mar 12;4(3):460-78. doi: 10.3390/jcm4030460.
-

Characterization of Incidental Liver Lesions: Comparison of Multidetector CT versus Ultrasonography

Hanady Elyas Osman

Radiologic Sciences Program, Batterjee Medical College, Jeddah, Saudi Arabia

Abstract

Background: Due to recent advancements in imaging techniques, as well as the widespread use of routine medical exams and screenings, incidental liver lesions are now more frequently discovered by ultrasound (US). Physicians must decide whether to simply follow up when incidental liver lesions are discovered in the US or to order additional imaging tests for lesion classification. The goal of our study was to identify liver lesions using multidetector computed tomography (MDCT) and US.

Methods and Results: A total of 50 participants were selected from a variety of male and female patients with abdominal pain and suspected liver diseases, and received a CT triphasic scan and US at the Royal Care International Hospital, Ibn Alhaitham Diagnostic Center, Alfaisal Specialized Hospital, and the Department of Diagnostic Radiology in the CT department of Sudan from April 2018 to May 2020.

The results of the ultrasound scanning (liver lesions and related findings) performed on patients before the CT scanning indicated that ascites + liver lesions was predominant (48.6%). The incidental liver lesions that take peripheral nodular enhancement by MDCT when contrast media is injected, were liver metastases (30%), hemangioma (14%), and hepatocellular carcinoma (10%). Liver cysts represent 10(20%) of the total cases of lesions that were non-enhanced by CT, with a few cases of liver cirrhosis (2%), hepatosplenomegaly (2%), and cyst + hepatitis (2%). We found a significant relationship between peripheral nodular enhancement for liver lesions by MDCT and non-enhancing liver lesions ($P=0.001$).

Conclusion: The US and CT scan findings have a statistically significant relationship ($P\leq 0.017$). Contrast-enhanced CT performs better at diagnosing liver lesions than does standard US. (**International Journal of Biomedicine. 2023;13(1):84-90.**)

Keywords: liver lesions • multidetector computed tomography • ultrasonography • contrast-enhanced computed tomography

For citation: Osman HE. Characterization of Incidental Liver Lesions: Comparison of Multidetector CT versus Ultrasonography International Journal of Biomedicine. 2023;13(1):84-90. doi:10.21103/Article13(1)_OA10

Abbreviations

CT, computed tomography; CM, contrast media; DP, delayed phase; EAP, early arterial phase; HCC, hepatocellular carcinoma; MDCT, multidetector computed tomography; MRI, magnetic resonance imaging; PVP, portal venous phase; US, ultrasound.

Introduction

With technological advancements in ultrasound (US), multidetector computed tomography (MDCT), and magnetic resonance imaging (MRI), we are now better able to identify low-contrast lesions and small hepatic lesions that would have gone undetected a few years ago.^(1,2)

A significant contribution to the assessment of patients with liver illness has been made by multiphase, contrast-enhanced dynamic computed tomography (CT) of the entire liver. Any lesion in the liver that is not part of the normal parenchyma and that causes structural or functional abnormalities in the hepatobiliary system is referred to as a *focal liver lesion*.⁽³⁾

MDCT has entered clinical use over the past few years. Compared to standard abdominal X-rays, CT scans of the liver and biliary tract can offer more detailed information about the liver, gallbladder, and related structures. This can help reveal more about injuries and/or diseases of the liver and biliary

*Corresponding author: Dr. Hanady Elyas Osman, Assistant Professor in Diagnostic Radiology, Radiologic Sciences Program, Batterjee Medical College, Jeddah, Saudi Arabia. E-mail: hanadyelyas86@gmail.com.

tract. The placement of needles during liver biopsies or the aspiration (extraction) of fluid from the area of the liver and/or biliary tract may also be visualized using CT scans of the liver and biliary tract.⁽⁴⁾

Ultrasonography is noninvasive, reasonably priced, and widely available. Many clinicians request it as the initial imaging modality for assessing the upper abdomen, including the liver, to quickly and efficiently narrow the differential diagnosis. Ultrasonography is particularly helpful in differentiating between cystic and solid lesions.^(5,6)

The liver has two blood supplies, and it is known that the time between the start of the contrast inflow from the portal vein and the start of the contrast inflow from the arteries defines the duration of the virtual hepatic arterial phase. Contrast agents can help characterize and detect localized liver lesions more accurately than US. Since diagnosing these lesions depends mostly on contrast resolution, a good contrast-to-noise ratio is crucial for successful lesion detection. The contrast is dependent on both the liver parenchyma and the CT attenuation of the localized lesion. The most popular imaging technique to identify and characterize hepatic metastasis is MDCT.⁽⁷⁾

Materials and Methods

The investigation was carried out concurrently at the Royal Care International Hospital, Ibn Alhaitham Diagnostic Center, Alfaisal Specialized Hospital, and the Department of Diagnostic Radiology in the CT department of Sudan from April 2018 to May 2020. A total of 50 participants were selected from a variety of male and female patients with abdominal pain and suspected liver diseases, and received a CT triphasic scan and US.

Inclusion and exclusion criteria

All patients who underwent abdominal CT and sonography aged between 25-85 years with abdominal pain and suspected liver diseases were included. Children, hepatectomy patients' and normal patients after sonogram were excluded from the study.

Patient position and techniques

Alfaisal Specialized Hospital. The patient was in the supine position with feet-first scanning. We used Toshiba Asteion-4, a 4-slice CT scanner with 120 KVP, and 200 MAS. A triphasic protocol A triphasic protocol (sure start protocol) was started after obtaining a scout view of one slice above the liver before starting the scan's early arterial phase (EAP), portal venous phase (PVP), and delayed phase (DP) with an automatic injection flow rate of 4ml/sec and an 18-gauge needle for injection.

The Royal Care International Hospital. The triphasic protocol was used with a Toshiba 64-slice (Aquilion) CT scanner (120 KVP, 125 MAS) and automatic injection of 70-100 ml Omnipaque contrast medium at a flow rate of 3.5 ml/sec. The scans were taken in the EAP, PVP, and DP. After the injection, the scan starts instantly, and the DP is performed 10 minutes later. Slice thickness is 5mm per slice, the patient position is supine, and each water bottle contains 10ml of the oral contrast medium (500 ml total).

The Ibn Alhaitham Diagnostic Center. The triphasic protocol was used with a Toshiba 4-slice CT scanner (Japan), using 120 KVP, 125 MAS. A triphasic protocol starts with an EAP scan (20 seconds after injection), a PVP scan (40 seconds after injection), and a DP scan (5-10 minutes after injection). The scans are taken at each phase automatically using 75 ml of Omnipaque contrast medium (40-50 ml for pediatric, according to weight). After the injection, the scan starts immediately, and the DP is performed 10 minutes later. Slices are 10 mm thick, and each water bottle contains 10 ml of the 500 ml oral contrast medium. The coronal region is the first slice, followed by the plain film without contrast medium and triphasic protocol scanning with contrast medium.

The Antalya Medical Center. The patient was supine with feet-first scanning from the sternal angle to the symphysis pubis. The CT machine (USA) was an 8-slice, bride-speed model (120 KVP, 165 MAS). The triphasic protocol is also used, starting with the automatic injection of 75 ml of Omnipaque contrast medium for adults at a flow rate of 3.5 ml/sec, followed by scans of the EAP, PVP, and DP. The scan immediately starts with a slice thickness of 5mm, and the reconstruction method takes 2.5 mm.

According to the triphasic protocol, the first scan is without contrast medium on plain film, followed by the scout (coronal section). Phased array transducers that operate between 3MHz and 5MHz are used to perform abdominal US.⁽⁸⁾

Statistical analysis was performed using statistical software package SPSS version 23.0 (Armonk, NY: IBM Corp.). Group comparisons were performed using chi-square test with Yates correction. A probability value of $P < 0.05$ was considered statistically significant.

Ethical approvals were obtained from the Radiologic Sciences Program, Batterjee Medical College (Jeddah, Saudi Arabia). The data was only used for study purposes without individual details identifying the participant.

Results

By convenient sampling, we selected 50 patients (22 men and 28 women), who underwent CT triphasic scans. The age distribution of the study sample participants was as follows: 25-34 years [3(6%)], 35-44 years [12(24.0%)], 45-54 years [18(36%)] and ≥ 65 years [17(34%)], with a mean age of 59.28 ± 12.67 years, minimum age of 27 years and maximum age of 85 years (Fig. 1).

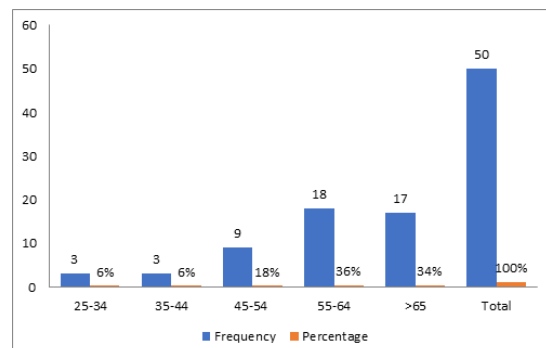


Fig. 1. The age distribution of the study sample participants.

The results of the ultrasound scanning (liver lesions and related findings) performed on patients before the CT scanning indicated that ascites+ liver lesions was predominant (48.6%) (Table 1).

Table 1.

The US scanning findings.

Diagnosis	Percentages (%)
Ascites + liver lesions	48.0
Liver lesions + hepatosplenomegaly	6.0
Multiple focal subdiaphragmatic + subcapsular lesions+ multiple mesenteric and para-aortic lymphadenopathies	6.0
Liver lesion + pancreatic tumor	6.0
Liver cyst	4.0
Liver mass	4.0
Hydatid liver cyst	2.0
Abdominal and pelvic mass + bilateral ovarian dermoid cysts	2.0
Liver lesions + prostate cancer	2.0
Fatty liver	2.0
HCC	2.0
Liver lesions + adnexal mass	2.0
Liver lesions + hemoperitoneum	2.0
Liver lesions + old TB granuloma	2.0
Liver lesions + sigmoid tumor	2.0
Hepatosplenomegaly + portal hypertension	2.0
Liver metastases	2.0
Liver mass+ right inguinal hernia	2.0
Liver lesions + right renal stone	2.0
Total	100.0

The incidental liver lesions characterized by CT were liver metastases (30%), liver cyst (20%), liver hemangioma (14%) and HCC (10%) (Table 2).

Table 2.

CT scanning results (liver lesions and associated findings).

Diagnosis	Percentages (%)
Liver metastases	30.0
Cyst	20.0
Hemangioma	14.0
HCC	10.0
HCC + liver cirrhosis	8.0
Liver abscess	6.0
Cyst + hepatitis	2.0
Hemangioma + old calcified granuloma	2.0
Hepatosplenomegaly	2.0
Liver cirrhosis	2.0
Liver metastases + hepatosplenomegaly	2.0
Liver metastases + lymphoma	2.0
Total	100.0

The incidental liver lesions that take peripheral nodular enhancement by MDCT when CM is injected, were liver metastases (30%), hemangioma (14%), and HCC (10%) (Table 3 A). Liver cysts represent 10(20%) of the total cases of lesions that were non-enhanced by CT, with a few cases of liver cirrhosis (2%), hepatosplenomegaly (2%), and cyst + hepatitis (2%) (Table 3B). We found a significant relationship between peripheral nodular enhancement for liver lesions by MDCT and non-enhancing liver lesions ($P=0.001$). When the US and CT scan findings were compared, a statistically significant relationship ($P\leq 0.017$) was found (Table 4).

Table 3A.

Peripheral nodular enhancement for liver lesion by MDCT.

CT (diagnosis)	Peripheral nodular enhancement
Hemangioma	7
	14.0%
Hemangioma + old calcified granuloma	1
	2.0%
HCC	5
	10.0%
HCC + liver cirrhosis	4
	8.0%
Liver abscess	3
	6.0%
Liver metastases	15
	30.0%
Liver metastases + hepatosplenomegaly	1
	2.0%
Liver metastases + lymphoma	1
	2.0%
Total	36
	72.0%

Table 3B.

Non-enhance liver lesions characterized by MDCT

CT (diagnosis)	Non-enhance enhancement
Cyst	10
	20.0%
Cyst + hepatitis	1
	2.0%
Hepatosplenomegaly	1
	2.0%
Liver cirrhosis	1
	2.0%
Liver metastases	1
	2.0%
Total	14
	28.0%

Table 4.

Ultrasonographic findings cross-tabulated with CT scanning diagnosis.

US Report (Diagnosis)	CT Report (Diagnosis)											Total
	Cyst	Cyst + hepatitis	Hemangioma + old calcified granuloma	HCC	HCC+ liver cirrhosis	Hepatosplenomegaly	Liver abscess	Liver cirrhosis	Liver metastases	Liver metastases + hepatosplenomegaly	Liver metastases + lymphoma	
Abdominal and pelvic mass + ovarian dermoid cysts/adnexa	-	-	2.0%	-	-	-	-	-	2.0%	-	-	4.0%
Ascites/ hepatic lesion	12.0%	2.0%	8.0%	8.0%	4.0%	-	4.0%	-	10.0%	-	-	48.0%
Liver lesions + prostate cancer	-	-	-	-	-	-	-	-	2.0%	-	-	2.0%
Fatty liver	-	-	-	-	-	2.0%	-	-	-	-	-	2.0%
HCC	-	-	2.0%	-	-	-	-	-	-	-	-	2.0%
Hepatic lesion + hemoperitoneum	-	-	2.0%	-	-	-	-	-	-	-	-	2.0%
Hepatic lesion + hepatosplenomegaly	-	-	2.0%	-	-	-	-	-	2.0%	2.0%	-	6.0%
Hepatic lesion + old TB granuloma	-	-	-	2.0%	-	-	-	-	-	-	-	2.0%
Hepatic lesion + sigmoid tumor	-	-	-	-	-	-	-	-	2.0%	-	-	2.0%
Hepatosplenomegaly + portal hypertension	-	-	-	-	2.0%	-	-	-	-	-	-	2.0%
Hydatid liver cyst	2.0%	-	-	-	-	-	-	-	-	-	-	2.0%
Liver cyst	2.0%	-	-	-	-	-	2.0%	-	-	-	-	4.0%
Liver mass	-	-	-	-	-	-	-	-	4.0%	-	-	4.0%
Liver metastases	-	-	-	-	-	-	-	-	2.0%	-	-	2.0%
Multiple focal subdiaphragmatic + subcapsular lesions, multiple mesenteric + para-aortic lymphadenopathies	-	-	-	-	2.0%	-	-	2.0%	-	-	2.0%	6.0%
Pancreatic tumor + multiple hepatic lesion	4.0%	-	-	-	-	-	-	-	2.0%	-	-	6.0%
Right inguinal hernia + liver mass	-	-	-	-	-	-	-	-	2.0%	-	-	2.0%
RT renal stone+ hepatic lesion	-	-	-	-	-	-	-	-	2.0%	-	-	2.0%
Total	20.0%	2.0%	16.0%	10.0%	8.0%	2.0%	6.0%	2.0%	30.0%	2.0%	2.0%	100.0%
P-value	≤0.017											

Discussion

In patients with liver lesions, the aim of imaging is crucial to identify and characterize those lesions and to

determine what is the most frequent lesion diagnosed by MDCT and US. CT scans are performed on patients with hepatic malignancies to rule out the presence of metastases and estimate the degree of local involvement. From our

study, we found that a liver abscess is characterized by a thick, irregular wall, internal echogenicity or debris, and flow signals in the wall. Hemangioma is a homogeneous echogenic lesion with an echogenic peripheral rim and no or few peripheral or intralesional flow signals. Heterogeneous echogenic lesions, hypoechoic rims, and peripheral or internal artery flow signals are all characteristics of liver metastases. A heterogeneous echogenic lesion with a target sign, hypoechoic halo, and little to no peripheral flow signals is liver metastasis.⁽⁹⁾



Image 1. A 40-year-old male patient. Axial CT image arterial phase shows peripheral enhancement of hemangioma.

In our study, by convenient sampling, we selected 50 patients (22 men and 28 women), who underwent CT triphasic scans. The age distribution of the study sample participants was as follows: 25-34 years [3(6%)], 35-54 years [12(24.0%)], 55-64 years [18(36%)] and ≥ 65 years [17(34%)], with a mean age of 59.28 ± 12.67 years, minimum age of 27 years and maximum age of 85 years (Fig. 1).

Before getting a CT scan, patients had a US to check for liver lesions and other findings. In our cases (Table 1), liver lesions were found by ultrasonography and diagnosed following the above standards.⁽⁹⁾ However, lesions were not specifically mentioned; rather, they were only reported as liver lesions. Table 2 displays the CT scan results of liver lesions and related findings.

Although it might be challenging to differentiate hepatic lesions based solely on imaging criteria, some focal liver lesions have well-defined ultrasonic and CT characteristics. It is crucial to stress that the main goal of imaging the liver is to differentiate between benign, metastatic, and initial malignant lesions. The best method for imaging the liver to detect localized liver disease is still debatable.⁽¹⁰⁾

Imaging is essential to diagnosing and treating HCC patients. Dynamic cross-sectional CT imaging techniques have also been used for HCC diagnosis and staging, although ultrasound is currently the primary diagnostic imaging tool for HCC. The use of CT is supported by recent technological developments in CT that relate to reducing radiation exposure, optimizing tissue characterization, and developing targeted contrast agents in various enhancement phases. The liver

cirrhosis and HCC enhancement patterns are shown in Table 3 (A&B), respectively. We found a significant relationship between peripheral nodular enhancement for liver lesions by MDCT and non-enhancing liver lesions ($P=0.001$).

Until proven differently, a liver mass in a cirrhotic liver should be considered an HCC. Malignant and benign lesions are both diagnosed as liver masses in cirrhotic livers. Ultrasound was used to identify a hepatic mass, and contrast-enhanced MDCT was used to define the mass. The hepatic lesion and cirrhosis are described differently by each modality, depending on the presence of certain nodules and other elements. The characteristics of the liver masses and lesions in the cirrhotic and non-cirrhotic liver were demonstrated in the current study. HCC occurs as a supplementary improvement. Although ultrasound is the main surveillance imaging tool for HCC, dynamic contrast-enhanced CT and MRI are used primarily for diagnosis and staging of HCC.⁽¹¹⁾

Regarding the cysts, similar descriptions were given in the study by P. Kar and J. Rajat,⁽¹²⁾ which stated that on CT, cysts appear as a well-defined intrahepatic lesion with water attenuation (0-15 HU), round or oval with smooth thin walls and homogeneous appearance with no internal structures. Cases with cysts appear as non-enhanced in 11(22.0%) cases as hypo-dense non-enhancing focal lesions and no enhancement after contrast administration.



Image 2. A 85-year-old male patient. Axial abdominal contrast-enhanced CT shows HCC with liver cirrhosis

The liver abscess in the current study has been described as a peripheral nodular enhancement and rounded hypo-dense localized hepatic lesion in 3(6%) of the cases. According to prior research, the most effective approach for detecting liver abscesses is CT.^(12,13) There are limitations to the CT diagnosis of liver abscess. Sometimes, the CT's appearance is neither specific nor diagnostic. In the series described from our study, abscesses ranged in appearance from fluid-filled cavities with clean margins to ill-defined masses with densities somewhat lower than the liver's surrounding tissue. Similar findings were described in the series of Rubinson et al.,⁽¹⁴⁾ where the appearance of a hyperdense rim on a CT scan following contrast enhancement is thought to be

evidence of an abscess, as in our study findings. Rubinson with colleagues showed that CT scanning of the abdomen in 50 patients evaluated for suspected intraabdominal abscess resulted in an overall accuracy of 92 percent.⁽¹⁴⁾

The most widely used method for imaging the liver in Sudan is US, which is also the main method for looking for liver metastases in many nations. US diagnosis has a smaller role in the United States due to the relative accessibility of CT and less physician engagement in US performance. When there is little to no suspicion of metastases, US frequently finds liver masses in patients. The screening for metastases is done less often with US. Studies comparing US to other imaging modalities show that it has higher specificity but lower sensitivity. Metastases can be hypoechoic, hyperechoic, cystic, or diffuse when detected by US. Normal hepatic arteries are commonly displaced by metastases.⁽¹⁵⁾

When the US and CT scan findings were compared, a statistically significant relationship ($P \leq 0.017$) was found (Table 4). This indicates that liver lesions can be detected and identified via ultrasonography. Due to its superior spatial and contrast resolution, ultrasonography can provide information about the liver and liver masses without the need for contrast agents, unlike CT scans. Liver cysts were found and confidently diagnosed, and a variety of solid mass manifestations pointed to a particular diagnosis. An echogenic or isoechoic liver mass with a hypoechoic halo or rim suggested that it was likely cancerous. This was also mentioned in earlier studies, and masses with this morphologic characteristic prompted confirmatory imaging with CT scans, some of which revealed the same findings and others with different results.

The small sample size of our study, particularly for benign lesions, is one of its limitations. Further, there was no calculation of interobserver agreement for CT picture interpretation. The diagnosis in cases of localized lesions was dependent on the radiologist's judgment and the CT/US diagnostic criteria rather than a biopsy. Another potential drawback is that multiple CT scanners of various makes were used for the scans.

Conclusion

Anatomical normality, pathologic alterations, and relationships to neighboring structures can all be seen using the highly spatially resolved MDCT technology. Additionally, the speed of MDCT scanning has improved, enabling quick and precise multiphasic imaging with brief breath-holding intervals. The accuracy of the presentation of enhancement and through-plane resolution of multiphasic liver imaging have both been greatly enhanced by the combination of MDCT and optimized administration of the contrast-agent. We can find tiny lesions by using thinner slices. Finally, contrast-enhanced CT performs better at diagnosing liver lesions than does standard US. However, an abdominal MDCT exposes the patient to a large amount of radiation. Consequently, the number of required scans and the use of reduced collimation should be precisely adhered to for each patient, with regard to the individual clinical concern and history.

Acknowledgments

I would like to express my special appreciation and thanks to the staff at the Sudan University of Science and Technology, College of Medical Radiological Science and Radiology Department in Alfaisal Specialized Hospital, Ibn Alhaitham Diagnostic Centre, Antalya Medical Centre, and Royal Care International Hospital for their help in data collection.

Competing Interests

The author declares that there is no conflict of interest in this work.

References

1. Schwartz LH, Gandras EJ, Colangelo SM, Ercolani MC, Panicek DM. Prevalence and importance of small hepatic lesions found at CT in patients with cancer. *Radiology*. 1999 Jan;210(1):71-4. doi: 10.1148/radiology.210.1.r99ja0371. PMID: 9885589.
2. Khalil HI, Patterson SA, Panicek DM. Hepatic lesions deemed too small to characterize at CT: prevalence and importance in women with breast cancer. *Radiology*. 2005 Jun;235(3):872-8. doi: 10.1148/radiol.2353041099. Epub 2005 Apr 15. PMID: 15833992.
3. Wilson SR, Jang HJ, Kim TK, Burns PN. Diagnosis of focal liver masses on ultrasonography: comparison of unenhanced and contrast-enhanced scans. *J Ultrasound Med*. 2007 Jun;26(6):775-87; quiz 788-90. doi: 10.7863/jum.2007.26.6.775. PMID: 17526609.
4. Furuta A, Ito K, Fujita T, Koike S, Shimizu A, Matsunaga N. Hepatic enhancement in multiphasic contrast-enhanced MDCT: comparison of high- and low-iodine-concentration contrast medium in same patients with chronic liver disease. *AJR Am J Roentgenol*. 2004 Jul;183(1):157-62. doi: 10.2214/ajr.183.1.1830157. PMID: 15208131.
5. Adam A, Dixon AK, Gillard JH, Schaefer-Prokop C, Grainger RG, Allison DJ. Grainger & Allison's Diagnostic Radiology E-Book. Elsevier Health Sciences; 2014 Jun 16.
6. Rumack CM, Wilson SR, Charboneau JW. Diagnostic Ultrasound Volume 1. 3rd Edition, Elsevier Mosby, Philadelphia; 2005.
7. Kulinna C, Schima W. Imaging Features of Hepatic Metastases: CT and MR. In: Lencioni, R., Cioni, D., Bartolozzi, C. (Eds) Focal Liver Lesions. Medical Radiology. Springer, Berlin, Heidelberg; 2005.
8. Iannaccone R, Piacentini F, Murakami T, Paradis V, Belghiti J, Hori M, Kim T, Durand F, Wakasa K, Monden M, Nakamura H, Passariello R, Vilgrain V. Hepatocellular carcinoma in patients with nonalcoholic fatty liver disease: helical CT and MR imaging findings with clinical-pathologic comparison. *Radiology*. 2007 May;243(2):422-30. doi: 10.1148/radiol.2432051244. Epub 2007 Mar 13. PMID: 17356175.
9. Xu HX, Liu GJ, Lu MD, Xie XY, Xu ZF, Zheng YL, Liang JY. Characterization of small focal liver lesions using real-time contrast-enhanced sonography: diagnostic

- performance analysis in 200 patients. *J Ultrasound Med.* 2006 Mar;25(3):349-61. doi: 10.7863/jum.2006.25.3.349. PMID: 16495496.
10. Soyer P, Sirol M, Fargeaudou Y, Duchat F, Hamzi L, Boudiaf M, Aout M, Guerrache Y, Vicaut E, Rymer R. Differentiation between true focal liver lesions and pseudolesions in patients with fatty liver: evaluation of helical CT criteria. *Eur Radiol.* 2010 Jul;20(7):1726-37. doi: 10.1007/s00330-009-1708-8. Epub 2010 Jan 19. PMID: 20084385.
11. Davarpanah AH, Weinreb JC. The role of imaging in hepatocellular carcinoma: the present and future. *J Clin Gastroenterol.* 2013 Jul;47 Suppl:S7-10. doi: 10.1097/MCG.0b013e31827f0d3d. PMID: 23632342.
12. Kar P, Rajat J. Imaging of Space Occupying Lesions of Liver. *Medicine Update -2011.* Available from: <https://citeseerx.ist.psu.edu/document?repid=rep1&type=pdf&doi=255509ad2c77122b331a9a3874b45dc557e33b92>
13. Butt AS, Hamid S, Wadalawala AA, Ghufraan M, Javed AA, Farooq O, Ahmed B, Ul Haq T, Jafri W. Hepatocellular carcinoma in Native South Asian Pakistani population; trends, clinico-pathological characteristics & differences in viral marker negative & viral-hepatocellular carcinoma. *BMC Res Notes.* 2013 Apr 8;6:137. doi: 10.1186/1756-0500-6-137. PMID: 23566475; PMCID: PMC3637624.
14. Robison JG, Pollock TW. Computed tomography in the diagnosis and localization of intraabdominal abscesses. *Am J Surg.* 1980 Dec;140(6):783-6. doi: 10.1016/0002-9610(80)90117-8. PMID: 7457703.
15. Senturk S, Cetin B, Cengiz M, Bilici A, Ozekinci S. Dynamic multidetector computed tomography findings of hepatocellular carcinoma of hepatitis B virus-positive and -negative patients. *Cancer Imaging.* 2014 Apr 22;14(1):9. doi: 10.1186/1470-7330-14-9. PMID: 25608603; PMCID: PMC4331841.
-

Assessment of Pancreatic Duct Dilation in Patients with Pancreatic Cancer and Chronic Pancreatitis using Ultrasonography: A Retrospective Study

Zuhal Y. Hamd¹, Awadia Gareeballah^{2*}, Ahmed E. Abdelsalam³, Sumaiah S. Alshebl¹, Ghaida A. Aldawas¹, Rawabi M. Alqahtani¹, Riyaf A. Almuhatib¹, Rahaf F. Madani¹, Basim Abdullah Salih Alhomida⁴

¹Department of Radiological Sciences, College of Health and Rehabilitation Sciences, Princess Nourah bint Abdulrahman University, Riyadh, Saudi Arabia

² Department of Diagnostic Radiologic Technology, College of Applied Medical Science, Taibah University, Medina, Saudi Arabia

³Department of Ultrasound, Radiology Services Operations Administration, King Fahad Medical City, Riyadh, Saudi Arabia

⁴College of Medicine, Almaarefa University, Riyadh, Saudi Arabia

Abstract

Background: The present study aimed to assess the main pancreatic duct (PD) in patients with chronic pancreatitis (CP) and pancreatic cancer (PC) to determine the prevalence of dilation in both conditions.

Methods and Results: A retrospective study was conducted at King Fahad Medical City in Riyadh from December 2019 to March 2020 on the use of ultrasonography to assess PD in patients with PC and CP. The sample included 73 patients: 39 (21 females and 18 males) with PC and 34 (20 males and 14 females) with CP. The diameter of the main PD was measured by ultrasonography. The mean age for PC patients was 61.17 ± 13.96 years, and for CP patients was 42.14 ± 17.08 years ($P=0.000$). The diameter of the main PD in PC was 0.52 ± 0.22 cm, and in CP, it was 0.51 ± 0.28 cm ($P=0.865$). Our results suggest that the dilation of the PD is one feature that accompanies PC and CP. In our study, there was no significant difference in the prevalence of dilation in both conditions (64.1% and 64.7%). Additionally, PC is 2.4 times more likely to be associated with diabetes mellitus than CP.

Conclusion: PC occurs more commonly in the older age group, while CP occurs more commonly in the younger age group. Most cases of PC and CP were associated with dilation of the PD with no significant difference in the amount of dilation. (International Journal of Biomedicine. 2023;13(1):91-94.)

Keywords: pancreatic cancer • chronic pancreatitis • ultrasound • pancreatic duct dilatation

For citation: Hamd ZY, Gareeballah A, Abdelsalam AE, Alshebl SS, Aldawas GA, Alqahtani RM, Almuhatib RA, Madani RF, Alhomida BAS. Assessment of Pancreatic Duct Dilation in Patients with Pancreatic Cancer and Chronic Pancreatitis using Ultrasonography: A Retrospective Study. International Journal of Biomedicine. 2023;13(1):91-94. doi:10.21103/Article13(1)_OA11

Abbreviations

CP, chronic pancreatitis; ERCP, endoscopic retrograde pancreatography; MRCP, magnetic resonance cholangiopancreatography; PD, pancreatic duct; PC, pancreatic cancer.

Introduction

The pancreas is both an exocrine accessory digestive organ and a hormone-secreting endocrine gland. The

exocrine portion consists of acinar and duct tissue, and an endocrine portion is made up of islets of Langerhans. Chronic pancreatitis (CP) is a common chronic inflammatory disease that causes irreversible changes in the pancreatic parenchyma

and function. Pancreatic cancer (PC) is one of the most lethal diseases.⁽¹⁾ The most common type of PC begins in the cells that line the ducts (pancreatic ductal adenocarcinoma). Previous studies have suggested that CP markedly increases the risk of PC, varying from 2.2- to 26.7-fold.⁽¹⁻⁴⁾ Known risk factors for PC also include diabetes mellitus, obesity, cigarette smoking, family history of PC, heavy alcohol consumption, and a history of acute pancreatitis.⁽⁵⁾

Several imaging modalities, including abdominal ultrasonography, ERCP, MRCP, and CT, can be used to diagnose pancreatic disorders.^(6,7) A frequently encountered condition is a dilated pancreatic duct (PD). PD dilatation can be caused by cancers or benign neoplasms. Dilated PDs can result from pancreatic tumors and, under the right circumstances, may require endoscopic evaluation and therapy, including stenting and dilation. PD dilatation can occur secondary to CP and may or may not warrant endoscopic intervention, depending on the overall symptom profile. Finally, the PD may dilate due to aging or normal physiological processes.⁽⁸⁾ The PD assessment is important in the cases of PC and CP to aid in managing the disease. In cancer cases, PD dilatation is linked with the advanced stage.

The present study aimed to assess the main PD in patients with CP and pancreatic carcinomas to determine the prevalence of dilation in both conditions.

Materials and Methods

A retrospective study was conducted at King Fahad Medical City in Riyadh from December 2019 to March 2020 on the use of ultrasonography to assess PD in patients with PC and CP. The sample included 73 patients: 39 (21 females and 18 males) with PC and 34 (20 males and 14 females) with CP. Patients with other pancreatic diseases, such as acute pancreatitis, pancreatic cysts, or pancreatic stones, were excluded.

Ultrasound technique

The pancreas was examined by abdominal ultrasound scanning with a low-frequency curve transducer to maintain deep penetration and full clearance to improve image quality (Philips iU22 and GE logiq E9 XDclear 2.0 Ultrasound Machine). The pancreas was scanned with the patients in a state of fasting for at least 6 hours before the appointment to eliminate stomach gases, which usually obscure images of the pancreas when the patient is in the supine position. With the patient lying supine, the gel was applied to the patient's skin at the midline of the abdomen to eliminate the air between the transducer and the skin; transverse and longitudinal scanning of the pancreas was performed using B-mode grayscale image and color Doppler. The diameter of the main PD was measured at the body on the longitudinal view of the pancreas, between the upper edge of the anterior line and the posterior line of the main pancreatic duct. The normal limit of the main PD diameter in the area of the body was up to 2 mm; if the diameter is more than 2 mm, it is considered to be a dilated PD (Figure 1).

Statistical analysis was performed using statistical software package SPSS version 23.0 (Armonk, NY: IBM Corp.). Group comparisons were performed using chi-square

test with Yates correction. A probability value of $P < 0.05$ was considered statistically significant.

The study was conducted in accordance with the Declaration of Helsinki and approved by the Ethics Committee of Princess Nourah bint Abdulrahman University (No 20-0051), with institutional review board (IRB) approval from King Fahad Medical City. The data was only used for study purposes without individual details identifying the participant.

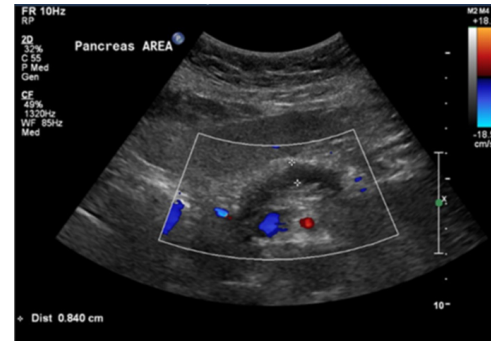


Fig. 1. US: pancreatic duct.

Results

PC was more common in the age group of >60 years. In contrast, CP occurred more in the groups of 29-39 years and 40-60 years. The mean age for PC patients was 61.17 ± 13.96 years, and for CP patients - 42.14 ± 17.08 years ($P=0.000$). The diameter of the main PD in PC was 0.52 ± 0.22 cm, and in CP, it was 0.51 ± 0.28 cm ($P=0.865$) (Table 1, Figure 2).

Table 1.

Demographic data and PD diameter in the study groups

Variables	PC	CP	P-value
Age, years	61.17 ± 13.96	42.14 ± 17.08	0.000
Mean diameter of PD, cm	0.52 ± 0.22	0.51 ± 0.28	0.865
Gender			
Male	18	20	0.280
Female	21	14	
Age group			
8-18 years	0	4	0.004
29-39 years	3	12	
40-60	17	13	
>60 years	19	5	
Total	39	34	

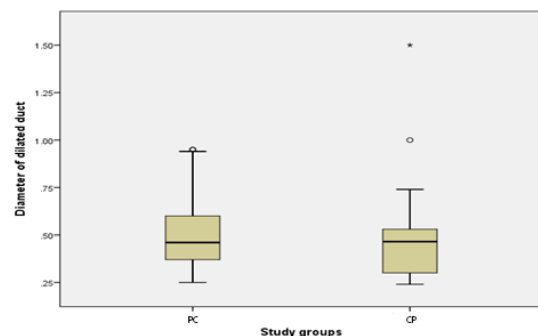


Fig. 2. PD diameter (cm) in the study groups.

This study found that PD dilation occurred in PC and CP with the same frequency, with no significant difference in the occurrence (Table 2, Figure 3).

Table 2.

The prevalence of PD dilation among the study groups.

PD dilation	PC	CP	P-value
Yes	25(64.1%)	22(64.7%)	0.957
No	14(35.9%)	12(35.3%)	

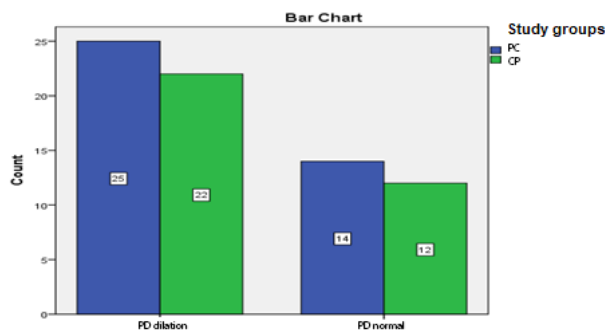


Fig. 3. The frequency of PD dilation in the study groups.

This study also found that PC was more likely to be associated with diabetes mellitus than CP (OR=2.42, 95%CI: 1.31-4.44, P=0.002) (Figure 4) The PD was more dilated in diabetic patients than in non-diabetic patients (Table 3, Figure 5).

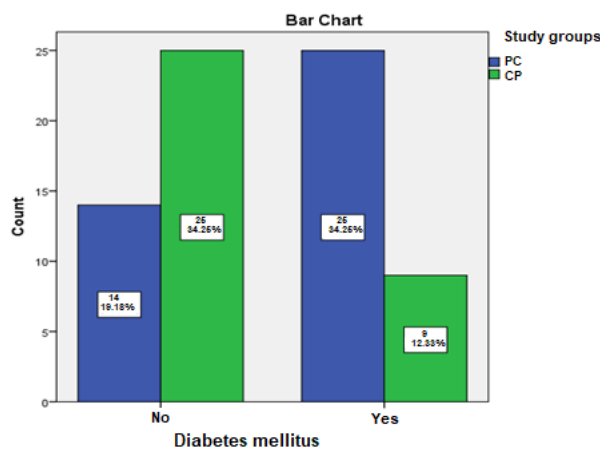


Fig. 4. The frequency of diabetes mellitus in the study groups.

Table 3.

The relative risk (RR) of PC in patients with history of diabetic mellitus related to CP.

	DM		Total	P-value	RR	95%CI
	No	Yes				
PC	14	25	39	0.004	2.42	1.32-4.44
CP	25	9	34			
Total	39	34	73			

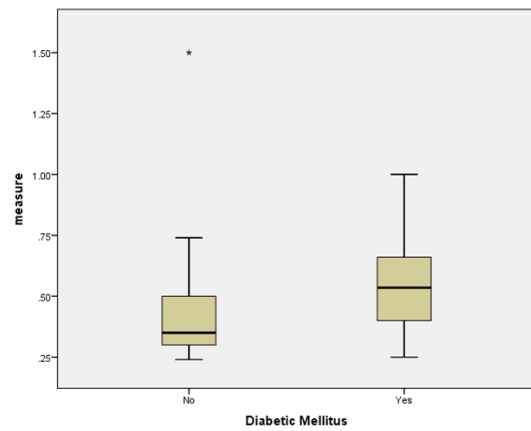


Fig. 5. The PD diameter (cm) in diabetic and non-diabetic patients.

Discussion

The majority of the burden of exocrine pancreatic disease is brought on by acute pancreatitis, chronic pancreatitis, and PC. Recurrent episodes of acute pancreatitis result in irreversible alterations indicative of CP.⁽⁹⁾

CP also has variances based on gender. Men are more likely than women to get CP, according to epidemiological studies, with a ratio of 4:5. Alcohol and tobacco use are also linked to CP in males (24:1) but not in females. In this study, CP occurred more commonly in males, while pancreatic carcinomas were more common in females. We also found that PC was more common in the age group of >60 and 40-60 years, with a mean age of 61.17 years. Moreover, the results showed that CP occurred more in younger age groups than in older ages, with a mean age of 42.14. A previous study stated that 90% of patients with newly diagnosed PC were over 55, and the risk of disease increased with age. PC rarely develops before the age of 30.⁽¹⁰⁾

In our study, 64.1% of the patients with PC had diabetes, and the risk of PC in diabetic patients was 2.4 times higher than in association with CP. Previous studies have found that diabetic patients have a twofold increased risk of developing PC. Although the association between diabetes and PC is complicated and assumed to be two-way, it has been shown that diabetes increases the likelihood of developing PC and worsens its symptoms. Compared to other types of cancers, the prevalence of diabetes among people with PC is exceptionally high.⁽¹¹⁾

Our results suggest that the dilation of the PD is one feature that accompanies PC and CP. In our study, there was no significant difference in dilation in both conditions (64.1% and 64.7%). Edge et al.⁽⁶⁾ found that the most common causes for dilatation of the main PD on CT were CP and PC. The result of the present study was consistent with the findings of Tanaka et al.,⁽¹²⁾ in which it was stated that in PC, the percentage of instances with a little dilation (<2 mm in diameter on ultrasound) of the main PD was 65% in the pre-cancer group, more than four years before the surgery for PC. One of the signs of PC is a slight dilation of the PD.^(6,12) The outcomes of the present study were also consistent with Luetmer et al., who found that PD dilation was found in 68% of CP.⁽¹³⁾

Conclusion

The present study concluded that pancreatic cancer occurs more commonly in the older age group, while chronic pancreatitis occurs more commonly in the younger age group. Additionally, pancreatic cancer is 2.4 times more likely to be associated with diabetes mellitus than chronic pancreatitis. Most cases of pancreatic cancer and chronic pancreatitis were associated with dilation of the main pancreatic duct with no significant difference in the amount of dilation.

Competing Interests

The authors declare that they have no competing interests.

References

1. Korpela T, Udd M, Mustonen H, Ristimäki A, Haglund C, Seppänen H, Kylänpää L. Association between chronic pancreatitis and pancreatic cancer: A 10-year retrospective study of endoscopically treated and surgical patients. *Int J Cancer*. 2020 Sep 1;147(5):1450-1460. doi: 10.1002/ijc.32971.
2. Malka D, Hammel P, Maire F, Rufat P, Madeira I, Pessione F, Lévy P, Ruszniewski P. Risk of pancreatic adenocarcinoma in chronic pancreatitis. *Gut*. 2002 Dec;51(6):849-52. doi: 10.1136/gut.51.6.849.
3. Kirkegård J, Mortensen FV, Cronin-Fenton D. Chronic Pancreatitis and Pancreatic Cancer Risk: A Systematic Review and Meta-analysis. *Am J Gastroenterol*. 2017 Sep;112(9):1366-1372. doi: 10.1038/ajg.2017.218.
4. Bansal P, Sonnenberg A. Pancreatitis is a risk factor for pancreatic cancer. *Gastroenterology*. 1995 Jul;109(1):247-51. doi: 10.1016/0016-5085(95)90291-0. PMID: 7797022.
5. Hassan MM, Bondy ML, Wolff RA, Abbruzzese JL, Vauthey JN, Pisters PW, et al. Risk factors for pancreatic cancer: case-control study. *Am J Gastroenterol*. 2007 Dec;102(12):2696-707. doi: 10.1111/j.1572-0241.2007.01510.x. Epub 2007 Aug 31. PMID: 17764494; PMCID: PMC2423805.
6. Edge MD, Hoteit M, Patel AP, Wang X, Baumgarten DA, Cai Q. Clinical significance of main pancreatic duct dilation on computed tomography: single and double duct dilation. *World J Gastroenterol*. 2007 Mar 21;13(11):1701-5. doi: 10.3748/wjg.v13.i11.1701
7. Issa Y, Kempeneers MA, van Santvoort HC, Bollen TL, Bipat S, Boermeester MA. Diagnostic performance of imaging modalities in chronic pancreatitis: a systematic review and meta-analysis. *Eur Radiol*. 2017 Sep;27(9):3820-3844. doi: 10.1007/s00330-016-4720-9.
8. Adler DG, Anderson MA. The Dilated Pancreatic Duct. *ERCP*. 2019;354-360. doi: 10.1016/B978-0-323-48109-0.00037-7.
9. Raimondi S, Lowenfels AB, Morselli-Labate AM, Maisonneuve P, Pezzilli R. Pancreatic cancer in chronic pancreatitis; aetiology, incidence, and early detection. *Best Pract Res Clin Gastroenterol*. 2010 Jun;24(3):349-58. doi: 10.1016/j.bpg.2010.02.007. PMID: 20510834.
10. Ozenoglu A. Relationship between diabetes, pancreatic cancer, and diet. *J Nutr Food Sci Metab*. 2022;1(1):1-5.
11. Setiawan VW, Stram DO, Porcel J, Chari ST, Maskarinec G, Le Marchand L, Wilkens LR, Haiman CA, Pandol SJ, Monroe KR. Pancreatic Cancer Following Incident Diabetes in African Americans and Latinos: The Multiethnic Cohort. *J Natl Cancer Inst*. 2019 Jan 1;111(1):27-33. doi: 10.1093/jnci/djy090.
12. Tanaka S, Nakaizumi A, Ioka T, Oshikawa O, Uehara H, Nakao M, Yamamoto K, Ishikawa O, Ohigashi H, Kitamura T. Main pancreatic duct dilatation: a sign of high risk for pancreatic cancer. *Jpn J Clin Oncol*. 2002 Oct;32(10):407-11. doi: 10.1093/jjco/hyf093.
13. Luetmer PH, Stephens DH, Ward EM. Chronic pancreatitis: reassessment with current CT. *Radiology*. 1989 May;171(2):353-7. doi: 10.1148/radiology.171.2.2704799.

Ultrasonographic Assessment of Normal Achilles Tendon Thickness and Width in the Asymptomatic Sudanese Population

Marwa H. Mohammed¹, Tasnim Badreldeen Elameen Abdalla¹, Raga Ahmed Abouraida², Magbool Alelyani², Awadia Gareeballah^{1,5}, Ala M. A Elgyoum³, Mogahid M. A. Zidan³, Abbas Omer⁴, Maisa Elzaki^{1,5}, Batil Alonazi⁶, Moram A. Fagiry⁶, Mustafa Z. Mahmoud^{6,7*}

¹Faculty of Radiology Science and Medical Imaging, Alzaiem Alazhari University, Khartoum, Sudan

²Department of Radiological Sciences, College of Applied Medical Sciences, King Khalid University, Abha, Saudi Arabia

³National Ribat University, Faculty of Radiology and Nuclear Medicine Science, Nile Street Burri, Khartoum, Sudan

⁴Radiological Sciences Department, Algahd International Colleges for Applied Medical Sciences, Al-Madinah Al-Munawwarah, Saudi Arabia

⁵Department of Diagnostic Radiological Technology, Faculty of Applied Medical Sciences, Taibah University, Al-Madinah Al-Munawwarah, Saudi Arabia

⁶Department of Radiology and Medical Imaging, College of Applied Medical Sciences in Al-Kharj, Prince Sattam bin Abdulaziz University, Al-Kharj 11942, Saudi Arabia

⁷Faculty of Health, University of Canberra, Canberra, ACT, Australia

Abstract

Background: The goal of this study was to measure normal Achilles tendon (AT) thickness and width in adult asymptomatic Sudanese people using high-resolution ultrasound.

Methods and Results: The study was conducted on members of a healthy Sudanese population (120 volunteers: 73/60.8% women and 47/39.2% men), who were chosen using simple random sampling. The study cases were all healthy people with no history of AT injuries or abnormalities. All patients were examined using a Toshiba Xairo200 linear transducer with a frequency range of 7-10MHz. All measurements were taken from a transverse scan at the calcaneus bone level of the AT insertion and 2 to 3cm above the calcaneus. The age group 20-27 had the most participants (44.2%), followed by 36-43 years (19.2%), 28-35 years (15.8%), 52-60 years (14.2%), and 44-51 years (6.7%). The study revealed that the mean age of participants was 34.19±12.29 years, height - 164±0.081 cm, weight - 67.22±15.97 kg, and BMI - 24.38±5.84 kg/m². The mean thickness and width of the AT were 4.36±0.81 mm and 21.85±3.23 mm, respectively, at its insertion into the calcaneus, and 4.63±0.77 mm and 12.20±1.37 mm, respectively, at the level 2-3 cm above the insertion. We found significant differences according to gender between the AT thickness and width at insertion into the calcaneus and above insertion and no statistically significant differences between the AT measurement's right and left side data.

Conclusion: The study found gender differences in the AT thickness and width at insertion into the calcaneus and 2-3 cm above the insertion. No statistically significant differences were detected between the AT measurement's right and left side data. Age, weight, height, and BMI correlated with the thickness and width of the AT at its insertion into the calcaneus and 2-3 cm above. Furthermore, additional research should be conducted using an extended field-of-view technology to measure the length of the AT tendon in the Sudanese population. (**International Journal of Biomedicine. 2023;13(1):95-100.**)

Keywords: Achilles tendon • high-resolution ultrasound • thickness

For citation: Mohammed MH, Abdalla TBE, Abouraida RA, Alelyani M, Gareeballah A, Elgyoum AMA, Zidan MMA, Omer A, Elzaki M, Alonazi B, Fagiry MA, Mahmoud MZ. Ultrasonographic Assessment of Normal Achilles Tendon Thickness and Width in the Asymptomatic Sudanese Population. International Journal of Biomedicine. 2023;13(1):95-100. doi:10.21103/Article13(1)_OA12

Introduction

Traditionally, conventional radiography was thought to be the primary tool for investigating bone and joint disorders. But now ultrasound (US) is taking on a larger role. Because of their superficial nature, the muscles, joints, connective tissues, and vascular structures of the upper and lower extremities are particularly well-suited for an ultrasound examination. As a result, over the last decade, ultrasound has played an important role, frequently serving as the primary tool for investigating many joint injuries and pathologies. In addition, when compared to other imaging technologies, such as MRI or CT scanning, ultrasound is very cost effective. For these reasons, the applications of musculoskeletal ultrasound have grown significantly in recent years.⁽¹⁾

Recent advancements in ultrasound system instrumentation and transducer technology promise a bright future for musculoskeletal disease research. Extended field-of-view imaging, harmonic tissue imaging, spatial compound imaging, and 1.5D transducer arrays are just a few of the advancements.⁽¹⁾ Transverse scans should be used for measurements.

Ultrasound (US) is thought to be the gold standard imaging technique for assessing tendons.⁽²⁾ To date, there is a noticeable lack of a standardized method for measuring AT thickness using US. In some studies, the insertion site of the tendon was used for measuring the thickness, while in others, the measurement was taken 2 or 3 cm proximal to the insertion site.⁽³⁻⁷⁾

The Achilles tendon (AT) has a thickness of 5 to 7 mm and a width of 12 to 15 mm at level 2 to 3 cm superior to its insertion into the calcaneus.⁽⁸⁾ Because the AT is the most commonly injured ankle tendon, it is critical to examine it from origin to insertion in both transverse and sagittal planes. The AT is most commonly injured 2-6 cm proximal to its insertion into the calcaneus, where a zone of relative vascularity exists.⁽⁹⁾

The goal of this study was to measure normal AT thickness and width in adult asymptomatic Sudanese people using high-resolution ultrasound.

Materials and Methods

The study was a descriptive cross-sectional study that took place at Prof. Abd Elsamad Mohammed Saleh X-ray and Ultrasound Training Center from April to September 2021. The study was conducted on members of a healthy Sudanese population (120 volunteers), who were chosen using simple random sampling. The study cases were all healthy people with no history of AT injuries or abnormalities. All subjects with a history of metabolic or inflammatory diseases, as well as those who have been treated with corticosteroids, were excluded from this study. All patients were examined using a Toshiba Xairo200 linear transducer with a frequency range of 7-10MHz.

The researcher filled out a data collection sheet that was designed to include all variables to satisfy the study and ultrasound examinations. The patient was lying prone on the examination table, with one foot hanging freely over the end of the table, slightly flexed.⁽⁹⁾ A coupling agent was required

to ensure good acoustic contact between the transducer and the skin, and complete sound beam transmission. Following informed consent, the patients' ankles were scanned with a linear transducer using the posterior approach technique.⁽¹⁰⁾

The AT was first imaged transversely from its insertion at the calcaneus to a level 2 to 3 cm above the insertion at the malleoli. The findings were then documented. All measurements were taken from a transverse scan at the calcaneus bone level of the AT insertion and 2 to 3cm above the calcaneus.

Statistical analysis was performed using statistical software package SPSS version 16.0 (SPSS Inc, Chicago, IL). Continuous variables with normal distribution were presented as mean (standard deviation [SD] and standard error of the mean [SEM]). Means of 2 continuous normally distributed variables were compared by independent samples Student's t-test. A 95% Confidence Interval (CI) of the difference was calculated. The frequencies of categorical variables were compared using Pearson's chi-squared test. A value of $P < 0.05$ was considered significant.

The study was conducted in accordance with the Declaration of Helsinki and approved by the Ethics Committee of Alzaiem Alazhari University (Khartoum, Sudan). The data was only used for study purposes without individual details identifying the participant. All patients gave verbal consent.

Results

A total of 240 ATs were scanned from 120 participants (73/60.8% women and 47/39.2% men), with 120 being right ATs and 120 being left ATs. The age group 20-27 had the most participants (44.2%), followed by 36-43 years (19.2%), 28-35 years (15.8%), 52-60 years (14.2%), and 44-51 years (6.7%) (Tables 1-9, Images 1-5).

Table 1.
Gender distribution of the study group.

Gender	Frequency	Percent	Valid Percent	Cumulative percent
Males	146	39.2	39.2	39.2
Females	94	60.8	60.8	100.0
Total	240	100.0	100.0	

Table 2.
Age distribution of the study group.

Age group	Frequency	Percent	Valid Percent	Cumulative percent
20- 27 years	106	44.2	44.2	44.2
28-35 years	38	15.8	15.8	60.0
36- 43 years	46	19.2	19.2	79.2
44- 51 years	16	6.7	6.7	85.8
52-60 years	34	14.2	14.2	100.0
Total	240	100.0	100.0	

Table 3.

Side distribution of AT measurements.

Side	Frequency	Percent	Valid Percent	Cumulative percent
Right	120	50.0	50.0	50.0
Left	120	50.0	50.0	100.0
Total	240	100.0	100.0	

Table 4.

Descriptive statistics for AT measurements, age, height, weight, and BMI.

Characteristics	n	Min	Max	Mean	SD
Age, year	240	20	60	34.19	12.29
Height, m	240	1.48	1.85	1.64	.0812
Weight, kg	240	37.00	120.0	67.22	15.97
BMI, kg/m ²	240	16	46	24.38	5.84
Thickness at insertion, mm	240	2.50	6.90	4.36	0.817
Width at insertion, mm	240	13.30	29.30	21.85	3.23
Thickness above insertion, mm	240	3.00	7.20	4.63	0.77
Width above insertion, mm	240	9.20	14.90	12.20	1.37
Valid N (list wise)	240				

Min - Minimum; Max - Maximum

Table 5.

Descriptive statistics for AT measurements according to gender.

A=Compare mean

Characteristics	Gender	n	Mean	SD	SEM
Thickness at insertion, mm	Males	94	4.61	0.62	0.064
	Females	146	4.20	0.88	.073
Width at insertion, mm	Males	94	22.99	2.83	0.29
	Females	146	21.12	3.27	0.27
Thickness above insertion, mm	Males	94	4.88	0.61	0.063
	Females	146	4.47	0.82	0.068
Width above insertion, mm	Males	94	12.76	1.18	0.12
	Females	146	11.83	1.36	0.11

Table 6.

Levene's test for equality of variances (Independent sample t-test) for gender groups

Characteristics	T	Df	Sig. (2-tailed)	Mean difference	Std. error difference	95% CI of the difference	
						Lower	Upper
Thickness at insertion, mm	3.932	238	0.000	0.41	0.10499	.20600	.61967
	4.226	235.764	0.000	0.41	0.09768	.22040	.60528
Width at insertion, mm	4.542	238	0.000	1.86	0.41142	1.05809	2.67907
	4.685	218.045	0.000	1.86	0.39888	1.08244	2.65472
Thickness above insertion, mm	4.115	238	0.000	0.40	0.09935	.21306	.60449
	4.376	232.676	0.000	0.40	0.09341	.22474	.59280
Width above insertion, mm	5.419	238	0.000	0.93	0.17188	.59288	1.27008
	5.594	218.481	0.000	0.93	0.16651	.60330	1.25965

Table 7.

Descriptive statistics for AT measurements according to right and left sides.

A=Compare mean

Characteristics	Side	n	Mean	SD	SEM
Thickness at insertion, mm	Right	120	4.36	0.80004	.07303
	Left	120	4.36	0.83819	.07652
Width at insertion, mm	Right	120	21.84	3.22898	.29476
	Left	120	21.87	3.25724	.29734
Thickness above insertion, mm	Right	120	4.60	0.77536	.07078
	Left	120	4.66	0.77865	.07108
Width above insertion, mm	Right	120	12.16	1.38963	.12685
	Left	120	12.24	1.36440	.12455

The study revealed that the mean age of participants was 34.19±12.29 years, height - 164±0.081 cm, weight - 67.22±15.97 kg, and BMI - 24.38±5.84 kg/m². The mean thickness and width of the AT were 4.36±0.81 mm and 21.85±3.23 mm, respectively, at its insertion into the calcaneus, and 4.63±0.77 mm and 12.20±1.37 mm, respectively, at the level 2-3 cm above the insertion.

Discussion

This result is consistent with the findings of a study by Beatrice et al.⁽¹¹⁾ The mean thickness of the AT above insertion was 5.1±0.63 mm, which agrees with the findings of Aydın et al.,⁽¹²⁾ who discovered that the mean thickness of the AT above insertion was 4.0±0.8mm in the healthy control group, but differs from the findings of van Schie et al.,⁽¹³⁾ who discovered that the mean AT thickness was 6.8 mm in the asymptomatic group.

Schmidt et al.⁽⁵⁾ have previously reported a difference of half a millimetre in the mean AT thickness of male and female healthy subjects. The sagittal diameter of the AT was 4.9 mm for women and 5.3 mm for men in a Spanish study,⁽¹⁴⁾ compared with 4.1 mm and 4.6 mm, respectively, in a study by Schmidt et al.⁽⁵⁾ Our study also discovered that in men, the mean thickness and width of the AT were 4.61±0.62 mm and 22.99±2.83 mm, respectively, at its insertion into the calcaneus, and 4.88±0.61 mm and 12.76±1.18 mm, respectively, at the level 2-3 cm above the insertion. In women, the mean thickness and width of the AT were 4.20±0.88 mm and 21.12±3.27 mm, respectively, at its insertion into the calcaneus, and 4.47±0.82 mm and 11.83±1.36 mm, respectively, at the level 2-3 cm above the insertion (Table 5). de Mello et al.⁽¹⁵⁾ found that the mean transverse diameter and anteroposterior diameter of the AT were 14.4±1.4 mm and 5.6±0.6 mm for males and 13.3±1.0 mm and 5.4±0.5 mm for females. We found significant differences according to gender between the AT thickness and width at insertion into the calcaneus and above insertion ($P<0.05$) (Table 6). This finding is consistent with the findings of de Mello et al.,⁽¹⁴⁾ whose measurements were significantly lower in females, and also agrees with a study done by Aydın et al.,⁽¹²⁾ who found a significant difference in the AT thickness in different genders (higher in males).

Table 8.

Levene's test for equality of variances (Independent sample t-test) for the right and left sides.

Characteristics	T	Df	Sig. (2-tailed)	Mean difference	Std. error difference	95% CI of the difference	
						Lower	Upper
Thickness at insertion, mm	.055	238	.956	.00583	.10578	-.20254	.21421
	.055	237.485	.956	.00583	.10578	-.20255	.21421
Width at insertion, mm	-.076	238	.940	-.03167	.41869	-.85647	.79314
	-.076	237.982	.940	-.03167	.41869	-.85647	.79314
Thickness above insertion, mm	-.565	238	.573	-.05667	.10031	-.25428	.14094
	-.565	237.996	.573	-.05667	.10031	-.25428	.14094
Width above insertion, mm	-.431	238	.667	-.07667	.17778	-.42689	.27356
	-.431	237.920	.667	-.07667	.17778	-.42689	.27356

Table 9.

Correlations between age, gender, height, weight, and BMI and all AT measurements.

Characteristics	Statistics	Age	Gender	Height	Weight	BMI	Side
Thickness at insertion	PC	.241**	-.247**	.351**	.577**	.451**	-.004
	Sig. (2-tailed)	.000	.000	.000	.000	.000	.956
Width at insertion	PC	.169**	-.282**	.368**	.364**	.226**	.005
	Sig. (2-tailed)	.009	.000	.000	.000	.000	.940
Thickness above insertion	PC	.231**	-.258**	.369**	.660**	.530**	.037
	Sig. (2-tailed)	.000	.000	.000	.000	.000	.573
Width above insertion	PC	.139*	-.331**	.416**	.490**	.331**	.028
	Sig. (2-tailed)	.031	.000	.000	.000	.000	.667
	N	240	240	240	240	240	240

PC -Pearson Correlation

** - Correlation is significant at the 0.01 level (2-tailed).

* - Correlation is significant at the 0.05 level (2-tailed).

The study also discovered that the mean thickness and width of the AT on the right side were 4.36±0.80 mm and 21.84±3.22 mm, respectively, at its insertion into the calcaneus, and 4.60±0.77 mm and 12.16±1.38 mm, respectively, at the level 2-3 cm above the insertion. The mean thickness and width of the AT on the left side were 4.36±0.83 mm and 21.87±3.26 mm, respectively, at its insertion into the calcaneus, and 4.66±0.78 mm and 12.24±1.36, respectively, at the level 2-3 cm above the insertion. We used the independent sample t-test to compare means and found no statistically significant differences between the AT measurement's right and left side data (Table 7, 8). Canbolat et al.⁽¹⁶⁾ also found that AT width and thickness showed no significant differences between the right and left side tendons.

Our study discovered statistically significant weak positive correlations between age and all AT measurements (Table 9). Statistically significant weak negative correlations were found between genders and all AT measurements. Moderate, significant positive correlations were found between the height and all AT measurements. Weight had a strong significant positive correlation with the AT thickness at insertion and a level above the insertion into the calcaneus, and a moderate, significant correlation with the AT width. Abate et al.⁽¹⁷⁾ noted that overweight, sedentary individuals showed Achilles tendon thickness values significantly higher than normal-weight sedentary individuals. BMI correlated strongly with the AT thickness above its insertion into the calcaneus and moderately with other AT measurements. According to the findings, there was no significant relationship between the side and the AT measurements (Table 7-9).



Image 1. Linear MSK ultrasound of the same patient. The left AT measurements (thickness at the AT insertion into the calcaneus and above insertion: 3.9 mm and 4.3 mm, respectively; the width at the AT insertion into the calcaneus and above insertion: 24.8 mm and 11.7mm, respectively).

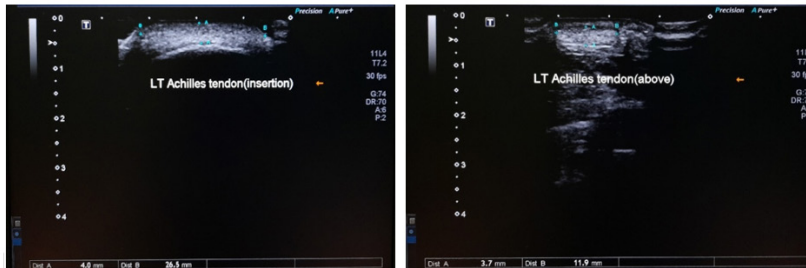


Image 2. Linear MSK ultrasound of a 26-year-old female patient. The left AT measurements (thickness at the AT insertion into the calcaneus and above insertion: 4.0 mm and 3.7 mm, respectively; the width at the AT insertion into the calcaneus and above insertion: 26.5 mm and 11.9 mm, respectively).



Image 3. Linear MSK ultrasound of the same patient. The right AT measurements (thickness at the AT insertion into the calcaneus and above insertion: 3.4 mm and 4.7 mm, respectively; the width at the AT insertion into the calcaneus and above insertion: 23.4 mm and 11.1 mm, respectively).

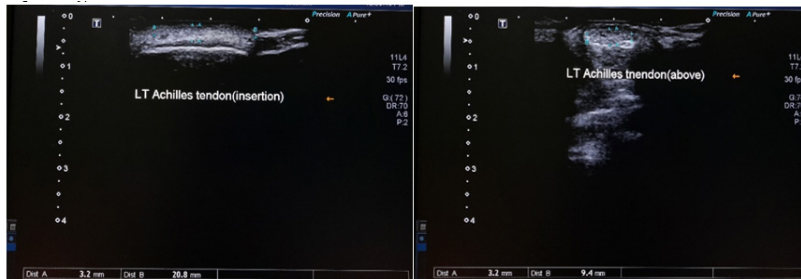


Image 4. Linear MSK ultrasound of a 26-year-old female patient. The left AT measurements (thickness at the AT insertion into the calcaneus and above insertion: 3.2 mm and 3.2 mm, respectively; the width at the AT insertion into the calcaneus and above insertion: 20.8 mm and 9.4 mm, respectively).



Image 5. Linear MSK ultrasound of the same patient. The right AT measurements (thickness at the AT insertion into the calcaneus and above insertion: 3.4 mm and 4.2 mm, respectively; the width at the AT insertion into the calcaneus and above insertion: 21.2 mm and 8.9 mm, respectively).

Conclusion

Our study found gender differences in the AT thickness and width at insertion into the calcaneus and at the level 2-3 cm above the insertion. Age, weight, height, and BMI correlated with the thickness and width of the AT at its insertion into the calcaneus and 2-3 cm above. All ultrasound departments should have a high-resolution musculoskeletal ultrasound. More research on athletes is needed to determine if sport affects AT size. Soldiers who have been standing on their feet for a long time should have more AT measurements taken. Children's reference value needs more research. Furthermore, additional research should be conducted using an extended field-of-view technology to measure the length of the AT tendon in the Sudanese population.

Competing Interests

The authors declare that they have no competing interests.

References

1. Czyrny Z. Standards for musculoskeletal ultrasound. *J Ultrason.* 2017 Sep;17(70):182-187. doi: 10.15557/JoU.2017.0027.
2. Grassi W, Filippucci E, Farina A, Cervini C. Sonographic imaging of tendons. *Arthritis Rheum.* 2000 May;43(5):969-76. doi: 10.1002/1529-0131(200005)43:5<969::AID-ANR2>3.0.CO;2-4.
3. Balint PV, Kane D, Wilson H, McInnes IB, Sturrock RD. Ultrasonography of enthesal insertions in the lower limb in spondyloarthritis. *Ann Rheum Dis.* 2002 Oct;61(10):905-10. doi: 10.1136/ard.61.10.905.
4. D'Agostino MA, Said-Nahal R, Hacquard-Bouder C, Brasseur JL, Dougados M, Breban M. Assessment of peripheral enthesitis in the spondylarthropathies by ultrasonography combined with power Doppler: a cross-sectional study. *Arthritis Rheum.* 2003 Feb;48(2):523-33. doi: 10.1002/art.10812.
5. Schmidt WA, Schmidt H, Schicke B, Gromnica-Ihle E. Standard reference values for musculoskeletal ultrasonography. *Ann Rheum Dis.* 2004 Aug;63(8):988-94. doi: 10.1136/ard.2003.015081.
6. Olivieri I, Barozzi L, Padula A, De Matteis M, Pierro A, Cantini F, Salvarani C, Pavlica P. Retrocalcaneal bursitis in spondyloarthritis: assessment by ultrasonography and magnetic resonance imaging. *J Rheumatol.* 1998 Jul;25(7):1352-7.
7. Filippucci E, Aydin SZ, Karadag O, Salaffi F, Gutierrez M, Direskeneli H, Grassi W. Reliability of high-resolution ultrasonography in the assessment of Achilles tendon enthesopathy in seronegative spondyloarthropathies. *Ann Rheum Dis.* 2009 Dec;68(12):1850-5. doi: 10.1136/ard.2008.096511. E
8. Rumack CM, Levine D. *Diagnostic ultrasound.* Fifth Edition. Elsevier, Inc; 2018.
9. Jacobson JA. *Fundamentals of Musculoskeletal Ultrasound.* Third Edition. Elsevier, Inc; 2018.
10. Kayser R, Mahlfeld K, Heyde CE. Partial rupture of the proximal Achilles tendon: a differential diagnostic problem in ultrasound imaging. *Br J Sports Med.* 2005 Nov;39(11):838-42; discussion 838-42. doi: 10.1136/bjism.2005.018416.
11. Beatrice S. F. Pang, Michael Ying. Sonographic measurement of Achilles tendons in asymptomatic subjects. *Hongkong* 1 Oct, 2006.
12. Aydın SZ, Filippucci E, Atagündüz P, Yavuz Ş, Grassi W, Direskeneli H. Sonographic measurement of Achilles tendon thickness in seronegative spondyloarthropathies. *Eur J Rheumatol.* 2014 Mar;1(1):7-10. doi: 10.5152/eurjrheum.2014.002.
13. van Schie HT, de Vos RJ, de Jonge S, Bakker EM, Heijboer MP, Verhaar JA, Tol JL, Weinans H. Ultrasonographic tissue characterisation of human Achilles tendons: quantification of tendon structure through a novel non-invasive approach. *Br J Sports Med.* 2010 Dec;44(16):1153-9. doi: 10.1136/bjism.2009.061010.
14. Civeira F, Castillo JJ, Calvo C, Ferrando J, de Pedro C, Martínez-Rodés P, Pocoví M. Tamaño del tendón de Aquiles por ecografía de alta resolución en población sana. Relación con las concentraciones lipídicas [Achilles tendon size by high resolution sonography in healthy population. Relationship with lipid levels]. *Med Clin (Barc).* 1998 Jun 20;111(2):41-4. Spanish.
15. de Mello RAF, Marchiori E, dos Santos AASMD, Neto GT. [Morphometric evaluation of Achilles tendon by ultrasound]. *Radiologia Brasileira.* 2006;39(3):161-165. [Article in in Portuguese].
16. Canbolat M, Ozba D, Ozdemir Z, Demirtafl G, Kafkas AS. Effects of physical characteristics, exercise and smoking on morphometry of human Achilles tendon: an ultrasound study. *Anatomy.* 2015;9(3):128-134.
17. Abate M, Schiavone C, Di Carlo L, Salini V. Achilles tendon and plantar fascia in recently diagnosed type II diabetes: role of body mass index. *Clin Rheumatol.* 2012 Jul;31(7):1109-13. doi: 10.1007/s10067-012-1955-y.

*Corresponding author: Prof. Mustafa Zuhair Mahmoud, Ph.D., Department of Radiology and Medical Imaging, College of Applied Medical Sciences in Al-Kharj, Prince Sattam bin Abdulaziz University, Al-Kharj 11942, Saudi Arabia. E-mail: zuhairmustafa4@hotmail.com

Stereological Measurement of the Volume of Medulla Oblongata in Young Adults from Magnetic Resonance Images using ImageJ Software

Abdalahim Y. Mohamed¹, Zuhail Y. Hamd^{2*}, Amal I. Alorainy², Awadia Gareeballah^{3,10}, Basim Abdullah Alhomida⁴, Nagwan Elhoussein⁵, Haya Abdulrahman Alshegri⁶, Sahar A. Mustafa⁷, Sara S. Albadri⁸, Wegdan Ahmed⁹

¹Anatomy Department, Faculty of Medicine, El Imam El Mahdi University, Sudan

²Department of Radiological Sciences, College of Health and Rehabilitation Sciences, Princess Nourah bint Abdulrahman University, Riyadh, Saudi Arabia

³Department of Diagnostic Radiology, College of Applied Medical Sciences, Taibah University, Medina, KSA

⁴College of Medicine Almaarefa University, Riyadh, Saudi Arabia

⁵Department of Diagnostic Radiology, College of Applied Medical Sciences, University of Ha'il, Ha'il, Saudi Arabia

⁶Medical Imaging Department, King Abdullah bin Abdul-Aziz University Hospital, Riyadh, Saudi Arabia

⁷Department of Radiological Sciences Alghad International Colleges for Applied Medical Sciences, Riyadh, Saudi Arabia

⁸Department of Radiological Sciences, Alghad International Colleges for Applied Medical Sciences, Alqassim, Saudi Arabia

⁹Anatomy Department, Faculty of Medicine, National University, Sudan

¹⁰Faculty of Radiological Sciences and Medical Imaging, Alzaiem Alazhari University, Khartoum Sudan

Abstract

Background: The aim of this study was to measure the volume of the medulla oblongata (MO) in young adult Sudanese from magnetic resonance images using ImageJ software.

Methods and Results: The study included 36 (18 males and 18 females) young adult Sudanese with normal brain MRI. The MO volume was measured from a T1-weighted MRI in healthy young adult Sudanese using ImageJ software to determine the effect of age, sex, and body mass index (BMI) on the MO volume. The study found that the stereological volume of MO was $717.39 \pm 82.31 \text{ mm}^3$ with significant differences between genders. The mean MO volume was greater in males than in females ($769.2 \pm 54.2 \text{ mm}^3$ and $665.7 \pm 73 \text{ mm}^3$, respectively. $P < 0.001$). There was an inverse, positive, moderately significant correlation between the age and MO volume ($r = -0.341$, $P < 0.05$). In contrast, there was no significant correlation between BMI and MO volume ($P > 0.05$).

Conclusion: Our study detected a significant difference between genders in MO volume, which was greater in males than in females. There is no significant correlation between MO volume and BMI. The size of the MO in individuals with normal brain MRI decreased gradually, by increasing age, from 20 to 40 years. (**International Journal of Biomedicine. 2023;13(1):101-105.**)

Keywords: medulla oblongata • magnetic resonance imaging • ImageJ software

For citation: Mohamed AY, Hamd ZY, Alorainy AI, Gareeballah A, Alhomida BA, Elhoussein N, Alshegri HA, Mustafa SA, Albadri SS, Ahmed W. Stereological Measurement of the Volume of Medulla Oblongata in Young Adults from Magnetic Resonance Images using ImageJ Software. International Journal of Biomedicine. 2023;13(1):101-105. doi:10.21103/Article13(1)_OA13

Abbreviations

BMI, body mass index; **MRI**, magnetic resonance imaging; **MO**, medulla oblongata.

Introduction

The medulla oblongata (MO) is the lower part of the brainstem, a cone-shaped neuronal mass. It lies anterior to the cerebellum; the midbrain lies at the upper part, where the pons sits in between. The MO joins the spinal cord inferiorly with the pons superiorly. The MO contains not only many cranial nerve nuclei⁽¹⁾ but also contains autonomic centers such as the cardiac, respiratory, and vasomotor centers, which regulate heart rate, breathing, and blood pressure, respectively.⁽²⁾

Generally, the size depends on several factors, such as age, gender, body size, and shape.⁽³⁾ Growing older begins with fertilization and continues throughout the life of individuals, with increasing cell numbers and sizes, which is demonstrated by some permanent physiological and structural changes.⁽⁴⁾ Numerous studies have been conducted to determine the volume of brain areas and their sex differences.⁽⁵⁻⁸⁾ Some studies show no gender phenotypic variation in the volume of brain structures,^(9,10) although, other studies have demonstrated that men have greater brain structure volumes than women.⁽¹¹⁻¹³⁾ This sexual dimorphism is explained by the fact that males have larger body sizes than females. There are few studies about the MO measurement. From available literature and published studies, there has yet to be any documentation of normal values of the MO. As a result, sex and time-of-life volumetric disparities in the MO have been interesting subjects for researchers. Thus, a thorough understanding of the asymmetrical construction of MO variations due to age and gender would be critical for an accurate diagnosis and neurosurgery procedure.

In our study, the MO volume was measured from a T1-weighted MRI in healthy young adult Sudanese using ImageJ software to determine the effect of age, sex, and BMI on the MO volume.

Materials and Methods

This cross-sectional descriptive study was conducted in the MRI department from February to October 2018. The study included 36 (18 males and 18 females) young adult Sudanese with normal brain MRI. The age of the participants ranged between 20 and 40 years. The participants were from different Sudanese tribes, and all of them were right-handed. The participants had no history of neurological or psychiatric diseases or congenital anomalies. Verbal consent from the department where the study was performed and from each participant included in the study sample was obtained after explaining the objectives of the study.

MRI protocol

The structured MRI was performed at the radiology department of Doctor's Hospital. Magnetic resonance procedure was carried out using 1.5 Tesla Philips scanners. T1-weighted images were acquired in 3D, utilizing Magnetization Prepared Rapid Acquisition (MP-RAGE), which results in excellent distinction between gray and white matter in the coronal slice. The acquisition time is 5 minutes and 18 seconds; the slice distance is 1.0 mm; the FOV is 250 reading, 192-millimeter phase, TR=1657 msec, TE=2.95 msec; the

bandwidth is 180 Hz/pixel, the flip angle is 15°, the ECHO spacing is 7 msec, the phase resolution is 100%, and the slice resolution is 50%. ImageJ (version 1.8.0_112) software was used to analyze MR images. ImageJ is available and free to download from the NIH website (<http://rsb.info.nih.gov/ij/>).

Protocol for measuring the MO using ImageJ software

The planimetry technique, which includes manually identifying the boundaries of the area of interest, was used to measure the cross-sectional area on ImageJ software.

The the images were processed according to the protocol prepared to analyze the MR images. Figure 1 shows step sequences for measurements of medulla oblongata volume using ImageJ software processing. The software automatically measures the medulla's sectional cut surface. The medulla volumes were calculated by multiplying the total sectional surface area by the section interval, as is shown in the formula: $V = \Sigma a \times t$, where V denotes the volume, t is the space between the studied sections, and Σa is the overall sectional area of the construction.

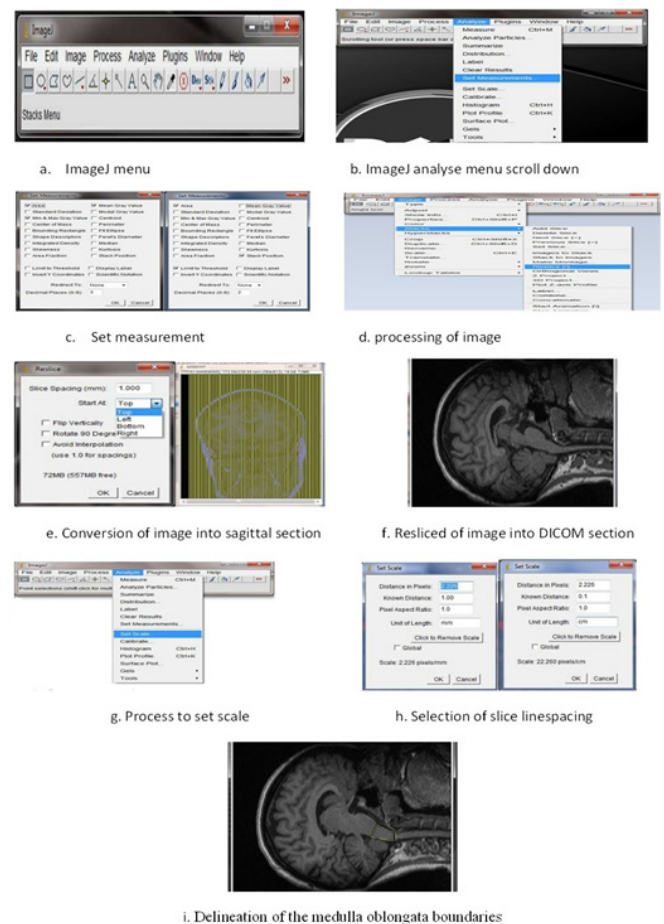


Fig. 1. Step sequences for measurements of medulla oblongata volume using ImageJ software processing.

Microsoft Excel was used to do the calculations and calculate the coefficient of error. The surface area data were transferred from ImageJ to an Excel spreadsheet. All the calculations were automated.

The study was approved by the Ethics Committee at Princess Nourah Bint Abdulrahman University, Riyadh, Saudi Arabia.

Statistical analysis was performed using statistical software package SPSS version 23.0 (Armonk, NY: IBM Corp.). Baseline characteristics were summarized as frequencies and percentages for categorical variables. Continuous variables with normal distribution were presented as mean (standard deviation [SD]). Means of 2 continuous normally distributed variables were compared by independent samples Student's t-test. Pearson's correlation coefficient (r) was used to determine the strength of the relationship between the two continuous variables. A probability value of $P < 0.05$ was considered statistically significant.

Results

The study found that the stereological volume of MO was $717.39 \pm 82.31 \text{ mm}^3$ with significant differences between genders. The mean MO volume was greater in males than in females (769.2 ± 54.2 and $665.7 \pm 73 \text{ mm}^3$, respectively, $P < 0.001$) (Figure 2). No significant differences in MO volume were found among the 2 age groups (20-30 years and 31-40 years) ($P > 0.05$) (Table 1). There was an inverse, positive, moderately significant correlation between the age and MO volume ($r = -0.341$, $P < 0.05$). In contrast, there was no significant correlation between BMI and MO volume ($P > 0.05$) (Table 2). On linear regression analysis, a weak linear relationship was found between the age and MO volume (Figure 3).

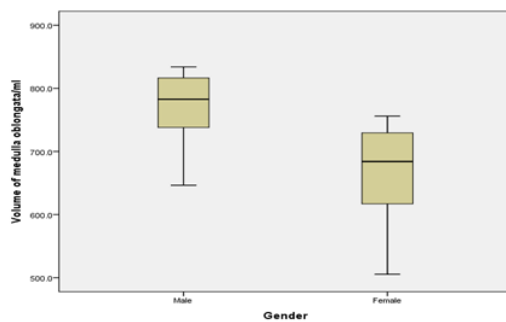


Fig. 2. The mean MO volume in males and females.

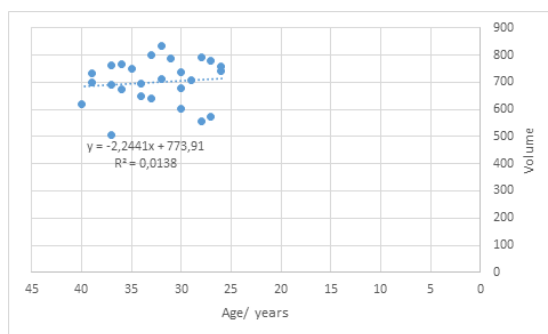


Fig. 3. Linear regression analysis: A weak linear relationship between the age and MO volume.

Table 1.

The mean MO volume in the age and gender groups.

Variable		n	The MO volume, mm^3	P-value
Gender	Male	18	769.16 ± 54.17	<0.0001
	Female	18	665.61 ± 73.06	
Age group	20-30 years	20	726.20 ± 84.61	0.481
	31-40 years	16	706.38 ± 80.67	
Total		36	717.39 ± 82.31	

Table 2.

Correlation between the age, BMI, and the MO volume.

Correlation		Age	BMI	MO
Age	Pearson Correlation	1	-0.123	-0.341
	Sig. (2-tailed)		0.473	0.042
	N	36	36	36
BMI	Pearson Correlation	-0.123	1	-0.069
	Sig. (2-tailed)	0.473		0.688
	N	36	36	36

Discussion

The brainstem is the control center of the human brain and connects the spinal cord to the cerebrum. Studying the effects of aging on the brainstem is important not only for understanding normal aging but also for comparing the pathophysiology of degenerative brain diseases and significant differences in brainstem size between males and females. Several studies have concluded that age-related changes in brainstem diameter are insignificant, while other studies have demonstrated a significant decrease in brainstem size with age. Studies describe specific brainstem growth patterns in different age groups.⁽¹⁴⁻¹⁷⁾

ImageJ is a software program that provides a variety of image processing procedures for two-dimensional (2D) and three-dimensional (3D) images. ImageJ includes various high-level image analysis methods in addition to basic image processing (filtering, edge detection, and resampling). ImageJ was created in Java. ImageJ can open a wide range of typical 2D image files and medical image data, such as MRI in DICOM format. The present study provided the normal value of the MO in the young adult Sudanese population from an MRI T1 image using the ImageJ software technique. The study demonstrated that males have a larger volume of MO than females. Our result is consistent with a study by Lee et al.,⁽¹⁸⁾ which explained the gender-related differences in the

MO volume by evolution and features of the male physique. Our study demonstrated an insignificant difference in the MO volume in the third and fourth decades of life. Lee et al. found no significant difference in MO volume between younger and older age groups, emphasizing that during these age periods, there is no synaptic loss. A study by Oguro⁽¹⁹⁾ clarified that supratentorial brain atrophy progressed by decades, with significant age-related atrophy in the tegmentum and pretectum of the midbrain and the base of the pons in men. In our study, there was significant age-related atrophy in the MO volume (by 2.2441mm³/year). Our results were inconsistent with Liptak,⁽²⁰⁾ who found no significant linear relationship with age in healthy subjects, but in multiple sclerosis patients, MO was reduced by 0.008 cm³/year.

A few studies assessed the MO volume using MRI. Most of the studies were conducted to evaluate the sagittal and AP measurement of the medulla. A study performed by Debnath et al.⁽²¹⁾ found that the cerebral peduncle, middle cerebellar peduncle, ventral midbrain thickness, midbrain height, pons, medulla, and spinal cord diameter, showed a steady and sharp increase in values from infancy and reached maximum values during the third decade, followed by a variable degree of decline in values. A study conducted in Sudan by Elameen et al.⁽²²⁾ found the diameter of MO decreased significantly and gradually after age 20. Singh et al.⁽²³⁾ found that the sagittal diameter of the MO and patient genders had no statistically significant association. The study also found that beyond age 50, the MO sagittal diameter reduced slightly, but after age 70, it decreased significantly. Ranganath et al.⁽²⁴⁾ found no significant differences in the AP diameter of the MO between genders; the AP diameter of the MO after 40 years of age at the cervical-medullary junction was significantly reduced. Our study reported that the MO volume was not significantly correlated with BMI.

Conclusion

Our study detected a significant difference between genders in MO volume, which was greater in males than in females. There is no significant correlation between MO volume and BMI. The size of the MO in individuals with normal brain MRI decreased gradually, by increasing age, from 20 to 40 years.

Competing Interests

The authors declare that they have no competing interests.

References

1. Snell RS. Clinical Neuroanatomy. 7th Edition. Philadelphia: Lippincott Williams & Wilkins; 2010.
2. Scanlon VC, Sanders T. Essentials of Anatomy and Physiology. 8th Edition, FA Davis; 2018 Oct 24.
3. Castell DO, Frank BB. Abdominal examination: role of percussion and auscultation. Postgrad Med. 1977 Dec;62(6):131-4. doi: 10.1080/00325481.1977.11714708.
4. Gocmen-Mas N, Pelin C, Canan S, Yazici AC, Zagyapan R, Senan S, Karabekir HS, Sahin B. Stereological evaluation of volumetric asymmetry in healthy human cerebellum. Surg Radiol Anat. 2009 Mar;31(3):177-81. doi: 10.1007/s00276-008-0424-4.
5. Allen JS, Damasio H, Grabowski TJ. Normal neuroanatomical variation in the human brain: an MRI-volumetric study. Am J Phys Anthropol. 2002 Aug;118(4):341-58. doi: 10.1002/ajpa.10092.
6. Allen JS, Damasio H, Grabowski TJ, Bruss J, Zhang W. Sexual dimorphism and asymmetries in the gray-white composition of the human cerebrum. Neuroimage. 2003 Apr;18(4):880-94. doi: 10.1016/s1053-8119(03)00034-x.
7. Blatter DD, Bigler ED, Gale SD, Johnson SC, Anderson CV, Burnett BM, Parker N, Kurth S, Horn SD. Quantitative volumetric analysis of brain MR: normative database spanning 5 decades of life. AJNR Am J Neuroradiol. 1995 Feb;16(2):241-51.
8. Filipek PA, Richelme C, Kennedy DN, Caviness VS Jr. The young adult human brain: an MRI-based morphometric analysis. Cereb Cortex. 1994 Jul-Aug;4(4):344-60. doi: 10.1093/cercor/4.4.344.
9. Barta P, Dazzan P. Hemispheric surface area: sex, laterality and age effects. Cereb Cortex. 2003 Apr;13(4):364-70. doi: 10.1093/cercor/13.4.364.
10. Nopoulos P, Flaum M, O'Leary D, Andreasen NC. Sexual dimorphism in the human brain: evaluation of tissue volume, tissue composition and surface anatomy using magnetic resonance imaging. Psychiatry Res. 2000 Feb 28;98(1):1-13. doi: 10.1016/s0925-4927(99)00044-x.
11. Acer N, Sahin B, Baş O, Ertekin T, Usanmaz M. Comparison of three methods for the estimation of total intracranial volume: stereologic, planimetric, and anthropometric approaches. Ann Plast Surg. 2007 Jan;58(1):48-53. doi: 10.1097/01.sap.0000250653.77090.97.
12. Kruggel F. MRI-based volumetry of head compartments: normative values of healthy adults. Neuroimage. 2006 Mar;30(1):1-11. doi: 10.1016/j.neuroimage.2005.09.063.
13. Mayhew TM, Olsen DR. Magnetic resonance imaging (MRI) and model-free estimates of brain volume determined using the Cavalieri principle. J Anat. 1991 Oct;178:133-44.
14. Elhussein N, Alkhatami AH, Ayad CE. Norms for Brain Stem: A morphometric MRI Based Study. IOSR Journal of Dental and Medical Sciences (IOSR-JDMS). 2017;16(6):74-79.
15. Suh JO, Joo YG, Suh SJ. MR measurement of normal brainstem diameter in Korean adults. Journal of the Korean Radiological Society. 1990 Aug 1;26(4):653-7. doi: 10.3348/jkrs.1990.26.4.653
16. Murshed KA, Ziylan T, Seker M, Cicekcibasi AE, Acikgozoglu S. Morphometric assessment of brain stem and cerebellar vermis with midsagittal MRI: the gender differences and effects of age. Neuroanatomy. 2003;2:35-8.
17. Raininko R, Autti T, Vanhanen SL, Ylikoski A, Erkinjuntti T, Santavuori P. The normal brain stem from infancy to old

*Corresponding author: Assistant Professor, Dr. Zuhail Y. Hamd, PhD, Department of Radiological Sciences, College of Health and Rehabilitation Sciences, Princess Nourah Bint Abdulrahman University, P.O. Box .84428, Riyadh 11671, Saudi Arabia. E-mail: zuhailhamd2019@gmail.com

- age. A morphometric MRI study. *Neuroradiology*. 1994 Jul;36(5):364-8. doi: 10.1007/BF00612119.
18. Lee NJ, Park IS, Koh I, Jung TW, Rhyu IJ. No volume difference of medulla oblongata between young and old Korean people. *Brain Res*. 2009 Jun 18;1276:77-82. doi: 10.1016/j.brainres.2009.04.027.
19. Oguro H, Okada K, Yamaguchi S, Kobayashi S. Sex differences in morphology of the brain stem and cerebellum with normal ageing. *Neuroradiology*. 1998 Dec;40(12):788-92. doi: 10.1007/s002340050685.
20. Liptak Z, Berger AM, Sampat MP, Charil A, Felsovalyi O, Healy BC, Hildenbrand P, Khoury SJ, Weiner HL, Bakshi R, Guttmann CR. Medulla oblongata volume: a biomarker of spinal cord damage and disability in multiple sclerosis. *AJNR Am J Neuroradiol*. 2008 Sep;29(8):1465-70. doi: 10.3174/ajnr.A1162.
21. Debnath J, Sharma V, Patrikar S, Krishna S, Shijith KP, Keshav RR. Normal measurements of brainstem and related structures for all ages: An MRI-based morphometric study. *Medical Journal Armed Forces India*. 2022. doi:10.1016/j.mjafi.2022.06.002
22. Elameen RAAE. Measurement of Normal Brainstem Diameter in Sudanese Population using MRI (Master dissertation, Sudan University of Science and Technology). 2016. Available from: <http://repository.sustech.edu/handle/123456789/15708>
23. Singh S, Sharma BR, Bhatta M, Poudel N. Measurement of anteroposterior diameters of normal brainstem by magnetic resonance imaging. *Journal of Gandaki Medical College-Nepal*. 2019;12(2):53-58. doi:10.3126/jgmcn.v12i2.27210
24. Ranganath A, Saklecha AK, Singh A, Vineela E. Age and gender differences in morphometric measurements of brain stem using magnetic resonance imaging in healthy Indian adults. *Journal of Datta Meghe Institute of Medical Sciences University*. 2022;17(1):21-24. doi:10.4103/jdmimsu.jdmimsu_238_22.
-

Vesicoureteral Reflux Grading using Different Imaging Techniques (MCUG, NM, and US): A Comparative Study

Awatif M. Omer^{1*}, Norah M. ALharbi², Nada F. Almohammadi², Ali S. Alsaadi², Amel F. Alzain¹, Meaad Z. Elbashir³, Sara Ali³, Maisa Elzaki¹

¹Department of Diagnostic Radiology Technology, College of Applied Medical Sciences, Taibah University, Almadinah Almunawwarah, Kingdom of Saudi Arabia

²King Salman Medical City, Almadinah Almunawwarah, Kingdom of Saudi Arabia

³Department of Diagnostic Radiology Technology, College of Applied Medical Sciences, Jazan University, Jazan, Kingdom of Saudi Arabia

Abstract

The aim of this study was to compare the different imaging procedures (micturating cystourethrogram [MCUG], nuclear medicine [NM], and ultrasound [US]) in the evaluation of vesicoureteral reflux (VUR).

Methods and Results: A retrospective study was conducted to compare different radiological investigations in the characterization and grading of VUR. In total, 93 patients (53 boys and 40 girls) with a mean age of 2.2 years were referred to the radiology department for exclusion or diagnosis of VUR. Age, sex, the pathway of obstruction, presence of VUR, degree of obstruction with VUR, presence of hydronephrosis, calcification, and grading according to MCUG were the main variables collected for US, NM, and MCUG.

Our results show that according to the frequency distribution, MCUG showed a higher sensitivity for detecting VUR and the degree of obstruction than the other imaging tools. US showed a higher sensitivity for the presence of hydronephrosis. The grading of VUR was more effectively detected by MCUG than by US and NM grading. We revealed a statistical association between VUR grades and the gender of a study's population, with a higher frequency of grade 5 in boys than in girls ($P=0.037$). Grades 3-5 showed higher frequencies in MCUG, in which the younger patients (0–50 weeks old) were more affected by obstruction and VUR than the other age groups. Moderate hydronephrosis was higher in boys than in girls ($P=0.006$).

Conclusion: The grading of VUR is more effectively detected by MCUG than by US and NM grading. (International Journal of Biomedicine. 2023;13(1):106-110.)

Keywords: vesicoureteral reflux • grading • micturating cystourethrogram

For citation: Omer AM, Alharbi NM, Almohammadi NF, Alsaadi AS, Alzain AF, Elbashir MZ, Ali S, Elzaki M. Vesicoureteral Reflux Grading using Different Imaging Techniques (MCUG, NM, and US): A Comparative Study. International Journal of Biomedicine. 2023;13(1):106-110. doi:10.21103/Article13(1)_OA14

Abbreviations

CL, the confidence level; ce-VUS, contrast-enhanced voiding urosonography; DMSA, dimercapto succinic acid; NM, nuclear medicine; NASHA/Dx, non-animal stabilized hyaluronic acid/dextranomer gel; MCUG, micturating cystourethrogram; RNC, radionuclide cystography; US, ultrasound; UTI, urinary tract infection; VUR, vesicoureteral reflux.

Introduction

The normal process and pathway of urination are affected by various pathological conditions involving interference with the normal passage of urine from the kidneys to the urinary bladder, which can result in infection of various

sites with various microorganisms, stones, strictures, or soft tissue masses. The normal process requires normal sphincters to judge the micturition, which is physiologically controlled by the normal innervation process.⁽¹⁾

Vesicoureteral reflux (VUR), the flow of urine back to the kidneys from the bladder, is a well-recognized, frequently

diagnosed, and understandable phenomenon.⁽²⁾ The big bang theory of reflux nephropathy postulates that renal parenchymal infection and scarring can result from the reflux of infected urine through the ureters to the upper renal tract.⁽³⁾ Pyelonephritis-induced renal scarring in childhood is a major risk factor for protein in the urine,⁽⁴⁾ renal hypertension, and renal failure.^(5,6) About 39%-40% of children with UTI presented with VUR.⁽⁷⁾

Untreated VUR can lead to various urinary tract manifestations, renal infections,^(8,9) pyelonephritis,⁽⁵⁾ and chronic renal failure (CRF) as a consequence of congenital renal hypoplasia.⁽¹⁰⁾ Gbadegesin et al.⁽⁶⁾ reported that VUR is a hereditary disease associated with a mutation in the gene encoding tenascin XB (TNXB in 6p21.3). One study on VUR after kidney transplantation found that 4.5% of patients had this disorder.⁽¹¹⁾

Imaging is an important step in the diagnosis and management of VUR, as it helps identify a congenital or acquired process due to anatomical or functional congenital abnormalities.⁽¹²⁾ VUR can be investigated using different methods to identify the grade of disease (VUR is graded 1–5, with 5 being the most severe);⁽¹³⁾ MCUG, also known as voiding cyst urography, is frequently used as a standard method of diagnosis, but because there are issues of increasing the radiation dose, some authors have introduced the use of ce-VUS,^(14,15) direct and indirect RNC,⁽¹⁵⁾ Tc-99m DMSA renal scintigraphy, and renal ultrasonography.⁽⁵⁾

Treatment of VUR is antibiotic prophylaxis or ureteral re-implantation to prevent complications.⁽¹⁶⁾ Serial imaging is required to identify the degree of resolution after antibiotic prophylaxis.⁽¹⁷⁾ Another method involving the endoscopic injection of NASHA/Dx (Deflux) was also introduced.⁽¹⁸⁾

The aim of this study was to compare the different imaging procedures (micturating cystourethrogram [MCUG], nuclear medicine [NM], and ultrasound [US]) in the evaluation of VUR.

Materials and Methods

A retrospective study was conducted to compare different radiological investigations in the characterization and grading of VUR. All examinations were carried out at King Salman bin Abdulaziz Medical City in Almadinah Almunawwarah from 2021 to 2022.

In total, 93 patients (53 boys and 40 girls) with a mean age of 2.2 years were referred to the radiology department for exclusion or diagnosis of VUR.

Age, sex, the pathway of obstruction, presence of VUR, degree of obstruction with VUR, presence of hydronephrosis, calcification, and grading according to MCUG were the main variables collected for US, NM, and MCUG.

MCUG was performed using the Luminos dRF Max Fluoroscopy machine produced by Siemens. The bladder was filled with 350 mg of Omnipaque (a contrast medium), diluted with normal saline, to visualize the urine pathway and identify any reflux. An ultrasound scan was performed with the patient in a supine position to identify the bladder, ureters, and kidneys, in order to determine the degree of hydronephrosis. Thirty-seven patients underwent successive

MCUG, ultrasound (Voluson E10), and renal scintigraphy scans (SPECT/CT, GE Healthcare).

Five grades of VUR were analyzed (Figure 1)⁽¹³⁾

Grade I: reflux into a nondilated ureter.

Grade II: reflux into the upper collecting system without dilatation.

Grade III: reflux into the dilated ureter and/or blunting of calyceal fornices.

Grade IV: reflux into a grossly dilated ureter.

Grade V: massive reflux, with significant ureteral dilatation and tortuosity and loss of the papillary impression.

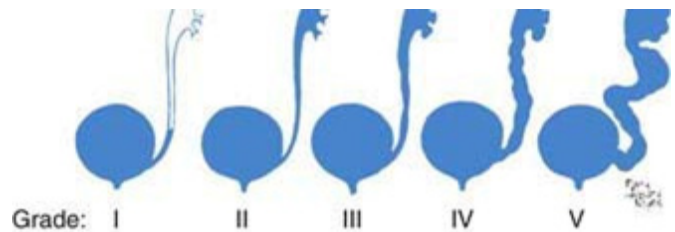


Fig. 1. The International Reflux Study Classification of I to V based on the appearance of the urinary tract on a contrast voiding cystourethrogram (VCUG).⁽¹³⁾

Statistical analysis was performed using statistical software package SPSS version 20.0 (SPSS Inc, Armonk, NY: IBM Corp). For descriptive analysis, results are presented as mean \pm standard deviation (SD). The independent t-test was applied to compare two groups for data with normal distribution. Group comparisons with respect to categorical variables are performed using chi-square test. A probability value of $P < 0.05$ was considered statistically significant.

Ethical approval for this study was obtained from the Ethical Committee at King Salman bin Abdulaziz Medical City (Almadinah Almunawwarah). Written informed consent was obtained from each patient's parent/guardian/ relative.

Results

An obstructed vesicoureteral junction was identified in 14 and 13 out of 37 patients in NM and US, respectively, while the same patients, in addition to the 65 patients, revealed obstructed pathways in the MCUG study (Table 1). Cross-tabulations revealed a statistical association between grades and the gender of a study's population, with a higher frequency of grade 5 in boys than in girls ($P=0.037$) (Table 2). Moderate hydronephrosis was higher in boys than in girls. ($P=0.006$) (Table 3). In our study, the more frequent grades were grades 3-5, with a higher percentage for grade 5 (Figure 2).

Our results show that according to the frequency distribution, MCUG showed a higher sensitivity for detecting VUR and the degree of obstruction than the other imaging tools. US showed a higher sensitivity for the presence of hydronephrosis. The grading of VUR was more effectively detected by MCUG than by US and NM grading.

Higher frequency ultrasounds were able to identify mild hydronephrosis, followed by moderate to severe conditions

with the possibility of no hydronephrosis (Figure 3). Grades 3-5 showed higher frequencies in MCUG, in which the younger patients (0–50 weeks old) were more affected by obstruction and VUR than the other age groups (Figure 4). Notably, there was a significant correlation between the degree of hydronephrosis and gender.

Table 1.

Different imaging procedures (MCUG, NM, and ultrasound) in the evaluation of VUR according to the degree of the vesicoureteral junction obstruction.

Vesicoureteral junction	NM	US	MCUG
Obstruction	14	13	92
No obstruction	8	5	1
Not clear obstruction	15	19	0
Total	37	37	93

Table 2.

Cross-tabulation of VUR grade and sex.

		VUR grading (MCUG)					Total	Statistics
		Grade 1	Grade 2	Grade 3	Grade 4	Grade 5		
Sex	Boys	2	2	8	13	26	51	Yates' $\chi^2 = 6.581$ $P\text{-value} = 0.160$
	Girls	1	7	11	8	11		
Total		3	9	19	21	37	89	
P-value		0.794*	0.059*	0.131	0.625	0.037		

*-P-value in chi-square test with Yates' correction

Table 3.

Cross-tabulation of the hydronephrosis by US grade and sex.

		Hydronephrosis by US				Total	Statistics
		Mild	Moderate	Severe	No hydronephrosis		
Sex	Boys	19	16	10	5	50	$\chi^2=12.059$ $P=0.008$
	Girls	18	3	5	12		
Total		37	19	15	17	88	
P-value		0.378	0.006	0.398	0.011		

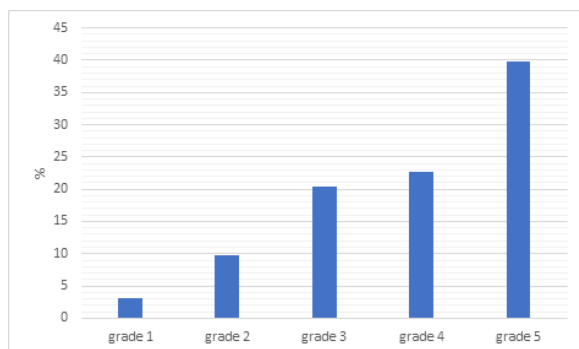


Fig. 2. Reflux grading according to MCUG.

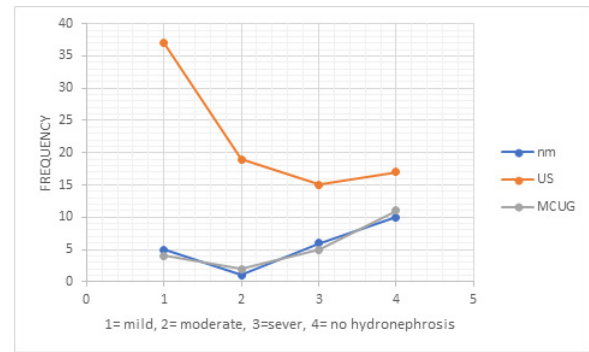


Fig. 3. Hydronephrosis grading.

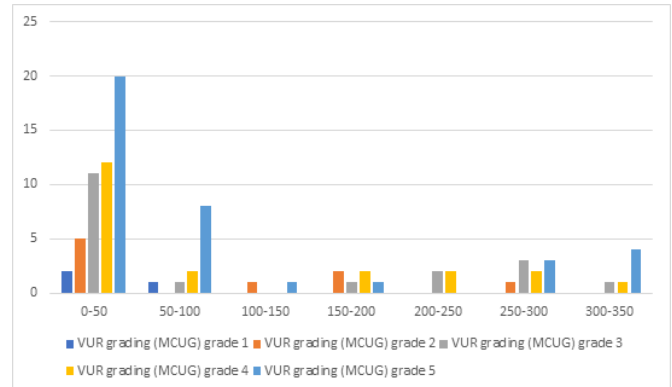


Fig. 4. Cross-tabulation of the VUR grade and age groups (in weeks)

Discussion

Identification of the reflux process in childhood genitourinary disease is considered an important step in identifying the treatment lines. The MCUG image shows (Figure 5) marked retention of contrast reaching both kidneys, an ultrasound of the same patient shows a dilated calyceal system, and a DMSA scan shows prominent hyperactive kidneys. We compared pathway obstructions seen in 37 NM scans with 93 MCUG scans. The results showed X-ray scans to be more sensitive in grading VUR than the other imaging procedures, which indicated that complete urinary tract obstructions are not frequently seen. An obstructed vesicoureteral junction was identified in 14 and 13 out of 37 patients in NM and US, respectively, while the same patients, in addition to the 55 patients, revealed obstructed pathways in the MCUG study (Table 1).



Fig. 5. VUR grading with MGUC (A), a dilated calyceal system showing the degree of hydronephrosis (B), and an NM scan of dilated kidneys (C)

We observed that obstruction could be confirmed after a few minutes of voiding in NM scans, as was seen in Papadopoulou et al.⁽¹⁹⁾ MCUG is indicated for patients with recurrent UTI, UTI with fever, bladder outlet obstruction, and abnormal US scans to exclude dysfunctional voiding as a result of a neurogenic bladder. International guidelines identify 5 grades of VUR. In our study, the more frequent grades were grades 3-5, with a higher percentage for grade 5 (Figure 2).

All advanced grades of VUR showed a variable degree of dilatation, which indicates the presence of hydronephrosis. All compression revealed that US imaging is the best method of quantifying such a condition, with MCUG and DMSA scans being the least effective. Higher frequency ultrasounds were able to identify mild hydronephrosis, followed by moderate to severe conditions with the possibility of no hydronephrosis. Braga et al.⁽²⁰⁾ identified hydronephrosis as a major risk factor for VUR.

Correlation analysis was done to investigate the gender effect on the presence and grading of VUR using various imaging modalities. The male gender was predominant in this study, and other authors reported similar results.^(20,21) Cross-tabulations revealed a statistical association between grades and the gender of a study's population, with a higher frequency of grade 4 and grade 5 in boys than in girls (Table 2). A statistical association was noted between the degree of hydronephrosis and gender; however, mild hydronephrosis occurs at the same frequency in females and males. Moderate to severe hydronephrosis was higher in boys than in girls (Table 3).

The study also indicated a statistical association between VUR grades and age group, with children aged 0–50 weeks having a predominantly higher frequency of grade 5. Chang et al.⁽²²⁾ obtained a similar result, noting that children aged 0.3–1.3 years have a higher frequency of VUR than other age groups.

Conclusion

VUR can be congenital or acquired.⁽²³⁾ Our results reveal the importance of the choice of imaging procedure in grading VUR (MCUG), ascertaining the presence of hydronephrosis (US), and identifying related factors that lead to VUR. The grading of VUR is more effectively detected by MCUG than by US and NM grading. Such knowledge is necessary to determine the best treatment for the patient, to ensure early management, and to avoid possible complications, such as renal scarring and agenesis, in follow-up care.

Competing Interests

The authors declare that they have no competing interests.

References

1. Mullins LJ, Conway BR, Menzies RI, Denby L, Mullins JJ. Renal disease pathophysiology and treatment: contributions from the rat. *Dis Model Mech*. 2016 Dec 1;9(12):1419-1433.

doi: 10.1242/dmm.027276.

2. Decter RM. Update on vesicoureteral reflux: pathogenesis, nephropathy, and management. *Rev Urol*. 2001 Fall;3(4):172-8.
3. Williams DI. Commentary at International Pediatric Nephrology Association Meeting; 1977; Helsinki, Finland.
4. Basic J, Golubovic E, Miljkovic P, Bjelakovic G, Cvetkovic T, Milosevic V. Microalbuminuria in children with vesicoureteral reflux. *Ren Fail*. 2008;30(6):639-43. doi: 10.1080/08860220802134805.
5. Temiz Y, Tarcan T, Onol FF, Alpay H, Simşek F. The efficacy of Tc99m dimercaptosuccinic acid (Tc-DMSA) scintigraphy and ultrasonography in detecting renal scars in children with primary vesicoureteral reflux (VUR). *Int Urol Nephrol*. 2006;38(1):149-52. doi: 10.1007/s11255-005-3829-6.
6. Gbadegesin RA, Brophy PD, Adeyemo A, Hall G, Gupta IR, Hains D, Bartkowiak B, Rabinovich CE, Chandrasekharappa S, Homstad A, Westreich K, Wu G, Liu Y, Holanda D, Clarke J, Lavin P, Selim A, Miller S, Wiener JS, Ross SS, Foreman J, Rotimi C, Winn MP. TNXB mutations can cause vesicoureteral reflux. *J Am Soc Nephrol*. 2013 Jul;24(8):1313-22. doi: 10.1681/ASN.2012121148.
7. Méndez R, Somoza I, Tellado MG, Liras J, Sánchez A, Pais E, Vela D. Predictive value of clinical factors for successful endoscopic correction of primary vesicoureteral reflux grades III-IV. *J Pediatr Urol*. 2006 Dec;2(6):545-50. doi: 10.1016/j.jpuro.2005.11.012.
8. Garin EH, Campos A, Homsy Y. Primary vesicoureteral reflux: review of current concepts. *Pediatr Nephrol*. 1998 Apr;12(3):249-56. doi: 10.1007/s004670050448.
9. Ascenti G, Chimenz R, Zimbaro G, Mazziotti S, Scribano E, Fede C, Ricca M. Potential role of colour-Doppler cystosonography with echocontrast in the screening and follow-up of vesicoureteral reflux. *Acta Paediatr*. 2000 Nov;89(11):1336-9. doi: 10.1080/080352500300002534.
10. Marra G, Oppezzo C, Ardissino G, Daccò V, Testa S, Avolio L, Taioli E, Sereni F; ItalKid Project. Severe vesicoureteral reflux and chronic renal failure: a condition peculiar to male gender? Data from the ItalKid Project. *J Pediatr*. 2004 May;144(5):677-81. doi: 10.1016/j.jpeds.2004.01.043.
11. Mastro Simone S, Pignata G, Maresca MC, Calconi G, Rabassini A, Butini R, Fandella A, Di Falco G, Chiara G, Caldato C, et al. Clinical significance of vesicoureteral reflux after kidney transplantation. *Clin Nephrol*. 1993 Jul;40(1):38-45.
12. Miyakita H, Hayashi Y, Mitsui T, Okawada M, Kinoshita Y, Kimata T, Koikawa Y, Sakai K, Satoh H, Tokunaga M, Naitoh Y, Niimura F, Matsuoka H, Mizuno K, Kaneko K, Kubota M. Guidelines for the medical management of pediatric vesicoureteral reflux. *Int J Urol*. 2020 Jun;27(6):480-490. doi: 10.1111/iju.14223.
13. Elder JS. Vesicoureteral reflux. In: Kliegman R, Nelson WE, eds. *Nelson Textbook of Pediatrics*. 19th ed. Philadelphia, PA: Elsevier/Saunders; 2011:1834-1838.

*Corresponding author: Awatef M. Omer, Ph.D. Department of Diagnostic Radiology Technology, College of Applied Medical Sciences, Taibah University, Almadinah Almunawwarah, Kingdom of Saudi Arabia. E-mail: Awatefomer222@hotmail.com

14. Darge K, Troeger J. Vesicoureteral reflux grading in contrast-enhanced voiding urosonography. *Eur J Radiol.* 2002 Aug;43(2):122-8. doi: 10.1016/s0720-048x(02)00114-6.
 15. Bosio M. Cystosonography with echocontrast: a new imaging modality to detect vesicoureteric reflux in children. *Pediatr Radiol.* 1998 Apr;28(4):250-5. doi: 10.1007/s002470050343.
 16. Jodal U, Smellie JM, Lax H, Hoyer PF. Ten-year results of randomized treatment of children with severe vesicoureteral reflux. Final report of the International Reflux Study in Children. *Pediatr Nephrol.* 2006 Jun;21(6):785-92. doi: 10.1007/s00467-006-0063-0.
 17. Cannon GM Jr, Arahna AA, Graham DA, Passerotti CC, Silva A, Retik AB, Nguyen HT. Improvement in vesicoureteral reflux grade on serial imaging predicts resolution. *J Urol.* 2010 Feb;183(2):709-13. doi: 10.1016/j.juro.2009.10.037.
 18. Banker H, Aeddula NR. Vesicoureteral reflux. InStatPearls [Internet] 2022 Aug 10. StatPearls Publishing.
 19. Papadopoulou F, Efremidis SC, Oiconomou A, Badouraki M, Panteleli M, Papachristou F, Soteriou I. Cyclic voiding cystourethrography: is vesicoureteral reflux missed with standard voiding cystourethrography? *Eur Radiol.* 2002 Mar;12(3):666-70. doi: 10.1007/s003300101108. Epub 2001 Sep 18. Erratum in: *Eur Radiol* 2002 Jan;12(1):260. Economou Anastasia [corrected to Oiconomou Anastasia]. PMID: 11870484.
 20. Braga LH, Farrokhyar F, D'Cruz J, Pemberton J, Lorenzo AJ. Risk factors for febrile urinary tract infection in children with prenatal hydronephrosis: a prospective study. *J Urol.* 2015 May;193(5 Suppl):1766-71. doi: 10.1016/j.juro.2014.10.091.
 21. Anand S, Sandlas G, Pednekar A, Jadhav B, Terdal M. A Comparative Study of the Ergonomic Risk to the Surgeon During Vesicoscopic and Robotic Cross-Trigonal Ureteric Reimplantation. *J Laparoendosc Adv Surg Tech A.* 2021 Aug 27. doi: 10.1089/lap.2021.0471.
 22. Chang JW, Liu CS, Tsai HL. Vesicoureteral Reflux in Children with Urinary Tract Infections in the Inpatient Setting in Taiwan. *Clin Epidemiol.* 2022 Mar 12;14:299-307. doi: 10.2147/CLEP.S346645.
 23. Bartik ZI, Sillén U, Djos A, Lindholm A, Fransson S. Whole exome sequencing identifies KIF26B, LIFR and LAMC1 mutations in familial vesicoureteral reflux. *PLoS One.* 2022 Nov 23;17(11):e0277524. doi: 10.1371/journal.pone.0277524.
-

Characterization of Primary and Malignant Liver Lesions using Texture Analysis

Abdalrafia Balla Mohammed^{1,2}, Mohammed Garelnabi³, Asma Alamin³, Muna A M A Ali Abushanab³, Kawthar Moh. Sharif⁴, Anna Mohamed Ahmed⁵, Hamid Osman^{6*}

¹Radiology Department, Alshaab Teaching Hospital, Khartoum, Sudan

²Faculty of Radiography and Medical Imaging, National University Sudan, Khartoum, Sudan

³College of Medical Radiological Science, Sudan University of Science and Technology, Khartoum, Sudan

⁴Radiology Department, Al Ghad International College of Applied Medical Sciences, Dammam, Saudi Arabia

⁵Department of Radiological Sciences, College of Applied Medical Sciences, King Khalid University, Abha, Saudi Arabia

⁶Department of Radiologic Sciences, College of Applied Medical Science, Taif University, Taif, Saudi Arabia

Abstract

Texture analysis can be used as a classification approach to describe microscopic changes in the liver. In our study, a total of 260 patients aged 4 to 90 underwent successful liver ultrasound examinations using a General Electric ultrasound machine (21045-87) with a 3.5MHz curve-linear transducer, typically used to scan the liver. The liver was scanned in multiple planes (transverse, sagittal, and oblique) to analyze the lesion based on shape, position, size, and echogenicity. Then the pictures were retrieved and classified into 5 categories: normal, a liver cyst, a hydatid cyst, hepatocellular carcinoma (HCC), and liver metastases. All pictures were 512 x512 pixels with 8-bit gray-level and were encoded in DICOM format; then three FOS features (mean, entropy, and energy, obtained from the intensity function of the images) were calculated for each ROI through all images using a 3x3 window size, and the data were processed for stepwise linear discriminant (SW-LD) analysis. The classification matrix of the original and predicted groups, using the discriminant function, presents the classification accuracy of each class in which 99.2% of normal liver was correctly classified and 75.6%, 81.4%, 100.0%, and 100.0% classification sensitivity for liver cyst, HCC, hydatid cyst, and liver metastases, respectively, with the highest predictive overall accuracy of 89.1%. (**International Journal of Biomedicine. 2023;13(1):111-114.**)

Keywords: liver • focal liver lesions • ultrasound • texture analysis • first order statistics

For citation: Mohammed AB, Garelnabi M, Alamin A, Abushanab M, Sharif KM, Ahmed AM, Osman H. Characterization of Primary and Malignant Liver Lesions using Texture Analysis. International Journal of Biomedicine. 2023;13(1):111-114. doi:10.21103/Article13(1)_OA15

Abbreviations

FOS, first order statistics; FLL, focal liver lesions; HCC, hepatocellular carcinoma; ROI, region of interest.

Introduction

Focal liver lesions are described as solid or liquid-containing masses that are not part of the normal anatomy of

the liver and may be distinguished from it utilizing imaging techniques.^(1,2)

They might be benign, cancerous, or metastatic. Benign lesions that are commonly found include pyogenic liver

abscess, localized nodular hyperplasia, simple cyst, hydatid cyst, and hemangioma.⁽³⁾ Due to the prevalence of a wide diversity of sonographic appearances, even within certain classes of focal liver lesions (FLL), differential diagnosis in FLL patients using B-mode (US) images is extensive.^(4,5)

Even so, B-mode ultrasonography⁽⁶⁾ is the preferred method for characterizing FLL due to its non-radioactive, non-invasive, low-cost, and real-time imaging characteristics. There is a particular disadvantage associated with using B-mode ultrasound for the FLL diagnosis, namely limited sensitivity for detecting small FLL developed (less than 2cm) in the cirrhotic liver, which is already nodular and coarse textured.⁽⁷⁾

The sonographic appearance of HCC, a typical hemangioma, and typical metastases are highly overlapping; the sonographic appearance of cystic metastases and a typical cyst often overlap.⁽⁸⁾ Even for seasoned radiologists, distinguishing tumor-affected tissue is a difficult task. The definitive diagnosis frequently necessitates invasive treatments such as needle biopsy or even surgery, which can be dangerous. New computer-aided image-processing technologies (particularly texture analysis) combined with effective classification algorithms can significantly enhance diagnosis accuracy. Those approaches, which extract information not generally recognized by the human eye, could reduce or even eliminate the need for intrusive procedures.⁽⁹⁾ One of the most important issues to address when performing computer-aided image analysis is the objective and explicit categorization of image regions. The texture of studied image regions could be one of the most valuable sources of information.⁽¹⁰⁾ The texture analysis entails obtaining a set of numerical parameters (referred to as texture characteristics) to characterize the ROI specified in the organs under investigation. Each texture parameter reflects a specific texture property, such as coarseness, homogeneity, or local contrast. A wide range of approaches to extracting texture features has been researched thus far.⁽¹¹⁾ Texture analysis is an important aspect of picture processing. It is a collection of mathematical strategies for quantifying the different gray levels in an image in terms of intensity and distribution. The texture is the spatial organization of gray levels in pixels in a location. As a result, it can be classified into two types: periodic texture and random texture. As a result, we can distinguish between structural and statistical techniques to calculate a number of mathematical factors that characterize texture. The study of periodic or regular textures lends itself better to structural techniques. Statistical methods, on the other hand, are employed to describe fine and non-homogeneous structures with no apparent regularity. As a result, this approach is commonly used in medical imaging.⁽¹²⁾ A texture is perceived as a quantitative measure of the organization of intensities in an area via a statistical approach. Based on the number of pixels required to define the feature, statistical methods are classified as first-order, second-order, higher-order, and spectral statistics.⁽¹³⁾

To calculate texture, first order statistics (FOS) measures are applied to the image histogram. The fundamental advantage of this strategy is its simplicity in characterizing data using

standard descriptors. For any surface, or image, grey levels are in the range $0 \leq i \leq N_g - 1$, where N_g is the total number of distinct grey levels. If $N(i)$ is the number of pixels with intensity i and M is the total number of pixels in an image, it follows that the histogram, or pixel occurrence probability, is given by $P(i) = N(i)/M$

Texture analysis techniques are commonly employed in image-processing disciplines such as classification, segmentation, and synthesis. Image classification aims to organize diverse images or image portions into distinct categories.⁽¹⁴⁾ Texture analysis methods are particularly suited to this since they provide unique information on the texture, or spatial variation, of pixels of the region in question. Image segmentation problems aim to define boundaries between distinct image sections. Image texture synthesis is essential in 3D computer graphics applications, where the goal is to build highly complex and realistic-looking surfaces.⁽¹⁵⁾ In general, seven characteristics are computed that are typically employed to define the qualities of the image histogram, and hence image texture. These are the following: mean, variance, coarseness, skewness, kurtosis, energy, and entropy.⁽¹⁶⁾

Materials and Methods

A total of 260 patients aged 4 to 90 underwent successful liver ultrasound examinations using a General Electric ultrasound machine (21045-87) with a 3.5MHz curve-linear transducer, typically used to scan the liver.

The study was conducted between 2016 to 2019. All participants provided written informed consent.

The liver was scanned in multiple planes (transverse, sagittal, and oblique) to analyze the lesion based on shape, position, size, and echogenicity. Then the pictures were retrieved and classified into 5 categories: normal, a liver cyst, hydatid cyst, hepatocellular carcinoma (HCC), and liver metastases. All pictures were 512 x 512 pixels with 8-bit gray-level and were encoded in DICOM format; then three FOS features (mean, entropy, and energy, obtained from the intensity function of the images) were calculated for each ROI through all images using a 3x3 window size, and the data were processed for stepwise linear discriminant (SW-LD) analysis. Studies with normal liver texture were performed as a control group. The obtained results are shown in Table 1 and Figures 1-4.

Results and Discussion

FOS was used to extract characteristics from ultrasound images in this investigation. Characteristics, which included mean, energy, and entropy, revealed a significant association with the studied 5 classes. All of these parameters were calculated for all images. The data were then ready for discrimination, which was performed using a stepwise technique to select the most significant feature that can be used to classify the classes in ultrasound liver images.

The results show a high concentration of components around the class centers, resulting in a significant difference between the classes (Figure 1).

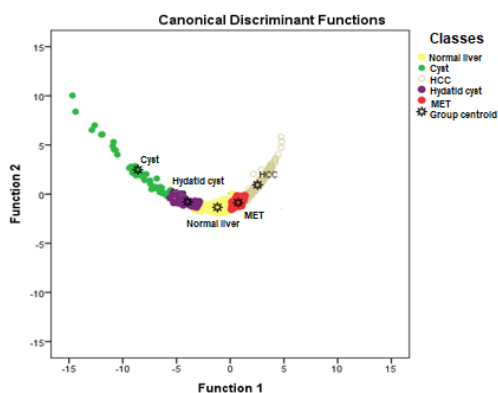


Fig. 1. Scatter plot of the classes using discriminant function and center of classes.

The classification matrix of the original and predicted groups, using the discriminant function, presents the classification accuracy of each class in which 99.2% of normal liver was correctly classified and 75.6%, 81.4%, 100.0%, and 100.0% classification sensitivity for liver cyst, HCC, hydatid cyst, and liver metastases (MET), respectively, with the highest predictive overall accuracy of 89.1% (Table 1).

Table 1.

The classification matrix of the original and predicted groups using the discriminant function.

Classes	Predicted Group Membership					Total
	Normal liver	Cyst	HCC	Hydatid Cyst	Metastasis	
Normal liver	99.2%	0.0	0.0	0.0	0.8	100.0
Cyst	0.0	75.6%	0.0	24.4%	0.0	100.0
HCC	0.0	0.0	81.4%	0.0	18.6	100.0
Hydatid Cyst	0.0	0.0	0.0	100.0%	0.0	100.0
Metastases	0.0	0.0	0.0	0.0	100.0%	100.0

There was a high concentration of features around the class centers, resulting in a significant disparity across the 5 classes. From the standpoint of discriminant power in terms of applied characteristics, entropy, like the mean, can successfully discriminate between all classes. The mean and entropy can successfully distinguish cysts and HCC from the rest of the tissue. Still, they are ineffective in distinguishing metastases and HCC since they have comparable average group levels. Textural heterogeneity and overlaps are observed.

Finally, the energy emphasizes HCC more than the other tissue types (Figures 2-4).

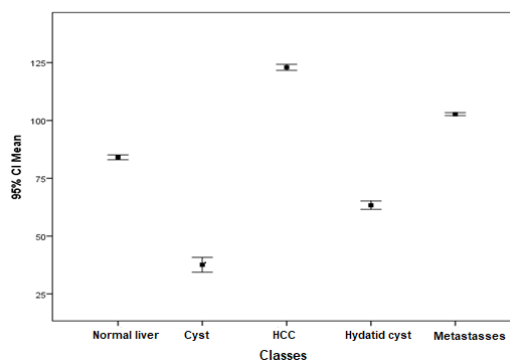


Fig. 2. An error bar of 5 classes using the mean feature with the standard error.

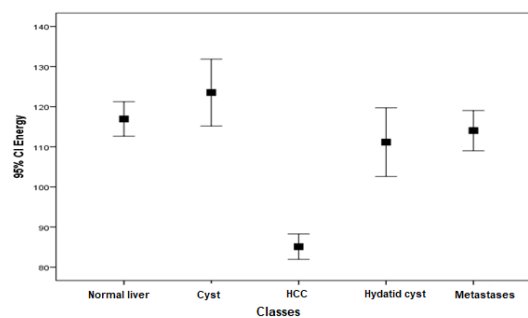


Fig. 3. An error bar of 5 classes using the energy feature with the standard error.

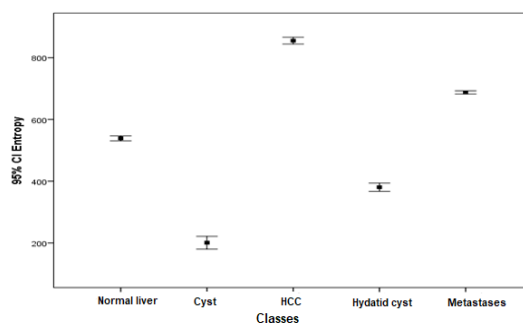


Fig. 4. An error bar of 5 classes using the entropy feature with the standard error.

Conclusion

Based on textural features, excellent discrimination between benign and malignant liver lesions can be achieved, and this serves as a secondary method for further characterization of the lesion. The texture reveals a different underlying pattern in the normal liver than do benign and malignant liver lesions, with an overall classification accuracy of 89.1%. Texture analysis can be used as a classification approach to describe microscopic changes in the liver. To summarize the findings of this study, the following equation should be used to classify liver tissue as normal, cyst, HCC, hydatid cyst, or liver metastases (MET), with the highest value receiving the most votes.

$$\text{Normal liver} = (35.6 \times \text{mean}) + (0.2 \times \text{Energy}) + (-4.2 \times \text{Entropy}) - 365.8$$

Cyst = $(25.7 \times \text{mean}) + (0.19 \times \text{Energy}) + (-3.1 \times \text{Entropy}) - 185.4$

HCC = $(35.8 \times \text{mean}) + (0.17 \times \text{Energy}) + (-4.2 \times \text{Entropy}) - 411.0$

Hydatid cyst = $(32.95 \times \text{mean}) + (0.185 \times \text{Energy}) + (-3.95 \times \text{Entropy}) - 303.19$

MET = $(36.4 \times \text{mean}) + (.205 \times \text{Energy}) + (-4.31 \times \text{Entropy}) - 400.4$

Competing Interests

The authors declare that they have no competing interests.

References

1. Suganya R, Rajaram S. Content Base Image Retrieval of Ultrasound Liver Diseases Based on Hybrid Approach. American Journal of Applied Sciences. 2012;9(6):938-945.
2. Pons F, Llovet JM. Approaching focal liver lesions. Rev Esp Enferm Dig. 2004 Aug;96(8):567-73; 573-7. doi: 10.4321/s1130-01082004000800006. PMID: 15449988.
3. Kumar P, Hegde P, Kumar BN, et al. A comparative study of Ultrasound and CT finding in focal liver lesions. Int Bio Med Res, 2014;5(3);4362-4369.
4. Namasivayam S, Salman K, Mittal PK, Martin D, Small WC. Hypervascular hepatic focal lesions: spectrum of imaging features. Curr Probl Diagn Radiol. 2007 May-Jun;36(3):107-23. doi: 10.1067/j.cpradiol.2006.12.004. PMID: 17484954.
5. Mittelstaedt CA. Ultrasound as a useful imaging modality for tumor detection and staging. Cancer Res. 1980 Aug;40(8 Pt 2):3072-8. PMID: 7397702.
6. Bates J. Abdominal Ultrasound How, Why, and When. The 2nd edition. Churchill Livingstone Oxford, 2004.
7. Virmani J, Kumar V, Kalra N, Khandelwal N. SVM-based characterization of liver ultrasound images using wavelet packet texture descriptors. J Digit Imaging. 2013 Jun;26(3):530-43. doi: 10.1007/s10278-012-9537-8.
8. Mittal D, Kumar V, Saxena SC, Khandelwal N, Kalra N. Neural network based focal liver lesion diagnosis using ultrasound images. Comput Med Imaging Graph. 2011 Jun;35(4):315-23. doi: 10.1016/j.compmedimag.2011.01.007.
9. Roux C, Coatrieux JL. Contemporary perspectives in three-dimensional biomedical imaging. Stud Health Technol Inform. 1997;30:1-393. PMID: 10168097.
10. Haralick RM. Statistical and structural approaches to texture. Proc. IEEE 1979;67:786-804.
11. Galloway MM. Texture analysis using gray level run lengths. Computer Graphics and Image Processing. 1975;4:172-179.
12. Sassi OB, Sellami L, Slima MB. Improved spatial gray level dependence matrices for texture analysis. International Journal of Computer Science & Information Technology (IJCSIT).2012;4(6):209- 219.
13. Gunasundari S, Janakiraman. A Study of Textural Analysis Methods for the Diagnosis of Liver Diseases from Abdominal Computed Tomography. International Journal of Computer Applications. 2013;74(11):7-13.
14. Pietikainen MK. Texture analysis in machine vision. World Scientific Publishing. 2000:981-02- 4373-1.
15. Mirmehdi M, Xie X, Suri J. Handbook of texture analysis. Imperial College Press, 2008:1- 84816-115-18.
16. Tuceryan M, Jain AK. Texture analysis. In: Chen CH, Pau LF, Wang PSP, editors. The handbook of pattern recognition and computer vision. 2nd ed. World Scientific Publishing Co. Singapore 1998: ISBN 9-810- 23071-0.

**Corresponding author: Prof. Hamid Osman Hamid
Department of Radiologic Sciences, College of Applied Medical
Science, Taif University, Taif, Saudi Arabia. E-mail: hamidssan@
yahoo.com*

Evaluation of Traumatic Knee Joint Injuries Using Magnetic Resonance Imaging

Mona Elhaj^{1*}, Amin Elzaki¹, Amel F. Alzain², Hanan Elnor¹, Wisal B Hassan¹, Mogahid Zidan³, Samih Kajoak¹, Shahd Alamri¹, Hajar Aljuaid¹, Njood Almuthafari¹, Fi Alshehri¹

¹Department of Radiological Sciences, College of Applied Medical Sciences, Taif University, Taif, Saudi Arabia

²Collage of Medical Applied Science, Taibah University, Department of Diagnostic Radiology Technologies, Almadinah Almunawara, Saudi Arabia

³Faculty of Radiology and Nuclear Medicine Science, The National Ribat University, Khartoum, Sudan

Abstract

Background: MRI is a widely used modality for diagnosing patients with knee complaints, and it has increasingly replaced diagnostic arthroscopy in this regard. The current research aimed to study the assessment of traumatic knee injuries using MRI, to identify any correlations between the type of tissue damage and age, to determine the ligaments most frequently involved, and to compare the frequency of knee injuries in athletes to those in the general population.

Methods and Results: This cross-sectional study included 150 patients with a history of knee injuries who were referred for knee MRI. The study was carried out in the radiology departments of two hospitals (King Faisal Hospital and King Abdulaziz Specialist Hospital, Taif, Saudi Arabia). Medical reports were collected from March 2021 to April 2022. The largest number of affected males were in the age group of 20-30 years; the largest number of affected females were in the age groups of 51-60 years and >60 years. Most athletic patients were in the age group of 20-30 years of age. The anterior cruciate ligament (51.9%) and meniscus (43.1%) were the most affected parts of the knee joint in patients of all ages. Joint effusions and cysts were found in 74.4% and 21.6%, respectively, among all age groups. A torn disc was found in 4 cases, only in male patients aged <20 to 40 years.

Conclusion: A non-invasive, radiation-free procedure, MRI facilitates accurate "lesion mapping," which is important in the diagnosis and follow-up of traumatic knee injuries. (**International Journal of Biomedicine. 2023;13(1):115-119.**)

Keywords: knee joint • ligament • meniscus • MRI

For citation: Elhaj M, Elzaki A, Alzain AF, Elnor H, Hassan WB, Zidan M, Kajoak S, Alamri S, Aljuaid H, Almuthafari N, Alshehri F. Evaluation of Traumatic Knee Joint Injuries Using Magnetic Resonance Imaging. International Journal of Biomedicine. 2023;13(1):115-119. doi:10.21103/Article13(1)_OA16

Abbreviations

ACL, anterior cruciate ligament; **CT**, computed tomography; **FSE**, fast spin echo; **LCL**, lateral collateral ligament; **MRI**, magnetic resonance imaging; **MCL**, medial collateral ligament, **PCL**, posterior cruciate ligament.

Introduction

The knee joint is the largest in the human body.⁽¹⁾ A form of synovial hinge joint allows for flexion, extension, and external and internal rotation.^(2,3) The knee joint is responsible

for weight-bearing and mobility.⁽⁴⁾ It is made up of bones (the femur, tibia, patella), ligaments (the anterior and posterior cruciate ligaments [ACL, PCL], and medial and lateral collateral ligaments [MCL, LCL]), tendons, and menisci; the medial and lateral menisci act as cushions.^(4,5) Ligament and

meniscal injuries are more common, more varied, and more severe in young athletes than other types of injuries and linked with a high rate of morbidity, which necessitates surgical care and a lot of rest.⁽⁶⁾ Joint damage has been identified as a significant risk factor for onset of osteoarthritis.^(6,7)

Despite the importance of clinical evaluation in diagnosing ligament and meniscal injury, painful stress tests are not always successful in the acute phase of the injury. In the event of a knee joint injury, medical assessment, radiographs, and even a CT scan are insufficient to diagnose certain internal joint derangements. As a result of its superior soft tissue contrast resolution and multiplanar imaging capabilities,⁽⁶⁾ MRI is a widely used modality for diagnosing patients with knee complaints, and it has increasingly replaced diagnostic arthroscopy in this regard. With the ability to examine different anatomy and pathology, ranging from ligamentous injuries to articular cartilage lesions, MRI is considered the optimal imaging and diagnostic method for the knee joint.^(8,9)

The use of MRI in diagnostic imaging of the knee has revolutionized the field.⁽¹⁰⁾ MRI offers superior soft tissue contrast and can analyze soft tissue and bony structures in several imaging planes, giving it a significant advantage over other imaging techniques. A non-invasive, radiation-free procedure, MRI facilitates accurate “lesion mapping,” which is important in the diagnosis and follow-up of traumatic knee injuries.^(7,11) In addition, MRI is a cost-effective technique as it reduces unnecessary surgical and arthroscopic interventions.^(7,12,13) Early detection of knee injuries is critical for avoiding the long-term implications of delayed treatment.^(14,15)

Materials and Methods

Study population

This study was cross-sectional in design. Medical reports of 150 patients were collected from March 2021 to April 2022. The study was carried out in the radiology departments of two hospitals (King Faisal Hospital and King Abdulaziz Hospital). Ethical approval for this study was obtained from the Research and Studies Department at the Directorate of Health Affairs at Taif City, The Ministry of Health (IRB Registration Number with KACST, KSA: HAP-02-T-067, approval number 674; on 02/02/2022). All participants provided written informed consent.

Data collection

Patients were examined using a Philips Gyroscan ACS-NT 1.5T MRI scanner and Siemens Magnetom Skyra 3T scanner. Fast spin echo (FSE) imaging, in combination with fat suppression (FS) MRI techniques, was used to improve the sensitivity and specificity of MRI in identifying ligament damage. The sequence was as follows: axial FSE (proton density or fat-saturated T2-weighted sequence), coronal FSE (proton density and/or fat-saturated T2-weighted sequence), and sagittal FSE (proton density with/without fat saturation and fat-saturated T2-weighted ± T1-weighted sequence)

MRI image analysis

The knee MRI scans were assessed for the presence of knee injuries. Two radiologists with more than five years of experience in musculoskeletal system imaging interpreted all

scans in consensus to decrease the inter- and intra-observer variability error/detection rate.

The MCL and LCL injuries were diagnosed in the axial and coronal FSE. The imaging features of ligament injury appeared as discontinuity of medial meniscofemoral and meniscotibial ligaments with a wavy form of the ligament.

In addition, the tears were diagnosed when the obtained signal intensity was increased on proton-density-weighted (PDw) and fat-saturated, T2-weighted images.

Finally, some imaging features appeared in some patients with knee injuries, such as bone contusion, anterior translation of the tibia, meniscal injury, and a joint effusion.

The statistical analysis was performed using the statistical software Microsoft Excel.

Results

A total of 150 patients (121[80.7%] males and 29[19.3%] females) were examined by MRI and presented with clinically suspected knee joint abnormalities, given the presence of a knee injury history. The mean age for males and females was 35.4 and 47.7 years, respectively. The largest number of males (35.5%) were in the age group of 20-30 years; the largest number of females were in the age groups of 51-60 years and >60 years (24.1% in both cases). In contrast, the age group of >60 years was smallest for males (5.8%), and the groups of 20-30 years and <20 years were smallest for females (6.9% in both cases) (Table 1).

Table 1.

Distribution of patients according to age and gender.

Age-group (years)	Male n (%)	Female n (%)	Total n (%)
<20	10 (8.3)	2 (6.9)	12 (8.0)
20-30	43 (35.5)	2 (6.9)	45 (30.0)
31-40	35 (28.9)	6 (20.7)	41 (27.3)
41-50	17 (14.0)	5 (17.2)	22 (14.7)
51-60	9 (7.4)	7 (24.1)	16 (10.7)
>60	7 (5.8)	7 (24.1)	14 (9.3)
Total	121 (80.7)	29 (19.3)	150 (100%)

In our study, 53(35.3%) of the patients were athletes. Most athletic patients were in the age group of 20-30 years of age. The age group of >60 years was the smallest (1.9%). Most athletic patients were male (92.5%), and only 7.5% were female (Table 2).

The ACL (51.9%) and meniscus (43.1%) were the most affected parts of the knee joint in patients of all ages (Table 3). For males, the ACL (53.7%) was the most affected, followed by the meniscus (41.1%). In contrast, the meniscus was most affected for females (53.8%), followed by the ACL (42.3%) (Table 4). Joint effusions and cysts were found in 74.4% and 21.6%, respectively, among all age groups (Table 5). Joint

effusions affected 75.9% of males and 68.6% of females, followed by cysts, which were identified in 19.1% of males and 31.4% of females (Table 6). A torn disc was found in 4 cases, only in male patients aged <20 to 40 years (Table 7).

Table 2.

Distribution of athletic patients (n=53) according to age

Age group (years)	Athletic patients n (%)
<20	3 (5.7)
20-30	22 (41.5)
31-40	14 (26.4)
41-50	11 (20.8)
51-60	2 (3.8)
>60	1 (1.9)

Table 3.

Distribution of patients according to the relationship between knee injuries (n=160) and age

Age group (years)	ACL	PCL	MCL	LCL	Meniscus	Patellar
<20	5	0	0	0	0	0
20-30	31	0	1	1	17	1
31-40	25	2	0	0	20	0
41-50	11	0	0	0	13	1
51-60	3	1	0	0	8	0
>60	8	1	0	0	11	0
Total	83(51.9%)	4(2.5%)	1(0.6%)	1(0.6%)	69(43.1%)	2(1.3%)

Table 4.

Distribution of patients according to the relationship between knee injury (n=160) and gender

Gender	ACL n(%)	PCL n(%)	MCL n(%)	LCL n(%)	Meniscus n(%)	Patellar n(%)	Total n(%)
Male	72(53.7)	3(2.2)	1(0.75)	1(0.75)	55(41.0)	2(1.5)	134(83.8)
Female	11(42.3)	1(3.8)	0(0)	0(0)	14(53.8)	0(0)	26(16.2)

Table 5.

Distribution of patients according to the relationship between pathology and age.

Age-group (years)	Normal	Joint effusion	Cyst	Fusion	Fracture
<20	0	12	0	0	0
20-30	4	40	4	0	1
31-40	4	37	10	0	1
41-50	1	18	8	2	1
51-60	1	13	8	0	2
>60	1	11	8	0	0
Total	11	131	38	2	5

Table 6.

Distribution of patients according to the relationship between pathology and gender.

Gender	Joint effusion	Cyst	Fusion	Fracture	Total
Male	107 (75.9%)	27 (19.1%)	2 (1.4%)	5 (3.5%)	141(80.1%)
Female	24 (68.6%)	11 (31.4%)	0	0	35 (19.9%)

Table 7.

Distribution of patients according to the relationship between a torn disc and age.

Ages (years)	Torn disc
<20	1 (25%)
20-30	1 (25%)
31-40	2 (50%)
41-50	0
51-60	0
>60	0
Total	4 (100%)

Figure 1 presents MRI images of the knee of a 45-year-old male who presented with pain and swelling in his left knee after a twisting injury.

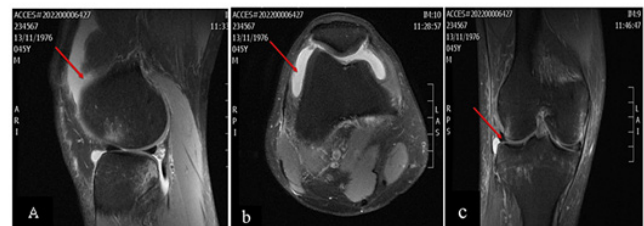


Fig. 1. MRI images of the knee for a 45-year-old male who presented with pain and swelling in his left knee after a twisting injury:

A): Sagittal FS PD-FSE image demonstrates moderate to severe joint effusion (red arrow); (B): Axial FS PD-FSE image indicates moderate to severe joint effusion (red arrow); (C): Coronal FS PD-FSE image shows a lateral meniscus posterior horn tear (red arrow).

Discussion

The increased resolution and precision of MRI have caused it to become recognized as the optimal method for imaging patients with trauma to the knee.⁽¹⁶⁾ Its diagnostic performance has been demonstrated to be superior to physical investigations for recognizing damage to the menisci and ligaments.⁽¹⁷⁾

The current research aimed to study the assessment of traumatic knee injuries using MRI, to identify any correlations between the type of tissue damage and age, to determine the ligaments most frequently involved, and to compare the frequency of knee injuries in athletes to those in the general population.

In our study, the male-to-female ratio was 4:1. The mean age for males and females was 35.4 and 47.7 years, respectively. Our gender/age findings were in accordance with a study by Umap et al.,⁽⁶⁾ which aimed at evaluating traumatic knee joint injuries with MRI. In a study by Yawn et al.,⁽¹⁸⁾ injured men were younger than injured women and more likely to have an injury during a sports activity, whereas women's injuries were more likely to result from non-sports-related falls. Knee sprain or strain was the most common final diagnosis (36%) among 664 patients with an isolated acute knee injury.

In the current study, the ACL (51.9%) and meniscus (43.1%) were the most affected in patients of all ages. In a study by Hetta et al.,⁽¹⁹⁾ among 25 patients who had sports-related knee injuries, 15(60%) had ACL injuries, 2(8%) had PCL injuries, 10(40%) had meniscal injuries, 8(32%) had collateral ligament injuries, 5(20%) had bone injuries, and 2(8%) had muscular injuries. Comparing the results from MRI findings of sport-related knee injuries with arthroscopic or surgical findings, Lazarova and Gligorievski⁽²⁰⁾ found that the accuracy of MRI in detecting the meniscal lesion was 66.7% for the complete meniscal lesion and 85.7% for the incomplete meniscal lesion. In detecting the ACL lesion, the accuracy of MRI was 85.7% for the complete ACL lesion and 80.8% for the partial ACL lesion.

In our study, the joint effusion (74.4%) and cysts (21.6%) were the most common pathologies among all age groups. Mahmoud et al.⁽²¹⁾ found that joint effusion was found on MRI in 63.8% of cases among 58 patients with knee joint pain. Our results align with those of Nasir,⁽²²⁾ in that males are more likely than females to present with joint effusion. However, the studies disagree in that, in the present work, cysts were more commonly identified in women.

Previous studies evaluated the spinal factors and the development of knee osteoarthritis. Tsuji et al.⁽²³⁾ reported that the presence of patella-femoral pain correlated well with the sacral inclination and knee flexion position and with changes in lumbar kyphosis. They called this correlation the "knee-spine syndrome." Murata et al.⁽²⁴⁾ suggested that degenerative changes in the knee might be a factor in the development of loss of lordosis. Tauchi et al.⁽²⁵⁾ showed that an increase in spinal inclination angle (OR=1.073, $P<0.05$) was significantly associated with knee osteoarthritis. In the current study population, a torn disc was noted in males aged <20-40 years.

Our study had several limitations. First, the number of subjects was relatively small. Second, the data collected also had no information about the sporting discipline. Thus, it is necessary to conduct further research, considering these limitations.

In conclusion, MRI is one of the imaging modality choices for rapidly diagnosing the knee joint injury and evaluating its condition. MRI can also be used instead of more invasive modalities in patients with traumatic knee injuries.

Competing Interests

The authors declare that they have no competing interests.

References

1. Kulowski J. Flexion contracture of the knee: the mechanics of the muscular contracture and the turnbuckle cast method of treatment; with a review of fifty-five cases. 1932. Clin Orthop Relat Res. 2007 Nov;464:4-10. doi: 10.1097/BLO.0b013e31815760ca.
2. Gupton M, Munjal A, Terreberry RR. Anatomy, Hinge Joints. StatPearls. StatPearls Publishing.
3. Rytter S, Egund N, Jensen LK, Bonde JP. Occupational kneeling and radiographic tibiofemoral and patellofemoral osteoarthritis. J Occup Med Toxicol. 2009 Jul 13;4:19. doi: 10.1186/1745-6673-4-19.
4. Saavedra MÁ, Navarro-Zarza JE, Villaseñor-Ovies P, Canoso JJ, Vargas A, Chiapas-Gasca K, Hernández-Díaz C, Kalish RA. Clinical anatomy of the knee. Reumatol Clin. 2012 Dec-2013 Jan;8 Suppl 2:39-45. doi: 10.1016/j.reuma.2012.10.002.
5. Fox AJ, Bedi A, Rodeo SA. The basic science of human knee menisci: structure, composition, and function. Sports Health. 2012 Jul;4(4):340-51. doi: 10.1177/1941738111429419.
6. Umap R, Anurag B, Bagale D, Shattari N: Evaluation of Traumatic Knee Joint Injuries with MRI. IJCMSR. 2018, 3:10.21276/ijcmsr.2018.3.3.17
7. Heidari B. Knee osteoarthritis prevalence, risk factors, pathogenesis and features: Part I. Caspian J Intern Med. 2011 Spring;2(2):205-12.
8. Chien A, Weaver JS, Kinne E, Omar I: Magnetic resonance imaging of the knee. polradiol. 2020, 85:509-531. 10.5114/pjr.2020.99415
9. Vincent JP, Magnussen RA, Gezmez F, Uguen A, Jacobi M, Weppe F, Al-Saati MF, Lustig S, Demey G, Servien E, Neyret P. The anterolateral ligament of the human knee: an anatomic and histologic study. Knee Surg Sports Traumatol Arthrosc. 2012 Jan;20(1):147-52. doi: 10.1007/s00167-011-1580-3.
10. Shapiro L, Staroswiecki E, Gold G. Magnetic resonance imaging of the knee: optimizing 3 Tesla imaging. Semin Roentgenol. 2010 Oct;45(4):238-49. doi: 10.1053/j.ro.2009.12.007.
11. Crema MD, Marra MD, Guermazi A, Bohndorf K, Roemer FW. Relevant traumatic injury of the knee joint-MRI follow-up after 7-10 years. Eur J Radiol. 2009 Dec;72(3):473-9. doi: 10.1016/j.ejrad.2008.08.001.
12. Bridgman S, Richards P, Walley G, Clement D, MacKenzie G, Al-Tawarah Y, et al. DOES A KNEE MAGNETIC RESONANCE IMAGING SCAN FOR PATIENTS ON WAITING LISTS FOR KNEE ARTHROSCOPY REDUCE THE NUMBER OF ARTHROSCOPIES?. Orthop Procs. 2006;88-B(SUPP_II):253-253. doi:10.1302/0301-620X.88BSUPP_II.0880253
13. van Oudenaarde K, Swart NM, Bloem JL, Bierma-Zeinstra SMA, Algra PR, Bindels PJE, Koes BW, Nelissen RGHH, Verhaar JAN, Luijsterburg PAJ, Reijnen M, van den Hout WB. General Practitioners Referring Adults to MR Imaging for Knee Pain: A Randomized Controlled Trial to

*Corresponding author: Mona Elhaj, Department of Radiological Sciences, College of Applied Medical Sciences, Taif University, Taif, Saudi Arabia. E-mail: mesheekh@tu.edu.sa

- Assess Cost-effectiveness. *Radiology*. 2018 Jul;288(1):170-176. doi: 10.1148/radiol.2018171383.
14. Matherne TH, Monu JU, Schruoff L, Neitzschman HR. Avulsions around the knee portend instability. *Emerg Radiol*. 2005 Jun;11(4):213-8. doi: 10.1007/s10140-005-0415-2.
15. Rossi R, Dettoni F, Bruzzone M, Cottino U, D'Elcio DG, Bonasia DE. Clinical examination of the knee: know your tools for diagnosis of knee injuries. *Sports Med Arthrosc Rehabil Ther Technol*. 2011 Oct 28;3:25. doi: 10.1186/1758-2555-3-25.
16. Gupta MK, Rauniyar MK, Karn NK, Sah PL, Dhungel K, Ahmad K. MRI evaluation of knee injury with arthroscopic correlation. *J Nepal Health Res Counc*. 2014 Jan;12(26):63-7.
17. Refaat M, El Shazly E, Elsayed A. Role of MR Imaging in Evaluation of Traumatic Knee Lesions. *BMFJ*. 2020, 37:77-86. 10.21608/bmfj.2020.110137
18. Yawn BP, Amadio P, Harmsen WS, Hill J, Ilstrup D, Gabriel S. Isolated acute knee injuries in the general population. *J Trauma*. 2000 Apr;48(4):716-23. doi: 10.1097/00005373-200004000-00021.
19. Hetta W, Niazi G. MRI in assessment of sports related knee injuries. *The. EJRN*. 2014;45:1153-1161.
20. Lazarova A, Gligorievski A. Evaluation of Knee Sport Injuries with Magnetic Resonance Images. *GMR*. 2022;6(4). doi: 10.31031/GMR.2022.06.000645
21. Z. Mahmoud M, Fagiry M, Al-Motrifi A, Sulieman A. Magnetic Resonance Imaging Findings in Knee Joint Pain at King Saud Medical City, Saudi Arabia. *IJSR*. 2013;2:4-7.
22. Nasir AI. The role of magnetic resonance imaging in the knee joint injuries. *IJRMS*. 2013;1:1-7.
23. Tsuji T, Matsuyama Y, Goto M, Yimin Y, Sato K, Hasegawa Y, Ishiguro N. Knee-spine syndrome: correlation between sacral inclination and patellofemoral joint pain. *J Orthop Sci*. 2002;7(5):519-23. doi: 10.1007/s007760200092.
24. Murata Y, Takahashi K, Yamagata M, Hanaoka E, Moriya H. The knee-spine syndrome. Association between lumbar lordosis and extension of the knee. *J Bone Joint Surg Br*. 2003 Jan;85(1):95-9. doi: 10.1302/0301-620x.85b1.13389.
25. Tauchi R, Imagama S, Muramoto A, Tsuboi M, Ishiguro N, Hasegawa Y. Influence of spinal imbalance on knee osteoarthritis in community-living elderly adults. *Nagoya J Med Sci*. 2015 Aug;77(3):329-37.
-

Radiomorphometric Indicators, their Reliability in Detecting Early Signs of Osteoporosis in Menopausal Women

Merita Shkodra-Brovina

The Ss. Cyril and Methodius University, Skopje, North Macedonia

Abstract

Background: The aim of this study was to evaluate the diagnostic value of panoramic radiography and the radiomorphometric indices in osteoporosis identification.

Methods and Results: The research included 60 women (average age of 62.90 ± 7.07 years) in the postmenopausal stage who were subjected to an assessment of bone density through the DEXA test and were divided into 2 groups based on the value of the DEXA test from the lumbar region (L1-L4): Main group (MG) included 30 women with osteoporosis (T-score < -2.5) and Comparison group (CG) included 30 women without osteoporosis (T-score > -2.5). Panoramic radiography were used to assess the mandibular cortical index (MCI), mental index (MI), panoramic mandibular index (PMI).

Based on the porosity level, Klemetti et al.(1994) has categorized MCI into three categories (C1, C2, and C3). MCI-C1, which represents the normal appearance of the lower jaw cortex without changes in bone quality, was found only in CG in 63.33%. MCI-C2 and MCI-C3 were found in 70% and 30% of cases, respectively, in MG. In CG, MCI-C2 was found in 36.67% of cases and MCI-C3 in 0% of cases. There was a significant difference between the two study groups in the distribution of MCI ($P=0.000$). MI below 3 mm was found in 19(63.33%) of cases in CG and 27(90.00%) in MG (OR=5.211, 95% CI: 1.278-21.237, $P=0.0213$). PMI below 0.3 mm was found in 7(23.33%) of cases in CG and 19(63.33%) in MG (OR=5.675 95% CI: 1.841-17.494, $P=0.0025$).

MCI sensitivity and specificity for osteoporosis were 70% (95% CI: 50.60%-85.27%) and 63.33% (95% CI: 43.86%-80.07%), respectively; PPV, NPV, and accuracy were 65.62% (95% CI: 53.03%-76.35%), 67.86% (95% CI: 53.41%-79.54%) and 66.67% (95% CI: 53.31%-78.31%), respectively. MI sensitivity and specificity at a cutoff point of 3 mm for osteoporosis were 90% (95% CI: 73.47%-97.89%) and 36.67% (95% CI: 19.93%-56.14%), respectively; PPV, NPV, and diagnostic accuracy were 58.70% (95% CI: 51.35%-65.67%), 78.57% (95% CI: 53.18%-92.21%) and 63.33% (95% CI: 49.90%-75.41%), respectively. PMI sensitivity and specificity at a cutoff point of 0.3 mm for osteoporosis were 63.33% (95% CI: 43.86%-80.07%) and 76.67% (95% CI: 57.72%-90.07%), respectively; PPV, NPV, and diagnostic accuracy were 73.08% (95% CI: 57.32%-84.58%), 67.65% (95% CI: 55.66%-77.69%) and 70.00% (95% CI: 56.79%-81.15%), respectively.

Conclusion: Panoramic radiography can be a useful tool to identify early signs of osteoporosis by using the evaluation of radiomorphometric indices. MCI, MI, and PMI can be potential screening tools for initial BMD loss. (*International Journal of Biomedicine. 2023;13(1):120-126.*)

Keywords: osteoporosis • panoramic radiography • radiomorphometric indices • mandibula

For citation: Shkodra-Brovina M. Radiomorphometric Indicators, their Reliability in Detecting Early Signs of Osteoporosis in Menopausal Women. *International Journal of Biomedicine. 2023;13(1):120-126. doi:10.21103/Article13(1)_OA17*

Abbreviations

BMD, bone mineral density; **BMI**, body mass index; **DEXA**, dual-energy x-ray absorptiometry; **LR**, likelihood ratio; **MCI**, mandibular cortical index; **MI**, mental index; **MF**, mental foramen; **MC**, mandibular cortex; **MCW**, mandibular cortical width; **NPV**, negative predictive value; **PMI**, panoramic mandibular index; **PPV**, positive predictive value; **PR**, panoramic radiography.

Introduction

Osteoporosis is a metabolic disease of bones, which is characterized by a decrease in bone strength and an increase

in the predisposition for fractures. The disease derives from micro-articular change with specific emphasis on trabecular bone, and most frequent fractures occur on the spine, wrist, and hip bones due to the predominance of trabecular bone

tissue in these structures. The disease affects more than 10 million people in the USA. Each year an estimated 1.5 million individuals suffer a fracture due to bone disease. Worldwide, osteoporosis causes 8.9 million fractures annually.⁽¹⁾ Besides the risk of fractures, osteoporosis is considered to be one of the most serious diseases due to the high degree of disability and the large number of people who remain bedridden as a result of severe complications. Disease usually develops in a progressive but latent form. In the overwhelming majority of cases, patients do not know that they suffer from the disease until the fractures occur. Fractures in these cases are the result of moderate knocks, but also cases of spontaneous fractures are not rare.⁽²⁾

Due to the high level of morbidity and its consequences, prevention and research to detect the early signs of disease are a priority among clinicians and researchers.

Osteoporosis is defined based on bone mineral density (BMD) values, referring to criteria determined by the World Health Organization (WHO). For body BMD values measured by DEXA scans, the WHO has defined a number of threshold values for osteoporosis. These values are based on units of standard deviation (SD) and are described as T- or Z-scores. T-score is a statistical definition that indicates the difference between a patient's BMD and the mean bone density of a normal population aged 20–30 years (reference population).⁽³⁾ This value shows the difference in terms of SDs. According to the WHO classification system, T-scores under the value of -2.5 are considered as osteoporosis, and between -1 and -2.5 as osteopenia; a T-score at -1.0 and above is normal.

Access to examination tests using DEXA equipment is problematic, especially in developing countries and underdeveloped countries. Even in countries where equipment is available, cost reimbursement is at a low level due to the high cost of the examination.⁽⁴⁾

Osteoporosis affects women three times more than men. The disease progresses significantly with age, when many etiological factors complement each other and favor the disease development. Estrogen is a hormone that plays a key role in bone metabolism and the deposition of bone mass during puberty. With the decrease in the level of estrogen in a very complex metabolic process, the level of bone mass loss increases, which usually begins approximately at the age of 50, except for health conditions that are accompanied by a deficit of estrogen hormone. It is considered that in the first 5 years of menopause, women lose up to 25% of their bone mass. Each year this loss is between 1% and 5%, with an average annual loss of about 2% of bone mass. BMI is also directly related to osteoporosis. Weight loss also causes the inability to produce estrogen from adipose cells, which are considered the second most important producer of estrogen in the body after the ovaries. In the European population, the risk of fracture increases below the BMI threshold of 19 kg/m².^(4,5)

Research regarding the correlation between osteoporosis and oral health dates to the 1960s. Osteoporotic changes affect both jaws, especially the lower jaw since the lower jaw consists of the cortical part of the bone, which surrounds the trabecular tissue structure of bone. The buccal cortex distal from the mental foramen (MF) is considered to be the most suitable

part to evaluate the loss of bone density. Many researchers have been focused on finding radio morphometric indicators that would serve to identify early signs of osteoporosis in panoramic radiography of women with low bone density with the aim of referring them to specialists in this area for final diagnosis. For this purpose, several radiomorphometric indices have been used, such as mandibular cortical index (MCI), mental index (MI), and panoramic mandibular index (PMI), which are considered to have the highest significance to identify early signs of osteoporosis. MCI is a qualitative index that is attributed to the visibility of the lower edge cortex of the mandible distal from the MF on both sides. Based on the porosity level, Klemetti et al.⁽⁶⁾ has categorized MCI into three categories: C1—the endosteal cortical margin is even and sharp on both sides, normal cortex; C2—moderately eroded cortex: the endosteal margin shows semilunar defects resulting from lacunar resorption, or forms endosteal cortical residues; C3—severely eroded or porous cortex: the cortex forms dense layers of endosteal and clearly porous cortical residues.

MI index refers to the width of the mandibular cortex in the region below the MF. Sizes under 3mm are considered abnormal values. PMI is the ratio between MI and distance from the lower edge of the MF to the lower edge of the mandible on both sides of the lower jaw—the method according to Benson et al.⁽⁷⁾ Values below 0.3mm are considered abnormal sizes.⁽⁸⁻¹²⁾

The aim of this study was to evaluate the diagnostic value of PR and the radiomorphometric indices in osteoporosis identification.

Materials and Methods

A total of 60 patients aged 50–80 years (average age of 62.90±7.07 years with min/max of 51/77) included in this research were informed regarding the research and its purpose and, in a voluntary manner, agreed to be part of this research project by signing a voluntary declaration of their inclusion in research in the presence of a second witness. Before initiating medical procedures, patients have carefully read the information letter regarding details of inclusion in the research.

Inclusion criteria: women aged 50-80 in the natural postmenopausal stage that have undergone an examination to assess BMD with DEXA test, and the final diagnosis by a nuclear medicine specialist.

Exclusion criteria: patients with diseases that affect the condition of bones (hyperparathyroidism, carcinoma with metastases, and patients receiving therapy that affects bone metabolism); women in the unnatural postmenopausal stage.

The research included 60 women in the postmenopausal stage who were subjected to an assessment of bone density through the DEXA test and were divided into 2 groups based on the value of the DEXA test from the lumbar region (L1-L4):

- Main group (MG) included 30 women with osteoporosis (T-score <-2.5)

- Comparison group (CG) included 30 women without osteoporosis (T-score >-2.5)

BMI was measured using calculations according to WHO standards, and underweight was identified as <18.5 kg/m², normal weight as 18.5-24 kg/m², and overweight as 25-29 kg/m².

Radiological analysis

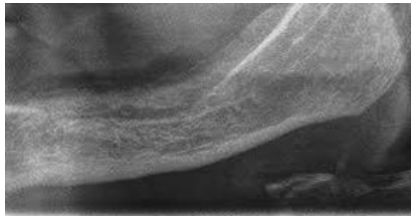
The DEXA test was done at the Nuclear Radiology Clinic of Kosovo University Clinical Center using the MEDILIN NK apparatus (MEDIX DR 2020).

Panoramic radiography was performed using Sirona Orthopos E2D. Radiological measurements were performed using the Sidexis SG system software. The following morphometric indices were assessed:

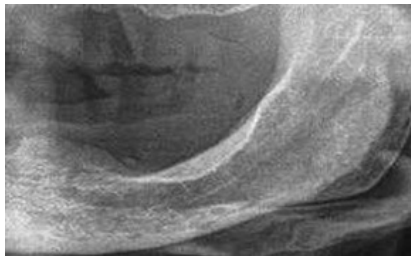
MCI: Visibility assessment of the lower edge of the mandible, distal from the MF, was done twice in timeframe intervals of 3 weeks. Based on the MC visibility assessment, patients were classified into three categories (C1-C3) according to Klemetti et al.⁽⁶⁾ (Figure 1).



A



B



C

Fig. 1. MCI categories (C1-C3) according to Klemetti et al.⁽⁶⁾
 A - Normal mandibular cortex with well-defined edges
 B - Mandibular cortex with medium porosity and lacunar changes
 C - Mandibular cortex with eroded cortex and visible deposits

MI: The MCW in PR was measured using the method according to the technique described by Lengerton,⁽¹³⁾ as follows: First, the MF is identified, then a line was drawn from the lower end of the MF in a perpendicular direction parallel to the mandible axis to the lower end of the mandible. The other drawn line touches the edges of the mandible base in the region of the MF. At the place where these two lines meet,

forming a straight right angle, the thickness of the mandible cortex is measured. The average width the lower edge border of the mandible under the MF gives values of the MI. Cortex thickness below 3 mm is considered an abnormal (reduced) value.

PMI: After identifying the MF, a perpendicular line is drawn from the lower edge of the MF to the lower edge of the mandible cortex. The ratio between MI and h (distance from the lower edge of the MF to the mandible lower edge) gives the data for the PMI values. PMI below 0.3mm is considered an abnormal (reduced) value. Measurements were performed on both sides of the mandible, and the average value was calculated, which gives the final result of PMI (Figure 2).

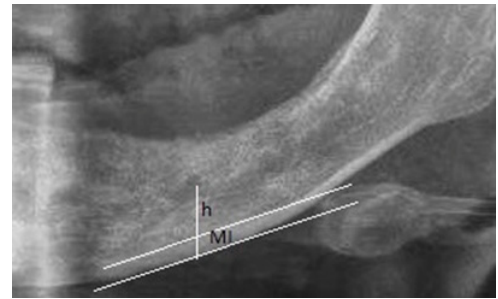


Fig.2. The distance between the two parallel lines represents the MI (MCW). PMI is the ratio between the MI and the distance from the lower border of MF to the lower border of the mandibula. $PMI=MI/h$.

Statistical analysis was performed using statistical software package SPSS version 23.0 (IBM Corp. Released 2019. IBM SPSS Statistics for Windows, Version 23.0. Armonk, NY: IBM Corp). Baseline characteristics were summarized as frequencies and percentages for categorical variables and as mean \pm SD for continuous variables. Inter-group comparisons were performed using Student's t-test. The Mann-Whitney U Test was used to compare the differences between the two independent groups (for nonparametric data). Categorical variables were analyzed using the Chi-square test with Yates' correction or, Fisher's exact test (2-tail), when appropriate. Odds ratios (ORs) and 95% confidence intervals (CIs) were calculated using logistic regression. We calculated the sensitivity, specificity, positive predictive value, negative predictive value, and likelihood ratios to determine the diagnostic value of signs. The area under the receiver operator characteristic (ROC) curve (AUC) using the MCW was measured to evaluate the diagnostic efficacy of the MCW. A probability value of $P<0.05$ was considered statistically significant.

The study was conducted in accordance with the Declaration of Helsinki and approved by the Ethics Committee of the Ss. Cyril and Methodius University, Skopje, North Macedonia. All participants provided written informed consent.

Results

The range and degree of significance of characteristics of subjects participating in research are shown in Table 1. Age

difference between the two study groups was insignificant ($P=0.787$). T-score <-2.5 was found in all women of MG. In CG, 21(70%) had T-score of -1 up to -2.5 and 9(30%) had T-score >-1 . BMI of CG women was higher than in MG women with osteoporosis ($P=0.011$). We did not find a significant difference between study groups regarding the time of menopause beginning ($P=0.052$).

Table 1.

Characteristics of subjects participating in research.

Characteristics	MG (n=30)	CG (n=30)	P-level
Age			
Mean ± SD	63.37±6.32	62.90±7.07	0.787
Min/Max	52/76	51/77	
Median	61	61	
DEXA test			
Mean ± SD	-2.98±0.76	-1.6±0.40	0.000
Min/Max	1.90/ -2.5	-2.10/ -0.40	
Median	-2.70	-1.10	
BMI			
Mean ± SD	27.25±1.95 kg/m ²	28.81±2.62 kg/m ²	0.011
Min/Max	27.70/22.50	24.66/34.60	
Median	27.70	29.79	
DEXA test values			
DEXA, T score <-2.5	30 (100%)	0 (0.00%)	0.000
DEXA, T score -1.0-2.5	0 (0.00%)	21 (70%)	
DEXA, T score >-1	0 (0.00%)	9(30%)	
Menopause stage			
Early stage <50 years	13 (43%)	6 (20.0%)	0.052
Normal stage >50 years	17 (56.7%)	24 (80%)	

MCI-C1, which represents the normal appearance of the lower jaw cortex without changes in bone quality, was found only in CG in 63.33%. MCI-C2 and MCI-C3 were found in 70% and 30% of cases, respectively, in MG. In CG, MCI-C2 was found in 36.67% of cases and MCI-C3 in 0% of cases. There was a significant difference between the two study groups in the distribution of MCI ($P=0.000$). MI below 3 mm was found in 19(63.33%) of cases in CG and 27(90.00%) in MG (OR=5.211, 95% CI: 1.278 to 21.237, $P=0.0213$). PMI below 0.3 mm was found in 7(23.33%) of cases in CG and 19(63.33%) in MG (OR=5.675, 95% CI: 1.841 to 17.494, $P=0.0025$) (Table 2).

Radiomorphometric indices were used to predict the osteoporosis disease. Through the Entry method, global accuracy of this model to predict osteoporosis was 65%. Sensitivity reaches 66.7% and specificity 63.30%. In determining the importance of radiomorphometric indices

in predicting osteoporosis, it was found that MCI has the greatest impact (Wald index = 6.296/ $P=0.012$), followed by PMI (Wald index =1.340/ $P=0.247$), and the lowest impact by MI (Wald index = 0.847/ $P=0.357$) (Table 3). Patients with MCI-C2 with moderate porosity of MC have a higher risk of developing osteoporosis (Exp(B)=4.130, 95% CI: 1.364 to 12.507, $P<0.012$) than patients with normal MC or MCI-C1. When the value of PMI increases by 0.1 mm, the chances of developing osteoporosis decrease by 42.2% (Exp(B)=0.578, 95% CI: 0.228 to 1.463); PMI impact is estimated to be insignificant ($P>0.05$). When the MI values increase by 1mm, the risk of osteoporosis decreases by 31.8%, (Exp(B)=0.682, 95% CI: 0.302 to 1.540, $P>0.05$) with an insignificant impact.

ROC analysis (MCI (1), MI, PMI) of the expected probability of detecting osteoporosis is presented in Figure 3. ROC zone was 0.720. In all possible pairs in which one has osteoporosis, and the other does not have osteoporosis, this model will determine the acceptable probability of osteoporosis.

Table 2.

The values of MCI, MI, and PMI in the study groups.

Characteristics	MG (n=30)	CG (n=30)	Statistics
MCI			
C1 Normal cortex	0	19 (63.33%)	Yates' $\chi^2= 26.695$ Yates' $P=0.0000$
C2 Moderate porosity of cortex	21 (70%)	11 (36.67%)	
C3 High porosity of cortex	9 (30%)	0 (0.00%)	
MI			
Normal value > 3 mm	3 (10%)	11 (36.67%)	OR= 5.211 95% CI (1.278-21.237) Z =2.303 $P=0.0213$
Reduce value < 3 mm	27 (90%)	19 (63.33%)	
PMI			
Normal value > 0.3 mm	11 (36.67%)	23 (76.67%)	OR= 5.675 95% CI (1.841-17.494) Z =3.023 $P=0.0025$
Reduce value < 0.3 mm	19 (63.33%)	7 (23.33%)	

Table 3.

Binary logistic regression for the prediction of osteoporosis

		B	S.E.	Wald	df	Sig.	Exp(B)	95% CI for EXP(B)	
								Lower	Upper
Step1 ^a	MCI (1)	1.418	0.565	6.296	1	0.012	4.130	1.364	12.507
	MI	0.382	0.415	0.847	1	0.357	0.682	0.302	1.540
	PMI	0.549	0.474	1.340	1	0.247	0.578	0.228	1.463
	Constant	0.464	1.114	0.173	1	0.677	1.590		
a. Variable(s) entered on step 1: MCI (1), MI, PMI.									

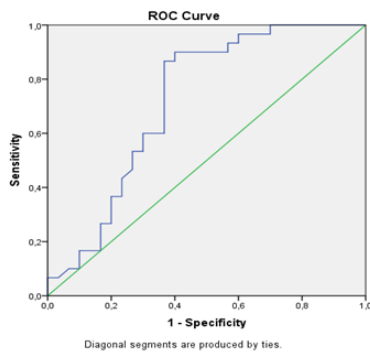


Fig. 3. Receiver Operating Characteristic (ROC) curve analysis to assess the probability of detecting osteoporosis.

Table 4 presents the sensitivity, specificity, positive predictive value, negative predictive value, and likelihood ratios to determine the diagnostic value of MCI, MI, and PMI. MCI sensitivity and specificity for osteoporosis were 70% (95% CI: 50.60% to 85.27%) and 63.33% (95% CI: 43.86% to 80.07%), respectively (code 1 is applied to MCI-C2, code 0 for MCI-C1 and MCI-C3); PPV, NPV, and accuracy were 65.62% (95% CI: 53.03% to 76.35%), 67.86% (95% CI: 53.41% to 79.54%) and 66.67% (95% CI: 53.31% to 78.31%), respectively.

MI sensitivity and specificity at a cutoff point of 3 mm for osteoporosis were 90% (95% CI: 73.47% to 97.89%) and 36.67% (95% CI: 19.93% to 56.14%), respectively (for MI < 3 mm, code 1 is applied; for MI > 3 mm, code 0 is applied); PPV, NPF, and diagnostic accuracy were 58.70% (95% CI: 51.35% to 65.67%), 78.57% (95% CI: 53.18% to 92.21%) and 63.33% (95% CI: 49.90% to 75.41%), respectively.

PMI sensitivity and specificity at a cutoff point of 0.3 mm for osteoporosis were 63.33% (95% CI: 43.86% to 80.07%) and 76.67% (95% CI: 57.72% to 90.07%), respectively (for PMI < 3 mm, code 1 is applied, code 0 for PMI > 3 mm); PPV, NPF, and diagnostic accuracy were 73.08% (95% CI: 57.32% to 84.58%), 67.65% (95% CI: 55.66% to 77.69%) and 70.00% (95% CI: 56.79% to 81.15%), respectively (Table 4).

Table 4.

Sensitivity and specificity of MCI, MI and PMI in identifying women with osteoporosis.

Index	Sensitivity Value (95% CI)	Specificity Value (95% CI)	PPV Value (95% CI)	NPV Value (95% CI)	+LR Value (95% CI)	-LR Value (95% CI)	Disease prevalence Value (95% CI)	Accuracy Value (95% CI)
MCI (any cortical shape)	70.00% (50.60%-85.27%)	63.33% (43.86%-80.07%)	65.62% (53.03%-76.35%)	67.86% (53.41%-79.54%)	1.91 (1.13-3.23)	0.47 (0.26-0.87)	50% (36.81%-63.19%)	66.67% (53.31%-78.31%)
MI < 3 mm (MCW)	90.00% (73.47%-97.89%)	36.67% (19.93%-56.14%)	58.70% (51.35%-65.67%)	78.57% (53.18%-92.21%)	1.42 (1.06-1.91)	0.27 (0.08-0.88)	50.00% (36.81%-63.19%)	63.33% (49.90%-75.41)
PMI < 0.3 mm	63.33% (43.86%-80.07%)	76.67% (57.72%-90.07%)	73.08% (57.32%-84.58%)	67.65% (55.66%-77.69%)	2.71 (1.34-5.48)	0.48 (0.29-0.80)	50% (36.81%-63.19%)	70% (56.79%-81.15%)

Discussion

The progressive but latent development of osteoporosis disease has directed many researchers to investigate more practical and accessible methods with the aim of identifying the early stages of osteoporosis. This will bring great benefits to science, medicine, the country, and its citizens since the disease manifests itself with severe complications of fractures that are accompanied by a long rehabilitation period and, at the same time, high costs for the country to reimburse health expenses.

Panoramic radiography and radiomorphometric indices have for a long time been considered a very practical option for identifying silent signs of osteoporosis, keeping in mind easy access to equipment frequently used in clinical dental practice, and technical advantages that offer a wide graphic area with easy identification of referral points.

In this study, the obtained data were compared based on research purposes. From women in the postmenopausal phase in both study groups, we received data from their anamnesis for the timeframe beginning with the menopause phase, dividing them into the group that had an early onset of menopause prior to the age of 50 and those that had a normal transition in the menopause time period, which is considered to be after the age of 50.

Data from our analysis show no significant correlation between the time of menopause onset and the DEXA test. This can be attributed to a small research sample because many studies have found a close connection between osteoporosis and menopause, attributing this connection to the action of rapid decline in estrogen hormone levels at this stage of life. Estrogen is considered as the key hormone that plays an essential role in complicated osteoblastic and osteolytic metabolic processes. Roberts et al.⁽⁹⁾ concluded that the thinning of the MC in women begins at the age of 42.5. A study in Saudi Arabia,⁽⁵⁾ which included 431 women in the postmenopausal phase, found a close correlation between the years that passed from the beginning of menopause and osteoporosis, classifying menopause as one of the risk factors for osteoporosis disease. It is considered that osteoporosis has a close correlation with body BMI.

The second source of estrogen after the ovaries is adipose cells. European women with osteoporosis are more prone to suffer fractures if the BMI is below the threshold of 19 kg/m^2 .^(8,9,14)

In our study, in women with T-score >-2.5 , BMI was significantly greater than in women with T-score <-2.5 . Numerous studies have been done with the aim of determining the reliability of the MCI as a qualitative index that describes morphological changes in the mandible cortex distally from the MF and the connection with the DEXA test. In 1998, Horner and Dalvin concluded that there is a correlation between BMD and MCI. A study by Devlin et al.,⁽¹⁰⁾ which included 671 postmenopausal women 45 to 70 years of age, found that only those patients with the thinnest mandibular cortices ($\text{MCW} < 3 \text{ mm}$) should be referred for further osteoporosis investigation. Dutra et al.⁽¹¹⁾ concluded that the thickness of the cortical mandibular bone is highly influenced by age. Taguchi et al.⁽¹²⁾ found that MCW determined from panoramic radiographs can be used to identify undetected low calcaneus BMD in young adult men, but not in young adult women (40 years) Ledgerton et al.⁽¹⁵⁾ found that that MI and PMI showed a significant, negative correlation with age. MCI also showed an age-related distribution.

The findings of our research are in line with the conclusions above: we found reduced MI values of less than 3mm in 90% of women with osteoporosis.^(10-12,15) Our data align with the conclusions of White et al.,⁽¹⁶⁾ who emphasized the validity of MI in detecting low BMD values in the research done with 227 Japanese women. Also, Langerton et al.⁽¹⁵⁾ have highlighted the high identification potential of MI and PMI in detecting osteoporosis. Our findings regarding MI and PMI ability in detecting osteoporosis align with the authors mentioned above.^(8-12,15,16) Drozdowska et al.⁽¹⁷⁾ concluded that MCI is not efficient enough to distinguish edentulous women with osteoporosis. The efficacy of the panoramic-based mandibular indices in diagnosing osteopenia/osteoporosis was low to moderate: specificity (ranging from 31% to 81%), sensitivity (ranging from 21% to 93%), negative and positive predictive values (ranging from 47% to 83% and 40% to 79%, respectively).

The present study sufficiently demonstrates the reliability of the radiomorphometric indices in identifying menopausal women with a greater risk of osteoporosis. Further studies need to be carried out with a much larger population to ascertain the efficacy of these indices.

Conclusion

MCI presents a moderate sensitivity (70%) with low specificity (63.33%) to detect early signs of osteoporosis, but the C3 category corresponds to overall bone condition and can be used by dentists to refer patients for final examination and diagnosis. MI at a cutoff point of 3 mm presents the moderate-high sensitivity (90%) for detecting bone mass loss, but the MI specificity is extremely low (36.67%). The efficacy of the PMI at a cutoff point of 0.3 mm is characterized by low sensitivity (63.33%) in diagnosing osteoporosis, but the PMI specificity is moderate (76.67%). PR can be a useful tool to

identify early signs of osteoporosis by using the evaluation of radiomorphometric indices. MCI, MI, and PMI can be potential screening tools for initial BMD loss.

Disclosures

None

References

1. Office of the Surgeon General (US). Bone Health and Osteoporosis: A Report of the Surgeon General. Rockville (MD): Office of the Surgeon General (US); 2004. PMID: 20945569.
2. Lippuner K, von Overbeck J, Perrelet R, Bosshard H, Jaeger P. Incidence and direct medical costs of hospitalizations due to osteoporotic fractures in Switzerland. *Osteoporos Int.* 1997;7(5):414-25. doi: 10.1007/pl00004149.
3. World Health Organization: Assessment of fracture risk and its application to screening for postmenopausal osteoporosis. Technical report series 843. 1994, Geneva: WHO.
4. Hernlund E, Svedbom A, Ivergård M, Compston J, Cooper C, Stenmark J, McCloskey EV, Jönsson B, Kanis JA. Osteoporosis in the European Union: medical management, epidemiology and economic burden. A report prepared in collaboration with the International Osteoporosis Foundation (IOF) and the European Federation of Pharmaceutical Industry Associations (EFPIA). *Arch Osteoporos.* 2013;8(1):136. doi: 10.1007/s11657-013-0136-1.
5. Who scientific group on the assessment of osteoporosis at primary health care level Summary Meeting Report Brussels, Belgium, 5-7 May 2004. Available at: <https://www.who.int/chp/topics/Osteoporosis>
6. Klemetti E, Kolmakov S, Kröger H. Pantomography in assessment of the osteoporosis risk group. *Scand J Dent Res.* 1994 Feb;102(1):68-72. doi: 10.1111/j.1600-0722.1994.tb01156.x.
7. Benson BW, Prihoda TJ, Glass BJ. Variations in adult cortical bone mass as measured by a panoramic mandibular index. *Oral Surg Oral Med Oral Pathol.* 1991 Mar;71(3):349-56. doi: 10.1016/0030-4220(91)90314-3.
8. Halling A, Persson GR, Berglund J, Johansson O, Renvert S. Comparison between the Klemetti index and heel DXA BMD measurements in the diagnosis of reduced skeletal bone mineral density in the elderly. *Osteoporos Int.* 2005 Aug;16(8):999-1003. doi: 10.1007/s00198-004-1796-x.
9. Roberts M, Yuan J, Graham J, Jacobs R, Devlin H. Changes in mandibular cortical width measurements with age in men and women. *Osteoporos Int.* 2011 Jun;22(6):1915-25. doi: 10.1007/s00198-010-1410-3.
10. Devlin H, Karayianni K, Mitsa A, Jacobs R, Lindh C, van der Stelt P, Marjanovic E, Adams J, Pavitt S, Horner K. Diagnosing osteoporosis by using dental panoramic radiographs: the OSTEODENT project. *Oral Surg Oral Med*

*Correspondence: Merita Shkodra-Brovina, Faculty of Dentistry, the Ss. Cyril and Methodius University, Skopje, North Macedonia. E-mail: meritabrovina@gmail.com

- Oral Pathol Oral Radiol Endod. 2007 Dec;104(6):821-8. doi: 10.1016/j.tripleo.2006.12.027.
11. Dutra V, Devlin H, Susin C, Yang J, Horner K, Fernandes AR. Mandibular morphological changes in low bone mass edentulous females: evaluation of panoramic radiographs. *Oral Surg Oral Med Oral Pathol Oral Radiol Endod.* 2006 Nov;102(5):663-8. doi: 10.1016/j.tripleo.2006.02.023.
12. Taguchi A, Sugino N, Miki M, Kozai Y, Mochizuki N, Osanai H, Yamada S, Kuroiwa H, Fujiki T, Uchida K, Yoshinari N, Kashima I. Detecting young Japanese adults with undetected low skeletal bone density using panoramic radiographs. *Dentomaxillofac Radiol.* 2011 Mar;40(3):154-9. doi: 10.1259/dmfr/30045588.
13. Ledgerton D, Horner K, Devlin H, Worthington H. Panoramic mandibular index as a radiomorphometric tool: an assessment of precision. *Dentomaxillofac Radiol.* 1997 Mar;26(2):95-100. doi: 10.1038/sj.dmfr.4600215.
14. Balto KA, Gomaa MM, Feteih RM, AlAmoudi NM, Elsamanoudy AZ, Hassanien MA, Ardawi MM. Dental Panoramic Radiographic Indices as a Predictor of Osteoporosis in Postmenopausal Saudi Women. *J Bone Metab.* 2018 Aug;25(3):165-173. doi: 10.11005/jbm.2018.25.3.165.
15. Ledgerton D, Horner K, Devlin H, Worthington H. Radiomorphometric indices of the mandible in a British female population. *Dentomaxillofac Radiol.* 1999 May;28(3):173-81. doi: 10.1038/sj/dmfr/4600435.
16. White SC, Taguchi A, Kao D, Wu S, Service SK, Yoon D, Swei Y, Nakamoto T, Tanimoto K. Clinical and panoramic predictors of femur bone mineral density. *Osteoporos Int.* 2005 Mar;16(3):339-46. doi: 10.1007/s00198-004-1692-4.
17. Drozdowska B, Pluskiewicz W, Tarnawska B. Panoramic-based mandibular indices in relation to mandibular bone mineral density and skeletal status assessed by dual energy X-ray absorptiometry and quantitative ultrasound. *Dentomaxillofac Radiol.* 2002 Nov;31(6):361-7. doi: 10.1038/sj.dmfr.4600729.
-

Association of Plasminogen Activator Inhibitor-1 4G/5G and Angiotensin-Converting Enzyme I/D Polymorphisms with Recurrent Pregnancy Loss in Sudanese Women: A Case-Control study

Hanan K. Ahmed¹, Amanda G. Elgoraish¹, Selma Elmalieh Abdalla²,
Asaad MA. Babker^{3*}, Ayman Hussien Alfeel³, Amin Omer Ibrahim Abbas⁴,
Khalid Abdelsamea Mohamedahmed⁵, Salaheldein G Elzaki¹

¹Tropical Medicine Research Institute, Khartoum, Sudan

²Sudan University of Sciences and Technology, Khartoum, Sudan

³College of Health Sciences, Gulf Medical University, Ajman, United Arab Emirates

⁴Department of Clinical Medicine, Faculty of Medicine, Al-Rayan Colleges, Saudi Arabia

⁵Department of Hematology and Immunology, Faculty of Medical Laboratory Sciences,
University of Gezira, Wad Medani, Sudan

Abstract

The aim of our study was to investigate the relationship between the *ACE* I/D and *PAI-1* 4G/5G polymorphisms and recurrent pregnancy loss (RPL) in Sudanese women.

Methods and Results: A total of 232 people participated in this case-control study, including 119 women who had been diagnosed with RPL (Case group) and 113 healthy women (Control group). The case group (RPL) consisted of Sudanese women (mean age of 31.3±5.9 years) who had at least three unfavorable pregnancy outcomes. Women in the control group (Control) were matched by age (mean age of 30.3±5.4 years), had at least two healthy pregnancies, and had no history of unfavorable pregnancy outcomes or recurrent losses. Genomic DNA samples were isolated from the whole blood by using the GF-1 Blood DNA Extraction Kit (Vivantis Technologies Sdn. Bhd., Malaysia). The status of the *PAI-1* 4G/5G and *ACE* I/D polymorphism was determined by PCR.

Analysis of the multiplicative and additive models for the *ACE* I/D polymorphism showed a significant risk of RPL with the carriage of the D allele (OR=2.07, 95% CI: 1.28-3.35, *P*=0.003) and the homozygous DD genotype (OR=2.40, 95% CI: 1.34-4.29, *P*=0.008). The multiplicative and additive models for the *PAI-1* 4G/5G polymorphism showed a significant risk of RPL with the carriage of the 4G allele (OR=3.11, 95% CI: 2.12-4.58, *P*=0.000) and the homozygous 4G/4G genotype (OR=3.09, 95% CI: 1.77-5.39, *P*=0.000). However, the carriage of risk-polymorphic markers, the *ACE* I/D and *PAI-1* 4G/5G polymorphisms, was not associated with the number of RPL. The combined carriage of the homozygous DD genotype and heterozygous ID genotype of the *ACE* I/D polymorphism with the homozygous 4G/4G genotype of the *PAI-1* 4G/5G polymorphism occurs significantly more often in RPL women than healthy women (*P*=0.000 and *P*=0.019, respectively). Carriage of the *PAI-1* 5G/5G genotype in healthy women was not associated with the *ACE* I/D polymorphism.

Conclusion: Testing for the *ACE* I/D and *PAI-1* 4G/5G polymorphisms should be part of the standard examination for patients with RPL. (International Journal of Biomedicine. 2023;13(1):127-133.)

Keywords: angiotensin-converting enzyme • plasminogen activator inhibitor-1 • recurrent pregnancy loss

For citation: Ahmed HKF, Elggourish AGA, Abdullah SE, Babker AMA, Alfeel AH, Abbas AOI, Mohamedahmed KA, Elzaki SG. Association of Plasminogen Activator Inhibitor-1 4G/5G and Angiotensin-Converting Enzyme I/D Polymorphisms with Recurrent Pregnancy Loss in Sudanese Women: A Case-Control study. International Journal of Biomedicine. 2023;13(1):127-133. doi:10.21103/Article13(1)_OA18

Abbreviations

ACE, angiotensin-converting enzyme; AT-II, angiotensin II; PAI-1, plasminogen activator inhibitor-1; PCR, polymerase chain reaction; RPL, recurrent pregnancy loss; RAS, renin-angiotensin system.

Introduction

According to conventional wisdom, three or more consecutive pregnancy losses constitute recurrent pregnancy loss (RPL). The American Society for Reproductive Medicine (ASRM) has described RPL as two or more miscarriages. A clinically confirmed pregnancy loss, which affects 2%-5% of fertile women, occurs when the pregnancy spontaneously terminates before 20 weeks.⁽¹⁾ RPL is a complex disorder with a poorly known pathogenesis.⁽²⁾ Multiple factors—including chromosomal anomalies, anatomical conditions, and endocrine, immunological, and infectious diseases—are thought to affect RPL.⁽³⁻⁵⁾ The identifiable reasons for RPL include genetic abnormalities, structural abnormalities, infection, endocrine abnormalities, immune dysfunction, and thrombophilic disorders.⁽⁶⁾

The renin-angiotensin system (RAS), a hormone-signaling cascade, plays an important role in regulating blood pressure levels and fluid balance. Circulating angiotensin II (AT-II) is the main effector of the RAS. The angiotensin-converting enzyme (ACE) is a key enzyme (a zinc metallopeptidase) that plays a role in generating AT-II by catalyzing the extracellular conversion of the decapeptide angiotensin I. The ACE hydrolyzes a number of other substrates, but probably the most important is the potent vasodilator bradykinin. Endocrine secretions from the decidua, placenta, and ovary affect RAS throughout gestation. For example, estrogen increases angiotensinogen synthesis by the liver, leading to increased serum AT-II.⁽⁷⁾ The uteroplacental unit is where RAS components are expressed, highlighting the significance of its local role.⁽⁸⁾ The uteroplacental RAS plays a crucial role in regenerating the endometrium after shedding, decidualization, implantation, and placentation.⁽⁹⁾ In addition, local RAS participates in the production of prostaglandin, the release of estradiol, and the control of blood flow to the placenta and uterus.⁽¹⁰⁾

The *ACE* gene is known to contain a polymorphism consisting of either the insertion (I) or deletion (D) of a 287bp Alu repetitive sequence inside intron 16. Notably, the D allele and the DD genotype are associated with elevated levels of ACE.⁽¹¹⁻¹³⁾ Homozygotes for the I allele may display as low as half of the plasma ACE level, compared to the homozygotes for the D allele, whereas the ID heterozygotes display an intermediate level.⁽¹⁴⁾

PAI-1, a single-chain glycoprotein member of the superfamily of serine-protease inhibitors, is one of the most important inhibitors of plasma fibrinolytic activity. PAI-1 is the principal inhibitor of the tissue-type plasminogen activator (t-PA) and the urinary-type plasminogen activator (u-PA). The increased expression of PAI-1 in vivo suppresses fibrinolysis, consequently leading to pathological fibrin deposition and tissue damage.^(15,16)

A number of studies have reported that *PAI-1* gene polymorphism is possibly associated with hypofibrinolysis and thrombotic complications.⁽¹⁷⁾ An association between the promoter -675 4G/5G polymorphism of the *PAI-1* gene and plasma PAI-1 concentrations has been suggested.^(18,19) Homozygosity for the deletion genotype (4G/4G) has been

associated with PAI-1 concentrations higher than those associated with the insertion genotype (5G/5G), causing reduced fibrinolytic activity, thereby increasing the risk of venous thromboembolism.^(20,21) The 5G homozygotes have the lowest PAI-1 concentrations.⁽²¹⁻²³⁾ However, such a relationship is still under study and, for some aspects, controversial.⁽²⁴⁻²⁷⁾

A number of previous studies have investigated the association of the *PAI-1* 4G/5G and *ACE* I/D polymorphisms with infertility, recurrent miscarriage, and major pregnancy complications.^(17,28-32)

The aim of our study was to investigate the relationship between the *ACE* I/D and *PAI-1* 4G/5G polymorphisms and RPL in Sudanese women.

Materials and Methods

Due to restricted resources, a total of 232 people participated in this case-control study, including 119 women who had been diagnosed with RPL (Case group) and 113 healthy women (Control group). The study was conducted from February 2019 to February 2020 at Omdurman Medical Hospital in Sudan. The case group (RPL) consisted of Sudanese women (mean age of 31.3±5.9 years) who had at least three unfavorable pregnancy outcomes. Women in the control group (Control) were matched by age (mean age of 30.3±5.4 years), had at least two healthy pregnancies, and had no history of unfavorable pregnancy outcomes or recurrent losses. The inclusion criteria for the Case group were three or more RPLs in a row without a known reason for the abortion. Exclusion criteria included a history of vascular thrombotic disease, fetal congenital malformations, fetal chromosomal anomalies, uterine abnormalities, or a known reason for the abortion.

A structured questionnaire was used to collect data regarding the age, medical history, family history, and obstetric history of the cases and controls.

After interviewing each participant and obtaining their verbal and written agreement, five ml of venous blood was taken from each and placed into a specific container. Patient name, medical record number, collection date, and time were written on the labels of the samples.

DNA extraction and quantification

Genomic DNA samples were isolated from the whole blood by using the GF-1 Blood DNA Extraction Kit (Vivantis Technologies Sdn. Bhd., Malaysia) according to the manufacturer's protocol. Until PCR analysis, DNA was stored in a -20°C freezer. The DNA concentration was determined at a wavelength of 260 nm using a GeneQuant spectrophotometer (Amersham Biosciences, UK).

Detection of the *PAI-1* 4G/5G polymorphism

The *PAI-1* 4G/5G polymorphism was tested by the amplification refractory mutation system-polymerase chain reaction (ARMS-PCR) technique,⁽³³⁾ using an upstream control primer (5'-AAGCTTTTACCATGGTAACCCCTGGT-3'), a 4G or 5G allele-specific primer (5'-AGAGTCTGGACACGTGGG GA-3' and 5'-AGAGTCTGGACACGTGGGGG-3', respectively), and a common downstream primer (5'-TGCAGCCAGCCACGTGATTGTCTAG-3'). 138 and

139-bp fragments for 4G and 5G alleles, respectively, at an annealing temperature of 55°C, and a 257-bp fragment for positive control were obtained from amplification by these primers. The conditions for the PCR reaction were denaturation at 95°C for 3 min, followed by 30 cycles of denaturation at 95°C for 20 s, annealing at 55°C for 10 s, and extension at 72°C for 20 s, followed by a final extension at 72°C for 3 min. The PCR products were fractionated by 2% agarose gel electrophoresis and visualized under UV light.

Detection of the *ACE* I/D polymorphism

For the *ACE* I/D polymorphism, the following primers (F:5'-CTGGAGACCACTCCCATCCTTCT-3' and R: 5'-GATGTGGCCATCACATTCGTCAGAT-3') were used to amplify the region of Alu insertion (intron 16). In order to avoid the mistyping of ID genotype as DD due to preferential amplification of the shorter D allele, a separate PCR was carried out in all the DD samples.⁽³⁴⁾ All PCR products were visualized after electrophoresis on a 2% agarose gel and ethidium bromide staining. Two alleles were identified: a 490-bp fragment I (with the insertion) and a 190-bp fragment D (without the insertion). Two bands (490 and 190 bp) were detected in heterozygous samples.

Statistical analysis was performed using statistical software package SPSS version 24.0 (Armonk, NY: IBM Corp.). The frequency distribution of genotypes for the studied polymorphic loci was checked for compliance with the Hardy–Weinberg equilibrium (HWE). Differences in the allele and genotype distribution between the groups were assessed by Chisquare test or Chisquare test with the Yates' correction, when appropriate. Odds ratios (ORs) and 95% confidence intervals (CIs) were calculated. Two genetic models were analyzed: the additive inheritance model (Cochran-Armitage Linear Trend Test) and the multiplicative inheritance model.

Results

In Case group women, 30(25.2%) had ≥ 4 RPL and 89(74.8%) had < 4 RPL (Table 1). The frequency distribution of alleles of the *ACE* I/D polymorphism showed that the carriage of the D allele prevailed in RPL patients more than in controls (86.6% vs. 75.7%; $\chi^2=9.025$, $P=0.0027$). The frequency distribution of alleles of the *PAI-1* 4G/5G polymorphism showed that the carriage of the 4G allele was greater in RPL patients than in controls (72.3% vs. 45.6%; $\chi^2=34.216$, $P=0.0000$) (Table 2).

Table 1.

Baseline characteristics of the study groups.

Variable	RPL (n=119)	Control (n=113)	P-value
Age, years	31.3 \pm 5.9	30.3 \pm 5.4	0.180
RPL number, n (%)	<4	89 (74.8%)	-
	≥ 4	30 (25.2%)	-

Table 2.

The frequency distribution of alleles and genotypes of the *ACE* I/D and *PAI-1* 4G/5G polymorphisms in the study groups.

Gene	Genotype Allele	RPL (n=119)	Control (n=113)	Statistics
<i>ACE</i> Genotype	II	7(5.9%)	1(9.7%)	$\chi^2=8.986$ $P=0.0112$
	ID	18(15.1%)	33(29.2%)	
	DD	94(79.0%)	69(61.1%)	
Allele	I	32(13.4%)	55(24.3%)	$\chi^2=9.025$ $P=0.0027$
	D	206(86.6%)	171(75.7%)	
<i>PAI-1</i> Genotype	5G/5G	7(5.9%)	38(33.6%)	$\chi^2=33.111$ $P=0.0000$
	4G/5G	52(43.7)	47(41.6%)	
	4G/4G	60(50.4%)	28(24.8%)	
Allele	5G	66(27.7%)	123(54.4%)	$\chi^2=34.216$ $P=0.0000$
	4G	172(72.3%)	103(45.6%)	

The distribution of polymorphic markers of the *ACE* I/D and *PAI-1* 4G/5G polymorphisms in controls was in HWE (Table 3).

Analysis of the multiplicative and additive models for the *ACE* I/D polymorphism showed a significant risk of RPL with the carriage of the D allele (OR=2.07, 95% CI: 1.28-3.35, $P=0.003$) and the homozygous DD genotype (OR=2.40, 95% CI: 1.34-4.29, $P=0.008$) (Tables 4 and 5).

The multiplicative and additive models for the *PAI-1* 4G/5G polymorphism showed a significant risk of RPL with the carriage of the 4G allele (OR=3.11, 95% CI: 2.12-4.58, $P=0.000$) and the homozygous 4G/4G genotype (OR=3.09, 95% CI: 1.77-5.39, $P=0.000$) (Tables 4 and 5).

However, the carriage of risk-polymorphic markers, the *ACE* I/D and *PAI-1* 4G/5G polymorphisms, was not associated with the number of RPL (Table 6).

The combined carriage of the homozygous DD genotype and heterozygous ID genotype of the *ACE* I/D polymorphism with the homozygous 4G/4G genotype of the *PAI-1* 4G/5G polymorphism occurs significantly more often in RPL women than healthy women ($P=0.000$ and $P=0.019$, respectively). Carriage of the *PAI-1* 5G/5G genotype in healthy women was not associated with the *ACE* I/D polymorphism (Table 7).

Discussion

Pregnancy complications can affect the mother's health, the baby's health, or both. Two or more consecutive pregnancy losses constitute RPL, the causes of which are unidentifiable in 40%-50% of pregnancy losses.⁽³⁵⁾ However, thrombophilic disorders and hypofibrinolysis were demonstrated to be risk factors in a majority of women with RPL. *PAI-1* plasma levels in RPL patients are increased, compared to women with healthy pregnancies.⁽³⁶⁾

The most common polymorphisms studied for association with RPL are thrombophilic gene polymorphisms.⁽³⁷⁻³⁹⁾ Among all the thrombophilic genes, functional *PAI-1*-6754G/5G polymorphism is one of the most frequently analyzed *PAI-1* genetic variants. However, the contribution of *PAI-1*-6754G/5G to unexplained RPL has remained controversial.⁽⁴⁰⁾

Table 3.

The distribution of polymorphic markers of the ACE I/D and PAI-1 4G/5G polymorphisms in RPL patients and controls.

Gene	Polymorphism	Genotype	RPL (n=119)	HWE (n=113)	χ^2	P	Control	HWE	χ^2	P	Allele	Frequency of alleles	
												RPL	Control
ACE	I/D	DD	0.790	0.749	5.09	0.025	0.611	0.572	2.08	0.15	D	0.866	0.757
		ID	0.151	0.233			0.292	0.368			I	0.134	0.243
		II	0.059	0.018			0.097	0.059					
PAI-1	4G/5G	4G/4G	0.504	0.522	0.44	0.51	0.248	0.208	1.62	0.2	4G	0.723	0.456
		4G/5G	0.437	0.401			0.416	0.496			5G	0.277	0.544
		5G/5G	0.059	0.077			0.336	0.296					

Table 4.

Genetic predisposition to RPL (the multiplicative inheritance model)

Gene	Polymorphism	Allele	Frequency of alleles		χ^2	P	OR (95%CI)
			RPL (n=119)	Control (n=113)			
ACE	I/D	I	0.134	0.243	9.03	0.003	0.48 (0.30-0.78)
		D	0.866	0.757			2.07 (1.28-3.35)
PAI-1	4G/5G	4G	0.723	0.456	34.22	0.000	3.11 (2.12-4.58)
		5G	0.277	0.544			0.32 (0.22-0.47)

Table 5.

Genetic predisposition to RPL (the additive inheritance model [CATT])

Gene	Polymorphism	Genotype	RPL (n=119)	Control (n=113)	χ^2	P	OR (95%CI)
ACE	I/D	DD	0.790	0.611	7.06	0.008	2.40 (1.34-4.29)
		ID	0.151	0.292			0.43(0.23-0.82)
		II	0.059	0.097			0.58 (0.22-1.55)
PIA-1	4G/5G	4G/4G	0.504	0.248	30.65	0.000	3.09 (1.77-5.39)
		4G/5G	0.437	0.416			1.09 (0.65-1.83)
		5G/5G	0.059	0.336			0.12 (0.05-0.29)

Table 6.

Polymorphic markers the ACE I/D and PAI-1 4G/5G polymorphisms and the number of RPL

Gene	Polymorphism	RPL number		P	χ^2
		<4 (n=98)	≥4 (n=21)		
ACE	D/D	77(78.6)	17(81.0)	0.947	0.109*
	D/I	15(15.3)	3(14.3)		
	I/I	6(6.1)	1(4.8)		
PAI-1	5G/5G	4(4.1)	3(14.3)	0.141	3.92
	4G/5G	42(42.9)	10(47.6)		
	4G/4G	52(53.1)	8(38.1)		

*Yates' chi-square

Table 7.

The combined carriage of the ACE I/D and PAI-1 4G/5G polymorphism genotypes in the study groups.

ACE		PIA-1			P	χ^2
		5G/5G	4G/5G	4G/4G		
D/D	RPL (n=94)	6(6.4%)	44(46.8%)	44(46.8%)	0.000	19.93
	Control (n=69)	21(30.4%)	32(46.4%)	16(23.2%)		
I/D	RPL (n=18)	0	6(33.3%)	12(66.7%)	0.019	7.933*
	Control (n=33)	12(36.4%)	11(33.3%)	10(30.3%)		
I/I	RPL (n=7)	1(14.3%)	2(28.6%)	4(57.1%)	0.482	1.461*
	RPL (n=11)	5(45.5%)	4(36.4%)	2(18.2%)		

*Yates' chi-square

A meta-analysis by Li et al.⁽⁴¹⁾ that included 22 studies with 4306 cases and 3076 controls showed that *PAI-1* 4G/5G polymorphism is associated with an increased RPL risk ($P=0.0003$), especially in the Caucasian subgroup ($P<0.001$). Other studies suggest that *PAI-1*-6754G/5G alone is not responsible for RPL.^(42,43)

Many studies have indicated that ACE affects hemostasis through different mechanisms, including platelet aggregation, blood clotting, and fibrinolysis.⁽⁴⁴⁻⁴⁶⁾ Endothelial PAI-1 synthesis is induced by AT-II, which is generated by ACE.

Results of a study performed by Buchholz et al.⁽²⁸⁾ showed that homozygosity for the D allele of the *ACE* gene, which results in elevated PAI-1 concentrations and hypofibrinolysis, is associated with an elevated risk of recurrent spontaneous miscarriages, and the combination of the DD genotype with 4G/4G genotype of the *PAI-1* promoter, which further increases PAI-1 plasma levels, is significantly more frequent in patients with recurrent spontaneous miscarriages than in controls.

In a study by Fazelnia et al.,⁽⁴⁴⁾ there was a significant association between the DD genotype of the *ACE* I/D polymorphism and RPL in women from the north of Iran (OR=2.04; 95% CI=0.94-4.44; $P=0.036$) with unexplained RPL. The D allele of the *ACE* I/D polymorphism was also significantly associated with the RPL (OR=1.59; 95% CI=1.05-2.41; $P=0.013$).

A systematic review and meta-analysis by Su et al.⁽⁴²⁾ were conducted to investigate the association between the *PAI-1* 4G/5G and *ACE* I/D polymorphisms with idiopathic RPL. Case-control studies comprising a total of 2820 RPL patients and 3009 controls were analyzed. Meta-analyses showed a significant association between *ACE* I/D polymorphism and idiopathic RPL [OR=1.29, 95% CI: 1.02-1.62]. There were no associations between *PAI-1* 4G/5G polymorphism and RPL in studies including more than two or three recurrent abortions.

A study performed by Aarabi et al.⁽⁴³⁾ investigated the *PAI-1* 4G/5G and *ACE* I/D polymorphisms in association with RPL in Iranian patients and normal healthy controls. Patients with the homozygote 4G/4G genotype were significantly more prone to RPL than others (OR=11.0, 95% CI: 2.3-52.4). For the *ACE* I/D polymorphism, no such association was found. A study performed by Shakarami et al.⁽⁴⁷⁾ also showed that patients with a homozygote 4G mutation were significantly more prone to RPL than the control group (OR: 4.63, % 95 CI: 1.55-13.84); at the same time, there were no significant associations between the *ACE* D allele or DD genotype and RPL.

Coulam et al.⁽³⁷⁾ found that women with a history of implantation failure after IVF-embryo transfer displayed a higher prevalence of the *PAI-1* 4G/5G mutations than controls ($P=0.007$). In a study by Goodman et al.,⁽⁴⁸⁾ a total of 550 women with a history of RPL were examined for the association of specific inherited thrombophilias and RPL. It was found that the *PAI-1* 4G/5G polymorphism correlated significantly with RPL, compared with controls ($P=0.009$). In contrast, Wolf et al.⁽³⁰⁾ did not find an association between the *PAI-1* 4G/4M polymorphism and RPL.

In our study, the combined carriage of the homozygous DD genotype and heterozygous ID genotype of the *ACE* I/D polymorphism with the homozygous 4G/4G genotype of the *PAI-1* 4G/5G polymorphism occurs significantly more often in RPL women than in healthy women ($P=0.000$ and $P=0.006$, respectively). In contrast, Goodman et al.⁽⁴⁸⁾ showed that homozygosity for the D allele of the *ACE* gene and the combination of the D/D genotype with two 4G alleles of the *PAI-1* promoter gene were not associated with a significant increase in the risk of recurrent miscarriage.

Conclusion

Our results showed a significant risk of RPL development with the carriage of the D allele and the homozygous DD genotype of the *ACE* I/D polymorphism and of the 4G allele and the homozygous 4G/4G genotype of the *PAI-1* 4G/5G polymorphism in Sudanese women. The combined carriage of the homozygous DD genotype and heterozygous ID genotype of the *ACE* I/D polymorphism with the homozygous 4G/4G genotype of the *PAI-1* 4G/5G polymorphism occurs significantly more often in RPL women than healthy Sudanese women. Testing for the *ACE* I/D and *PAI-1* 4G/5G polymorphisms should be part of the standard examination for patients with RPL.

Acknowledgments

We gratefully acknowledge the participants that contributed to this study and offer our special appreciation and thanks to the staff of the Omdurman Maternity Hospital in Sudan for their help in data collection.

Competing Interests

The authors declare that they have no competing interests.

References

1. El Hachem H, Crepau V, May-Panloup P, Descamps P, Legendre G, Bouet PE. Recurrent pregnancy loss: current perspectives. *Int J Womens Health*. 2017 May 17; 9:331-345. doi: 10.2147/IJWH.S100817. PMID: 28553146; PMCID: PMC5440030.
2. Pei CZ, Kim YJ, Baek KH. Pathogenetic factors involved in recurrent pregnancy loss from multiple aspects. *Obstet Gynecol Sci*. 2019 Jul; 62(4):212-223. doi: 10.5468/ogs.2019.62.4.212. Epub 2019 Jun 17. PMID: 31338338; PMCID: PMC6629979.
3. Hyde KJ, Schust DJ. Genetic considerations in recurrent pregnancy loss. *Cold Spring Harb Perspect Med*. 2015 Feb 6;5(3):a023119. doi: 10.1101/cshperspect.a023119. PMID: 25659378; PMCID: PMC4355257.

*Corresponding author: Associate Prof. Asaad Mohammed M. A. Babker, PhD. College of Health Sciences, Gulf Medical University, Ajman, United Arab Emirates. E-mail: azad.88@hotmail.com

4. Babker AM, Gameel FE. Methylenetetrahydrofolate reductase c677t polymorphism in Sudanese women with recurrent spontaneous abortions. *Kuwait Medical Journal*. 2016;48(2):100–104.
5. Babker AM, Gameel FE. Molecular Characterization of Prothrombin G20210A gene Mutations In pregnant Sudanese women with spontaneous recurrent abortions. *Rawal Medical Journal*. 2015 Apr 1;40(2):207-9.
6. Rai R, Regan L. Recurrent miscarriage. *Lancet*. 2006 Aug 12;368(9535):601-11. doi: 10.1016/S0140-6736(06)69204-0. PMID: 16905025.
7. Brown MA, Gallery ED, Ross MR, Esber RP. Sodium excretion in normal and hypertensive pregnancy: a prospective study. *Am J Obstet Gynecol*. 1988 Aug;159(2):297-307. doi: 10.1016/s0002-9378(88)80071-1. PMID: 3044110.
8. Lumbers ER, Pringle KG. Roles of the circulating renin-angiotensin-aldosterone system in human pregnancy. *Am J Physiol Regul Integr Comp Physiol*. 2014 Jan 15;306(2):R91-101. doi: 10.1152/ajpregu.00034.2013.
9. Irani RA, Xia Y. Renin angiotensin signaling in normal pregnancy and preeclampsia. *Semin Nephrol*. 2011 Jan;31(1):47-58. doi: 10.1016/j.semnephrol.2010.10.005.
10. Gintoni I, Adamopoulou M, Yapijakis C. The Angiotensin-converting Enzyme Insertion/Deletion Polymorphism as a Common Risk Factor for Major Pregnancy Complications. *In Vivo*. 2021 Jan-Feb;35(1):95-103. doi: 10.21873/invivo.12236.
11. Rigat B, Hubert C, Alhenc-Gelas F, Cambien F, Corvol P, Soubrier F. An insertion/deletion polymorphism in the angiotensin I-converting enzyme gene accounting for half the variance of serum enzyme levels. *J Clin Invest*. 1990 Oct;86(4):1343-6. doi: 10.1172/JCI114844.
12. Cambien F, Poirier O, Lecerf L, Evans A, Cambou JP, Arveiler D, Luc G, Bard JM, Bara L, Ricard S, et al. Deletion polymorphism in the gene for angiotensin-converting enzyme is a potent risk factor for myocardial infarction. *Nature*. 1992 Oct 15;359(6396):641-4. doi: 10.1038/359641a0.
13. Villard E, Tiret L, Visvikis S, Rakotovo R, Cambien F, Soubrier F. Identification of new polymorphisms of the angiotensin I-converting enzyme (ACE) gene, and study of their relationship to plasma ACE levels by two-QTL segregation-linkage analysis. *Am J Hum Genet*. 1996 Jun;58(6):1268-78.
14. McKenzie CA, Julier C, Forrester T, McFarlane-Anderson N, Keavney B, Lathrop GM, Ratcliffe PJ, Farrall M. Segregation and linkage analysis of serum angiotensin I-converting enzyme levels: evidence for two quantitative-trait loci. *Am J Hum Genet*. 1995 Dec;57(6):1426-35. Erratum in: *Am J Hum Genet* 1996 Mar;58(3):648.
15. Weisberg AD, Albornoz F, Griffin JP, Crandall DL, Elokda H, Fogo AB, Vaughan DE, Brown NJ. Pharmacological inhibition and genetic deficiency of plasminogen activator inhibitor-1 attenuates angiotensin II/salt-induced aortic remodeling. *Arterioscler Thromb Vasc Biol*. 2005 Feb;25(2):365-71. doi: 10.1161/01.ATV.0000152356.85791.52.
16. Aso Y. Plasminogen activator inhibitor (PAI)-1 in vascular inflammation and thrombosis. *Front Biosci*. 2007 May 1;12:2957-66. doi: 10.2741/2285.
17. Khosravi F, Zarei S, Ahmadvand N, Akbarzadeh-Pasha Z, Savadi E, Zarnani AH, Sadeghi MR, Jeddi-Tehrani M. Association between plasminogen activator inhibitor 1 gene mutation and different subgroups of recurrent miscarriage and implantation failure. *J Assist Reprod Genet*. 2014 Jan;31(1):121-4. doi: 10.1007/s10815-013-0125-8.
18. Kohler HP, Grant PJ. Plasminogen-activator inhibitor type 1 and coronary artery disease. *N Engl J Med*. 2000 Jun 15;342(24):1792-801. doi: 10.1056/NEJM200006153422406.
19. Baglin T. Inherited and acquired risk factors for venous thromboembolism. *Semin Respir Crit Care Med*. 2012 Apr;33(2):127-37. doi: 10.1055/s-0032-1311791
20. Margaglione M, Grandone E, Vecchione G, Cappucci G, Giuliani N, Colaizzo D, Celentano E, Panico S, Di Minno G. Plasminogen activator inhibitor-1 (PAI-1) antigen plasma levels in subjects attending a metabolic ward: relation to polymorphisms of PAI-1 and angiotensin converting enzyme (ACE) genes. *Arterioscler Thromb Vasc Biol*. 1997 Oct;17(10):2082-7. doi: 10.1161/01.atv.17.10.2082.
21. Dawson SJ, Wiman B, Hamsten A, Green F, Humphries S, Henney AM. The two allele sequences of a common polymorphism in the promoter of the plasminogen activator inhibitor-1 (PAI-1) gene respond differently to interleukin-1 in HepG2 cells. *J Biol Chem*. 1993 May 25;268(15):10739-45.
22. Mansfield MW, Stickland MH, Grant PJ. Environmental and genetic factors in relation to elevated circulating levels of plasminogen activator inhibitor-1 in Caucasian patients with non-insulin-dependent diabetes mellitus. *Thromb Haemost*. 1995 Sep;74(3):842-7.
23. Eriksson P, Kallin B, van 't Hooft FM, Båvenholm P, Hamsten A. Allele-specific increase in basal transcription of the plasminogen-activator inhibitor 1 gene is associated with myocardial infarction. *Proc Natl Acad Sci U S A*. 1995 Mar 14;92(6):1851-5. doi: 10.1073/pnas.92.6.1851.
24. Mannucci PM, Mari D, Merati G, Peyvandi F, Tagliabue L, Sacchi E, Taioli E, Sansoni P, Bertolini S, Franceschi C. Gene polymorphisms predicting high plasma levels of coagulation and fibrinolysis proteins. A study in centenarians. *Arterioscler Thromb Vasc Biol*. 1997 Apr;17(4):755-9. doi: 10.1161/01.atv.17.4.755.
25. Rizzo MR, Ragno E, Barbieri M, De Lucia D, Manzella D, Tagliamonte MR, Colaizzo D, Margaglione M, Paolisso G. Elevated plasma activator inhibitor 1 is not related to insulin resistance and to gene polymorphism in healthy centenarians. *Atherosclerosis*. 2002 Feb;160(2):385-90. doi: 10.1016/s0021-9150(01)00575-5.
26. Bladbjerg EM, Andersen-Ranberg K, de Maat MP, Kristensen SR, Jeune B, Gram J, Jespersen J. Longevity is independent of common variations in genes associated with cardiovascular risk. *Thromb Haemost*. 1999 Sep;82(3):1100-5.
27. Barbieri M, Rizzo MR, Ragno E, Grella R, Manzella D, Carbonella M, Saccomanno F, Paolisso G. Insulin resistance, plasma PAI-1 levels and PAI-1 gene polymorphism in healthy centenarians. *J Endocrinol Invest*. 2002;25(10 Suppl):110-2.
28. Buchholz T, Lohse P, Rogenhofer N, Kosian E, Pihusch R, Thaler CJ. Polymorphisms in the ACE and PAI-1 genes are associated with recurrent spontaneous miscarriages. *Hum Reprod*. 2003 Nov;18(11):2473-7. doi: 10.1093/humrep/deg474.
29. Jeddi-Tehrani M, Torabi R, Zarnani AH, Mohammadzadeh A, Arefi S, Zeraati H, Akhondi MM, Chamani-Tabriz L, Idali F, Emami S, Zarei S. Analysis of plasminogen activator inhibitor-1, integrin beta3, beta fibrinogen, and methylenetetrahydrofolate reductase polymorphisms in Iranian women with recurrent pregnancy loss. *Am J Reprod Immunol*. 2011 Aug;66(2):149-56. doi: 10.1111/j.1600-0897.2010.00974.x.

30. Wolf CE, Haubelt H, Pauer HU, Hinney B, Krome-Cesar C, Legler TJ, Hellstern P, Emons G, Zoll B, Köhler M. Recurrent pregnancy loss and its relation to FV Leiden, FII G20210A and polymorphisms of plasminogen activator and plasminogen activator inhibitor. *Pathophysiol Haemost Thromb*. 2003 May-Jun;33(3):134-7. doi: 10.1159/000077821.
31. Wang Z, Wang P, Wang X, He X, Wang Z, Xu D, Hu J, Wang B. Significant association between angiotensin-converting enzyme gene insertion/deletion polymorphism and risk of recurrent miscarriage: a systematic review and meta-analysis. *Metabolism*. 2013 Sep;62(9):1227-38. doi: 10.1016/j.metabol.2013.03.003.
32. Zhang S, Wang J, Wang B, Ping Y, Ma X. Strong association between angiotensin I-converting enzyme I/D polymorphism and unexplained recurrent miscarriage of Chinese women--a case-control study. *Reprod Sci*. 2011 Aug;18(8):743-6. doi: 10.1177/1933719111415865.
33. Shaghghi Z, Bonyadi M, Somi MH, Khoshbaten M. Association of plasminogen activator inhibitor-1 gene polymorphism with inflammatory bowel disease in Iranian Azeri Turkish patients. *Saudi J Gastroenterol*. 2014 Jan-Feb;20(1):54-8. doi: 10.4103/1319-3767.126322.
34. Shanmugam V, Sell KW, Saha BK. Mistyping ACE heterozygotes. *PCR Methods Appl*. 1993 Oct;3(2):120-1. doi: 10.1101/gr.3.2.120.
35. Jaslow CR, Carney JL, Kutteh WH. Diagnostic factors identified in 1020 women with two versus three or more recurrent pregnancy losses. *Fertil Steril*. 2010 Mar 1;93(4):1234-43. doi: 10.1016/j.fertnstert.2009.01.166.
36. Gris JC, Neveu S, Mares P, Biron C, Hedon B, Schved JF. Plasma fibrinolytic activators and their inhibitors in women suffering from early recurrent abortion of unknown etiology. *J Lab Clin Med*. 1993 Nov;122(5):606-15.
37. Coulam CB, Jeyendran RS, Fishel LA, Roussev R. Multiple thrombophilic gene mutations rather than specific gene mutations are risk factors for recurrent miscarriage. *Am J Reprod Immunol*. 2006 May;55(5):360-8. doi: 10.1111/j.1600-0897.2006.00376.x.
38. Robertson L, Wu O, Langhorne P, Twaddle S, Clark P, Lowe GD, Walker ID, Greaves M, Brenkel I, Regan L, Greer IA; Thrombosis: Risk and Economic Assessment of Thrombophilia Screening (TREATS) Study. Thrombophilia in pregnancy: a systematic review. *Br J Haematol*. 2006 Jan;132(2):171-96. doi: 10.1111/j.1365-2141.2005.05847.x.
39. Torabi R, Zarei S, Zeraati H, Zarnani AH, Akhondi MM, Hadavi R, Shiraz ES, Jeddi-Tehrani M. Combination of thrombophilic gene polymorphisms as a cause of increased the risk of recurrent pregnancy loss. *J Reprod Infertil*. 2012 Apr;13(2):89-94.
40. Ye Y, Vattai A, Zhang X, Zhu J, Thaler CJ, Mahner S, Jeschke U, von Schönfeldt V. Role of Plasminogen Activator Inhibitor Type 1 in Pathologies of Female Reproductive Diseases. *Int J Mol Sci*. 2017 Jul 29;18(8):1651. doi: 10.3390/ijms18081651.
41. Li X, Liu Y, Zhang R, Tan J, Chen L, Liu Y. Meta-analysis of the association between plasminogen activator inhibitor-1 4G/5G polymorphism and recurrent pregnancy loss. *Med Sci Monit*. 2015 Apr 11;21:1051-6. doi: 10.12659/MSM.892898.
42. Su MT, Lin SH, Chen YC, Kuo PL. Genetic association studies of ACE and PAI-1 genes in women with recurrent pregnancy loss: a systematic review and meta-analysis. *Thromb Haemost*. 2013 Jan;109(1):8-15. doi: 10.1160/TH12-08-0584.
43. Aarabi M, Memariani T, Arefi S, Aarabi M, Hantoosh Zadeh S, Akhondi MA, Modarressi MH. Polymorphisms of plasminogen activator inhibitor-1, angiotensin converting enzyme and coagulation factor XIII genes in patients with recurrent spontaneous abortion. *J Matern Fetal Neonatal Med*. 2011 Mar;24(3):545-8. doi: 10.3109/14767058.2010.511331.
44. Fazelnia S, Farazmandfar T, Hashemi-Soteh SM. Significant correlation of angiotensin converting enzyme and glycoprotein IIIa genes polymorphisms with unexplained recurrent pregnancy loss in north of Iran. *Int J Reprod Biomed*. 2016 May;14(5):323-8.
45. Sayed-Tabatabaei FA, Oostra BA, Isaacs A, van Duijn CM, Wittman JC. ACE polymorphisms. *Circ Res*. 2006 May 12;98(9):1123-33. doi: 10.1161/01.RES.0000223145.74217.e7.
46. Ueda S, Elliott HL, Morton JJ, Connell JM. Enhanced pressor response to angiotensin I in normotensive men with the deletion genotype (DD) for angiotensin-converting enzyme. *Hypertension*. 1995 Jun;25(6):1266-9. doi: 10.1161/01.hyp.25.6.1266.
47. Shakarami F, Akbari MT, Zare Karizi S. Association of plasminogen activator inhibitor-1 and angiotensin converting enzyme polymorphisms with recurrent pregnancy loss in Iranian women. *Iran J Reprod Med*. 2015 Oct;13(10):627-32.
48. Goodman C, Hur J, Goodman CS, Jeyendran RS, Coulam C. Are polymorphisms in the ACE and PAI-1 genes associated with recurrent spontaneous miscarriages? *Am J Reprod Immunol*. 2009 Dec;62(6):365-70. doi: 10.1111/j.1600-0897.2009.00744.x.
-

The Impact of Single-Nucleotide Polymorphisms in Regulatory Genes on the Development of Severe Acne

Alexander G. Rumyantsev^{1,2}, Olga M. Demina^{1,2}

¹Dmitry Rogachev National Medical Research Center of Pediatric Hematology, Oncology and Immunology

²Pirogov Russian National Research Medical University
Moscow, the Russian Federation

Abstract

Background: The pathogenesis of acne is multifactorial, and it was traditionally believed that four different processes play a decisive role in the development of the disease: the increased production of sebum, changes in keratinization processes leading to the formation of comedones, bacterial colonization of hair follicles by *Cutibacterium acnes* (*C. acnes*; formerly called *Propionibacterium acnes*), and synthesis of pro-inflammatory mediators in the pilosebaceous unit.

The role of genetic factors in the development of acne has been repeatedly discussed and continues to be the subject of discussion among scientists. The currently available data from various studies on genetic associations in acne are contradictory, which makes it relevant to address the problem of searching and analyzing the molecular mechanisms of the influence of regulatory genes in the pathogenesis of acne.

The aim of this study was to identify and analyze SNPs in the regulatory genes (*GATA1*, *GATA2*, *GATA2-AS1* [*GATA2 Antisense RNA 1*], *NFKB2*, *NFKBIA*, and *NFKB1*) in patients with severe acne.

Methods and Results: A prospective, open, non-randomized, single-center comparative study was conducted between 2017-2020. The study included 50 (29 men and 21 women) patients (the main group [MG]) with severe acne aged from 15 to 46 years (the median age of 23.2 years) and 20 (13 men and 7 women) apparently healthy individuals (the comparison group [CG]) aged from 16 to 40 years (the median age of 19.4 years). Molecular genetic diagnostics was performed using high-throughput DNA sequencing—next-generation sequencing (NGS). The results of our study made it possible to identify SNPs in regulatory genes (*GATA1*, *GATA2*, *GATA2-AS1* [*GATA2 Antisense RNA 1*], *NFKB2*, *NFKBIA*, and *NFKB1*) associated with the development of severe acne.

Conclusion: The revealed SNPs within the *GATA1*, *GATA2*, *GATA2-AS1* [*GATA2 Antisense RNA 1*], *NFKB2*, *NFKBIA*, and *NFKB1* genes in patients with severe acne probably indicate the involvement of regulatory transcription factors in the pathogenesis of acne. (**International Journal of Biomedicine. 2023;13(1):134-140.**)

Keywords: regulatory gene • single nucleotide polymorphism • acne

For citation: Rumyantsev AG, Demina OM. The Impact of Single-Nucleotide Polymorphisms in Regulatory Genes on the Development of Severe Acne. International Journal of Biomedicine. 2023;13(1):134-140. doi:10.21103/Article13(1)_OA19

Abbreviations

IL, interleukin; **IGF-1**, insulin-like growth factor-1; **NGS**, next-generation sequencing; **NF-κB**, nuclear factor kappa B; **SNP**, single nucleotide polymorphism; **TNF**, tumor necrosis factor; **TGF**, transforming growth factor.

Introduction

Currently, acne remains one of the most common dermatoses and, according to the Global Burden of Disease, affects about 85% of people aged 12-25 years. The

pathogenesis of acne is multifactorial, and it was traditionally believed that four different processes play a decisive role in the development of the disease:⁽¹⁻³⁾

- Androgen-induced increased sebum production
- Altered keratinization with the formation of comedones

- Bacterial colonization of hair follicles by *Cutibacterium acnes* (*C. acnes*; formerly called *Propionibacterium acnes*)
- Inflammation with the synthesis of pro-inflammatory mediators in the pilosebaceous unit

The role of genetic factors in the development of acne has been repeatedly discussed and continues to be the subject of discussion among scientists. An analysis of the risk of developing acne based on family history and in twins showed a significant genetic contribution of susceptibility to acne with a heritability of 78% and 81%, respectively.

According to a genome-wide association analysis performed by Navarini et al.,⁽⁴⁾ in the United Kingdom, three genome-wide significant associations were identified: 11q13.1 (rs478304, $P_{\text{combined}}=3.23 \times 10^{-11}$, OR=1.20), 5q11.2 (rs38055, $P_{\text{combined}}=4.58 \times 10^{-9}$, OR=1.17) and 1q41 (rs1159268, $P_{\text{combined}}=4.08 \times 10^{-8}$, OR=1.17) were identified in patients with severe acne. All three loci contain genes linked to the TGF β cell signaling pathway, namely OVOL1, FST, and TGF β 2. At the same time, the OVOL1 and TFGB2 transcripts had a reduced expression in the affected skin compared to normal. These data support a key role in the dysregulation of TGF β -mediated signaling in acne susceptibility.

In another study,⁽⁵⁾ two new acne susceptibility loci were identified at 11p11.2 (DDB2, rs747650, $P_{\text{combined}}=4.41 \times 10^{-9}$ and rs1060573, $P_{\text{combined}}=1.28 \times 10^{-8}$) and 1q24.2 (SELL, rs7531806, $P_{\text{combined}}=1.20 \times 10^{-8}$) that are involved in androgen metabolism, inflammation processes and scar formation in severe acne.

An analysis of the results of another GWAS study of severe adolescent acne in 928 European Americans found the most significant association with the rs4133274 SNP on chromosome 8q24 ($P=1.7 \times 10^{-6}$). An allele variant of this SNP (G allele) was associated with an increased risk of severe adolescent acne with OR=4.01 (95% CI: 2.37-6.82).⁽⁶⁾

Combined analysis performed in a meta-analysis by Yang et al. revealed a significant association between the *TNF- α* -308G/A polymorphism and acne vulgaris risk under a recessive model (OR=2.73, 95% CI: 1.37-5.44, $P=0.004$ for AA vs. AG + GG). Subgroup analysis by ethnicity showed that the acne vulgaris risk associated with the *TNF- α* -308G/A polymorphism was significantly elevated among Caucasians under the recessive model (OR=2.34, 95% CI: 1.13-4.86, $P=0.023$).⁽⁷⁾

According to Tasli et al.,⁽⁸⁾ the *IGF-1* cytosine-adenine (CA) repeat polymorphism was associated with the development of acne in the Turkish population.

A systematic review of 51 articles covering Asians and Caucasians found 60 genes/loci and their 100 variants implicated in acne. Detailed analysis showed that most of the studied genes/loci were located in the intron, coding region/ missense, and promoter regions. The commonly studied candidate genes/gene families include TNF, IL, and cytochrome P450 (CYP) gene families. As a result, it was shown that most of the analyzed gene variants exhibited insignificant pooled odds ratio (pOR) and significant heterogeneity between studies. The authors found that the *TNF* rs1800629 A allele carriers and the *CYP17A1* rs743572 T allele carriers had significantly reduced mild acne risk [pOR=

0.60, 95% CI: 0.33-0.86] and severe acne risk (pOR=0.59, 95% CI: 0.40-0.79), respectively, across populations. Overall, the *FST* (follistatin) rs629725 A allele showed a moderately increased risk for acne (pOR=1.19, 95% CI: 1.14-1.23). At the same time, there was no association of acne development with the *TIMP2* (TIMP 2 metalloproteinase inhibitor) rs8179090 and *CYP11A1* rs4646903 (pOR=0.96, 95% CI: 0.80-1.12; OR=0.95, 95% CI: 0.83-1.08, respectively). The authors also discovered 15 new SNPs in the 3'UTR region of the Toll-like receptor 4 (*TLR4*) gene associated with acne.⁽⁹⁾

The currently available data from various studies on genetic associations in acne are contradictory, which makes it relevant to address the problem of searching and analyzing the molecular mechanisms of the influence of regulatory genes in the pathogenesis of acne.

The aim of this study was to identify and analyze the SNPs in the regulatory genes (*GATA1*, *GATA2*, *GATA2-AS1*, *NFKB2*, *NFKB1A*, and *NFKB1*) in patients with severe acne.

Materials and Methods

Our prospective, open, non-randomized, single-center comparative study was conducted between 2017-2020. The study included 50 patients (the main group [MG]) with SA aged between 15 and 46 years (the median age of 23.2 years) and 20 apparently healthy individuals (the comparison group [CG]) aged between 16 and 40 years (the median age of 19.4 years). MG and CG were comparable in age and sex characteristics.

Molecular-genetic diagnostics was carried out by the method of high-throughput DNA sequencing (next-generation sequencing) in the Department of Molecular Genetics at the *NMRC PHOI*, named after Dmitry Rogachev (Moscow, Russia). Genomic DNA was isolated from whole blood samples of examined patients using the CellSep Advanced Kit (DiaSorin Ireland Ltd., Ireland) according to the manufacturer's instructions.

To assess the population frequencies of the identified variants, we used the the international project gnomAD Exomes (ExAC) data for exon variants and the gnomAD Genomes database for intron variants. For computer assessment of the pathogenicity of the missense variants we found, the programs for predicting the pathogenicity of amino acid substitutions (*SIFT*, *PolyPhen-2*, *PROVEAN*, *UMD Predictor*) were used. The *MutationTaster*, *Human Splicing Finder*, and *NNSplice* programs were used for computer prediction of the effect of changes in the splicing sites or areas adjacent to the splicing site.

The study of the functional significance of the complement system genes in the biological pathways of the body was carried out using an online program (<https://www.genecards.org/cgi-bin/carddisp.pl?gene>) that employs the STRING database (<https://version11.string-db.org/cgi/network.pl?taskId=5WAhRP62DcT8>) of known and predicted interactions, including direct and functional associations. The program performs mathematical prediction based on Genomic Context Predictions, High-throughput Lab Experiments, (Conserved) Co-Expression, and Automated Textmining

databases. The STRING database currently covers 24,584,628 proteins from 5,090 organisms.^(10,11)

Statistical analysis was performed using the statistical software package XLSTAT 2019. The normality of the distribution of continuous variables was tested by the Shapiro-Wilk test. For descriptive analysis, results are presented as median (Me), first quartile (Q1), and third quartile (Q3). Differences of continuous variables were tested by the Mann-Whitney *U*-test. Group comparisons with respect to categorical variables are performed using the chi-square test. Odds ratios (ORs) and their 95% confidence intervals (CIs) were calculated to determine associations between the SNPs and severe acne. A probability value of $P < 0.05$ was considered statistically significant.

This study was approved by the Ethics Committee of the PRNRMU of the Ministry of Healthcare of the Russian Federation and complied with Ethical Principles for Medical Research Involving Human Subjects, adopted by the 18th WMA General Assembly, Helsinki, Finland, June 1964, and amended by the 59th WMA General Assembly, Seoul, Republic of Korea, October 2008. All patients gave their written informed consent.

Results

All patients of the MG suffered from a severe form of acne, which was clinically characterized by multiple open and closed comedones, deep inflammatory papules, pustules, and nodules merging into conglomerates, atrophic scars, post-inflammatory stagnant-cyanotic spots with predominant localization on the skin of the face, back and chest. The skin in the lesions had a greasy appearance; subjective sensations were characterized by mild to moderate pain aggravated by movement and palpation.

We stratified the studied SNPs in exons, in introns, in the 3'UTR, 5'UTR, and splicing regions according to their regulatory significance in the genes *GATA1*, *GATA2*, *GATA2-AS1*, *NFKB2*, *NFKB1A*, and *NFKB1*. Characteristics of SNPs in exons of the *GATA2*, *NFKB1*, and *NFKB2* genes in patients with acne are presented in Table 1. In the *GATA1*, *GATA2-AS1*, and *NFKB1A* genes, we did not identify polymorphic loci in exons.

Four of the 5 SNPs in exons of the studied genes [*GATA2* (rs34799090) (OR=2.055, 95% CI: 0.096-43.775, $P=0.644$), *NFKB2* (rs199577673) (OR=1.221, 95% CI: 0.049-30.606, $P=0.903$), *NFKB1* (rs146936581) (OR=1.221, 95% CI: 0.048-30.6064, $P=0.903$), *NFKB1* (rs4648072) (OR=1.221, 95% CI: 0.049-30.605, $P=0.903$)] probably could be associated with the development of severe acne ($P > 0.05$). Whereas one SNP (rs2335052) of the *GATA2* gene (OR=0.705, 95% CI: 0.284-1.748, $P=0.451$) are likely to have a protective effect. Characteristics of SNPs in introns of the *GATA1*, *GATA2*, and *GATA2-AS1* genes in patients with acne are presented in Table 2.

We identified 11 SNPs in the introns of the studied genes for the first time that have not been previously described in any disease. It was found that in one SNP of the *GATA1* gene (.), defined by us for the first time, the frequency of the alternative allele was significantly different between MG and CG ($P=0.009$), and OR=11 (95% CI: 1.189-101.717, $P=0.034$) indicates a significant association with

the development of severe acne. For the *NFKB2* (rs4919632) SNP we identified, the frequency of the alternative allele was significantly different between the MG and the CG ($P=0.049$), and OR=18.76 (95% CI: 0.946-371.894, $P=0.049$) indicates a significant association with the risk of acne formation.

The OR results showed that one SNP of the *GATA2* gene, 2 SNPs of the *GATA1* gene, 13 SNPs of the *NFKB2* gene, and 23 SNPs of the *NFKB1A* gene probably could be associated with the development of severe acne ($P > 0.05$). At the same time, the remaining SNPs of the studied genes (OR from 0.13 to 0.92) are likely to have a protective effect ($P > 0.05$). We identified two SNPs in the *GATA2* gene (one in the splicing zone, one in the 5'UTR) and two SNPs in the *NFKB2* gene, for the first time in acne patients. Two SNPs in the *NFKB1* gene loci rs386357216 and rs4648143 with ORs > 1 indicate a possible association with severe acne. Four SNPs in the *GATA2* gene and 6 SNPs in the *NFKB2* gene are likely to have a protective effect (Table 3).

Discussion

The results of our study made it possible to identify SNPs in regulatory genes (*GATA1*, *GATA2*, *GATA2-AS1* [GATA2 Antisense RNA 1], *NFKB2*, *NFKB1A*, and *NFKB1*) associated with the development of severe acne.

The *GATA1* (GATA Binding Protein 1) gene encodes a protein belonging to the GATA family of transcription factors. The *GATA1* protein plays an important role in erythroid development by regulating the switch of fetal hemoglobin into adult hemoglobin. In addition, the *GATA1* gene controls the differentiation of megakaryocytes, platelets, and basophils, and regulates the apoptotic signaling pathway. Mutations in this gene have been associated with X-linked dyserythropoietic anemia. It is important that the *GATA1* gene is located on the X chromosome (p11.23), which leads to X-linked inheritance. Notably, different positions of pathogenic *GATA1* variants result in a wide variety of phenotypes, spanning ineffective erythropoiesis, thrombocytopenia, and thrombocytopathy. A significant association of one SNP (.) in the *GATA1* gene with the risk of developing severe acne (OR=11, 95% CI: 1.189-101.717, $P=0.034$) indicates the involvement of regulatory transcription factors in the pathogenesis of acne.

The *GATA2* (GATA Binding Protein 2) gene encodes a member of the GATA family of zinc-finger transcription factors that are named for the consensus nucleotide sequence they bind in the promoter regions of target genes. The encoded protein plays an essential role in regulating the transcription of genes involved in the development and proliferation of hematopoietic and endocrine cell lineages. The *GATA2* gene also regulates endothelin-1 gene expression in endothelial cells. The *GATA2* SNPs identified in our study showed a probable association with the risk of acne.

The *GATA2-AS1* (GATA2 Antisense RNA 1) gene, an RNA gene, is associated with the lncRNA class. It showed that *GATA2-AS1* positively regulates *GATA2* expression at the post-transcriptional level. *GATA2* is combined with the *GATA2-AS1* promoter to enhance *GATA2-AS1* expression. Our data regarding the *GATA2-AS1* SNPs showed a probable association with the risk of the SA development.

Table 1.**Characteristics of SNPs within exons of the GATA2, NFKB1, NFKB2 genes in acne patients**

Gene	Chr: Position (hg19)	SNPid	Exon numbers	Type and position of substitution	P-value (Z-test for proportion)	OR (95% CI) P-value
GATA2	3:128204951	rs2335052	3	c.G490A: p.A164T (nonsynonymous)	0.449	0.705 (0.284 - 1.748) P=0.451
GATA2	3:128204960	rs34799090	3	c.C481G: p.P161A (nonsynonymous)	0.368	2.055 (0.096 - 43.775) P=0.644
NFKB2	10:104161032	rs199577673	18	c.G2167A: p.D723N	0.525	1.221 (0.049 - 30.606) P=0.903
NFKB1	4:103500158	rs146936581	8	c.G689A: p.R230H	0.526	1.221 (0.048 - 30.606) P=0.903
NFKB1	4: 103518700	rs4648072	15	c.A1516G: p.M506V	0.525	1.221 (0.049 - 30.605) P=0.903

Table 2.**Characteristics of SNPs within introns of the GATA1, GATA2, GATA2-ASI, NFKB2, NFKB1A, and NFKB1 genes in acne patients.**

Gene	SNPid	Chr: Position (hg19)	Type of substitution	P-value (Z-test for proportion)	OR (95% CI) P-value
GATA2	rs2713603	3:128200534	G>A	0.406	0.728 (0.344 - 1.542), P=0.408
GATA2	rs11708606	3:128200806	G>A	0.665	0.777 (0.248 - 2.438), P=0.666
GATA2	rs55914222	3:128202943	G>C	0.139	0.191 (0.017 - 2.179), P=0.183
GATA2	rs73862209	3:128207423	C>T	0.367	2.056 (0.096 - 43.775), P=0.644
GATA2-ASI	rs559062253	3:128211729	G>A	0.335	0.388 (0.053 - 2.852), P=0.352
GATA1	(.)	X:48649428	->G	0.009	11 (1.189 - 101.717), P=0.034
GATA1	rs62600348	X:48649449	T>G	0.650	2.481 (0.048 - 127.204), P=0.651
GATA1	rs66717003	X:48649456	T>G	0.650	2.481 (0.048 - 127.204), P=0.650
NFKB2	rs76034131	10:104154581	G>A	0.525	1.221 (0.048 - 30.606), P=0.903
NFKB2	rs1572532	10:104154683	C>T	0.651	2.481 (0.048 - 127.204), P=0.651
NFKB2	rs36226954	10:104155345	T>C	0.791	0.791 (0.139 - 4.504), P=0.792
NFKB2	rs61873662	10:104155823	A>T	0.525	1.221 (0.048 - 30.606), P=0.903
NFKB2	(.)	10:104156392	->T	0.414	1.411 (0.615 - 3.237), P=0.415
NFKB2	rs776641137	10:104156856	C>A	0.525	1.221 (0.048 - 30.606), P=0.903
NFKB2	rs12772374	10:104156911	A>G	0.702	1.235 (0.416 - 3.659), P=0.702
NFKB2	(.)	10:104157588	C>G	0.525	1.221 (0.048 - 30.606), P=0.903
NFKB2	rs7897947	10:104157711	T>G	0.118	0.488 (0.196 - 1.215), P=0.123
NFKB2	rs4919632	10:104157727	C>T	0.049	18.76 (0.946 - 371.894), P=0.049
NFKB2	rs45487496	10:104157947	C>A	0.149	4.664 (0.252 - 86.351), P=0.301
NFKB2	rs3740418	10:104158933	C>G	0.414	1.411 (0.615 - 3.237), P=0.415
NFKB2	rs11574849	10:104159696	G>A	0.532	1.524 (0.401 - 5.781), P=0.535
NFKB2	rs201550645	10:104160934	C>T	0.525	1.221 (0.048 - 30.606), P=0.903
NFKB2	rs72845693	10:104161168	G>A	0.526	1.221 (0.049 - 30.606), P=0.903
NFKB2	(.)	10:104161323	G>A	0.112	0.131 (0.005 - 3.284), P=0.216
NFKB2	rs11574852	10:104161475	A>C	0.113	0.131 (0.005 - 3.285), P=0.216

Table 2 (continued).

Characteristics of SNPs within introns of the *GATA1*, *GATA2*, *GATA2-AS1*, *NFKB2*, *NFKB1A*, and *NFKB1* genes in acne patients.

Gene	SNPid	Chr: Position (hg19)	Type of substitution	P-value (Z-test for proportion)	OR (95% CI) P-value
<i>NFKB2</i>	rs11574853	10:104161796	T>A	0.005	0.053 (0.003 - 1.057), P=0.054
<i>NFKB2</i>	rs7077329	10:104161967	T>C	0.526	0.770 (0.343 - 1.730), P=0.527
<i>NFKB1A</i>	rs149524774	14:35871327	G>A	0.525	1.221 (0.048 - 30.606), P=0.903
<i>NFKB1A</i>	rs1022714	14:35871407	A>G	0.574	1.269 (0.551 - 2.929), P=0.575
<i>NFKB1A</i>	rs5026132	14:35871441	A>G	0.629	1.199 (0.573 - 2.514), P=0.629
<i>NFKB1A</i>	rs2233419	14:35871960	G>A	0.101	3.352 (0.730-15.395), P=0.119
<i>NFKB1A</i>	rs2233418	14:35872068	G>A	0.564	0.587 (0.094 - 3.656), P=0.569
<i>NFKB1A</i>	rs2233417	14:35872094	C>T	0.101	3.352 (0.730 - 15.395), P=0.119
<i>NFKB1A</i>	(.)	14:35872170	C>T	0.525	1.221 (0.049 - 30.606), P=0.903
<i>NFKB1A</i>	rs3138054	14:35872307	C>T	0.287	2.007 (0.544 - 7.405), P=0.295
<i>NFKB1A</i>	rs2233416	14:35872765	G>A	0.231	3.391 (0.410 - 28.038), P=0.257
<i>NFKB1A</i>	rs2233415	14:35872792	A>G	0.499	0.761 (0.345 - 1.679), P=0.499
<i>NFKB1A</i>	(.)	14:35872837	TC>-	0.113	0.251 (0.040 - 1.567), P=0.139
<i>NFKB1</i>	rs41477752	4:103446824	T>-	0.872	1.206 (0.121 - 11.953), P=0.872
<i>NFKB1</i>	(.)	4:103454926	C>T	0.525	1.221 (0.048 - 30.606), P=0.903
<i>NFKB1</i>	rs230526	4:103458825	A>G	0.445	1.334 (0.635 - 2.804), P=0.44
<i>NFKB1</i>	rs230525	4:103458877	G>A	0.345	1.434 (0.676 - 3.041), P=0.346
<i>NFKB1</i>	(.)	4:103458890	AC>-	0.445	1.334 (0.635 - 2.804), P=0.446
<i>NFKB1</i>	rs2293970	4:103487982	A>T	0.872	1.206 (0.122 - 11.953), P=0.872
<i>NFKB1</i>	rs230496	4:103488491	G>A	0.513	1.279 (0.609 - 2.685), P=0.514
<i>NFKB1</i>	rs909332	4:103497875	A>T	0.872	1.206 (0.122 - 11.953), P=0.872
<i>NFKB1</i>	(.)	4:103501611	A>G	0.525	1.221 (0.048 - 30.606), P=0.903
<i>NFKB1</i>	rs1598858	4:103506095	A>G	0.702	0.864 (0.411 - 1.821), P=0.703
<i>NFKB1</i>	rs1020760	4:103514445	C>G	0.829	0.922 (0.441 - 1.928), P=0.829
<i>NFKB1</i>	rs4648049	4:103514737	C>T	0.872	1.206 (0.122 - 11.953), P=0.873
<i>NFKB1</i>	rs4648050	4:103514741	T>C	0.869	1.065 (0.500 - 2.269), P=0.869
<i>NFKB1</i>	rs749750576	4:103516042	G>A	0.525	1.221 (0.048 - 30.606), P=0.903
<i>NFKB1</i>	rs4648073	4:103518843	G>T	0.872	1.206 (0.121 - 11.953), P=0.872
<i>NFKB1</i>	(.)	4:103527605	TAAG>_	0.525	1.221 (0.048 - 30.6062), P=0.903
<i>NFKB1</i>	rs4648095	4:103527876	T>C	0.872	1.206 (0.122 - 11.953), P=0.872
<i>NFKB1</i>	rs4648097	4:103528128	G>A	0.367	2.055 (0.096 - 43.775), P=0.644
<i>NFKB1</i>	(.)	4:103528780	G>C	0.112	0.131 (0.005 - 3.284), P=0.216
<i>NFKB1</i>	rs4648104	4:103531991	G>C	0.139	0.191 (0.016 - 2.178), P=0.183
<i>NFKB1</i>	rs56207297	4:103533052	G>A	0.268	2.907 (0.146 - 7.579), P=0.483
<i>NFKB1</i>	rs4648110	4:103533821	T>A	0.118	0.512 (0.219 - 1.195), P=0.121
<i>NFKB1</i>	rs4648117	4:103534557	C>T	0.872	1.206 (0.122 - 11.953), P=0.873

Table 3.**Characteristics of SNPs within 3'UTR, 5'UTR and splicing area of the GATA2, NFKB2, NFKBIA and NFKB1 genes in acne patients**

Gene	SNPId	Chr: Position (hg19)	3'UTR/ 5'UTR/ splice site	Type and position of substitution	P-value (Z-test for proportion)	OR (95% CI) P-value
GATA2	rs10934857	3:128199662	UTR3	c.*200C>T	0.639	0.807 (0.330 - 1.976), P=0.640
GATA2	rs1806462	3:128206618	UTR5	c.-744G>T	0.255	0.642 (0.299 - 1.379), P=0.257
GATA2	rs2335237	3:128206710	UTR5	c.-836A>C	0.195	0.607 (0.284 - 1.297), P=0.198
GATA2	rs7611275	3:128206759	UTR5	c.-885G>C	0.086	0.278 (0.059 - 1.305), P=0.105
GATA2	(.)	3:128206766	splicing	Exon 2:UTR5	0.525	1.221 (0.049 - 30.606), P=0.903
GATA2	(.)	3:128207240	UTR5	c.-1366C>G	0.525	1.221 (0.048 - 30.606), P=0.903
NFKB2	rs11574842	10:104154068	UTR5	724:c.-1649C>T	0.525	1.221 (0.048 - 30.606), P=0.903
NFKB2	(.)	10:104154327	UTR5	724:c.-1390del-	0.302	0.655 (0.293 - 1.467), P=0.304
NFKBIA	rs696	14:35871093	UTR3	c.*126G>A	0.914	0.960 (0.461 - 2.00), P=0.914
NFKBIA	(.)	14:35871140	UTR3	c.*79_ *77delAGA	0.499	0.393 (0.024 - 6.455), P=0.513
NFKBIA	rs8904	14:35871217	UTR3	c.*2C>T	0.914	0.960 (0.461 - 2.00), P=0.914
NFKBIA	(.)	14:35873938	UTR5	c.-89_ 88insCGTCCCGC	0.917	0.928 (0.227 - 3.783), P=0.917
NFKB1	rs2272676	4:103423326	splicing	Exon 1: UTR5	0.345	0.696 (0.328 - 1.4771), P=0.346
NFKB1	rs386357216	4:103534740	splicing	Exon 23:c.2746+2->A	0.665	1.625 (0.176 - 15.00), P=0.668
NFKB1	rs4648143	4:103537774	UTR3	c.*23G>A	0.525	1.221 (0.048 - 30.606), P=0.903

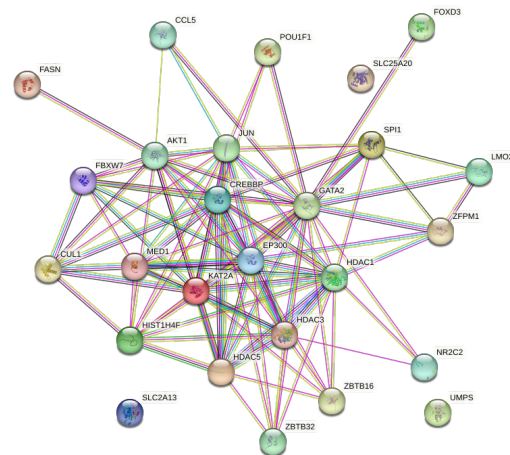
The *NFKB2* (Nuclear Factor Kappa B Subunit 2) gene encodes a subunit of the transcription factor complex nuclear factor-kappa-B (NF- κ B). The NF- κ B complex is expressed in numerous cell types and functions as a central activator of genes involved in inflammation and immune function. The protein encoded by this gene can function as both a transcriptional activator and repressor, depending on its dimerization partner. Our data regarding SNP (rs4919632) in the *NFKB2* gene with an increased frequency of the alternative allele in the MG with OR=18.76 (95% CI: 0.946-371.894, P=0.049) probably indicates a significant association with the development of severe acne.

The *NFKBIA* (NFKB Inhibitor Alpha) gene encodes a member of the NF-kappa-B inhibitor family, which contains multiple ankyrin repeat domains. The encoded protein interacts with REL dimers to inhibit NF-kappa-B/REL complexes, which are involved in inflammatory responses. The *NFKBIA* SNPs we identified showed a probable association with the risk of developing acne.

The *NFKB1* (Nuclear Factor Kappa B Subunit 1) gene encodes a 105 kD protein, which can undergo cotranslational processing by the 26S proteasome to produce a 50 kD protein. The 105 kD protein is a REL protein-specific transcription inhibitor, and the 50 kD protein is a DNA-binding subunit of the NF- κ B protein complex. The *NFKB1* SNPs we identified showed a probable association with the risk of developing acne.

The results of our study made it possible to identify SNPs in regulatory genes (*GATA1*, *GATA2*, *GATA2-AS1*

[*GATA2* Antisense RNA 1], *NFKB2*, *NFKBIA*, and *NFKB1*) associated with the development of severe acne. The gene-gene interactions are shown in Figure 1.

**Fig.1.** The gene-gene interactions.

<https://string-db.org/cgi/network?taskId=bnPlpAhhFXnY&sessionId=b1VYAaiLUmdh>

Conclusion

Transcription factors have previously been defined as “non-drug-responsive” targets, except ligand-inducible nuclear receptors. More excellent knowledge of these

transcription factors, namely their structures and functions, including expression and degradation, as well as their ability to interact with cofactors, has changed this hypothesis.

NF- κ B is a pleiotropic transcription factor present in almost all cell types. It is the endpoint of a series of signal transduction events initiated by various stimuli related to many biological processes, such as inflammation, immunity, differentiation, cell growth, tumorigenesis, and apoptosis. NF- κ B is a transcriptional regulator activated by various intra- and extracellular stimuli such as cytokines, free radicals, ultraviolet radiation, and bacterial or viral products. Activated NF- κ B translocates to the nucleus and stimulates the expression of genes involved in a wide range of biological functions. Impaired NF- κ B activation is associated with several inflammatory diseases, while persistent inhibition of NF- κ B results in inappropriate immune cell development or stunted growth. The identified polymorphic loci in the regulatory genes are likely to disturb the regulation of the inflammatory response, which can lead to the formation of a prolonged torpid course of acne.

The revealed SNPs within the *GATA1*, *GATA2*, *GATA2-ASI* [GATA2 Antisense RNA 1], *NFKB2*, *NFKB1A*, and *NFKB1* genes in patients with severe acne probably indicate the involvement of regulatory transcription factors in the pathogenesis of acne.

Competing Interests

The authors declare that they have no competing interests.

References

- Williams HC, Dellavalle RP, Garner S. Acne vulgaris. *Lancet*. 2012 Jan 28;379(9813):361-72. doi: 10.1016/S0140-6736(11)60321-8. Epub 2011 Aug 29. Erratum in: *Lancet*. 2012 Jan 28;379(9813):314. PMID: 21880356.
- Tang HY, Xiao B, Liu X, Yang GL. [Signaling Pathways in the Pathogenesis of Acne Vulgaris]. *Zhongguo Yi Xue Ke Xue Yuan Xue Bao*. 2020 Aug 30;42(4):559-561. doi: 10.3881/j.issn.1000-503X.11470. [Article in Chinese].
- Hazarika N. Acne vulgaris: new evidence in pathogenesis and future modalities of treatment. *J Dermatolog Treat*. 2021 May;32(3):277-285. doi: 10.1080/09546634.2019.1654075.

- Navarini AA, Simpson MA, Weale M, Knight J, Carlavan I, Reiniche P, et al.; Acne Genetic Study Group; Willis C, Déret S, Voegel JJ, Spector T, Smith CH, Trembath RC, Barker JN. Genome-wide association study identifies three novel susceptibility loci for severe Acne vulgaris. *Nat Commun*. 2014 Jun 13;5:4020. doi: 10.1038/ncomms5020.
- He L, Wu WJ, Yang JK, Cheng H, Zuo XB, Lai W, et al. Two new susceptibility loci 1q24.2 and 11p11.2 confer risk to severe acne. *Nat Commun*. 2014;5:2870. doi: 10.1038/ncomms3870.
- Zhang M, Qureshi AA, Hunter DJ, Han J. A genome-wide association study of severe teenage acne in European Americans. *Hum Genet*. 2014 Mar;133(3):259-64. doi: 10.1007/s00439-013-1374-4.
- Yang JK, Wu WJ, Qi J, He L, Zhang YP. TNF-308 G/A polymorphism and risk of acne vulgaris: a meta-analysis. *PLoS One*. 2014 Feb 3;9(2):e87806. doi: 10.1371/journal.pone.0087806.
- Tasli L, Turgut S, Kacar N, Ayada C, Coban M, Akcilar R, Ergin S. Insulin-like growth factor-I gene polymorphism in acne vulgaris. *J Eur Acad Dermatol Venereol*. 2013 Feb;27(2):254-7. doi: 10.1111/j.1468-3083.2011.04299.x.
- Heng AHS, Say YH, Sio YY, Ng YT, Chew FT. Gene variants associated with acne vulgaris presentation and severity: a systematic review and meta-analysis. *BMC Med Genomics*. 2021 Apr 13;14(1):103. doi: 10.1186/s12920-021-00953-8.
- GeneCards: The Human Gene Database. <https://www.genecards.org/>
- STRING resource. <https://version11.string-db.org/>.
- Freson K, Wijngaerts A, Van Geet C. GATA1 gene variants associated with thrombocytopenia and anemia. *Platelets*. 2017 Nov;28(7):731-734. doi: 10.1080/09537104.2017.1361525.
- Huilgol D, Venkataramani P, Nandi S, Bhattacharjee S. Transcription Factors That Govern Development and Disease: An Achilles Heel in Cancer. *Genes (Basel)*. 2019 Oct 12;10(10):794. doi: 10.3390/genes10100794.
- Zhong Z, Umemura A, Sanchez-Lopez E, Liang S, Shalpour S, Wong J, et al. NF- κ B Restricts Inflammation Activation via Elimination of Damaged Mitochondria. *Cell*. 2016 Feb 25;164(5):896-910. doi: 10.1016/j.cell.2015.12.057.

*Corresponding author: Olga M. Demina, PhD. Dmitry Rogachev National Research Center of Pediatric Hematology, Oncology and Immunology. Moscow, Russia. E-mail: demina.75@mail.ru

Detection of *Actinobacillus actinomycetemcomitans* DNA in Patients with Partial and Complete Dentures by Real-Time PCR

Enis Veseli^{1*}, Gloria Staka^{1,2}

¹Department of Prosthodontics, Dental School, Faculty of Medicine,
University of Pristina, Pristina, Kosovo

²University Dentistry Clinical Center of Kosovo, Pristina, Kosovo

Abstract

Background: The purpose of the present study was to detect *Actinobacillus actinomycetemcomitans* (Aa) using RT-PCR in patients with complete and partial edentulism before (T0) and three months after (T3) treatment with removable partial dentures (RPD) and complete dentures (CD), respectively, to compare the data between these two research groups.

Methods and Results: The sample comprised 60 patients: 33 men and 27 women, aged 48 to 76 years. The patients were divided into two groups. Group 1 included 30 patients with partial edentulism who were treated with RPD. Group 2 included 30 patients with complete edentulism who were treated with CD. The samples from Group 1 were taken from the gingival sulcus of the abutment teeth by means of sterile paper points. For Group 2, the samples were taken with a sterile swab from the dorsum of the tongue. The samples were taken in T0 and T3 intervals. To detect Aa DNA, we used RT-PCR and ParodontoScreen REAL-TIME PCR Detection Kit (DNA-TECHNOLOGY). Bacterial load levels of species were conventionally represented in logarithm (Lg) of genome equivalents per sample. The results were also presented in three ranges depending on the level of bacterial load: normal (<4.0 Lg), mild/moderate (≥4.0 Lg), and severe (>5.0 Lg).

The study found a significant difference in the amount of Aa between the T0 and T3 intervals only in patients treated with RPD (0.87±1.58 Lg vs. 1.28 ±1.96 Lg, $P=0.004$). Patients treated with CD, however, did not differ significantly in the amount of Aa between the T0 and T3 intervals (0.03±0.16 Lg vs. 0). The average bacterial load in patients with RPD was significantly higher than in those with CD three months after treatment ($P=0.02$). Of the 30 patients with RPD, 2(6.7%) had a severe range, 2(6.7%) had a mild/moderate range, and 26(86.7%) had a normal range. The 30 CD patients all had a normal range. There was no significant difference in the prevalence range of bacterial load level with Aa between groups (Fisher's Exact Test = 3.537, $P=0.113$) / Monte Carlo Sig. (2-sided) / 0.105–0.121). However, in general, RPD causes a significant increase in Aa, so the level of periodontal pathogens may be higher in RPD patients than in CD patients. (**International Journal of Biomedicine. 2023;13(1):141-145.**)

Keywords: *Actinobacillus actinomycetemcomitans* • real-time PCR • dentures

For citation: Veseli E, Staka G. Detection of *Actinobacillus actinomycetemcomitans* DNA in Patients with Partial and Complete Dentures by Real-Time PCR. International Journal of Biomedicine. 2023;13(1):141-145. doi:10.21103/Article13(1)_OA20

Abbreviations

CD, complete dentures; RPD, removable partial dentures; RT-PCR, real-time polymerase chain reaction.

Introduction

The oral cavity is a suitable environment that provides multiple habitats for colonizing microorganisms, including viruses, bacteria, and fungi. The role of some of them is already known in the development of various oral diseases, including caries and periodontitis. Still, recent research has

shown that these microorganisms are also implicated in heart disease, gastrointestinal infections, and malignant diseases.⁽¹⁻³⁾

Researchers have observed that certain microorganisms colonize specific areas, including removable partial dentures (RPD) and complete dentures (CD). Due to the properties of the dentures' acrylic surface and the acidic action that saliva has on the prosthesis, affecting the creation of pores, the dentures

become a suitable area for the adhesion of microorganisms.⁽⁴⁾ These microorganisms have the potential to develop biofilm, thus influencing the appearance of local changes in the oral cavity.

The clinical condition that most often appears in users of removable dentures is prosthetic stomatitis, which is characterized by inflammatory changes in the oral mucosa. Different factors affect the development of prosthetic stomatitis, including a poor adaptation of prostheses, long-term treatment with antibiotics, and fungal infection resulting from *Candida albicans*.⁽⁵⁾

Although most of the literature in this area has focused on *Candida albicans*, there is growing evidence to suggest that the use of CD and RPD also causes microbial changes, including changes in the level of periodontal pathogens.⁽⁶⁻⁹⁾

Some of these studies have reported changes occurring in the level of red-complex bacteria. Still, the literature is deficient in reporting the level of *Actinobacillus actinomycetemcomitans* (Aa), considering the risk factors associated with it, which are not limited to the area of the mouth but also extend to the general condition of a person's organism.^(10,11)

Accordingly, the purpose of the present study was to detect Aa using RT-PCR in patients with complete and partial edentulism before (T0) and three months after (T3) treatment with RPD and CD, respectively, to compare the data between these two research groups.

Materials and Methods

The sample comprised 60 patients: 33 men and 27 women, aged 48 to 76 years. The patients were divided into two groups. Group 1 included 30 patients with partial edentulism who were treated with RPD. Group 2 included 30 patients with complete edentulism who were treated with CD.

Inclusion criteria: patients' ability and willingness to cooperate, an indication for treatment with RPD and CD. Exclusion criteria: antimicrobial therapy and using immunosuppressants in the previous 90 days, temporomandibular joint problems, severe periodontal conditions.

CD was made of acrylic resin, and RPD was made of acrylic resin with a metal frame.

Sample collection

The samples from Group 1 were taken from the gingival sulcus of the abutment teeth by means of sterile paper points. For Group 2, the samples were taken with a sterile swab from the dorsum of the tongue. The samples were taken in T0 and T3 intervals. We placed the samples in sterile test tubes containing the physiological solution and sent them to the appropriate microbiological laboratory.

RT-PCR

To detect Aa, we used RT-PCR and ParodontoScreen REAL-TIME PCR Detection Kit (DNA-TECHNOLOGY). The laboratory stages are described in detail on the company's website.⁽¹²⁾ Bacterial load levels of species were conventionally represented in logarithm (Lg) of genome equivalents per sample. The results were also presented in three ranges

depending on the level of bacterial load: normal (<4.0 Lg), mild/moderate (≥4.0 Lg), and severe (>5.0 Lg).

Statistical analysis was performed using statistical software package SPSS version 21.0 (SPSS Inc, Armonk, NY: IBM Corp). For descriptive analysis, results are presented as mean (M) ± standard deviation (SD), 95% Confidence Interval (95% CI), Minimum, and Maximum. Differences in attributive series between the patient groups were tested using Pearson Chi-square / Monte Carlo Sig. (2-sided), Fisher's Exact Test / Monte Carlo Sig (2-sided). The Kruskal-Wallis H test/one way ANOVA was used to compare groups. In all cases, a probability value of $P < 0.05$ was considered statistically significant.

Ethical approval for this study was obtained from the Ethical Committee of the University Clinical Center of Pristina, Pristina, Kosovo (protocol number 378/19). All participants provided written informed consent.

Results

Table 1 provides descriptive statistics on the value of Aa bacterial load in patients with RPD and CD. The study found a significant difference in the amount of Aa between the T0 and T3 intervals only in patients treated with RPD (0.87 ± 1.58 Lg vs. 1.28 ± 1.96 Lg, $P = 0.004$). Patients treated with CD, however, did not differ significantly in the amount of Aa between the T0 and T3 intervals (0.03 ± 0.16 Lg vs. 0).

Table 1.

The value of the Aa bacterial load before (T0) and 3 months after (T3) of treatment with RPD and CD.

Dentures	T	n	Mean	-95% CI	+95% CI	Min	Max	SD	Z	P
	T0	30	0.87	0.28	1.46	0	5.2	1.58		
RPD	T3	30	1.28	0.55	2.01	0	6.1	1.96	2.1	0.04
	T0	30	0.03	-0.03	0.09	0	0.9	0.16		
CD	T3	30	0			0	0	0	/	/

The average bacterial load in patients with RPD was significantly higher than in those with CD three months after treatment ($P = 0.02$) (Table 2).

Table 2.

The difference in the Aa bacterial load 3 months after prosthetic treatment.

<i>Actinobacillus actinomycetemcomitans</i> (3 months after treatment)	n	A	RPD	CD
			R:53.23	35
RPD	30	1597		0.02
CD	30	1050	0.02	

R: statistical variables; A: amounts

The prevalence range of bacterial load levels in the groups are presented in Table 3. Of the 30 patients with RPD, 2(6.7%) had a severe range, 2(6.7%) had a mild/moderate range, and 26(86.7%) had a normal range. The 30 CD patients all had a normal range. There was no significant difference in the prevalence range of bacterial load level with Aa between groups (Fisher's Exact Test = 3.537, $P=0.113$) / Monte Carlo Sig. (2-sided) / 0.105–0.121). However, in general, RPD causes a significant increase in Aa, so the level of periodontal pathogens may be higher in RPD patients than in CD patients.

Table 3.

The prevalence range of the Aa bacterial load levels in the study groups.

		<i>Actinobacillus actinomycetemcomitans</i> (3 months after)			Total
		Severe	Mild/moderate	Normal	
RPD	Count	2	2	26	30
	%	6.67%	6.67%	86.67%	100.0%
CD	Count	0	0	30	30
	%	0%	0%	100%	100.0%
Total	Count	2	2	56	60
	%	3.33%	3.33%	93.33%	100.0%

Discussion

The main characteristic of the RT-PCR method used in our research is that it monitors the amplification of the DNA molecule in real time, not at the end, as in the conventional polymerase chain reaction. Using the molecular genetic method to detect Aa by isolating bacterial DNA is significantly more suitable than the culture method used in previous studies, due to the molecular method's sensitivity, speed, and reliability.⁽¹³⁾ Therefore, the use of RT-PCR was suitable for this study.

In this study, we initially detected Aa in both groups of patients, namely 1(3.3%) of the edentulous patients and 8(26%) of the partially edentulous patients. The higher number of patients with Aa in the latter group may be attributed to the periodontal space in patients with teeth, providing a favorable environment in the oral cavity for anaerobic species. This theory is consistent with previous research: O'Donnell et al.⁽¹⁴⁾ found higher levels of certain periodontal pathogens on the tooth surface than on the oral mucosa, and Gazdek et al.⁽¹⁵⁾ observed lower levels of Aa in edentulous patients than in partially edentulous ones. Moreover, our results are in agreement with a series of studies,^(6,16,17) which found that Aa colonizes even in edentulous conditions; however, our results are in contrast to the previous study by Danser et al.,⁽¹⁸⁾ which did not identify the presence of Aa in bacterial

samples collected from edentulous patients. These data provide significant information that the presence of Aa in the oral cavity of edentulous patients may be a major source of future bacterial colonization of dental implants.⁽¹⁹⁾ This information may influence how peri-implants are developed. At any rate, Aa is an anaerobic bacterium that plays a role in the destruction of the periodontium and has a significant impact on the development of systemic diseases such as heart disease, diabetes mellitus, and dementia;^(10,11) accordingly, we strongly encourage patients to maintain proper oral hygiene and denture care.

Another important objective of this study was the detection of Aa after treatment with removable prostheses. Based on our microbiological analyses, Aa was absent in edentulous patients three months after CD insertion. In contrast to our study, Andjekovic et al. observed an increase in Aa six months after treatment with CD. This difference may be attributed to the shorter follow-up time in our study than in the previous study.⁽²⁰⁾

On the other hand, in our study the level of Aa increased significantly in patients treated with RPD. Our results are consistent with the findings of Costa et al., who observed a general increase of microorganisms, including Aa, six months after treatment with RPD.⁽²¹⁾ Thus, based on the study's results three months after beginning therapy with RPD, the future risk of developing periodontal diseases in the supporting teeth is high when using RPD. These findings suggest more excellent oral hygiene and denture care over time. Moreover, we found that the bacterial load of Aa in patients after treatment with RPD is significantly higher than after treatment with CD. This may be attributed to the greater microbial diversity of dental plaque compared to the oral mucosa, since dental plaque may be a more hospitable environment for the growth of microorganisms.⁽²²⁾

However, dietary changes that occur due to the placement of RPD are also important factors that could influence the level of bacterial load. Al-Hamd et al. found that dietary changes and poor oral hygiene significantly impact the composition of oral microflora.⁽²³⁾ In addition, removable prostheses can be a source of infection in cases where, after laboratory procedures, the prosthetic appliance has not been adequately disinfected, resulting in the transfer of bacteria from the dental laboratory to the new prosthesis.⁽²⁴⁾ Other factors that could influence the level of Aa and were not considered in the study are the degree of porosity of the prosthesis and the design of the framework of RPD. Both factors have been observed to play an important role in microbial diversity over time.^(25,26) Thus, the proper management of removable prostheses to reduce bacterial colonization should be a major focus of future research.

Conclusion

Within the limits of this study, we can state: (1) RT-PCR analysis detected Aa in both study groups at the T0 time interval, but three months (T3) after the initial sample collection, Aa was detected only in patients treated with RPD; and (2) at T3, a significant difference emerged between the two groups, with RPD wearers having a higher level of Aa than CD wearers.

Acknowledgments

We thank Julie Stiegemeier, Ph.D., from Scribbr (info@scribbr.com), for editing a draft of this manuscript.

Competing Interests

The authors declare that they have no competing interests.

References

- Zhang JS, Chu CH, Yu OY. Oral Microbiome and Dental Caries Development. *Dent J (Basel)*. 2022 Sep 30;10(10):184. doi: 10.3390/dj10100184. PMID: 36285994; PMCID: PMC9601200.
- Di Stefano M, Polizzi A, Santonocito S, Romano A, Lombardi T, Isola G. Impact of Oral Microbiome in Periodontal Health and Periodontitis: A Critical Review on Prevention and Treatment. *Int J Mol Sci*. 2022 May 5;23(9):5142. doi: 10.3390/ijms23095142. PMID: 35563531; PMCID: PMC9103139.
- Peng X, Cheng L, You Y, Tang C, Ren B, Li Y, Xu X, Zhou X. Oral microbiota in human systematic diseases. *Int J Oral Sci*. 2022 Mar 2;14(1):14. doi: 10.1038/s41368-022-00163-7. PMID: 35236828; PMCID: PMC8891310.
- Monteiro DR, de Souza Batista VE, Caldeirão ACM, Jacinto RC, Pessan JP. Oral prosthetic microbiology: aspects related to the oral microbiome, surface properties, and strategies for controlling biofilms. *Biofouling*. 2021 Apr;37(4):353-371. doi: 10.1080/08927014.2021.1912741. Epub 2021 Jun 17. PMID: 34139899.
- Sartawi SY, Abu-Hammad S, A Salim N, Al-Omouh S. Denture Stomatitis Revisited: A Summary of Systematic Reviews in the Past Decade and Two Case Reports of Papillary Hyperplasia of Unusual Locations. *Int J Dent*. 2021 Oct 13;2021:7338143. doi: 10.1155/2021/7338143. PMID: 34691183; PMCID: PMC8528609.
- Yasui M, Ryu M, Sakurai K, Ishihara K. Colonisation of the oral cavity by periodontopathic bacteria in complete denture wearers. *Gerodontology*. 2012 Jun;29(2):e494-502. doi: 10.1111/j.1741-2358.2011.00506.x. Epub 2011 Sep 19. PMID: 21929616.
- Cortelli JR, Aquino DR, Cortelli SC, Nobre Franco GC, Fernandes CB, Roman-Torres CV, Costa FO. Detection of periodontal pathogens in oral mucous membranes of edentulous individuals. *J Periodontol*. 2008 Oct;79(10):1962-5. doi: 10.1902/jop.2008.080092. PMID: 18834252.
- Fernandes CB, Aquino DR, Franco GC, Cortelli SC, Costa FO, Cortelli JR. Do elderly edentulous patients with a history of periodontitis harbor periodontal pathogens? *Clin Oral Implants Res*. 2010 Jun;21(6):618-23. doi: 10.1111/j.1600-0501.2009.01892.x. Epub 2010 Mar 11. PMID: 20337663.
- Mine K, Fueki K, Igarashi Y. Microbiological risk for periodontitis of abutment teeth in patients with removable partial dentures. *J Oral Rehabil*. 2009 Sep;36(9):696-702. doi: 10.1111/j.1365-2842.2009.01982.x. Epub 2009 Jul 23. PMID: 19650858.
- Ozuna H, Snider I, Belibasakis GN, Oscarsson J, Johansson A, Uriarte SM. *Aggregatibacter actinomycetemcomitans* and *Filifactor alocis*: Two exotoxin-producing oral pathogens. *Front Oral Health*. 2022 Aug 15;3:981343. doi: 10.3389/froh.2022.981343. PMID: 36046121; PMCID: PMC9420871.
- Oscarsson J, Claesson R, Lindholm M, Höglund Åberg C, Johansson A. Tools of *Aggregatibacter actinomycetemcomitans* to Evade the Host Response. *J Clin Med*. 2019 Jul 22;8(7):1079. doi: 10.3390/jcm8071079. PMID: 31336649; PMCID: PMC6678183.
- DNA-Technology. ParodontoScreen [Internet]. Online information available at: <https://dna-technology.com/equipmentpr/pcr-kits-microbiome-composition-screening/parodontoscreen>. (Accessed 21 Dec 2022).
- Van der Weijden F, Rijnen M, Valkenburg C. Comparison of three qPCR-based commercial tests for detection of periodontal pathogens. *Sci Rep*. 2021 Mar 17;11(1):6141. doi: 10.1038/s41598-021-85305-3. PMID: 33731742; PMCID: PMC7969924.
- O'Donnell LE, Robertson D, Nile CJ, Cross LJ, Riggio M, Sherriff A, Bradshaw D, Lambert M, Malcolm J, Buijs MJ, Zaura E, Crielaard W, Brandt BW, Ramage G. The Oral Microbiome of Denture Wearers Is Influenced by Levels of Natural Dentition. *PLoS One*. 2015 Sep 14;10(9):e0137717. doi: 10.1371/journal.pone.0137717. PMID: 26368937; PMCID: PMC4569385.
- Gazdeck RK, Fruscione SR, Adami GR, Zhou Y, Cooper LF, Schwartz JL. Diversity of the oral microbiome between dentate and edentulous individuals. *Oral Dis*. 2019 Apr;25(3):911-918. doi: 10.1111/odi.13039. Epub 2019 Feb 10. PMID: 30657624.
- Sachdeo A, Haffajee AD, Socransky SS. Biofilms in the edentulous oral cavity. *J Prosthodont*. 2008 Jul;17(5):348-56. doi: 10.1111/j.1532-849X.2008.00301.x. PMID: 18355168.
- de Waal YC, Winkel EG, Raangs GC, van der Vusse ML, Rossen JW, van Winkelhoff AJ. Changes in oral microflora after full-mouth tooth extraction: a prospective cohort study. *J Clin Periodontol*. 2014 Oct;41(10):981-9. doi: 10.1111/jcpe.12297. Epub 2014 Sep 4. PMID: 25065274.
- Danser MM, van Winkelhoff AJ, de Graaff J, Loos BG, van der Velden U. Short-term effect of full-mouth extraction on periodontal pathogens colonizing the oral mucous membranes. *J Clin Periodontol*. 1994 Aug;21(7):484-9. doi: 10.1111/j.1600-051x.1994.tb00412.x. PMID: 7929861.
- Srinivas S, Ravi MB, Ram K, Jaishankar Homberhalli HP, Nagaraja MS, Gowrav MP, Ramesh K. Antibacterial Efficacy of Hubballi Propolis against *Aggregatibacter Actinomycetemcomitans* One of the Major Causative Organisms of Perimplantitis: An *In vitro* Study. *J Pharm Bioallied Sci*. 2022 Jul;14(Suppl 1):S595-S599. doi: 10.4103/jpbs.jpbs_653_21. Epub 2022 Jul 13. PMID: 36110765; PMCID: PMC9469338.
- Andjelkovic M, Sojic LT, Lemic AM, Nikolic N, Kannosh IY, Milasin J. Does the Prevalence of Periodontal Pathogens Change in Elderly Edentulous Patients after Complete

*Corresponding author: Enis Veseli, Department of Prosthodontics, Dental School, Faculty of Medicine, University of Pristina, Pristina, Kosovo. E-mail: enis.veseli@uni-pr.edu

- Denture Treatment? J Prosthodont. 2017 Jul;26(5):364-369. doi: 10.1111/jopr.12402. Epub 2015 Nov 30. PMID: 26619204.
21. Costa L, do Nascimento C, de Souza VO, Pedrazzi V. Microbiological and clinical assessment of the abutment and non-abutment teeth of partial removable denture wearers. Arch Oral Biol. 2017 Mar; 75:74-80. doi: 10.1016/j.archoralbio.2016.11.002. Epub 2016 Nov 3. PMID: 27825678.
22. Zaura E, Keijser BJ, Huse SM, Crielaard W. Defining the healthy «core microbiome» of oral microbial communities. BMC Microbiol. 2009 Dec 15;9:259. doi: 10.1186/1471-2180-9-259. PMID: 20003481; PMCID: PMC2805672.
23. Al-Ahmad A, Roth D, Wolkewitz M, Wiedmann-Al-Ahmad M, Follo M, Ratka-Krüger P, Deimling D, Hellwig E, Hannig C. Change in diet and oral hygiene over an 8-week period: effects on oral health and oral biofilm. Clin Oral Investig. 2010 Aug;14(4):391-6. doi: 10.1007/s00784-009-0318-9. Epub 2009 Jul 22. PMID: 19626350.
24. Moodley KL, Owen CP, Patel M. Quantitative Analysis of Selected Microorganisms Present at Various Sites in a Prosthetics Clinic and Dental Laboratory during Complete Denture Fabrication. Int J Environ Res Public Health. 2020 May 12;17(10):3345. doi: 10.3390/ijerph17103345. PMID: 32408512; PMCID: PMC7277632.
25. Delgado AHS, Carvalho J, Borrecho G, Nascimento T, Silva ME, Félix SA, Mendes JJ. *In situ* Multispecies Colonization of An Acrylic Resin: Comparison to Oral Microbiome and Potential for Inflammatory Response. Contemp Clin Dent. 2018 Jul-Sep;9(3):400-405. doi: 10.4103/ccd.ccd_141_18. PMID: 30166834; PMCID: PMC6104353.
26. Ao A, Wakabayashi N, Nitta H, Igarashi Y. Clinical and microbiologic effects of lingual cervical coverage by removable partial dentures. Int J Prosthodont. 2013 Jan-Feb;26(1):45-50. doi: 10.11607/ijp.3061. PMID: 23342333.
-

The Color Differences in Cervical, Middle and Incisal Segments of Maxillary Frontal Teeth

Teuta Pustina Krasniqi^{1*}, Edit Xhajanka², Zana Lila Krasniqi¹, Linda Dula¹, Tetore Olloni¹

¹Department of Prosthetic Dentistry, Dental Branch, Faculty of Medicine, University of Pristina, Pristina, Kosovo

²Department of Prosthetic Dentistry, Medical University of Tirana, Tirana, Albania

Abstract

The purposes of our study were to apply criteria of color differences among parameters L*, a*, and b* in three vestibular segments (cervical, middle, and incisal) of the maxillary frontal teeth.

Methods and Results: This study included 255 dentistry students who volunteered to participate in this study. The color of the central incisors, lateral incisors, and canines of the maxilla was measured by the probe tip of the spectrophotometer Vita Easyshade® (Germany).

The color parameters L*, a*, and b* in the maxillary anterior teeth differed not only from one another but also from one segment to another segment of the same tooth. The differences in color between the maxillary anterior teeth are evident; especially, these differences in color were noticed between the maxillary incisors and canines. It was concluded that the differences were of high significance between maxillary incisors and canines. The significant differences in frontal teeth were stronger between the cervical and middle segments than between these segments and incisal segments. (**International Journal of Biomedicine, 2023;13(1):146-150.**)

Keywords: maxillary frontal teeth • color • tooth segments

For citation: Krasniqi TP, Xhajanka EX, Krasniqi ZL, Dula L, Olloni T. The Color Differences in Cervical, Middle and Incisal Segments of Maxillary Frontal Teeth. International Journal of Biomedicine. 2023;13(1):146-150. doi:10.21103/Article13(1)_OA21

Introduction

To avoid the artificial look and reproduce the color of porcelain appliances as close to the original color as possible, matching natural maxillary anterior teeth is of high esthetic importance in the dental work routine. Because visual perceptions might be inaccurate and flawed, digital systems for matching color are preferred.

Spectrophotometers, colorimeters, and imaging systems are useful and relevant tools for tooth color measurement and analysis, and for quality control of color reproduction.⁽¹⁾

The future of digital dentistry is in the design of integrated approaches providing personalized treatments to patients. In addition, esthetic dentistry can benefit from

those advances by developing models allowing a complete characterization of tooth color and enhancing the accuracy of dental restorations.⁽²⁾

Dental spectrophotometers provide the highest overall accuracy and precision among different shade selection methods, while needing clinical settings to control related effective factors, conditions and technological improvement to perform optimally.⁽³⁾ The impact of color science can be seen on various restorative materials, ranging from ceramics to maxillofacial prosthetic materials.⁽⁴⁾

The teaching of esthetic dentistry in North American dental schools is highly variable and, in many schools, is shared among different disciplines. Dental schools should work together to establish the parameters for teaching this subject and should formulate the necessary standards for education and research in this new field. The majority of the studies of tooth color determinations with digital devices were based on color parameters established in 1976 by the Commission Internationale de l'Eclairage (CIE).⁽⁵⁾

**Corresponding author: Prof. Teuta Pustina Krasniqi, Department of Prosthetic Dentistry, Dental Branch, Faculty of Medicine, University of Pristina, Pristina, Kosovo. E-mail:teuta.pustina@uni-pr.edu*

In the literature, color is described based on the Munsell color space in terms of lightness, chroma, and hue. The CIE $L^*a^*b^*$ color space has a vertical axis that indicates relative lightness or darkness. The two horizontal axes represent the amounts of a^* ~ red/green and b^* ~ yellow/blue. In the $L^*a^*b^*$ color space, L^* is a measure of the lightness of an object, which represents the quantity of light reflected by an object; a^* is a measure of redness/ $a > 0$ /or greenness/ $a < 0$; and b^* is a measure of yellowness/ $b > 0$ /or blueness/ $b < 0$. Chroma is the strength or dominance of the hue; it can also be described as a saturation of color. Hue describes a dimension of color.⁽⁶⁾

Differences in lightness, chroma, and hue of pairs of natural anterior teeth, are important for providing more accurate information on color for the production of dentures with a natural appearance.⁽⁷⁾

Goodkind and Schwabacher,⁽⁸⁾ in a colorimetric study of maxillary anterior teeth, concluded that the best representation of tooth color was in the vestibular middle third of the tooth; women's teeth were lighter, less chromatic, and less reddish-colored than men's; aging produced darker and more reddish teeth; cuspid teeth were darker than incisors; central incisors had the highest lightness.

Seghi et al.⁽⁹⁾ found that the photo-electric tristimulus colorimeter showed the best overall performance on porcelain surfaces, supporting its use as a valuable tool for evaluating color in dentistry.

Tooth color determination has attracted attention in the field of dentistry. It can be measured by visual perception and via digital instruments. The Munsell system created by A. Munsell is presently one of the most popular spaces for measuring object color and is widely used in virtually all fields.⁽¹⁰⁾ It is one of the uniform color spaces defined by CIE in 1976 in order to reduce one of the major problems of the original Yxy space: equal distances on the x, y chromaticity diagram. In this space, L^* indicates lightness, and a^* and b^* are the chromaticity coordinates. The a^* and b^* indicate color directions: $+a^*$ is the red direction, $-a^*$ is the green direction, $+b^*$ is the yellow direction, and $-b^*$ is the blue direction. The center is achromatic; as the a^* and b^* values increase and the point moves out from the center, the saturation of the color increases.⁽¹¹⁾ Improved shade guides, availability of shade-taking devices, and research in the area of human color vision have improved the potential of clinicians to achieve excellent color-matched restorations. An understanding of the appearance attributes of natural teeth is required, along with new shade guides and shade-taking instruments, to maximize shade-matching results.⁽¹²⁾ Many investigators from a range of different countries have reported L^* , a^* , and b^* values for teeth measured in vivo using instrumental techniques such as spectrophotometers, colorimeters, and image analysis of digital images. In general, these studies show a large range in L^* , a^* , and b^* values, but consistently show that there is a significant contribution of b^* value or yellowness in natural tooth color.⁽¹³⁾

The purposes of our study were to apply criteria of color differences among parameters L^* , a^* , and b^* in three vestibular segments of the maxillary frontal teeth.

Materials and Methods

This study included 255 subjects. The study was performed in the Dental Branch, Faculty of Medicine, University of Pristina. The dentistry students volunteered to participate in this study. The criteria for involvement in the study were to have intact teeth without any pigments, decay, or other elements that could affect the tooth color.

The color of the central incisors, lateral incisors, and canines of the maxilla was measured by the probe tip of the spectrophotometer Vita Easyshade® (VITA Zahnfabrik H. Rauter GmbH and Co. KG, Bad Sackingen, Germany) (Figure 1).

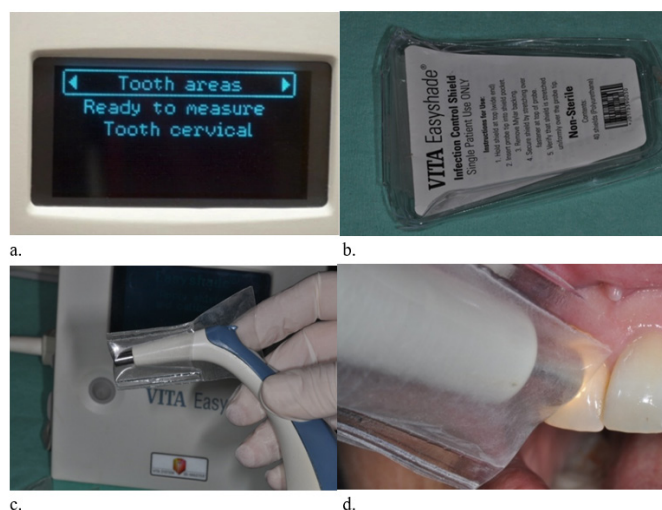


Fig. 1. a. Program Tooth Areas of the spectrophotometer Vita Easyshade®; b. Infection control shield; c. The infection control shield placed on the probe tip; d. Digital measuring of the tooth color.

Before measurements in every volunteer, an infection control shield was placed on the probe tip. The program Tooth Areas in the spectrophotometer Vita Easyshade® enables measuring tooth color in three segments of the vestibular surface of the tooth: cervical, middle, and incisal. The L^* a^* b^* parameters of the tooth color were collected.

In previous studies,^(13,14) variations of color coordinates have been reported for human teeth in the range of $L^*=60-95$ (where 0=black and 100=white), $b^*=8-25$ (positive values designate colors towards yellow, negative values designate colors towards blue), and $a^*=-2$ to $+10$ (negative values designate colors towards green, positive values designate colors towards red).

Statistical analysis was performed using the Statistica 7.1 software package (Stat-Soft Inc., USA). A Bonferroni test, a series of t-tests performed on each pair of groups, was applied. A probability value of $P < 0.05$ was considered statistically significant.

Ethical approval for this study was obtained from the Ethical Committee of the University of Pristina. All participants provided written informed consent.

Results

Table 1. shows the results of differences between mean values of L* for the target tooth, in the distribution of Central Incisor/Lateral Incisor/Canine (CI/LI/C) and their segments, Cervical/Middle/Incisal (Cs/Ms/Is), analyzed with Bonferroni Post Hoc Test.

The mean L* for CI/Cs (85.39) was significantly higher than for CI/Ms (83.15) and CI/Is (79.56) of the same tooth ($P < 0.001$ in both cases). The mean L* for CI/Cs (85.39) was significantly greater than for LI/Ms (82.85) and LI/Is (80.34) and for C/Cs (82.23), C/Ms (80.21) and C/Is (77.54) ($P < 0.001$ in all cases). The mean L* for CI/Ms (83.15) was significantly greater than for CI/Is (79.56), LI/Is (80.34), C/Ms (80.21), and C/Is (77.54) ($P < 0.001$ in all cases). The mean L* for CI/Is (79.56) was significantly less than for LI/Cs (83.57), LI/Ms (82.85), and C/Cs (82.23) ($P < 0.001$ in all cases); at the same time, it was significantly greater than for C/Is (77.54) ($P < 0.01$). The mean L* for LI/Cs (83.75) was significantly greater than for LI/Is (80.34), C/Ms (80.21), and C/Is (77.54) ($P < 0.001$ in all cases). The mean L* for LI/Ms (82.85) was significantly greater than for LI/Is (80.34) and C/Ms (80.21) ($P < 0.001$ in both cases). The mean L* for LI/Is (80.34) was significantly less than for C/Cs (82.23) ($P < 0.01$) and significantly greater than for C/Is (77.54) ($P < 0.001$). The mean L* for C/Cs (82.23) was significantly greater than for C/Ms (80.21) and C/Is (77.54) ($P < 0.01$ in both cases). The mean L* for C/Ms (80.21) was significantly greater than for C/Is (77.54) ($P < 0.001$).

Table 1.
Bonferroni Post Hoc Test / L*

Bonferroni test; variable L *											
	Tooth	Seg- ment	(1) 85.39	(2) 83.15	(3) 79.56	(4) 83.75	(5) 82.85	(6) 80.34	(7) 82.23	(8) 80.21	(9) 77.54
1	CI	C		***	***	*	***	***	***	***	***
2	CI	M	***		***			***		***	***
3	CI	I	***	***		***	***		***		**
4	LI	C	*		***			***		***	***
5	LI	M	***		***			***		***	
6	LI	I	***	***		***	***		**		***
7	C	C	***		***			**		**	***
8	C	M	***	***		***	***		**		***
9	C	I	***	***	*	***	***	***	***	***	

*- $P < 0.05$; **- $P < 0.01$; ***- $P < 0.001$

Table 2 shows the differences in mean values of parameter a* (red/green) for the target tooth, in the distribution of CI/LI/C and their segments (Cs/Ms/Is).

The mean a* for CI/Cs (-1.14) was significantly higher than for CI/Ms (-1.59) and CI/Is (-1.80) of the same tooth ($P < 0.001$ in both cases). The mean a* for CI/Cs (-1.14) was significantly less than for LI/Cs (-0.44) ($P < 0.001$) and was significantly higher than for LI/Is (-1.47) ($P < 0.05$). The mean a* for CI/Cs (-1.14) was significantly less than for C/Cs (0.79), C/Ms (0.58), and C/Is (0.11) ($P < 0.001$ in all cases). The mean a* for CI/Ms (-1.59) was significantly less than for LI/Cs (-0.44) and LI/Ms (-1.09) and for C/Cs (0.79), C/Ms (0.58) and C/Is (0.11) ($P < 0.001$ in all cases). The mean a* for CI/Is (-1.80) was significantly less than for LI/Cs (-0.44) ($P < 0.001$), LI/Ms (-1.09) ($P < 0.001$) and LI/Is (-1.47) ($P < 0.05$), and for C/Cs (0.79), C/Ms (0.58), and C/Is (0.11) ($P < 0.001$ in all cases). The mean a* for LI/Cs (-0.44) was significantly higher than for LI/Ms (-1.09) and LI/Is (-1.47) ($P < 0.001$ in both cases); at the same time, it was significantly less than for and for C/Cs (0.79), C/Ms (0.58) and C/Is (0.11) ($P < 0.001$ in all cases). The mean a* for LI/Ms (-1.09) was significantly higher than for LI/Is (-1.47) ($P < 0.001$); at the same time, it was significantly less than for C/Cs (0.79), C/Ms (0.58) and C/Is (0.11) ($P < 0.001$ in all cases). The mean a* for LI/Is (-1.47) was significantly less than for C/Cs (0.79), C/Ms (0.58) and C/Is (0.11) ($P < 0.001$ in all cases). The mean a* for C/Cs (0.79) was significantly higher than for C/Is (0.11) ($P < 0.001$) and the mean a* value for C/Ms (0.58) was significantly higher than for C/Is (0.11) ($P < 0.001$).

Table 2.
Bonferroni Post Hoc Test/Parametar a*

Bonferroni test; variable a*											
	Tooth	Seg- ment	(1) -1.14	(2) -1.59	(3) -1.80	(4) -0.44	(5) -1.09	(6) -1.47	(7) 0.79	(8) 0.58	(9) 0.11
1	CI	C		***	***	***		*	***	***	***
2	CI	M	***			***	***		***	***	***
3	CI	I	***			***	***	*	***	***	***
4	LI	C	***	***	***		***	***	***	***	***
5	LI	M		***	***	***		**	***	***	***
6	LI	I	*		*	***	**		***	***	***
7	C	C	***	***	***	***	***	***			***
8	C	M	***	***	***	***	***	***			***
9	C	I	***	***	***	***	***	***	***	***	

*- $P < 0.05$; **- $P < 0.01$; ***- $P < 0.001$

Table 3 shows the differences in mean values of parameter b* (yellow/blue) for the target tooth, in the distribution of CI/LI/C and their segments (Cs/Ms/Is). The mean b* for CI/Cs (21.62) was significantly higher

than for CI/Ms (18.22) and CI/Is (16.42) of the same tooth ($P<0.001$ in both cases). The mean b^* for CI/Cs (21.62) was significantly higher than for LI/Ms (19.47) and LI/Is (17.08) ($P<0.001$ in both cases). The mean b^* for CI/Cs (21.62) was significantly less than for C/Cs (29.39), C/Ms (26.59) and C/Is (24.02) ($P<0.001$ in all cases). The mean b^* for CI/Ms (18.22) was significantly higher than for CI/Is (16.42) ($P<0.001$) and LI/Is (17.08) ($P<0.05$); at the same time, it was significantly less than for LI/Cs (21.98), C/Cs (29.30), C/Ms (26.59) and C/Is (24.02) ($P<0.001$ in all cases). The mean b^* for CI/Is (16.42) was significantly less than for LI/Cs (21.98), LI/Ms (19.47), C/Cs (29.39), C/Ms (26.59), and C/Is (24.02) ($P<0.001$ in all cases). The mean b^* for LI/Cs (21.98) was significantly higher than for LI/Ms (19.47) and LI/Is (17.08) of the same tooth ($P<0.001$ in both cases); at the same time, it was significantly less than for C/Cs (29.39), C/Ms (26.59) and C/Is (24.02) ($P<0.001$ in all cases). The mean b^* for LI/Ms (19.47) was significantly higher than for LI/Is (17.08) ($P<0.001$); at the same time, it was significantly less than for C/Cs (29.39), C/Ms (26.59) and C/Is (24.02) ($P<0.001$ in all cases). The mean b^* for LI/Is (17.08) was significantly less than for C/Cs (29.39), C/Ms (26.59) and C/Is (24.02) ($P<0.001$). The mean b^* for C/Cs (29.39) was significantly higher than for C/Ms (26.59), C/Is (24.02) ($P<0.001$ in both cases), and the mean b^* for C/Ms (26.59) was significantly higher than for C/Is (24.02) ($P<0.001$).

obtained data showed that the cervical segment of the frontal teeth of the maxilla has higher lightness than the middle and incisal segments.

Schwabacher et al.⁽¹⁵⁾ found that correlations between hue, lightness, and chroma were not significant for incisal and cervical sites. For the middle site, these Munsell color coordinates were highly correlated and closely confined to a planar region of the color space, described by a single equation.

In a study by Çetin et al.,⁽¹⁶⁾ based on the right-left localization variable, L^* (Right L^* : 79.7, Left L^* : 80.2, $P<0.001$), and a^* parameters showed statistical higher (Right a^* : -0,1 / Left a^* : -0.2, $P=0.020$) values in general.

Zhao and Zhu,⁽¹⁷⁾ using a fiber-optic spectrophotometer (FMC-9204, Kunming, China) for in vivo color measurements of 410 healthy maxillary anterior teeth of 70 Kunming residents aged 18 to 70, showed that the color of the maxillary anterior teeth was related to tooth position: the central incisor had the highest value of L^* , and the canine had the lowest. The canine was also redder, yellower, and more saturated.

Savas et al.⁽¹⁸⁾ performed a spectrophotometric color analysis of maxillary permanent central incisors based on apical developmental stage, age, and gender groups. Digital images were quantified by non-contact spectrophotometry to determine the tooth color. Each tooth's color shade and L^* , a^* , and b^* values were recorded. A statistically significant difference was found between the 7- to 12-year-old and 13- to 18-year-old age groups in the general tooth shade and its L^* value in the overall, cervical, middle, and incisal sites ($P<0.05$). The authors concluded that there is a strong relationship between the apical developmental stages of the teeth and the L^* values.

Dozic et al.⁽¹⁹⁾ found a relation in color between the maxillary incisors and canines, which was stronger between the cervical than between the middle and incisal segments. In a study by Tabatabaian et al.,⁽²⁰⁾ central and lateral teeth showed color matches in middle and incisal regions, while lateral and canine teeth disclosed color matches in cervical regions.

In a study by Dozic et al.,⁽²¹⁾ the color relation between three tooth segments (cervical, middle, and incisal) in vital upper central incisors, using digital photography was determined. The authors found statistically significant linear correlations for L^* and b^* between the three tooth segments (cervical, middle, and incisal) (all $r's \geq 0.06$, $P<0.001$). The correlation coefficient for a^* was lower compared to L^* and b^* values.

Table 3.

Bonferroni Post Hoc Test - Parameter b^*

Bonferroni test; variable b^*											
	Tooth	Seg-ment	(1) 21.62	(2) 18.22	(3) 16.42	(4) 21.98	(5) 19.47	(6) 17.08	(7) 29.39	(8) 26.59	(9) 24.02
1	CI	C		***	***		***	***	***	***	***
2	CI	M	***		***	***	**	*	***	***	***
3	CI	I	***	***		***	***		***	***	***
4	LI	C		***	***		***	***	***	***	***
5	LI	M	***	**	***	***		***	***	***	***
6	LI	I	***	*		***	***		***	***	***
7	C	C	***	***	***	***	***	***		***	***
8	C	M	***	***	***	***	***	***	***		***
9	C	I	***	***	***	***	***	***	***	***	

*- $P<0.05$; **- $P<0.01$; ***- $P<0.001$

Discussion

Our results show that values of L^* were higher for CI/Cs than for LI/Cs, LI/Ms, LI/Is, C/Cs, C/Ms, and C/Is. Thus, the

Conclusion

The color parameters L^* , a^* , and b^* in the maxillary anterior teeth differ not only from one another but also from one segment to another segment of the same tooth. The differences in color between the maxillary anterior teeth are evident; especially, these differences in color were noticed between the maxillary incisors and canines. It was concluded that the differences were of high significance between

maxillary incisors and canines. The significant differences in frontal teeth were stronger between the cervical and middle segments than between these segments and incisal segments. The clinical implication of this study is a way to provide proper shade selection, especially when the color of the teeth is measured visually; dentists and assisting staff should concentrate on the cervical and middle segments of the tooth. It is an essential basic step to achieve perfect esthetic results. The color of the teeth is influenced by many factors, causing subjective differences. Color differences should also be considered when producing denture teeth, to come as close as possible to the natural color.

Competing Interests

The authors declare that they have no competing interests.

References

1. Chu SJ, Trushkowsky RD, Paravina RD. Dental color matching instruments and systems. Review of clinical and research aspects. *J Dent.* 2010;38 Suppl 2:e2-16. doi: 10.1016/j.jdent.2010.07.001. Epub 2010 Aug 1. PMID: 20621154.
2. Carrillo-Perez F, Pecho OE, Morales JC, Paravina RD, Della Bona A, Ghinea R, Pulgar R, Pérez MDM, Herrera LJ. Applications of artificial intelligence in dentistry: A comprehensive review. *J Esthet Restor Dent.* 2022 Jan;34(1):259-280. doi: 10.1111/jerd.12844. Epub 2021 Nov 29. PMID: 34842324.
3. Tabatabaian F, Beyabanaki E, Alirezaei P, Epakchi S. Visual and digital tooth shade selection methods, related effective factors and conditions, and their accuracy and precision: A literature review. *J Esthet Restor Dent.* 2021 Dec;33(8):1084-1104. doi: 10.1111/jerd.12816. Epub 2021 Sep 9. PMID: 34498789.
4. Bhat V, Prasad DK, Sood S, Bhat A. Role of colors in prosthodontics: application of color science in restorative dentistry. *Indian J Dent Res.* 2011 Nov-Dec;22(6):804-9. doi: 10.4103/0970-9290.94675. PMID: 22484875.
5. Gordan VV, Abu-Hanna A, Mjör IA. Esthetic dentistry in North American dental schools. *J Can Dent Assoc.* 2004 Apr;70(4):230. PMID: 15120016.
6. CIE (Commission Internationale de l'Eclairage). Colorimetry – Technical Report. CIE Pub. No. 15. 3rd ed. Vienna: Bureau Central de la CIE; 2004.
7. Eiffler C, Cevirgen E, Helling S, Zornek J, Pritsch M, Hassel AJ. Differences in lightness, chroma, and hue in the anterior teeth of quinquagenarians and septuagenarians. *Clin Oral Investig.* 2010 Oct;14(5):587-91. doi: 10.1007/s00784-009-0331-z. Epub 2009 Aug 18. PMID: 19688229.
8. Goodkind RJ, Schwabacher WB. Use of fiber-optic colorimeter for in vivo color measurements of 2830 anterior teeth. *J Prosthet Dent.* 1987;58:535–42. [https://doi.org/10.1016/0022-3913\(87\)90380-5](https://doi.org/10.1016/0022-3913(87)90380-5).
9. Seghi RR, Johnston WM, O'Brien WJ. Performance assessment of colorimetric devices on dental porcelains. *J Dent Res.* 1989 Dec;68(12):1755-9. doi: 10.1177/00220345890680120701. PMID: 2600256.
10. Paravina RD, Powers JM. *Esthetic Color Training in Dentistry*. Chapter 2. Elsevier Mosby, 2004.
11. Ragain JC. A Review of Color Science in Dentistry: Colorimetry and Color Space. *J Dent Oral Disord Ther.* 2016;4(1):1-5
12. Brewer JD, Wee A, Seghi R. Advances in color matching. *Dent Clin North Am.* 2004 Apr;48(2):v, 341-58. doi: 10.1016/j.cden.2004.01.004. PMID: 15172604.
13. Joiner A, Hopkinson I, Deng Y, Westland S. A review of tooth colour and whiteness. *J Dent.* 2008;36 Suppl 1:S2-7. doi: 10.1016/j.jdent.2008.02.001. PMID: 18646363.
14. Zhu H, Lei Y, Liao N. [Color measurements of 1,944 anterior teeth of people in southwest of China-discreption]. *Zhonghua Kou Qiang Yi Xue Za Zhi.* 2001 Jul;36(4):285-8. PMID: 11718012. [Article in Chinese].
15. Schwabacher WB, Goodkind RJ, Lua MJ. Interdependence of the hue, value, and chroma in the middle site of anterior human teeth. *J Prosthodont.* 1994 Dec;3(4):188-92. doi: 10.1111/j.1532-849x.1994.tb00153.x. PMID: 7866499.
16. Çetin C. , Eroğlu E. , Küçükeşmen C. , Özişçi Ö. CIE L*a*b* Color Analyses of Anterior Maxillary Teeth According to Gender and Localization. *Süleyman Demirel Üniversitesi Sağlık Bilimleri Dergisi.* 2019; 10(4): 448-453.
17. Zhao Y, Zhu J. In vivo color measurement of 410 maxillary anterior teeth. *Chin J Dent Res.* 1998 Dec;1(3):49-51. PMID: 10557174.
18. Savas S, Kavrik F, Yasa B, Kucukyilmaz E. Spectrophotometric color analysis of maxillary permanent central incisors in a pediatric population: a preliminary study. *Int J Paediatr Dent.* 2017 Sep;27(5):420-427. doi: 10.1111/ipd.12276. Epub 2016 Nov 24. PMID: 27882626.
19. Dozić A, Kleverlaan CJ, Aartman IH, Feilzer AJ. Relations in color among maxillary incisors and canines. *Dent Mater.* 2005 Mar;21(3):187-91. doi: 10.1016/j.dental.2004.03.005. PMID: 15786586.
20. Tabatabaian F, Ourang SA, Khezri AS, Namdari M. Are there any color match and color correlation between maxillary anterior teeth? *J Esthet Restor Dent.* 2022 Mar;34(2):397-404. doi: 10.1111/jerd.12845. Epub 2022 Jan 4. PMID: 34981888.
21. Dozic A, Kleverlaan CJ, Aartman IH, Feilzer AJ. Relation in color of three regions of vital human incisors. *Dent Mater.* 2004 Nov;20(9):832-8. doi: 10.1016/j.dental.2003.10.013. PMID: 15451238.

Correlation of Herd Immunity to Measles Vaccination Rate and Disease Incidence

Edita Goranci Haxhiu¹, Isme Humolli^{1*}, Donjeta Pllana²

¹Department of Epidemiology, Faculty of Medicine, University of Prishtina

²Department of Microbiology, National Institute of Public Health of Kosovo
Prishtina, Kosovo

Abstract

Background: Measles is one of the most contagious diseases faced by humans. Despite considerable progress, measles remains one of the leading global causes of death among children.

Methods and Results: The seroprevalence of antibodies against measles in Kosovo was determined with a serological survey of measles. In total, 768 participants aged between 3 days and 45 years of both sexes were included. Enzyme-linked immunosorbent assay results revealed total seropositivity of 74.5% (95% CI: 0.70–0.88) among participants. Those in the unvaccinated 0–1.9-year age group had the lowest seropositivity (33.2%). The 2–6-year age group, which received one dose of the vaccine, had higher seropositivity (78.6%) than the youngest group. The 8–17-year age group, which received two doses of the measles vaccine, had significantly higher seropositivity (91.3%) than the 2–6-year age group. The highest level of seropositivity (93.4%) was observed in the 18–45-year age group. An analysis of sex-specific IgG antigen levels indicated that female participants had significantly higher seropositivity than male participants ($P < 0.01$).

Conclusion: The seroprevalence of measles antibodies in Kosovo has not yet reached the required 95% threshold, and the threat of a possible measles epidemic exists. An immunization strategy that targets vulnerable groups and the entire population is required. (International Journal of Biomedicine. 2023;13(1):151-155.)

Keywords: measles • seroprevalence • vaccination

For citation: Haxhiu EG, Humolli I, Pllana D. Correlation of Herd Immunity to Measles Vaccination Rate and Disease Incidence. International Journal of Biomedicine. 2023;13(1):151-155. doi:10.21103/Article13(1)_OA22

Abbreviations

MMR, measles–mumps–rubella; MCV, measles-containing vaccine; NTU, NovaTec Units.

Introduction

Measles is one of the most contagious diseases faced by humans.⁽¹⁾ Despite considerable progress in reducing the incidence of measles, it remains one of the leading global causes of death among children.⁽²⁾ To control measles and prevent outbreaks and deaths, vaccination coverage rates with

the required MCV1 and MCV2 vaccines must reach and be maintained at 95% at the national and sub-national levels.⁽¹⁾ Global MCV1 coverage has stagnated at 84%–85% for over a decade. Although a safe and cost-effective vaccine is available, global measles deaths have continued to climb and surged worldwide in 2019, when the highest number of reported cases in the previous 23 years were reported.⁽¹⁾

Measles outbreaks continue to occur in countries in which the population is unvaccinated or under-vaccinated, as well as in countries with highly vaccinated populations.⁽³⁾ Despite the universal use of the two-dose trivalent measles–mumps–rubella (MMR) vaccine in the past two decades,

*Corresponding author: Prof. Dr. Isme Humolli, Ph.D.,
Department of Epidemiology, University of Prishtina, Prishtina,
Kosovo. E-mail: Isme.humolli@uni-pr.edu

outbreaks of these diseases still occur in countries with high vaccine uptake, giving rise to concerns about the primary and secondary failure of MMR vaccine components.⁽⁴⁾

In addition to the factors presented above, the COVID-19 pandemic has considerably disrupted health services worldwide because of associated healthcare staff shortages and the requirement for social distancing.⁽⁵⁾ The suspension of measles campaigns because of the COVID-19 pandemic in some countries will inevitably lead to an increase in measles cases in these countries.⁽⁶⁾ The WHO has targeted measles for elimination by 2020, an ostensibly challenging goal.⁽⁷⁾ The organization assumes that the recommended measles vaccination coverage rates will generate and maintain the herd immunity required to prevent the transmission of measles in the community.⁽⁸⁾

During the 2000–2020 period, measles vaccination prevented an estimated 31.7 million deaths globally, making the measles vaccine one of the most cost-effective programs in public health.⁽³⁾ Several countries that have achieved sustained measles control now demonstrate that the level of measles-specific IgG antibodies declines with time from vaccination. Given the strong epidemiologic evidence for population-level protection, the implications of declining measles-specific IgG antibody levels to the maintenance of measles eradication remain unclear.⁽⁹⁾

Before the introduction of the mandatory measles vaccine in Kosovo in 1971, large outbreaks of measles were recorded every 1–3 years. No cases of measles were registered between 2000 and 2017. During the 2017–2018 measles outbreak, 749 confirmed cases and two deaths were recorded. At the beginning of the outbreak, most confirmed cases were among hard-to-reach children from vulnerable groups; the outbreak then spread to the entire population.⁽¹⁰⁾ During the same period, a total of 41,000 confirmed measles cases, including 37 deaths that occurred in the first six months of 2018, were reported in seven European countries.⁽¹¹⁾

In Kosovo, the vaccination of individuals aged 0–18 years is in accordance with the Health Law, the Public Health Law, and the Law on Prevention and Control of Communicable Diseases.⁽¹²⁾ The vaccination calendar is dynamic and varies according to the epidemiological situation in the country and abroad. Children who receive one dose of BCG (Bacille Calmette-Guerin), three doses of IPV (Inactivated polio vaccine), DPT (diphtheria, pertussis, tetanus), HepB, (Hepatitis B), HiB (Haemophilus influenza type B), and one dose of MMR by the age of 12 months are considered; however, unregistered children and those who are hard to reach remain high-risk groups. The decrease in the vaccination coverage rate during the past 3 years has been driven by several factors: the COVID-19 pandemic, the difficulty reaching unregistered hard-to-reach children, the false association of the MMR vaccine with autism, and religious beliefs. The national level of vaccination coverage is satisfactory for registered children.

The purpose of the study was to assess the seroprevalence of measles-specific antibodies in 768 participants aged 0–45 years in Kosovo, where measles vaccination rates have been high (>95%), and cases have been very low for decades. We further aimed to identify possible demographic factors

associated with the seroprevalence of measles antibodies, MMR vaccination coverage, and the incidence of measles in Kosovo during the 2012–2021 period. Our main objective was to provide scientific evidence for ways to eliminate measles and guide relevant strategies to achieve eradication, protect public health, offer safe vaccines, and identify the additional vaccination coverage required to establish herd immunity against measles.

Material and Methods

The study was approved by the Ethical Committee of the Medical Faculty of the University of Pristina in Kosovo and was based on the committee's methodology. Written informed consent was obtained from each research participant (or the participant's parent/guardian).

The seroprevalence of antibodies against measles was determined using a serological survey of measles in Kosovo. Sera collection was conducted from 2017 to 2021. In total, 768 participants aged 3 days to 45 years of both sexes (48.7% male and 51.3% female) were included in the study. Using the Kish method,⁽¹³⁾ a representative sample was obtained from seven Kosovo regions (29 municipalities). Participants included in the research were healthy and active. Individuals who were infected during the 2017–2018 measles outbreak were excluded from antibody seroprevalence analysis. The numbers of sera by age group varied from 150 to 241. All participants were divided into four age groups: 0–1.9 years (n=190), 2–6 years (n=187), 8–17 years (n=150), and 18–45 years (n=241). Personal information, including sex, age or date of birth, measles vaccination, and sampling date, was collected. We assessed the correlation between MMR vaccination coverage and disease incidence in 2012–2021. Vaccination history was collected from the Immunization Program Management Database. Measles incidence data were obtained from the National Institute of Public Health annual reports for Communicable Diseases in Kosovo.

Serological tests were performed in the laboratory of the microbiology department of the Institute of Public Health. All samples were tested using the NovaTec (222 Thomas Ave, Baltimore, MD 21225, USA) enzyme-linked immunosorbent assay. A commercial kit was used for the qualitative determination of IgG antibodies against the measles virus in human serum or plasma. Samples were kept at 2–8°C if the assay was performed within 5 days of sample collection; otherwise, samples were aliquoted and were deep-frozen at –20°C. Samples were processed according to the First In, First Out principle. Washing was performed using automatic Tecan (Seestrasse 103, 8708 Mannedorf, Switzerland) equipment. Negative and positive controls were included in each enzyme-linked immunosorbent assay kit calibrator. A house control was included in each round of testing. Sensitivity diagnostic performance was 97%, and specificity was 100%. Results were calculated based on the protocol and were evaluated qualitatively as positive (>11NTU), negative (<9NTU), and intermediary (9–11NTU). Sera with intermediary values were subjected to repeated testing; in cases of repeated results, a new sample was requested.

Statistical analysis was performed using the SPSS Version 26.0 (IBM Corp. Released 2019. IBM SPSS Statistics for Windows, Version 26.0. Armonk, NY: IBM Corp) statistical software package. Participants' demographic characteristics were analyzed using the descriptive method. The association between MMR vaccination coverage and the measles incidence rate was analyzed using Pearson's correlation. The Mann–Whitney test was used to determine the difference between male and female participants in measles-specific IgG levels. The association between age and measles-specific IgG levels was assessed using the Kruskal–Wallis test. A *p*-value less than 0.05 was considered statistically significant.

Results

Participants in the unvaccinated 0–1.9-year age group had the lowest seropositivity (33.2%). The 2–6-year age group, which received one dose of the vaccine (93.3% MCV1), had higher seropositivity (78.6%) than the youngest group. Higher seropositivity (91.3%) was observed in the 8–17-year age group, which received two doses of the MMR vaccine (96% MCV1, MCV2), than in the 2–6-year age group. The highest level of seropositivity (93.4%) was observed in the 18–45-year age group. The total seropositivity of participants was 74.5% (95% CI: 0.70–0.88; Table 1).

Table 1.

Participant characteristics and measles seroprevalence results of study participants

Age group (years)	Male (n)	Female (n)	IgG positive (n)	IgG negative (n)	Median IgG (IU/mL)	Seroprevalence (%)	95 % CI
0–1	102	88	63	127	0.14	33.2	0.12–0.16
2–6	88	99	147	40	0.79	78.6	0.71–0.91
8–17	76	74	137	13	0.97	91.3	0.85–1.07
18–45	108	133	225	16	1.23	93.4	1.11–1.39

A comparison by sex of IgG levels indicated that female participants had a significantly higher seropositivity rate than male participants ($P < 0.01$, Figure 1).

Figure 2 illustrates that the 0–1.9-year age group, which was not vaccinated with MMR, had significantly lower quantities of IgG than age groups that were vaccinated with one or two doses of MMR. The differences increase with age and there are significant statistical differences ($P < 0.01$).

Figure 3 shows a correlation between national MMR vaccine coverage and the incidence of measles per 100,000 inhabitants (0.89) from 2012 to 2021. The average vaccination

coverage from 2012 to 2019 was 95.2%, and it decreased by 5% during the COVID-19 pandemic. Vaccination coverage was higher at the beginning of the measles outbreak 2017–2018 than in 2012–2016 because of the vaccination campaigns undertaken during that period.

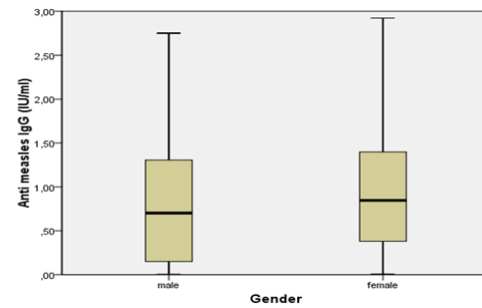


Fig. 1. Measles-specific IgG levels by sex.

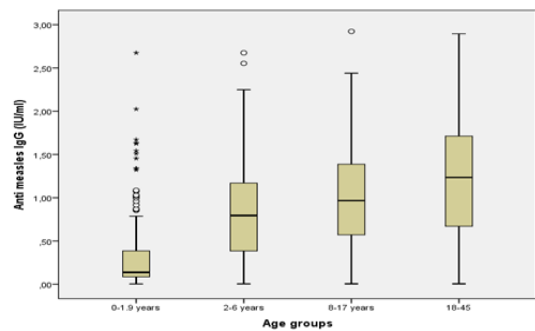


Fig. 2. Ig G levels by age groups.

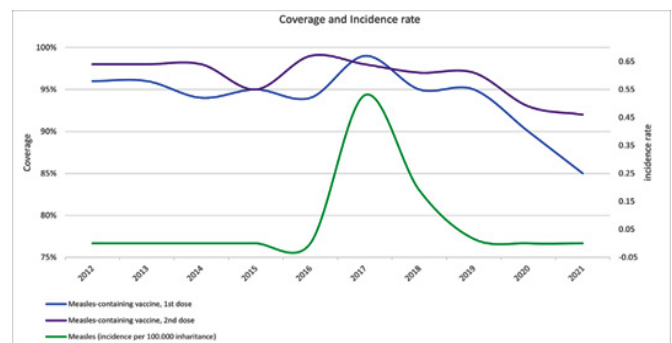


Fig. 3. National MMR vaccine coverage and measles incidence (2012–2021).

Figure 4 illustrates MMR vaccine coverage by Kosovo municipality. Findings indicate that most municipalities are within the national coverage level. The highest coverage was achieved in the municipalities of Hani i Elezit, Istog, Mamusha, Theranda, and Dragash—which are above the threshold of the national coverage level—whereas the municipalities of Gjilan, Prishtina, Lipjan, Peja, and Fushë Kosova were below the national threshold and had the highest incidence of measles during the 2017–2019 outbreak.

Discussion

Our results showed that 74.5% (95% CI: 0.70%–0.88%) of participants enrolled in the study had positive titers of measles-specific IgG antibodies. We assessed the seroprevalence of measles-specific antibodies, the influence of demographic factors, including age and sex, on measles-specific IgG levels, MMR coverage, and the incidence of measles. Compared with the results of other studies,^(14,15) the seropositivity results in our study were lower and were within an 80–96% range, similar to rates observed in Poland.⁽¹⁶⁾ The lower ratio of seropositivity in our study was found in the 0–1.9-year age group, which was unvaccinated.

Sex is a well-known biological variable that influences vaccine-induced immune responses.⁽¹⁷⁾ Consistent with the findings of previous reports, female participants in this study cohort had higher levels of measles-specific IgG than male participants (Figure 1). Higher measles-specific IgG levels in females could be explained by a stronger initial humoral immune response to measles vaccines⁽¹⁸⁾ or a slower waning of measles immunity in females than in males.⁽¹⁹⁾ In contrast to the results of Shoho et al.,⁽²⁰⁾ in our study, we observed a higher titer of antibodies in the group vaccinated with two vaccines than in the group that received one dose of the MMR vaccine. The titer among participants in the 18–45-year age group was higher than reported in other studies⁽²¹⁾ and was similar to values reported in studies conducted in Italy⁽²²⁾ and the Czech Republic.⁽²³⁾ Vaccination coverage with MMR in Kosovo from 2012 to 2019 was 95.2% and declined by 5% during the COVID-19 pandemic. The incidence of measles was 0.89 per 100,000 inhabitants during the 2017–2019 outbreak. Measles outbreaks mainly occur in unvaccinated or under-vaccinated populations. Vaccine failure and waning immunity may be contributing factors to measles outbreaks in the immunized population.⁽²⁴⁾ A threshold of 93–95% is needed to stop measles transmission.⁽²⁵⁻²⁶⁾

Conclusion

The population immunity level in Kosovo may still be below the criteria required for achieving eradication, and further population immunity is required. To keep measles under control, we must establish a high level of herd immunity, prevent and control the transmission of measles, and reduce infectious sources. An important measure is to encourage vaccination among family members of children to protect vulnerable infants from infection. Our study impacts public health by providing evidence of the low seroprevalence of measles in the population. Therefore, results could have implications for achieving the goal of measles elimination. Furthermore, low measles seroprevalence indicates the need to monitor routine immunization practices, especially vaccine storage and cold chain maintenance—processes that may lead to low serologic responses. Our findings highlight a low level of measles seroprevalence and suggest a high risk of measles outbreaks. Results further indicate the likely need to reevaluate the MMR vaccination program in Kosovo to increase herd immunity.

Acknowledgments

We thank Anahid Pinchis from Edanz (www.edanz.com/ac) for editing a draft of this manuscript.

Competing Interests

The author declares that there is no conflict of interest in this work.

References

1. WHO. History of the Measles Vaccine. Available from: <https://www.who.int/news-room/spotlight/history-of-vaccination/history-of-measles-vaccination>
2. World Health Organization (WHO). Measles fact sheet N286. Geneva: WHO; November 2015 [updated 2016 Mar].
3. Dixon MG, Ferrari M, Antoni S, Li X, Portnoy A, Lambert B, Hauryski S, Hatcher C, Nedelec Y, Patel M, Alexander JP Jr, Steulet C, Gacic-Dobo M, Rota PA, Mulders MN, Bose AS, Rosewell A, Kretsinger K, Crowcroft NS. Progress Toward Regional Measles Elimination - Worldwide, 2000-2020. *MMWR Morb Mortal Wkly Rep.* 2021 Nov 12;70(45):1563-1569. doi: 10.15585/mmwr.mm7045a1.
4. Schenk J, Abrams S, Theeten H, Van Damme P, Beutels P, Hens N. Immunogenicity and persistence of trivalent measles, mumps, and rubella vaccines: a systematic review and meta-analysis. *Lancet Infect Dis.* 2021 Feb;21(2):286-295. doi: 10.1016/S1473-3099(20)30442-4.
5. Nelson R. COVID-19 disrupts vaccine delivery. *Lancet Infect Dis.* 2020 May;20(5):546. doi: 10.1016/S1473-3099(20)30304-2.
6. Durrheim DN, Andrus JK, Tabassum S, Bashour H, Githanga D, Pfaff G. A dangerous measles future looms beyond the COVID-19 pandemic. *Nat Med.* 2021 Mar;27(3):360-361. doi: 10.1038/s41591-021-01237-5.
7. Orenstein WA, Hinman A, Nkowane B, Olive JM, Reingold A. Measles and Rubella Global Strategic Plan 2012-2020 midterm review. *Vaccine.* 2018 Jan 11;36 Suppl 1:A1-A34. doi: 10.1016/j.vaccine.2017.09.026.
8. World Health Organization Regional Office for Europe (2014) Eliminating measles and rubella. Framework for the verification process in the WHO European Region. Copenhagen, WHO Regional Office for Europe; 2014. Available from: https://www.euro.who.int/__data/assets/pdf_file/0009/247356/Eliminating-measles-and-rubella-Framework-for-the-verification-process-in-the-WHO-European-Region.pdf
9. Gidding HF, Quinn HE, Hueston L, Dwyer DE, McIntyre PB. Declining measles antibodies in the era of elimination: Australia's experience. *Vaccine.* 2018 Jan 25;36(4):507-513. doi: 10.1016/j.vaccine.2017.12.002.
10. National Institute of Public Health of Kosovo. [Communicable diseases in Kosovo, 2017. Annual report].
11. Kmietowicz Z. Measles: Europe sees record number of cases and 37 deaths so far this year. *BMJ.* 2018 Aug 20;362:k3596. doi: 10.1136/bmj.k3596.
12. Ligjet - Ministria e Shendetesise. Available from: <https://msh.rks-gov.net/sq/legjislacioni/ligjet/>
13. Kish L. A procedure for objective respondent selection

within the household. *Journal of the American Statistical Association*. 1949;44:92-115.

14. Poethko-Müller C, Mankertz A. Sero-epidemiology of measles-specific IgG antibodies and predictive factors for low or missing titres in a German population-based cross-sectional study in children and adolescents (KiGGS). *Vaccine*. 2011 Oct 19;29(45):7949-59. doi: 10.1016/j.vaccine.2011.08.081.

15. Gallone MS, Germinario C, Larocca A, Tafuri S. Long time immunogenicity of measles vaccine in the vaccination era: An open question. *Hum Vaccin Immunother*. 2017 Jan 2;13(1):117-119. doi: 10.1080/21645515.2016.1227519.

16. Holka J, Pawlak K, Ciepiela O. Seroprevalence of IgG antibodies against measles in a selected Polish population - do we need to be re-vaccinated? *Cent Eur J Immunol*. 2019;44(4):380-383. doi: 10.5114/ceji.2019.92789.

17. Klein SL, Flanagan KL. Sex differences in immune responses. *Nat Rev Immunol*. 2016 Oct;16(10):626-38. doi: 10.1038/nri.2016.90.

18. Quach HQ, Ovsyannikova IG, Grill DE, Warner ND, Poland GA, Kennedy RB. Seroprevalence of Measles Antibodies in a Highly MMR-Vaccinated Population. *Vaccines (Basel)*. 2022 Nov 3;10(11):1859. doi: 10.3390/vaccines10111859.

19. Kontio M, Jokinen S, Paunio M, Peltola H, Davidkin I. Waning antibody levels and avidity: implications for MMR vaccine-induced protection. *J Infect Dis*. 2012 Nov 15;206(10):1542-8. doi: 10.1093/infdis/jis568.

20. Shoho Y, Kimura T, Yanagawa Y, Saito A, Inoue T, Suto C, Tsunekawa K, Araki O, Nara M, Tokue Y, Murakami M. Vaccination Status and Antibody Titers against Rubella and

Measles among Japanese Female College Students Majoring in Childcare between 2015 and 2018. *Tohoku J Exp Med*. 2018 Oct;246(2):73-79. doi: 10.1620/tjem.246.73.

21. Bolotin S, Severini A, Hatchette T, McLachlan E, Savage R, Hughes SL, et al. Assessment of population immunity to measles in Ontario, Canada: a Canadian Immunization Research Network (CIRN) study. *Hum Vaccin Immunother*. 2019;15(12):2856-2864. doi: 10.1080/21645515.2019.1619402.

22. Anichini G, Gandolfo C, Fabrizi S, Miceli GB, Terrosi C, Gori Savellini G, Prathyumnann S, Orsi D, Battista G, Cusi MG. Seroprevalence to Measles Virus after Vaccination or Natural Infection in an Adult Population, in Italy. *Vaccines*. 2020; 8(1):66. doi: 10.3390/vaccines8010066

23. Tomášková H, Zelená H, Kloudová A, Tomášek I. Serological survey of measles immunity in the Czech Republic, 2013. *Cent Eur J Public Health*. 2018 Mar;26(1):22-27. doi: 10.21101/cejph.a5251.

24. Hayman DTS. Measles vaccination in an increasingly immunized and developed world. *Hum Vaccin Immunother*. 2019;15(1):28-33. doi: 10.1080/21645515.2018.1517074.

25. Funk S. Critical immunity thresholds for measles elimination. *Cmmid*. 2019. Available from: https://terrace.who.int/mediacentre/data/sage/SAGE_Docs_Ppt_Oct2017/10_session_measles_and_rubella/Oct2019_session10_Presentation3_measles_elimination.pdf

26. Zhang Z, Chen M, Wang Y, Li J, Li X, Lu L. Seroepidemiology of measles in Beijing, China: a cross-sectional study. *Hum Vaccin Immunother*. 2019;15(9):2112-2116. doi: 10.1080/21645515.2019.1581527.



Correlates of Satisfaction among Hospitalized Patients in Kosovo

Haxhi Kamberi^{1,2}, Naim Jerliu^{3,4*}, Genc Burazeri^{5,6}

¹Regional Hospital "Isa Grezda", Gjakova, Kosovo

²Faculty of Medicine, University of Gjakova "Fehmi Agani", Gjakova, Kosovo

³National Institute of Public Health of Kosovo, Prishtina, Kosovo

⁴Faculty of Medicine, University of Prishtina "Hasan Prishtina", Prishtina, Kosovo

⁵Department of Public Health, Faculty of Medicine, University of Medicine, Tirana, Albania

⁶Department of International Health, School of CAPHRI, Care and Public Health Research Institute, Maastricht, The Netherlands

Abstract

Background: The aim of our study was to assess selected sociodemographic correlates of satisfaction among hospitalized patients in Kosovo.

Methods and Results: A cross-sectional study was conducted in May-June 2022, including a representative sample of 508 hospitalized patients (58.1% women and 41.9% men) aged ≥ 18 years. A structured 19-item questionnaire about patient satisfaction with hospital services was used for data collection. Each item was measured on a Likert scale ranging from 1 (very satisfied) to 5 (very unsatisfied). A summary score was calculated for all 19 items related to the level of satisfaction among hospitalized patients ranging from 19 (highest level of satisfaction) to 95 (lowest level of satisfaction). Binary logistic regression was used to assess the association of the summary score of satisfaction (19-item instrument, dichotomized in the analysis into "satisfied" vs. "unsatisfied" based on the median value of the summary score) with sociodemographic factors, general health status, and duration of hospitalization.

In multivariable-adjusted logistic regression models controlling in a backward stepwise procedure for all sociodemographic factors, health status, and duration of hospitalization, patients' dissatisfaction was significantly associated with urban residence (OR=1.52, 95%CI: 1.00-2.31), income level (OR_[low vs. high income]=2.44, 95%CI: 1.18-5.06) and health status (OR_[poor vs. good health]=7.95, 95%CI: 4.43-14.24).

Conclusion: Our findings point to a significantly higher dissatisfaction level among urban patients, low-income individuals, and patients with poor general health status. Healthcare providers and policymakers in Kosovo and other similar countries should be aware of the importance of continuous quality improvement of hospital services to increase, among other things, the satisfaction level of hospitalized patients. (**International Journal of Biomedicine. 2023;13(1):156-160.**)

Keywords: healthcare • hospitals • Kosovo • patient satisfaction

For citation: Kamberi H, Jerliu N, Burazeri G. Correlates of Satisfaction among Hospitalized Patients in Kosovo. International Journal of Biomedicine. 2023;13(1):156-160. doi:10.21103/Article13(1)_OA23

Introduction

Patient satisfaction is determined by the opinions of the patients regarding the overall experience of health care received from health professionals.⁽¹⁾ As such, patient

satisfaction is naturally connected with the quality of care provided by health professionals and the organizational environment of the concerned health institutions/facilities.^(2,3)

It has been convincingly argued that patient satisfaction influences adherence to treatment, utilization of health services, and general attitudes toward the healthcare system.⁽¹⁾ Furthermore, patient satisfaction provides valuable clues about medical care and is recognized as an important dimension of quality of care in hospital settings and beyond, also including such factors as communication and interaction with medical staff.⁽⁴⁻⁶⁾

*Corresponding author: Naim Jerliu, MD, PhD, Faculty of Medicine "Hasan Prishtina," University of Prishtina & National Institute of Public Health of Kosovo, Prishtina, Kosovo. E-mail: naim.jerliu@uni-pr.edu

Indeed, the manner in which the medical staff communicates with patients has a significant effect on patient satisfaction, by not applying a dominant position, being caring and committed to patients, and exhibiting positive attitudes – which all have a strong influence on the functioning of the relationship between health personnel and patients.^(7,8)

Kosovo is a small country in the Western Balkans that is still striving for international recognition almost 15 years after declaring its independence. Even with the ongoing profound reforms in the health sector, mainly aiming toward establishing a social health insurance system, the health status of the general population in Kosovo exhibits worse indicators than do members of the European Union.^(9,10) Current reforms in the health sector in Kosovo are also concerned with the hospital services, which absorb most of the health care funds. A previous report has documented a range of factors influencing patient satisfaction in hospital settings in Kosovo, including age, education, length of hospitalization, and related cost.⁽¹¹⁾ However, to date, there is no systematic documentation of patient satisfaction in hospital settings in Kosovo, particularly assessments based on a solid methodology, including representative samples of patients and standardized measuring instruments.

In this context, our aim was to assess selected sociodemographic correlates of satisfaction among hospitalized patients in Kosovo.

Methods

A cross-sectional study was conducted in May-June 2022, including a representative sample of hospitalized patients in the following three main regions of Kosovo (Gjakova, Peje, and Prizren). More specifically, our study included a consecutive sample of 520 patients aged ≥ 18 years who were hospitalized in the regional hospitals during the aforementioned period. The minimum sample size necessary for inclusion in this study was calculated as 476 patients, but we decided to approach 520 patients to account for potential non-response. Of 520 patients invited, 508 (97.7%) of them agreed to participate, and 295 (58.1%) were women.

The level of satisfaction of hospitalized patients was based on an adapted version of the EUROPEP instrument,⁽¹²⁾ which had been previously validated in the context of primary healthcare services in Kosovo.⁽¹³⁾ The adapted measuring instrument included 19 items inquiring about patient satisfaction with the following dimensions: availability of healthcare personnel, medical care received, attitudes of the healthcare personnel, and communication and interaction with the healthcare personnel. Each item of the instrument was measured on a Likert scale ranging from 1 (very satisfied) to 5 (very unsatisfied).

A summary score was calculated for all 19 items related to the level of satisfaction among hospitalized patients ranging from 19 (highest level of satisfaction) to 95 (lowest level of satisfaction). In the analysis, the summary score was dichotomized into “satisfied” vs. “unsatisfied” based on its median value.

Furthermore, information about demographic factors, general self-perceived health status, and duration of hospitalization was collected for all study participants.

Statistical analysis was performed using statistical software package SPSS version 19.0 (SPSS Inc, Armonk, NY: IBM Corp). Fisher’s exact test was used to compare differences in sociodemographic factors and general health status between patients who were satisfied and those who were unsatisfied with hospital services. Binary logistic regression was used to assess the association of the summary score of satisfaction (19-item instrument, dichotomized in the analysis into “satisfied” vs. “unsatisfied” based on the median value of the summary score) with sociodemographic factors, general health status, and duration of hospitalization. Initially, crude (unadjusted) odds ratios (ORs), their respective 95% confidence intervals (95% CIs), and P-values were calculated. Subsequently, all variables were entered in a backward stepwise procedure with a P-value to exit set at $P > 0.10$. Multivariable-adjusted ORs, their respective 95% CIs, and P-values were calculated for the variables retained in the final models. In all cases, a probability value of $P \leq 0.05$ was considered statistically significant.

The study was approved by the Ethics Commission and Council of the Faculty of Medicine, University of Gjakova.

Results

The mean age of the hospitalized patients included in this study was 45.4 ± 18.2 years (median age: 45 years; interquartile range: 28-60 years; range: 18-87 years). About two-thirds of participants resided in urban areas; the absolute majority (92%) were ethnic Albanians; 62% were currently married; 35% had 0-8 years of education; 44% were unemployed; 14% were poor, and one out of four participants reported a poor general health status irrespective of the condition leading to current hospitalization.

Female patients were more satisfied than males: 54% vs. 44%, respectively; $P=0.03$ (Table 1). Furthermore, the prevalence of satisfaction with hospital services was higher among the following categories: ethnic Albanians, compared to the other ethnic groups (51% vs. 35%, respectively; $P=0.06$); highly educated participants, compared especially with their low-educated counterparts (60% vs. 43%, respectively; $P=0.02$); employed vs. retired individuals (56% vs. 36%, respectively; $P=0.01$); high-income participants, compared to their low-income counterparts (67% vs. 23%, respectively; $P < 0.001$); and individuals who reported a good general health status, compared to those who said poor health status (73% vs. 21%, respectively; $P < 0.001$). Conversely, there were no significant differences in the satisfaction level of hospitalized patients depending on their marital status or place of residence (Table 1).

Table 2 presents the crude (unadjusted) and multivariable-adjusted association of the level of satisfaction (dichotomized into “satisfied” vs. “unsatisfied”) with sociodemographic factors, general health status, and duration of hospitalization among patients included in this study. In crude binary logistic regression models, patients’ dissatisfaction was significantly

related to the male gender (OR=1.48, 95%CI: 1.04-2.11), age (OR_[for an increment of 1 year]=1.02, 95%CI: 1.01-1.03), minority groupings (OR=1.96, 95%CI: 1.02-3.76), low education (OR=1.96, 95%CI: 1.23-3.13), retirement (OR=2.26, 95%CI: 1.34-3.81), low income (OR=7.0, 95%CI: 3.69-13.3), and poor general health status (OR=10.26, 95%CI: 6.04-17.4). Conversely, there was no significant association with marital status or place of residence, notwithstanding the higher odds of dissatisfaction among urban residents, compared with their rural counterparts.

In multivariable-adjusted logistic regression models controlling in a backward stepwise procedure for all sociodemographic factors, health status, and duration of hospitalization, patients' dissatisfaction was significantly associated with urban residence (OR=1.52, 95%CI: 1.00-2.31), income level (OR_[low vs. high income]=2.44, 95%CI: 1.18-5.06) and general health status (OR_[poor vs. good health]=7.95, 95%CI: 4.43-14.24) (Table 2).

Table 1.

Distribution of the level of satisfaction by selected socio-demographic factors and health status in a sample of hospitalized patients in Kosovo (n=508)

Sociodemographic factors and general health status	Satisfied (n=253)	Unsatisfied (n=255)	P [†]
<u>Gender</u>			
Men	94 (44.1)*	119 (55.9)	0.031
Women	159 (53.9)	136 (46.1)	
<u>Place of residence</u>			
Urban areas	160 (48.0)	173 (52.0)	0.305
Rural areas	93 (53.1)	82 (46.9)	
<u>Marital status</u>			
Not married	95 (48.5)	101 (51.5)	0.649
Married	158 (50.6)	154 (49.4)	
<u>Ethnicity</u>			
Other ethnic groups	15 (34.9)	28 (65.1)	0.055
Albanian	238 (51.2)	227 (48.8)	
<u>Education level</u>			
Low	76 (43.2)	100 (56.8)	0.018
Middle	103 (49.3)	106 (50.7)	
High	73 (59.8)	49 (40.2)	
<u>Employment</u>			
Employed	109 (55.6)	87 (44.4)	0.008
Unemployed	112 (50.0)	112 (50.0)	
Retired	31 (35.6)	56 (64.4)	
<u>Income level</u>			
High	116 (67.1)	57 (32.9)	<0.001
Average	121 (45.8)	143 (54.2)	
Low	16 (22.5)	55 (77.5)	
<u>Health status</u>			
Good	154 (73.3)	56 (26.7)	<0.001
Average	73 (41.7)	102 (58.3)	
Poor	26 (21.1)	97 (78.9)	

* Absolute numbers and row percentages (in parenthesis).

† P-values from Fisher's exact test.

Table 2.

Association of patients' dissatisfaction with sociodemographic factors, general health status, and duration of hospitalization: results from binary logistic regression.

Variable	Unadjusted models*			Multivariable-adjusted models [†]		
	OR	95%CI	P	OR	95%CI	P
<u>Gender</u>						
Men	1.48	1.04-2.11	0.030			
Women	1.00	Reference				
Age (years)	1.02	1.01-1.03	<0.001			
<u>Place of residence</u>						
Urban areas	1.23	0.85-1.77	0.275	1.52	1.00-2.31	0.049
Rural areas	1.00	Reference		1.00	Reference	
<u>Marital status</u>						
Not married	1.09	0.76-1.56	0.634			
Married	1.00	Reference				
<u>Ethnicity</u>						
Other ethnic groups	1.96	1.02-3.76	0.044			
Albanian	1.00	Reference				
<u>Education level</u>			0.019(2) [‡]			
Low	1.96	1.23-3.13	0.005			
Middle	1.53	0.98-2.41	0.064			
High	1.00	Reference	-			
<u>Employment</u>			0.009(2)			
Unemployed	1.25	0.85-1.84	0.251			
Retired	2.26	1.34-3.81	0.002			
Employed	1.00	Reference	-			
<u>Income level</u>			<0.001(2)			0.025(2)
Low	7.00	3.69-13.3	<0.001	2.44	1.18-5.06	0.017
Average	2.41	1.61-3.58	<0.001	1.64	1.05-2.57	0.029
High	1.00	Reference	-	1.00	Reference	-
<u>Health status</u>			<0.001(2)			<0.001(2)
Poor	10.26	6.04-17.4	<0.001	7.95	4.43-14.24	<0.001
Average	3.84	2.50-5.90	<0.001	3.15	2.00-4.97	<0.001
Good	1.00	Reference	-	1.00	Reference	-
Duration of hospitalization (days)	1.03	0.99-1.08	0.121			

* Odds ratios (OR: "unsatisfied" vs. "satisfied"), 95%CI and P-values from binary logistic regression. Range of the summary score (dichotomized into satisfied vs. unsatisfied based on its median value) was from 19 (the highest level of satisfaction) to 95 (the lowest level of satisfaction among hospitalized patients).

† All variables presented in the table were entered in a backward stepwise model with a P-value to exit set at P>0.10. Empty cells represent the variables removed from the final model.

‡ Overall P-value and degrees of freedom (in parentheses).

Discussion

The main findings of our study consist of a significantly lower satisfaction level among patients residing in urban areas, individuals with low socioeconomic status, and those who perceived their general health status as poor irrespective of

their current hospitalization. The associations of dissatisfaction with the place of residence and especially with income level and general health status were strong and persisted upon adjustment for a range of other sociodemographic characteristics, including age, gender, educational attainment, employment, ethnicity, and marital status—even after controlling for length of the current episode of hospitalization.

A previous study conducted in Kosovo reported a significant association between satisfaction level and education,⁽¹¹⁾ whereas, in our study, income level was a more powerful predictor than educational attainment. In a study by AA conducted in Kosovo,⁽¹¹⁾ length of hospitalization was reported as a significant determinant of patient satisfaction, a finding which was not evident in our study, even in crude (unadjusted) analysis. Our study included patients admitted to public hospitals, whereas a previous study carried out in Kosovo included patients admitted to both public and private hospitals.⁽¹¹⁾ Therefore, a comparison of the findings between these two studies should be made with caution, because sociodemographic characteristics of the patients admitted to public hospitals in Kosovo may differ from those hospitalized in private facilities.

A study conducted in Spain⁽¹⁴⁾ reported an association of patient satisfaction with age, education level, marital status, sex, and length of hospitalization. Conversely, in our study, none of these factors was significantly related to patient satisfaction in multivariable-adjusted analyses. Instead, low income was strongly associated with patient dissatisfaction in our study. However, the Spanish study did not find any significant association with employment status.

A study conducted in Serbia⁽¹⁵⁾ has not provided information about the association of patient satisfaction with sociodemographic factors but has reported on the most influential institutional/organizational factors for patient satisfaction, that is, the admission process, doctor care, staff care, and technology tools.

In crude (unadjusted) models, age was significantly related to satisfaction level in our study, but in the opposite direction to previous reports from other studies conducted elsewhere.^(16,17) Hence, some previous studies have evidenced a higher satisfaction level among older patients, whereas we found an inverse association which, nevertheless, disappeared upon adjustment for other sociodemographic characteristics.

We found a higher satisfaction level among women, a finding compatible with a previous study,⁽¹⁶⁾ whereas some other studies have reported an opposite finding.^(14,18,19) Our finding about a higher satisfaction level among rural residents is interesting. Rural patients may report a higher satisfaction level due to their lower expectations, whereas urban residents may have much higher expectations of medical encounters. However, the finding on urban/rural differences in satisfaction levels requires further replication in future studies in Kosovo and other similar settings.

In any case, our study may be prone to several limitations related to sample representativeness, the possibility of information bias, and study design. Our study included a sample of patients pertinent to three regional hospitals in Kosovo; therefore, findings from this study may

not be generalizable to all hospitals in Kosovo. The instrument we used to assess satisfaction level has been previously validated in primary healthcare settings in Kosovo.⁽¹³⁾ Still, the possibility of information bias cannot be excluded, as hospitalized patients may differ from primary healthcare users. Furthermore, associations observed in cross-sectional studies do not imply causality.

Irrespective of the aforementioned potential limitations, our study provides useful evidence about important sociodemographic correlates of dissatisfaction among hospitalized patients in Kosovo. Our findings point to a significantly higher dissatisfaction level among urban patients, low-income individuals, and patients with poor general health status. Healthcare providers and policymakers in Kosovo and other similar countries should be aware of the importance of continuous quality improvement of hospital services to increase, among other things, the satisfaction level of hospitalized patients.

Competing Interests

The authors declare that they have no competing interests.

References

1. Feleke AA, Demise YA, Garede MG. Patient Satisfaction and Associated Factors on In-patient Nursing Service at Public Hospitals of Dawro zone, Southern Ethiopia. *Int J Car Sci*. 2020;13(2):1411-20.
2. Molla M, Berhe A, Shumye A, Adama J. Assessment of adult patients satisfaction and associated factors with nursing care in Black Lion Hospital, Ethiopia; institutional based cross sectional study. *International Journal of Nursing and Midwifery*. 2014;6(4):49-57.
3. Woldeyohanes TR, Woldehaimanot TE, Kerie MW, Mengistie MA, Yesuf EA. Perceived patient satisfaction with in-patient services at Jimma University Specialized Hospital, Southwest Ethiopia. *BMC Res Notes*. 2015 Jul 1;8:285. doi: 10.1186/s13104-015-1179-8. PMID: 26126658; PMCID: PMC4487793.
4. Schoenfelder T, Klewer J, Kugler J. Determinants of patient satisfaction: a study among 39 hospitals in an in-patient setting in Germany. *Int J Qual Health Care*. 2011 Oct;23(5):503-9. doi: 10.1093/intqhc/mzr038. Epub 2011 Jun 29. PMID: 21715557.
5. Manary MP, Boulding W, Staelin R, Glickman SW. The patient experience and health outcomes. *N Engl J Med*. 2013 Jan 17;368(3):201-3. doi: 10.1056/NEJMp1211775. Epub 2012 Dec 26. PMID: 23268647.
6. Doyle C, Lennox L, Bell D. A systematic review of evidence on the links between patient experience and clinical safety and effectiveness. *BMJ Open*. 2013 Jan 3;3(1):e001570. doi: 10.1136/bmjopen-2012-001570. PMID: 23293244; PMCID: PMC3549241.
7. Schmid Mast M, Hall JA, Roter DL. Disentangling physician sex and physician communication style: their effects on patient satisfaction in a virtual medical visit. *Patient Educ Couns*. 2007 Sep;68(1):16-22. doi: 10.1016/j.pec.2007.03.020. Epub 2007 May 4. PMID: 17482418.

8. Schmid Mast M, Hall JA, Roter DL. Caring and dominance affect participants' perceptions and behaviors during a virtual medical visit. *J Gen Intern Med.* 2008 May;23(5):523-7. doi: 10.1007/s11606-008-0512-5. Epub 2008 Feb 8. PMID: 18259824; PMCID: PMC2324145.
 9. The World Bank. Life expectancy at birth in Kosovo. <https://data.worldbank.org/indicator/SP.DYN.LE00.IN?locations=XK> (accessed: 30 November, 2022).
 10. Agency of Statistics, Republic of Kosovo. Health statistics, 2020. Pristina, 2021. <https://ask.rks-gov.net/media/6320/statistikat-e-shendetesise-2020.pdf> (accessed: 30 November, 2022).
 11. Hoxha R, Kosevska E, Berisha M, Ramadani N, Jerliu N, Zhjeqi V, Gashi S. Predictive factors for patient satisfaction in public and private hospitals in Kosovo. *SEEJPH.* 2019;12(1). Doi: 10.4119/seejph-2362
 12. Wensing M. Europep 2006. Revised Europep instrument and user manual; 2006. <https://www.yumpu.com/en/document/view/20032561/europep-2006-topas-europe> (accessed: 30 November, 2022).
 13. Kamberi H, Tanushi V, Kadrija M, Kamberi S, Jerliu N. Level of satisfaction and socio-demographic correlates among users of primary health care services in Kosovo. *SEEJPH.* 2022. doi: 10.11576/seejph-5922.
 14. Quintana JM, González N, Bilbao A, Aizpuru F, Escobar A, Esteban C, San-Sebastián JA, de-la-Sierra E, Thompson A. Predictors of patient satisfaction with hospital health care. *BMC Health Serv Res.* 2006 Aug 16;6:102. doi: 10.1186/1472-6963-6-102. PMID: 16914046; PMCID: PMC1579213.
 15. Damnjanović V, Janičić R, Jovanović V. Factors affecting patient satisfaction in the health care sector in Serbia. *Srp Arh Celok Lek.* 2018;146(9-10):506-11.
 16. Hargraves JL, Wilson IB, Zaslavsky A, James C, Walker JD, Rogers G, Cleary PD. Adjusting for patient characteristics when analyzing reports from patients about hospital care. *Med Care.* 2001 Jun;39(6):635-41. doi: 10.1097/00005650-200106000-00011. PMID: 11404646.
 17. Jaipaul CK, Rosenthal GE. Are older patients more satisfied with hospital care than younger patients? *J Gen Intern Med.* 2003 Jan;18(1):23-30. doi: 10.1046/j.1525-1497.2003.20114.x. PMID: 12534760; PMCID: PMC1494807.
 18. Nguyen Thi PL, Briçon S, Empereur F, Guillemin F. Factors determining inpatient satisfaction with care. *Soc Sci Med.* 2002 Feb;54(4):493-504. doi: 10.1016/s0277-9536(01)00045-4. PMID: 11848270.
 19. Crow R, Gage H, Hampson S, Hart J, Kimber A, Storey L, Thomas H. The measurement of satisfaction with healthcare: implications for practice from a systematic review of the literature. *Health Technol Assess.* 2002;6(32):1-244. doi: 10.3310/hta6320. PMID: 12925269.
-

Knowledge, Attitude, and Perception Among the Dental Students During the COVID-19 Pandemic in Kosovo

Vlorë Hysenaj Cakolli¹, Valë Hysenaj Hoxha², Valbona Ferizi³, Lulëjeta Ferizi Shabani^{4,5*}

¹Department of Periodontology Alma Mater Europaea, Campus College “Rezonanca”, Prishtina, Republic of Kosovo

²Department of Pediatric and Preventive Dentistry, School of Dental Medicine, University of Prishtina, Prishtina, Republic of Kosovo

³Obstetrics and Gynecology Clinic, University Clinical Center of Kosovo, Prishtina, Republic of Kosovo

⁴Department of Pediatric Dentistry Alma Mater Europaea, Campus College “Rezonanca”, Prishtina, Republic of Kosovo

⁵Department of Pediatric and Preventive Dentistry, University Dentistry Clinical Center of Kosovo, Prishtina, Republic of Kosovo

Abstract

Background: The current pandemic of the coronavirus disease COVID-19 has affected almost all countries of the world. Dental students are exposed to a high risk of contracting COVID-19 due to direct contact with patients. Thus, the objectives of this study were to determine the knowledge, perceived risk, and preventive behaviors regarding COVID-19.

Methods and Results: A total of 157 dental students from the first to the fifth year of studies, regardless of gender, were included in this cross-sectional study. Data were collected using a questionnaire distributed to dental students at the College to ensure unbiased responses. The questionnaire, based on information provided by WHO and the CDC on SARS-CoV-2 and COVID-19, contains sociodemographic questions and 19 questions exploring knowledge about the definition, symptoms, source of infection, routes of transmission, treatment, vaccination, and stress related to COVID-19.

Most of the dental students recognized the acronym COVID-19 (51%) and knew all the symptoms of the disease (62.4%), as well as the way of transmission (100.0%). Moreover, 85.4% of them had a lot of knowledge about the preventive measures against COVID-19, and 99.4% thought that dentists were a group at risk of infection. About 64.3% of students had been infected with COVID-19, but most of them (63.5%) were treated only with vitamins and paracetamol. Regarding vaccination, 94.9% of dental students were vaccinated: 75.8% of them had received two doses of the vaccine, 13.4% of them three doses, while 6.4% had received only one dose. A small percentage were not vaccinated at all (5.1%), and the reason for this was their allergies and fear of vaccines (37.5%). Nevertheless, several dental students felt that they did not have enough information about the vaccine and its safety (34.4%). The pandemic affected the depression of 49.0% of dental students, and a large percentage of them felt tired of the continued news about COVID-19 (91.7%).

Conclusion: The findings show a very high number of dental students who had good knowledge about the COVID-19 pandemic. However, we recommend informing and educating dental students about the COVID-19 pandemic and the importance of vaccination, but also about mental health care. (*International Journal of Biomedicine*. 2023;13(1):161-167.)

Keywords: COVID-19 • knowledge • attitude • dental students

For citation: Cakolli VH, Hoxha VH, Ferizi V, Shabani LF. Knowledge, Attitude, and Perception Among the Dental Students During the COVID-19 Pandemic in Kosovo. *International Journal of Biomedicine*. 2023;13(1):161-167. doi:10.21103/Article13(1)_OA24

Abbreviations

COVID-19, coronavirus disease of 2019; **CDC**, Centers for Disease Control and Prevention; **PPE**, personal protective equipment; **SARS-Cov-2**, severe acute respiratory syndrome coronavirus 2; **WHO**, World Health Organization.

Introduction

The coronavirus (COVID-19) infection spread completely around the world, and authorities in 227 countries and territories have reported about 666.9 million Covid19 cases and 6.7 million deaths since China reported its first cases to the WHO in December 2019.⁽¹⁾ Within a week of the disease's appearance, over 107 nations around the world had closed all schools, affecting the lives of more than 862 million students around the world.⁽²⁾

The COVID-19 pandemic and the various measures introduced to slow its spread have significantly affected the day-to-day lifestyle and mental well-being of the general public; however, many higher education students have found themselves in a unique situation, perhaps isolated in a household with others they do not know well.⁽³⁾

The impact of COVID-19 on the dental community is evident. Dental education programs and academic activities have also suffered from the ramifications of the pandemic.⁽⁴⁾ Students face an increasingly uncertain environment, where financial and health shocks (for example, lack of resources to complete their studies or fear of becoming seriously ill), along with the transition to online learning, may have affected their academic performance, educational plans, current labor market participation, and expectations about future employment.⁽⁵⁾

Students have been impacted by the COVID-19 pandemic in multiple ways: threats to their own and their family's health, the closure of schools and pivoting to online learning, a long summer of physical distancing, and then the challenge of returning to school in the fall of 2020.⁽⁶⁾

Since dentistry students are in close contact with people affected during this pandemic, they must have sufficient knowledge of COVID-19, and it is believed that this will affect their preventive behaviors.⁽⁷⁾ When the first case of COVID-19 in Kosovo was announced in March 2020, dental students had insufficient awareness, and they did not have sufficient knowledge of this viral infection. This knowledge involves using all barriers, such as facemasks, eye protection with lateral shields, and protective clothing, adequate disinfection of clinical premises, and proper sterilization of the dental equipment and instruments.^(8,9)

The high prevalence of anxiety, fear, stress, and depressive symptoms among the students might be due to the disruption created by the COVID-19 pandemic in their academic life. This sudden disruption has a long-term effect on their future career, health, and personal life.⁽¹⁰⁾

This current study is directed toward determining the level of knowledge, attitude, and perception among dental students during the COVID-19 pandemic.

Materials and Methods

Study Design and Sampling Procedures

A cross-sectional study was conducted in a sample of dental students (n=157) attending Alma Mater Europaea, Campus College "Rezonanca" (Pristina, Kosovo) to investigate the perceptions of the students regarding theoretical knowledge and stress as a result of the COVID-19 pandemic. Therefore,

students were invited to participate anonymously in completing a questionnaire between October 2022 and November 2022, after the start of work at the College after the COVID-19 pandemic. Regarding the gender distribution, 81(51.6%) were females and 76(48.4%) were males. Students' distribution per year of studies was as follows: the first year 38(24.2%), the second year 29(18.5%), the third year 31(19.7%), the fourth year 34(21.7%), and the fifth year 25(15.9%).

Data Collection and Ethical Considerations

Data were collected using a questionnaire distributed to dental students at the College to ensure unbiased responses. The questionnaire, based on information provided by WHO and the CDC on SARS-CoV-2 and COVID-19, contains sociodemographic questions and 19 questions exploring knowledge about the definition, symptoms, source of infection, routes of transmission, treatment, vaccination, and stress related to COVID-19.

Before answering the questions, the respondents were informed that their participation in the questionnaire survey was voluntary and anonymous. Ethical approval of the study was obtained from the Ethic Committee of the Alma Mater Europaea, Campus College "Rezonanca," Prishtina, Kosovo (AD-4012/22,12.07.2022). Completing and submitting the questionnaire was considered to be a student's informed consent to participate in this study.

Survey Instrument

The questionnaire was constructed in Albanian for the present study and then translated into English. For the English version, a pilot study was conducted on ten dental students to test the questionnaire to ensure both the understanding of the meaning of the questions and the accuracy of their translation into English.

A face-to-face validation was conducted by asking ten dental students to answer the questionnaire. This phase was conducted to test and judge the items of the study instrument in terms of clarity of wording, readability, and likelihood of respondents answering the questions. The questionnaire was edited accordingly after the face-to-face validation. A pilot study was then carried out among 20 dental students as a preliminary analysis to evaluate the reliability of the questionnaire using Cronbach's alpha.

The questionnaires were divided into four sections and had a total of 19 questions. The first section contained demographic details like gender, age group, areas, and years of studies. Sections 2, 3, and 4 assessed the dental students' general knowledge about COVID-19 (7 questions; Q1-Q7), knowledge of whether they had been affected by COVID-19, diagnosis, treatment, and vaccination doses (9 questions; Q8-Q16), and information about the stress they had due to COVID-19 (3 questions; Q17-Q19).

The inclusion criteria for this study were dental students in the private College of Alma Mater Europaea Campus College "Rezonanca". The exclusion criteria were respondents who submitted incomplete survey questionnaires or denied consent to participate.

Statistical analysis was performed using Microsoft Excel (MS Office 2010 Microsoft Corp., Redmond, WA, USA) and statistical software package SPSS version 21.0 (SPSS Inc,

Armonk, NY: IBM Corp). Baseline characteristics were summarized as frequencies and percentages for categorical variables. Group comparisons were performed using chi-square tests or, alternatively, Fisher's exact test. A probability value of $P < 0.05$ was considered statistically significant.

Results

Sociodemographic Data

Of all the students, 72(45.9%) belonged to the age group of 19-20 years, 60(38.2%) to the age group of 21-22 years, 17(10.8%) to the age group of 23-24 years, while only 8(5.1%) students were over 25 years old. According to the residents, 128(81.5%) of the students were from urban areas, and 29(18.5%) of the students were from rural areas. Students' distribution per year of studies is presented in Table 1.

Table 1.

Sociodemographic characteristics of dental students.

Variables	n	%
Gender		
F	81	51.6
M	76	48.4
Age group		
19-20	72	45.9
21-22	60	38.2
23-24	17	10.8
25 +	8	5.1
Area		
Urban	128	81.5
Rural	29	18.5
Year of studies		
1	38	24.2
2	29	18.5
3	31	19.7
4	34	21.7
5	25	15.9
Total	157	100.0

Dental Students' Knowledge of Covid-19

The students' knowledge about COVID-19 is presented in Table 2. In all the questions asked, it is apparent that the students gave correct answers. Only one student did not know what the acronym COVID-19 was, while the majority of students (51.0%) were aware that the acronym COVID-19 represents coronavirus, a disease caused by an influenza virus, or a disease caused by SARS-CoV-2 ($P < 0.0001$) (Table 2).

About 62.4% of respondents were able to identify all of the possible symptoms of COVID-19 infection at the time the study was conducted. Most of the participants considered respiratory complications in the lungs (19.1%) and temperature and cough (18.5%) as important symptoms of the disease ($P < 0.0001$).

All participants gave correct answers regarding the fact that COVID-19 is a contagious disease and transmitted from the infected person to other individuals, whereas 85.4% thought that effective preventive measures were washing hands with an alcohol-based disinfectant, wearing a mask, and avoiding social contacts ($P < 0.0001$).

Table 2.

Dental students' knowledge of COVID-19.

Variables	n	%	P-value
Q1. What do you identify with the acronym COVID-19?			
A coronavirus	26	16.6	<0.0001
Disease caused by an influenza virus	4	2.5	
Disease caused by SARS-CoV-2	46	29.3	
All previous answers are correct	80	51.0	
I do not know	1	0.6	
Q2. What are the symptoms of COVID-19?			
Temperature and cough	29	18.5	<0.0001
Gastrointestinal symptoms	0	0.0	
Respiratory complications in the lungs	30	19.1	
All previous answers are correct	98	62.4	
I do not know	0	0.0	
Q3. Is COVID-19 a contagious disease?			
Yes	157	100.0	NA
No	0	0.0	
I do not know	0	0.0	
Q4. How is COVID-19 transmitted?			
From the infected person to others	157	100.0	NA
Through contact with domestic animals	0	0.0	
Through food	0	0.0	
I do not know	0	0.0	
Q5. Which of these measures prevents the spread of the virus?			
Washing hands with an alcohol-based disinfectant	3	1.9	<0.0001
Wearing a mask	14	8.9	
Avoiding social contacts	5	3.2	
All previous answers are correct	134	85.4	
I do not know	1	0.6	
Q6. Currently, how can patients be treated?			
According to the doctor's instructions	118	75.2	<0.0001
With antibiotics	3	1.9	
With antivirals	2	1.3	
Vaccinations	34	21.6	
I do not know	0	0.0	
Q7. Do you think that dentists are among the groups at risk of infection with COVID-19?			
Yes	156	99.4	<0.0001
No	1	0.6	
I do not know	0	0.0	

Regarding the treatment of COVID-19, the results show that the majority of students (75.2%) considered that the treatment should be based on the doctor's instructions, and only 1.3% thought that the treatment should be conducted by using antivirals ($P < 0.0001$).

However, regarding the fact that dentists are among the groups at risk of infection with COVID-19, 99.4% of dental students agreed ($P < 0.0001$).

Data Related to Infection, Diagnostic Method, Treatment and Vaccination of Dental Students

As shown in Table 3, about 64.3% of students had been infected with COVID-19 ($P < 0.0001$): while 39.6% of them were diagnosed by testing in a public hospital and 60.4% in a private clinic ($P = 0.0001$). Despite this, fortunately, the majority of students (62.4%) were treated only with vitamins and paracetamol ($P = 0.047$). More than half of the students expressed that they are not afraid of the Omicron variant. 94.9% were vaccinated against COVID-19: 75.8% received

two doses of the vaccine, 13.4% three doses, while 6.4% had only received one dose ($P<0.0001$). A small percentage of dental students (5.1%) were not vaccinated at all, and the reason for this is that they are allergic or afraid of the vaccine against COVID-19 (37.5%).

The majority of students did not know or estimate that vaccination would not be mandatory every 6 months (37.6%) and also agreed that they had sufficient information about the vaccine and its safety (49.0%) ($P<0.0001$).

Table 3.

Data related to infection, diagnosis method, treatment, and vaccination of dental students.

Variables	n	%	P-value
Q8. Have you been infected with COVID-19?			
Yes	101	64.3	<0.0001
No	56	35.7	
Q9. If you have been infected with COVID-19, where were you diagnosed?			0.0001
With a test in a public hospital	40	39.6	
With a test in a private clinic	61	60.4	
Q10. If you have had COVID-19, what have you been treated with?			0.047
I was hospitalized	3	3.0	
With antibiotics	19	18.8	
Only with vitamins and paracetamol	63	62.4	
I have not received any therapy	16	15.8	
Q11. Are you afraid of the Omicron variant of the COVID-19 virus?			<0.0001
Yes	27	17.2	
No	120	76.4	
I do not know	10	6.4	
Q12. Are you vaccinated against COVID-19?			<0.0001
Yes	149	94.9	
No	8	5.1	
Q13. If you are vaccinated, how many doses of the vaccine did you receive?			<0.0001
Just one dose	10	6.4	
Two doses	119	75.8	
Three doses	21	13.4	
No dose	7	4.5	
Q14. If you have never been vaccinated against COVID-19, why did you do this?			0.882
I'm allergic	3	37.5	
I am afraid of vaccines in general	2	25.0	
I am afraid of the vaccine against COVID-19	3	37.5	
Q15. Do you think that the vaccination will be done every 6 months, for a longer time (several years)?			<0.0001
Yes	39	24.8	
No	59	37.6	
I do not know	59	37.6	
Q16. Do you think you have enough information about the vaccines against COVID-19 and their safety?			<0.0001
Yes	77	49.0	
No	54	34.4	
I do not know	26	16.6	

Information Related to the Stress Dental Students Have Due to COVID-19

From the results given in Table 4, we could not find any significant difference regarding the depression of dental

students during the pandemic period. As can be seen, 49.0% of dental students had shown depressed behavior, while 51.0% denied that they felt depressed. Of all students surveyed, 91.7% were tired of hearing news about COVID-19, and 58.6% thought the world would not be the same because of the COVID-19 pandemic ($P<0.0001$).

Table 4.

Information related to the stress dental students have due to COVID-19.

Variables	n	%	P-value
Q17. Have you felt depressed due to isolation during the pandemic period?			0.811
Yes	77	49.0	
No	80	51.0	
Q18. Are you tired of the pandemic and hearing the news about COVID-19?			<0.0001
Yes	144	91.7	
No	13	8.3	
Q19. Do you think that the world will not be the same because of the COVID-19 pandemic?			<0.0001
Yes	92	58.6	
No	46	29.3	
I do not know	19	12.1	

Discussion

COVID-19 still poses a problem for dentists and all medical professionals because they are at persistent risk of infection. For this reason, it is very important that beginning with students, their knowledge about COVID-19 is constantly evaluated.

However, more than two years have passed since the world's population has been affected by COVID-19, so there are still not many studies that evaluate the knowledge of students regarding this disease. Dentistry students are future professionals; therefore, they should definitely have knowledge about the spread of pandemic diseases, because they are in direct contact with the oral cavity of patients, with dental materials and contaminated dental instruments, and in this way, can contribute to the spread of the pandemic disease.⁽¹¹⁾ Therefore, in this study, we analyzed dental students' knowledge of the novel coronavirus and identified gaps in current knowledge and misunderstanding among the dental student population.

Our study revealed encouraging results among dentistry students in Kosovo, where most of them had knowledge related to what COVID-19 is, its symptoms, way of transmission, and treatment. These results reveal that students actually demonstrated overall good knowledge of COVID-19. This finding is consistent with previous studies regarding students' knowledge of COVID-19.⁽¹¹⁻¹³⁾

Above all, it is important that dentists know the preventive measures against COVID-19. Most of the students in our research (85.4%) gave correct answers regarding preventive measures. The same results were presented by Khader Y et al.,⁽¹⁴⁾ who found that most dentists reported cleaning and disinfecting hands and surfaces that came into

contact with patients known to have COVID-19 or suspected of it, and wearing personal protective equipment (PPE) could help prevent transmission from patients with known or suspected COVID-19.

Dental healthcare workers are considered to be the frontline in the current pandemic.⁽¹⁵⁾ The main reason they are at risk is because of the proximity with the patient during the treatment when it is well known that the disease is also spread through respiratory droplets that we breathe through our nose and mouth.^(16,17) All students in our study agreed that dentists belong to the group of health professionals most at risk from COVID-19. Other authors have given the same opinion in their studies.^(15,18-20)

However, many measures have been used to prevent the transmission of COVID-19 in dental environments, starting from the use of PPE, ventilation of the dental environment after each patient, meticulous hand hygiene, and sterilization procedures aimed at deactivating, destroying or removing pathogens from any surface or instrument. In addition, patients complete screening questionnaires for COVID-19, and the patient's body temperature is measured before each visit to the dentist.⁽²¹⁾ While patients were treated only in urgent cases, and all patients with any symptoms consistent with COVID-19, with a positive test, or possible previous exposure were postponed for at least 2 weeks.⁽¹⁶⁾

In Kosovo, not only government hospitals but also numerous private clinics have the ability and license to perform laboratory diagnostics of COVID-19. According to the results of our study, a large percentage of students (64.3%) were infected with COVID-19, and the largest percentage were diagnosed in a private clinic (61.5%). Our results are higher than other studies regarding the infection of dental students with COVID-19.^(22,23) Fortunately, most of the dental students were treated only with symptomatic therapy. Infections among dental students were due to the nature of the dental practice, which exposes students to bodily fluids from the patient, including blood and saliva, and the way the virus is transmitted through contact with respiratory droplets from an infected individual.⁽²⁴⁾

After two years had passed since the pandemic was present in the world, the Omicron variant began to spread as a mutation of COVID-19. This variant was unknown, and cases increased dramatically, again causing travel restrictions to prevent transmission of the disease and fear among the world's population.^(25,26) Despite this, our study shows that most dental students were not afraid of the Omicron variant. This is probably related to what was said above that most students infected with COVID-19 were treated with symptomatic therapy, so they did not take the spread of a new variant of Omicron as a concern.

When working with patients, dentists and dental students must follow strict workplace protocols to prevent the spread of disease. Vaccination against COVID-19 remains the most valuable solution to this day. Although it has been documented that conspiracy beliefs and misconceptions about immunity have limited student acceptance of the vaccine, our study nevertheless shows a high vaccination rate among dental students (94.9%) with two doses of the vaccine. High results

regarding the vaccination of dental students were also given by Schmidt J. et al.,⁽²³⁾ where the vaccination rate among students was 93.8%, and 75.4% of respondents supported mandatory COVID-19 vaccination for healthcare professionals. Kateeb E et al.⁽²²⁾ found that 57.8% of dental students in Palestinian educational institutions were willing to be vaccinated against COVID-19 when it became available. On the other hand, a small number of dental students were not vaccinated, and the reasons for this were an allergy, fear of the vaccine against COVID-19 (42.8%), and lack of information about the vaccine (34.4%). Other studies also found that insufficient knowledge about vaccines was a predictor of COVID-19 vaccine hesitancy among healthcare workers globally.^(27,28)

The pandemic has impacted global communities in different ways. Besides the influence on physical health, it also affects people psychologically because of the risk of developing pandemic fatigue.⁽²⁹⁾ Most of the dental students in our study did not indicate that they felt depressed due to isolation during the COVID-19 pandemic (51%), although a slightly lower percentage admitted that isolation during the pandemic had caused them depression (49.0%). On the other hand, almost all dental students were tired of constantly hearing news about the pandemic, and they thought that the world would not be the same because of it. Our results are similar to a study by Ali S et al.⁽³⁰⁾ regarding the dental students being tired of hearing about COVID-19.

The main strength of the current study is that this is the first study conducted among dental students in Kosovo regarding knowledge of the COVID-19 pandemic. Therefore, the knowledge obtained from this study is important for public health and for preventive measures that public and private faculties should implement. Another strong point of this study is that it shows dental students' knowledge of the COVID-19 pandemic is quite high, indicating dental professionals' knowledge about preventive measures against it.

This study also has some limitations. First, this study is limited to only private dental college students. Second, the sample size is relatively small, and the results are not generalizable to other private and public dental colleges. Therefore, it is recommended that further studies be conducted using larger samples in different dental and medical educational institutions in Kosovo.

Conclusion

The current investigation found that most of the dental students in Kosovo had good knowledge about the etiology and way of transmission, clinical features, treatment modalities, and dental preventive measures against COVID-19. Most students knew that vaccination was the best method to prevent the spread of the pandemic. However, some students hesitated in this direction due to their lack of knowledge about the vaccine. Also, dental students showed fatigue from the amount of information related to COVID-19.

We recommend using this opportunity to educate students further to widen their knowledge not only about preventing the spread of the pandemic but also about the importance of vaccination against COVID-19.

Competing Interests

The author declares that there is no conflict of interest in this work.

References

- World Health Organization. Coronavirus disease (COVID-19) pandemic. Available at: <https://www.who.int/emergencies/diseases/novel-coronavirus-2019>
- Armstrong-Mensah E, Ramsey-White K, Yankey B, Self-Brown S. COVID-19 and Distance Learning: Effects on Georgia State University School of Public Health Students. *Front Public Health*. 2020 Sep 25;8:576227. doi: 10.3389/fpubh.2020.576227.
- Dong Q, Kuria A, Weng Y, Liu Y, Cao Y. Impacts of the COVID-19 epidemic on the department of stomatology in a tertiary hospital: A case study in the General Hospital of the Central Theater Command, Wuhan, China. *Community Dent Oral Epidemiol*. 2021 Dec;49(6):557-564. doi: 10.1111/cdoe.12680.
- Meng L, Hua F, Bian Z. Coronavirus Disease 2019 (COVID-19): Emerging and Future Challenges for Dental and Oral Medicine. *J Dent Res*. 2020 May;99(5):481-487. doi: 10.1177/0022034520914246.
- Nahar Z, Sohan M, Supti KF, Hossain MJ, Shahriar M, Bhuiyan MA, Islam MR. Prevalence and associated risk factors for mental health problems among female university students during COVID-19 pandemic: A cross-sectional study findings from Dhaka, Bangladesh. *Heliyon*. 2022 Oct;8(10):e10890. doi: 10.1016/j.heliyon.2022.e10890.
- Schwartz KD, Exner-Cortens D, McMorris CA, Makarenko E, Arnold P, Van Bavel M, Williams S, Canfield R. COVID-19 and Student Well-Being: Stress and Mental Health during Return-to-School. *Can J Sch Psychol*. 2021 Jun;36(2):166-85. doi: 10.1177/08295735211001653.
- Wee EG, Giri MS, Sundram TK, Venudran CV. COVID-19: Knowledge, attitude and preventive behaviors of medical and dental students. *Int J Biomed Clin Sci*. 2020;5:236–56. doi: 10.13140/RG.2.2.28763.18722
- Almulhim B, Alassaf A, Alghamdi S, Alroomy R, Aldhuwayhi S, Aljabr A, Mallineni SK. Dentistry Amidst the COVID-19 Pandemic: Knowledge, Attitude, and Practices Among the Saudi Arabian Dental Students. *Front Med (Lausanne)*. 2021 Apr 7;8:654524. doi: 10.3389/fmed.2021.654524
- Tian Z, Stedman M, Whyte M, Anderson SG, Thomson G, Heald A. Personal protective equipment (PPE) and infection among healthcare workers - What is the evidence? *Int J Clin Pract*. 2020 Nov;74(11):e13617. doi: 10.1111/ijcp.13617.
- Patsali ME, Mousa DV, Papadopoulou EVK, Papadopoulou KKK, Kaparounaki CK, Diakogiannis I, Fountoulakis KN. University students' changes in mental health status and determinants of behavior during the COVID-19 lockdown in Greece. *Psychiatry Res*. 2020 Oct;292:113298. doi: 10.1016/j.psychres.2020.113298.
- Karaaslan F, Dikilitaş A, Aydin EÖ. Comparison of COVID-19 relevant knowledge and attitudes of clinical and preclinical dental students in Turkey. *Balkan J Dent Med*. 2020;24(3):127-33. doi: 10.2478/bjdm-2020-0021.
- Umezudike KA, Isiekwe IG, Fadeju AD, Akinboboye BO, Aladenika ET. Nigerian undergraduate dental students' knowledge, perception, and attitude to COVID-19 and infection control practices. *J Dent Educ*. 2021 Feb;85(2):187-196. doi: 10.1002/jdd.12423.
- Peng Y, Pei C, Zheng Y, Wang J, Zhang K, Zheng Z, Zhu P. A cross-sectional survey of knowledge, attitude and practice associated with COVID-19 among undergraduate students in China. *BMC Public Health*. 2020 Aug 26;20(1):1292. doi: 10.1186/s12889-020-09392-z.
- Khader Y, Al Nsour M, Al-Batayneh OB, Saadeh R, Bashier H, Alfaqih M, Al-Azzam S, AlShurman BA. Dentists' Awareness, Perception, and Attitude Regarding COVID-19 and Infection Control: Cross-Sectional Study Among Jordanian Dentists. *JMIR Public Health Surveill*. 2020 Apr 9;6(2):e18798. doi: 10.2196/18798.
- Wolf TG, de Col L, Banihashem Rad SA, Castiglia P, Arghittu A, Cannavale M, Campus G. How the COVID-19 Pandemic Affects Risk Awareness in Dentists: A Scoping Review. *Int J Environ Res Public Health*. 2022 Apr 20;19(9):4971. doi: 10.3390/ijerph19094971.
- Levit M, Levit L. Infection Risk of COVID-19 in Dentistry Remains Unknown: A Preliminary Systematic Review. *Infect Dis Clin Pract (Baltim Md)*. 2021 Mar;29(2):e70-7. doi: 10.1097/IPC.0000000000000939.
- Marya A, Karobari MI, Selvaraj S, Adil AH, Assiry AA, Rabaan AA, Horn R, Venugopal A, Messina P, Scardina GA. Risk Perception of Various Protective Measures by Dentists Across Various Countries. *Int J Environ Res Public Health*. 2021 May 29;18(11):5848. doi: 10.3390/ijerph18115848.
- Izzetti R, Nisi M, Gabriele M, Graziani F. COVID-19 Transmission in Dental Practice: Brief Review of Preventive Measures in Italy. *J Dent Res*. 2020 Aug;99(9):1030-8. doi: 10.1177/0022034520920580.
- Peng X, Xu X, Li Y, Cheng L, Zhou X, Ren B. Transmission routes of 2019-nCoV and controls in dental practice. *Int J Oral Sci*. 2020 Mar 3;12(1):9. doi: 10.1038/s41368-020-0075-9.
- Madathil S, Siqueira WL, Marin LM, Sanauilla FB, Faraj N, Quiñonez CR, McNally M, Glogauer M, Allison P. The incidence of COVID-19 among dentists practicing in the community in Canada: A prospective cohort study over a 6-month period. *J Am Dent Assoc*. 2022 May;153(5):450-9. doi: 10.1016/j.adaj.2021.10.006.
- Lo Giudice R. The Severe Acute Respiratory Syndrome Coronavirus-2 (SARS CoV-2) in Dentistry. Management of Biological Risk in Dental Practice. *Int J Environ Res Public Health*. 2020 Apr 28;17(9):3067. doi: 10.3390/ijerph17093067.
- Kateeb E, Danadneh M, Pokorná A, Klugarová J, Abdulqader H, Klugar M, Riad A. Predictors of Willingness to Receive COVID-19 Vaccine: Cross-Sectional Study of Palestinian Dental Students. *Vaccines (Basel)*. 2021 Aug 26;9(9):954. doi: 10.3390/vaccines9090954.

*Corresponding author: Luljeta Ferizi Shabani, Professor Assistant, Alma Mater Europaea, Campus College Rezonanca, and University Dentistry Clinical Center of Kosovo, Prishtina, Republic of Kosovo. E-mail: luljetaferizi@gmail.com

23. Schmidt J, Vavrickova L, Micopulos C, Suchanek J, Pilbauerova N, Perina V, Kapitan M. COVID-19 among Czech Dentistry Students: Higher Vaccination and Lower Prevalence Compared to General Population Counterparts. *Vaccines (Basel)*. 2022 Nov 14;10(11):1927. doi: 10.3390/vaccines10111927.
24. Lestari W, Yazid NH, Azhar ZN, Ismail A, Sukotjo C. Impact of COVID-19 on Malaysian dental students' physical, mental, financial and academic concerns. *BMC Oral Health*. 2022 Feb 23;22(1):46. doi: 10.1186/s12903-022-02081-w.
25. Thurzo A, Urbanová W, Waczulíková I, Kurilová V, Mriňáková B, Kosnáčová H, Gális B, Varga I, Matajs M, Novák B. Dental Care and Education Facing Highly Transmissible SARS-CoV-2 Variants: Prospective Biosafety Setting: Prospective, Single-Arm, Single-Center Study. *Int J Environ Res Public Health*. 2022 Jun 23;19(13):7693. doi: 10.3390/ijerph19137693.
26. Mehta S, Singh Gambhir R, Singh B, Goel R, Singh Ghuman K, Aggarwal A. Covid-19 update: Omicron variant - a new emerging threat. *Rocz Panstw Zakl Hig*. 2022;73(1):13-6. doi: 10.32394/rpzh.2022.0198.
27. Biswas N, Mustapha T, Khubchandani J, Price JH. The Nature and Extent of COVID-19 Vaccination Hesitancy in Healthcare Workers. *J Community Health*. 2021 Dec;46(6):1244-51. doi: 10.1007/s10900-021-00984-3.
28. Riad A, Huang Y, Abdulqader H, Morgado M, Domnori S, Koščík M, Mendes JJ, Klugar M, Kateeb E, Iads-Score. Universal Predictors of Dental Students' Attitudes towards COVID-19 Vaccination: Machine Learning-Based Approach. *Vaccines (Basel)*. 2021 Oct 10;9(10):1158. doi: 10.3390/vaccines9101158.
29. Cleofas JV, Oducado RM. Optimistic but tired of hearing about COVID: optimism as a predictor of COVID-19 information and behavioral fatigue among Filipino youth. *Social Sci J*. 2021 Oct 9:1-11. doi: 10.1080/03623319.2021.1986300.
30. Ali S, Alam BF, Farooqi F, Almas K, Noreen S. Dental and Medical Students' Knowledge and Attitude toward COVID-19: A Cross-Sectional Study from Pakistan. *Eur J Dent*. 2020 Dec;14(S 01):S97-S104. doi: 10.1055/s-0040-1719219.
-

Primary Mucinous Cystadenocarcinoma of the Testis: A Case Report and Literature Review

Labinot Shahini^{1,2}, Artan Elshani³, Valon Cena², Vasiona Dermaku², Altina Metushi²,
Sefedin Muçaj^{1,4*}

¹Faculty of Medicine, University of Prishtina “Hasan Prishtina”, Prishtina, Kosovo

²Institute of Pathology, University Clinical Center of Kosovo, Prishtina, Kosovo

³Clinic of Urology, University Clinical Center of Kosovo, Prishtina, Kosovo

⁴National Institute of Public Health of Kosovo, Prishtina, Kosovo

Abstract

Primary mucinous cystadenocarcinoma (MCA) of the testis is extremely rare, only 10 cases having been reported to date. Metastases of mucinous adenocarcinomas that have originated in different sites can mimic primary MAC and must be included in the differential diagnosis. We report a case of primary MCA of the tunica vaginalis testis in a 28-year-old patient who presented with a painless mass on the left side of the scrotum. We present the clinical and pathological characteristics to contribute to the further understanding of these rare tumors. Mucinous cystadenocarcinoma of the testis is extremely rare, particularly in individuals younger than 40 years. Histological examination, immunohistochemical analysis, and clinical examination to exclude metastases from other organs are necessary for a definitive diagnosis. (**International Journal of Biomedicine. 2023;13(1):168-171.**)

Keywords: mucinous cystadenocarcinoma • ovarian-type surface epithelial neoplasm • testicular adenocarcinoma

For citation: Shahini L, Elshani A, Cena V, Dermaku V, Metushi A, Muçaj S. Primary Mucinous Cystadenocarcinoma of the Testis: A Case Report and Literature Review. International Journal of Biomedicine. 2023;13(1):168-171. doi:10.21103/Article13(1)_CR1

Introduction

Ovarian-type surface epithelial tumors very rarely present as primary neoplasms of the testis.⁽¹⁾ The mucinous subtype is particularly rare, only approximately 30 cases having been published to date,⁽²⁾ only 10 of which were primary MCA of the testis.⁽³⁻¹²⁾

Case Report

A 28-year-old man presented with painless swelling of the left testis that he had first noticed 1 month before. On physical examination, there was no erythema, and no lymph nodes were palpable. Ultrasound examination showed a mainly hypoechoic, heterogenous, cystic lesion on the lateral surface of the left testis. Laboratory examination showed a serum alpha-fetoprotein concentration of 3.27 ng/mL (normal range: 0–20 ng/mL) and the β -human chorionic gonadotrophin of 0.112 mU/mL (normal range: 0.5–2.67 mU/mL). Other hematological and biochemical findings were within normal

reference ranges. Computed tomography of the abdomen and pelvis confirmed the ultrasound findings and did not detect any lesions in the peripheral lymph nodes or other organs. A chest radiograph was normal.

A biopsy of the nodule was obtained, resulting in a histopathological diagnosis of the primary mucinous cystadenocarcinoma of the testis. The patient accordingly underwent total radical left orchiectomy. Grossly, the tumor consisted of irregular tissue with mucinous elements. Microscopically, it consisted of glandular formations and cystic spaces lined with ciliated, cylindrical, epithelial cells. Some malignant goblet cells with intracellular mucin were noted, as were wide mucinous pools with scattered neoplastic cells. The tumor stroma was composed of a dense inflammatory, predominantly mononuclear, infiltrate and proliferation of wide blood vessels containing erythrocytes. The patient was discharged on Day 4 of the hospital stay and referred to an oncology center. Immunohistochemical analysis was positive for CK 20, carcinoembryonic antigen, and MUC2 and negative for CK7, vimentin, thyroid transcription factor 1, and WT1.



Fig. 1

Figure 1. Photograph of the cut surface of the testis with spermatic cord showing a mucinous cystic mass replacing the testicular parenchyma.

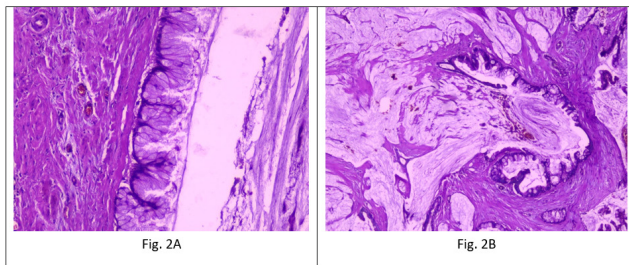


Figure 2. Photomicrographs showing a moderately differentiated, cystic, malignant neoplasm with mucinous differentiation and irregular glands lined with single or multiple layers of columnar epithelium containing mucin. Papillary growth was also observed in some areas. Stain: H&E; Magnification: A, 40 \times ; B, 200 \times

Discussion

Primary ovarian-type surface epithelial tumors of the mucinous subtype are very rare. The first case, a cystadenoma in an 11-year-old boy, was reported in 1959.⁽¹³⁾ These tumors are classified as benign, borderline, and malignant.⁽¹⁴⁾ They are almost identical to their ovarian counterparts, with some key differences: they are not as large and more often present as unilocular cystic tumors.⁽³⁾ Ovarian-type testicular tumors generally present as unilateral, painless, scrotal masses, often accompanied by a hydrocele. They can be para- or intratesticular, the former generally arising from the tunica vaginalis of the testis.⁽¹⁵⁾ Gross examination typically shows cystic masses with gelatinous material.⁽⁴⁾ Mucinous tumors vary microscopically according to whether they are benign or malignant. Benign tumors generally have cystic spaces and tumor glands with endocervical-type epithelium, whereas borderline, malignant, and mucinous carcinomas characteristically feature intestinal-type epithelium.⁽¹⁶⁾ Our patient's tumor had these gross and histological features. Immunohistochemical staining of primary

mucinous cystadenocarcinoma of the testis can reportedly be positive for cytokeratins, carcinoembryonic antigen, cancer antigen 125, epithelial membrane antigen, carbohydrate antigen 19-9, and cytokeratin CAM 5.2.⁽⁶⁾ These tumors have a higher incidence in older individuals than do other testicular tumors, typically presenting in the fifth and sixth decade of life.^(3,17) However, our review of cases of primary mucinous cystadenocarcinoma of the testis showed a similar incidence across age groups. Based on our research and experience, at 28 years of age, our patient is the youngest yet reported.

The origin of mucinous tumors of the testis remains unclear. Many hypotheses concerning their histogenesis have been proposed. One widely accepted theory is that these tumors originate from Müllerian remnants in the appendix testis or extra testicular scrotal tissue. Another theory suggests that they may originate in Müllerian metaplasia of the tunica vaginalis.^(15,18) Others have argued that intratesticular lesions may arise from mesothelial inclusions or represent monodermal teratomas.⁽¹⁷⁾

Because mucinous tumors of the testis are rare, metastasis of mucinous tumors to the testis is more common than primary mucinous cystadenocarcinoma. It is, therefore, important to exclude the possibility of a metastasis mimicking the primary mucinous cystadenocarcinoma of the testis. It has been estimated that 53% of mucinous tumors in the testis are metastases from other sites. Metastatic testicular tumors most commonly originate from mucinous carcinomas of the colon, stomach, pancreas, prostate, and appendix.^(7,20-23) Metastases from other sites can be distinguished from primary testicular mucinous cystadenocarcinoma by their multifocality, growth in the testicular interstitium, and prominent vascularity.^(4,7,19) Another important point of differentiation is that testicular metastases can be bilateral.⁽¹⁵⁾ Immunohistochemical positivity in primary ovarian epithelial mucinous carcinomas is not completely specific and may overlap with positivity in mucinous metastases from other sites.⁽⁹⁾ However, it has been reported that immunohistochemical staining for CK7, MUC2, MUC5AC, and MUC6 may be helpful in the differential diagnosis of metastatic mucinous tumors of the testis.⁽⁷⁾ A combination of immunohistochemical studies and clinical correlations is therefore needed to make the correct diagnosis.

Other differential diagnoses include primary testicular tumors, such as mesothelioma, adenocarcinoma of the rete, appendix testis, epididymis, and germ cell tumors.^(6,16,24) Mesothelioma of the tunica vaginalis can be excluded by histological differences, such as a lack of psammoma bodies, low cellularity, intestinal type, and ciliated serous morphology, as well as the immunohistochemical profile.^(6,24) The possible diagnosis of adenocarcinoma of the rete testis, appendix testis, or epididymis can be eliminated by the parenchymal location of the tumor and the specific histological features.⁽⁶⁾ These lesions are located in the extra scrotal region, and their histological characteristics include tubular and tubule-papillary structures lined by cuboidal cells.⁽²⁵⁾

Germ cell tumors can be excluded by the presence of a ciliated serous component, psammomatous calcification, and a lack of teratomatous elements,^(5,26) the latter being a feature of most reported cases and the present case. Germ cell tumors

also differ in the age of onset, generally presenting at younger ages.⁽²⁷⁾ Another differential diagnosis is mucinous tumors of the appendix or peritoneal surfaces in an inguinal hernia sac, the distinction relying on the location of the neoplasm within a hernial sac and the presence of a prominent, extracellular mucinous component.^(4,17)

The prognosis and treatment of patients with primary mucinous cystadenocarcinoma of the testis differ depending on the benign or malignant nature of the tumor. The most common treatment is radical orchiectomy and follow-up.⁽²⁾ The prognosis of primary mucinous cystadenocarcinoma of the testis remains unclear because of their rarity. Our literature review yielded 10 previous cases of primary mucinous cystadenocarcinoma of the testis; 4 of these patients had developed distant metastases, and 2 had died within months of the diagnosis.^(3,4,7,9)

Conclusion

Mucinous cystadenocarcinoma of the testis is extremely rare, particularly in individuals younger than 40 years. Histological examination, immunohistochemical analysis, and clinical examination to exclude metastases from other organs are necessary for a definitive diagnosis.

Informed written consent was obtained from the patient to publish this case report and any accompanying medical images.

Acknowledgments

We thank Dr Trish Reynolds, MBBS, FRACP, from Edanz (<https://www.edanz.com/ac>) for editing a draft of this manuscript.

Competing Interests

The authors declare that they have no competing interests.

References

1. Young RH, Scully RE. Testicular and paratesticular tumors and tumor-like lesions of ovarian common epithelial and müllerian types. A report of four cases and review of the literature. *Am J Clin Pathol.* 1986 Aug;86(2):146-52. doi: 10.1093/ajcp/86.2.146.
2. Hao C, Kang C, Kang X, Yu Z, Li T, Xue J. Primary Borderline Mucinous Testicular Tumor: A Case Report and Literature Review. *Front Oncol.* 2021 Mar 9;10:619774. doi: 10.3389/fonc.2020.619774.
3. Azuma T, Matayoshi Y, Nagase Y. Primary mucinous adenocarcinoma of the testis. *Case Rep Med.* 2012;2012:685946. doi: 10.1155/2012/685946.
4. Ulbright TM, Young RH. Primary mucinous tumors of the testis and paratestis: a report of nine cases. *Am J Surg Pathol.* 2003 Sep;27(9):1221-8. doi: 10.1097/00000478-200309000-00005.
5. Celdrán JO, Rodríguez CS, Valverde FM, Compiano LO. Primary mucinous cystadenocarcinoma of the testis: An extremely rare ovarian-type surface epithelial carcinoma. *J Cancer Res Ther.* 2015 Jul-Sep;11(3):647. doi: 10.4103/0973-1482.143363.
6. Iuga AC, Mull J, Batra R, Miller W. Mucinous cystadenocarcinoma of the testis: a case report. *Hum Pathol.* 2011 Sep;42(9):1343-7. doi: 10.1016/j.humpath.2010.11.021.
7. Tanriverdi O, Tarimer ML, Pak CD, Uylas S, Alkan A, Dere Y, Yazici A, Sen S, Sahin H. Management of a patient with primary mucinous testicular adenocarcinoma as a rare case with adjuvant and metastatic sequential treatments. *J Oncol Pharm Pract.* 2020 Sep;26(6):1520-1523. doi: 10.1177/1078155220903374.
8. Lei H, Lai L, Xu H, Bai S, Shi M, Yang L. Primary mucinous adenocarcinoma of the testis: A case report and review of the literature. *Front Oncol.* 2021;10:32-34.
9. Maruschke M, Schmidt W, Casper J, Hakenberg OW. Ovarian type surface epithelial carcinoma of the testis with delayed metastatic spread. *Urol Int.* 2008;81(1):119-21. doi: 10.1159/000137653.
10. Teo CH, Chua WJ, Consigliere DT, Raju GC. Primary intratesticular mucinous cystadenocarcinoma. *Pathology.* 2005 Feb;37(1):92-4. doi: 10.1080/00313020400024832.
11. Di Franco CA, Porru D, Viglio A, Paulli M, Rovereto B. Primary paratesticular mucinous "ovarian-type" adenocarcinoma: A rare case of scrotal tumor in a patient with history of bilateral cryptorchidism. *World J Nephrol Urol.* 2015;4:260-263.
12. Rao NB, Sudhkar G, Swathi VR, Kumar AH. Mucinous adenocarcinoma of testis: A rare case report. *J Evol Med Dental Sci.* 2015;4:13144.
13. KELLERT E. An ovarian type pseudomucinous cystadenomainthescrotum. *Cancer.* 1959 Jan-Feb;12(1):187-90. doi: 10.1002/1097-0142(195901/02)12:1<187::aid-cncr2820120124>3.0.co;2-h.
14. Funada S, Yoshida T, Ito M, Kono F, Segawa T. Primary borderline mucinous tumors of the testis: a case report and literature review. *Case Rep Oncol Med.* 2015;2015:863745. doi: 10.1155/2015/863745.
15. Lin MS, Ayala AG, Ro JY. Ovarian-type tumors (Mullerian tumors) of the testis: clinicopathologic findings with recent advances. *Ann Urol Oncol.* 2019;2:36-45.
16. Ali TZ, Parwani AV. Benign and Malignant Neoplasms of the Testis and Paratesticular Tissue. *Surg Pathol Clin.* 2009 Mar;2(1):61-159. doi: 10.1016/j.path.2008.08.007.
17. Amin MB. Selected other problematic testicular and paratesticular lesions: rete testis neoplasms and pseudotumors, mesothelial lesions and secondary tumors. *Mod Pathol.* 2005 Feb;18 Suppl 2:S131-45. doi: 10.1038/modpathol.3800314.
18. Raspollini MR, Montagnani I, Montironi R, Lopez-Beltran A. Ovarian epithelial-stromal tumors and similar lesions in the testis. In *Gynecologic and Urologic Pathology*. In: Raspollini MR, Beltran AL, editors. Cambridge University Press, UK, 2019:62-83.
19. Elliott JE, Klein JR, Drachenberg DE. Primary testicular mucinous neoplasms: case report and literature review. *Can*

*Corresponding author: Sefedin Muçaj, Faculty of Medicine, University of Prishtina "Hasan Prishtina," Street Lagjja e spitallit p.n. 10000, Pristina, Kosovo. E-mail: sefedin.mucaj@uni-pr.edu

- Urol Assoc J. 2010 Aug;4(4):E112-5. doi: 10.5489/cuaj.894.
20. Seo IY, Kim SG, Han WC, Rim JS. Paratesticular mucinous cystadenocarcinoma: metastasis from pancreatic cancer. *Int J Urol*. 2004 Dec;11(12):1147-9. doi: 10.1111/j.1442-2042.2004.00964.x.
21. Bunn R, Liu S, Stokes S, Turner J, Louie-Johnsun M. Mucinous Lung Adenocarcinoma Metastasis to Testis in a 29 Year Old-A Case Report. *Urology*. 2018 Aug;118:3-5. doi: 10.1016/j.urology.2018.01.016.
22. Kim YW, Kim JW, Kim JH, Lee J, Lee E, Kim MY, Yang HK, Chang H. Metastatic testicular tumor presenting as a scrotal hydrocele: An initial manifestation of pancreatic adenocarcinoma. *Oncol Lett*. 2014 Jun;7(6):1793-1795. doi: 10.3892/ol.2014.2009.
23. Jesus CM, Goldberg J, Camargo JL. Single testicular metastasis mimicking primary testicular neoplasm: a rare manifestation of prostate cancer. *Int Braz J Urol*. 2005 Jan-Feb;31(1):54-6. doi: 10.1590/s1677-55382005000100011.
24. Bürger T, Schildhaus HU, Inniger R, Hansen J, Mayer P, Schweyer S, Radzun HJ, Ströbel P, Bremmer F. Ovarian-type epithelial tumours of the testis: immunohistochemical and molecular analysis of two serous borderline tumours of the testis. *Diagn Pathol*. 2015 Jul 22;10:118. doi: 10.1186/s13000-015-0342-9.
25. Çoban G, Yildiz P, Tuğçe K, Ersöz C. Histopathological features of paratesticular solid tumors: 5 years experience. *IKSSTD*. 2020;12:130–135.
26. Kim G, Kwon D, Na HY, Kim S, Moon KC. Mucinous Cystadenoma of the Testis: A Case Report with Immunohistochemical Findings. *J Pathol Transl Med*. 2017 Mar;51(2):180-184. doi: 10.4132/jptm.2016.08.30.
27. Dieckmann KP, Richter-Simonsen H, Kulejewski M, Ikogho R, Zecha H, Anheuser P, Pichlmeier U, Isbarn H. Testicular Germ-Cell Tumours: A Descriptive Analysis of Clinical Characteristics at First Presentation. *Urol Int*. 2018;100(4):409-419. doi: 10.1159/000488284.
-

Anaplastic Pleomorphic Xanthoastrocytoma, WHO Grade 3, Located on the Hippocampal Region: A Case Report

Serbeze Kabashi-Muçaj^{1,2}, Agon Mekaj³, Mentor Petrela⁴, Besim Latifi⁵, Gentian Kaloshi⁴,
Flaka Pasha^{1,2}, Kreshnike Dedushi Hoti^{1,2}, Arben Rroji⁶, Labinot Shahini^{1,7}, Fjolla Hyseni⁸,
Sefedin Muçaj^{*1,9}

¹Faculty of Medicine, University of Prishtina “Hasan Prishtina”, Prishtina, Kosovo

²Clinic of Radiology, University Clinical Center of Kosovo, Prishtina, Kosovo

³Clinic of Neurosurgery, University Clinical Center of Kosovo, Prishtina, Kosovo

⁴Neurosurgery UHC “Mother Teresa”, Tirana, Albania

⁵Department of Pathology, Ashford and St. Peter’s Hospitals NHS Trust, Chertsey, United Kingdom

⁶Clinic of Radiology, UHC “Mother Teresa”, Tirana, Albania

⁷Institute of Pathology, University Clinical Center of Kosovo, Prishtina, Kosovo

⁸NYU Langone Health, New York, United States

⁹National Institute of Public Health of Kosovo, Prishtina, Kosovo

Abstract

Anaplastic pleomorphic xanthoastrocytoma (APXA) is a rare and aggressive brain tumor that requires a multidisciplinary approach for proper diagnosis and treatment. This case report presents the case of a 15-year-old male patient diagnosed with APXA in the left temporal region. The patient underwent a combination of imaging studies, including MRI, followed by a biopsy of the tumor tissue and surgery. The patient was then closely monitored for recurrence and progression of the tumor, and further received six cycles of chemotherapy and radiation therapy.

This report aims to provide detailed information about the diagnostic process for APXA, which can be challenging due to its similarity to other tumors, such as pilocytic astrocytoma. Additionally, the report highlights the varying treatment options and outcomes for patients with APXA, as well as the importance of close monitoring for the recurrence and progression of the tumor. More research is needed to fully understand the best treatment options for APXA and to improve outcomes for patients diagnosed with this rare and aggressive brain tumor. (**International Journal of Biomedicine. 2023;13(1):172-176.**)

Keywords: anaplastic pleomorphic xanthoastrocytoma • brain tumor • hippocampus • MRI • biopsy

For citation: Kabashi-Muçaj S, Mekaj A, Petrela M, Latifi B, Kaloshi G, Pasha F, Hoti KD, Rroji A, Shahini L, Hyseni F, Muçaj S. Anaplastic Pleomorphic Xanthoastrocytoma, WHO Grade 3, Located on the Hippocampal Region: A Case Report International Journal of Biomedicine. 2023;13(1):172-176. doi:10.21103/Article13(1)_CR2

Introduction

Anaplastic pleomorphic xanthoastrocytoma (APXA) is a rare and malignant brain tumor characterized by its pleomorphic cells and xanthomatous material. First described in 1979,⁽¹⁾ it was later recognized as a separate entity from pleomorphic xanthoastrocytoma (PXA) in 1993 and classified as a World Health Organization (WHO) grade III tumor

in 2016.⁽²⁾ APXAs are more commonly found in adults and typically occur in the brain’s cerebral hemispheres.

Despite aggressive treatment, the prognosis for APXA is generally poor, with a 5-year overall survival rate of around

**Corresponding author: Prof. Assoc. Dr. Sefedin Muçaj, Faculty of Medicine, University of Prishtina “Hasan Prishtina”, Prishtina, Kosovo. E-mail: sefedin.muçaj@uni-pr.edu*

42% due to its infiltrative nature and the difficulty of treating it. Additionally, there is limited data on the incidence of APXA as it is a rare type of brain tumor. Studies have shown that PXA and APXA together make up less than 1% of all astrocytomas, and the majority of cases are found in children and adolescents, with a median age of onset at 22 years old.⁽³⁾ However, more research is needed to fully understand the incidence and prevalence of APXA in the world.

Clinicians need to be familiar with the clinical and pathological characteristics of APXA to make an accurate diagnosis and provide appropriate treatment. Treatment options for APXA may include surgery, radiation therapy, and chemotherapy. However, due to the rarity of this type of tumor, there is limited data and research available on it. Therefore, it is important to consult with experts in the field and to participate in clinical trials to improve the knowledge and the outcomes for APXA patients.

This case report aims to share in-depth information about the diagnosis, treatment, and outcome of a patient with APXA, a rare and aggressive type of brain tumor. Additionally, this report aims to bring attention to the rarity of this type of tumor, the difficulty in differentiating it from pilocytic astrocytoma, and the aggressive nature of APXA. It also emphasizes the importance of close monitoring and exploring various treatment options for patients with APXA.

Case Presentation

This case report presents a 15-year-old male patient admitted to the hospital with a left temporal lobe lesion. He had no prior medical history but had recently been experiencing episodes of speech aphasia and loss of consciousness, which had become more frequent in the past few weeks. His parents reported that the patient has been experiencing these symptoms for over a year and they had become increasingly aggressive in the past 2-3 months. The patient was prescribed antiepileptic therapy but was not compliant. The neurologist requested a brain MRI, which revealed a mass in the left mesial-temporal region that appeared hypointense on T1 and hyperintense on T2. The lesion enhanced heterogeneously after intravenous contrast injection. The radiological features favored a diagnosis of pilocytic astrocytoma, but other possibilities, such as APXA and gangliocytoma were also considered, based on the location of the mass.

On December 2022, the patient underwent surgery, which was performed through neuron navigation, with a left temporal basal mini craniotomy and a subtemporal approach. The lesion was infiltrative, white-gray, aspirable, and had no cleavage plain. A gross total resection (GTR) was achieved. The initial diagnosis was pilocytic astrocytoma.

Further examination of the tissue (Figure 1) revealed features of APXA, a highly malignant tumor with a high potential to recur and progress despite initial treatment. The patient had been experiencing headaches, vertigo, nausea, behavioral changes, and aphasia for some time.

Treatment for APXA typically involves a combination of surgery, radiation therapy, and chemotherapy. In this case, the patient underwent radiation therapy according to the ACNS 0423 protocol of the Children's Oncology Group, including concomitant radio-chemotherapy with temozolomide (90 mg/m²/day for 42 days) and radiation therapy treatment with a total dose of 54.0 Gy, followed with a boost of 5.4 Gy. One month after the end of radiotherapy, the patient started adjuvant chemotherapy consisted of up to 6 cycles of CCNU 90 mg/m² on day 1 and temozolomide 160 mg/m²/day ×5 every 6 weeks.

Neuroimaging of the course of the disease is presented in Figures 2 and 3. It was proposed that a head and spinal cord MRI should be performed after 6 months. There was no evidence of the expansive relapse process after reevaluation with intravenous contrast brain MRI after 6 months.

The neurologist should discuss the case again with the pathologist to seek further data on the *BRAF* V600E mutation and any chromosomal analysis (*CDKN2A*, chromosome 1q, 9p, 10p, 12q, 18q).

APXA can be difficult to differentiate from other types of gliomas, particularly pilocytic astrocytomas, due to their similar radiographic and histologic features. However, APXA is characterized by its high degree of pleomorphism and atypia, as well as the presence of mitotic figures and lack of Rosenthal fibers, which are characteristic of pilocytic astrocytomas. The prognosis for APXA is generally poor, with a high potential for recurrence and progression despite initial treatment. Close monitoring and further treatment options, such as re-operation or additional radiation therapy and/or chemotherapy, should be considered for patients with APXA, especially those with a recurrence of the tumor.

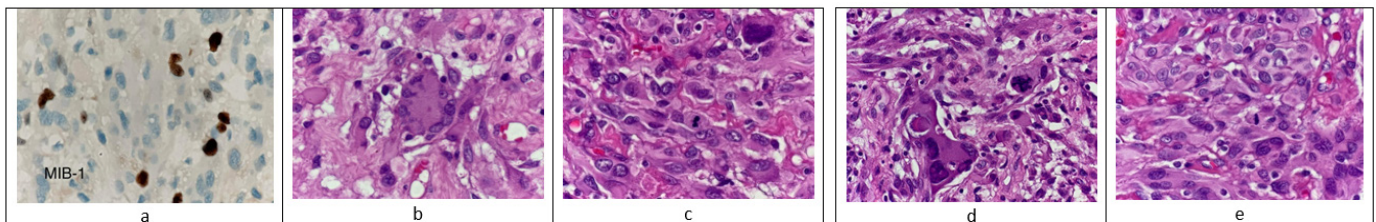


Fig. 1. Microscopic images of the patient. A. Positivity of MIB-1 after staining with immunohistochemistry. B. Multinucleated cell at 400X magnification. C. D and E. Proliferation of markedly pleomorphic cells, with variation in sizes and shapes. There is focally seen lymphocytic infiltration. Neoplastic cells show prominent eosinophilic cytoplasm with intracytoplasmic vacuoles. Mitotic figures are seen (400X).

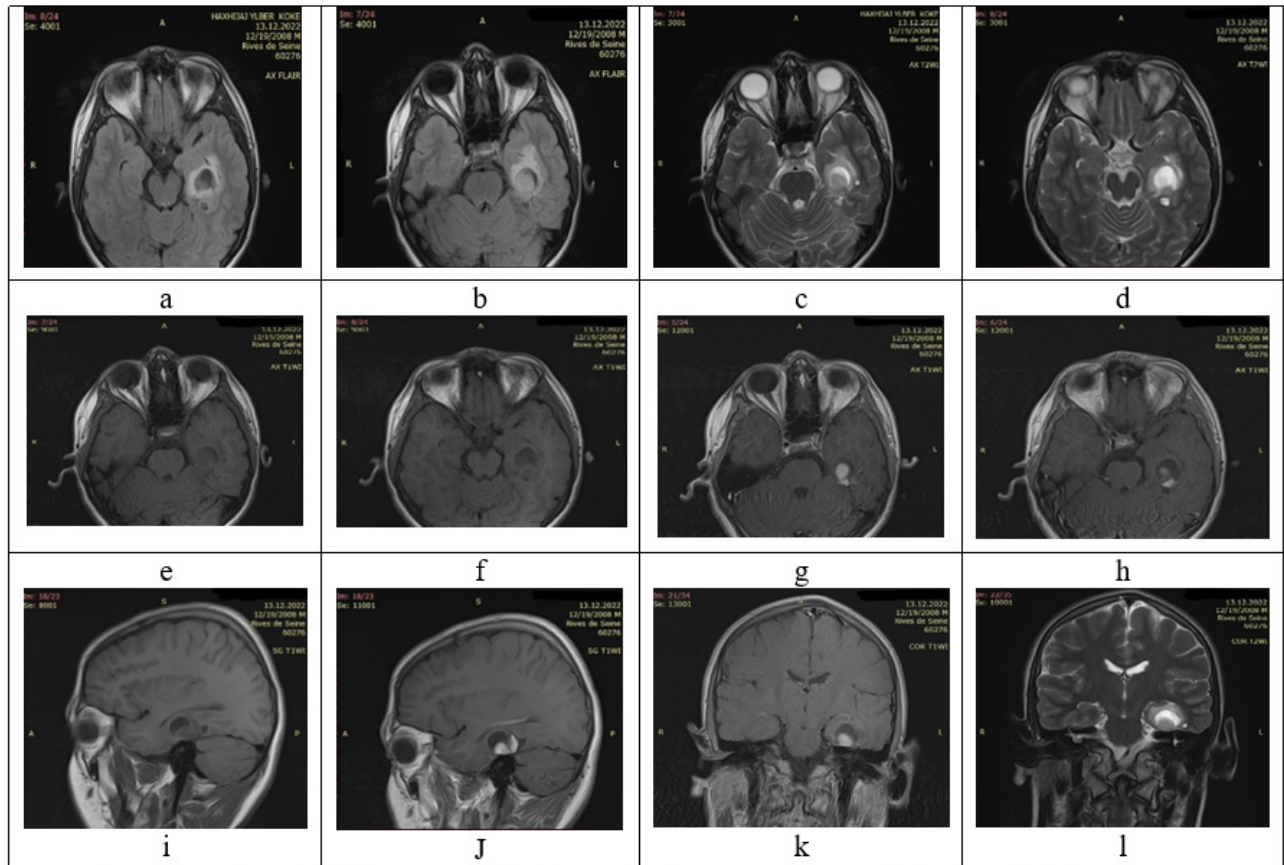


Fig. 2. Preoperative images. MR images revealing a well-circumscribed, heterogeneous tumor with solid-cystic components in the left temporal lobe, approximately 26x20 mm in size, with peritumoral edema presented on axial Flair (a,b), on axial T2 images showing proximal cystic components 18mm very hyperintense (c,d). In T1, before the contrast, the cystic component is hypointense, while the solid part is isointense (e,f). After the gadolinium contrast application, there is the pathological enhancement of the solid component, mainly heterogeneous in the form of the nodule with a tracheal extension over the tentorium (g,h), while T1 in the sagittal plane before and after gadolinium, the pathological enhancement of the solid component is presented (i,j). Coronal T1 post-gadolinium (k) and coronal T2 (l) MR images.

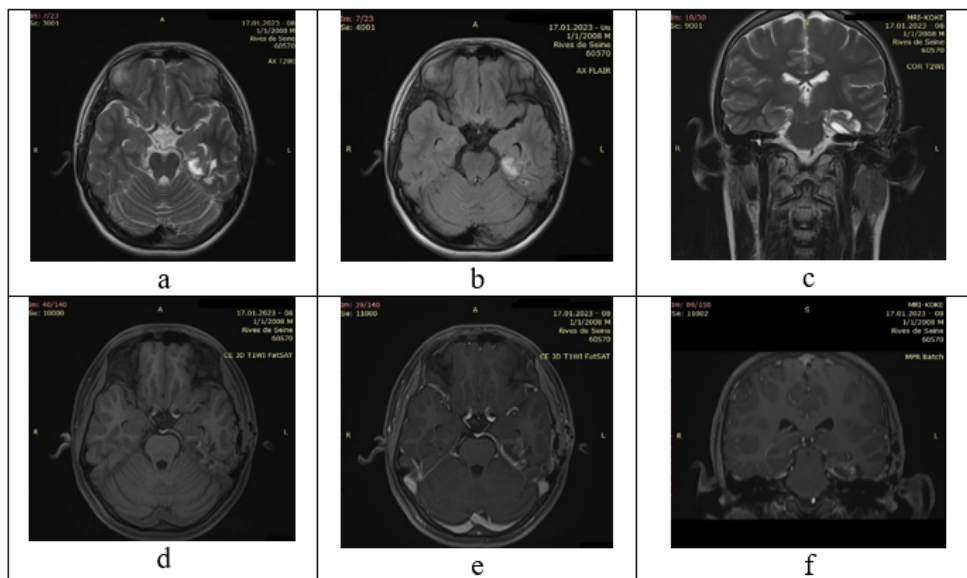


Fig. 3. MR images one month after the surgical resection reveal a well-limited postoperative parenchymal defect, mostly homogeneous, with porencephalic cystic components in the left temporal lobe, without peritumoral edema. Axial T2 images show porencephalic cystic components approximately 14x8mm, very hyperintense, with the expansion of the left temporal horn (a). Axial Flair presents postoperative cicatricial edema, not expansive edema (b). Coronal T2 clearly shows the postoperative defect (c). In T1 before the contrast, we notice a hypointense cystic component, while the solid component is not present, there is methemoglobin retention (d), after the gadolinium contrast, we have very discrete pathological marginal enhancement of the postoperative defect (e), while in T1 in the coronal plane after gadolinium is presented the discrete marginal pathological enhancement from the postoperative porencephalic cystic component (f).

Discussion

This case report explains in detail the diagnosis and treatment of a 15-year-old male patient with APXA in the left temporal region. APXA is a rare type of brain tumor, with an estimated incidence of only 0.1%-0.2% of all brain tumors.⁽⁴⁾ However, the exact incidence of APXA worldwide is not well-established, as it is a rare tumor and data is limited. A study published in the *Journal of Neuro-Oncology* found that the incidence of APXA in the United States is 1-2 cases per million per year.⁽⁴⁾ It is important to note that the true incidence may be higher, as the tumor can be misdiagnosed as other types of brain tumors. Due to its rarity, there is limited data and research available on the incidence of APXA worldwide.

APXA primarily affects individuals in their second decade of life, with an average age of presentation being 47.7 years old, as reported by She et al.⁽⁵⁾ These tumors are commonly found in the cerebral hemispheres and do not involve the dura mater. They are often difficult to distinguish from other types of desmoplastic neuroepithelial neoplasms, such as gliosarcoma, desmoplastic infantile ganglioglioma, and desmoplastic cerebral astrocytoma of infancy, due to their similar clinical, radiological, and pathologic features.⁽⁶⁾ Additionally, epithelioid glioblastoma can also resemble APXA due to similar histopathological characteristics.^(7,8)

MRI is an important tool in the diagnosis of APXA, as it can provide useful information about the size, perilesional edema, infiltration, hemorrhage, and necrosis of the tumor. Previous case reports have shown that APXA tumors are larger than pilocytic astrocytoma due to an increased mitotic rate of more than five mitoses per 10 high-power fields.⁽¹⁾ Additionally, APXA tumors have been found to have more significant tumoral enhancement and perilesional edema compared to PXA tumors.

There have been various attempts to develop tools to differentiate between PXA and APXA, such as the ratio between diffusion-weighted imaging (DWI) and apparent diffusion coefficient (ADC) values,⁽⁹⁻¹¹⁾ which aims to assess the differences between the two tumors based on the nuclear to cytoplasmic ratio. Another study reported that increased microvascular proliferation in anaplastic tumors increases the relative cerebral blood volume (rCBV) value, which is correlated with cellular proliferation in high-grade gliomas, and in modern MRI techniques, rCBV is considered a significant marker for tumor vascularity. However, these case studies have a small sample size, making generalization difficult.⁽¹²⁻¹⁴⁾

Currently, there is no standard postoperative therapy for APXA as the rarity of the tumor makes it challenging to develop a treatment protocol. Surgical resection and stereotactic radiation therapy are effective in achieving long-term control, but conventional radiotherapy and chemotherapy are not proven to have been beneficial in the treatment of APXA. Stereotactic radiosurgery may have the potential to reverse progression, but more research is needed to confirm its effectiveness.

It is important to note that due to the rarity of APXA, the true incidence may be higher than reported, and the tumor can

be misdiagnosed as other types of brain tumors. More research is needed to better understand the incidence, diagnosis, and treatment of APXA.

Conclusion

This case report aims to provide detailed information about the diagnosis, treatment, and outcome of a patient with APXA. The rarity of this tumor, the differential diagnosis with pilocytic astrocytoma, and the aggressiveness of the APXA tumor are highlighted in this report. Additionally, the importance of close monitoring and further treatment options for patients with APXA is emphasized. Despite the rarity of this tumor and the lack of standard postoperative therapy, surgical resection and stereotactic radiation therapy have been reported to provide long-term control in some cases. However, more research is needed to fully understand the best treatment options for APXA and to improve outcomes for patients diagnosed with this rare and aggressive brain tumor.

Competing Interests

The authors declare that they have no competing interests.

References

1. Kepes JJ, Rubinstein LJ, Eng LF. Pleomorphic xanthoastrocytoma: a distinctive meningocerebral glioma of young subjects with relatively favorable prognosis. A study of 12 cases. *Cancer*. 1979 Nov;44(5):1839-52. doi:10.1002/1097-0142(197911)44:5<1839::aid-cnrcr2820440543>3.0.co;2-0.
2. Louis DN, Perry A, Reifenberger G, von Deimling A, Figarella-Branger D, Cavenee WK, et al. The 2016 World Health Organization Classification of Tumors of the Central Nervous System: a summary. *Acta Neuropathol*. 2016 Jun;131(6):803-20. doi: 10.1007/s00401-016-1545-1.
3. Giannini C, Scheithauer BW, Burger PC, Brat DJ, Wollan PC, Lach B, et al. Pleomorphic xanthoastrocytoma: what do we really know about it? *Cancer*. 1999 May 1;85(9):2033-45.
4. Ronsley R, Dunham C, Yip S, Brown L, Zuccato JA, Karimi S, et al. A case series of pediatric survivors of anaplastic pleomorphic xanthoastrocytoma. *Neurooncol Adv*. 2021 Jan 30;3(1):vdaa176. doi: 10.1093/noajnl/vdaa176.
5. She D, Liu J, Xing Z, Zhang Y, Cao D, Zhang Z. MR Imaging Features of Anaplastic Pleomorphic Xanthoastrocytoma Mimicking High-Grade Astrocytoma. *AJNR Am J Neuroradiol*. 2018 Aug;39(8):1446-1452. doi: 10.3174/ajnr.A5701.
6. Shao LW, Wang FL. Anaplastic pleomorphic xanthoastrocytoma. *Chin J Contemp Neurol Neurosurg*. 2017;17:616-625.
7. Alexandrescu S, Korshunov A, Lai SH, Dabiri S, Patil S, Li R, et al. Epithelioid Glioblastomas and Anaplastic Epithelioid Pleomorphic Xanthoastrocytomas--Same Entity or First Cousins? *Brain Pathol*. 2016 Mar;26(2):215-23. doi: 10.1111/bpa.12295.
8. Broniscer A, Tatevossian RG, Sabin ND, Klimo P Jr, Dalton J, Lee R, et al. Clinical, radiological, histological and molecular characteristics of paediatric epithelioid glioblastoma.

- Neuropathol Appl Neurobiol. 2014 Apr;40(3):327-36. doi: 10.1111/nan.12093.
9. Fornasa F. Diffusion-weighted Magnetic Resonance Imaging: What Makes Water Run Fast or Slow? *J Clin Imaging Sci.* 2011;1:27. doi: 10.4103/2156-7514.81294.
10. Wang J, Takashima S, Takayama F, Kawakami S, Saito A, Matsushita T, et al. Head and neck lesions: characterization with diffusion-weighted echo-planar MR imaging. *Radiology.* 2001 Sep;220(3):621-30. doi: 10.1148/radiol.2202010063.
11. Sasaki M, Eida S, Sumi M, Nakamura T. Apparent diffusion coefficient mapping for sinonasal diseases: differentiation of benign and malignant lesions. *AJNR Am J Neuroradiol.* 2011 Jun-Jul;32(6):1100-6. doi: 10.3174/ajnr.A2434.
12. Aronen HJ, Pardo FS, Kennedy DN, Belliveau JW, Packard SD, Hsu DW, et al. High microvascular blood volume is associated with high glucose uptake and tumor angiogenesis in human gliomas. *Clin Cancer Res.* 2000 Jun;6(6):2189-200.
13. Buckley DL. Uncertainty in the analysis of tracer kinetics using dynamic contrast-enhanced T1-weighted MRI. *Magn Reson Med.* 2002 Mar;47(3):601-6. doi: 10.1002/mrm.10080.
14. Lev MH, Ozsunar Y, Henson JW, Rasheed AA, Barest GD, Harsh GR 4th, et al. Glial tumor grading and outcome prediction using dynamic spin-echo MR susceptibility mapping compared with conventional contrast-enhanced MR: confounding effect of elevated rCBV of oligodendrogliomas [corrected]. *AJNR Am J Neuroradiol.* 2004 Feb;25(2):214-21. Erratum in: *AJNR Am J Neuroradiol.* 2004 Mar;25(3):B1.
-



RETRACTIONS

**RETRACTED: Mitochondrial tRNA^{Leu}(UUR) Mutations
in Patients with Essential Hypertension**

International Journal of Biomedicine

Editorial Retraction

International Journal of Biomedicine has retracted the article titled “Mitochondrial tRNA^{Leu}(UUR) Mutations in Patients with Essential Hypertension” (Khan I, Lizhe A, Zhiqiang L. Mitochondrial tRNA^{Leu}(UUR) Mutations in Patients with Essential Hypertension. *International Journal of Biomedicine*. 2022;12(3):444-449. doi: 10.21103/Article12(3)OA18). The above article has been retracted as a result of concerns regarding the use of raw Figures 1-4 by one of the authors upon which the presented research has been based. The article is therefore being retracted due to concerns regarding the reliability of the data. All authors agree to the retraction of the article. The retracted article will remain online to maintain the scholarly record, but it will be digitally watermarked on each page as “Retracted.”(***International Journal of Biomedicine*. 2023;13(1):177.**)

For citation: *International Journal of Biomedicine*. RETRACTED: Mitochondrial tRNA^{Leu}(UUR) Mutations in Patients with Essential Hypertension. *International Journal of Biomedicine*. 2023;13(1):177. doi: 10.21103/Article13(1)_ER.

IJB M

INTERNATIONAL JOURNAL OF BIOMEDICINE

Instructions for Authors

International Journal of Biomedicine (IJBM) publishes peer-reviewed articles on the topics of basic, applied, and translational research on biology and medicine. International Journal of Biomedicine welcomes submissions of the following types of paper: Original articles, Reviews, Perspectives, Viewpoints, and Case Reports.

All research studies involving animals must have been conducted following animal welfare guidelines such as *the National Institutes of Health (NIH) Guide for the Care and Use of Laboratory Animals*, or equivalent documents. Studies involving human subjects or tissues must adhere to the *Declaration of Helsinki and Title 45, US Code of Federal Regulations, Part 46, Protection of Human Subjects*, and must have received approval of the appropriate institutional committee charged with oversight of human studies. Informed consent must be obtained.

Pre-submissions

Authors are welcome to send an abstract or draft manuscript to obtain a view from the Editor about the suitability of their paper. Our Editors will do a quick review of your paper and advise if they believe it is appropriate for submission to our journal. It will not be a full review of your manuscript.

Manuscript Submission

Manuscript submissions should conform to the guidelines set forth in the Recommendations for the Conduct, Reporting, Editing and Publication of Scholarly Work in Medical Journals (ICMJE Recommendations), available from www.ICMJE.org.

Original works will be accepted with the understanding that they are contributed solely to the Journal, are not under review by another publication, and have not previously been published except in abstract form.

All manuscripts must be submitted through the International Journal of Biomedicine's online submission system (www.ijbm.org/submission.php). Manuscripts must be typed, double-spaced using a 14-point font, including references, figure legends, and tables. Leave 1-inch margins on all sides. Assemble the manuscript in this order: Title Page, Abstract, Key Words, Text (Introduction, Methods, Results, and Discussion), Acknowledgments, Sources of Funding, Disclosures, References, Tables, Figures, and Figure Legends. References, figures, and tables should be cited in numerical order according to first mention in the text.

The preferred order for uploading files is as follows: Cover letter, Full Manuscript PDF (PDF containing all parts of the manuscript including references, legends, figures and tables), Manuscript Text File (MS Word), Figures (each figure and its corresponding legend should be presented together), and Tables. Files should be labeled with appropriate and descriptive file names (e.g., SmithText.doc, Fig1.eps, Table3.doc). Text, Tables, and Figures should be uploaded as separate files. (Multiple figure files can be compressed into a Zip file and uploaded in one step; the system will then unpack the files and prompt the naming of each figure. See www.WinZip.com for a free trial.)

Authors who are unable to provide an electronic version or have other circumstances that prevent online submission must contact the Editorial Office prior to submission to discuss alternate options (editor@ijbm.org).

Cover Letter

The cover letter should be saved as a separate file for upload. In it, the authors should (1) state that the manuscript, or parts of it, have not been and will not be submitted elsewhere for publication; (2) state that all authors have read and approved the manuscript; and (3) disclose any financial or other relations that could lead to a conflict of interest. If a potential conflict exists, its nature should be stated for each author. When there is a stated potential conflict of interest a footnote will be added indicating the author's equity interest in or other affiliation with the identified commercial firms.

The corresponding author should be specified in the cover letter. All editorial communications will be sent to this author. A short paragraph telling the editors why the authors think their paper merits publication priority may be included in the cover letter.

Types of articles

Original articles

Original articles present the results of original research. These manuscripts should present well-rounded studies reporting innovative advances that further knowledge about a topic of importance to the fields of biology or medicine. These can be submitted as either a full-length article (no more than 6,000 words, 4 figures, 4 tables) or a Short Communication (no more than 2,500 words, 2 figures, 2 tables). An original

article may be Randomized Control Trial, Controlled Clinical Trial, Experiment, Survey, and Case-control or Cohort study.

Case Reports

Case reports describe an unusual disease presentation, a new treatment, a new diagnostic method, or a difficult diagnosis. The author must make it clear what the case adds to the field of medicine and include an up-to-date review of all previous cases in the field. These articles should be no more than 5,000 words with no more than 6 figures and 3 tables. Case Reports should consist of the following headings: Abstract (no more than 100 words), Introduction, Case Presentation (clinical presentation, observations, test results, and accompanying figures), Discussion, and Conclusions.

Reviews

Reviews analyze the current state of understanding on a particular subject of research in biology or medicine, the limitations of current knowledge, future directions to be pursued in research, and the overall importance of the topic. Reviews could be non-systematic (narrative) or systematic. Reviews can be submitted as a Mini-Review (no more than 2,500 words, 3 figures, and 1 table) or a long review (no more than 6,000 words, 6 figures, and 3 tables). Reviews should contain four sections: Abstract, Introduction, Topics (with headings and subheadings, and Conclusions and Outlook.

Perspectives

Perspectives are brief, evidenced-based and formally structured essays covering a wide variety of timely topics of relevance to biomedicine. Perspective articles are limited to 2,500 words and usually include ≤ 10 references, one figure or table. Perspectives contain four sections: Abstract, Introduction, Topics (with headings and subheadings), Conclusions and Outlook.

Viewpoints

Viewpoint articles include academic papers, which address any important topic in biomedicine from a personal perspective than standard academic writing. Maximum length is 1,200 words, ≤ 70 references, and 1 small table or figure.

Manuscript Preparation

Title Page

The first page of the manuscript (title page) should include (1) a full title of the article, (2) a short title of less than 60 characters with spaces, (3) the authors' names, academic degrees, and affiliations, (4) the total word count of the manuscript (including Abstract, Text, References, Tables, Figure Legends), (5) the number of figures and tables, and (6) the name, email address, and complete address of corresponding author.

Disclaimers. An example of a disclaimer is an author's statement that the views expressed in the submitted article are his or her own and not an official position of the institution or funder.

Abstract

The article should include a brief abstract of no more than 200 words. Limit use of acronyms and abbreviations. Define at first use with acronym or abbreviation in parentheses. The abstract should be structured with the following headings: Background, Methods and Results, and Conclusions. The

Background section should describe the rationale for the study. Methods and Results should briefly describe the methods and present the significant results. Conclusions should succinctly state the interpretation of the data. Authors should supply a list of up to four key words not appearing in the title, which will be used for indexing. The key words should be listed immediately after the Abstract. Use terms from the Medical Subject Headings (MeSH) list of Index Medicus when possible.

Main text in the IMRaD format

Introduction should describe the purpose of the study and its relation to previous work in the field; it should not include an extensive literature review.

Methods should be concise but sufficiently detailed to permit repetition by other investigators. Previously published methods and modifications should be cited by reference. A subsection on statistics should be included in the Methods section.

Results should present positive and relevant negative findings of the study, supported when necessary by reference to Tables and Figures.

Discussion should interpret the results of the study, with emphasis on their relation to the original hypotheses and to previous studies. The importance of the study and its limitations should also be discussed.

The IMRaD format does not include a separate Conclusion section. The conclusion is built into the Discussion. More information on the structure and content of these sections can be found in the Recommendations for the Conduct, Reporting, Editing and Publication of Scholarly Work in Medical Journals (ICMJE Recommendations), available from www.ICMJE.org.

Acknowledgments, Sources of Funding, and Disclosures

Acknowledgments: All contributors who do not meet the criteria for authorship should be listed in an acknowledgments section. Examples of those who might be acknowledged include a person who provided purely technical help, writing assistance, or a department chairperson who provided only general support. Authors should declare whether they had assistance with study design, data collection, data analysis, or manuscript preparation. If such assistance was available, the authors should disclose the identity of the individuals who provided this assistance and the entity that supported it in the published article.

Sources of Funding: All sources of financial support for the study should be cited on the title page, including federal or state agencies, nonprofit organizations, and pharmaceutical or other commercial sources.

Disclosure and conflicts of interest: All authors must disclose any financial or other relations that could lead to a conflict of interest. If a potential conflict exists, its nature should be stated for each author. All sources of financial support for the study should be cited, including federal or state agencies, nonprofit organizations, and pharmaceutical or other commercial sources. Please use ICMJE Form for Disclosure of Potential Conflicts of Interest (<http://www.icmje.org/conflicts-of-interest/>).

References

References should follow the standards summarized in the NLM's International Committee of Medical Journal Editors (ICMJE) Recommendations for the Conduct, Reporting,

Editing and Publication of Scholarly Work in Medical Journals: Sample References webpage (www.nlm.nih.gov/bsd/uniform_requirements.html) and detailed in the NLM's Citing Medicine, available from www.ncbi.nlm.nih.gov/books/NBK7256/. MEDLINE abbreviations for journal titles (www.ncbi.nlm.nih.gov/nlmcatalog/journals) should be used. The first six authors should be listed in each reference citation (if there are more than six authors, "et al" should be used following the sixth). Periods are not used in authors' initials or journal abbreviations. Examples of journal reference style:

Journal Article: Serruys PW, Ormiston J, van Geuns RJ, de Bruyne B, Dudek D, Christiansen E, et al. A Poly(lactide Bioresorbable Scaffold Eluting Everolimus for Treatment of Coronary Stenosis: 5-Year Follow-Up. *J Am Coll Cardiol*. 2016;67(7):766-76. doi: 10.1016/j.jacc.2015.11.060.

Book: Murray PR, Rosenthal KS, Kobayashi GS, Pfaffler MA. *Medical Microbiology*. 4th ed. St. Louis: Mosby; 2002.

Chapter in Edited Book: Meltzer PS, Kallioniemi A, Trent JM. Chromosome alterations in human solid tumors. In: Vogelstein B, Kinzler KW, editors. *The Genetic Basis of Human Cancer*. New York: McGraw-Hill; 2002:93-113.

References should be numbered consecutively in the order in which they are first mentioned in the text. Identify references in text, tables, and legends by Arabic numerals in parentheses and listed at the end of the article in citation order.

Tables

Tables should be comprehensible without reference to the text and should not be repetitive of descriptions in the text. Every table should consist of two or more columns; tables with only one column will be treated as lists and incorporated into the text. All tables must be cited in the text and numbered in order of appearance. Tables should include a short title. Place explanatory matter in footnotes, not in the heading. Explain all nonstandard abbreviations in footnotes, and use symbols to explain information if needed. Each table submitted should be double-spaced, each on its own page. Each table should be saved as its own file as a Word Document. Explanatory matter and source notations for borrowed tables should be placed in the table footnote.

Figures and Legends

All illustrations (line drawings and photographs) are classified as figures. All figures should be cited in the text and numbered in order of appearance. Figures should be provided in .tiff, .jpeg or .eps formats. Color images must be at least 300 dpi. Gray scale images should be at least 300 dpi. Line art (black and white or color) and combinations of gray scale images and line art should be at least 1,000 dpi. The optimal size of lettering is 12 points. Symbols should be of a similar size. Figures should be sized to fit within the column (86 mm) or the full text width (180 mm). Line figures must be sharp, black and white graphs or diagrams, drawn professionally or with a computer graphics package. Legends should be supplied for each figure and should be brief and not repetitive of the text. Any source notation for borrowed figures should appear at the end of the legend. Figures should be uploaded as individual files.

Units of Measurement

Measurements of length, height, weight, and volume should be reported in metric units (meter, kilogram, or liter) or their decimal multiples. Temperatures should be in degrees

Celsius. Blood pressures should be in millimeters of mercury. All measurements must be given in SI or SI-derived units. Drug concentrations may be reported in either SI or mass units, but the alternative should be provided in parentheses where appropriate.

Style and Language

The journal accepts manuscripts written in English. Spelling should be US English only. The language of the manuscript must meet the requirements of academic publishing. Reviewers may advise rejection of a manuscript compromised by grammatical errors. Non-native speakers of English may choose to use a copyediting service.

Abbreviations and Symbols

Use only standard abbreviations; use of nonstandard abbreviations can be confusing to readers. Avoid abbreviations in the title of the manuscript. The spelled-out abbreviation followed by the abbreviation in parenthesis should be used on first mention unless the abbreviation is a standard unit of measurement.

Drugs should be referred to by their generic names. If proprietary drugs have been used in the study, refer to these by their generic name, mentioning the proprietary name, and the name and location of the manufacturer, in parentheses.

Permissions

To use tables or figures borrowed from another source, permission must be obtained from the copyright holder, usually the publisher. Authors are responsible for applying for permission for both print and electronic rights for all borrowed materials and are responsible for paying any fees related to the applications of these permissions. This is necessary even if you are an author of the borrowed material. It is essential to begin the process of obtaining permission early, as a delay may require removing the copyrighted material from the article. The source of a borrowed table should be noted in a footnote and of a borrowed figure in the legend. It is essential to use the exact wording required by the copyright holder. A copy of the letter granting permission, identified by table or figure number, should be sent along with the manuscript. A permission request form is provided for the authors use in requesting permission from copyright holders.

Open Access Policy

All articles published by International Journal of Biomedicine are made freely and permanently accessible online immediately upon publication, without subscription charges or registration barriers. Articles published under an IMRDC user license are protected by copyright and may be used for non-commercial purposes. A copy of the full text of each Open Access article is archived in an online repository separate from the journal. The International Journal of Biomedicine's articles are archived in Scientific Electronic Library (Russian Science Citation Index). The authors can also self-archive the final publisher's version/PDF on personal website, departmental website, institutional repository with a link to publisher version.

Users may access, download, copy, translate, text and data mine (but may not redistribute, display or adapt) the articles for non-commercial purposes provided that users cite the article using an appropriate bibliographic citation (i.e. author(s), journal, article title, volume, issue, page numbers, DOI and the link to the definitive published PDF version on www.ijbm.org).

Article Processing Charges

When a paper is accepted for publication, the author is issued an invoice for payment of Article Processing Charge (APC). APC can be paid by the author or on their behalf, for example, by their institution or funding body.

APC helps IMRDC recover the costs of publication—including peer review management, production of the journal printed version, and online hosting and archiving, as well as inclusion in citation databases, enabling electronic citation in other journals that are available electronically. IJBM publishes all content Open Access and makes the content freely available online for researchers and readers.

IJBM charges a processing fee of \$120.00 per printed black and white journal page and \$220.00 per printed page of color illustrations. IJBM charges a processing fee of \$100.00 per page in the case of online-only publications. For online-only publications, all illustrations submitted in color will be published in color online, at no cost to the author.

Under IJBM's existing policy, certain categories of authors are eligible for a discount. The amount of discount depends on factors such as country of origin, position of the author in the institute and quality and originality of the work. Young researchers and first time authors may also qualify for

a discount. To apply for a discount, please contact our office using the 'Contact Us' page or send email to the Publisher (editor@ijbm.org) with the following information:

- Your name and institution with full address details
- Reason for applying for a waiver
- Title of your paper
- Country of residence of any co-authors.

Page Proofs

Page proofs are sent from the Publisher electronically and must be returned within 72 hours to avoid delay of publication. Generally, peer review is completed within 3-4 weeks and the editor's decision within 7-10 days of this. It is therefore very rare to have to wait more than 6 weeks for a final decision.

IMRDC Author Services

If you need help preparing a manuscript for submission, our publisher, IMRDC, offers a range of editorial services for a fee, including Advanced Editing and Translation with Editing. Please note that use of IMRDC Author Services does not guarantee acceptance of your manuscript.

It is important to note that when citing an article from IJBM, the correct citation format is **International Journal of Biomedicine**.
